

PREPRINTS

Symposia

Characterization and Chemistry of Oil Shales

**(Cosponsored by Division of Petroleum Chemistry
and Division of Fuel Chemistry)**

*Co-chairmen, J. Y. Shang
H. L. Feldkirchner*

DIVISION OF PETROLEUM CHEMISTRY, INC.



American Chemical Society

SYMPOSIUM ON CHARACTERIZATION AND CHEMISTRY OF OIL SHALES
PRESENTED BEFORE THE DIVISIONS OF FUEL CHEMISTRY AND
PETROLEUM CHEMISTRY, INC.
AMERICAN CHEMICAL SOCIETY
ST. LOUIS MEETING, APRIL 8 - 13, 1984

CHEMICAL CHARACTERIZATION OF AN OIL SHALE BED LYING WITHIN THE
HEATH FORMATION, FERGUS COUNTY, MONTANA

By

F. N. Abercrombie, P. D. Derkey and J. A. Daniel
Montana Bureau of Mines and Geology, Montana College of Mineral Science and Technology
Butte, Montana 59701

INTRODUCTION

Over 1,200 ft of core from the Heath Formation were obtained during an exploratory drilling project by the Montana Bureau of Mines and Geology in 1982. The results of that project are detailed in Derkey (1). Data derived from that study indicate that a thin, metalliferous oil-shale zone occurs in six of seven core holes over a 130-sq mi area (Figure 1). The average thickness of this oil shale zone is 6.2 ft. It has a weighted average* oil yield of 10.4 gal per short ton and is enriched in molybdenum, nickel, vanadium and zinc. Chromium is only locally anomalous.

Vine and Tourtelot (2, 3) were the first workers to describe the Heath Formation as containing above-average amounts of chromium and nickel. A decade later, Desborough and others (4) and Desborough and Poole (5) reported anomalous values of molybdenum, nickel, vanadium and zinc in the Heath Formation. Cox and Cole (6) summarized previous work concerning the oil potential of the Heath Formation. Published oil yields from within the study area range from 0 to 26.4 gal per short ton (4, 6-8).

EXPERIMENTAL

Sampling

Samples consisted of 0.5- to 2.6-ft core intervals, each generally representing a single lithology. The cores were cut along the longitudinal axis to provide a repository sample (1/4), lithological sample (1/2) and chemical analysis sample (1/4). The chemical analysis sample was crushed to 1/4-3/8 size and split at the Laramie Energy Technology Center (Wyoming), U. S. Department of Energy. The A split was taken for Fischer-Assay analysis while the B split was returned to the Montana Bureau of Mines and Geology. The B splits were dried at 110°C for 1 hr and pulverized using a Bico-Braun rotary pulverizer with alumina plates. The individual sample pulps were blended and placed in Kraft paper envelopes.

Fischer Assay

The Fischer Assay (ASTM D3904-80) was carried out in Laramie under the direction of Laurence G. Trudell for the entire 1,224-ft thickness of recovered drill core.

Sample Dissolution

Digestion A - 2-Gram samples were treated by a combined wet acid digestion of 6 ml HNO_3 /2 ml HC10_4 /2 ml H_2SO_4 taking the samples to dense fumes of $\text{HC10}_4/\text{H}_2\text{SO}_4$. After evaporating to near dryness, the cool pastes were treated with 4.7 ml HCl and 1.3 ml HNO_3 . After mild heating and cooling, the samples were diluted to 100 ml.

Digestion B - 2-Gram samples were roasted for 4 hr at 450°C. Mixed acid consisting of 2 ml HF /2 ml HNO_3 /6 ml HCl was added and heated slowly until evaporated to near dryness. The acid treatment was repeated. After evaporating to near dryness 1 ml HNO_3 and 3 ml HCl was added and evaporated to near dryness twice. 1.6 ml HNO_3 and 4.6 ml HCl was added, heated, cooled and diluted to 100 ml.

Extraction

2-Gram portions of selected shales were extracted with xylene using a Soxhlet extractor

* Average value for stratigraphic unit, weighted for sample interval thickness. Weighted average = $\sum (\text{sample concentration} \times \text{sample interval thickness}) / (\text{total interval thickness})$.

(Corning 3480) for 48 hours. The extractor and upper section of the boiling flask were insulated in order to increase the extraction temperature. After cooling, the xylene-oil extract solution was filtered through .45 μ membrane filters to remove shale fines. The xylene was removed from the extracted oil using a rotary evaporator (water aspirator; 50°C bath). The extracted oil was then weighed.

Dilution of Oils

The oil distillates from Fischer Assay, the oils recovered by xylene extraction, and oil standards were diluted 1 to 20 (w/v) in xylene. Conostan 21TM blended oil (21 elements at 900 ppm), 5000 ppm Conostan cobalt single element oil and Conostan 75 base oil were similarly diluted in xylene. The diluted standards were mixed and diluted with 1:20 Conostan 75 base oil-xylene providing serial dilutions at decade levels from 500 to 0.05 ppm element.

Carbon Analyses

Total carbon content of selected shales was determined by ASTM D-3178-73. Carbonate content of the shales was determined by addition of 10% (v/v) H₂SO₄ to the shale contained in a flask connected to an Orsat gas buret. The solution was heated to boiling and flooded with water to transfer all the evolved gases into the buret. The evolved sulfur oxides and hydrocarbons were removed by absorption in permanganate and silver sulfate/sulfuric acid solutions, respectively. The carbon dioxide was then determined volumetrically by difference after absorption with saturated potassium hydroxide solution.

Atomic Absorption Analysis - Cobalt

The cobalt analysis of shale acid digests was accomplished using a Perkin-Elmer 603 following the manufacturer's instructions (direct nebulization, 240.7 nm, air-acetylene and background correction).

Multi-Element Analysis

Multi-element analysis of the oil shale digests and oil-xylene mixtures was accomplished using an Applied Research Laboratories Model 34000 induction coupled argon plasma emission spectrometer. Forward powers of 1600 and 2000 watts (2-turn load coil) were used for aqueous acid digests and xylene solutions, respectively. The manufacturer's operating instructions were followed with the exception that sample uptake was controlled by a Gilson Minipuls IITM peristaltic pump. A computer iteration (9) which computes a correction factor (similar to an internal standard) was used to correct for the matrix effect caused by the varying concentration of the major elements in the shale.

Reflectance Measurements

A Leitz, incident-light microscope with oil immersion objectives was used to identify coal macerals and to assess sediment thermal maturity. Reflectance of the maceral vitrinite was measured with a MPV compact system photometer using methods outlined by Stach (10) and International Committee for Coal Petrology (11). Fifty measurements per polished plug for 2 plugs per sample were taken for a total of 13 core samples of coal collected from both above and below the oil shale zone. For each sample, 50 measurements were taken with polarized light and 50 with non-polarized light, always using a 546-nm interference filter. Mean vitrinite reflectance (R₀) was measured, rather than mean maximum reflectance.

RESULTS AND DISCUSSION

A single oil shale zone within the Heath Formation is correlated over a 130-sq mi area based on stratigraphic position, relatively high Fischer-Assay oil yields, and enriched metal content (1). The oil shale unit generally thickens eastward, ranging from 4.0 ft thick at the western edge of the study area to 3.4 and 5.7 ft thick in the central part of the area to 10.5 ft thick at the area's eastern edge.

Oil Yield and Organic Carbon

The average thickness of the oil shale is 6.2 ft. It has a weighted average oil yield of 10.4 gal per short ton and a weighted average organic carbon content of 11.4%. Oil yields of individual samples range from 3.1 to 20.0 gal per short ton. An almost 1:1 relationship exists between oil yield and organic carbon content (Figure 2). A similarly close relationship also has been reported for the Sunbury Shale and the Cleveland high-grade zone of the Ohio Shale in northeastern Kentucky (12).

Weighted average oil yield generally decreases as the unit thickens. Weighted average values range from 12.0 to 15.7 gal per short ton for 3.4- to 5.7-ft-thick oil shale in the western

and central parts of the study area to 8.1 and 8.6 gal per short ton for 10.5-ft-thick oil shale at the eastern edge of the area based on data from 24 samples from 6 core holes.

Metal Content

Evaluation of Digestion Procedures - Replicate samples of 25 selected shales were analyzed by the two digestion procedures. The replication scheme included triplicate digestions by each procedure for 6 samples and duplicate digestions by each procedure for 2 samples; single digestions by each procedure were carried out for the remaining 17 samples. The plasma emission analyses for digestions A and B of sample nos. 32779, 32780 and 32781 are presented in Table I for selected elements. The HF-aqua regia digestion (digestion B) yielded better precision and dissolved more of the sample as demonstrated by significantly higher values obtained for Al, Fe, Mn, Nb, Ti, V and Zr and somewhat higher values for Mg, Na, Li and Sr. The elements Ca, Mn and Ag were definitely more soluble in the nitric/perchloric/sulfuric acid digestion (digestion A); and Cd, Cr, Cu, P and Zr were somewhat more soluble in digestion A. The elements Mo, Ni and Pb were dissolved equally by the two digestions. Digestion B was selected for the digestion of the remaining samples because of its overall efficiency and ease of implementation compared to digestion A.

TABLE I

COMPARISON OF ACID DIGESTION PROCEDURES

<u>Sample Number</u>	<u>Digestion Procedure</u> ^a	<u>Ca</u> <u>%</u>	<u>K</u> <u>%</u>	<u>Al</u> <u>%</u>	<u>Mn</u> <u>ppm</u>	<u>Cr</u> <u>ppm</u>	<u>Cu</u> <u>ppm</u>	<u>Mo</u> <u>ppm</u>
33085	A	7.9	.29	.97	190	49	31	130
		8.9	.22	.72	190	41	31	130
	B	17.1	.71	2.00	230	83	43	140
		16.8	.70	2.01	220	77	40	130
33086	A	6.3	.63	2.2	190	140	46	200
		3.4	.59	2.0	160	130	36	170
		10.0	.31	1.0	190	90	53	200
	B	12.8	1.05	3.6	200	190	58	200
		12.0	.98	3.4	200	180	54	200
		12.5	.99	3.5	200	180	54	200
33087	A	11.4	.11	.30	270	23	21	46
		9.1	.14	.41	260	27	19	49
	B	12.5	.30	.41	290	46	25	43
		12.4	.29	.49	290	47	28	46

<u>Sample Number</u>	<u>Digestion Procedure</u> ^a	<u>Nb</u> <u>ppm</u>	<u>Ni</u> <u>ppm</u>	<u>Pb</u> <u>ppm</u>	<u>Sr</u> <u>ppm</u>	<u>V</u> <u>ppm</u>	<u>Zn</u> <u>ppm</u>
33085	A	4.4	112	23	180	231	570
		4.9	112	30	210	190	560
	B	4.8	110	16	390	370	610
33086	A	4.4	102	7	400	360	580
		4.5	150	21	180	610	1160
		3.9	130	18	140	550	970
	B	6.1	160	54	240	370	1190
		3.9	150	27	360	830	1230
		2.7	140	22	360	810	1170
33087	A	3.5	150	27	350	800	1170
		4.7	41	33	160	90	21
	B	4.4	41	28	120	110	24
		8.2	33	11	240	180	25
		11.4	35	18	240	180	21

a. See text.

Several pulverized samples were split in triplicate to provide control samples. The second and third splits were sent to the U. S. Geological Survey in Denver for Chemical analysis. The comparison of these data is given in Table II. The agreement between the data from the three laboratories using two different instrumental procedures is very good.

TABLE II

COMPARISON OF MBMG AND USGS ANALYTICAL RESULTS OF SELECTED ELEMENTS FOR SIX BLACK SHALE CORE SAMPLES OF THE HEATH FORMATION FROM THE COX RANCH BOREHOLE

Sample No. and Oil Yield	Element	MBMG Metal Values (ppm)			USGS Metal Values (ppm)		
		ICP Emission Spectroscopy			X-Ray Fluorescence (Poole written commun. 1983)	ICP Emission Spectroscopy, (Lichte, written commun., 1983)	
32780 (7.5 gal/ton)	Cr	196	192	196	--	170	170
	Mo	206	205	208	200	200	200
	Ni	154	152	155	100	140	150
	V	860	865	868	800	840	850
	Zn	1190	1130	1133	800	1000	1100
32804 (no oil)	Cr	116	121	117	--	110	110
	Mo	18	20	17	<20	16	14
	Ni	61	70	62	<100	60	58
	V	154	159	156	<100	160	150
	Zn	72	100	81	<100	90	90
32809 (no oil)	Cr	55	57	58	--	55	56
	Mo	2	5	3	<20	4	3
	Ni	58	57	58	<100	56	55
	V	61	62	63	<100	63	63
	Zn	45	36	33	<100	40	30
32829 (18.3 gal/ton)	Cr	330	336	346	--	300	300
	Mo	690	703	717	700	670	680
	Ni	562	576	594	750	550	560
	V	2149	2209	2234	2500	2200	2200
	Zn	4948	5091	5127	3500	4700	4700
32844 (trace oil)	Cr	112	118	125	--	110	110
	Mo	5	9	7	<20	8	6
	Ni	70	76	82	<100	74	77
	V	138	148	152	<100	150	140
	Zn	19	72	32	<100	30	30
32951 (14.7 gal/ton)	Cr	593	600	602	--	--	--
	Mo	289	291	288	300	--	--
	Ni	313	319	320	300	--	--
	V	1312	1324	1324	1500	--	--
	Zn	2746	2761	2763	2000	--	--

-- Not determined.

Roasted Shale - Analysis of 95 roasted samples (digestion B) of the Heath Formation interbedded shale and limestone unit indicates that the enclosed oil shale zone is enriched in molybdenum, nickel, vanadium and zinc in six of seven core holes and in chromium in two of the six core holes. Weighted average values of these metals for the interbedded unit (excluding the oil shale zone) exceed average values for black shales but do not exceed thresholds that delineate metal-rich black shales as defined by Vine and Tourtelot (3).

Weighted average values for the oil shale in six core holes are 385 ppm Cr, 352 ppm Mo, 269 ppm Ni, 948 ppm V and 1,737 ppm Zn. These weighted average values reach a maximum of 525 ppm Cr, 515 ppm Mo, 326 ppm Ni, 1,088 ppm V and 2,420 ppm Zn in individual core holes. In comparison, weighted average values for the sampled portion of the interbedded unit (excluding the oil shale zone) in six core holes are 106 ppm Cr, 144 ppm Mo, 104 ppm Ni, 234 ppm V and 329 ppm Zn. These weighted average values reach a maximum of 221 ppm Cr, 178 ppm Mo, 154 ppm Ni, 374 ppm V and 816 ppm Zn in individual core holes.

The distribution of weighted average chromium, molybdenum, nickel, vanadium, zinc and oil values for the oil shale zone shows that chromium is a fairly good indicator of oil content, a fact which holds true for individual samples. Chromium and vanadium are enriched only within the oil zone. Chromium is enriched in all samples which yielded 14 or more gal oil per short ton, whereas vanadium is enriched in some, but not all, samples which yielded 6.6 or more gal oil per short ton. Molybdenum, nickel and zinc are less closely associated with oil yield. Molybdenum is

enriched sporadically throughout the interbedded shale and limestone unit of the Heath Formation; high molybdenum values do not always correspond to high oil yields for individual samples. Nickel and zinc, for the most part, are enriched within the oil shale zone; a few high values occur in the enclosing interbedded shale and limestone unit. As with molybdenum, high nickel and zinc values do not necessarily correspond to high oil yields for individual samples.

Comparison of metal abundance of the Heath oil shale zone with other Paleozoic-age black shales of the United States indicates that the zone is most similar to the Sunbury Shale in north-eastern Kentucky.

Fischer-Assay Oil Distillate - Metal values for oil distillates produced from 20 samples of the oil shale by the Fischer-Assay procedure are extremely low compared to values for corresponding roasted shale samples. Average values of selected metals in oil distilled from the oil shale zone are <1 ppm Cr, <1 ppm Mo, 7 ppm Ni, 23 ppm V and 2 ppm Zn based on weighted average values from six core holes. The major portion of these metals remained behind in the spent shale, as is shown by analysis of the spent shale.

Fischer-Assay Spent Shale - Metal values for 5 samples of the oil shale zone from which an oil product was removed by Fischer-Assay distillation are slightly higher than values for corresponding roasted shale samples (Table III). In comparison, the Fischer-Assay oil distillates have a very low metal content. Removal of the oil distillate has benefited the spent shale slightly.

TABLE III

COMPARISON OF MBMG EMISSION SPECTROSCOPY RESULTS OF SELECTED ELEMENTS FOR VARIOUS FRACTIONS OF FIVE METAL- AND OIL-RICH OIL SHALE SAMPLES

Sample Interval No. Oil Yield and Drill Hole	Element	Metal Content (ppm)				
		Shale Fractions			Oil Fractions	
		Oil Shale ^a	Fischer-Assay Spent Shale ^b	Inorganic Fraction ^c	Fischer- Assay Oil ^d	Organic Fraction ^e
32951/33520 (14.7 gal/ton) Cox Ranch	Cr	598 ^f	630	607	<1	<1
	Mo	290 ^f	318	289	1	1
	Ni	317 ^f	347	319	4	1
	V	1320 ^f	1399	1215	20	45
	Zn	2758 ^f	2982	2807	3	<1
33026/33521 (18.0 gal/ton) Beaver	Cr	621	692	664	<1	<1
	Mo	337	354	359	<1	<1
	Ni	356	398	364	10	4
	V	1413	1510	1412	10	15
	Zn	4203	4471	4371	3	<1
33107/33523 (19.9 gal/ton) Middle Bench	Cr	572	634	594	<1	<1
	Mo	483	558	500	<1	1
	Ni	407	478	416	11	<1
	V	1657	1848	1481	50	13
	Zn	3176	3723	3353	2	<1
33216/33522 (14.0 gal/ton) Red Hill	Cr	569	630	541	<1	<1
	Mo	298	333	291	<1	7
	Ni	307	344	296	6	3
	V	1410	1510	1178	25	99
	Zn	2221	2502	2243	2	<1
33358/33524 (20.0 gal/ton) Heath	Cr	700	811	700	<1	<1
	Mo	397	429	367	<1	<1
	Ni	398	443	365	9	7
	V	1586	1723	1374	21	53
	Zn	3490	3953	3494	2	<1

a. 500°C ash of core sample.

b. Core sample from which Fischer-Assay oil was distilled at 500°C.

c. Inorganic fraction of core sample derived by low temperature xylene extraction technique.

d. Oil derived from core sample by the modified Fischer-Assay procedure.

e. Organic fraction of core sample derived by low temperature xylene extraction technique.

f. Average value

Inorganic Fraction - Metal values for the inorganic fraction of 5 samples of the oil shale zone in which xylene was used to disassociate the inorganic and organic fractions at a low temperature (120°C) are slightly less than values for corresponding roasted shale samples (Table III).

Organic Fraction - Metal values for the organic fraction of 5 samples of the oil shale zone in which xylene was used to disassociate the inorganic and organic fractions at a low temperature (120°C) are extremely low and very similar to values for corresponding Fischer-Assay oil distillates (Table III).

The xylene extracted fractions also exhibit color and odor properties which are different from those of the Fischer distillates. The color of the xylene extracted oil fractions ranged from dark yellow to red-brown. The xylene-extracted oil fractions did not have any odor. The Fischer distillates were often composed of 3 phases (water, dark brown oil and light gray grease). The Fischer distillates all possessed a strong, sharp, biting odor that is often associated with crude oil.

Reflectance

Average vitrinite reflectance values range from 0.49 to 0.64% reflectance for samples from a coal bed that occurs just below the oil shale zone (Table IV). This range indicates an immature to incipiently oil-mature coal bed and, thus, less oil-mature overlying rocks, if thermal maturity in this area is directly related to sediment burial depth.

TABLE IV
REFLECTANCE (% R_o) DATA

Core Hole	Depth (ft)	Sample Number	Number of Measurements	R _o (%)
Beaver	159 ^a	33508	100	0.53
Cottonwood	101 ^a	33507	100	0.53
Middle Bench	65 ^a	33506	100	0.55
Red Hill	248 ^a	33505	100	0.49
Heath	284 ^a	33504	100	0.49
Cox Ranch	117	33509	100	0.55
	185	33510	100	0.61
	436	33500	100	0.70
Potter Creek	254 ^a	33513	100	0.57
	258 ^a	33512	100	0.64
	289	33503	---	contaminated
	312	33514	100	0.73
	324	33515	100	0.83

a. Coal bed which occurs just below the oil shale zone.

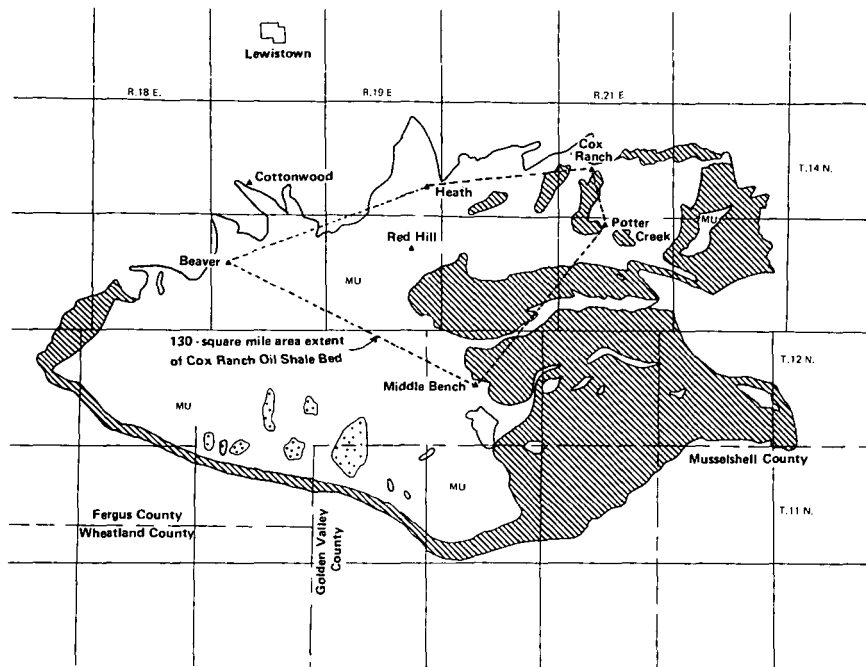
Reflectance values increase rapidly in the Potter Creek drill hole from 0.57% R_o (incipiently mature) at 254 ft depth to 0.83% R_o (oil-mature) at 324 ft depth. This rapid increase is probably due to the intrusion of a 6-ft-thick lamprophyre sill or dike at 340 ft depth, 16 ft below the lowermost coal. The high, 0.70% R_o value for the lowermost coal in the Cox Ranch core hole may also be the result of igneous activity; however, igneous rocks were not intersected in this core hole.

Conclusion

Shale samples from the Heath Formation have been analyzed to characterize their oil and metal content. The objective of this program was to determine whether or not these shales possessed any economic resource value. Early discussions about the Heath oil shale reasoned that a "low" oil yield shale might have economic value if metals in the shale were contained in the shale oil distillate as metal porphyrins. The emission spectrometric analysis of Fischer-Assay oil distillates proved that no significant amount of metals was found in the distillate. While the Fischer Assay does not provide an exact measure of the oil shale retorting process, we believe the data imply that commercial scale retorting of the Heath oil shale will not recover significant levels of metals.

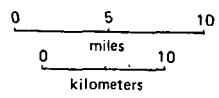
We also subjected the Heath oil shale to solvent extraction to determine whether or not the retorting temperatures might be pyrolyzing any metal organic complexes in the shale. Emission spectrometric analysis of the xylene extracted oil found no significant metal content in the extracted oil. This final test suggests that the metal content is not carried by the labile organic fraction of the oil shale. The metal values of the Heath shale probably can not be economically recovered from

FIGURE 1



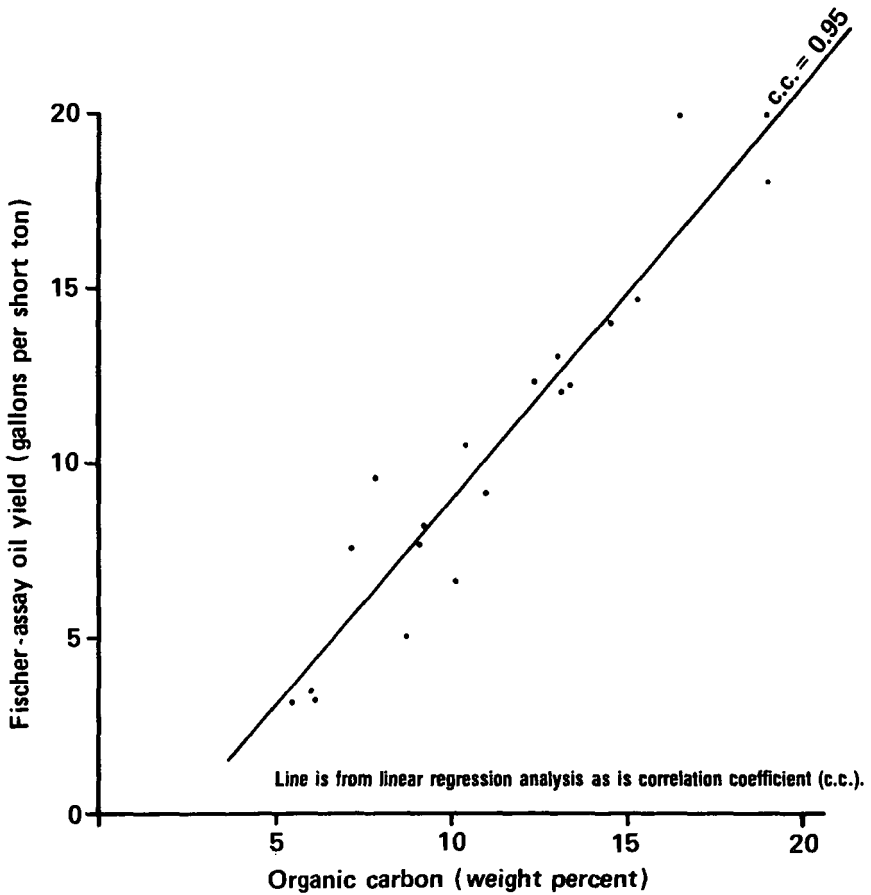
EXPLANATION

-  Post - Pennsylvanian strata
-  Pennsylvanian strata
-  Mississippian strata
-  Pre - Mississippian strata
-  MBMG core hole



**Generalized geologic map of central Montana
showing location of MBMG core holes**

FIGURE 2



Plot of Fischer-assay oil yield vs. organic carbon for the oil shale bed based on 20 samples from 6 core holes.

the shale concurrent with a shale oil recovery process. This property does not enhance the economic potential of the Heath oil shale as an oil and metal resource.

LITERATURE CITED

- (1) Derkey, P. D., "Oil and Metal Potential of the Heath Formation, Fergus County, Montana", Montana Bureau of Mines and Geology Open-File Report 110, p. 86 (1983).
- (2) Vine, J. D. and Tourtelot, E. B., "Geochemical Investigations of Some Black Shales and Associated Rocks", U. S. Geological Survey Bulletin 1314-A, p. 43 (1969).
- (3) Vine, J. D. and Tourtelot, E. B., "Geochemistry of Black Shale Deposits--A Summary Report", Economic Geology, 65, 253-272 (1970).
- (4) Desborough, G. A., Poole, F. G. and Green, G. N., "Metaliferous Oil Shales in Central Montana and Northeastern Nevada", U. S. Geological Survey Open-File Report 81-121, 1. 14 (1981).
- (5) Desborough, G. A. and Poole, F. G., "Metal Concentrations in Marine Black Shales of Western United States", Soc. of Mining Engineers of AIME, Preprint no. 82-58, p. 14 (1982).
- (6) Cox, W. E. and Cole, G. A., "Oil Shale Potential in the Heath and Tyler Formations, Central Montana", Montana Bureau of Mines and Geology Geologic Map 19, 2 sheets (1981).
- (7) Cox, W. E., "Fergus County Research Project--Evaluation of Heath-Tyler Oil Shales, With Laboratory Analyses by John W. Blumer", Montana Bureau of Mines and Geology Open-File Report M.B.M.G 15, p. 85 (1973).
- (8) Miller, R. N., "Oil Shales in Montana", B. S. Thesis, Montana School of Mines, Butte, p. 78 (1953).
- (9) Abercrombie, F. N. and Olmstead, W., "A Computer Approach to True Internal Standardization for Induction Coupled Plasma-Emission Spectroscopy", in preparation.
- (10) Stach, E., Stach's Textbook of Coal Petrology (2nd edition), Berlin, Gebruder Borntraeger, Berlin, p. 428 (1975).
- (11) International Committee for Coal Petrology, "International Handbook of Coal Petrography (2nd edition)", Centre National de la Recherche Scientifique, Paris, unpaginated looseleaf book (1963). (Supplements published in 1971, 1975.)
- (12) Robl, T. L., Beard, J. G., Kepferle, R. C., Pollock, J. D., Koppelaar, D. W., Thomas, G. A., Bland, A. E., Cislser, K., Barron, L. S. and Kung, J., "Resource Assessment of Oil-Bearing Shales in Lewis and Fleming Counties, Kentucky", Insti. for Mining and Minerals Research Technical Report, Univ. of Kentucky, Lexington, 2 volumes (not paginated) (1980).

SYMPOSIUM ON CHARACTERIZATION AND CHEMISTRY OF OIL SHALES
PRESENTED BEFORE THE DIVISIONS OF FUEL CHEMISTRY AND
PETROLEUM CHEMISTRY, INC.
AMERICAN CHEMICAL SOCIETY
ST. LOUIS MEETING, APRIL 8 - 13, 1984

RAPID HEAT-UP ASSAY FOR EASTERN OIL SHALES

By

C. A. Audeh

Mobil Research and Development Corporation, Central Research Division, P. O. Box 1025
Princeton, New Jersey 08540

INTRODUCTION

Interest in the exploitation of eastern oil shales is related to the economics of their location. Advantages such as the availability of the needed water resources and a labor pool with experience in mining as well as processing are usually cited in favor of the future development of these shales. Also, the proximity of the markets of the east coast to the resource makes their development attractive. However, eastern shales, in general, give low oil yields in the Fischer Assay. Since the Fischer Assay has been considered as a means of predicting oil yield from commercial processing of oil shale (1), the exploitation of eastern shales based on this yield evaluation becomes doubtful.

Many eastern shale deposits have been analyzed (2, 3) and assessed as to their commercial prospects (2) on the basis of their oil yield, carbon content and thickness. In general, eastern shales can be matched with samples from western shales with the same carbon content. However, the Fischer Assay yield of oil from a western shale exceeds that from an eastern shale with the same carbon content. For example, whereas a western shale with 13.6 wt % organic carbon yields 11.4 wt % oil (about 30 gallons per ton, g/t) an eastern shale with 13.7 wt % organic carbon yields 4.6 wt % oil (about 12 g/t) (4). These yields correspond to 73% and 30% conversion of organic carbon to oil.

Several reports (5-7) have suggested that oil yields from eastern shales are influenced by the rate at which the retorting temperature is reached. Thus, it was reported that when the rate of heat-up was increased to 55°C/min, vs. 12°C/min for the Fischer Assay (8), an oil yield 125% of Fischer Assay was obtained (5). Further, at much higher heat-up rates, 6,000°C/min (7) and 33,000°C/min (6), an increase of up to 140% of Fischer Assay oil yield was calculated. These calculated yields, however, were estimates based on the residual carbon content of the shale after retorting under Fischer Assay conditions and upon retorting in a fluidized bed unit (6). Yields were also calculated by measurement of relative areas under a chromatogram and elemental analyses of the spent shales (7). Although yields of shale oil were determined (5) or estimated (6, 7), oil characterization was not reported.

Clearly, there is no standard retorting procedure comparable to the Fischer Assay that is applicable to eastern shales wherein rapid heat-up (RHU) to the desired pyrolysis temperature could be used for determining the potential oil yield of an oil shale. Oil yield and oil properties are two essential characteristics needed for economic assessment of a shale resource. Thus, the development of a rapid heat-up assay for eastern shales that can generate collectible quantities of oil that could be characterized is necessary. Such an assay has been developed and it is proposed that it be adopted as a common procedure for determining the oil yield from shales under rapid heat-up conditions.

EXPERIMENTAL

Retort

Figure 1 depicts the rapid heat-up retort used in these experiments. The retort was constructed from two 6" x 6" stainless steel plates, 1/8" thick and a standard bolted flat flange. A 1/4" spacer was used along three edges of the plates to create a 6" x 6" x 1/4" "pocket" with a capacity of at least 100 gm. At the bottom of the pocket reactor (PR), a sweep gas inlet was connected to a diffuser through a plenum. The PR was sealed by bolting the loose top flange to the flange attached to the body of the retort. A high temperature gasket was placed between the two flanges to prevent product leakage. Two thermocouples, placed halfway in the bed of shale, were used to observe the temperature in the retort. The temperature was continuously monitored and recorded on a strip chart recorder. Products were allowed to leave the PR through an outlet connected to

the recovery system by a glass ball joint.

Retort Heater

A fluidized sand bath was used in all experiments. The sand bath temperature was set to about 575°C and maintained at that temperature.

Oil Recovery System

The system described in the Fischer Assay (8) was modified by using a -10°C bath for the centrifuge tube and by circulating -10°C coolant in an efficient glass condenser. However, other arrangements could be used to achieve the desired recovery of oil, as for example those described in (1, 5 and 9).

Gas Measurement

H₂S was removed as cadmium sulfide and the non-condensable gas was measured by means of a wet test meter.

Retorting Procedure

The loaded PR was connected to the inert gas lines and the flow adjusted to 10-15 ml/min. When the desired sand bath temperature (575°C) was reached, the PR was dropped into the bath and the product outlet immediately connected to the recovery system. As the inside temperature of the PR approached 480-485°C, the temperature of the sand bath was allowed to cool to about 515°C so that the retort temperature did not exceed 500-505°C. This temperature was then maintained for 30 minutes.

Oil Shale Samples

The various samples of oil shale used were collected from Bullitt County, Kentucky. Each sample was crushed and sieved. Particles, 16/28 and 28/35 mesh were collected. In some cases, a 16/35 mesh fraction was collected. All crushed samples were stored under argon.

RESULTS AND DISCUSSION

Retort Heat-Up Profiles

In a Fischer Assay, it is generally stated (1, 5-7) that the heat-up rate is 12°C/min. However, in the required heat-up profile (8), six distinct and different heat-up rates can be identified. These are:

- | | | | |
|----|-----------|------------------------|----------|
| 1. | 0-10 min | the rate is < 1°C/min | to 30°C |
| 2. | 10-20 min | the rate is 20°C/min | to 225°C |
| 3. | 20-30 min | the rate is 12.5°C/min | to 350°C |
| 4. | 30-36 min | the rate is 10°C/min | to 410°C |
| 5. | 36-44 min | the rate is 8°C/min | to 475°C |
| 6. | 44-55 min | the rate is 4°C/min | to 500°C |

Also, this profile corresponds to the temperature of the base of the Fischer retort and not the shale in the retort. By modifying the Fischer retort to allow for the measurement of its internal temperature, it was determined that there is a difference of about 70°C between the shale nearest the wall of the retort and its center. Even shale < 1/4" from the retort wall is 17°C cooler than the base.

For the RHU assay described, the actual temperature of the shale was measured and in the resultant profile, three distinct and different heat-up rates were identified. These were:

- | | | | |
|----|-------------|------------------------|----------|
| 1. | 0-2.5 min | the rate was 114°C/min | to 310°C |
| 2. | 2.5-5.0 min | the rate was 56°C/min | to 450°C |
| 3. | 5-7.5 min | the rate was 20°C/min | to 498°C |

However, since the bed of shale in the RHU retort is 1/4" in thickness, no temperature gradient was detectable across the 6" x 6" x 1/4" retort. It is estimated that the 1/4" bed is made up of about 10 shale particles and, since heat was uniformly applied from all directions, the heat-up profile of each 1/8" of shale is also uniform. Thus, overall, it was concluded that all the shale was retorted at the same temperature.

In control experiments, it was observed that two effects influence the observed decrease in heat-up rate: First, Δt , the difference between the temperature of the sand bath and the bed temperature of the retort. Second, the formation of oil during retorting. As the internal temperature increases and Δt becomes small, heat transfer is reduced and as oil is formed, the demand for energy increases. Both effects work in the direction of reducing the heat-up rate. It was not possible to study these effects separately; however, it was observed that when oil formation started the heat-up rate always decreased.

Oil formation was accompanied by the formation of gas. Also, about 90% of the oil produced was recovered during the 375-475°C temperature interval, which corresponds to a period of

about 2 minutes. This is in contrast with the Fischer Assay in which the same temperature interval corresponds to about 12 minutes during which less than 50% of the oil is collected. As pointed out earlier, the temperature of the shale in a Fischer retort does not correspond to that of the base of the retort and there exists within the retort a significant temperature gradient. Thus, whereas oil generation in the RHU retort proceeds uniformly and at the same temperature throughout the bed, in the Fischer retort, it proceeds across steep temperature gradients in time and space.

Yield of Products

Rapid heat-up to retorting temperatures results in a higher oil yield than that obtained in the Fischer Assay, Table I. All the eastern shales tested gave from about 150% to 200% of Fischer Assay. This observation is consistent with predicted increases for eastern shales and is achieved at lower heat-up rates than the 6,000-30,000°C calculated (6, 7). It also confirms the directional increase based on experiments carried out at a heat-up rate of about 50°C/min.

TABLE I
YIELDS OF OIL FROM FISCHER ASSAY AND RAPID HEAT-UP ASSAY OF OIL SHALES

Sample	Fischer Assay Gallons/Ton	Rapid Heat-Up Gallons/Ton
Kentucky, Bullitt Co.		
1 B	9.4	17.4
1 C	8.7	17.9
1 D	9.3	18.4
1 E	11.5	21.3
Drum	10.8	16.2

The other yields determined, Table II, were those of the gas that did not condense in the product recovery system, H₂S and retort water. It was observed that the volume of gas generated in RHU retorting was greater than that generated in the Fischer Assay. In contrast, the amount of water collected was the same and that of hydrogen sulfide smaller.

TABLE II
YIELD OF OIL, GAS AND H₂S FROM FISCHER ASSAY (FA)^a AND
RAPID HEAT-UP ASSAY (RHUA)^b

Sample I. D.	Oil, % Wt		Oil G/T		Gas 1/100g		H ₂ S, % Wt	
	FA	RHUA	FA	RHUA	FA	RHUA	FA	RHUA
1B	3.5	6.9	9.4	17.4	1.41	ND*	0.9	0.7
1C	3.2	7.1	8.7	17.9	1.61	2.03	1.9	1.6
1D	3.5	7.3	9.3	18.4	1.74	2.03	1.2	0.8
1E	4.4	8.5	11.5	21.3	1.82	2.68	1.5	1.2
Drum	4.3	6.3	11.3 ^c	16.0 ^d	1.20	1.60	1.1	0.9

- a. Heat-up to 500°C at - 12°C/min, 1/2 hr at 500°C.
- b. Heat-up to 500°C at an initial rate of about 100°C/min, 1/2 hr at 500°C.
- c. Average of 3 determinations; 11.8, 10.8 and 11.4 G/T.
- d. Average of 3 determinations; 15.8, 15.8 and 16.3 G/T.

* ND - Not determined.

H₂S formation during retorting has been studied previously for western shale (10). However, little or no information is available for eastern shales (11). In all the experiments carried out, significant amounts of H₂S equivalent to about 1% S by wt of the sample retorted were formed. The source of H₂S is organically combined sulfur and pyrite (10). Both types of S are present in the shale. The kerogen contains the organic sulfur, which upon retorting, is converted to product oil and H₂S. Pyrite, on the other hand, does not form H₂S in the absence of a hydrogen source. During retorting several hydrogen sources are available for the pyrite/H reactions. Kerogen, oil-forming intermediates, hydrocarbons in the product oil as well as the oil's various heteroatomic species and steam are likely H-sources.

In separate experiments, the dependence of the formation of H₂S from pyrite on a source of hydrogen was confirmed. By treating a spent shale, obtained as a result of a Fischer Assay, with steam, significant amounts of H₂S were generated. H₂S was also formed in significant amounts when a sulfur-free crude oil fraction was retorted in the presence of pyrite-containing spent shale.

During the retorting of an eastern shale the appropriate environment exists for the reaction of pyrite with a hydrogen source. Also in the Fischer Assay the time the hydrogen source could be in contact with the pyrite is 10 times as long as that in the RHU assay. This difference could be the reason for the lower yield of H₂S generated by RHU than that generated in the Fischer Assay.

Product Properties

Gas - Increasing the heat-up rate during retorting generates a larger volume of gas/100 gms of oil shale than that generated in a Fischer Assay. This increase in gas yield was not the same for all the shales studied. For example, one eastern shale sample tested generated about 15% more gas, another generated 50% more. The increases in gas yield, however, were accompanied by increases of 100% and 85% in the Fischer Assay yield, respectively. It is possible that some correlation could be established between gas yield in the RHU assay and that of the Fischer, however, the data available so far are not sufficient for this purpose.

The composition of RHU gas shows little variation for different shale samples. Also, the differences in concentration between the main components of RHU and the Fischer Assay gases are minimal, Table III. An interpretation of this observation is consistent with the thermal treatment of the shale in the two assay procedures. Since, in both assays, the maximum temperature to which the oil shale and the product oil are exposed is the same, the extent of thermal cracking to lighter fragments would be similar. This observation is consistent with that made for delayed coking of petroleum residual oil wherein it is higher temperatures, not longer times, that result in secondary cracking of product oil and produce a change in the composition of the gas generated (12).

TABLE III

YIELD AND COMPOSITION OF GAS FROM FISCHER AND RHU RETORTING OF
A BULLITT COUNTY, KENTUCKY, OIL SHALE (SAMPLE 1D)

Retort	Fischer	PR
Heat-up rate, °C/min	12	100 ^a
Gas, liters/100gm, H ₂ S free	1.74	2.03
H ₂ S, % Wt	1.2	0.8
Gas Analysis, Mol %		
H ₂	40.6	39.6
CH ₄	27.0	26.4
C ₂ H ₄	2.1	2.2
C ₂ H ₆	3.1	2.1
C ₃ H ₆	3.1	2.1
C ₃ H ₈	2.9	2.7
C ₄ H ₈	1.6	0.5
C ₄ H ₁₀	1.7	0.9
CO	2.6	4.0
CO ₂	9.0	12.0
Gas + H ₂ S, 1/100 g	2.53	2.56
% H ₂ S	31	21
% Gas	69	79

a. Initial heat-up rate.

Oil - As with the Fischer Assay, the amounts of oil generated in the RHU assay vary with the oil shale used. Also, because of the batch nature of both assays and the size of sample, 100 gms., these amounts of oil are necessarily small. Thus, the extent to which the assay oils can be tested is limited. For these experiments, the same tests were carried out on oils produced from both assays. In Table IV, data are present for product oils obtained for one eastern shale. The differences in properties are typical and the data shown for oils obtained from the two assay procedures are consistent with data obtained for other eastern shale samples.

TABLE IV

COMPARISON OF PROPERTIES OF SHALE OIL OBTAINED FROM FISCHER AND RHU RETORTING OF A BULLITT, COUNTY, KENTUCKY OIL SHALE (DRUM SAMPLE)

<u>Retort</u>	<u>Fischer</u>	<u>RHU</u>
Heat-up rate, °C/min	12	100 ^a
Oil yield G/T	10.8	16.2
% Wt	4.3	6.3
Spent shale, % wt	92	88
Gas yield, liters/100 gm	1.2	1.6
H ₂ S yield, % wt	1.1	0.9
Water, % wt	1.5	1.7
Oil Properties		
Gravity, °API	26.1	21.6
Specific gravity, 60°F/60°F	0.8978	0.9242
Pour point, °F	-50	-40
Aromatic carbon, %	40	41
Elemental Analysis, wt %		
C	84.42	84.59
H	11.09	10.52
N	1.35	1.14
S	1.81	1.64
Distillation, ASTM D2887, %		
C ₅ - 400°F	24	22
400 - 550	18	13
550 - 710	27	19
710 - 1000	30	45
1000°+	< 1	1
Shale, Spent and (Fresh)		
Elemental Analysis, % Wt		
C (Fresh)	8.88 (12.60)	7.39
H	0.55 (1.32)	0.34
N	0.33 (0.38)	0.36
S	5.86 (6.58)	5.50
Ash, % wt	88.3 ----	86.6
Pyritic sulfur	---- (6.42)	----

a. Initial heat-up rate.

A salient and consistent observation is the difference in the gravity between oil collected from the Fischer Assay and that from the RHU assay. Invariably, a difference in gravity of about 4-5° API is observed. RHU oils are denser, i. e., have the lower API gravity. This reduction in API gravity is consistent with the idea that oil precursors are thermally converted to oil products with a wide range of molecular weight. Since, in the RHU assay, the time taken to reach retorting temperatures is short and a stripping gas is used, the heavier components are removed from the retort rapidly and are condensed in the oil with the lighter components. In the Fischer Assay, these conditions do not prevail. Some of the heavier components partially condense and remain with the shale or are further cracked to form the lighter products. Another observation supports this interpretation. The boiling point distribution of RHU assay oil shows larger amounts of the 700°F+ distillate than that of the Fischer Assay product. In both assays, however, the distillate contains little or no 1000°F+ residue, reflecting the - 930°F maximum retorting temperature of both tests.

Another difference between the oils is in the hydrogen to carbon ratio. RHU assay oil H/C ratio again reflects the heavier nature of the product oil. Whereas Fischer Assay oil typically has

RAPID HEAT-UP RETORT

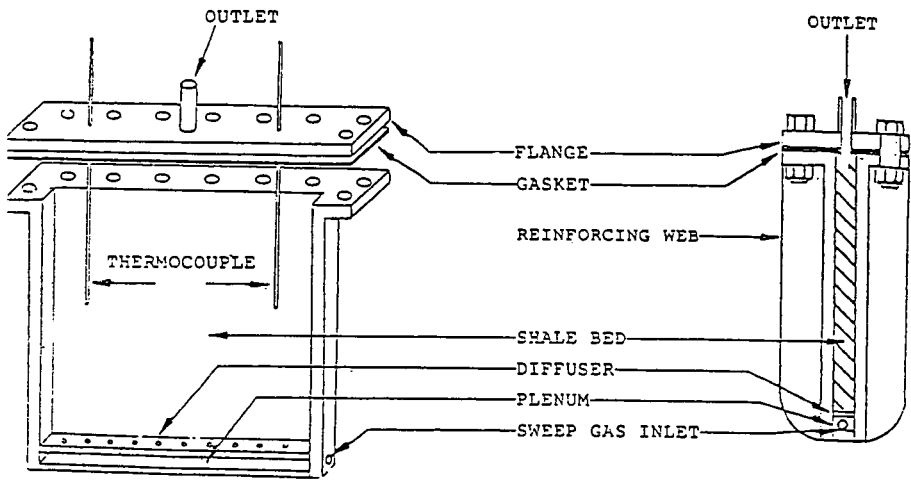


Figure 1

10.5-11% wt hydrogen, that of RHU assay is about 1% lower for the same carbon content. This observation is consistent with the boiling range shift towards heavier distillates and is in agreement with the qualitative assessment described as a chromatographically "unresolved hump in the C₂₀-C₃₀ range" obtained from fluidized bed pyrolysis of eastern oil shale (13). It is also supported by studies of Kuckersite shales in fixed bed retorting (14).

Sulfur and nitrogen concentrations in the RHU assay oils are similar to those of the Fischer Assay oils. The available data point towards a dependence of S and N content of the oil on the S and N concentration of the raw shale. However, these data are not sufficient for developing a correlation that would predict the sulfur and nitrogen concentrations of the product oil. As mentioned earlier, pyrite is a common component of eastern shales and this has to be taken into consideration when developing the sulfur correlation.

The pour points of the eastern shale oils produced were below -40°F. Little or no dependence on retorting method was observed for this property.

Carbon type distribution, aromatic and aliphatic, in the oils produced by the two assays was the same. Oil from the Fischer Assay had 40% aromatic carbon and that from the RHU assay 41%. Considering the accuracy of the nmr determination this result shows that RHU retorting of a shale does not change this characteristic of the product oil. Although a boiling point shift towards heavier products was observed, this change was either averaged over both types of carbon or were too small for detection by ¹³C nmr.

Spent Shale

Elemental analyses of spent shale produced by RHU retorting confirmed the increased conversion of kerogen carbon to product oil. Both carbon and hydrogen in the spent shale reflected the improvement in the conversion of kerogen to products. However, duplicate results for some samples were inconsistent. Particularly troublesome were hydrogen determinations on the spent shales. Directionally, however, the reduced hydrogen content of spent shale from RHU and Fischer Assays was correct.

CONCLUSIONS

A rapid heat-up assay for eastern shales that can generate collectible quantities of oil that can be characterized has been developed. It is proposed that it be adopted as a common procedure for determining the oil yield of an eastern shale.

LITERATURE CITED

- (1) Goodfellow, L. and Atwood, M. T., Proc. 7th Oil Shale Symp. Quart CSM, 69, 205 (1974).
- (2) Janka, J. C. and Dennison, J. M., Symp. papers: Synthetic Fuels from Oil Shale, Atlanta, GA, p. 21 (1979).
- (3) Smith, J. W. and Young, N. B., Chem. Geology, 2, 157 (1967).
- (4) Miknis, F. P. and Mactel, G. E., Proc. 14th Oil Shale Symp., p. 270 (1981).
- (5) Rubel, A. M. and Coburn, T. T., Proc. 1981 Eastern Oil Shale Symp., p. 151 (1981).
- (6) Margolis, M. J., Ibid., p. 151.
- (7) Reasoner, J. W., Sturgeon, L., Naples, K. and Margolis, M. J., *ibid.*, p. 11.
- (8) ASTM D 3904-80.
- (9) Wallman, P. H., Tam, P. W. and Spars, B. G., ACS Symp. Series No. 163, Paper No. 7, p. 93.
- (10) Burnham, A. K., Kirman Bey, N. and Koskinas, G. J., *ibid.*, paper No. 5, p. 61.
- (11) Rostam-Abadi, M. and Mickelson, R. W., 91st Natl. Meeting AIChE, Detroit, Paper 16B, (1981).
- (12) Audeh, C. A. and Yan, T. Y., ACS Symp. Series 202, Coke Formation on Metal Surfaces, ACS, Washington, D.C. (1982).
- (13) Burnham, A. K., Richardson, J. H. and Coburn, T. T., UCRL-87587, Preprint (1982).
- (14) Urove, K. E., Khimiya Tverdogo Roplica, 10, No. 5, 33 (1976).

SYMPOSIUM ON CHARACTERIZATION AND CHEMISTRY OF OIL SHALES
PRESENTED BEFORE THE DIVISIONS OF FUEL CHEMISTRY AND
PETROLEUM CHEMISTRY, INC.
AMERICAN CHEMICAL SOCIETY
ST. LOUIS MEETING, APRIL 8 - 13, 1984

INVESTIGATION OF ORGANIC PRODUCTS FROM THE THERMAL TREATMENT OF
GREEN RIVER OIL SHALE WITH METHANOL AND WATER

By

S-L. Chong and J. F. McKay
Western Research Institute*, Laramie, Wyoming 82071

INTRODUCTION

Recovery of organic material from Green River oil shale has been extensively studied. Conventional retorting methods including Fischer Assay (1), aboveground retorts (2, 3) and in situ retorts (4), recover only about 65% or less of the organic material (kerogen plus bitumen); however, this is accomplished at the expense of large amounts of char remaining on the spent shale. Different retorting methods have been applied to increase oil yields, such as hydrogenation (5) and atmospheric steam pyrolysis (6). One highly efficient method is supercritical fluid extraction which has been developed in the last two decades. Water (7), carbon monoxide and water (8), methanol and water (9) and toluene (10) have been used as supercritical extraction solvents to extract shale oil from Green River oil shale with much higher yields than obtainable by no-solvent heating techniques. The methanol-water mixture investigated in this laboratory was found to be highly efficient in recovering organics from Green River oil shale (9). At 400°C and 31.2 MPa (4525 psig), 90% of organic materials in the shale were produced as liquid oil and only 2% as gases. This high yield is very impressive and leads us to further investigate the composition of the products. The total liquid oils obtained at temperatures of 300 to 425°C were fractionated into various compound types and compared. The degree of pyrolysis at different temperatures was determined by the distribution of *n*-alkanes and *n*-carboxylic acids. The function of methanol in the treatment of Green River oil shale is also discussed.

EXPERIMENTAL PROCEDURE

Materials

The oil shale sample used was a 271.2 L/T (65 gal/ton) Green River oil shale from the Mahogany Zone of the Piceance Creek Basin near Rifle, Colorado and contained about 37.3% organic material. The oil shale was ground and screened to -150 μ m (-100 mesh) before treatment.

Silica gel (CC-7 Special) was purchased from Mallinckrodt Co. Silver nitrate on silica gel was prepared by mixing 20 g silver nitrate (Reagent Grade) (dissolved in 100 mL water) and 100 g silica gel. The mixture was dried at 100-120°C for 7 hours, placed in a desiccator and stored in the dark.

n-Pentane and methylene chloride were Burdick-Jackson, distilled in glass. Diethyl ether was Reagent Grade.

Extract Preparation

Oil shale samples were heated independently at temperatures of 300, 350, 375, 400 and 425°C for 1 hour at a charged argon pressure of 3.5 MPa (500 psig) in a 1-liter reaction vessel constructed of Inconel-600. The heating rate for this reaction vessel was about 2°C/min. Forty grams of shale and 120 mL each of methanol and water were used in each run. The experimental procedure was the same as used by Cummins and Robinson (8). The reacted shale and oil was Soxhlet extracted with the benzene-methanol azeotrope and the methanol-water solution also containing some oil was extracted with diethyl ether followed by methylene chloride. After extractions, the solvent was stripped from each extract using a rotary-film evaporator. The combined extracts (total liquid oil) were then separated into different compound types.

Separation Procedure

The separation scheme shown in Figure 1 is similar to that used previously (11) except that a separation of olefins using silver nitrate-silica gel was added. Twenty grams of 20% silver nitrate on silica gel was packed in a column (45 cm x 1.5 cm OD) for each 0.2 g alkanes plus

* Formerly Laramie Energy Technology Center.

olefins, and the column was wrapped with aluminum foil to prevent photodecomposition of the silver nitrate. Alkanes were eluted with 100 mL n-pentane and olefins were eluted with 100 mL of 50/50 n-pentane/diethyl ether. Alkanes were further separated by 5A molecular sieves into n-alkanes and branched-plus-cyclic alkanes (12).

Carboxylic acid methyl esters were prepared in the following way. The acids extracted from the anion resin were first refluxed with the $\text{BF}_3\text{-CH}_3\text{OH}$ complex in benzene for 4 hours and then water was added to react with the excess BF_3 . The esterified acids obtained were then charged to a fresh IRA-904 anion resin column and the carboxylic acid methyl esters were eluted from the column with cyclohexane.

Gas Chromatography

Both n-alkanes and carboxylic acid methyl esters were analyzed using a Hewlett-Packard 5830A gas chromatograph equipped with a 25 m x 0.2 mm ID SP2100 fused silica capillary column and a flame ionization detector. The gas chromatograph (GC) oven was programmed from 100 to 275°C at 3°C/min and maintained at 275°C for 50 min. Response factors were determined for standard $\text{C}_{15}\text{-C}_{32}$ n-alkanes and $\text{C}_{14}\text{-C}_{32}$ n-carboxylic acid methyl esters. The weight percent of each component was calculated by multiplying the peak area with its GC response factor.

RESULTS AND DISCUSSION

Extract Composition

The recoveries of liquid organic material from the treatment of Green River oil shale with a methanol-water mixture at various supercritical conditions were calculated as weight percent of total organic material in the shale (37.3% is 100%) and are given in Table I. Also, the elemental analyses and the molecular weights of the extracts are presented. Incidentally, the ash contents of all extracts were found to be less than 1%. The experimental results show that the recoveries of liquid organics increase with the increasing temperature from 300 to 400°C; however, at 425°C the recovery decreased apparently due to decomposition of liquid organics to gases. This is believed to be true because a significant pressure increase was observed on the pressure gauge after the experiment. The atomic H/C ratio of the liquid oil decreased from 1.66 to 1.52 as temperature increased from 300 to 425°C. The higher atomic H/C ratio at 300 and 350°C suggests that at these temperatures, aliphatic components are more easily generated than aromatic components. Above 350°C, the atomic H/C ratio decreased toward that (1.54) of Green River oil shale kerogen. At 425°C, a slight loss of hydrogen occurs as evidenced by the lower atomic H/C ratio (1.52). These results suggest that the improved recovery at the increased temperatures come mostly from recovery of more aromatic components. As with most other retort methods, as the temperature increases, oxygen and sulfur decrease and nitrogen increases.

TABLE I

WEIGHT PERCENT OF ORGANIC MATERIAL RECOVERED, ELEMENTAL ANALYSES AND MOLECULAR WEIGHTS OF EXTRACTS

Sample	% of Organic Material Recovered	Operating pressure MPa	Wt % of Extract					Atomic H/C Ratio	Molecular Weight
			C	H	N	S	O		
Extract									
300°C	13.6	18.5	78.4	10.8	1.3	1.1	6.6	1.66	
350°C	26.6	24.7	79.8	11.0	1.6	-	5.8	1.65	515
375°C	52.3	27.6	79.0	10.6	1.9	1.0	5.4	1.60	572
400°C	89.5	31.2	80.4	10.5	2.6	0.5	3.7	1.57	452
425°C	83.3	35.8	82.9	10.5	2.5	0.1	3.7	1.52	
Kerogen ^a			80.5	10.3	2.4	1.0	5.8	1.54	

a. Smith, J. W., U. S. BuMines Rept. of Inv. 5725, 16 pp (1961).

Degree of Pyrolysis

The distribution of n-alkanes and n-carboxylic acids has been found to be sensitive to thermal conditions (13, 14). The odd-even predominance (OEP) of n-alkanes and the even-odd predominance (EOP) of n-carboxylic acids, as calculated by the method described by Scanlan and Smith (13), generally decrease with increased temperature.

For an immature oil shale, the OEP of extractable n-alkanes is very high; however, OEP decreases to about 1 as the maturity of the oil shale increases (15). In the treatment of Green

River oil shale with methanol and water, the OEP of n-alkanes was studied and found to decrease with the increased temperature. A plot of OEP of n-C₃₁H₆₄ against temperature is shown in Figure 2. The OEP of n-alkanes for the benzene-extracted bitumen and Fischer Assay oil of the shale are also shown in Figure 2 for comparison. The OEP for a Fischer Assay oil (obtained by heating Green River oil shale at an effective temperature of 475°C and representing only 65% of organics in the raw shale) was found to be 2.2. At 400°C with a maximum oil yield (89.5%), the OEP of n-C₃₁H₆₄ produced from methanol-water treatment was found to be 2.4, which is slightly higher than that from Fischer Assay. These results show that pyrolysis in the methanol-water treatment at 400°C is definitely not more severe than the pyrolysis in the Fischer Assay method. Therefore, the high oil yield must be caused by a combination of pyrolysis and supercritical solvent extraction effect.

The EOP distribution of n-carboxylic acids was studied by analyzing the carboxylic acid methyl esters. The normalized weight percent of n-carboxylic acid methyl esters was obtained from their weight percents calculated from GC. Figure 3 shows the EOP of n-C₃₁H₆₃COOH as a function of temperature, the EOP also decreased with increased temperature. In general, the EOP values of n-carboxylic acids are a few units higher than the OEP values of the corresponding n-alkanes. The decrease in the OEP of n-alkanes and the EOP of n-carboxylic acids with the increased temperatures in the methanol-water treatment suggest that the OEP and EOP values can be used as good thermal indicators for the supercritical fluid extraction process.

The amounts of olefins obtained at different temperatures were also measured and are presented in Table II. The results show that the amount of olefins stays fairly constant from 300 to 425°C, contrary to the general increase of olefins with the increased temperature of heating during Fischer Assay or retorting (about 10% at 475°C). If this trend is maintained, then it suggests that the presence of methanol and water suppressed the formation of olefins.

TABLE II
THE AMOUNT OF OLEFINS AT DIFFERENT TEMPERATURES

Temperature, °C	Olefins, Wt % of Extract
300	3.1
350	3.2
375	2.3
400	2.6
425	3.0

Function of Methanol

The experimental conditions in this work were above the critical temperature and pressure of methanol. (The critical temperature and pressure of methanol are 240°C and 7.96 MPa (1154 psig), respectively.) Undoubtedly, methanol acts as a "super" solvent in the methanol-water treatment of Green River oil shale due to the high near-liquid density of the supercritical gases. In addition, methanol seems to be incorporated into the products because the infrared spectra of the extract at all temperatures contained a significant carbonyl absorption at 1730 cm⁻¹. (Extract from the water-only-run does not have this intense IR absorption.) The infrared spectrum of the extract obtained at 400°C is shown in Figure 4. After compound-type separations, this absorption peak appeared in both the hydrocarbon and base fractions, as shown in Figure 5. Absorption at 1730 cm⁻¹ is generally due to some type of carboxyl group. However, the hydrocarbon fraction is not expected to contain polar groups such as carboxylic acids because the anion resin in the separation scheme should retain all of the carboxylic acids. Therefore, it must be due to a less polar carboxyl group, for example, carboxylic acid methyl esters.

A labelled ¹³CH₃OH-CH₃OH(1.3/98.7)/H₂O experiment with Green River oil shale at 400°C was performed to further prove that esterification had occurred in the treatment. The extracts obtained from the unlabelled and the labelled experiments were analyzed by ¹³C NMR, and the NMR spectra are shown in Figure 6. The peak at 51.4 ppm (due to ¹³CH₃O group of methyl esters) in Figure 6B is much higher than that in Figure 6A showing the incorporation of ¹³CH₃OH into esters, in agreement with the infrared data. Thus, this data shows that the reaction of methanol with carboxylic acids (16) and carboxylic acid salts (17) in Green River oil shale is possible and the products are methyl esters (18).

The maximum increased weight percent (X) for the oil yield due to the incorporation of methanol can be calculated from the following equation:

$$X = \frac{MW_i}{MW_{A+S}} \times P_{A+S} \times 100$$

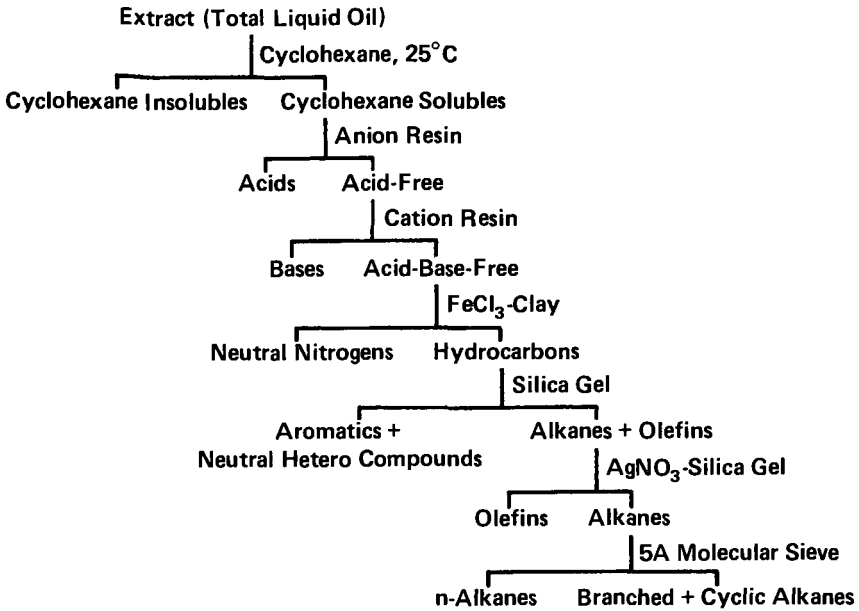


Figure 1. The separation scheme for the extracts from the methanol-water treatment of Green River oil shale.

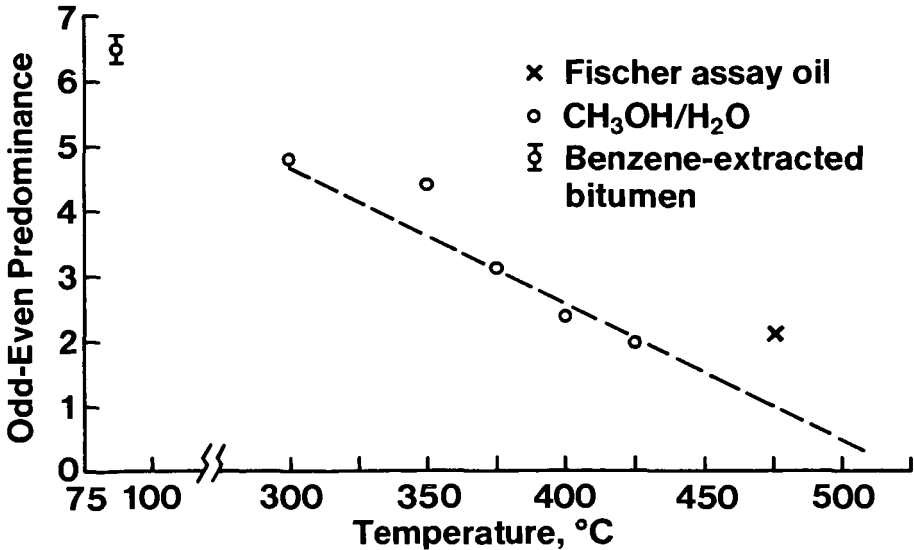


Figure 2. Changes of odd-even predominance of $n\text{-C}_{31}\text{H}_{64}$ with temperature in the methanol-water treatment.

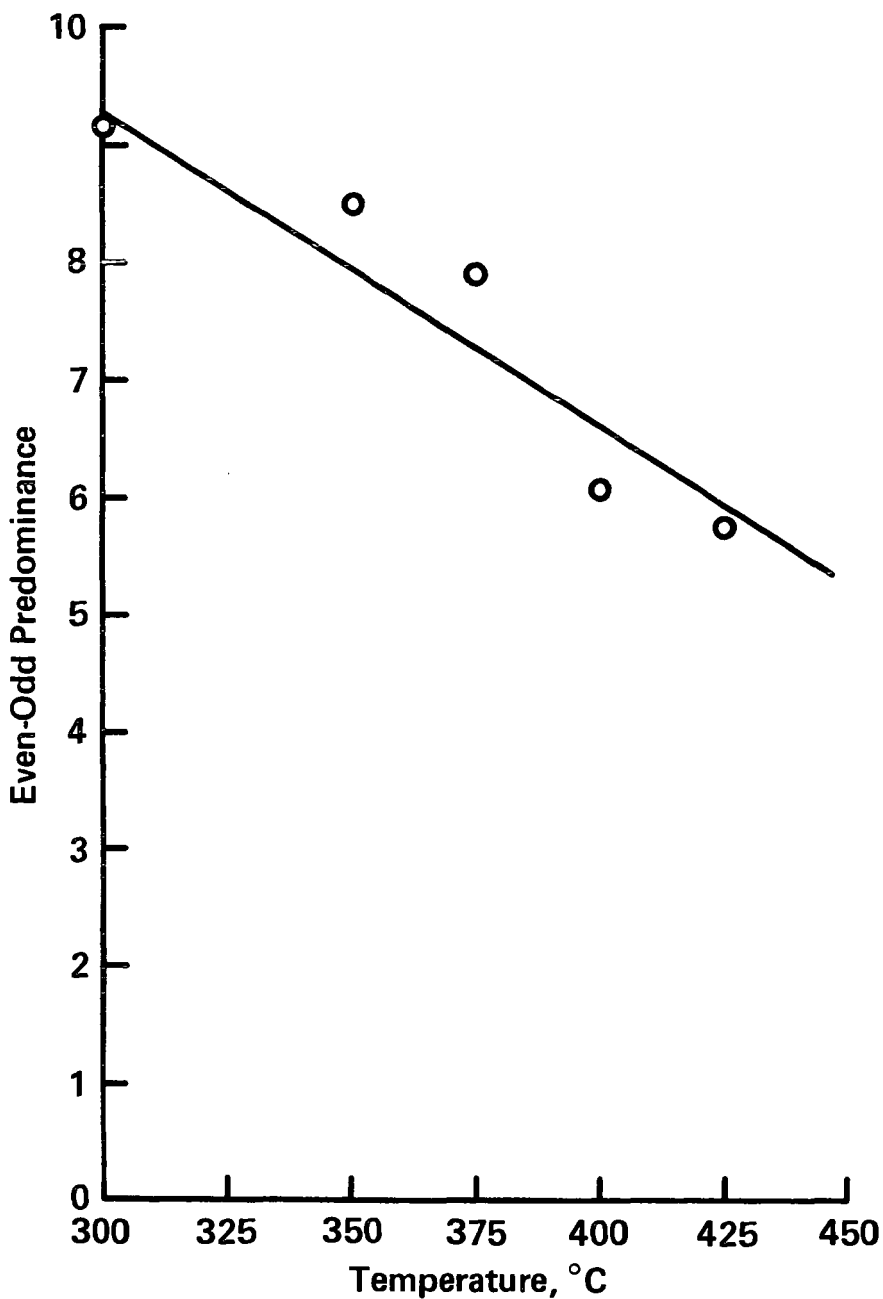


Figure 3. Changes of even-odd predominance of $n\text{-C}_{31}\text{H}_{63}\text{COOH}$ with temperature in the methanol-water treatment.

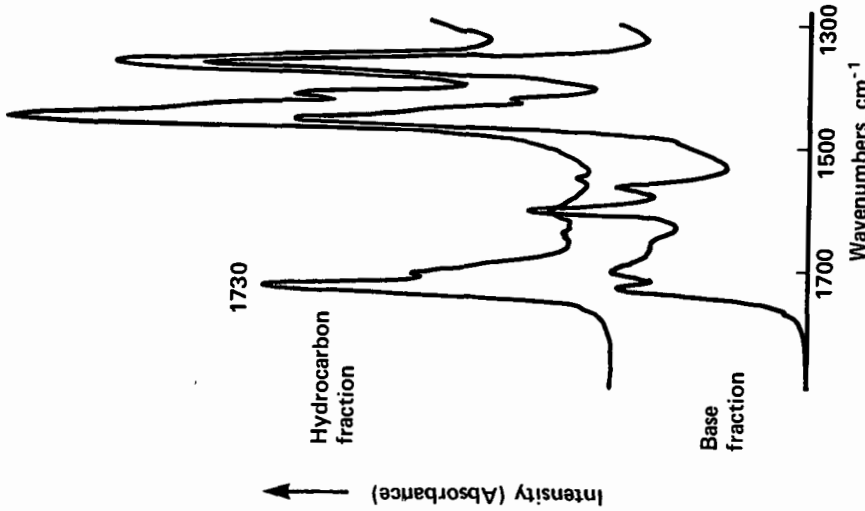


Figure 5. Partial infrared spectra of hydrocarbon fraction and base fraction from the methanol-water treatment of Green River oil shale at 400°C (in CH_2Cl_2).

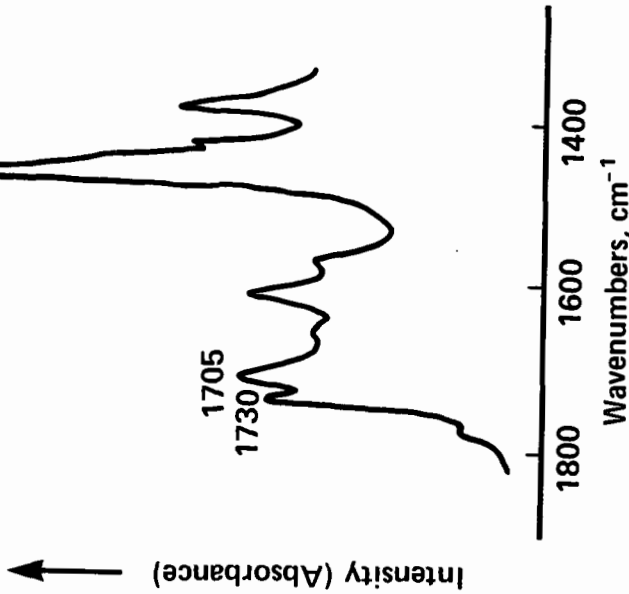


Figure 4. Partial infrared spectrum of extract from the methanol-water treatment of Green River oil shale at 400°C (in CH_2Cl_2).

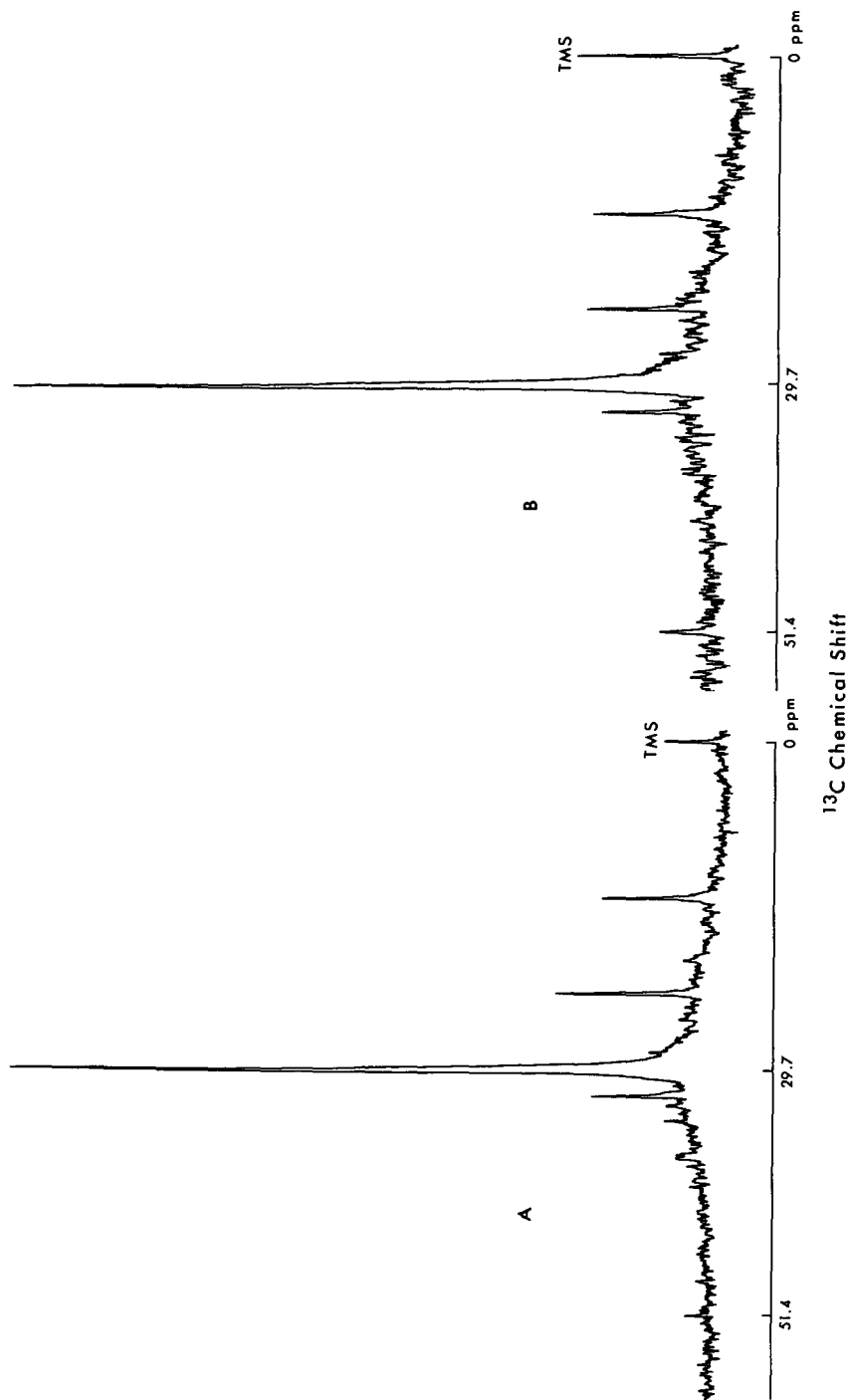


Figure 6. ^{13}C NMR spectrum of extract from $^{13}\text{CH}_3\text{OH}-\text{H}_2\text{O}$ experiment at 400°C .

where MW_i is the increased molecular weight for carboxylic acids and carboxylic acid salts due to incorporation of methanol, MW_{A+S} is the average molecular weight of carboxylic acids and carboxylic acid salts and P_{A+S} is the weight percent of carboxylic acids and carboxylic acid salts in the organic materials of the shale. Almost all of carboxylic acids found in the shale sample are monocarboxylic acids (16) so that a replacement of H by CH_3 only increases molecular weight by 14. If carboxylic acid salts are involved in the reaction, the replacement of a cation by CH_3 will only decrease the molecular weight because the cations found are sodium, calcium, aluminum, copper, etc. (17). MW_{A+S} is about 500 and P_{A+S} was found to be 20% (16). Based on these numbers, X is calculated to be 0.56%. This calculation shows that the incorporation of methanol is not enough to account for the increased oil yield found in the methanol-water treatment.

CONCLUSIONS

At 300 and 350°C, a methanol-water mixture generated more aliphatic organic materials from Green River oil shale than at higher temperatures. As the temperature of the treatment increased from 350 to 425°C, the atomic H/C ratio of the extract decreased towards that of Green River oil shale kerogen, suggesting that more aromatic components are generated at higher temperatures. In addition, the odd-even predominance of n-alkanes and the even-odd predominance of n-carboxylic acids were shown to be good thermal indicators for the supercritical fluid extraction process. The higher oil yield in the methanol-water treatment of Green River oil shale is apparently contributed to both by pyrolysis and by the supercritical solvent effect. There is evidence of methanol incorporation into the liquid oils in the methanol-water treatment, but not near enough to account for the higher oil yield.

ACKNOWLEDGMENT

For the ^{13}C NMR analyses and interpretation, we thank Mr. Gary Propeck and Dr. Daniel Netzel.

LITERATURE CITED

- (1) Annual Book of ASTM Standards, D3904-80.
- (2) Henderson, T. A., *Quart. Colo. School Mines*, **69** (3), 45 (1974).
- (3) Harak, A. E., Dockter, L. A. and Cohns, H. W., U. S. Bureau of Mines, Rept. Inv. 7995, 31 pp. (1974).
- (4) Sohns, H. W. and Carpenter, H. C., *Chem. Eng. Prog.*, **62** (8), 75 (1966).
- (5) LaRue, D. M. and Wise, R. L., LERC/Tech. Progress Report 77/2, 30 pp. (1977).
- (6) Campbell, J. H. and Taylor, J. R., Lawrence Livermore Laboratory, Univ. California, UCID 17770, 20 pp. (1978).
- (7) McCollum, J. D. and Quick, L. M., U. S. Patent 4,151,068, April 24, 1979.
- (8) Cummins, J. J. and Robinson, W. E., U. S. Dept. of Energy, Rept. Inv. LERC/RI-78/1, 19 pp. (1978).
- (9) McKay, J. F., Chong, S-L. and Gardner, G. W., ACS Geochemistry Div. Abstract, Abstract No. 25, New York, August 23-28, 1983.
- (10) Compton, L. E., Preprints, ACS, Div. Fuel Chem., **28** (4), 205, Washington, D. C., August 28-September 2, 1983.
- (11) Chong, S-L., Cummins, J. J. and Robinson, W. E., Preprints, ACS, Div. Fuel Chem., **21** (6), 26, August 29-September 3, 1976.
- (12) O'Connor, J. G., Burow, F. H. and Norris, M. S., *Anal. Chem.*, **34** (1), 82 (1962).
- (13) Scanlan, R. S. and Smith, J. E., *Geochim. Cosmochim. Acta*, **34**, 611 (1970).
- (14) Kvenvolden, K. A., *J. Amer. Oil Chem. Soc.*, **44**, 628 (1967).
- (15) Martin, R. L., Winters, J. C. and Williams, J. A., *Nature*, **199**, 110 (1963).
- (16) Chong, S-L., Chapter in "Chemical and Geochemical Aspects of Fossil Energy Extraction", T. F. Yen, F. K. Kawashara and R. Hertzberg, eds., Ann Arbor Science, 143 (1983).
- (17) Chong, S-L. and McKay, J. F., to be published in *Fuel*.
- (18) Chong, S-L. and McKay, J. F., ACS Geochemistry Div. Abstract, Abstract No. 36, Washington, D. C., August 28-September 2, 1983.

SYMPOSIUM ON CHARACTERIZATION AND CHEMISTRY OF OIL SHALES
PRESENTED BEFORE THE DIVISIONS OF FUEL CHEMISTRY AND
PETROLEUM CHEMISTRY, INC.
AMERICAN CHEMICAL SOCIETY
ST. LOUIS MEETING, APRIL 8 - 13, 1984

ELECTRON PARAMAGNETIC RESONANCE AND THERMOGRAVIMETRIC INVESTIGATIONS OF
THE PYROLYSIS OF EASTERN SHALES

By

N. S. Dalal and M. S. Suryan
Chemistry Department, West Virginia University, Morgantown, West Virginia 26506
and
M. S. Shen and K. H. Casleton
Morgantown Energy Technology Center, Morgantown, West Virginia 26505

INTRODUCTION

The organic matter in oil shale is composed mostly of kerogen (insoluble in common organic solvents) with a few percent soluble bitumen. When Green River oil shale is heated to 573 K, natural bitumen can be removed thermally from oil shale. The chromatogram of thermally separated bitumen is identical to that of the solvent-extracted bitumen (1). At temperatures above 573 K, the kerogen decomposes to bitumen and subsequently bitumen to oil and gas (2, 3). While considerable work has been done using Electron Paramagnetic Resonance (EPR) on coal (4, 5) and western oil shale (6, 7), relatively little is known about eastern shales. EPR measurements yield direct, in situ information on the kinetics of the organic-free radicals present in heated shale and natural bitumen. The present work was undertaken as a correlated EPR and TGA investigation of eastern shales to elucidate the pyrolysis mechanisms of these shales.

EXPERIMENTAL

Oil shale samples used in the present study are Kentucky Sunbury oil shale and Tennessee U. S. oil shale. Chemical analyses of the oil shales are given in Table I.

TABLE I
CHEMICAL PROPERTIES OF OIL SHALES

Type of Oil Shale/ Analysis Items, Wt %	Sunbury Oil Shale Kentucky	U. S. Oil Shale Tennessee
Hydrogen	1.55	1.31
Nitrogen	0.53	0.36
Total carbon	14.07	11.49
Oxygen (by difference)	3.30	0.04
Silicon, SiO ₂	66.70	60.74
Aluminum, Al ₂ O ₃	20.00	13.76
Iron, Fe ₂ O ₃	7.80	15.30
Calcium, CaO	0.20	8.47
Magnesium, MgO	1.40	1.52
Sodium, Na ₂ O	1.14	0.67
Potassium, K ₂ O	5.10	4.91
Phosphorus, P ₂ O ₅	0.24	0.17
Titanium, TiO ₂	0.72	0.88
Sulfur, SO ₃	0.52	1.01

EPR measurements were made with a Brüker-IBM EPR spectrometer Model ER 200D fitted with an NMR gaussmeter and a digital frequency counter for measuring the microwave frequency. The peak-to-peak line widths, ΔH_{pp} , were measured by using a Brüker NMR gaussmeter. The data acquisition and reduction was carried out with a Brüker Model Aspects 2000 computer. The in situ, high-temperature EPR measurements were made with a Brüker high-temperature cavity Model 4114 HT. The g -values and the line widths, ΔH_{pp} , were measured by the least squares fitting of the observed signals using the Aspects 2000 computer.

The oil shale sample was heated at $\sim 8\text{K}/\text{min}$. in 40° intervals, the temperature was stabilized for ~ 15 minutes, and then the EPR spectrum was recorded. The sample temperature was measured with a chromel-alumel thermocouple located close to the sample. The temperature stability was $< 1\text{K}$ over a 20-minute period.

The TGA experiments were carried out by a DuPont 951 thermogravimetric balance interfaced with a DuPont 1090 thermal analyzer. Details of the TGA measurements are given elsewhere (8).

RESULTS AND DISCUSSION

Figure 1 shows typical TG and DTG curves for Kentucky Sunbury shale (8). There are two major peaks from the derivative weight loss/temperature curve. The first peak begins about 20°C and ends about 100°C while the second peak begins about 350°C and ends about 550°C . It is likely that the first peak represents the volatilization of water, while the second peak represents the decomposition of pyrolytic bitumen. The differential weight variation between two peaks is considered to be the decomposition of natural bitumen and kerogen.

Figure 2 shows typical EPR scans for the two samples: (a) for the Sunbury oil shale and (b) for the U. S. oil shale. Both spectra consists mainly of some broad signals covering a range of about 1000 G over which are superimposed sharp lines from organic-free radicals (indicated with arrows) at g -values around 2.006 ± 0.001 . It may be noted that the broad signals, attributable to Fe_2O_3 , Fe_3O_4 or related impurity, are more abundant in the U. S. shale than the Sunbury oil shale.

Figures 3 and 4, respectively, show the measured temperature dependence of the free radical concentration (c) as measured by the area under the signal corrected by the high-temperature Curie-Weiss behavior, the peak-to-peak line widths (ΔH_{pp}) in Gauss and the line positions (g -values). Figure 3 is for the U. S. oil shale and Figure 4 shows similar results for the Sunbury oil shale. In both cases, part (a) shows temperature dependence of the g -values, and (b) and (c) are those of the peak-to-peak line width (ΔH_{pp}) for the free radical EPR signal and the free radical concentrations, respectively. It is seen that, in both cases, the free radical concentration is fairly constant up to about 300K and then rises steeply, especially around $600 \pm 10\text{K}$. A close correlation between the sharp increase in free radical concentration for the Sunbury shale shown in Figure 4 with the maximum in the DTG curve for Sunbury shale in Figure 1. For the U. S. oil shale, there are two somewhat unresolved peaks. For the Sunbury shale, a peak and a shoulder are also visible in about the same temperature range, but here the peak resolution is even less.

The peak-to-peak line width, ΔH_{pp} , of the EPR derivative signals from the two shales showed strikingly different temperature dependence. With the increase in temperature, the line width of the U. S. shale is fairly constant up to about 600 K, exhibits a sharp increase around 620 K and then drops sharply to about 60% of the maximum value at about 800 K. It is noted that the minimum line width occurs at about the same temperatures as that corresponding to the maximum in the free radical concentration.

The peak-to-peak line width (ΔH_{pp}) for the Sunbury shale shows a steady decrease from about 200 K to a minimum at about 560 K and then increases to about the original value at about 800 K, the maximum temperature in our measurements on this shale. We found that, for this shale, an excessive microwave loss in the cavity due to some change in the shale prevented us from EPR measurements at higher temperature (the mechanism for this microwave loss is unclear but experiments are in progress). Once again, the minimum in the ΔH_{pp} occurs at about the temperature of the start of the smaller peak in the free radical concentration. However, the excessive microwave loss for this sample might be the cause of the broadening of ΔH_{pp} above 600 K.

The g -values of both samples exhibit a fairly small ($< 0.1\%$) but steady increase with temperature. The broad maxima in the g -value plots occur roughly at the temperature of the maxima in the free radical concentration for both shales.

The results of Figures 3 and 4 clearly demonstrate that the free radical concentration changes by nearly one order of magnitude for both shales as the results of pyrolysis. It is clear that the line widths (ΔH_{pp}) also change drastically as a result of the heating, indicating that pyrolysis results in probably new types of free radicals, different from those already present in the shale sample. This conclusion is supported by plot (a) wherein the g -values also exhibit a definite slowly increasing trend with temperature increase.

Sample: KENTUCKY SHALE
 Size: 59.96 mg
 Rate: 10 DEG/MIN 100CC N2/MIN

TGA

Date: 6-Oct-83 Time: 22:45:45
 File: SUNBURY.07
 Operator: M. SHEN

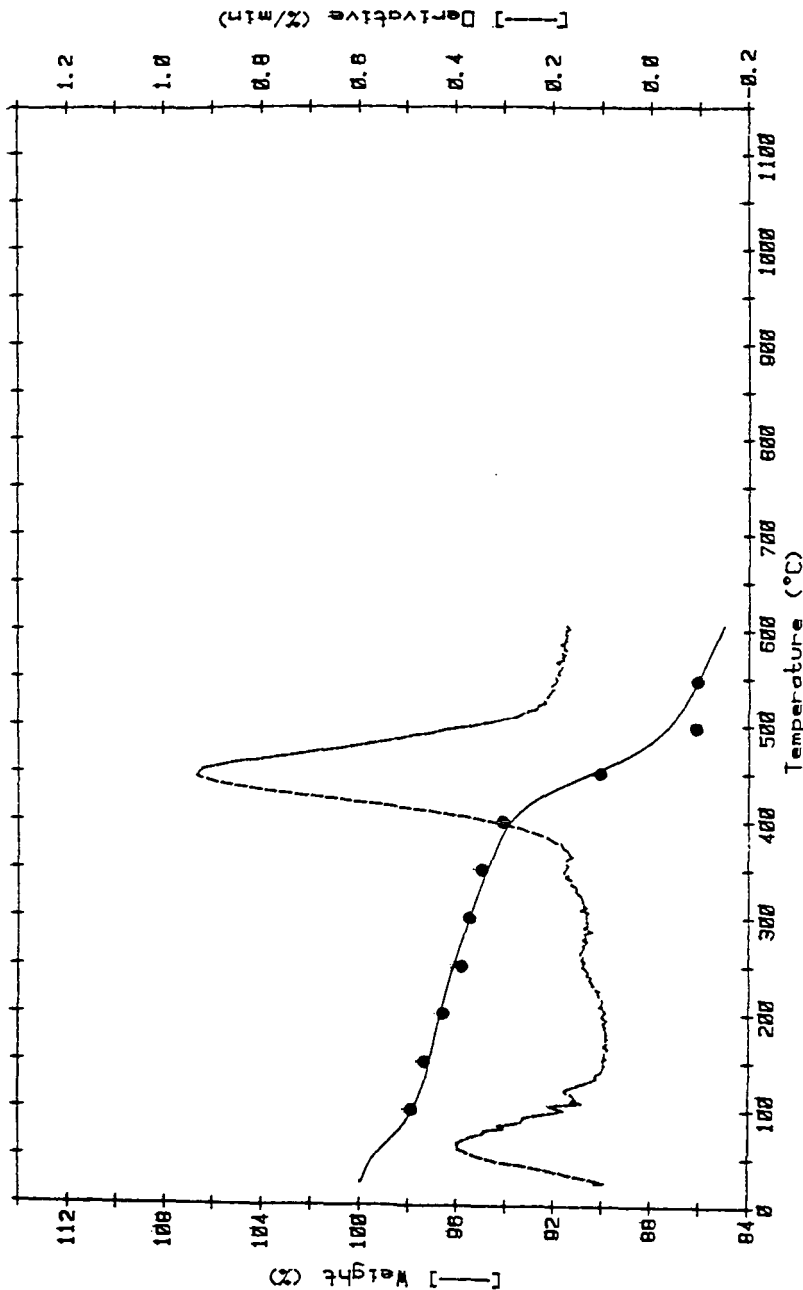


Figure 1. Typical TG and DTG curves for Kentucky's Sunbury oil shale.

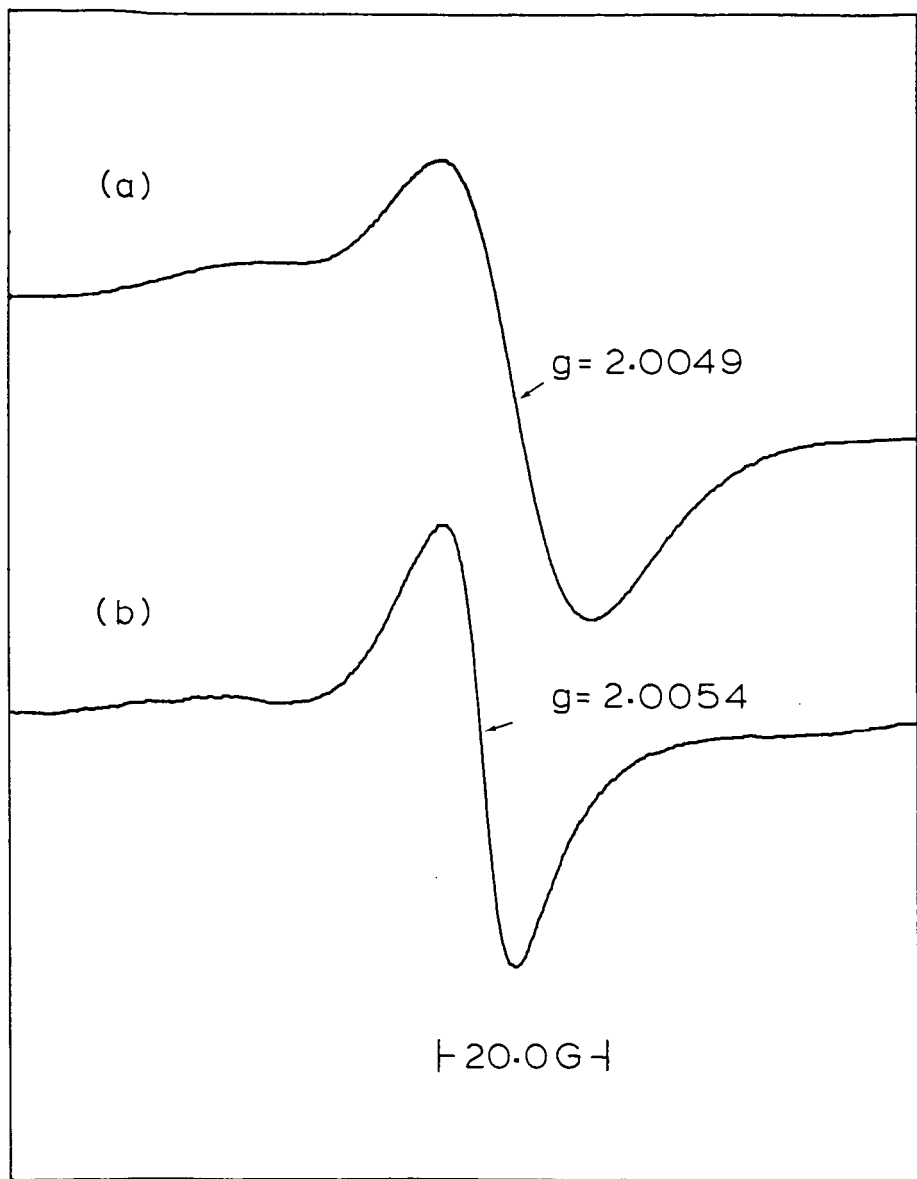


Figure 2. Typical EPR spectra of (a) Kentucky's Sunbury oil shale and (b) Tennessee's U. S. oil shale.

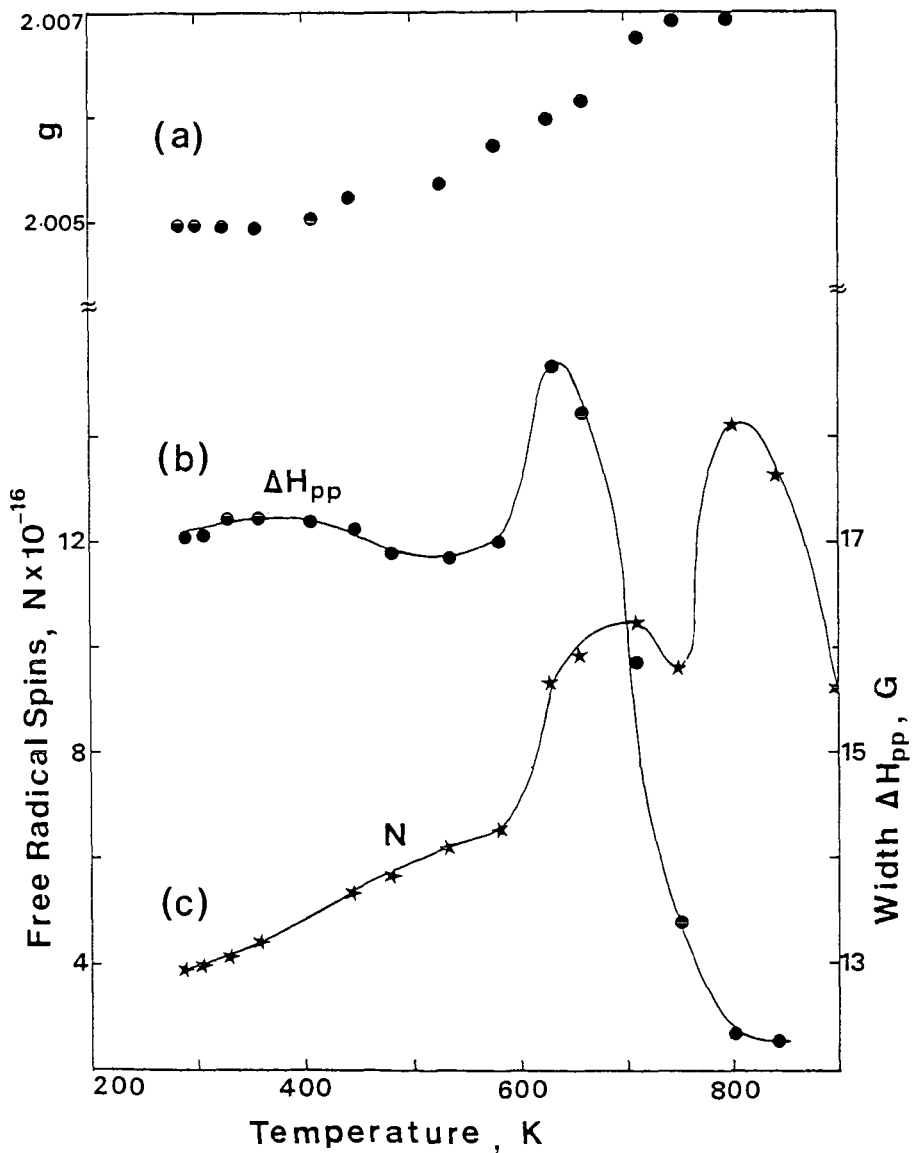


Figure 3. Temperature dependence of the EPR parameters for Tennessee's U. S. oil shale: (a) G-values, (b) peak-to-peak line widths and (c) concentration of the radicals relative to room temperature.

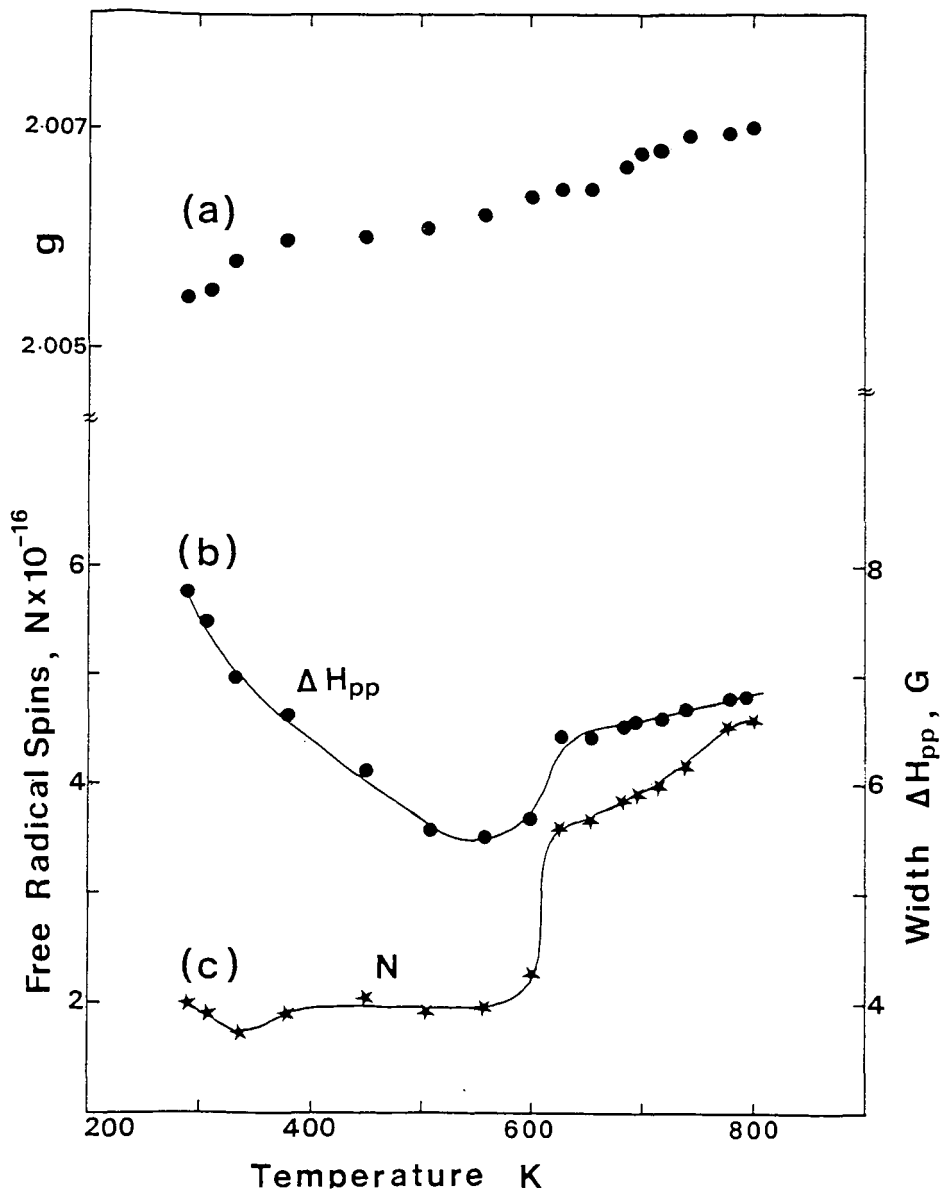


Figure 4. Temperature dependence of the EPR parameters for Kentucky's Sunbury oil shale: (a) g-values, (b) peak-to-peak line widths and (c) relative concentration.

We note that the decrease in ΔH_{pp} concomitant with the increase in the free radical intensity might also be interpreted simply as a result of spin exchange narrowing, as is well known to happen for concentrated spin systems. However, the comparison with g -values suggests that the linewidth change is perhaps more likely to be due to the formation of new species of radicals.

As far as the identification of the radicals is concerned, it is clear from the g -values (being close to the free electron g -value of 2.0023) that the radicals are all fairly similar in nature. Comparison with the pyrolysis results of Retcofsky et al. on coal samples suggests that the radicals are essentially π -type delocalized hydrocarbon radicals. The increase of the g -value over 2.0023 shows that the free electron resides also partly on heteroatoms with spin-orbit coupling larger than carbon, possibly oxygen, sulfur or nitrogen.

Figures 3 and 4 show that the g -values of the two shale samples are nearly the same (2.007) at the high temperature end. The significant positive deviation from the free electron value of 2.0023 suggests that the free radicals in both shales are essentially of the same nature; the deviation being largely due to the spin-orbit coupling of a heteroatom in the free radical structure. However, the data on chemical analysis (Table I) show that nitrogen and oxygen are significantly larger in Sunbury oil shale than in the U. S. oil shale while the sulfur is larger in the U. S. oil shale. Since sulfur has much larger spin-orbit coupling constant than oxygen or nitrogen, the presence of sulfur in a radical will cause its g -value to be much higher than that for a similar radical containing oxygen or nitrogen. The present EPR data show that the g -values for both samples are nearly the same. Thus, these results indicate that the newly formed free radicals in the U. S. oil shale are preferentially formed around the sulfur moiety.

Another interpretation of the line width decrease at high temperature is that the decrease results from the loss of hydrogens on pyrolysis, as found for coal samples. This interpretation implies that the original cause of the EPR line width is the dipolar coupling between the unpaired electron of the free radical and the protons from the C-H hydrogens. However, there is no direct proof for this hypothesis. We plan to carry out electron-nuclear double resonance (ENDOR) studies to clarify the origin of the line widths and to identify the structures of the produced organic radicals.

LITERATURE CITED

- (1) Scrima, D. A., Yen, T. F. and Warren, P. L., *Energy Sources*, Vol. 1, No. 3, 321-336 (1974).
- (2) Hubbard, A. B. and Robinson, W. E., *Report Investigation*, U. S. Bureau of Mines, No. 4744 (1950).
- (3) Allred, V. D., *Chem. Eng. Prog.*, **62**, 55-60 (1966).
- (4) See, for example, Retcofsky, H. L., *Coal Science*, **1**, 43-82 (1982).
- (5) Petrakis, L. and Grandy, D. W., in *Proc. Am. Inst. Phys. Conf. on Chemistry and Physics on Coal Utilization*, Morgantown, WV, pp. 101-120 (1980).
- (6) Villey, M., Estrade-Swarthropf, H. and Conrad, J., *Revue de L'Institut Francais du Petrole*, **36**, 3-16 (1981).
- (7) Marchand, A. and Conrad, J., in *Kerogen*, B. Durand, ed., Editions Technip, Paris, 243-270 (1980).
- (8) Shen, M. S., Fan, L. S. and Casleton, K. H., *Symp. on Characterization and Chemistry of Oil Shale*, the 188th Natl. Amer. Chem. Soc. Meeting, At. Louis, Missouri, April 8-13, 1984.

SYMPOSIUM ON CHARACTERIZATION AND CHEMISTRY OF OIL SHALES
PRESENTED BEFORE THE DIVISIONS OF FUEL CHEMISTRY AND
PETROLEUM CHEMISTRY, INC.
AMERICAN CHEMICAL SOCIETY
ST. LOUIS MEETING, APRIL 8 - 13, 1984

OIL SHALE DEPOSITS IN JORDAN

By

Y. M. Hamarneh
Laboratories Division, Natural Resources Authority, The Hashemite Kingdom of Jordan

INTRODUCTION

Occurrences of oil shale have been reported in most of the Jordanian districts. The geological studies and exploration for water, oil and minerals showed that oil shale is widely distributed in many parts of the country, either outcropping at the surface or encountered in exploratory wells. The following are the main localities of oil shale (Figure 1): (a) in northern Jordan (Irbid District), for example at Yarmouk river, Buweida and Beit Ras villages and at Risha H-4 area in the north-eastern Panhandle; (b) in Central Jordan (Karak District) in the area between Al-Husseinieh in the south and Daba'a in the north along the Desert Highway and also in El-Lajjun area; (c) Southern Jordan (Ma'an Area) at Jafr area; (d) West Bank - Nabi Musa Area.

The average thickness of oil shale deposits varies from 30 m in El-Lajjun area to 400 m in the Yarmouk area. A conservative estimate of oil shale reserves in Jordan is 50 billion tons (1). What is really important is not the total reserves that may exist but the minable reserves. This includes deposits with favorable characteristics for large scale, economical development.

The Natural Resources Authority has been exploring oil shale deposits using the following guidelines: favorable conditions for surface mining, such as minimum overburden, absence of significant structural disturbances and absence of intrusive rock bodies or limitation of thickness of these bodies; number and thickness of oil shale layers, oil shale oil content, moisture content and other adequate properties for processing; adequate reserves to justify installing a commercial processing plant.

The deposits in Central Jordan have been selected for detailed studies because they are the shallowest known deposits which offer favorable mining conditions, the area is traversed by main roads in the central part of the country where a reasonable infrastructure exists and reasonable amounts of groundwater are available for the industrial utilization. Among the deposits in Central Jordan, El-Lajjun has been selected for feasibility studies.

EL-LAJJUN OIL SHALE DEPOSIT

The El-Lajjun oil shale deposit is located in the western part of Central Jordan, midway between Qatrana and Karak, approximately 110 km south of Amman. It is 10 km long and 2-2.5 km wide. The rocks which occur in the investigated area are limestones, marls, cherts, shales and phosphates of Campanian Maestrichtian to Holocene ages. In the investigated area, the outstanding feature is the El-Lajjun graben which controls morphological depression bordered from east and west by faults striking generally N-S. The bituminous facies in the area occurs in the upper portion of the phosphorite unit as well as in the chalk-marl unit in which the best grades of oil shale occur. The average thickness of oil shale is 30 m. The stratigraphy of the bituminous layers of the chalk-marl unit is based on drill hole data. On the basis of the oil content determined by Fischer Assay, the bituminous sequence of the chalk-marl unit has been subdivided into several sub-units (2). The deposit is a homogeneous one. This is clearly shown from the uniformity of lithology (as shown in Figure 2) as well as the average contents of several constituents as moisture, oil and sulfur.

The following sub-units have been recognized from bottom to top: P is the uppermost bituminous part of the phosphorite unit which reaches about 7 m in thickness; its average oil content is between 5.5 and 7.5%, with a very high P_2O_5 and rather varying $CaCO_3$ content. A has the highest oil content (12.6%), is the thickest (12-18 m) and it has high sulfur content (3-5%). AL includes the dolomitic limestone (Arbid Limestone); it is slightly bituminous (approximately 3% oil). B consists of the section between the Arbid limestone and the first concretionary limestone and is characterized by high oil yield (12.3%), the highest SiO_2 (26.1%) and the lowest $CaCO_3$ content (33%). C is relatively thin (5-6 m) and has a low oil content (7.8%); its $CaCO_3$ content is greater than that of sub-unit B (53%) and the SiO_2 content is less (11.5%). D reaches a maximum thickness of 11 m; its average oil content is 11.1%. E is approximately 27 m thick and consists of an average of 6% oil; its $CaCO_3$ content (56%) is higher than in sub-unit D and the Al_2O_3 content is the highest in the

whole bituminous sequence (6.7%); its average P_2O_5 content falls below 2%. F reaches about 17 m and the average oil content 4%; its $CaCO_3$ content exceeds 7%, as in sub-unit G. G has an average oil content of 4.3%.

TABLE I
AVERAGE CHEMICAL COMPOSITION AND PROPERTIES OF EL-LAJJUN
STRATIGRAPHIC SUBUNITS

Sub-Unit	Oil %	Moisture %	Sulfur %	$CaCO_3$ %	Corg. %	Gross C. Value (KJ/Kg)	Al_2O_3 %	P_2O_5 %	SiO_2 %	Thickness (m)
G	4.3	3.6	1.9	73.9	6.3	2580	2.5	0.5	5.5	7
F	3.4	2.3	1.7	71.1	5.6	2050	3.1	1.3	6.7	17
E	5.7	2.8	2.6	56.0	8.6	4180	4.8-6.7	1.75	12.4	4-23
D	11.1	3.4	3.3	45.0	12.8	6850	5.0-5.7	3.35	13.3	2-11
C	7.8	2.2	2.3	53.0	9.8	4700	4.2-4.8	3.3	11.5	5-6
B	12.3	3.1	3.2	33.0	14.0	8100	2.6-2.9	3.6	26.1	8-11
AL	5.2	2.3	1.7	60.0	6.2	4090	2.1-6.6	3.0	22.0	1-2
A	12.6	1.9	3.5	46.0	14.5	8170	3.4-3.5	2.7	14.6	12-18
P	6.1	1.8	1.9	45.0	8.3	4200	1.1-1.4	9.7	9.1	2-6

One hundred and thirteen boreholes were drilled in the area during the periods 1968/69, 1979, 1982. The drilled thickness varies between 1.4 to 86.5 m. The core recovery in the oil shale and the overlying chalky marl and phosphorite was excellent (over 85%). A new drilling program started April 1983, aiming to provide accurate figures for the reserves of the different sub-units. Upon the completion of the new drilling program, the core-hole spacing will become 300 m.

The total oil shale reserves was calculated to be 1.3 billion tons with an average stripping ratio of overburden to bituminous marl of 0.9 : 1, which indicates favorable conditions for open pit mining.

OIL SHALE COMPOSITION, SHALE OIL YIELDS AND PROPERTIES

Previous Activities

The analysis started in 1968. Fischer analysis in which the oil shale was pyrolyzed up to 320°C gave amounts of oil, water, gas and residue (spent shale). Other analysis included the determination of organic matter, sulfur, moisture, trace elements and other inorganic constituents. Representative samples were analyzed in different institutions and organizations such as U. S. G. S., BGR, IGS, BP, USSR. The results of these investigations were reflected in the reports submitted to the N.R.A. by Speers of the BP (5), Dinneen USGS (3), Jacobs BGR (4) and Hamarneh NRA (6, 7). This program was terminated by NRA in 1960 because oil prices were low at that time.

As oil prices were continuously increasing from 1973 onward, NRA resumed its studies of this deposit in 1979. Omary of NRA reviewed previous work done (8). This was followed by a detailed study by M. Abu Ajamieh (9). Further studies of El-Lajjun deposit were conducted in 1979 by NRA in cooperation with the Federal Institute of Natural Resources and Geosciences (BGR) of the Federal Republic of Germany. The work done in that program included completion of 1:10,000 geological map, electric resistivity survey, additional coredrilling and laboratory tests.

In 1982-1983, a new drilling program started with aim to drill about 60 boreholes in the southern part of the deposit including laboratory analysis of core samples to assess the reserves in the area.

Composition of Oil Shale

Analysis of some representative samples are given in Table II. All the analysis of core samples leads to the following conclusions: the yields of low temperature carbonization (Fischer Assay), especially the oil content, is one of the main parameters that determine the suitability of the deposit to be used as a source of oil production; the oil content by pyrolysis to 520°C, in the whole deposit varies from 0.5 to 18.5%, the average is 10% and recoverable oil reaches 161.5 L/t. The organic carbon determined by the Leco analyzer after the removal of carbonate by dilute HCl showed that El-Lajjun oil shale contains organic material, relatively uniform in composition, and correlates well (0.986) with the oil yield as shown in Figure 3; determination of organic carbon is less expensive than oil content and may replace the Fischer Assay. Mean gross calorific value was 2000 Kcal/Kg and correlate well with organic carbon as shown in Figure 4; therefore, we can estimate the gross calorific value from the content of organic carbon.

TABLE II
CHEMICAL COMPOSITION OF RAW SHALE, SHALE OIL AND ASH

<u>Fischer Assay</u>			
Oil %	16.7	8.0	13.4
Water %	2.1	3.3	2.6
Spentshale %	76.5	83.0	80.3
Gas and loss	4.6	5.7	3.7
Spec. Gr. of oil 60°F 60°F	0.968	0.964	0.977
<u>Carbon</u>			
<u>Raw Shale</u>			
Total C	27.2	18.7	25.2
Mineral C	5.19	5.48	3.57
Mineral C (Calculated CaCO_3)	43.2	45.6	29.7
Organic C (Calculated total organic matter)	22.0	13.2	21.6
<u>Spent Shale</u>			
Total C	15.2	9.9	15.80
Mineral C	5.87	3.3	6.86
Organic C	9.3	6.6	8.90
<u>Total Sulfur Raw Shale</u>			
<u>Fraction of Shale Oil Obtained from F. A.</u>			
Saturated Hydrocarbons	9.62	9.06	8.01
Aromatic Hydrocarbons	75.77	78.00	76.32
Asphaltic Compounds	14.61	12.96	15.67
<u>Soluble Bitumen from Raw Shale</u>			
Methanol Soluble	1.78	1.41	0.86
Chloroform-soluble	3.18	2.20	2.77
Total Meth. Chl. Sol.	4.96	3.61	3.63
<u>Spectrographic Analysis of Raw Shale Ash</u>			
Ash %	54.55	67.67	54.73
Si	>10	>10	>10
Al	2	2	3
Ca	>10	>10	>10
Mg	0.7	0.7	0.7
Na	0.3	0.3	0.2
P	3	2	1.5
Tl	0.1	0.15	0.2
Mn	0.005	0.005	0.005
Ag	0.00015	0.0001	0.0003
B	0.007	0.007	0.007
Ba	0.015	0.001	0.001
V	0.05	0.05	0.03
Zn	0.15	0.15	0.07
Sr	0.15	0.1	0.15
Ni	0.05	0.03	0.03
CO	<0.0007	<0.0007	<0.0007
Cu	6.05	0.03	0.03
Cr	0.15	0.07	0.10
MO	0.05	0.03	0.03
Pb	0.003	0.003	<0.001
Zr	0.007	0.007	0.007

On the basis of the gross calorific values in parallel with other geological and chemical data, we conclude that the high grade oil shale, which is available in considerable amounts, contains sufficient energy for generating electricity by direct combustion methods if a modern process is used, which overcomes the obstacle of the high sulfur content (2.6-3.5%) and which operates mainly at temperatures below the initial deformation temperatures of carbonates (1215-1410°C) to

avoid fouling on the heating surfaces. High percentage of CaCO_3 in the ash leads to cementation, which may impede operation of the ash disposal system. The presence of P_2O_5 reduces efficiency of electrostatic precipitators. The total sulfur content determined by wet chemical methods and by Leco combustion in oxygen varies from 0.4% to 4% and gradually decreases from bottom to top (Table I), correlating with average content of the organic carbon; the high sulfur content in the re-tarted oil indicates that a considerable part of the sulfur is chemically bound to the organic material. The moisture content determined by drying at 105°C and by Dean and Stark method seldom exceeds 6%, so that predrying won't be necessary. Density was 1.9 g/cm^3 . The mineral composition, determined mainly by X-ray diffraction, as a whole, is uniform with depth; it is in Table III. The chemical composition determined by wet chemical analysis and X-ray fluorescence is in Table IV.

TABLE III
MINERALOGICAL COMPOSITION OF OILSHALE
Average %

Calcite	20-80%	45
Quartz	10-40%	20
Kaolinite	5-10%	10
Apatite	4-14%	6
Dolomite	2-36%	3
Feldspar	5	
Pyrite	5	
Muscovite-illite	5	rare
Geothite	5	rare
Gypsum	5	rare
Opal	present	

TABLE IV
INORGANIC CHEMICAL ANALYSIS OF OILSHALE
Range Wt %

SiO_2	4.65-41.63
TiO_2	0.03- 0.38
Al_2O_3	0.97- 9.26
Fe_2O_3	0.41- 3.57
MnO	0.01
MgO	0.17- 8.17
CaO	15.32-45.67
Na_2O	0.00- 0.33
K_2O	0.02- 0.56
P_2O_5	0.47-14.67
SO_3	0.07- 6.73
L. O. I.	27.9 -45.9

Differential thermal analysis (DTA) and the thermogravimetric analysis (TGA) were conducted on the shale. When calibrated, the DTA curve can be used to determine the heating value of the fuel and to obtain the kinetic data with the development of appropriate procedure. The DTA tests with a heating rate of $10^\circ\text{C}/\text{min}$ showed the following heat effects:

1. $30^\circ\text{-}150^\circ$ endothermic release of the adsorbed water.
2. $150^\circ\text{-}55.0^\circ$ exothermic reaction of the first organic complex.
3. $420^\circ\text{-}520^\circ$ exothermic roasting of the pyrites.
4. $480^\circ\text{-}520^\circ$ exothermic dehydration of the phosphate complex.
5. $450^\circ\text{-}800^\circ$ exothermic reaction of the second organic complex.
6. $790^\circ\text{-}940^\circ$ endothermic dissociation of dolomite.
7. 920° endothermic dissociation of calcite.

From TGA the ignition temperature, char burn out, % of ash and % of moisture can be identified.

The tests showed three reaction phases; (a) 250-500°C, (b) 500-700°C and (c) 700-1000°C. Ignition occurs at 250°C and the burn out is completed at 500°C; in this interval, the highest loss in wt was recorded. This is an important factor to determine the retorting temperature. The loss in weight above 700°C depends on the carbonate content of the oil shale.

Fischer Assay product composition is in Tables V-VII.

TABLE V

COMPOSITION AND PROPERTIES OF FISCHER ASSAY PRODUCTS

Shale Oil		
Specific gravity	15°/16°	0.936
Elemental Composition %		
C		78.55
H		9.74
S		8.50
N+O+Cl		3.21
Group Components of the Shale Oil %		
Paraffins		17.7
Olefins		13.1
Aromatics and Sulfo-Organic Compounds		56.1
Oxygen compounds		13.1
Nickel in ppm		8
Vanadium in ppm		9

TABLE VI

FRACTION CHARACTERISTICS OF THE SHALE OIL

	Fractions				
	1	2	3	4	5
Yield, % by wt	4.2	11.9	26.8	23	24.8
Boiling temp. °C	100	100-200	200-300	300-391	391-445
Sp. gravity 16/16	0.750	0.851	0.915	0.962	0.974
Refractive index	1.4300	1.4600	1.502	1.5262	1.5472
Sulfur content %	3.88	9.5	9.5	8.5	6.2
Oxygen content %	0.66	0.88	1.26	1.46	1.66

TABLE VII

GROUP CHEMICAL COMPOSITION OF THE GAS

Gas

The group chemical composition of the gas is given below:

CO ₂ % Vol	14.5
H ₂ S	26.2
CO	1.0
H ₂	21.6
Olefins	9.3
Paraffins	28.4

The calorific value of the gas was found to be 9400 Kcal/M³.

The following oriented balance may be concluded, taking into consideration that the total organic matter content in the raw shale is 24.3%; oil 54.7%, water 5.8%, gas 18.3% and residue (spent shale) 21.2%. This indicates that the remaining energy can be used in a suitable process to generate heat.

EXPLORATION AND UTILIZATION OF EL-LAJJUN OIL SHALE

Oil shale is the only known fossil energy resource in Jordan. Therefore, the possibility of its exploration is of national importance.

Mining

The near-the-surface El-Lajjun deposit with its favorable stripping ratio 1:1 is best mined by open-pit methods. The kind of open-pit mining depends on the scale of the intended utilization.

Crushing

Grindability of the oil shale was evaluated according to the Hardgrove and VT1 scale. The Hardgrove grindability tests revealed indices of 20.1-43.6 by VT1 scale 0.61-0.97. This shows that El-Lajjun oil shale is more difficult than the hardest coal to grind. Provision in the conceptual design should be made for additional power requirements in the preparation process and higher wear rates in mills and transference facilities.

Utilization

On the basis of studies concluded on the El-Lajjun oil shale, utilization can be by direct combustion or retorting.

Direct combustion estimates were made for areas where petroleum is in short or uncertain supply and where oil shale can be mined by open-pit. Utilization of oil shale would be on a large scale. Direct combustion is considered if the heating value of the oil shale exceeds 1000 kcal/kg or if the organic matter is more than 15%. Problems may arise due to the high ash content of the oil shale (52.07-57.29%), flue gases, corrosion and sintering and smelting of the ash in the furnace. The known processes for direct combustion are: dust-fired plant, classical fluidized bed and circulating fluidized bed. The dust-fired plants operate at temperatures above 900°C with short gas/oil shale reaction time. This results in sintering and smelting of the ash in the furnace and in high SO₂ emissions in the waste gas, which does not only cause environmental pollution but the corrosion of the plant. The desulfurization even with the high Ca content of the oil shale is insufficient. In contrast, the classical fluidized bed operating under temperatures below 800° avoids melting of the ash and minimizes the sulfur problems. The circulating fluidized bed combustion is suited for the low combustion of all fuels and is characterized by intensive internal and external solids recycle (10). The circulating fluid bed is thus in the transition region between the classical fluidized bed and pneumatic transport. The major advantages of the system can be summarized as follows: the temperature of combustion can be adjusted to any desired level below the fusion point of the ashes. The ashes after combustion do not fuse so that they do not deposit on any walls. The ashes act as fluidizing medium and take a major part in the heat transfer of the system. High heat transfer coefficients in the fluid bed allow lower metal surface areas. Uniform temperature in the whole reactor results from solids recirculation. Fast desulfurization results from neutralization by the lime with longer and better contact between the particles. Formation of harmful NOX gases in the reactor is low due to staged combustion at low temperatures.

Retorting is applicable if the oil yield by Fischer Assay from oil shale exceeds 7% or if the organic matter is more than 25%. To this extent, a modern economic process should fulfill the following requirements: simple construction, high reliability in operation, low investment and operation costs with an oil production of nearly 100% of the Fischer Assay, low water requirements, continuous operation and minimum environmental pollution.

In direct-heating processes, the necessary heat is generated by feeding air into the retort and burning part of the organic material contained in the shale. The yield reach 85% of the Fischer Assay yield and a low calorific value gas (5000 KJ/m³) is produced.

Indirect heating processes are characterized by separation of the combustion gases from the retorts. Heat carriers, such as spent shale, sand, ceramic balls or hot gasses, are used. The processes reach 100% of the Fischer Assay yield and produce high-grade gas (35000-38000 KJ/m³). The thermal efficiency is high if the residual energy of the retorted shale is used.

The Prefeasibility Study for a 50,000 bbl/day retorting plant showed the following results: The Retorting Plant will require a mine of 25 million tons/year capacity and will produce products the quantity of which after upgrading will be as follows: 4660 T/d of crude oil, 38° API and 0.5% S, 2020 T/d Naptha 55° API and 0.3% S, 510 T/d L. P. G. gas, 1690 T/d sulfur and 310 MW of electricity, 190 MW of which will be used in the plants and the rest will be connected to the national grid.

Utilization of Retorted Products

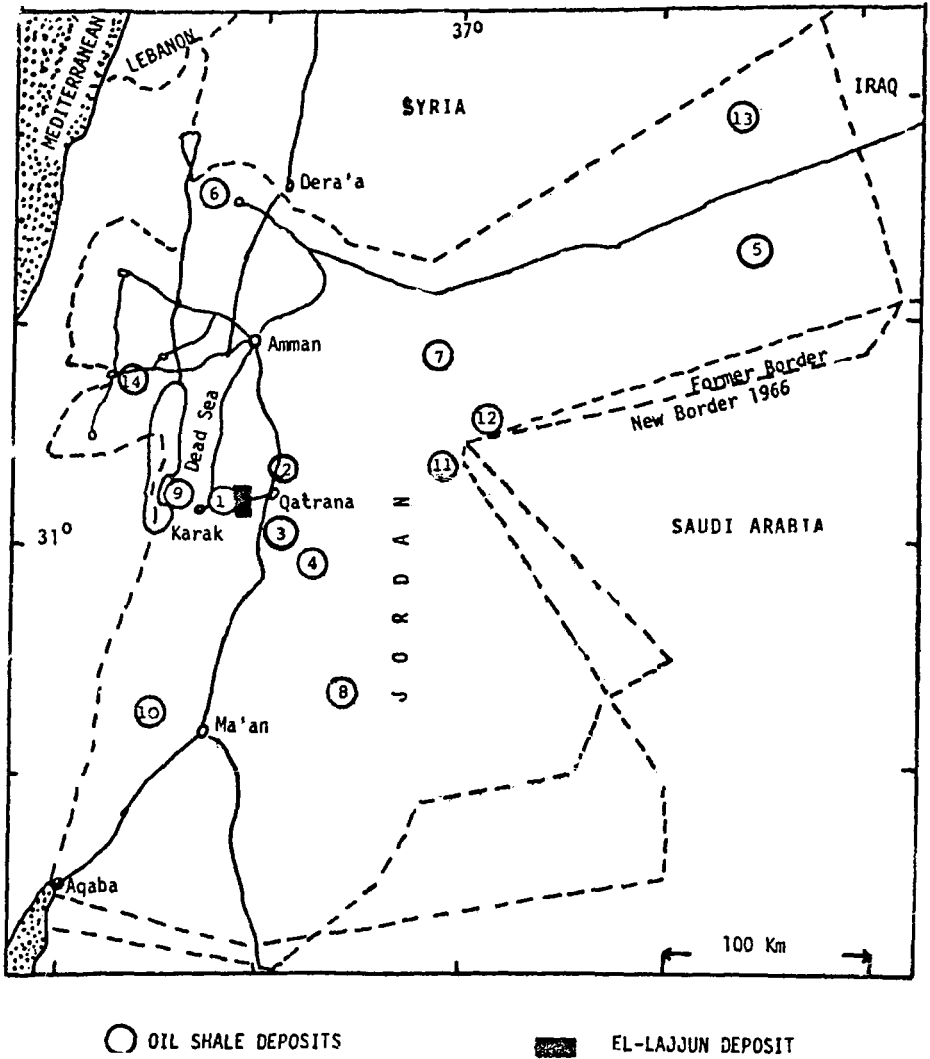
Retorted products are oil, gas, water (and other byproducts).

The crude shale oil is rich in sulfur and nitrogen. By upgrading (hydrotreating and distilling the crude shale oil) it is transformed to gasoline, kerosene, gas oil, fuel oil, etc.

Depending on the retorting process, the calorific values of the gas varies from 5000-38000 KJ/m³. The hydrogen for hydrogenation can be processed from this gas. Besides, gas can be utilized for many purposes including power generation.

Spent shale, in general, can be used for soil stabilization, road construction and cement production, but, in the case of El-Lajjun oil shale, the spent shale is undesired byproduct and can only be dumped because of the high P₂O₅ content.

FIGURE 1: LOCATION OF OIL SHALE DEPOSITS IN JORDAN



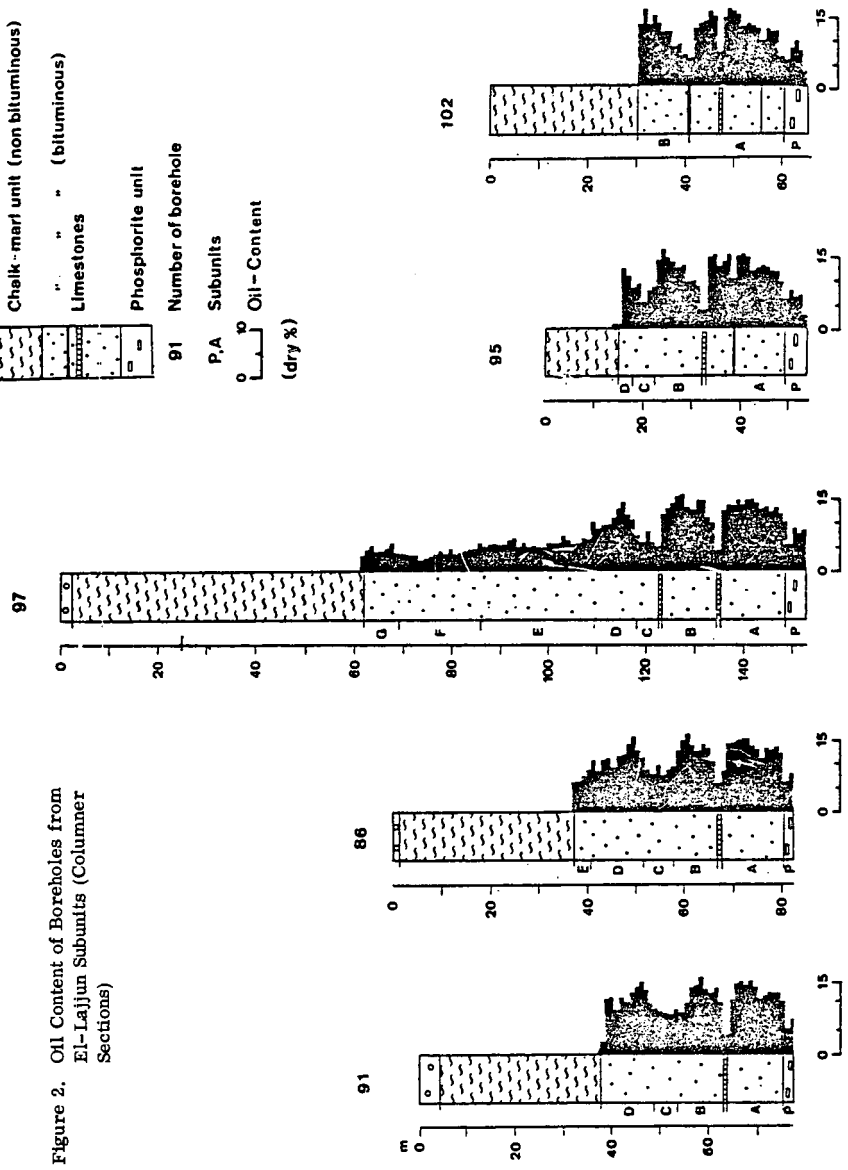
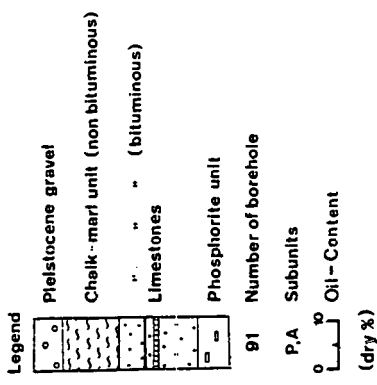


Figure 2. Oil Content of Boreholes from El-Lajjun Subunits (Columnar Sections)

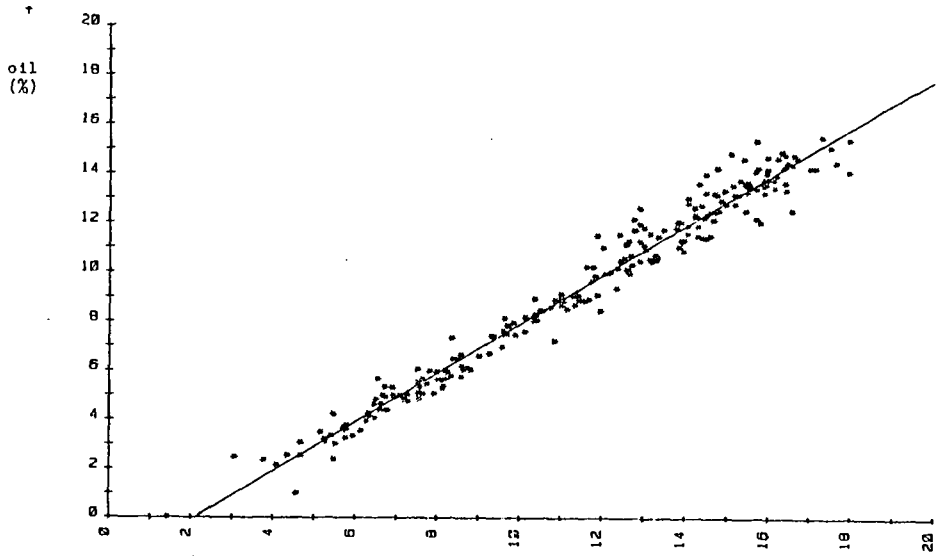


Figure 3. Relationship of Oil Content to Organic Carbon Content

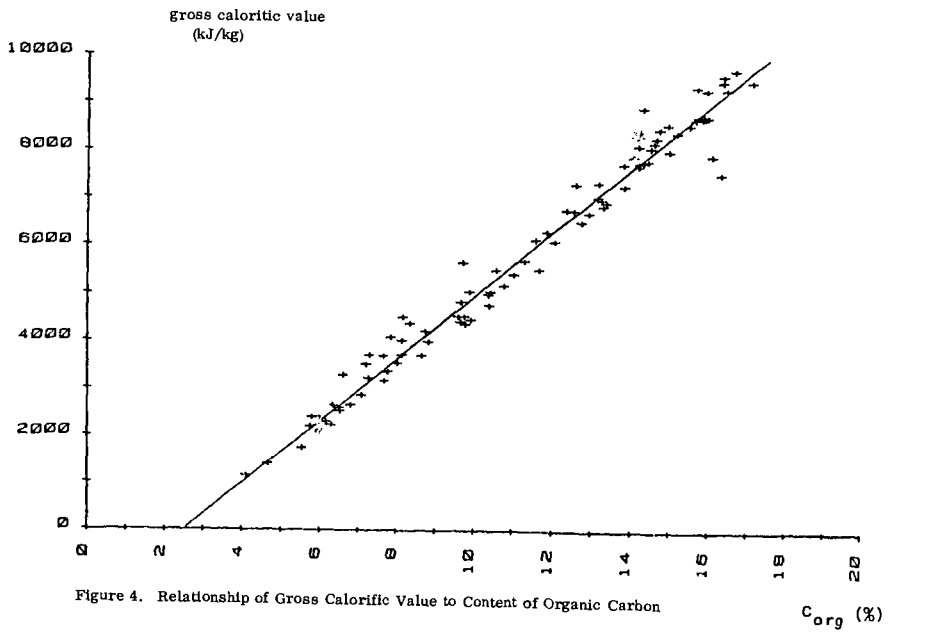


Figure 4. Relationship of Gross Calorific Value to Content of Organic Carbon

After the removal of phenols, which exists in adequate quantities, the water can be used to moisten the dry and dusty spent shale to prevent it from being blown away by the wind or in the retorting plant itself, although it may increase the operation costs. The most serious problem for the potential utilization of the El-Lajjun oil shale deposit is the amount of water required by the retorting process, combustion of residual carbon, refining of the crude shale oil and for consolidating the spent shale or the ash in the dump area. The retorting plant should use the minimum amount of feed water and cooling should be largely done by air coolers. The area of El-Lajjun forms part of a large ground water basin. Ground water occurs in layers underlying the bituminous formation. Evaluation of the ground water potential in the area is in progress. The results obtained are encouraging.

ACKNOWLEDGMENT

The author wishes to express his thanks and gratitude to Eng. M. Abu Ajamieh, Director of Geological Survey and Bureau of Mines, whose suggestions, discussions and reviewing this report were indeed valuable. The author is indebted to the entire staff of the Laboratories Division for their cooperation. Thanks are also due to Mrs. Y. Salah for typing this report.

LITERATURE CITED

- (1) Nimry, Y., Abu Ajamieh, M., Omari, K., Daghestani, F. and Hamarneh, Y., Oil Shale in Jordan (1981).
- (2) Hufnagel, H., Scmitz, H. H. and El Kaysi, K., Investigation of the El-Lajjun Oil Shale Deposit, Hannover (1980).
- (3) Dinnen, G. V., Evaluation of Investigation of the Oil Shale Resources of Jordan and Comments on their Utilization, U. S. Bureau of Mines (1970).
- (4) Jacob, H., Analysis of Five Core Samples of El-Lajjun Bituminous Marl, Central Jordan, unpublished report (1969).
- (5) Speers, G. C., El-Lajjun Oil Shale Deposit Jordan, NRA and BP Research Centre (1969).
- (6) Hamarneh, Y. and Gubergritz, M., Techno-Chemical Characteristics of El-Lajjun Oil Shale, Institute of Chem. Estonian Academy of Science Tallin (1969).
- (7) Klesment, I., Riken, U., Eizen, O. and Hamarneh, Y., The Chemical Composition of Jordanian Shale Oil, Institute of Chem. Estonian Academy of Science Tallin (1970).
- (8) Omary, K., El-Lajjun Oil Shale Deposit NRA (1978).
- (9) Abu Ajamieh, M., An Assessment of the El-Lajjun Oil Shale Deposit NRA (1980).
- (10) The Proceeding of the Sixth Internatl. Conf. on Fluidized Bed Combustion (1980).

SYMPOSIUM ON CHARACTERIZATION AND CHEMISTRY OF OIL SHALES
PRESENTED BEFORE THE DIVISIONS OF FUEL CHEMISTRY AND
PETROLEUM CHEMISTRY, INC.
AMERICAN CHEMICAL SOCIETY
ST. LOUIS MEETING, APRIL 8 - 13, 1984

NMR AND ESR CHARACTERIZATION OF OIL SHALES

By

J. W. Harrell, Jr., Taro Kohno and Fayequa Banu
Department of Physics and Astronomy, University of Alabama, University, Alabama 35486
and
H. S. Hanna
Mineral Resources Institute, University of Alabama, University, Alabama 35486

INTRODUCTION

NMR and ESR have proven to be very useful methods for studying various properties of fossil fuels. Although most studies have been applied to coals, in recent years an increasing emphasis has been placed on using magnetic resonance to study oil shales. One of the most important recent developments involves the use of C-13 NMR. Using cross-polarization and magic-angle spinning, separate aliphatic and aromatic C-13 peaks can be resolved (1). It has been shown for oil shales that the Fischer Assay determination of oil yield is strongly correlated with the aliphatic signal (2, 3).

Proton NMR has also been useful in characterizing oil shales. Several investigators have shown that the total proton NMR signal is linearly correlated with the oil yield if oil shale samples of a similar type are compared (4-7). Temperature-dependent relaxation time measurements can also be useful. Miknis and Wetzel (5) reported T_1 values of a Western shale and its kerogen concentrate which had a temperature dependence which reflected some characteristic motion of the kerogen. Harrell and Kohno (8) have shown that $T_{1\rho}$ measurements can also be useful in identifying molecular motions. Lynch and co-workers (9) have shown that transient second moment measurements can help to identify thermal changes that occur in shales when they are heated.

Although a considerable amount of ESR work has been done on coal (10), by comparison, very little work has been reported for oil shales. Eaton and co-workers (11, 12) have used ESR to study a set of Wyoming oil shale samples which were nearly all obtained from different depths from the same bore hole. They showed that the integrated intensity of the organic free radical signal was linearly correlated with the oil yield. Harrell and co-workers (8, 13) have recently shown that the ESR spectra of Eastern U. S. oil shales are more intense and complex than those of Western oil shales.

In this paper, we present temperature-dependent T_1 and $T_{1\rho}$ results and ESR and ENDOR measurements on Eastern and Western U. S. oil shales.

EXPERIMENTAL

Samples

Most of the oil shale samples and their oil Fischer Assays were supplied by the Mineral Resources Institute of the University of Alabama. Two additional Western shale samples from Colorado were supplied by Exxon Research and Engineering Company. Untreated or raw shale samples (with associated oil Fischer Assays in gallons per ton, GPT) were from the following locations: Madison Co., Alabama (12.3 GPT), Limestone Co., Alabama (16 GPT), Dekalb Co., Alabama (~1 GPT), Franklin Co., Tennessee (9.5 GPT), Powel Co., Kentucky (16.9 GPT), Wyoming (60 GPT) and Colorado (25 and 33 GPT). The beneficiation products of Madison Co., Alabama and Wyoming samples with different kerogen concentrations were prepared by fine grinding and flotation (14) and had Fischer Assays in the ranges 0.3 GPT to 27 GPT and 5 GPT to 91 GPT, respectively. Madison Co., Alabama spent shales were also used. The Alabama and Tennessee shales were from the Chattanooga formation, the Kentucky shale was from the New Albany formation, the Wyoming shale was from the Mahogany Zone formation and the Colorado shales were from the Green River formation. The Dekalb Co., Alabama shales were deformed shale from a geologically folded region.

NMR

The pulse NMR system consisted of a 36 MHz Spin-Lock CPS-2 spectrometer controlled by an external digital pulse programmer. Free-induction-decay signals were recorded on a Nicolet

Explorer III digital oscilloscope which was interfaced to a microcomputer for signal averaging of weak signals. Temperature control was achieved by a gas-flow system with an electronic regulator. T_1 measurements were made using a saturation- τ -90° pulse sequence and $T_{1\rho}$ measurements were made using a 90° pulse followed by a 90° phase-shifted spin-locking pulse of variable length.

ESR and ENDOR

ESR measurements were made on X-band and K-band systems which employed 17 kHz and 33.5 kHz field modulation frequencies. Spin concentration measurements were made at K-band by digitally integrating the first-harmonic signal. Signals were compared with the signal from a fixed amount of Cr^{3+} which was placed near the shale in the ESR cavity and which had a sufficiently different g-factor so that almost no signal overlap with the shale occurred. The Cr^{3+} was calibrated against a ruby standard obtained from the National Bureau of Standards. Saturation measurements of the line components were made at X-band using second-harmonic detection because of the better resolution as compared to the first-harmonic signal. G-factor measurements were made at K-band using second-harmonic detection. ENDOR measurements were made at X-band using field modulation and second-harmonic detection.

RESULTS

NMR

In general, the T_1 and $T_{1\rho}$ relaxation measurements were nonexponential and were characterized by a distribution of relaxation times. For simplicity effective T_1 and $T_{1\rho}$ values, defined as $t_{1/2}/\ln 2$, were determined. For T_1 , $t_{1/2}$ was the time for the longitudinal magnetization to recover to within one-half of the thermal equilibrium value following a saturation sequence. For $T_{1\rho}$, $t_{1/2}$ was the duration of a spin-locking pulse in a $T_{1\rho}$ sequence such that the transverse magnetization decayed by a factor of one-half.

T_1 and $T_{1\rho}$ values for all of the raw shales were measured as a function of temperature from about -135°C to 280°C. Results for the Limestone Co., Alabama and Wyoming shales are shown in Figures 1 and 2 as representative results for the Eastern and Western shales. The T_1 values for all of the samples had a temperature dependence which was similar to that shown in Figures 1 and 2, although the magnitudes varied from shale to shale. At room temperature, the T_1 's ranged from a low of 4 ms for the Kentucky shale to a high of 40 ms for the Madison Co., Alabama shale. For all samples, essentially no variation in T_1 with temperature was observed below room temperature. T_1 increased with increasing temperature starting in the range from about 20°C to 85°C. For some samples a shallow T_1 minimum was also observed in this temperature region. When the samples were evacuated overnight, T_1 was observed to either increase or to remain unchanged. The greatest change, a factor of about two, occurred for the Limestone Co., Alabama shale, as shown in Figure 1, while essentially no change occurred for the Madison Co., Alabama shale.

The $T_{1\rho}$ values of all of the Eastern shales were nearly the same both in magnitude and in temperature dependence. Almost no change occurred in $T_{1\rho}$ as a function of temperature except for a slight increase in $T_{1\rho}$ at the highest temperatures for some of the samples. The Limestone Co., Alabama $T_{1\rho}$ values shown in Figure 1 had about the same dependence upon H_1 over the entire temperature range. When H_1 was increased from 3 G to 16 G, $T_{1\rho}$ increased by a factor of about two.

The $T_{1\rho}$ results for the Western shales exhibited the most detail of all of the relaxation measurements. Both Colorado shales gave $T_{1\rho}$ results almost identical to those shown in Figure 2 for the Wyoming shale. A broad minimum centered at -75°C and a sharp minimum centered at 182°C were detected. The dependence upon H_1 in the vicinity of the low-temperature minimum was about the same as for the Eastern shales. However, a stronger H_1 dependence was detected near the high-temperature minimum, with the largest dependence detected on the low-temperature side of the minimum. In contrast to the T_1 case, almost no change was observed in $T_{1\rho}$ for either Eastern or Western shales after they were evacuated.

ESR and ENDOR Spectra

All oil shale samples exhibited ESR signals which were characteristic of organic free radicals. In addition, weak vanadium signals in the Eastern shales and manganese signals in the Western shales could be detected.

The organic free radical spectra of all of the raw Eastern oil shales were similar to the Madison Co., Alabama spectrum shown in Figure 3. Three well-defined components can be easily detected in this X-band spectrum. At K-band these components were more clearly resolved. G-factors measured at K-band were 2.0028, 2.0018 and 2.0006, from left to right. The sample used to obtain the spectrum of Figure 3 consisted of finely ground particles which had been exposed to air for about 30 minutes before the spectrum was obtained. When the sample was evacuated overnight and the spectrum remeasured, an additional sharp component appeared in the spectrum as shown in

Figure 4. This peak overlaps the broad low-field component but appears to have a slightly smaller g-factor. This peak was even more intense in the spectrum of a fresh sample which was crushed to millimeter-size pieces and quickly measured in air.

The saturation behavior of a Madison Co., Alabama oil shale spectrum taken in air is shown in Figure 5. As indicated in the figure, the amplitude of the spectrum at four different positions is plotted as a function of relative microwave power. Because of the overlap of the spectral components, this curve does not accurately represent the saturation behavior of the individual components. However, it is quite clear that the high-field peak is easily saturated relative to the other peaks.

All of the raw Eastern oil shale samples had line components with g-factors and widths which were approximately the same as those for the Madison Co., Alabama shale, although the relative amplitudes of the components varied. Beneficiated Madison Co., Alabama samples exhibited spectra which had less resolution than those which were obtained from the raw, untreated Eastern shales. Spent Madison Co., Alabama shales showed a single broad in-phase component and no out-of-phase component, implying a very short T_1 . The Western shale spectra consisted primarily of a single broad component. In addition, some Western spectra exhibited a weak, sharp component which had a g-factor approximately the same as that of the high-field component in the Eastern shales.

ENDOR spectra were measured from a Madison Co., Alabama shale sample in order to obtain information about the nuclear environment of the free radicals. Both in-phase and out-of-phase ENDOR signals were measured from different parts of the ESR spectrum. Figure 6 shows in-phase and out-of-phase spectra obtained from the low-field part of the ESR signal. Although the signal is displayed in the figure as positive, it is actually negative. Only a broad matrix ENDOR signal centered at the free-proton frequency of 13.8 MHz was obtained. Similar signals were obtained from other parts of the ESR spectrum. Because of the overlap of the individual ESR line components and because of the weak signal-to-noise ratio, no significant differences in the hyperfine interactions of the different components could be determined.

Spin Concentrations

Spin concentrations were determined for raw, untreated shales, for beneficiated Madison Co., Alabama and Wyoming shales, and for spent beneficiated Madison Co., Alabama shales. When comparing raw shales, the spin concentration generally decreased as the Fischer Assay increased. The deformed Dekalb Co., Alabama shales, which had a Fischer Assay of about 1 GPT, had the largest spin concentration and the Wyoming shale, with a Fischer Assay of 60 GPT, had the smallest spin concentration.

Figure 7 is a plot of spin concentration as a function of the amplitude of the hydrogen free-induction-decay signal per unit mass of sample. This plot shows that when comparing beneficiated shales of a given type, that is, either the Madison Co., Alabama or the Wyoming shales, a linear relationship is seen to exist between the spin concentration and the hydrogen NMR signal. The graph shows that this linear relationship is preserved when the Madison Co., Alabama shales are pyrolyzed in the Fischer Assay process to yield spent shales. The spin concentration also appears to be linearly related to the hydrogen NMR signal for the raw Dekalb Co., Alabama deformed shales. The straight lines do not extrapolate through the origin.

DISCUSSION

NMR

There is strong evidence to suggest that interactions between protons and paramagnetic centers may be a significant T_1 relaxation mechanism in the oil shales. The T_1 values are much lower than one would expect due to other likely relaxation mechanisms. The weak temperature dependence below room temperature is typical of relaxation due to paramagnetic centers (15). The removal of paramagnetic oxygen by evacuation increases T_1 . Also, ESR shows that paramagnetic centers do exist in the shales. If paramagnetic centers do contribute significantly to the relaxation, then one might expect to observe a correlation between $1/T_1$ and the spin concentration; however, no such correlation was observed. However, in view of the complex and heterogeneous composition of the shales, this lack of correlation does not rule out this possible relaxation mechanism. It might be more reasonable, for example, to expect a correlation between $1/T_1$ and the number of spins per unit mass of total organic matter or per unit mass of aromatic material, rather than total sample mass. The high-temperature T_1 behavior suggests that there is some characteristic motion occurring in this range which is common to all the shales. This observation is in agreement with the work of Mknis and Wetzel (5).

It is difficult to determine what relaxation mechanisms are responsible for the $T_{1\rho}$ results, especially for the Eastern shales. The lack of variation in $T_{1\rho}$ for the Eastern shales from sample to sample and the observation that $T_{1\rho}$ does not change when the samples are evacuated

suggest that relaxation due to paramagnetic centers may not be very important. Since there is essentially no variation in $T_{1\rho}$ with temperature for the Eastern shales, no motional information can be obtained from the data. The reason for this lack of variation may be in part because the Eastern shales have a highly aromatic and somewhat rigid molecular structure.

In contrast with the Eastern shales, the $T_{1\rho}$ results for the Western shales provide clear evidence of molecular motion. The low-temperature $T_{1\rho}$ minimum is probably caused by the same type of motions that give rise to the high-temperature variation in T_1 . The high-temperature $T_{1\rho}$ minimum depicts a motion which cannot be observed in the T_1 data. Lynch et al. (9) have reported a second moment reduction in a highly aliphatic Australian shale at a temperature similar to that for the high-temperature $T_{1\rho}$ minimum. They liken the motion producing this reduction to a glass to rubber-type transition in an amorphous polymer. The high-temperature $T_{1\rho}$ measurements may be evidence of a similar type of motion.

Some insight in understanding the relaxation mechanisms involved in the oil shales might be obtained by making comparisons with simpler model systems such as polymers. For example, there are similarities between the results presented here and those found for poly(vinylidene fluoride) (PVF₂) in which slow spin diffusion was found to be important in explaining the $T_{1\rho}$ results (16).

ESR and ENDOR

The unusual nature of the ESR spectra of the Eastern shales is of particular interest. The two overlapping low-field components, including the oxygen effect, are similar to results which have been reported for bituminous coals (17, 18). However, the high-field peak is unusual in its combination of narrow line width, the ease with which it saturates and its low g -factor. To our knowledge, these spectra are unlike any other spectra which have been previously reported for fossil fuels.

Although the ENDOR results are unable to reveal differences between the nature of the different components of the Eastern ESR signals, the existence of a matrix ENDOR signal is evidence that some of the free radicals have a hydrogen environment. The difficulty of detecting separate ENDOR signals due to overlapping ESR line components might be partially resolved if ENDOR measurements were made at K-band where the line components are more widely separated. The ENDOR spectra in Figure 6 are similar to the negative ENDOR spectra obtained by Miyagawa et al. (17) for various components of bituminous coal from Alabama. However, we know of no other reported ENDOR spectra which have been obtained from oil shale.

The linear relationship that we have observed between the spin concentration and the hydrogen density as determined by the NMR signal for beneficiated samples suggests that the ESR signal is primarily of organic origin. The extrapolation of these straight lines to zero spin concentration suggests that there is an appreciable amount of hydrogen-bearing material in the shales which contain no free radicals.

The decrease in spin concentration with increasing oil yield that we have observed for the raw shales appears to differ from the linear relationship that Eaton and co-workers have observed (11). However, this apparent inconsistency may be resolved if one considers the free radicals to be based primarily in the aromatic fraction of the oil shale and the oil yield to depend primarily upon the aliphatic fraction.

CONCLUSIONS

It has been shown that relaxation measurements can be useful in characterizing motions in oil shales. High-temperature $T_{1\rho}$ measurements have been shown to be especially useful in showing molecular motions that may be related to the oil producing aliphatic part of the shale. However, in order to more fully exploit relaxation measurements, a more fundamental understanding of the relaxation mechanisms must be obtained.

Because the ESR spectra of the Eastern oil shales have been found to be so rich in detail, it may be possible to learn more about the nature of the free radicals in shales than is now known for coal, which has been studied much more extensively. Clearly, additional work on this subject should prove fruitful.

In order to more fully evaluate the utility of using spin concentrations as a measure of the resource potential of oil shales, measurements must be made on a larger number and a greater variety of shales.

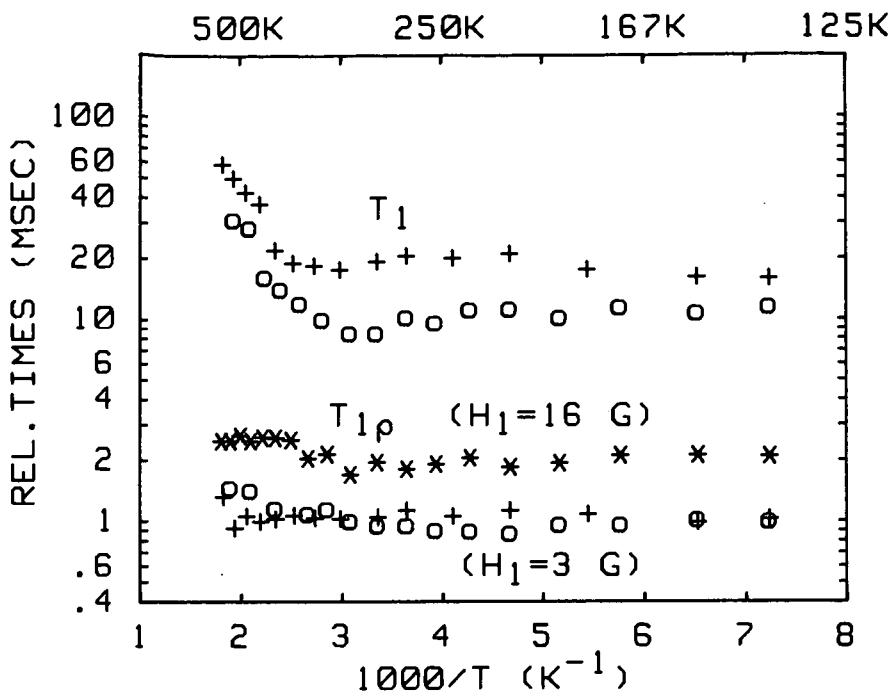


Figure 1. T_1 and $T_{1\rho}$ results for shale from Limestone Co., Alabama. Points indicated by (+) are for evacuated sample. Other points are for sample exposed to air.

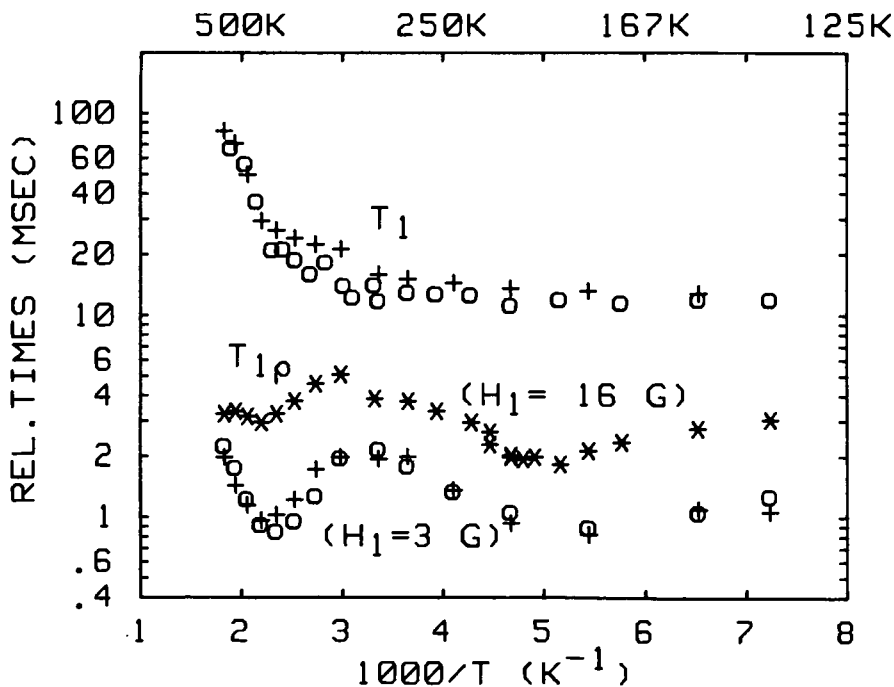


Figure 2. T_1 and $T_{1\rho}$ results for shale from Wyoming. Points indicated by (+) are for evacuated sample. Other points are for sample exposed to air.

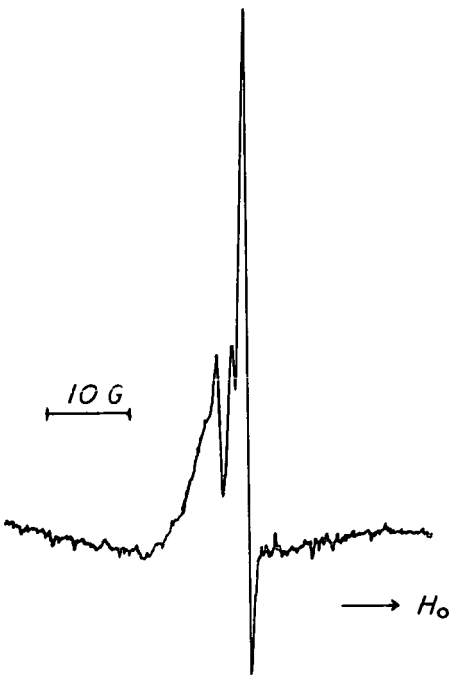


Figure 3. ESR spectrum of shale from Madison Co., Alabama exposed to air and taken at X-band using 2nd harmonic detection.

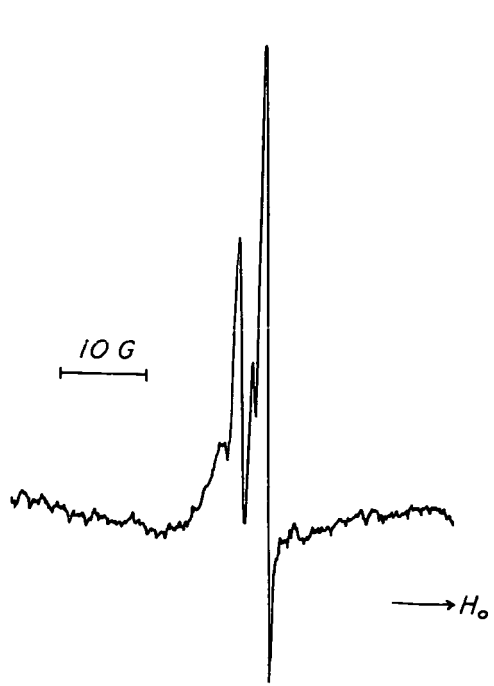


Figure 4. ESR spectrum of evacuated shale sample from Madison Co., Alabama.

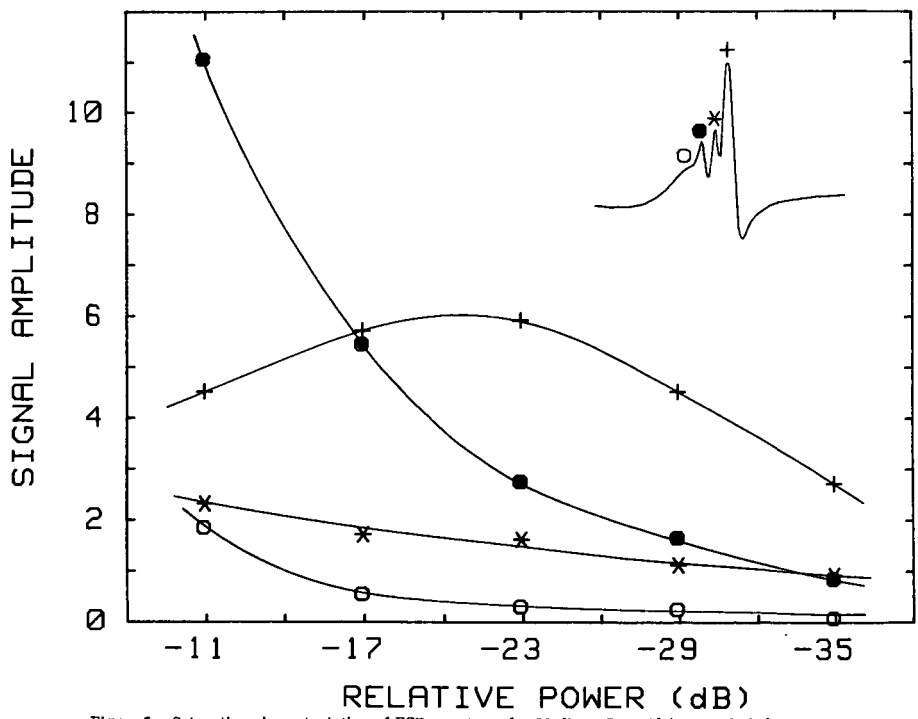


Figure 5. Saturation characteristics of ESR spectrum for Madison Co., Alabama oil shale.

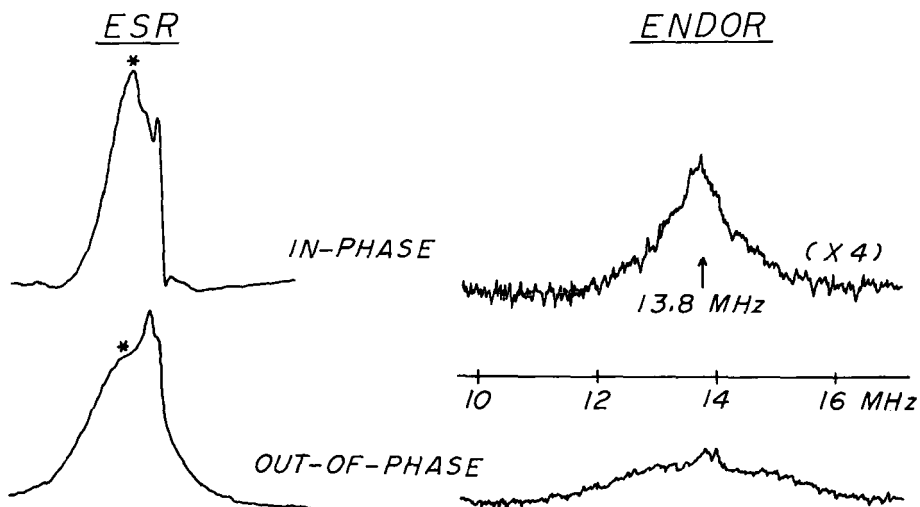


Figure 6. ENDOR spectra taken from low-field part of ESR signal.

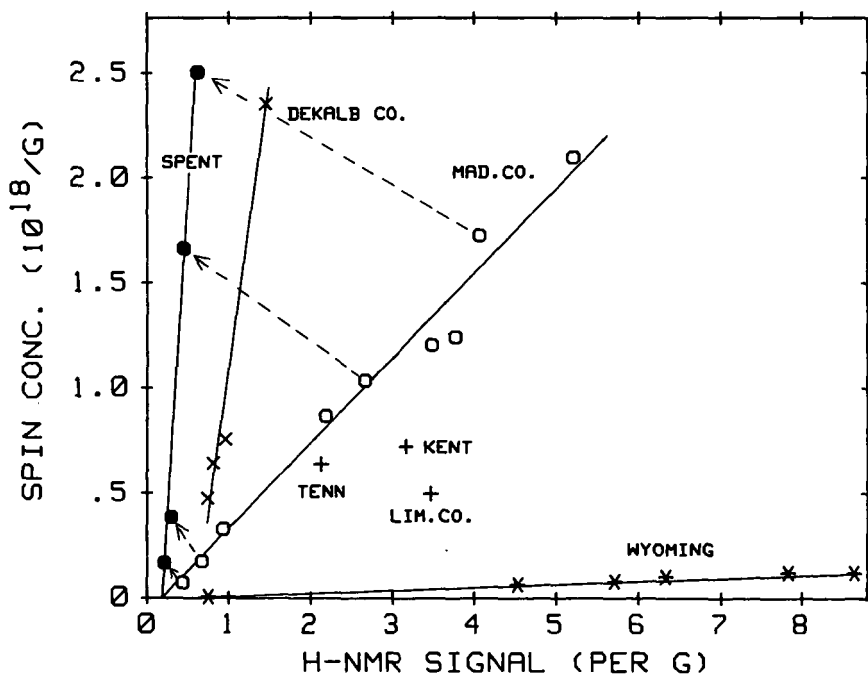


Figure 7. Spin concentration versus amplitude of proton free-induction-decay signal.

LITERATURE CITED

- (1) Resing, H. A. , Garroway, A. N. and Hazlett, R. N. , Fuel, 57, 450 (1978).
- (2) Maciel, G. E. , Bartuska, V. J. and Miknis, F. P. , Fuel, 57, 505 (1978).
- (3) Maciel, G. E. , Bartuska, V. J. and Miknis, F. P. , Fuel, 58, 155 (1979).
- (4) Miknis, F. P. , Decora, A. W. and Cook, G. L. , in Science and Technology of Oil Shales, T. F. Yen, ed. , Ann Arbor Science, Ann Arbor, 35 (1976).
- (5) Miknis, F. P. and Wetzal, D. A. , in Magnetic Resonance in Colloid and Interface Science, ACS Symp. Series No. 34, H. A. Resing and C. G. Wade, eds. , Washington, 182 (1976).
- (6) Sydansk, R. D. , Fuel, 57, 66 (1978).
- (7) Harrell, J. W. , Jr. , to appear in the proceedings of the 1982 Eastern Oil Shale Symp. held in Lexington, Kentucky, October 11-13, 1982.
- (8) Harrell, J. W. , Jr. and Kohno, T. , to appear in the proceedings of the NATO Advanced Study Insti. on Magnetic Resonance Techniques in Fossil Energy Problems held in Crete, July 3-15, 1983.
- (9) Lynch, L. J. , Webster, D. S. , Bacon, N. A. and Barton, W. A. , to appear in the proceedings of the NATO Advanced Study Insti. on Magnetic Resonance Techniques in Fossil Energy Problems held in Crete, July 3-15, 1983.
- (10) Marchand, A. and Conard, J. , in Kerogen, B. Durand, ed. , Technip, Paris, 243 (1980).
- (11) Sidwell, B. L. , McKinney, L. E. , Bozeman, M. F. , Egbujor, P. C. , Eaton, G. R. , Eaton, S. S. and Netzel, D. A. , Geochim. Cosmochim. Acta 43, 1337 (1979).
- (12) Eaton, G. R. and Eaton, S. S. , Fuel, 60, 67 (1981).
- (13) Harrell, J. W. , Jr. , Kohno, T. and Alexander, C. , to appear in the proceedings of the 1983 Eastern Oil Shale Symp. held in Lexington, Kentucky, November 13-16, 1983.
- (14) Hanna, H. S. and Lamont, W. E. , in Symp. papers on Synthetic Fuels From Oil Shales and Tar Sands, IGT, July, 1983, pp.295-321.
- (15) Abragam, A. , Principles of Nuclear Magnetism, Oxford Univ. Press, London, pp. 378-389 (1961).
- (16) McBrierty, V. J. , Douglass, D. C. and Weber, T. A. , J. Polym. Sci. , Polym. Phys. Ed. , 14, 1271 (1976).
- (17) Miyagawa, I. , Shibata, K. and Alexander, C. , in Abstracts of the 15th Biennial Conf. on Carbon, Philadelphia, PA, 464 (1981).
- (18) Das, U. , Doetschman, D. C. , Jones, P. M. and Lee, M. , Fuel, 62, 285 (1983).

SYMPOSIUM ON CHARACTERIZATION AND CHEMISTRY OF OIL SHALES
PRESENTED BEFORE THE DIVISIONS OF FUEL CHEMISTRY AND
PETROLEUM CHEMISTRY, INC.
AMERICAN CHEMICAL SOCIETY
ST. LOUIS MEETING, APRIL 8 - 13, 1984

A COMPARISON OF THERMAL DECOMPOSITION KINETICS
FOR SANTA ROSA AND UTAH TAR SAND

By

D. S. Thakur*, H. E. Nuttall, P. L. Shar and D. S. Lim
Department of Chemical and Nuclear Engineering
University of New Mexico, Albuquerque, New Mexico 87131

ABSTRACT

Recently, geological studies of many tar sand deposits have shown the distinctive nature and unique characteristics of each site. Similarly one might expect that since the geological history of deposits has varied, so will the chemical composition and pyrolysis kinetics be different for each site; however, very few comparative studies have been performed. Samples from Utah's Tar Sand Triangle and from New Mexico's Santa Rosa deposit were subjected to both isothermal and nonisothermal pyrolysis. From the resulting weight loss curves kinetic parameters were calculated and compared. Linear heating rates in the range of 1 to 50 degrees Centigrade per minute were used for the nonisothermal studies.

To analyze, compare, and determine kinetic parameters, the data were treated using the Coats-Redfern first order kinetic model and the three parameter statistical model of Anthony-Howard. As is often the case when using the Coats-Redfern model the nonisothermal data showed two distinct regions, i. e. , one below 425°C and the second between 425 and 500°C. When the activation energies were compared, the Tar Sand Triangle sample showed much greater activation energies for both temperature regions. The calculated Coats-Redfern activation energies for the 425-500°C temperature region are:

Sample Location	Activation Energy Kcal/mole
Utah Tar Sand Triangle	40.0
New Mexico Santa Rosa	26.0

These observed differences in activation energies for samples from two geologically different deposits indicates that there may be important chemical variations from site to site and that these differences should be considered in the design of commercial recovery processes.

*Internorth, Research Center, 4840 F Street, Omaha, Nebraska 68117

SYMPOSIUM ON CHARACTERIZATION AND CHEMISTRY OF OIL SHALES
PRESENTED BEFORE THE DIVISIONS OF FUEL CHEMISTRY AND
PETROLEUM CHEMISTRY, INC.
AMERICAN CHEMICAL SOCIETY
ST. LOUIS MEETING, APRIL 8 - 13, 1984

CHARACTERIZATION OF THE OIL SHALE OF THE
NEW ALBANY SHALE IN INDIANA

By

R. K. Leininger, J. G. Haller and N. R. Shaffer
Indiana Geological Survey, 611 N. Walnut Grove Avenue
Bloomington, Indiana 47405

ABSTRACT

In the 1920's chemical and mineralogic characterization of the New Albany Shale (Mississippian-Devonian) in Indiana showed the dark shale to be rich in organic material and have commercial possibilities. Projects in the 1960's resulted in disparaging descriptions of exiguous fossil record, monotonous mineralogy, and intractable chemistry. Since 1978 expanded efforts have yielded much new information but new problems as well.

Although organic carbon and total sulfur show positive correlation, two nearly exclusive populations exist. Material high in organic carbon is more depleted in C^{13} than material with less organic carbon. A bed usually at the top of the unit hosts anomalous accumulations of heavy metals and contains concentrations in similar ratios to those of sea water except for Mo and Pb and shows very negative δS^{34} . Heat content as Btu/lb, organic carbon (total less inorganic), and Fischer assay oil-yields generally correlate, but one is not an accurate predictor of the others.

SYMPOSIUM ON CHARACTERIZATION AND CHEMISTRY OF OIL SHALES
PRESENTED BEFORE THE DIVISIONS OF FUEL CHEMISTRY AND
PETROLEUM CHEMISTRY, INC.
AMERICAN CHEMICAL SOCIETY
ST. LOUIS MEETING, APRIL 8 - 13, 1984

THERMAL PROPERTIES OF AUSTRALIAN OIL SHALES: CHARACTERIZATION BY
THERMAL ANALYSIS AND INFRARED SPECTROPHOTOMETRY

By

J. H. Levy and W. I. Stuart
CSIRO, Division of Energy Chemistry, Lucas Heights Research Laboratories
Lucas Heights, NSW, Australia, 2232

INTRODUCTION

Thermal methods of analysis such as thermogravimetry (TG), derivative thermogravimetry (DTG), differential thermal analysis (DTA) and differential scanning calorimetry (DSC) are obvious choices for studying the thermal behavior and retorting properties of oil shales.

This paper describes work in which we combined TG, DTG and DSC techniques with infrared (ir) transmission spectrometry to provide pyrolysis and oxidative profiles as a means of characterizing and comparing Australian oil shales.

EXPERIMENTAL

Specimens of oil shale were obtained from the Condor, Duaringa, Julia Creek, Nagoorin, Rundle and Stuart deposits in Queensland; and from the Glen Davis and Hartley Vale torbanite deposits in New South Wales. Each specimen was ground in a Sieb mill and sieved. A sieved fraction (-1.4 to +0.6 mm) was chosen for analysis and ballmilled.

Kerogen concentrates were prepared by demineralizing the powdered oil shales with HCl and then HF solutions. Concentrates derived from Queensland shales contained 5-15% residual mineral matter with pyrite as a principal component. The torbanites do not contain pyrite and yield kerogen concentrates with less than 2% mineral matter.

TG and DTG curves were obtained by means of Cahn RH and RG thermobalances interfaced to an LSI-11 computer. Data were processed using a recursive digital filter as described elsewhere (1).

Differential scanning calorimetry was carried out using a Perkin-Elmer DTA 1700 in the DSC mode.

Solid-state ir spectra of oil shales, kerogen concentrates and residues were obtained using a pressed KBr disc technique. All spectra were measured on a JASCO A-302 ir spectrophotometer.

RESULTS AND DISCUSSION

The ir spectra of all kerogens are broadly similar. Table I lists the principal absorption bands which are common to samples of the oil shales and kerogen concentrates that we examined.

TABLE I

INFRARED SPECTRA OF KEROGENS

<u>Band Frequency cm⁻¹</u>	<u>Assignment</u>
3400	O-H stretch
2930	asym. stretch, CH ₂ alkyl
2860	sym. stretch, CH ₂ alkyl
1700	C=O stretch, ester, aldehyde, -COOH
1620	C-C vibration of aromatic rings
1465	asym. band of alkyl CH ₃ and CH ₂ groups
1375	mainly sym. band of CH ₃ groups

Note: A moderately intense band at 720 cm⁻¹ due to CH₂ rocking vibrations of non-cyclic hydrocarbons having more than four contiguous CH₂ groups is also prominent in spectra of NSW torbanite and Duaringa kerogen.

As Rouxhet et al. have shown (2), Ir spectra of coals, kerogens, humic substances and other carbonaceous solids are qualitatively alike, in the sense that they display the same major absorption bands. Nevertheless, the various kerogens display considerable differences in band intensities which permit useful qualitative comparisons. This is illustrated in Figure 1 with Ir spectra of Hartley Vale and Julia Creek kerogens. The aliphatic content of Hartley Vale kerogen is high, as shown by the intensity of bands at 2930, 2860, 1455 and 1375 cm^{-1} . Julia Creek kerogen, by contrast, is more aromatic, having weaker alkane bands and a correspondingly more intense aromatic band at 1620 cm^{-1} . The concentration of carboxylic groups in Julia Creek material is also much higher, as indicated by strong O-H stretching and C=O stretching bands at 3400 cm^{-1} and 1700 cm^{-1} , respectively. A comparison of Ir spectra of all the kerogen specimens shows the most aliphatic material to be the kerogen components of Hartley Vale, Glen Davis and Duinga shales. Kerogens of the Nagoorin carbonaceous and Condor carbonaceous shale are the most aromatic with Ir spectra similar to those of coals. The aromaticity of Condor brown, Julia Creek and Stuart shale lies in between the extremes represented by the torbanites and carbonaceous shales.

Compositional differences revealed by Ir spectrophotometry are reflected in the thermal behavior of the various kerogens, as the following discussion shows.

A common feature of kerogen pyrolysis is that decomposition of carboxylic groups dominates the early stages, from about 150 to 300°C for linear heating in nitrogen; this is indicated by a substantial reduction in O-H and C=O vibrational stretching bands at 3400 and 1700 cm^{-1} , respectively. Thus, the low concentration of -COOH groups observed for torbanite kerogen would account for the low rates of mass loss observed for Hartley Vale and Glen Davis oil shales below 300°C, as shown in Figure 2; conversely, TG-DTG pyrolysis curves for Julia Creek kerogen demonstrate that significant mass losses occur below 300°C, as one might predict from the comparatively high content of carboxylic groups indicated by the Ir data of Figure 1.

Figure 3 gives TG-DTG oxidative and pyrolysis profiles for two substantially aromatic shales (Nagoorin carbonaceous oil shale and a specimen obtained from the carbonaceous sequence of the Condor deposit). TG-DTG curves are also given for two shales with a high aliphatic component: Hartley Vale shale and a specimen from the Condor brown shale unit. A notable feature is that the total mass loss for combustion of Hartley Vale and Condor brown shale is only slightly greater than that obtained by pyrolytic decomposition in nitrogen. On the other hand, the mass loss by combustion of the Nagoorin and Condor carbonaceous shale is much greater than the corresponding mass loss by pyrolysis; that is, pyrolysis of the more aromatic kerogen yields a substantial amount of combustible residue. Mass losses for both pyrolysis and oxidation are given in Table II for a number of Australian oil shales.

TABLE II

THERMOGRAVIMETRIC ANALYSIS OF SOME AUSTRALIAN OIL SHALES

Shale	Mass Loss %		Mass Loss Ratio
	in air	in N ₂	Air:N ₂
Hartley Vale	53.8	52.5	1.03
Rundle	28.5	26.0	1.09
Condor brown	18.7	18.4	1.02
Julia Creek	32.4	23.5	1.38
Condor carbonaceous	43.9	26.9	1.63
Nagoorin	62.5	31.8	1.97

Other compositionally dependent features are demonstrated by TG-DTG oxidative profiles. In a separate study (3) we have used TG-DTG techniques, Ir transmission spectra and evolved gas analysis (EGA) to examine the oxidative properties of Australian oil shales and kerogen concentrates, and to identify the major oxidative stages in dynamic air atmospheres. This work showed that combustion of the kerogen component of shale occurs in two stages. Stage 1 involves near-complete combustion of aliphatic components, to yield a char containing aromatic moieties and (presumably) elemental carbon; and stage 2 is, therefore, combustion of the char residue. The various oxidation stages are illustrated in Figure 4 with TG-DTG curves for Condor carbonaceous, Rundle, Stuart and Julia Creek shales. Julia Creek shale shows a substantial weight loss between 650 and 800°C due to thermal decomposition of calcite and, in this respect, differs from the other shales. Common features shown in Figure 4 are two major DTG peaks at 280 and 420°C, respectively, denoting the two stages of kerogen combustion. Minor peaks at 450 (stage 3) and 600-666°C (stage 4) arise from combustion of pyrite as indicated by the following:

i. EGO measurements to 500°C (3) showed that SO₂ is the major gaseous species evolved during stage 3.

ii. Addition of pyrite to a kerogen concentrate derived from Condor brown shale enhances stages 3 and 4, as shown in Figure 5; the additional mass loss due to added pyrite is as one might expect, assuming that SO_2 and Fe_2O_3 were the products of pyrite combustion.

Although there appears a rough parallelism of ir spectra as indicators of aromaticity, as well as the ratio of the magnitudes of the first and second stages of combustion, we cannot assume that this ratio provides a quantitative measure of the ratio of aliphatic to aromatic constituents in raw shales, since heating may induce aromatization of cyclic hydrocarbons, and combustion of aromatic constituents could also occur during stage 1. But certainly, the results are consistent with a model for kerogen visualizing alkane, alkanone, carboxylic and various other reactive functional groups held within a polymeric and thermally more stable polynuclear aromatic framework.

Although we can relate TG-DTG curves to broad compositional features of Australian oil shales, there is no immediately apparent connection between thermal properties and type of precursor material as suggested by Earnest (4, 5). For example, petrology of Rundle, Stuart and Condor brown shales (6), shows the kerogen to be primarily of algal origin, with the colonial green alga *Pediastrum* as a major precursor. Julia Creek oil shale (7, 8) is a marine shale with planktonic or benthonic algae, dinoflagellate and arciatarch cysts as principal originating materials. Condor carbonaceous shale (6) is derived from higher plants in a forest swamp environment. Although a substantial calcite decomposition DTG peak reflects the marine origin of Julia Creek material, all these shales show qualitatively similar thermal behavior, with quantitative differences reflecting the degree of catagenesis rather than the nature of precursor organisms.

DSC curves show that for all shale specimens that we have examined by this technique, pyrolytic decomposition of the kerogen component is a weakly endothermic event. This can be seen from the data of Figure 6 and Table III. Figure 6 shows a DSC curve for a Julia Creek oil shale sample, with an endotherm for calcite decomposition at 810°C overshadowing the pyrolysis endotherm between 390 and 610°C , although mass loss due to pyrolysis is substantial (25% compared to 18% for the calcite decomposition). Table III lists enthalpy of pyrolysis for a number of samples. For calculating the values given in column 3 as MJ/kg contained kerogen, the kerogen content was taken as the total mass loss incurred during first and second stage combustion.

TABLE III
ENTHALPY OF PYROLYSIS

Sample	Enthalpy of Pyrolysis	
	MJ/kg raw shale	MJ/kg contained kerogen
Rundle oil shale	0.22	0.91
Condor carbonaceous shale	0.13	0.37
Condor brown shale	0.21	1.20
Julia Creek shale	0.13	0.48
Hartley Vale shale	0.12	0.22
Hartley Vale kerogen concentrate	-	0.22

Although the results of Table III are preliminary and incomplete, they indicate a substantial variability in thermal behavior of the various kerogen components of Australian oil shales. These DSC measurements are continuing as a means of relating oil shale composition and thermochemical behavior.

Table II shows that pyrolysis of the more aromatic and catagenetically more mature oil shales yields a carbonaceous residue that could represent a useful secondary heat source in the retorting process. With this in mind, we investigated combustion of a Nagoorin carbonaceous shale specimen and some pyrolyzed residues which were derived by linearly heating the raw shale in nitrogen to various stages of pyrolysis. Enthalpy values obtained from this study are listed in Table IV.

In a parallel study, we monitored changes in the ir spectrum of the shale at various stages of pyrolytic decomposition in nitrogen. The ir spectrum of the raw shale shows some bands due to mineral components (mainly kaolinite), but the principal bands of the kerogen component (Table I) are prominent. This kerogen is more advanced in catagenesis than the Julia Creek and Hartley Vale kerogens of Figure 1; a lower carbonyl/carboxyl functionality is evident by the 1700 cm^{-1} band appearing at reduced intensity as a shoulder to the prominent 1600 cm^{-1} band and alkyl groups are fewer as shown by comparatively weak C-H stretching bands near 2900 and 1400 cm^{-1} . Up to 580°C and 75% pyrolysis, the principal spectral changes are a diminution in the C=O band at 1700 cm^{-1} accompanied by loss of alkyl bands. At 75% pyrolysis, these bands are no longer evident. However, a band at 1620 cm^{-1} attributable to aromatic C-C vibrations, is still prominent at this stage of pyrolysis. On further pyrolysis, the aromatic band progressively diminishes and is

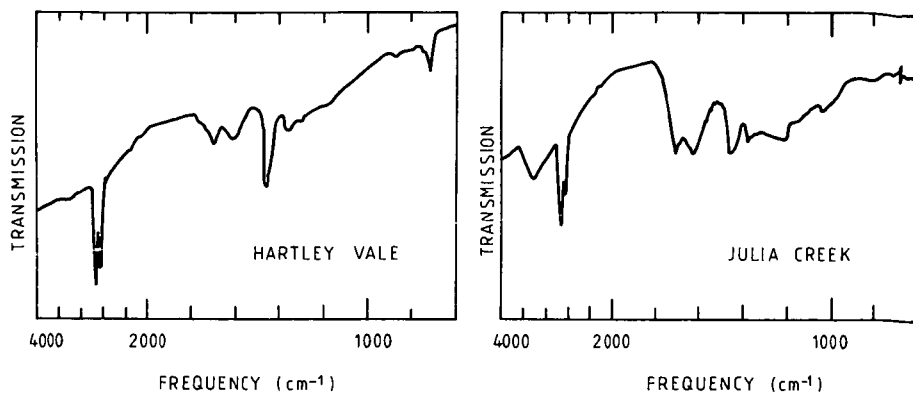


Figure 1. Infrared spectra of kerogen concentrates.

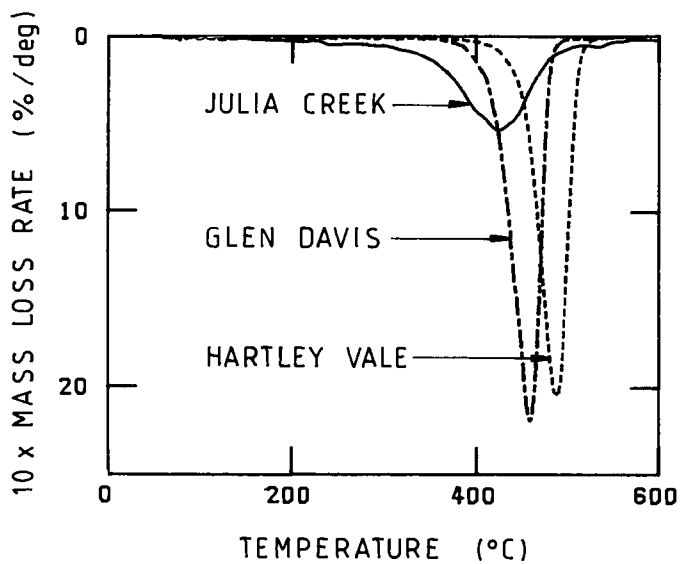


Figure 2. DTG curves for kerogens heated in nitrogen at 10°/min.

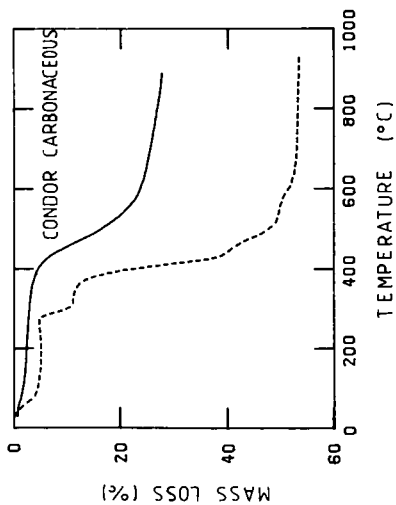
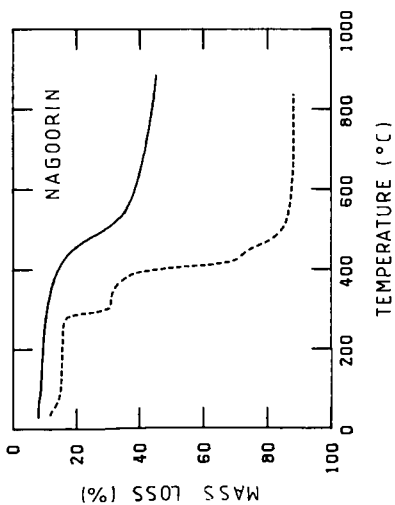
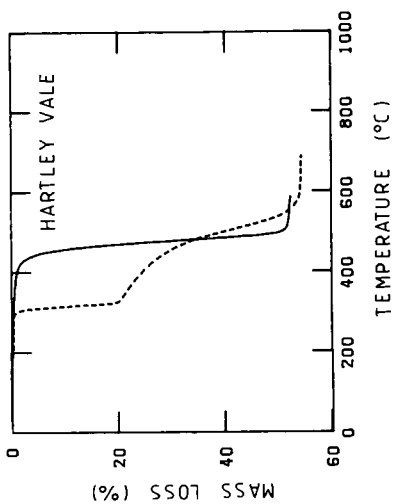
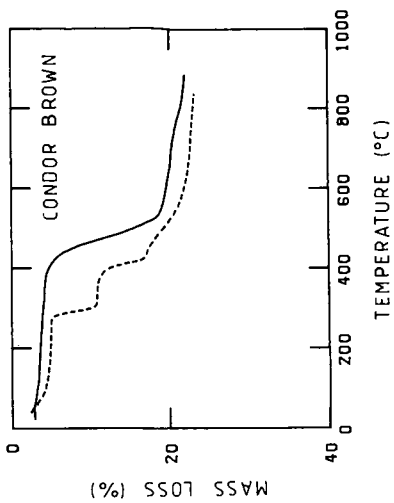


Figure 3. TG curves for Australian oil shales heated at 10°/min full curve - nitrogen, dashed curve - air.

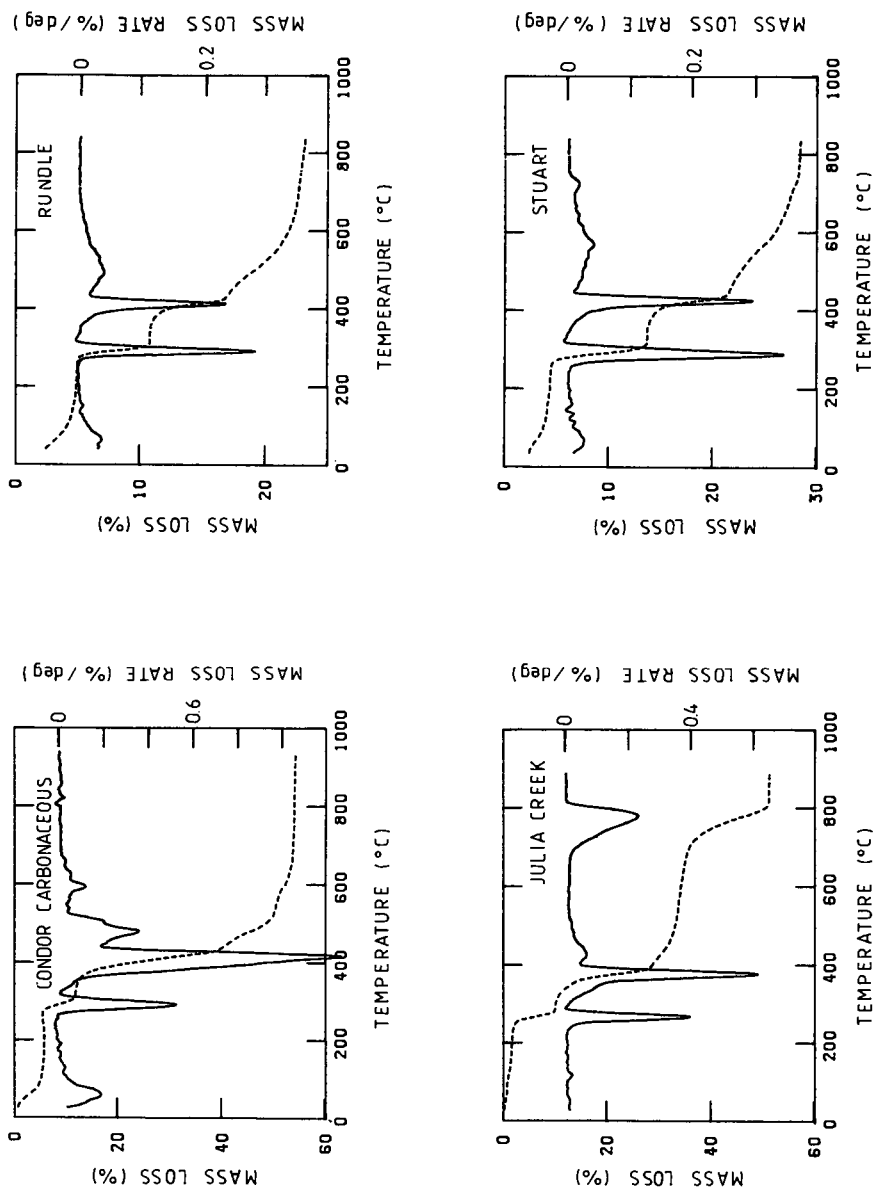


Figure 4. TG-DTG oxidative profiles for Australian oil shales heated in air at 10°/min.

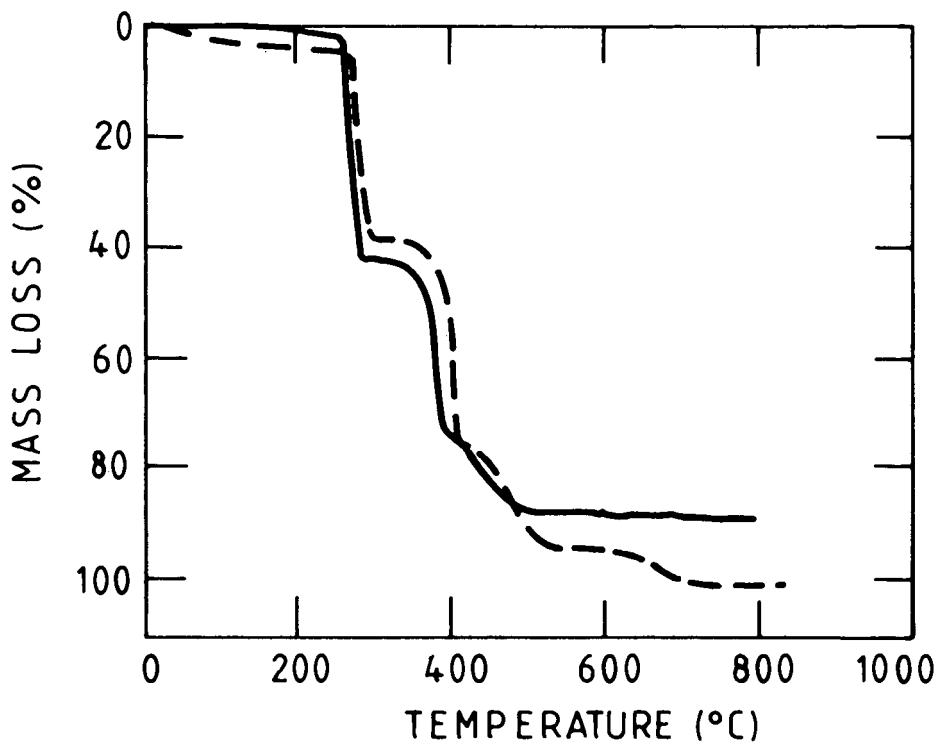


Figure 5. TG curve for Condor kerogen concentrate heated in air at 10°/min.
 Full line - kerogen with no added pyrite.
 Dashed line - with pyrite mixed into kerogen sample.

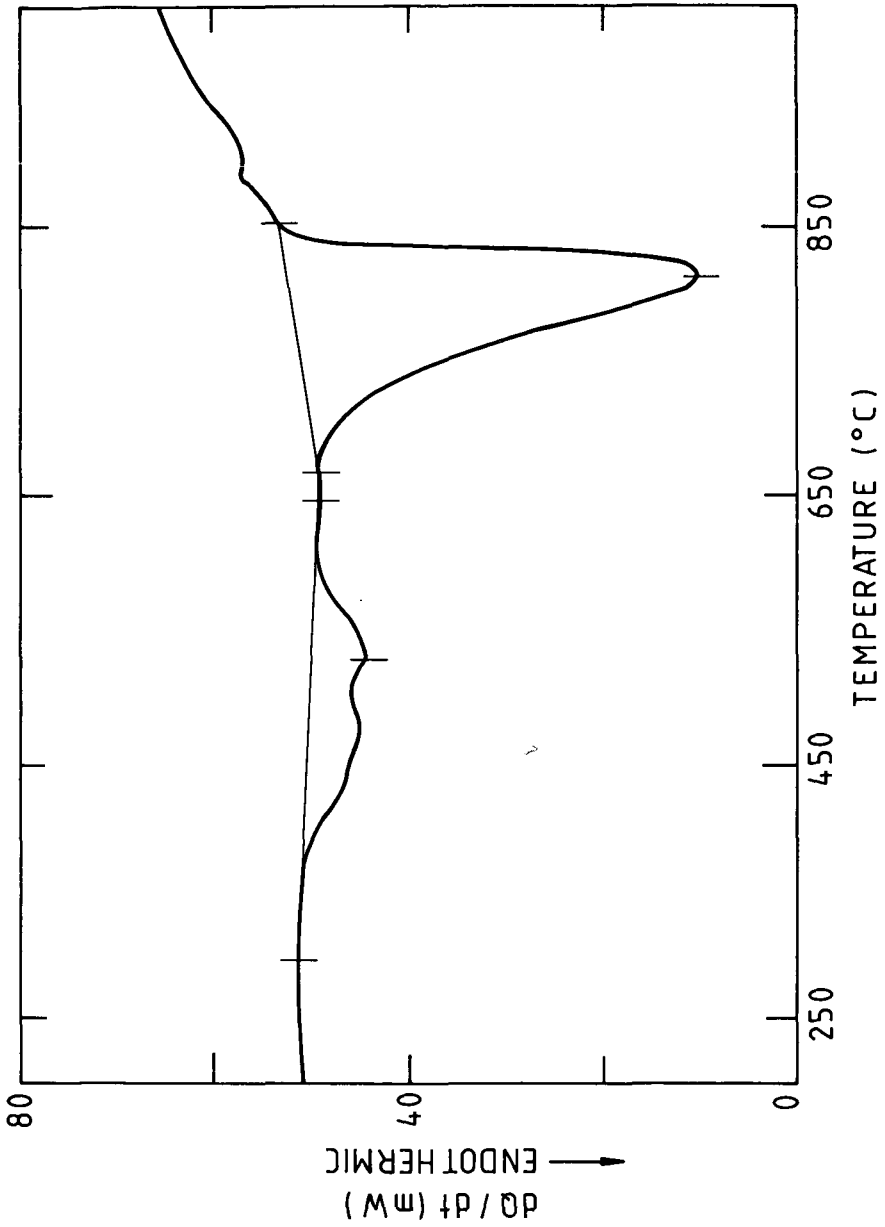


Figure 6. DSC curve for Julia Creek shale heated in nitrogen at 10°/min.

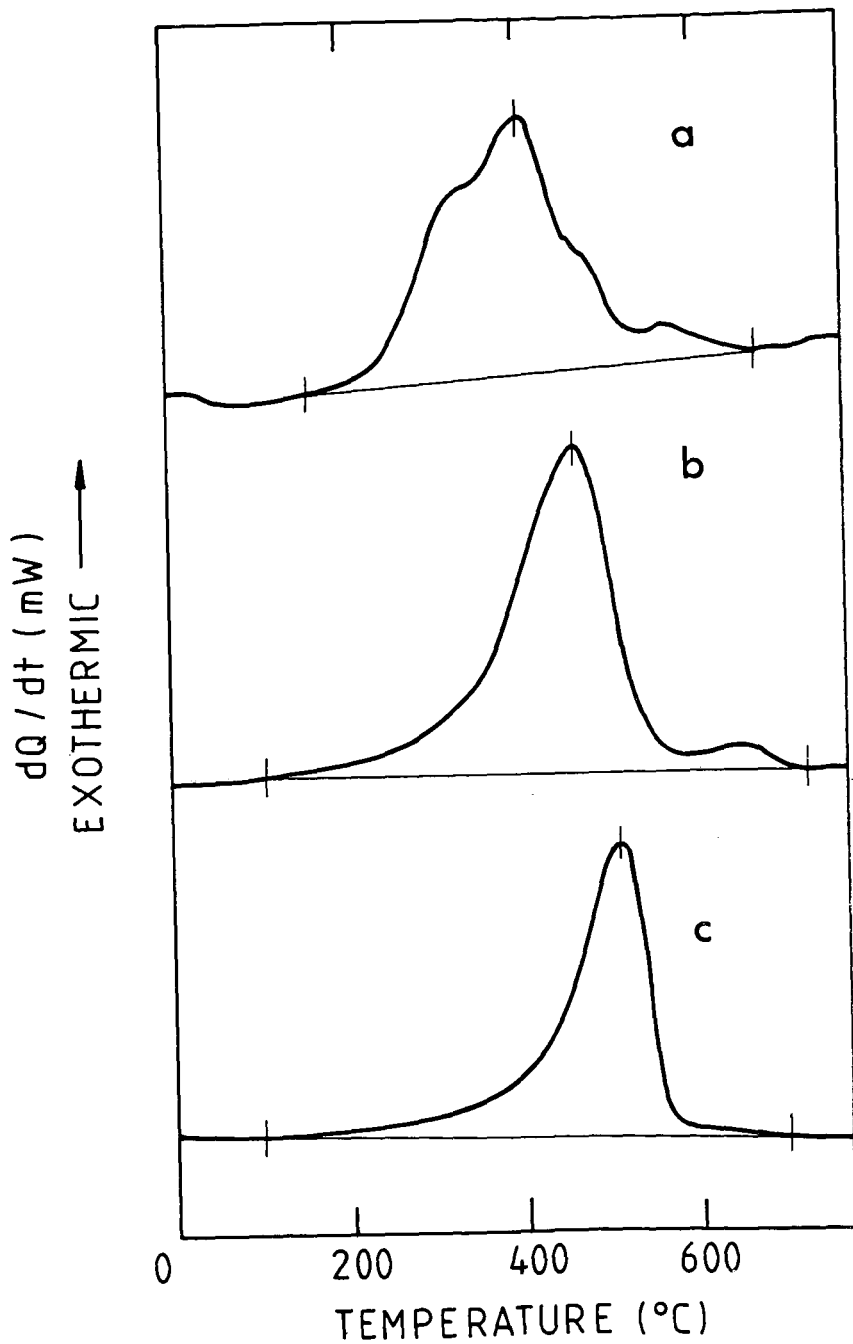


Figure 7. DSC combustion curves for Nagoorin shale and pyrolyzed residues heated in air at $10^{\circ}/\text{min}$.

- a. Raw shale
- b. Pyrolyzed residue (75% pyrolysis)
- c. Pyrolyzed residue (100% pyrolysis)

not detectable at 910°C; so pyrolysis of Nagoorin carbonaceous kerogen beyond 75% is a process of carbonization to give a final char which retains about 50% of the initial kerogen mass.

TABLE IV

ENTHALPY OF COMBUSTION IN AIR OF NAGOORIN OIL SHALE AND ITS VARIOUS PYROLYZED RESIDUES OBTAINED BY HEATING THE SHALE AT 10°/MIN IN A DYNAMIC NITROGEN ATMOSPHERE

Final T	% Pyrolysis	Enthalpy of Combustion	
		MJ/kg	MJ/kg
		Raw Shale	Pyrolyzed Residue
-	0	-11.0	-
300	8	-10.0	-10.9
580	75	- 8.6	-12.3
645	83	- 9.2	-13.5
780	97	- 8.3	-13.1
910	100	- 7.8	-12.6

Figure 7 shows DSC curves for combustion of the Nagoorin carbonaceous raw shale and some pyrolyzed residues. The combustion stages, shown clearly by DTG data, are not as well resolved in the DSC curve. Nevertheless, four exothermic stages can be distinguished for the raw shale, and identified by reference to TG-DTG profiles as discussed above. A major exothermic peak at 350°C is due principally to combustion of aliphatic components. The peak at 410°C corresponds to combustion of carbonaceous aromatic char, whilst two minor exotherms at higher temperatures arise from pyrite combustion. DSC curves for pyrolyzed residue show that with increasing pyrolysis, the first combustion peak diminishes and disappears, whereas the second peak shifts to higher temperatures. The fully pyrolyzed residue displays a single combustion peak at 509°C and the pyrite combustion exotherms are no longer evident; these may be eclipsed by peak shift but, more likely, decomposition of pyrite may have occurred during the final stages of pyrolysis.

ACKNOWLEDGMENTS

We gratefully acknowledge the donation of oil shale specimens by Southern Pacific Petroleum NL, Central Pacific Minerals NL, CSR Ltd and Esso Australia Ltd. We thank Mr. John Fursden and Mr. Alan Tomlinson of Perkin-Elmer (Australia) Pty Ltd for valuable technical advice and support.

LITERATURE CITED

- (1) Whittam, R. N., Levy, J. H. and Stuart, W. I., *Thermochim. Acta*, 57, 235 (1982).
- (2) Rouxhet, P. G., Robin, P. L. and Nicaise, G., in "KEROGEN : Insoluble Organic Matter From Sedimentary Rocks", B. Durand, ed., Editions Tech., Paris (1983).
- (3) Levy, J. H. and Stuart, W. I., *Thermochim. Acta*, in press.
- (4) Earnest, C. M., *ibid.*, 58, 271 (1982).
- (5) Earnest, C. M., *ibid.*, 60, 171 (1983).
- (6) Hutton, A. C., *Proc. First Australian Workshop on Oil Shale, Lucas Heights, Australia 18-19 May*, pp. 31-34 (1983).
- (7) Sherwood, N. R. and Cook, A. C., *ibid.*, pp. 35-38.
- (8) Glikson, M., *ibid.*, pp. 39-42.

SYMPOSIUM ON CHARACTERIZATION AND CHEMISTRY OF OIL SHALES
PRESENTED BEFORE THE DIVISIONS OF FUEL CHEMISTRY AND
PETROLEUM CHEMISTRY, INC.
AMERICAN CHEMICAL SOCIETY
ST. LOUIS MEETING, APRIL 8 - 13, 1984

THE HYDRORETORTING ASSAY - A NEW TECHNIQUE FOR OIL SHALE ASSESSMENT

By

P. A. Lynch and J. C. Janka
HYCRUDE Corporation, 10 West 35th Street, Chicago, Illinois 60616
and
F. S. Lau, H. L. Feldkirchner and H. A. Dirksen
Institute of Gas Technology, 3424 South State Street, Chicago, Illinois 60616

INTRODUCTION

The Modified Fischer Assay technique developed by the U. S. Bureau of Mines for evaluation of oil yields from oil shale evolved from tests originally designed to measure the potential liquid yield obtained in coal pyrolysis operations. During the early decades of this century, procedures and operating conditions for the Fischer Assay were gradually modified to bring the results into line with oil yields obtained by typical thermal retorting processes of the day. The resulting test is now an ASTM standard method (Designation, D3904-80). While modern thermal retorting processes - when applied to Western U. S. (Eocene Age) oil shales - may produce oil yields which differ slightly from the results of this Fischer Assay Test, their yields are sufficiently close for Fischer Assay results to be accepted as a standard for assessment of the size of oil shale resources.

With the development of the HYTORT Process, it became necessary to develop an assay technique capable of measuring the substantially greater oil yields obtained by hydroretorting. In the future, we believe that evaluation of the magnitude of many oil shale resources will require utilization of the Hydroretorting Assay test described in this paper, as well as the conventional Modified Fischer Assay technique. In some instances, these techniques produce results which differ by factors of four or even greater. Acceptance and use of the Hydroretorting Assay technique described in this paper will, therefore, become a prerequisite for complete understanding of a given oil shale resource.

SPECIFICATIONS FOR THE HYDRORETORTING ASSAY PROCEDURE

From the beginning of the Hydroretorting Assay development project, it was recognized that direct measurement of actual yields of oil and water produced by hydroretorting oil shale samples was required. Although indirect techniques were briefly considered, the need for repeated empirical calibration of such techniques while moving from one oil shale deposit to another constituted a significant drawback which eventually caused rejection of these approaches. The problem thus became development of a laboratory procedure for reaction of small samples of oil shale with hydrogen and the design and construction of prototype test equipment to carry out that procedure. After the problem had been so defined, the following criteria were established for the design of the hydroretorting assay unit.

- The procedure should be simple enough to be conducted by a technician.
 - The device used should be capable of field operation.
 - Reproducibility of results should be aided by means of computer control of the device.
 - In the prototype version, provision should be made for adjusting process conditions such as pressure, temperature, gas flow and heatup rate, to enable the operating conditions to be varied.
 - A 100-gram sample should be used, for consistency with the Modified Fischer Assay test procedure.
 - The device should be capable of duplicating the results of the Modified Fischer Assay.
- The Hydroretorting Assay unit depicted in Figure 1 meets these criteria.

DESCRIPTION OF THE PROTOTYPE HYDRORETORTING ASSAY UNIT

The Hydroretorting Assay unit is capable of operating from atmospheric pressure up to 1000 psig, at temperature up to 1200°F and with heatup rate as high as 25°F/min. The unit consists of a 7/8-inch diameter, 16-inch long reactor tube mounted concentrically within a pressure-

retaining shell, 1-1/2-inches in diameter and 31 inches in length. This unit is enclosed in a three-zone electrically heated furnace. A schematic diagram of the unit is shown in Figure 2. The heaters are computer-controlled to achieve the desired heatup rate, to maintain the reactor at the operating temperature for a predetermined period of time and to maintain isothermal conditions vertically in the shale sample. Reactor temperatures are measured by a multipoint thermocouple inserted in the shale bed. The metered feed gas (hydrogen or nitrogen) enters the bottom of the pressure shell, is preheated as it flows upward in the annular space surrounding the reactor tube and then enters the reactor and is cooled by an electric chiller. The condensibles are collected in a graduated glass container and the gaseous product is continuously depressurized and metered by a dry test meter prior to venting. Gas samples may be taken throughout the test if desired. Test data--temperatures, feed and product gas flow rates, and pressure--are continuously recorded.

Before conducting Hydroretorting Assay tests, representative shale samples are crushed to -8 mesh particle size and riffled into approximately 100-gram samples. The weight of the test sample is then recorded and the sample is charged into the reactor. The system is pressure-tested and purged with feed gas. The operating conditions are programmed into the microprocessor and a test is started by keying in the run command. The system is brought to the desired operating pressure and the gas flowrate is set. The furnace heaters are activated and adjusted to achieve the desired heatup rate. The reactor is maintained at the desired operating temperature for a predetermined period of time. At the end of the test, the furnace is shut down and the reactor is allowed to cool to about 200°F. The residual shale is removed and weighed; the liquid products collected in the graduated glass container are centrifuged; the water and oil volumes are measured; and the entire liquid sample is weighed. The unit is then ready for the next test. A typical output data sheet is shown in Figure 3. Tests take about four hours to complete.

A standardized set of assay conditions were established after a test program was conducted to survey results at various operating conditions and to compare them with larger scale HYTORT Process test results. These conditions are shown in Table I.

TABLE I
OPERATING CONDITIONS FOR THE STANDARD HYDRORETORTING ASSAY AND
FOR FISCHER ASSAY SIMULATION

	<u>Hydroretorting Assay</u>	<u>Fischer Assay Simulated</u>
Sample, wt, gm	100	100
Particle size	-8 Mesh	-8 mesh
Pressure, psig	1000	0
Heat-up rate, °F/min	25	22
Maximum temperature, °F	1000	932
Time at maximum temperature, min	30	40
Gal flow rate, SCF/hr	4 (H ₂)	0.1 (N ₂)

A standardization test series conducted on Indiana New Albany oil shale showed that Hydroretorting Assay tests on riffled splits of the same sample having a mean hydroretorting oil yield of 28.25 gal/ton exhibited a standard deviation of 1.23 gal/ton, or about 4%.

The Hydroretorting Assay test unit can also be operated with inert sweep gases at atmospheric pressure to provide an indication of oil yields in conventional, thermal retorting in a manner analogous to the Modified Fischer Assay.

Simulation of a conventional Modified Fischer Assay in this device requires a small flow of nitrogen because the Hydroretorting Assay unit reactor is shaped rather differently than a conventional Modified Fischer Assay retort. Tests were conducted on oil shale of the Western United States to determine the quality of simulation of Fischer Assay obtainable in the Hydroretorting Assay device. These test indicated that results within 2% of oil yields obtained by conventional Fischer Assay can be obtained in the Hydroretorting Assay under simulated Fischer Assay conditions. Agreement is excellent despite the use of nitrogen purge and the unit is capable of assessing oil shale response to conventional retorting as well as to hydroretorting.

Although the standardized hydroretorting test conditions which we have developed call for operation at 1000 psi, the Hydroretorting Assay unit can also be operated at other pressures. Temperature and heatup rate can also be varied. Therefore, the Hydroretorting Assay unit can serve as a first experimental step in determination of the economically-optimum conditions of operation for a given oil shale resource. Further, samples of product gas from the hydroretorting assay unit can be analyzed off-line using a mass spectrometer or a gas chromatograph. Coupled with ultimate analysis of raw and spent shale, this technique can be used to obtain the equivalent of a material

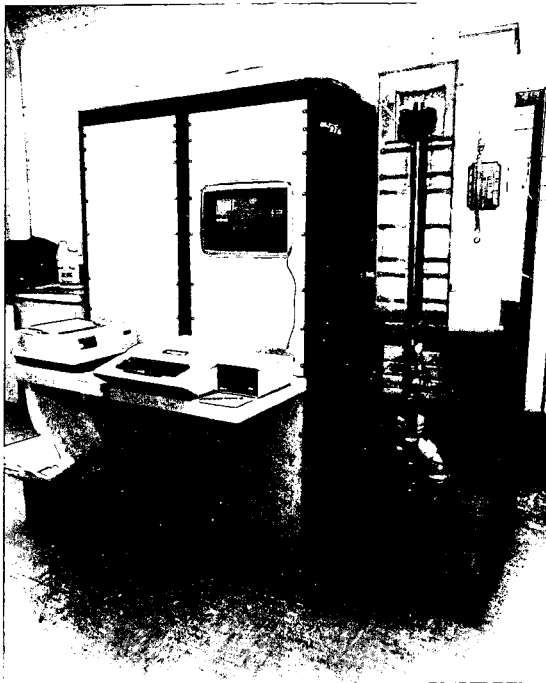


Figure 1. Hydroretorting Assay Unit

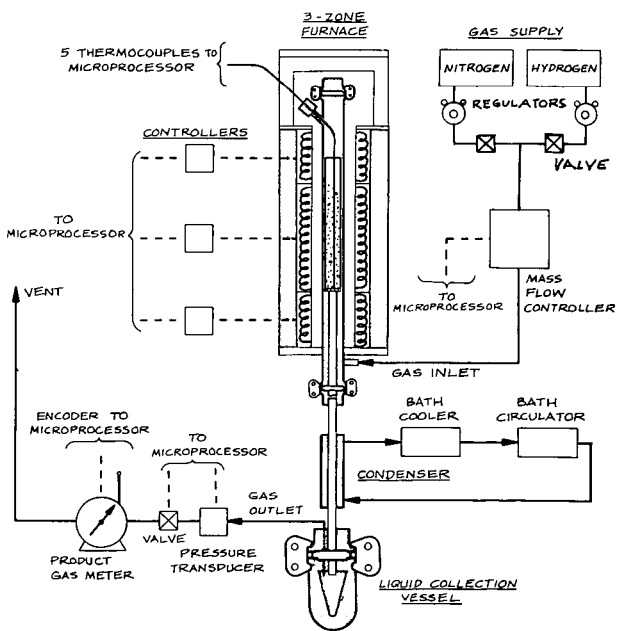


Figure 2
HYDRORETORTING ASSAY UNIT
SIMPLIFIED PROCESS FLOW DIAGRAM

COMPUTERIZED HYDRORETORTING ANALYSIS

RUN NUMBER	—
SAMPLE DESIGNATION	—
WEIGHT OF SAMPLE: GRAMS	100.06
GAS FLOW: SCFH	4.07
UNIT PRESSURE: PSIG	1000.4
RAMP: DEG./MIN.	24.26
MAXIMUM TEMPERATURE: °F	1005.8
TIME AT TEMPERATURE: MIN.	30
SOLIDS RESIDUE: GRAMS	74.53
TOTAL LIQUID PRODUCTS: CC.	19.8
VOLUME OF WATER: CC.	6.3
OIL PRODUCTION: GALS./TON	32.33

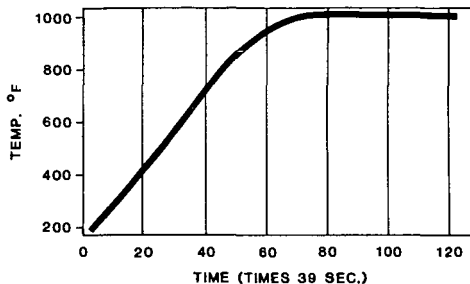


Figure 3. HYDRORETORTING ASSAY PRINTOUT

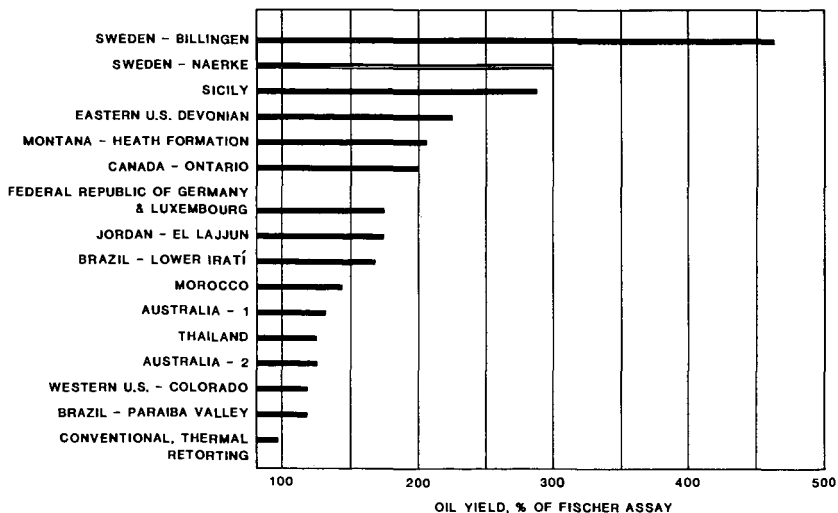


Figure 4. HYDRORETORTING ASSAY RESULTS FOR WORLD OIL SHALE SAMPLES

balance Fischer Assay for hydroretorting. Thus, the hydroretorting Fischer Assay unit has flexibility beyond that required for a device to merely measure oil yields.

HYDRORETORTING ASSAY TEST RESULTS

In co-operation with the U. S. Geological Survey and with various foreign survey personnel, HYCRUDE Corporation has conducted Hydroretorting Assay tests on samples from a number of the world's major oil shale resource areas. Selected test results are shown in Figure 4. These results indicate that the HYTORT Process can produce oil yields of over 400% of those obtained by conventional, thermal retorting in at least one instance, with a number of samples showing oil yields of more than 150% of Fischer Assay (Table II). In some instances, these results mean that oil yields over 30 gallons per ton can be produced from oil shale resources which would normally be considered too lean for commercial exploitation by conventional retorting processes.

TABLE II

SELECTED HYDRORETORTING ASSAY TEST RESULTS

Oil Shale Sample	Oil Yields	
	Fischer Assay gal/ton	Hydroretorting Assay gal/ton
Sweden - Billingen	3.8	17.5
Sweden - Naerke	10.9	32.3
Sicily	4.4	12.2
Indiana - New Albany	12.5	28.2
Montana - Heath Formation	16.2	33.6
Canada - Ontario	10.0	21.1
Jordan - El Lajjun (Sample 1)	20.3	33.8
Jordan - El Lajjun (Sample 2)	32.8	57.0

SYMPOSIUM ON CHARACTERIZATION AND CHEMISTRY OF OIL SHALES
PRESENTED BEFORE THE DIVISIONS OF FUEL CHEMISTRY AND
PETROLEUM CHEMISTRY, INC.
AMERICAN CHEMICAL SOCIETY
ST. LOUIS MEETING, APRIL 8 - 13, 1984

ANALYTICAL PYROLYSIS EVALUATION OF THE RETORTING POTENTIAL OF
KENTUCKY OIL SHALE

By

M. J. Margolis, D. N. Taulbee, A. M. Rubel and J. L. Howard
University of Kentucky Institute for Mining and Minerals Research, P. O. Box 13015
Lexington, Kentucky 40512

INTRODUCTION

The utilization of oil shale as a source of synthetic fuels has been increasingly promoted in recent years. While oil shales in the western United States have been extensively studied for many years, eastern shales have received serious consideration only recently.

The value of a shale resource is determined by a variety of factors. The mining and reclamation aspects of the resource, processing requirements, the product composition and the overall economics are some of the more significant variables. However, the overall resource quality, which is represented by its magnitude, accessibility and oil content, is perhaps the most important.

The standard measure of oil shale quality (oil yield potential) has been the Fischer Assay. In its various experimental forms, this assay results from the physical measurement of the amount of oil produced from the retorting of a shale sample under a standardized set of conditions. This assay and modified forms of it have, for the most part, been the accepted and standard basis for judging the retorting potential of shales worldwide.

The true utility of a standard assay is, however, its predictive ability. Fischer Assays have been shown to be an acceptable measure of the conventional retort potential of western U. S. shales. This, however, has not been shown to be true for eastern oil shales. The overwhelming acceptance of the Fischer Assay yield has, in large part, been responsible for underestimating the value of and, therefore overlooking, eastern oil shale as a synfuel resource. The current interest in eastern shale is due in part to the realization of its retorting characteristics and true oil generation potential.

Work at the Institute for Mining and Minerals Research (IMMR) (1, 2) and others (3, 4) have shown that the Fischer Assay of eastern oil shales typical of Kentucky are low with respect to the shale's true retorting potential. Retorting eastern oil shales under rapid heating, vacuum, steam addition, fluid bed, hydrogen atmosphere and donor solvent conditions (2, 5-8) have consistently produced yields in excess of Fischer Assay values. Assay yields have been exceeded by as much as 25-100% when eastern oil shales have been retorted under these conditions. A more complete discussion of eastern oil shale and their retorting characteristics can be found in the literature (9-12).

On an analytical scale, pyrolysis techniques have been used widely in many organic-analytical applications. Geochemical applications have included the evaluation of source rock potential and oil shale organic geochemistry (13-16). These techniques provide the opportunity to: pyrolyze materials under highly controlled thermal conditions, determine the material's response to pyrolysis and characterize the products of the pyrolysis.

Eastern shale oil yields are sensitive to retorting parameters and, in particular, to thermal conditions (1). The ability to carefully control thermal conditions in analytical pyrolysis experiments suggested that these techniques may be useful in evaluating shale retorting behavior. Preliminary evaluation of eastern oil shales by pyrolysis/gas chromatography analysis has examined the yield and product composition trends related to pyrolysis conditions (17, 18).

The work presented here represents an examination of an analytical pyrolysis technique as a method for determining oil shale retorting potential. A carefully selected and prepared set of oil shale samples was evaluated by three methods: Fischer Assay, bench scale fluid bed retorting and the analytical pyrolysis method described below.

EXPERIMENTAL METHODS

Oil Shale Samples

Samples of Sunbury, Cleveland and Huron shales obtained from a ninety foot oil shale core

were used for comparison of the pyrolysis and Fischer Assay yield determinations. A 1.5 inch diameter core (identified as "T-16") was drilled in Madison County, Kentucky and has been thoroughly characterized (19). Since only limited amounts of core material were available, additional samples from the Cleveland Member of the Ohio Shale and the New Albany Shale were selected for a further comparison of the pyrolysis measurement with Fischer Assay and fluid bed yields. Bulk samples of the Ohio Shale were obtained from Fleming County, Kentucky; samples of the New Albany Shale from Henryville, Indiana.

Shales were crushed, blended, sieved and split to produce representative and homogeneous aliquots for each of these analyses. Samples were prepared in 8 x 30, 18 x 20 and -325 mesh sizes for the Fischer Assay, fluid bed and pyrolysis methods, respectively. These samples were stored under an argon atmosphere until used.

Fischer Assay Analysis

The modified Fischer Assay procedure used at the IMMR has been described previously (1). These assays were performed on 100 gm aliquots in the stainless steel retort illustrated in Figure 1. A Lindberg electric furnace equipped with a programmable temperature controller was used to heat the retort under the following conditions: heated to 150°C for 30 minutes, increased from 150 to 550°C at a rate of 13±1°C/minute and held at 500°C for 20 minutes.

Oil yields were determined from the weight change of the entire liquid collection apparatus less the weight of water also collected (1). The density of each oil sample was determined on a Mettler DMA 40 density meter and was used to express oil weight on a gallons per ton (gal/t) oil yield basis.

Fluid Bed Retorting

A bench scale fluid bed retort, developed at the IMMR, used in this study is shown in Figure 2. Operating conditions for this unit were: a bed temperature of 550°C, helium gas at a linear fluidizing velocity of 25.6 m/min, a shale residence time of 20 min and a calculated theoretical heating rate of approximately 20,300°C/min. A detailed description of the operation and product trapping system used in this apparatus is given by Rubel et al. (20).

Analytical Pyrolysis

Oil shales were subjected to pyrolysis using a Chemical Data systems Model 820GS pyrolysis system. The instrument was operated in its "rapid P1/P2" mode and can be viewed as having essentially the instrumental configuration illustrated in Figure 3. In this mode of operation, the sample is heated to pyrolysis temperature under an inert atmosphere while the pyrolysate evolution is continuously monitored by a flame ionization detector (FID). The FID signal is recorded continuously and integrated by a Hewlett-Packard Model 3390A reporting integrator.

Small samples (3-5 mg) of -325 mesh shale are weighed into quartz capillaries (4 x 15 mm) and held in place with small quartz wool plugs. The sample is inserted into the pyrolysis chamber and is flushed for three minutes with helium. The sample is rapidly heated, under a 50 cc/minute helium flow, from ambient temperature (50-60°C) to 300°C, held at this temperature for nine minutes, heated at 60°C/minute to 600°C and held at this final temperature for fifteen minutes. The pyrolysis temperature program and the corresponding FID response are illustrated in Figure 4.

The FID is predominately sensitive to organic carbon containing compounds. The monitor's response, therefore, represents organic carbon pyrolysate and does not include significant contributions from water, carbon dioxide, hydrogen sulfide or other inorganic species. The material evolved up to 300°C represents the distillable (P1) fraction of the shale's organic content. The pyrolysis product (P2) is derived from the kerogen fraction of the shale. The total FID response (P1 + P2) per milligram of shale relative to that of a standard oil shale is the basis for correlating pyrolysis data to Fischer Assay.

RESULTS AND DISCUSSION

Shale Analyses

A complete discussion of the retorting and analytical characteristics of the T-16 core samples is beyond the scope of this work. These samples have been thoroughly examined and these results have been reported (19). Core data useful to the following discussion has been summarized in Table I along with data for the group of bulk samples.

Carbon and hydrogen analyses were determined using a Carlo-Erba Model 1106 elemental analyzer according to standard ASTM procedure D3178. Inorganic carbon was determined by measurement of acid-evolved carbon dioxide and was used to calculate organic carbon from total carbon.

TABLE I

SUMMARY OF CHARACTERISTICS FOR OIL SHALES

<u>Sample</u>	<u>Shale Designation</u>	<u>Depth Interval (ft.)</u>	<u>Organic Carbon (%)</u>	<u>Hydrogen/Carbon</u>
T-16 001	Sunbury	4-6.7	13.34	1.17
T-16 003	Cleveland	7-10	10.96	1.31
T-16 004	Cleveland	10-12	14.62	1.21
T-16 005	Cleveland	12-14	11.60	1.21
T-16 006	Cleveland	14-16	16.57	1.21
T-16 007	Cleveland	16-18	15.67	1.21
T-16 008	Cleveland	18-20	10.75	1.26
T-16 009	Cleveland	20-22	11.81	1.21
T-16 010	Cleveland	22-24	11.85	1.25
T-16 011	Cleveland	24-26	10.67	1.27
T-16 014	Cleveland	30-32.4	8.65	1.35
T-16 017	Huron	35.8-38	7.78	1.31
T-16 018	Huron	38-40	8.31	1.31
T-16 019	Huron	40.5-44	7.43	1.31
T-16 020	Huron	44-48	7.51	1.42
T-16 021	Huron	48-52	7.74	1.41
T-16 022	Huron	52-56	7.98	1.38
T-16 023	Huron	56-60	8.51	1.35
T-16 025	Huron	64-67	8.64	1.33
NALB-1	New Albany	-	13.31	1.28
NALB-2	New Albany	-	12.79	1.33
CLE 982C	Cleveland	-	11.65	1.41
CLE 82C	Cleveland	-	11.13	1.49

Yield Determinations

Fischer Assays were performed on the shales described above with mass and carbon balances in the 99-100% range. Oil yields were measured in weight percent and converted to gallons per ton using the individually determined oil densities. Oil yields, for the T-16 core samples, based on this classical method, varied from 7.1 to 19.0 gal/t. For Kentucky shales examined at the IMMR, Fischer Assay values parallel shale organic carbon content and yield about 1.1 gal/t for each weight percent organic carbon. The organic carbon versus Fischer Assay correlation (r) equalled 0.96 for the T-16 core samples. The data describing the Fischer Assay analyses are summarized in Table II.

Under fluid bed retorting conditions, oil yields from the bulk shale samples varied from 7.1 to 8.1% of the raw shale. Mass and carbon balances of 98 to 100% were obtained. These yields reflect a 130 to 145% enhancement of the values determined by Fischer Assay. This is presented in Table III.

Analytical Pyrolysis

Shale samples from the T-16 core were pyrolyzed as described earlier, and a value representing the FID response per milligram of shale was determined. This measurement reflects the amount of hydrocarbons evolved but is not used directly as an indication of yield. Because of potential day to day variations in the FID response, this value (response per mg) is normalized to that of a standard. The standard in this case was a shale sample with a known Fischer Assay value and permitted day to day comparison of our pyrolysis data and facilitated the conversion of response per milligram data to a gallons per ton basis. The data from other oil shales examined here were treated similarly. Table IV contains a summary of the normalized pyrolysis response data.

Data Correlations

Very good correlations were found between the normalized pyrolysis response values and the results from Fischer Assay. For T-16 core samples, the correlation (r) between the analytical pyrolysis and Fischer Assay data was 0.966. A similar relationship was found for the bulk shales examined. The T-16 core pyrolysis correlations with Fischer Assay and organic carbon are illustrated in Figure 5.

The fluid bed versus pyrolysis yield correlations for the bulk samples were also very good ($r=0.962$). Due to the nature of the fluid bed experiment and the method of oil collection, yield data were only available on a weight percent basis. The results summarizing the Fischer Assay,

fluid bed and pyrolysis evaluation of these samples are presented in Figure 6.

TABLE II
SUMMARY OF RESULTS FROM THE FISCHER ASSAY EVALUATION OF
T-16 CORE OIL SHALE SAMPLES

T-16 Sample	Fischer Assay (gal/t)	Fischer Assay (Wt %)	Oil Density
001	13.9	5.40	.932
003	13.2	5.01	.910
004	18.3	6.97	.913
005	13.9	5.23	.902
006	19.0	7.20	.908
007	17.6	6.68	.910
008	13.0	4.99	.920
009	13.7	5.19	.909
010	12.1	4.62	.914
011	12.9	4.92	.914
014	9.4	3.62	.924
017	9.3	3.44	.887
018	7.8	-	-
019	8.0	3.02	.906
020	7.8	2.96	.910
021	7.3	2.75	.902
022	9.6	3.63	.906
023	10.0	3.79	.909
025	9.3	3.51	.904

TABLE III
SUMMARY OF BULK SHALE RETORTING RESULTS FROM
FLUID BED AND FISCHER ASSAY EXPERIMENTS

Sample	Fischer Assay (Wt %)	Fluid Bed (Wt %)
NALB-1	6.1	8.1
NALB-2	5.9	7.8
CLE 982C	5.2	7.1
CLE 82C	4.7	6.7

The correlation of T-16 pyrolysis data with organic carbon (Figure 5b) is notably better than the correlation with Fischer Assay values (Figure 5a). Although the correlations for both sets of data are very good, the scatter in the pyrolysis versus organic carbon data appears smaller. In part, this reflects the smaller error associated with the determination of organic carbon as opposed to the greater experimental error associated with Fischer Assay determinations. The retorting assay methods have several contributing sources of error related to the control of thermal conditions, product trapping efficiency, product isolation, manipulative losses and density measurement among others. The pyrolysis approach has superior control over thermal parameters and no losses related to product handling. Potential problems related to reproducible FID response, standardization, weighing and sampling small samples and the preparation of representative samples exist. There are also several fundamental differences between retorting and analytical pyrolysis methods.

The measurement of yield by retorting assay methods are essentially volumetric determinations (gallons per ton) and reflect both the mass of organic matter produced and its density. The response of the FID in the pyrolysis experiment only reflects the mass of the organic matter evolved and, therefore, its yield is independent of product density. This difference between methods can be minimized by correlating oil yield data on a wt % rather than a gal/t basis. The uniformity in the oil densities for the T-16 products suggests similar pyrolysis correlation by either approach. The wt % based correlation between these methods for the T-16 core samples plotted in Figure 7 is virtually indistinguishable from the gal/t basis.

While retorting assay methods quantify yields on the basis of recovered liquid products, the FID based pyrolysis technique reflects the production of both gaseous and liquid hydrocarbons

without distinction. In the evaluation of the T-16 core shales, the amount of organic carbon evolved in the form of gases was fairly constant in the 1 to 2% range. This relatively small and constant amount of gaseous hydrocarbon contributes to the pyrolysis versus Fischer Assay correlation. The noncondensable hydrocarbon fraction is generally overlooked by retort assay methods and, in this regard, the FID response gives a more accurate measurement of the total hydrocarbon product evolved.

TABLE IV
SUMMARY OF NORMALIZED PYROLYSIS RESPONSE DATA FOR THE
T-16 CORE AND BULK OIL SHALE SAMPLES

Sample	Pyrolysis ^a Response	No. of Samples	Relative % Deviation
T-16 001 ^b	1.00	-	-
T-16 003	0.92 ± 0.02	5	2.2
T-16 004	1.17 ± 0.07	8	6.0
T-16 005	0.96 ± 0.04	7	4.2
T-16 006	1.33 ± 0.05	2	3.8
T-16 007	1.21 ± 0.04	5	3.3
T-16 008	0.93 ± 0.02	3	2.1
T-16 009	1.07 ± 0.04	2	3.7
T-16 010	1.00 ± 0.05	4	5.0
T-16 011	0.99 ± 0.05	4	5.1
T-16 014	0.77 ± 0.03	5	3.9
T-16 017	0.75 ± 0.02	3	2.7
T-16 018	0.73 ± 0.00	2	-
T-16 019	0.64 ± 0.05	3	7.8
T-16 020	0.71 ± 0.04	2	5.6
T-16 021	0.74 ± 0.04	4	5.4
T-16 022	0.72	1	-
T-16 023	0.83 ± 0.01	2	1.2
T-16 025	0.78 ± 0.05	8	6.4
NALB-1	1.13 ± 0.04	3	-
NALB-2	1.07 ± 0.01	3	-
CLE 982C	0.96 ± 0.05	3	-
CLE 82C	0.96 ± 0.01	3	-

a. Mean ± standard deviation.

b. Sample used as pyrolysis reference standard.

The work described above has been a part of an overall Kentucky oil shale resource characterization effort. The T-16 core has been extensively examined and the pyrolysis results closely parallel a variety of characterization parameters in addition to Fischer Assay values. A more complete discussion of the T-16 core trends appears elsewhere in the literature (19). The T-16 core samples represent a wide range of compositions with varied geologic ages, depth of burial, organic content and depositional history. For purposes of evaluating down core trends, the pyrolysis results compare very favorably to other measurements.

SUMMARY

It is evident from the data presented above that an analytical pyrolysis based assay is an acceptable alternative to more traditional methods. This approach was also shown to be predictive of the yield of several different shales under fluid bed retorting conditions. Further, there are several distinct advantages that the pyrolysis method offers. These principally relate to sample size requirements, speed of analysis and ancillary analytical capabilities.

Classical assay methods require large amounts of sample in comparison to an analytical pyrolysis technique. The Fischer Assay determinations described above used approximately 100 g and fluid bed evaluations normally consume more. While sample availability is not usually a factor in bulk sample analyses, it is a major limitation in evaluating drilled core. To measure Fischer Assay yields on a typical 1.5-inch diameter core, one-half of the core is consumed and material covering 2-foot intervals combined. The milligram scale pyrolysis sample requirement can preserve most of the core and provide more detailed yield and resource information as a result of the

substantially smaller sampling interval used. It is in the core analysis and resource characterization context that analytical pyrolysis may be of greatest use.

The pyrolytic analyses described here can be performed at a rate of nearly two per hour. Fischer Assays and fluid bed evaluations, however, require as much as two hours in retorting time alone.

The pyrolysis experiment described here represents only one aspect of the capabilities of this technique. The ability to carefully control the pyrolysis conditions (e.g., temperature limits, rates and residence times) should permit the evaluation of the relationship between yield and thermal treatment. The products from the above analytical pyrolysis were not examined but the capability to perform capillary gas chromatography is an additional feature of the Chemical Data Systems' 820 GS instrumentation. The integration of the pyrolysis yield, thermal treatment and product analysis capabilities are currently under evaluation in an effort to determine relationships between retorting conditions, product yield and product composition.

ACKNOWLEDGMENTS

The authors would like to acknowledge the contribution of many Institute staff members with particular thanks to Ms. Marlys Higgenbotham and Ms. Laura Tungate for the Fischer Assay and fluid bed retorting; Mr. Lance Barron and Dr. Thomas Robl for acquisition and preparation of the shales; Mr. Gerald Thomas and Dr. David Koppenaal for shale analyses; and Ms. Kathie Sauer for the preparation of this manuscript's graphics.

This work was conducted with support from the Kentucky Energy Cabinet at the Kentucky Center for Energy Research Laboratory.

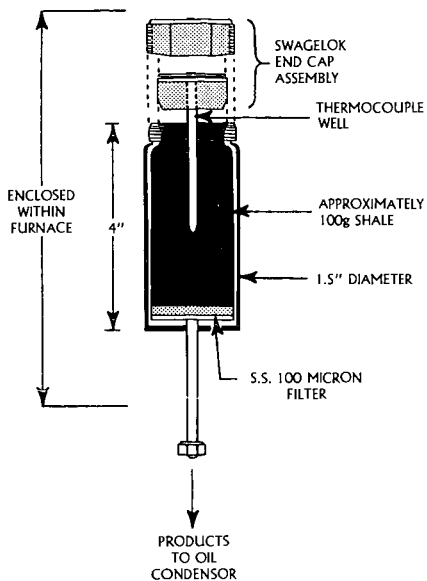


Figure 1. The modified Fischer Assay retort used to determine oil yields.

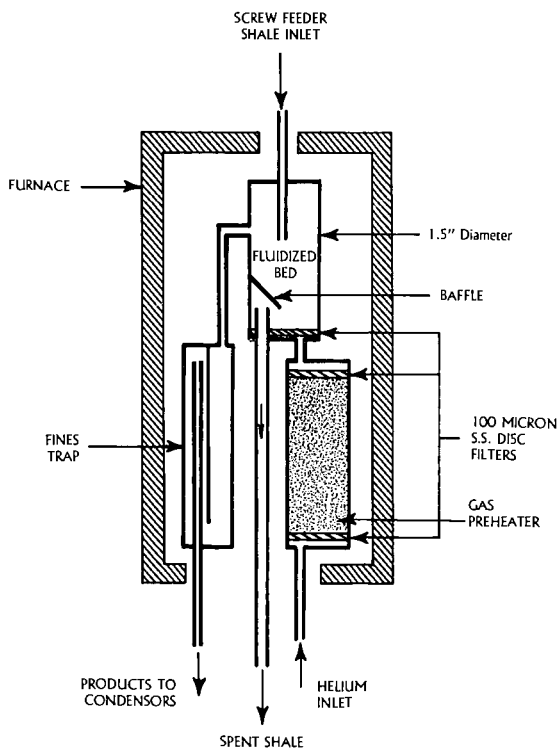


Figure 2. The fluid bed retort system developed at the IMHR for evaluating oil shale retorting under rapid heating and short product residence time conditions.

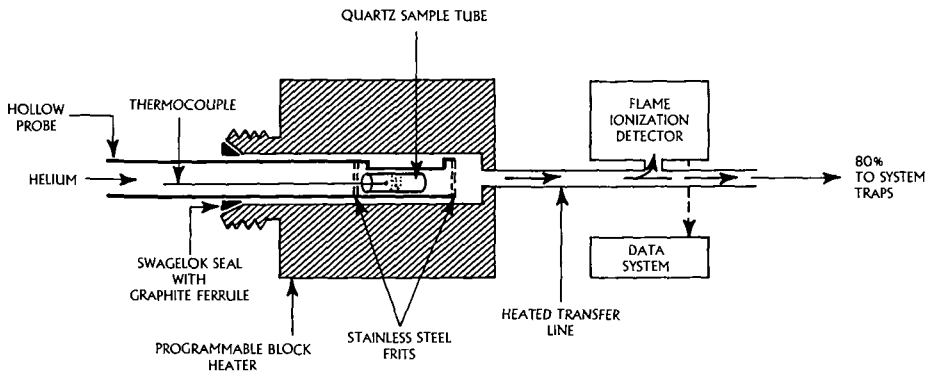


Figure 3. Simplified schematic of the Chemical Data Systems 820 GS pyrolysis system in its "rapid P1/P2" mode of operation.

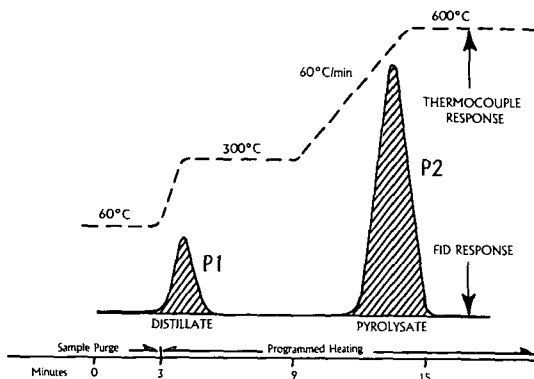


Figure 4. Illustration of the pyrolysis temperature program and the corresponding FID response reflecting pyrolysate evolution.

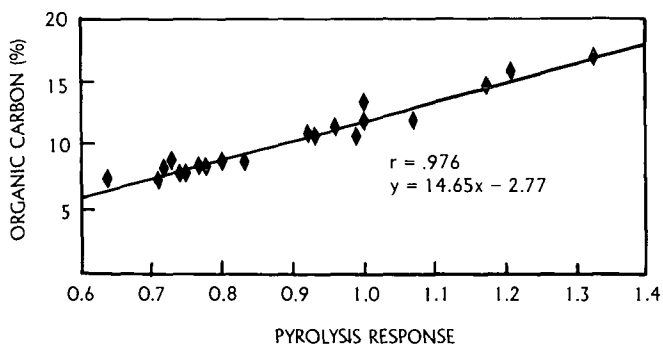
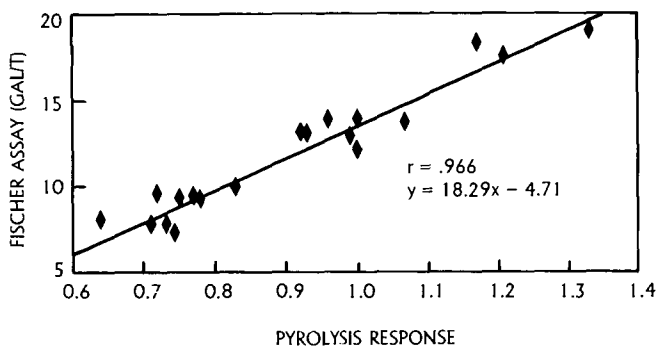


Figure 5. Normalized pyrolysis response data for T-16 core shales; correlations to: (a) Fischer Assay values and (b) organic-carbon content.

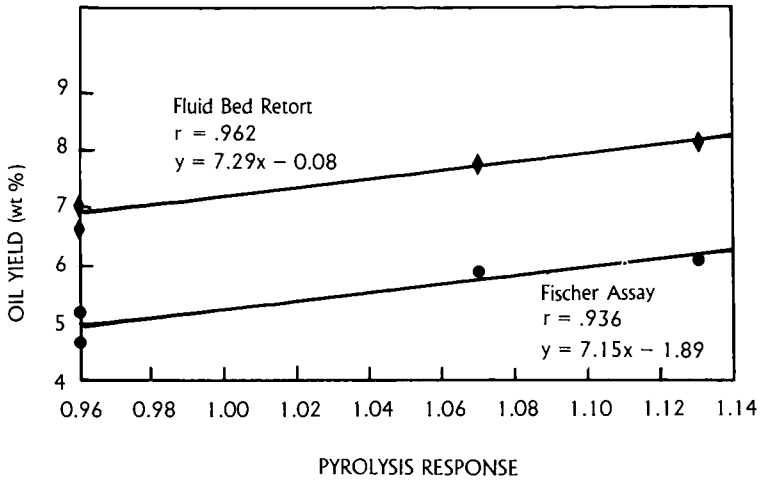


Figure 6. Correlation of normalized pyrolysis response with Fischer Assay and fluid bed yield data for a group of different bulk shales.

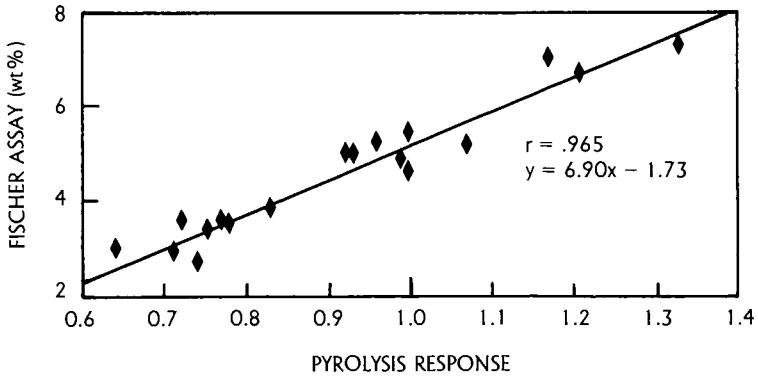


Figure 7. Normalized pyrolysis response data vs. Fischer Assay on a weight percent basis for T-16 core shales.

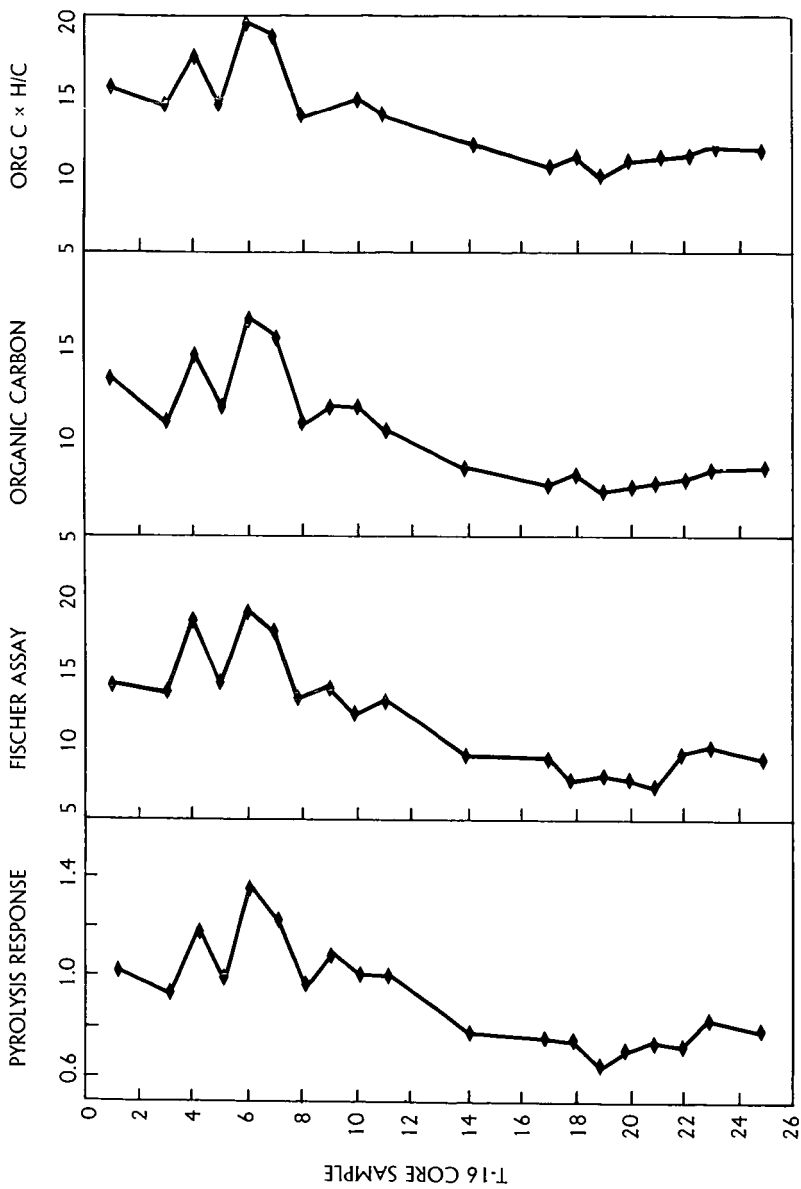


Figure 8. Comparison of pyrolysis, Fischer Assay, and organic carbon down core trends for T-16 shales.

LITERATURE CITED

- (1) Coburn, T. T., Rubel, A. M. and Henson, T. T., "Eastern Oil Shale Retorting I. Pyrolysis of the Sunbury Shale of Kentucky", University of Kentucky Inst. for Mining and Minerals Research, Report No. IMMR81/062 (1981).
- (2) Rubel, A. M. and Coburn, T. T., In: 1981 Eastern Oil Shale Symp. Proceedings, p. 21, Univ. of Kentucky Insti. for Mining and Minerals Research, Report No. IMMR82/066 (1982).
- (3) Richardson, J. H., Huss, E. B., Ott, L. L., Clarkson, J. E., Bishop, M. O., Taylor, J. R., Gregory, L. J. and Morris, C. J., UCID-19548, Lawrence Livermore Natl. Lab. (1982).
- (4) Burnham, A. K., Richardson, J. H. and Coburn, T. T., UCID-87587, Lawrence Livermore Natl. Lab. (1982).
- (5) Margolis, M. J., In: 1981 Eastern Oil Shale Symp., p. 151, Univ. of Kentucky Insti. for Mining and Minerals Research, Report No. IMMR82/066 (1982).
- (6) Margolis, M. J., Hagan, M., Cummins, W. and Toney, D., "Donor Solvent Extraction Behavior of Eastern Kentucky Oil Shale", Submitted to Fuel Processing Technology.
- (7) McKay, J. F. and Chong, S. L., In: Symp. Papers, Synthetic Fuels from Oil Shale and Tar Sands, p. 389, Insti. of Gas Technology, May 17-19 (1983).
- (8) Feldkirchner, H. L. and Janka, J. C., In: Symp. Papers, Synthetic Fuels from Oil Shale, Insti. for Gas Technology, December (1979).
- (9) "Synthetic Fuels from Oil Shale II, Symp. Papers", Nashville, TN, Insti. of Gas Technology, October 26-29 (1981).
- (10) "1981 Eastern Oil Shale Symp. Proceedings", Lexington, KY, Univ. of Kentucky Insti. for Mining and Minerals Research, November 15-17 (1981).
- (11) "1982 Eastern Oil Shale Symp. Proceedings", Lexington, KY, Univ. of Kentucky Insti. for Mining and Minerals Research, October 11-13 (1982).
- (12) "Synthetic Fuels from Oil Shale and Tar Sands Symp. Papers", Louisville, KY, Insti. of Gas Technology, May 17-19 (1983).
- (13) Espitalie, J., Laporte, J. L., Madec, M., Marquis, F., Leplat, P., Paulet, J. and Boutefeu, A., Rev. Inst. Fr. Pet. 32, 23-42 (1977).
- (14) Larter, S. R., J. Anal. Appl. Pyrolysis 4, 1-19 (1982).
- (15) Aizenshtat, Z., Israel J. Chem. 22, 266-272 (1982).
- (16) Leventhal, J. S., Chem. Geol. 18, 5-20 (1976).
- (17) Reasoner, J. W., Sturgeon, L., Naples, K. and Margolis, M. J., In: 1981 Eastern Oil Shale Symp. Proceedings, p. 11, Univ. of Kentucky Insti. for Mining and Minerals Research, Report No. IMMR82/066 (1982).
- (18) Reasoner, J. W., Naples, K. V. and Margolis, M. J., In: 1982 Eastern Oil Shale Symp. Proceedings, Univ. of Kentucky Insti. for Mining and Minerals Research, Report in press.
- (19) Rubel, A. M., Koppelaar, D. W., Taulbee, D. N. and Robl, T. L., In: 16th Oil Shale Symp. Proceedings, p. 132, Colorado School of Mines (1983).
- (20) Rubel, A. M., Margolis, M. J., Haley, J. K. and Davis, B. H., In: 1983 Eastern Oil Shale Symp. Proceedings, Univ. of Kentucky Insti. for Mining and Minerals Research (in press).

SYMPOSIUM ON CHARACTERIZATION AND CHEMISTRY OF OIL SHALES
PRESENTED BEFORE THE DIVISIONS OF FUEL CHEMISTRY AND
PETROLEUM CHEMISTRY, INC.
AMERICAN CHEMICAL SOCIETY
ST. LOUIS MEETING, APRIL 8 - 13, 1984

NMR MEASUREMENTS ON HEATED OIL SHALES

By

F. P. Miknis

Western Research Institute, P. O. Box 3395, University Station, Laramie, Wyoming 82071

INTRODUCTION

Many studies have been conducted in the past on various aspects of oil shale conversion; however, none have adequately addressed the basic chemistry involved during kerogen thermal decomposition (1). Instead, most of the studies have been concerned with the rate of kerogen conversion to products and average activation energies associated with the processes. Typically kerogen conversion is found to be a first order rate process and these data are used to provide a global or macroscopic description of kerogen conversion. The reason why structural information has not been obtained in previous work is that suitable analytical techniques have not been developed to provide such information. Now such techniques can provide information about the structure of kerogen and how the structure changes during heating. The most important technique is nuclear magnetic resonance (NMR) cross polarization (CP) with magic angle spinning (MAS).

In this paper, CP/MAS ^{13}C NMR techniques, with and without interrupted decoupling have been employed to measure changes in the organic carbon distribution of oil shales upon heating. The results suggest the potential of solid state ^{13}C NMR techniques for understanding the reaction chemistry during oil shale thermal decomposition.

EXPERIMENTAL

A rich, 72 gallons per ton (GPT) oil shale was used for this study. Samples for NMR analyses were prepared by interrupting the heating schedule of the standard Fischer Assay when the retort reaches intermediate temperatures of 400°, 425° and 450°C. A fourth experiment corresponds to interruption of the Fischer Assay immediately upon reaching the maximum temperature of 500°C. Identical samples of 72 GPT oil shale were used in each of these experiments. The retorted shale from the standard Fischer Assay of the feed material was used as a fifth sample for comparison with the partially retorted materials. The Fischer Assay is not designed for quenching the retorting when the experiment is interrupted and no special cooling provisions were incorporated into the apparatus for these experiments. As a result, no kinetic information was derived from these experiments.

^{13}C NMR measurements were made at 15 MHz ^{13}C frequency, 1-ms contact time and 1-s repetition rate. Interrupted decoupling spectra were recorded at a 75 μs interrupt time.

RESULTS AND DISCUSSION

The preliminary experiments have provided samples which qualitatively represent the expected gradation in shale properties with increasing temperature and residence time. The experimental yields are listed in Table I along with the elemental compositions of the product shale samples.

The oil and gas yields increase with temperature and residence time, while the water yield remains constant within experimental error. The water yields reflect the production of essentially all bound water below 400°C. The concentration of the principal elements decreases in the shale with the increase in oil and gas yields. Random fluctuations in the carbonate carbon content probably reflect inconsistencies in the mineral composition of the samples.

The CP/MAS ^{13}C NMR spectra (Figure 1) for the shale samples indicate a decrease in the aliphatic carbon content with increasing oil yield. This observation is consistent with previous studies which indicate that the oil and gas production are primarily due to aliphatic carbon conversion (2). However, the spectrum of the 450°C sample shows some broadening with the appearance of a shoulder at 19 ppm and some aliphatic carbon remains in the retorted shale from the standard Fischer Assay. These observations suggest that the aliphatic carbon in the partially retorted samples has a higher concentration of short chain alkyl substituents. The rich oil shale shows a tendency to coke in the Fischer Assay and the residual aliphatic carbon may reflect partial coking

where the aromatization is incomplete.

TABLE I
PRODUCT ANALYSES

Yields	Temperature at Interruption				Fischer Assay
	400°C	425°C	450°C	500°C	
Oil, % w	0.6	2.8	11.1	27.1	27.5
Gas, % w	0.6	1.6	2.5	4.9	6.3
Water, % w	2.2	2.4	2.6	2.2	2.2

Composition of Spent Shale Samples

Carbonate C, % w	3.6	6.4	8.0	6.3	6.0
Organic C, % w	29.7	24.2	17.7	5.9	6.1
Hydrogen, % w	4.0	3.5	2.6	0.4	0.3
Nitrogen, % w	1.0	0.9	0.8	0.5	0.5
Sulfur, % w	1.6	1.3	1.1	0.5	0.5

TABLE II
AROMATICITY MEASUREMENTS

Interruption Temperature	Carbon Aromaticity		Hydrogen Aromaticity Oil	Product Oil	
	Shale	Oil		Specific Gravity	H/C Ratio
400°C	0.30	0.12	0.035	-	-
425°C	0.33	0.24	0.045	-	1.74
450°C	0.39	0.26	0.041	0.892	1.74
500°C	0.73	0.31	0.051	0.907	1.65
Fischer Assay	0.79	0.29	0.056	0.909	1.66

The aromatic carbon bands in the CP/MAS ^{13}C NMR spectra are narrower at the higher temperatures and longer residence times. This observation suggests that the aromatic carbon becomes less substituted and more condensed. Similar behavior is observed for coals as a function of rank (3, 4). The partially retorted samples resemble oil shales of different "rank". In this analogy, the "rank" is artificially produced by heating to high temperatures for short periods of time as compared to slow heating over geologic time.

Liquid-state NMR measurements of the product oils are consistent with the solid-state CP/MAS ^{13}C NMR results. Both the ^{13}C and ^1H aromaticity values increase at the higher temperatures and longer residence times. These data represent a shortening of the aliphatic carbon chains. Also, some dehydrogenation reactions may conceivably occur at the higher temperatures. An observed increase in the oil specific gravity and a corresponding decrease in the H/C atomic ratio support the aromaticity data by NMR. These data are compared with the NMR measurements in Table II.

The partially retorted shale samples are also used to test interrupted decoupling techniques for supplementing CP/MAS in the application of ^{13}C NMR to solid shale samples. For these experiments, the ^{13}C NMR spectra are interrupted at 75 μs . The interrupted decoupling spectra are not scaled to zero time as suggested by Murphy et al. (5, 6) for quantitative measurements. Thus, in this paper the interrupted decoupling spectra are used for qualitative assessments. The interrupted decoupling technique discriminates between carbon with hydrogen directly attached and carbon which is not directly bonded to hydrogen. However, the technique does not completely suppress methyl carbon contributions to the spectra. In this preliminary application, the carbonyl region of the spectra (> 170 ppm) is enhanced and some shoulders in the spectra suggest the presence of phenolic carbon (150-160 ppm). The center of the aromatic carbon region in the spectra is shifted upfield and becomes narrower with increasing temperature and residence time. These observations suggest a trend from substituted quaternary aromatic carbon at low temperatures to more polycondensed quaternary aromatic carbon at higher temperatures. The residual aliphatic carbon in the fully retorted shale sample is not present in these spectra, suggesting that these carbons are secondary and tertiary aliphatic carbons.

While the NMR data for the heated shales are preliminary and qualitative, the chemical

Normal CP/MAS Spectra

72 G/T Raw Shale

400°C

425°C

450°C

500°C

Spent Shale

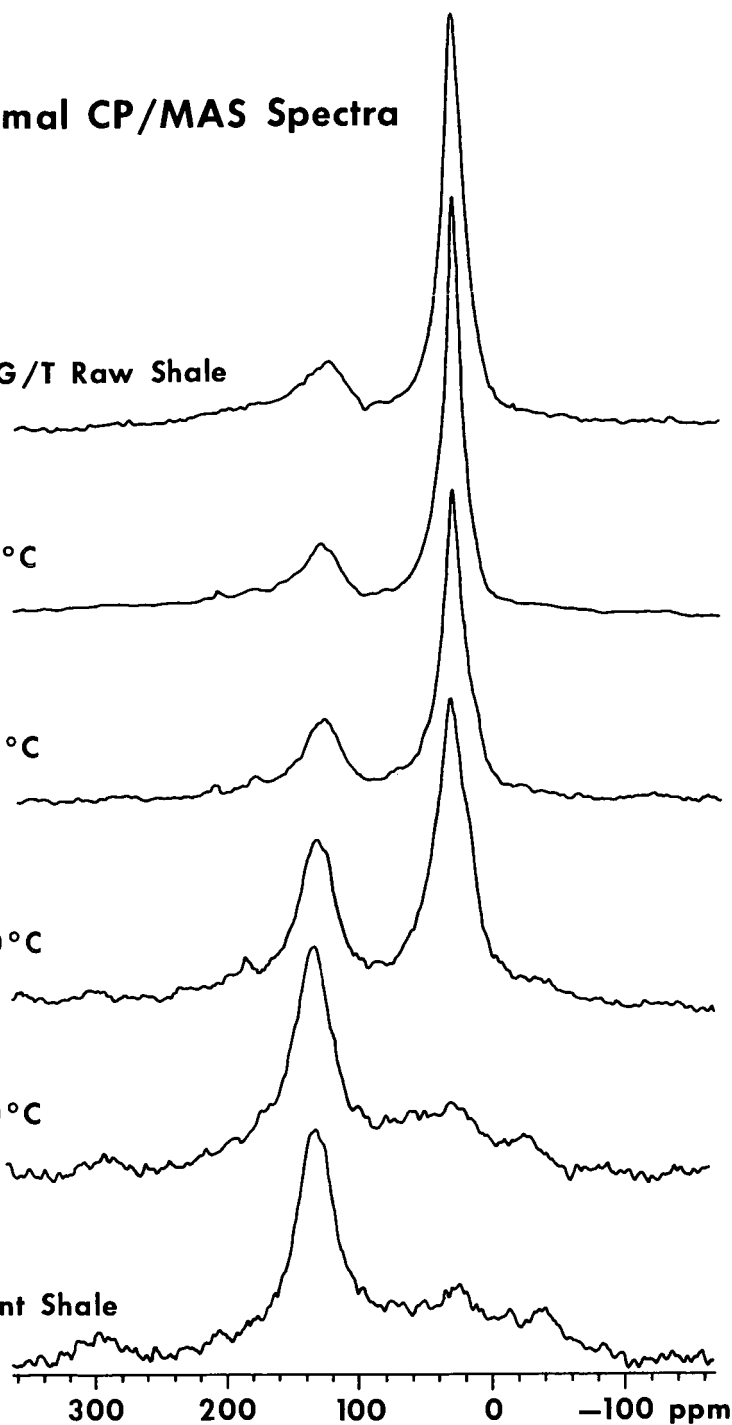


Figure 1. CP/MAS ^{13}C NMR Spectra of heated Colorado oil shale.

Interrupted Decoupling Spectra

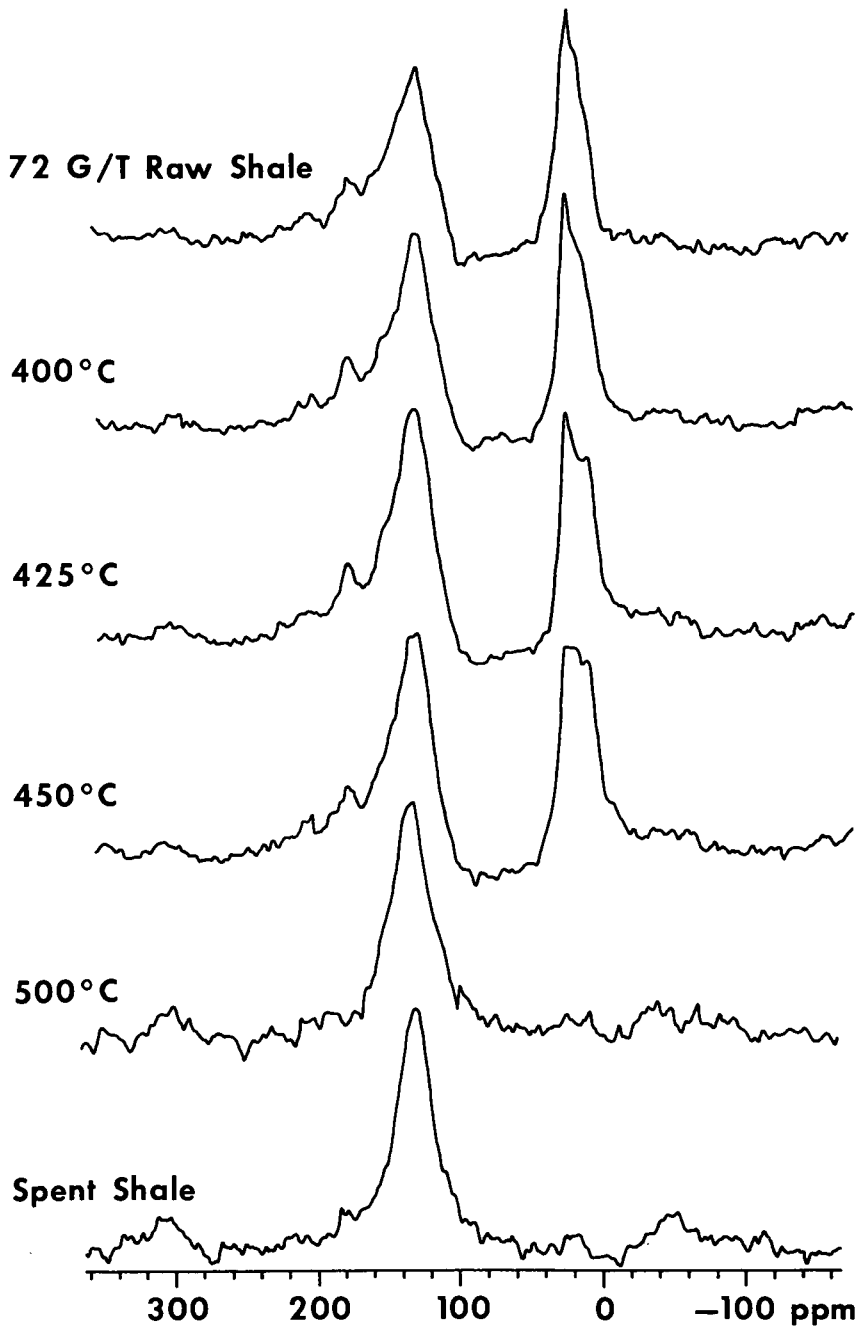


Figure 2. Interrupted decoupling spectra of heated Colorado oil shale. The interrupt time is $75 \mu\text{s}$.

information obtainable by CP/MAS ^{13}C NMR techniques make them attractive for the study of oil shale reaction kinetics. More detailed studies are in progress.

LITERATURE CITED

- (1) See for example: (a) Campbell, J. H., Koskinas, G. H., Stout, N. D. and Coburn, T. T., *In situ*, 2, 1 (1978); (b) Campbell, J. H., Koskinas, G. H. and Stout, N. D., *Fuel*, 57, 372 (1978); (c) Shih, S. M. and Sohn, H. Y., *Ind. Eng. Proc. Des. Dev.*, 19, 420 (1980); (d) Johnson, W. F., Walton, D. K., Kaller, H. H. and Louch, E. J., *Colorado School of Mines Quarterly*, 70, 237 (1975); (e) Nuttall, H. E., Guo, T. M., Schrader, S. and Thakur, D. S., in "Geochemistry and Chemistry of Oil Shales, F. P. Miknis and J. F. McKay, eds., ACS Symp. Series 230, 269-300 (1983).
- (2) Miknis, F. P., Netzel, D. A., Smith, J. W., Mast, M. A. and Maciel, G. E., *Geochim. et Cosmochim. Acta*, 46, 977 (1982).
- (3) Miknis, F. P., Sullivan, M., Bartuska, V. J. and Maciel, G. E., *Org. Geochem.*, 3, 19 (1981).
- (4) Dereppe, J. M., Boudou, J. P., Moreaux, C. and Durand, B., *Fuel*, 62, 575 (1983).
- (5) Murphy, P. D., Gerstein, B. C., Weinberg, V. L. and Yen, T. F., *Anal. Chem.*, 54, 522 (1982).
- (6) Murphy, P. D., Cassady, T. J. and Gerstein, B. C., *Fuel*, 61, 1233 (1982).

SYMPOSIUM ON CHARACTERIZATION AND CHEMISTRY OF OIL SHALES
PRESENTED BEFORE THE DIVISIONS OF FUEL CHEMISTRY AND
PETROLEUM CHEMISTRY, INC.
AMERICAN CHEMICAL SOCIETY
ST. LOUIS MEETING, APRIL 8 1 13, 1984

THE SOLID PHASE FUNCTIONAL GROUP APPROACH
TO OIL SHALE ANALYSIS

By

C. Costa Neto, H. T. Nakayama and F. R. Castro
Instituto de Quimica, Universidade Federal do Rio de Janeiro

ABSTRACT

Two classes of solid phase reagents have been devised to deal with the analysis of the soluble organic phases derived from oil shales (bitumens and tars). In the first—the solid phase organic functional group reagents—specific organic functional chromogenic reagents, bound to a solid matrix, were devised to determine the functional groups present in a bitumen or a tar (these are chemically complex, very dark media, where the functional groups are present in very low concentrations). The method is being also used for the quantitative determination of the groups. A second class of solid reagents was devised to fractionate bitumens and tars into isofunctional sets of compounds. In these reagents a specific functional group is bound to a solid matrix in such a way that after proper procedure—the solid phase extraction method—a class of substances is extracted from the mixture; e.g., acylhydrazides bound to a polymetacrylate matrix have been used to separate aldehydes and ketones from the Irati oil shale bitumen. In a third approach, functional groups of kerogens have been determined by the functional group marker method, where a marker is incorporated to the kerogen by means of the reaction of a marked functional group reagent with the kerogen. The quantitative determination of the marker incorporated to kerogen is a measure of the (minimum) amount of that functional group. Fluorescent markers are presently being used (through microscopy) to define the topographical distribution of organic functional groups in kerogens (surface).

SYMPOSIUM ON CHARACTERIZATION AND CHEMISTRY OF OIL SHALES
PRESENTED BEFORE THE DIVISIONS OF FUEL CHEMISTRY AND
PETROLEUM CHEMISTRY, INC.
AMERICAN CHEMICAL SOCIETY
ST. LOUIS MEETING, APRIL 8 - 13, 1984

GENERAL KINETIC MODEL OF OIL SHALE PYROLYSIS

By

A. K. Burnham and R. L. Braun
Lawrence Livermore National Laboratory, Livermore, California 94550

INTRODUCTION

Relatively simple effective kinetic expressions have been derived for oil evolution during pyrolysis of Green River oil shale: single first-order for slow and moderate heating rates (1, 2) and double first-order or single pseudo-nth-order for rapid isothermal pyrolysis (3-5). A number of workers (3, 4, 6-13) have investigated how secondary reactions (as influenced by pyrolysis heating rates, temperatures, residence times and pressure) can modify oil yield from that obtained under Fischer Assay (FA) conditions. They have found that the secondary reactions are very important, demonstrating that slow heating rates cause hetero-aromatic compounds in the oil to be converted to coke and that excessively high temperatures cause aliphatic structures to crack to gases.

While the qualitative aspects of oil-yield loss and quantitative relationships for some circumstances have been established, there is presently no mathematical formulation which can satisfactorily calculate the oil yield for any given oil shale heated under an arbitrary temperature-pressure-gas environment history. For example, Campbell et al. (7) demonstrated that the change in oil yield with pyrolysis heating rate is due to a competition between oil evaporation and coking. They developed a mechanism for oil coking that included an empirical rate constant for oil evaporation, but it cannot be used directly to calculate oil yields for conditions such as the interrupted heating schedules used by Stout et al. (6) or the elevated pressures used by Burnham and Singleton (12).

The mathematical model reported here is a first attempt at achieving our long-range goal of being able to calculate accurately the oil yield for any arbitrary pyrolysis conditions. As presently formulated, it is valid only for Green River oil shale, but it could be easily modified for other oil shales. A central feature of this model is that it divides the oil into 11 boiling-point fractions in order to treat evaporation more rigorously. This feature also allows cracking of heavy fractions to lighter fractions, enabling a calculation of the effect of pyrolysis conditions on the boiling-point distribution of the product oil. The model is tested under a wide range of pyrolysis conditions for which data are available in the literature. The model does very well generally, although certain limitations are demonstrated.

MODEL DESCRIPTION

The reactions defining the model and their associated rate constants are given in Table I. The properties of the oil components are given in Table II. Native bitumen is treated as being an initial oil content with properties described in Table II. The model assumes a uniformly reacting particle (no concentration or thermal gradients) and the absence of molecular oxygen. Formation of water from mineral dehydration and CO_2 from dolomite decomposition are included in order to properly calculate the residence time of the organic pyrolysis products inside the particle. The model also has the capability of an inert or H_2 sweep gas. Governing equations for the model are written as 67 first-order, nonlinear, ordinary equations specifying the rate of change of each gas, liquid and solid component in terms of the vaporization or chemical reactions. Some of the reactions are formulated to approach an equilibrium. This set of equations is solved simultaneously by LSODE (Livermore Solver for Ordinary Differential Equations) (14).

The kinetic parameters were taken as much as possible from the literature. Gas evolution kinetics, except those involving oil degradation, were taken (or derived in the case of CO_2) from the results of Campbell et al. (15) as modified by Huss and Burnham (16). For some reactions, it was necessary to use a distributed activation energy (17) in order to match observed results. Special numerical methods were developed for solving these reactions for arbitrary temperature history. We have also determined how these methods can be applied when the amount of a given component, such as a reaction intermediate, is not known at the beginning of the calculation.

TABLE II
PROPERTIES OF THE 11 OIL FRACTIONS

Fraction No.	Average Mol Wt (g/mol)	Average Normal	Wt % of Bitumen	Initial	Wt % of Oil	Wt % of Cokable	Relative Rate of Cracking (A_i)	Antoine Coeffs $\log P = A-B/(T-C)$		
		Boiling Point (°C)		Wt % of Shale				A(Pa)	B(Pa)	C(K)
1	86	69	0.0	3.85	3.9	1.0	20.725	2696.8	48.8	
2	114	126	0.0	5.10	11.8	2.1	20.824	3113.1	64.0	
3	142	174	0.7	6.73	19.7	3.8	20.881	3442.8	79.3	
4	177	226	5.0	7.69	25.6	6.5	21.017	3833.8	95.2	
5	212	271	16.0	8.65	29.6	10.0	21.065	4121.6	111.8	
6	261	323	20.3	10.10	33.5	15.8	21.031	4406.2	132.7	
7	317	374	10.8	10.58	37.4	24.2	21.213	4763.4	155.7	
8	380	422	10.2	12.40	43.4	35.4	21.276	5039.2	178.4	
9	464	476	14.7	14.23	47.3	53.8	21.343	5329.1	205.9	
10	562	525	13.0	12.02	51.3	80.8	21.400	5577.6	233.1	
11	703	594	9.3	8.65	55.2	153.8	21.494	5917.6	273.0	

To derive the rate expressions for oil coking, we attempted to mimic the reactions shown in Table I, in that the oil that cokes ($\text{CH}_{0.99}\text{N}_{0.038}\text{O}_{0.01}$) is more aromatic and high in nitrogen content than the average oil ($\text{CH}_{1.56}\text{N}_{0.021}\text{O}_{0.01}$). It was, therefore, assumed that only part of the oil, related to the ^{13}C NMR aromaticity, could coke. The relative amount of each oil fraction that could coke (shown in Table II) was then determined from the relative nitrogen contents. It is well known that the cracking rates of aliphatic compounds depend on their molecular weight. The relative rates, A_i , for cracking of the various oil fractions were calculated from the equation of Voge and Good (19). The preexponential factor was multiplied by a pressure-dependent factor derived from results given by Fabuss (20). The formalism for treating multicomponent oil cracking is then the same as used previously (10). Each of the oil fractions independently undergoes a first-order cracking reaction to generate coke, gas (CO , H_2 , CH_4 and CH_x) and lighter oil such that

$$\frac{dy_i}{dt} = \sum_{j=1}^{11} a_{ij} k_{c,j} y_j$$

where

y_i = the weight fraction of the i^{th} oil species

$k_{c,j}$ = the first-order rate coefficient for cracking j^{th} oil species

A_j = relative cracking rate of the j^{th} oil species,

and the stoichiometry factors are:

$$a_{ij} = -1 \quad \text{for } i = j$$

$$a_{ij} = 0 \quad \text{for } i > j$$

and

$$a_{ij} = 1/(j + 2.8) \quad \text{for } i < j$$

The latter stoichiometry factor is obtained by assuming that equal masses of each of the lighter oil fractions are created by cracking a heavier fraction (approximately true for Voge and Good's data (19)) and that the cracking products are always in the following relative mass ratio with respect to the gas product CH_x : coke, 0.632; CO , 0.0566; H_2 , 0.0314; CH_4 , 0.166; and Oil, 0.50.

The rate parameters for oil degradation could not be used directly because of a lack of data or a difference in formulation of the reactions. The activation energy for shale oil cracking was that determined (10) using an 11-component model for data between 500 and 650°C. The activation energy for oil coking was taken from Campbell et al. (7). The preexponential factors were then adjusted to give agreement with the experimental results of Burnham and Singleton (12), whose

measurements span the largest range of pyrolysis conditions. A close interplay was observed between coking and cracking. That is, reducing the coking rate coefficient caused a decrease in the amount of oil coked, but a nearly compensating increase occurred in the amount of oil cracked. This may be due to a decrease in the flux of sweep gas generated by the coking reaction, thus giving the oil a greater residence time for cracking to occur. The relative amounts of coking and cracking were adjusted using the estimation from oil biomarker content (12) that less than 5% of the oil yield loss at atmospheric pressure and about 10% of the oil yield loss at 2.7 MPa was due to oil cracking. Future experiments at variable porosity will be used to better decouple the liquid and vapor residence times, thereby helping to separate the relative contributions of coking and cracking. The amount of H_2 and CH_4 formed by oil coking was determined from previous data (7), but unlike the original work, we made a correction for the additional H_2 and CH_4 formed at slow heating rates by char pyrolysis.

RESULTS

We first developed an expression for the rate of water release because it has a large impact on the residence time of the generated oil. Our kinetic expression incorporates an equilibrium limitation for clay dehydration. A comparison between calculated time-dependent water production with the measurements of Burnham and Singleton (12) is shown in Figure 1. The agreement is excellent. Although the inhibition of clay dehydration by water vapor is well known (21-22), no suitable kinetics were available for illite, the principal clay in oil shale. Because our rate expression was derived empirically, caution should be used in applying it for pressures and heating rates much outside the range shown in Figure 1.

In Table III, we compare the oil yields calculated by our model with the experimental results of Burnham and Singleton (12). The yields agree very well except at the two extremes of pyrolysis conditions. It would have been possible to fit any subgroup more accurately by sacrificing agreement with the other experiments, but our objective was to see how general a pyrolysis model could be developed. The amount of oil degradation by each mechanism is also shown in Table III. In agreement with previous observations, most of the yield loss at atmospheric pressure is due to oil coking. Both coking and cracking become greater at 2.7 MPa because of longer liquid and gas residence times. Cracking becomes more important at higher pressures. Both oil liquid and oil vapor were allowed to crack, but most of the cracking was calculated to occur in the liquid, perhaps due to the greater mass concentration of the liquid oil compared with the oil vapor.

TABLE III

COMPARISON OF MODEL CALCULATIONS WITH DATA OF BURNHAM AND SINGLETON (12)

Heating Rate (°C/h)	Pressure (MPa)	Oil Yield, Wt % FA		Calculated Yield Loss	
		meas	calc	Coking	Cracking
720	0.1	100	106	5	0.1
110	0.15	97	100	11	0.2
11	0.15	86	89	21	1
1	0.15	77	79	29	3
108	2.7	78	81	22	8
9	2.7	73	70	28	13
1	2.7	72	62	33	16

Note: The maximum calculated oil yield is 111% FA.

Further comparisons of model calculations and measurements of Burnham and Singleton demonstrate the ability of the model to calculate accurately even some properties not used in developing the model. The agreement between observed and calculated oil evolution versus temperature shown in Figure 2 is very good. Most of the delay of oil evolution at increased pressure is predicted using our treatment of oil evaporation. The model has the capability of calculating the change in boiling point properties of the product oil as shown in Table IV. The agreement between observed and calculated gas evolution versus temperature shown in Figure 3 is also very good for the two experiments where data are available. As shown in Table V, the total amounts of H_2 , CH_4 and CH_x agree well for the near-atmospheric pressure cases, but significant discrepancies exist for the 2.7 MPa cases, especially for H_2 . These discrepancies are discussed in the next section.

We next compare our model calculations with the experiments of Stout et al. (6). These comparisons are especially significant because of the complicated temperature history of the experiments and because no comparisons were made during model development. In these

experiments, the oil shale was heated at 12°C/min to a preselected temperature between 250 and 450°C, held there for either 8, 80 or 800 h, then heated the rest of the way to 500°C at 12°C/min, as shown schematically in Figure 4a. A comparison of measured and calculated yields for these conditions is shown in Figure 4b. We represent the data by lines and the calculations by points because there were more experimental points than model calculations. The lines shown are those drawn by Stout et al. The experiments show that holding at about 350°C is the most sensitive for causing yield loss and that most of the yield loss is caused within 80 h. The model calculations reproduce these features. The model can also reproduce the reported gas compositions as shown in Figure 5.

TABLE IV
COMPARISON OF BOILING POINT DISTRIBUTIONS WITH DATA OF
BURNHAM AND SINGLETON (12)

Boiling Interval °C	Fischer Assay		1°C/h, 0.15 MPa		1°C/h, 2.7 MPa	
	exp	calc	exp	calc	exp	calc
<100	4.1	3.8	5.6	6.0	6.9	12.9
100-150	4.4	5.0	5.8	7.6	10.2	14.5
150-200	7.3	6.7	9.7	9.7	14.5	16.3
200-250	8.8	7.9	12.7	11.2	16.3	16.5 ^a
250-300	10.8	9.6	16.5 ^a	13.0	17.2 ^a	16.2
300-350	12.7	11.3	16.3	14.0 ^a	15.3	13.0
350-400	13.0	11.1	13.9	12.0	10.6	6.8
400-450	14.4 ^a	12.8	11.7	11.4	6.0	2.9
450-500	13.7	14.0 ^a	5.8	10.1	2.5	0.7
500-550	8.0	11.0	2.0	4.6	0.5	0.1
>550	2.8	6.8	0.0	0.4	0.0	0.0

a. The most abundant oil fraction.

TABLE V
COMPARISON OF CALCULATED GAS PRODUCTION WITH MEASUREMENTS OF
BURNHAM AND SINGLETON (12), IN UNITS OF MMOLE/kg

Heating Rate (°C/h)	Pressure (MPa)	H ₂		CH ₄		CH _x	
		meas	calc	meas	calc	meas	calc
720	0.1	160	175	107	100	111	109
110	0.15	220	207	127	106	105	112
11	0.15	324	353	184	182	134	125
1	0.15	366	508	205	267	121	147
108	2.7	127	317	252	154	159	183
9	2.7	91	482	374	250	160	249
1	2.7	43	632	312	343	93	294

The final comparisons presented are with experiments involving a gas sweep. Campbell et al. (7) showed that an inert gas sweep could reduce oil yield loss due to coking at low heating rates by increasing the rate of oil vaporization. A comparison between the calculated and observed effect of a gas sweep is shown in Figure 6. Although the general trend is correct, the calculation overestimates the effect. The principal reason is undoubtedly that the experiments have diffusion effects that the model does not take into account, even though the particle size used by Campbell et al. was small (<0.84 mm). A related problem is that the model calculates the same oil yield for Fischer Assay conditions and for pyrolysis at 500°C in a gas sweep. Although evidence is not unanimous (4), it appears most likely that the latter conditions produce 5 to 10% more oil (3, 10). It appears that the model has some problem in calculating the rate of degradation of the 10% most unstable oil. Finally, Herskowitz et al. (11) reported oil yields for pyrolysis of shale heated at 360°C/h and 2.6 MPa in rapidly flowing N₂ and H₂. They obtained 90% of Fischer Assay yield in N₂ and 117% in H₂. Using the same flowrates as in the experiments, the model calculated oil yields of 106% and 110%, respectively, of Fischer Assay yield. For comparison, the model calculated 106% of Fischer Assay yield at Fischer Assay pyrolysis conditions as shown in Table III. Apparently, the N₂ sweep in the experiments was not capable of completely counteracting the inhibiting effect of

pressure on oil evaporation because of intraparticle diffusion. The difference between experiment and calculation in H_2 indicates that the model does not yet account for all the beneficial aspects of H_2 pressure.

DISCUSSION

The results shown above demonstrate the wide-ranged ability of the model presented here. It is the only model to our knowledge that can calculate oil yields and evolution kinetics for an arbitrary temperature-pressure history. The model predicts decreased oil yield at lower heating rates and the maximum sensitivity to coke formation at 350°C. The model also predicts the delay of oil evolution and decreased oil yield at elevated pressures. The model also calculates the amount of unvaporized oil (bitumen) during the course of pyrolysis, although we have not attempted any comparisons to experiment.

The model does have some weaknesses. The calculated yields for Fischer Assay conditions and the Stout experiments (Figure 4) are systematically high by several percent. If we had limited our goal to modeling atmospheric pressure pyrolysis for heating rates of 720°C/h and lower, much better agreement could have been obtained. Instead, we adopted a maximum possible yield of 111% of the Fischer Assay value in order to account for rapid pyrolysis (3, 10) and high-pressure hydrogen experiments (11, 13) that obtain oil yields greater than Fischer Assay.

Another way of stating this problem is that the model overestimates the detrimental effect of pressure on oil yield, especially at slow heating rates. Because the calculated yield loss due to coking at slow heating rates does not increase much with increased pressure, the amount of oil cracking must be overestimated. We first attempted to solve this problem by not allowing liquid oil to crack, but a compensating increase in oil vapor cracking caused the oil yield to remain approximately constant. Since this paper was in draft form, we decided that the stoichiometry for oil cracking should be pressure dependent. Data of Voge and Good (22) indicate that the gas to light oil ratio of the cracking products decreases with increased pressure. Preliminary calculations using a pressure-dependent cracking stoichiometry indicate an improvement, but the model still overestimates the effect of heating rate at high pressure. This must be because the activation energy used for oil cracking is too low. It is also probably the reason why the cracking preexponential factor had to be reduced by a factor of 60 from that determined for shale oil between 500 and 650°C. Future work will explore the use of a higher activation energy.

Another apparent weakness is the calculation of too much hydrogen production at high pressure as shown in Table V. Increased H_2 production calculated by the model is due to oil coking and cracking. Our stoichiometry for these reactions was derived from atmospheric pressure experiments (6-8, 15). Apparently there are significant differences at higher pressures. One example of a difference is that alkenes are formed by oil cracking at atmospheric pressure, but none were formed from the cracking that occurred in the 2.7 Mpa, 1°C/h experiment, apparently because the hydrogen radicals are all captured by hydrocarbon radicals. Future work on model development will attempt to take this into account. The model also has a provision for reaction of H_2 with char to form methane, but its use has not yet been explored.

Although the model was designed to have the capability of allowing oil yields greater than obtained at Fischer Assay conditions, the model calculates nearly identical yields for pyrolysis at Fischer Assay conditions and for rapid pyrolysis in a sweep gas. Experiments indicate that the latter conditions give higher oil yields. Another weakness of the model for rapid pyrolysis involves hydrogen. Gas evolution kinetics have been reported by Richardson et al. (10) for isothermal fluidized-bed pyrolysis. They found that hydrogen (unlike other gases) did not reach its maximum rate of release until most of the oil was evolved, suggesting that it is formed by a reaction intermediate. In contrast, the model calculated that the maximum rate of hydrogen evolution was during the initial stages of kerogen pyrolysis, even though a major source of hydrogen is oil coking. A way to resolve this discrepancy is not yet apparent, but the problem emphasizes the importance of understanding the reactions of hydrogen for developing an improved general pyrolysis model.

A related problem is that the maximum possible oil yield is less than that attainable in high-pressure hydrogen. In the present model, the only way hydrogen can increase oil yield is by inhibiting oil coking. It appears necessary to include another mechanism in order to obtain higher yields in hydrogen than for flash pyrolysis. The recent ^{13}C NMR measurements of Herskowitz et al. (11) and Burnham and Happe (23) suggest how. High-pressure hydrogen appears to inhibit the formation of additional aromatic carbon during pyrolysis. Under a wide range of other conditions, the total amount of aromatic carbon in the oil and carbonaceous residue is roughly constant and nearly twice that present in the raw shale. These are important because our present model assumes that only part of the oil, roughly corresponding to the aromatic components, is susceptible to coking. Consequently, a higher fraction of the oil is likely to be susceptible to coking in the absence of added hydrogen donors. Therefore, it appears that the amount of oil susceptible to coking as well as the rate of coking should depend on hydrogen partial pressure.

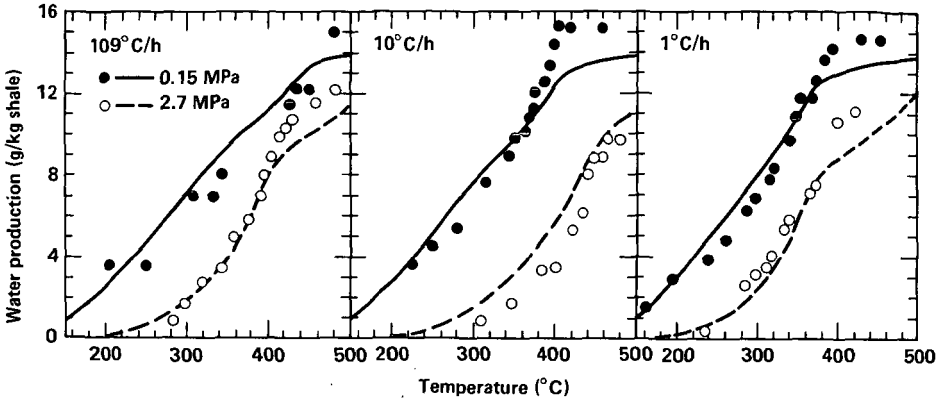


Figure 1. Comparison of calculated cumulative water production with measurements of Burnham and Singleton (12).

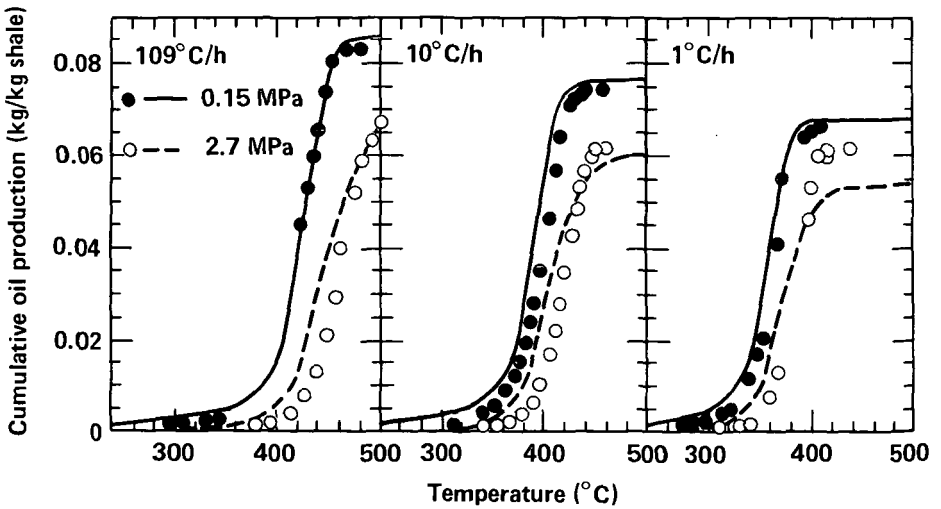


Figure 2. Comparison of calculated cumulative oil production with measurements of Burnham and Singleton (12).

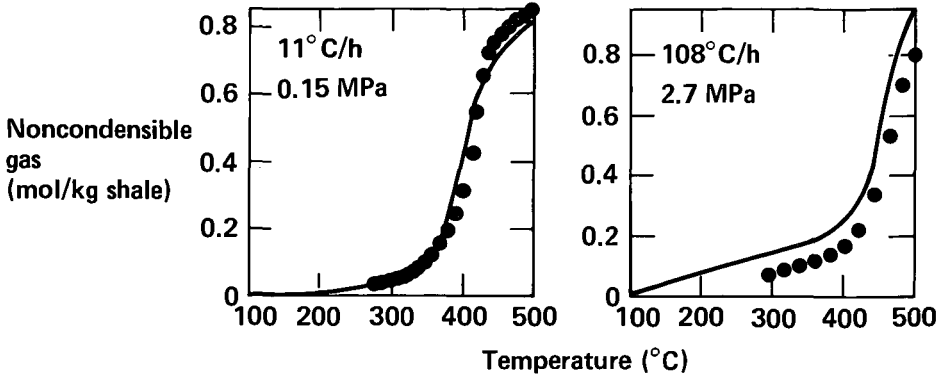


Figure 3. Comparison of calculated cumulative gas production with measurements of Burnham and Singleton (12).

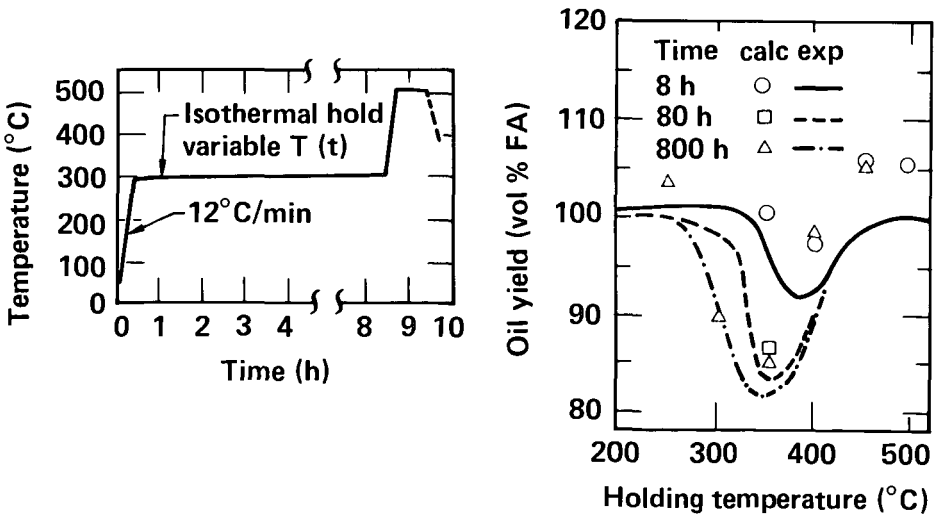


Figure 4. Thermal history of experiments by Stout et al. (6) and a comparison of calculated oil yields with their measurements.

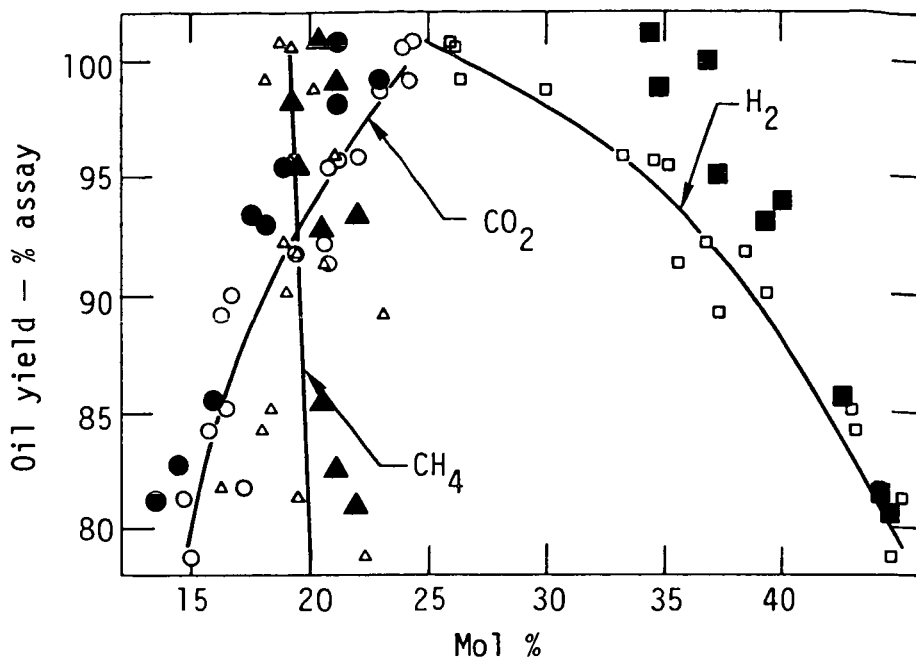


Figure 5. Comparison of calculated gas composition with results of Stout et al. (16).

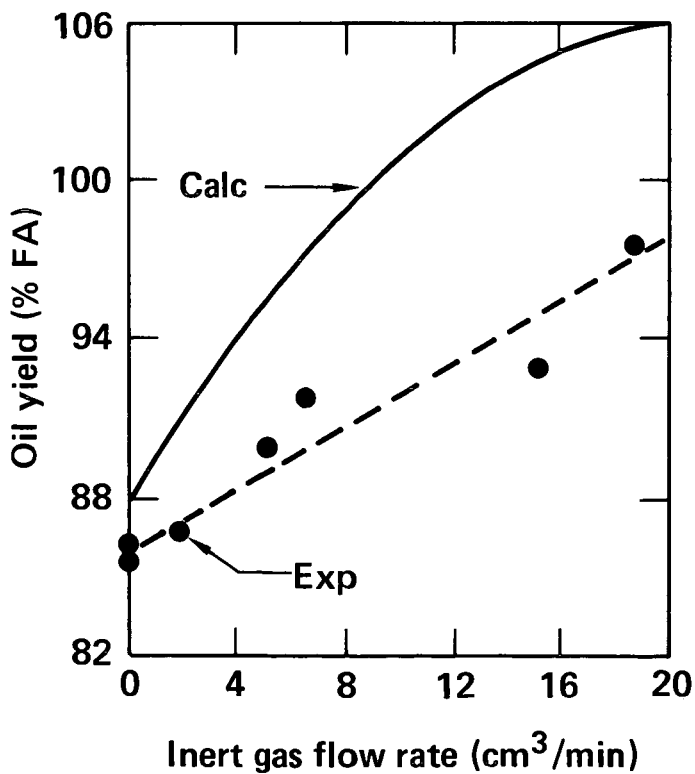


Figure 6. Comparison of calculated effect of flow rate with experiments of Campbell et al. (7).

ACKNOWLEDGMENTS

This work was supported by the offices of Basic Energy Sciences and Oil, Gas and Shale under contract W-7405-ENG-48.

LITERATURE CITED

- (1) Campbell, J. H., Koskinas, G. J. and Stout, N. D., *Fuel*, 57, 372 (1978).
- (2) Shih, S. M. and Sohn, H. Y., *Ind. Eng. Chem. Proc. Des. Dev.*, 19, 420 (1980).
- (3) Wallman, P. H., Tamm, P. W. and Spars, B. G., "Oil Shale, Tar Sands and Related Materials", ACS Symp. Series No. 163, H. C. Stauffer, ed., Washington, D. C., p. 93 (1981).
- (4) Richardson, J. H., Huss, E. B., Ott, L. L., Clarkson, J. E., Bishop, M. O., Taylor, J. R., Gregory, L. J. and Morris, C. J., "Fluidized-bed Pyrolysis of Oil Shale: Oil Yield, Composition and Kinetics", Lawrence Livermore Natl. Lab. Rept. UCID-19548 (1982).
- (5) Braun, R. L. and Burnham, A. K., *Oil Shale Project Quarterly Rept.*, Lawrence Livermore Natl. Lab. Rept. UCID-16986-82-2, p. 11 (1982).
- (6) Stout, N. D., Koskinas, G. J., Raley, J. H., Santor, S. D., Opila, R. L. and Rothman, A. J., *Colo. Sch. Mines Quart.*, 71, 153 (1976).
- (7) Campbell, J. H., Koskinas, G. J., Stout, N. D. and Coburn, T. T., *In Situ*, 2, 1 (1978).
- (8) Burnham, A. K., "Oil Shale, Tar Sands and Related Materials", ACS Symp. Series No. 163, H. C. Stauffer, ed., Washington, D. C., p. 39 (1981).
- (9) Thakur, D. S., Vora, J. P., Wilkins, E. S. and Nuttall, H. E., *Preprints, ACS, Div. Fuel Chem.*, 27 (2), 158 (1982).
- (10) Bissell, E. R., Burnham, A. K. and Braun, R. L., Lawrence Livermore Natl. Lab. Report UCRL-89976, submitted to I and EC Proc. Des. Dev. (1983).
- (11) Herskowitz, F., Olmstead, W. N., Rhodes, R. P. and Rose, K. D., "Chemistry and Geochemistry of Oil Shale", ACS Symp. Series 230, F. P. Miknis, ed., Washington, D. C., p. 301 (1983).
- (12) Burnham, A. K. and Singleton, M. F., "Chemistry and Geochemistry of Oil Shale", ACS Symp. Series 230, F. P. Miknis, ed., Washington, D. C., p. 335 (1983).
- (13) Well, S. A. and Rue, D. M., *Synthetic Fuels from Oil Shale II: Symp. Papers, Inst. Gas Technol.*, Chicago, IL, p. 217 (1982).
- (14) Hindmarsh, A. C., *ACM SIGNUM Newsletter*, 15 (4), 10 (1980).
- (15) Campbell, J. H., Gallegos, G. and Gregg, M., *Fuel*, 59, 727 (1980).
- (16) Huss, E. B. and Burnham, A. K., *Fuel*, 61, 1188 (1982).
- (17) Anthony, D. B. and Howard, J. B., *AIChE J.*, 22, 725 (1976).
- (18) Singleton, M. F., Koskinas, G. J., Burnham, A. K. and Raley, J. H., "Assay Products from Green River Oil Shale", Lawrence Livermore Natl. Lab. Rept. UCRL-53273 (1982).
- (19) Voge, H. H. and Good, G. M., *J. Am. Chem. Soc.*, 71, 593 (1949).
- (20) Fabuss, B. M., Smith, J. O. and Satterfield, C. N., *Advances in Petroleum Chem. and Refining*, 9, 157 (1964).
- (21) Brindley, G. W., Sharp, J. H., Patterson, J. H. and Narahari, B. N., *Amer. Min.*, 52, 201 (1967).
- (22) Stone, R. L. and Rowland, R. A., *Clays and Clay Minerals*, Proc. 3rd Nat. Conf., p. 103 (1955).
- (23) Burnham, A. K. and Happe, J. A., Lawrence Livermore Natl. Lab., Report UCRL-89977, submitted to *Fuel* (1983).

SYMPOSIUM ON CHARACTERIZATION AND CHEMISTRY OF OIL SHALES
PRESENTED BEFORE THE DIVISIONS OF FUEL CHEMISTRY AND
PETROLEUM CHEMISTRY, INC.
AMERICAN CHEMICAL SOCIETY
ST. LOUIS MEETING, APRIL 8 - 13, 1984

STRUCTURAL CHARACTERIZATION OF SUPERCRITICAL GAS EXTRACTS AND
RESIDUES OF FUSHUN AND MAOMING OIL SHALE

By

K. Z. Qin, R. A. Wang, S. S. Jia, Y. X. Lao and S. H. Guo
East China Petroleum Institute, Dongying, Shandong, PRE 22996-7

INTRODUCTION

An ideal degradation process used to elucidate oil shale kerogen structure involves cautious split of kerogen to such an appropriate extent that the high yield fragments will be soluble in common solvents for application of various instrumental analyses, yet still preserve most of kerogen structure in the fragments. Several investigators have employed different methods, such as mild thermosolvolytic by tetralin in autoclaves (1) and stepwise oxidation by alkaline potassium permanganate (2) to achieve these ends, yet the semicontinuous supercritical gas extraction (SCGE) appears to be a more effective means. During the process, kerogen matrix swells and loses its structure due to the dense phase solvent gas penetrating into the crosslinked network. As the framework of kerogen is broken down at the weakened linkages, the thermally depolymerized bitumen fragment just being extractable by supercritical gas escapes from the reaction zone immediately together with the gas stream and is condensed under reduced temperature and pressure, so the minimization of the secondary degradation occurs. Different Chinese oil shales have been extracted by supercritical toluene in a semicontinuous apparatus successfully (3), for instance, Maoming oil shale yields 79% of bitumen extracted on the basis of organic matter content at 385°C and 15 MPa with low yields of gas and water. Much valuable information can be provided by analyses of bitumen and its constituents. Furthermore, determination of the voidage and porous structure of extracted shale will reveal the distribution pattern of organic matter in the raw shale, since the major part of organic matter has been removed from its mineral matrix, which is primary inert to the extraction. The semi-quantitative data measured by porosimeter give a distinct description of that important physical property of oil shale. The present work is such an experiment with Fushun and Maoming oil shale, two of the most famous oil shale deposits in China.

EXPERIMENTAL

Extraction

The extraction was carried out in a home-made semi-continuous apparatus consisting of a stainless steel preheater and an extractor. For each run, 100 g of 20-60 mesh oil shale sample was charged. A constant flow rate stream of toluene was pumped upward through the extractor and a definite temperature and pressure were maintained automatically all over the extraction. Supercritical toluene carrying the dissolved bitumen was condensed in a water cooler, it was removed from the condensate at 80°C under vacuum and the extract obtained was preserved under nitrogen atmosphere. The extracted shale was discharged after cooling the system to room temperature by nitrogen.

Characterization of Extract

During the fractionating of the extract, asphaltenes were precipitated by heptane extraction. The solubles were fractionated by adsorption chromatography on alumina. The aliphatics, aromatics and resins were eluted successively with petroleum ether (b. p. 60-90°C), benzene and benzene-ethanol mixture (1:1 by volume).

Gas-liquid chromatographic analyses (GLC) of the aliphatics were carried out using a HP-5734-A chromatograph on a 12 m x 0.2 mm i. d. capillary column with ov-101 silicone fluid as stationary phase and He as carrier gas. The column was heated from 100°C to 280°C with a heating rate of 8°C/min. Combined gas chromatography-mass spectrometry analyses (GC-MS) were carried out using a Finnigan model 4201-c GC-MS and data reduction system. Separated components were identified by comparison of standard mass spectra.

Proton and C-13 nmr were performed for bitumen and its constituents on a Bruker WH-90 nmr spectrometer with CDCl₃ as solvent.

Molecular weights were determined using a Knauer vapor pressure osmometer with

benzene as solvent.

Proximate and ultimate analysis procedure follows that of National Standards of China for coals to solid samples and for petroleum products to bitumen samples.

Infrared spectra were measured by a Hitachi 260-50 grating spectrophotometer. Samples were prepared as smears on NaCl cells.

Characterization of Extracted Shale

Preliminary microscope examination shows that the pore size of extracted shale distributes in the range of macropores. A CARLO ERBA-1520 automatic mercury porosimeter was adapted to the determination. It was operated under 0-150 MPa of mercury for the pore radii range 50 to 75,000 Å. The samples were dried at 105°C for 2 hours before hand. Pore radius r is calculated by the Washburn equation in which surface tension of mercury is assumed to be 480 dyne/cm and contact angle, 140°.

True density of samples was determined by water pycnometer and particle density by mercury displacement. Total open pore volume was calculated by the difference between reciprocals of particle and true densities.

For the examination of mineral constituents, above mentioned infrared spectrophotometer was used. The samples were prepared as KBr pellets.

The porous structure of extracted shale was examined by a Hitachi HU-11A transmission electron microscope (TEM) using microtomy for section preparation. Morphology of the minerals was also examined by scanning electronic microscopy (SEM) techniques. (TEM was carried out by Beijing Petro-chemical Research Institute and SEM by Shengli Geological Research Institute.)

RESULTS AND DISCUSSION

Table I summarizes the ultimate analyses of organic matter, bitumen (SCGE) and its group constituents. Kerogen of Maoming and Fushun oil shale will be classified as type 1 according to H/C and O/C diagram suggested by Tissot et al. (4), as well as to their infrared spectra. Detailed analyses of these two shales and description of SCGE experiment conditions are stated elsewhere (3, 5).

TABLE I

ULTIMATE ANALYSIS OF ORGANIC MATTER, SCG EXTRACTS AND GROUP CONSTITUENTS

Sample	Origin	Ultimate Analysis (Wt %)						Weight Yield % (basis)	
		C	H	N	S	O	H/C		
Organic Matter	F	79.1	9.9	2.1	1.9	7.0	1.51	21.1	(d. a. f. shale)
SCG	M	79.4	9.7	1.6	1.1	8.2	1.46	19.2	(d. a. f. shale)
Extract	F	84.5	10.3	1.5	0.2	3.5	1.46	70.9	(org. matter)
Aliphatic fraction	M	84.1	10.1	1.5	0.6	3.7	1.44	79.1	(org. matter)
	F	-	-	-	-	-	-	8	(extract)
	M	-	-	-	-	-	-	7	(extract)
Aromatic Fraction	F	85.7	11.1	-	-	-	1.55	8	(extract)
	M	84.4	10.8	-	-	-	1.54	8	(extract)
Resins	F	79.6	9.4	1.7	0.4	8.9	1.42	52	(extract)
	M	79.9	9.6	1.5	0.3	8.7	1.44	43	(extract)
Asphaltenes	F	80.5	8.7	2.3	0.9	7.6	1.30	32	(extract)
	M	81.6	9.3	1.8	0.5	6.8	1.37	42	(extract)

F: Fushun oil Shale; M: Maoming oil shale.

GLC and GC-MS Analyses

Figure 1 is a total ionization plot of a gas chromatogram of the petroleum ether eluate of Maoming extract. It reveals primarily a homologous series of alkanes from C₁₂ to C₃₃, and also an olefin series, as the weaker peaks are adjacent to respective alkanes. The structure of some individual olefins has been identified as α -mono-olefins by computer comparison of mass spectra. Figure 1 shows that there is a distinct major peak of C₂₇ and the n-alkane homologues exhibited a predominance of odd carbon numbers over even ones, but no such regular pattern for the olefin series. The relative amount of olefins to alkanes decreases as the temperature of extraction goes down. It implies that olefins are the fragments split from the side chains of kerogen structure and unlike the alkanes are indigenous components. In the aliphatics, a lot of isoprenoids, steranes and pentacyclic triterpanes such as pristane, phytane, cholestane, ergostane, stigmastane, hopane and

their isomers and homologues have been verified by mass spectra. These biological markers are valuable to the geochemists for the studies of kerogen genesis and maturity.

GLC analysis of Fushun aliphatics gives analogous results to that of Maoming.

It is evident that branched and cyclic aliphatic structures are present. However, the overwhelming majority are the unbranched aliphatic hydrocarbons. As shown in Table I, the weight fraction of aliphatics reaches 7-8.5%. There is a considerable amount of alkanes in the total extract. Will all the alkanes be originally entrapped in the cage structure of kerogen matrix? It is an interesting problem of the kerogen structure, but it is not clear yet.

Structure Similarities Between Extract and Kerogen

A noticeable feature in Table I is the hydrogen carbon atomic ratio of the extracts which are very close to that of their kerogen matrix. Generally, a cracking process should give the light products a higher H/C than the crude stock, but a depolymerizing process gives the degradation products a same H/C as its precursor.

The infrared spectra of SCG extract bear striking resemblance to those of original kerogen. The strongest absorption bands are around 2920, 2855 and 1455 cm^{-1} contributed by CH_2 and CH_3 groups of aliphatics; another specific band at 720 cm^{-1} shows predominant $(\text{CH}_2)_n$ structures (n larger than 4), exists both in extract and kerogen.

The carbon aromaticities determined by proton nmr are 0.33 and 0.34 for Fushun and Maoming SCG extracts. Recently, we have got the information that the carbon aromaticities directly measured by C-13 nmr with cross polarization/magic angle spinning techniques carried out in Colorado State University for these two raw oil shales are 0.35 and 0.32, respectively (6). This fact may well be taken as one of the reliable indications of a polymer character of kerogen.

Asphaltene of bitumens extracted from oil shale at ordinary conditions is known as having similar structures of kerogen, SCG asphaltene, the major constituent of extract, will naturally give more similarities. For instance, carbon aromaticity of Maoming SCE asphaltene determined by C-13 nmr is 0.33; their X-ray diffraction curves are also having remarkable resemblance. A special report of this item is under preparation.

These structural similarities between SCG extract and kerogen lead to the conclusion that thermo-depolymerization is the main reaction experienced during SCGE and a great portion, if not all, of the kerogen matrix has characters of a multipolymer.

"Building Block" of Kerogen

Although the SCG extract is not just the "monomer" of the multipolymer structure of kerogen, it may be considered as a specimen composed of different "monomers" of kerogen. An average "building block" of kerogen can be described, therefore, with the group constituents used to describe a bitumen. The molecular ratio of these constituents in SCE extracts are tabulated as follows:

Group Constituent	Average M. W.		Weight Fraction		Molecular Fraction		Molecular Ratio	
	(VPO)							
	1	2	1	2	1	2	1	2
Aliphatics	330	326	0.07	0.08	0.17	0.19	1.0	1.0
Aromatics	390	390	0.08	0.08	0.16	0.15	0.9	0.8
Resins	690	710	0.43	0.52	0.49	0.53	2.9	2.8
Asphaltenes	1870	1667	0.42	0.32	0.18	0.14	1.0	0.8

Note: 1 - Maoming oil extract; 2 - Fushun oil shale extract.

Accordingly, average "building blocks" of kerogen keep their constitutional molecular numbers in the ratio of 1:1.3:1 approximately, so the unit weight of an average "building block" of these two kerogens may be estimated as 4400-4600. It has a good agreement with the results of our other work (7), in which the average unit weight was calculated from the correlation of refraction index, density, aromaticity and ultimate analyses of kerogens.

Density of Maoming and Fushun oil shale kerogen has been assessed to be nearly 1.10 (8); then the average molecular volume of a "building block" be spheric in form, the diameter of sphere would be 24Å. It appears somewhat smaller than the dimension of Green River oil shale kerogen, $39 \times 27 \times 25 \text{ Å}^3$, suggested by Yen (9), but still in the same magnitude order. Using ultimate analysis data of kerogen as those of "building block", their chemical formulas can be written as $\text{C}_{302}\text{H}_{440}\text{O}_{23}\text{N}_6\text{S}_2$ for Maoming and $\text{C}_{296}\text{H}_{446}\text{O}_{20}\text{N}_7\text{S}_2$ for Fushun. It is logical that the carbon constitutional fractions of SCG extract may be taken as those of kerogen (10) and are listed in Table II.

TABLE II
 PROTON MUR SPECTROSCOPY AND STRUCTURAL PARAMETERS OF SCG EXTRACT
 (per average molecule)

<u>Item</u>	<u>Fushun Extract</u>	<u>Maoming Extract</u>
Total C atoms	53.4	55.3
Total H atoms	77.9	79.6
Molecular Weight (VPO)	758	789
Hydrogen Distribution:		
aromatic	6.2	6.3
naphthenic	8.4	11.6
olefinic	0.3	0.5
alpha to ar. ring	10.7	13.0
beta to ar. ring	44.3	40.0
gama to ar. ring	8.1	8.1
Structural parameters:		
aromatic C fraction	0.33	0.34
naphthenic C fraction	0.16	0.23
paraffinic C fraction	0.51	0.43
no. of total rings	6.6	7.1
no. of aromatic rings	4.0	3.9
no. of naphthenic rings	2.2	3.2
no. of fused carbon	-0.5	-1.0

In the light of characterization of SCG extract, an aspect of the carbon skeleton structure of these two kerogens may be described. Nearly one half of the total carbon atoms are shown to be paraffinic, one third aromatic and the rest naphthenic. It appears more paraffinic in nature for Fushun kerogen but nearly the same aromatic for these two. It implies that they are close in maturity but perhaps differ in origin precursors to some extent. Unbranched long chains are the overwhelming majority in the paraffinic structure. For the cyclic ring cluster, aromatics are rather cata-condensed with long side chains and adjacent with naphthenics to form hydroaromatic structure. Several clusters linked randomly by different bridges constitute a unit "building block" of the multipolymer --oil shale kerogen.

Minerals in Extracted Shale

X-Ray diffraction and infrared spectra have identified that the bulk mineralogy of those two shales primarily consists of quartz, kaolinite and illite and with few percent of carbonates and pyrite (5). Small changes in sieve analysis of shales before and after extraction indicates that, despite the removal of most of the organic matter, no severe fragmentation of the shale results. This is consistent with SEM morphology observations, minerals are cemented together in various patterns with indigenous clay components to form a continuous phase although the individual inorganic crystals such as quartz and calcite are either partly or entirely encased by organic matter.

Some clay minerals such as montmorillonite will lose crystal layer water at 150-200°C. Samples of these two shales dried at 105°C have been further dehydrated in vacuo at 200°C for two hours, their weight loss is no more than 0.1%. It means that, for these two shales, loss of crystal layer water of clay may be ignored.

Siderite is the carbonate most sensitive to heat, beginning its decarbonization at 370°C. These two shales do contain a little carbonate but they are primarily calcite. The good balance of inorganic carbon dioxide of the shale before and after extraction shows that nearly all the carbonates remain unchanged in the residue.

Quartz and kaolinites are rather stable at extraction temperature. Thermogravimetric analysis of minerals of Maoming oil shale has shown that weight loss detected is negligible below 400°C (11).

The case of pyrite is somewhat different. It is reported (12) that pyrite crystals in the oil shale usually coated with a layer of organic matter are distributed evenly in the kerogen matrix. Microscopic examination has proved that Maoming and Fushun oil shale are not the exception. The finely dispersed bright points in the microphotograph of Maoming kerogen present a distinctive picture of pyrite distribution. As large amount of organic matter is extracted by the solvent, pyrite crystal in kerogen will be entrained with the extracts. The pyrite sulfur content of Maoming shale decreases from 0.96% to 0.57%, which affirms the loss of pyrite in extraction. Fushun oil shale has a lower pyrite content, its loss should be less.

Infrared spectra examinations of the shales before and after extraction show that the characteristic absorption bands of minerals, such as 3620-3670 cm^{-1} for kaolinite, 1070-1160 cm^{-1}

and 910-920 cm^{-1} for Si-O bond, 790-800 cm^{-1} for quartz, either the shape or the intensity, are unaltered; only the bands of pyrite (390, 410 cm^{-1}) are weakened.

Tisot et al. (13) observed that gypsum and iron oxide were formed in heat treatment of Green River oil shale at 750°F exposed to air. It is not the case here, since no oxidation will take place in SCGE process.

It comes to the conclusion that, under the operation conditions of SCGE, no remarkable change has happened to the minerals of these two shales. Accordingly, the pore volume increment and porous structure change of the shale due to the extraction are primarily caused by the removal of the organic matter, though the loss of some pyrite and other individual crystal particles must be borne in mind.

Pore Size Distribution and Pore Volume Increment

Figure 2 shows the relation between the pore radius and accumulative pore volume of two shales before and after SCGE. The solid lines (50-75,000 Å) are plotted according to the data of mercury porosimeter and prolonged in dotted lines (<50 Å) to the total pore volume points. The curve sections at radius larger than 500 Å of these two raw shales coincide with each other but diverge sharply in the smaller radius range. It shows that Maoming oil shale is abundant in micropores and has a much higher porosity (up to 20.9%) than that of Fushun (8.3%). It is not surprising that to such a high porosity of oil shale the average moisture content up to 17% is reported.

Data listed in Table III show that the pore volume increment measured is somewhat larger than the calculated volume of the extract, a little ineluctable loss of mineral slits may lead to the difference. However, it still confirms that the pore volume increment is mainly due to the removal of organic matter.

TABLE III

SOME PROPERTIES OF OIL SHALE AND SCG EXTRACTED SHALE

Item	Fushun		Maoming	
	Oil Shale	Ext. Shale	Oil Shale	Ext. Shale
Organic carbon, wt % ^a	16.3	4.9	17.5	4.4
Ash content, wt %	71.9	84.2	72.0	87.3
Mineral CO ₂ , wt %	3.0	3.5	1.4	1.7
Pyrite S, wt %	-	-	0.96	0.57
True density	2.0428	2.2852	2.0353	2.5731
Particle density	1.3594	1.7457	1.1337	1.4281
Total pore volume (ml/g)	0.083	0.298	0.209	0.494
Extracted shale yield, wt %		85.8		82.2
Pore volume increment (ml/g) ^b		0.173		0.197
Volume of extract (ml/g) ^b		14.0		17.5

a. All weight fractions are on dry basis.

b. On oil shale basis.

In Figure 3, the pore radius is plotted against the pore volume increment fraction, which is the quotient of pore volume increment of different radius and total volume increment. The curve represents distribution structure of organic matter in raw oil shale. Nearly 90% of the organic matter of Maoming oil shale is distributed in the size of radius 300-10,000 Å, one half of which being smaller than 1200 Å; for Fushun oil shale, the corresponding figures are 80-6,000 Å and 500 Å. It reveals that the organic matters of these shales are distributed very finely and evenly in the mineral matrix, especially for Fushun oil shale. The results are consistent with TEM porous structure examinations of the extracted shales. This is another significant difference in physical properties of these two oil shales.

From the view point of oil shale processing technology, the properties of porous structure and organic matter distribution structure are of great importance as related to the reaction mechanism and kinetics of the processes, such as drying, extraction, pyrolysis, gasification and combustion. During these fluid-solid multiphase processes, the fluid reactants should diffuse into the solid phase through the micropores, while the fluid reactants should do the opposite. In our experiments, either in the solvent extraction or in the low temperature oxidation, the reaction speed of Maoming oil shale is much faster than that of Fushun. The structural difference between the pore structure and organic matter distribution must be playing an important part, in addition to the factor of difference in chemical properties of kerogen.

Moreover, the moisture content of oil shale is usually directly related to its porosity. As

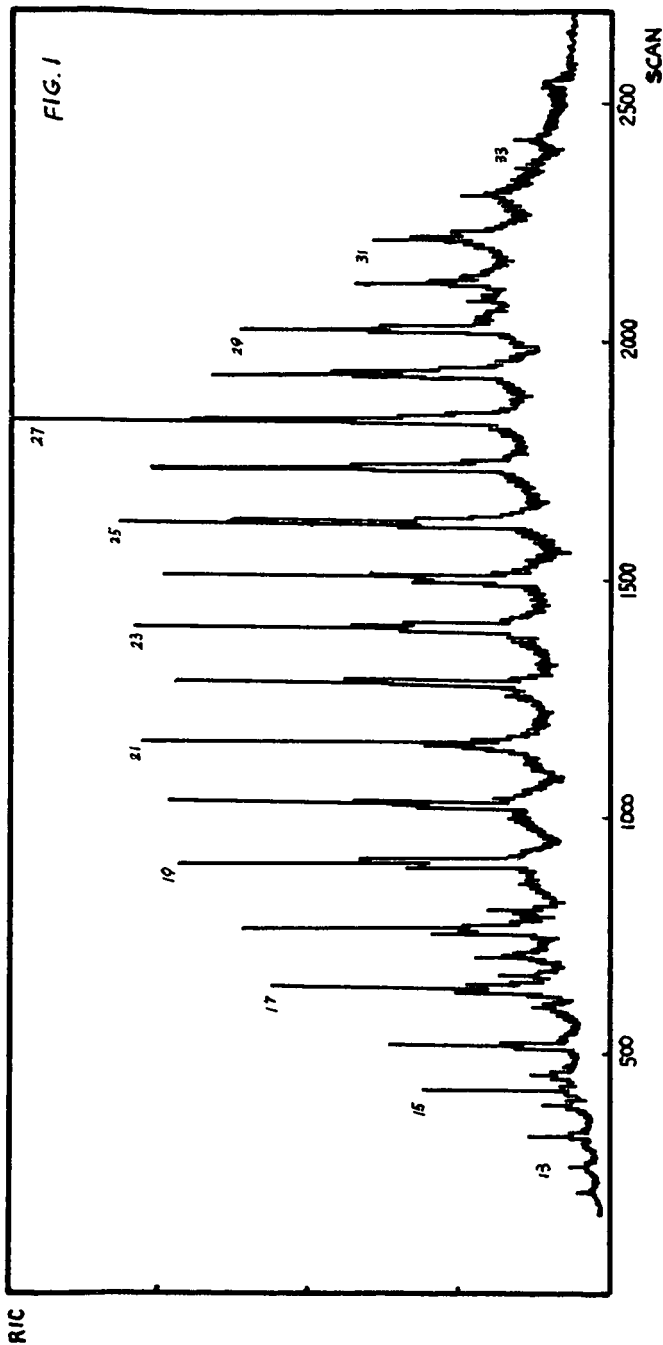


FIGURE 1 TOTAL IONIZATION PLOT OF GAS CHROMATOGRAM OF PETROLEUM ETHER
 ELUATE (MAOMENG OIL SHALE SCG EXTRACT)
 (Arabic numbers indicate number of carbons of n-alkanes)

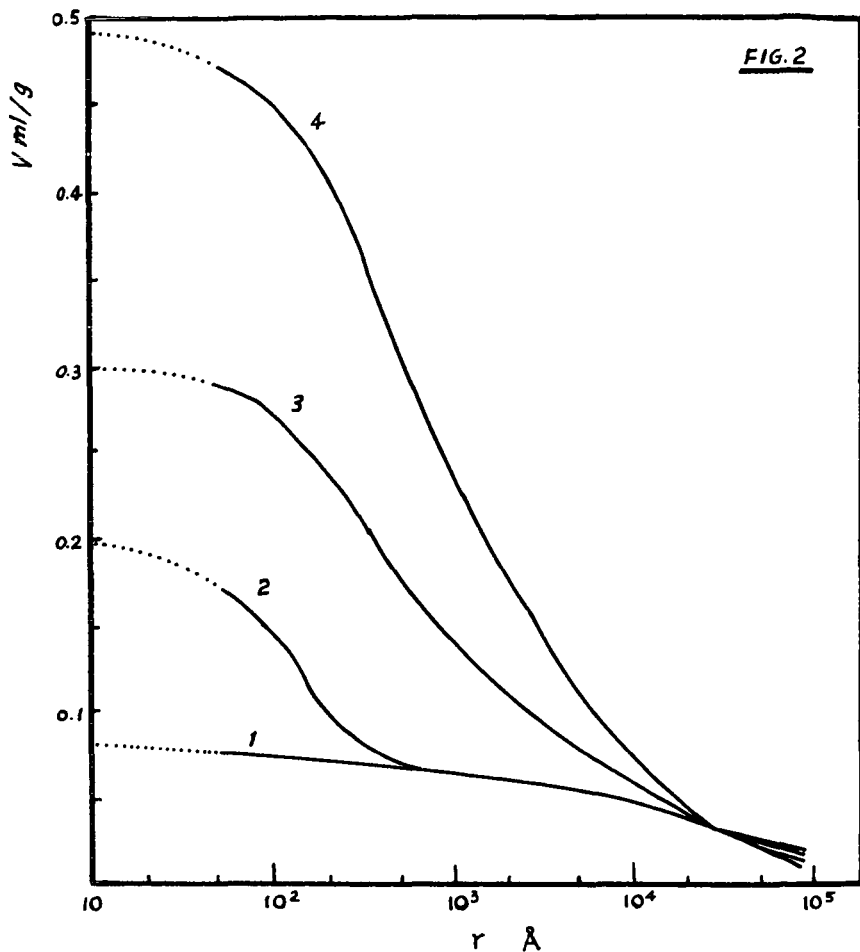


FIGURE 2 RELATION OF PORE RADIUS (r) AND ACCUMULATIVE PORE VOLUME (V)

- 1: Fushun oil shale
- 2: Maoming oil shale
- 3: Fushun extracted shale
- 4: Maoming extracted shale

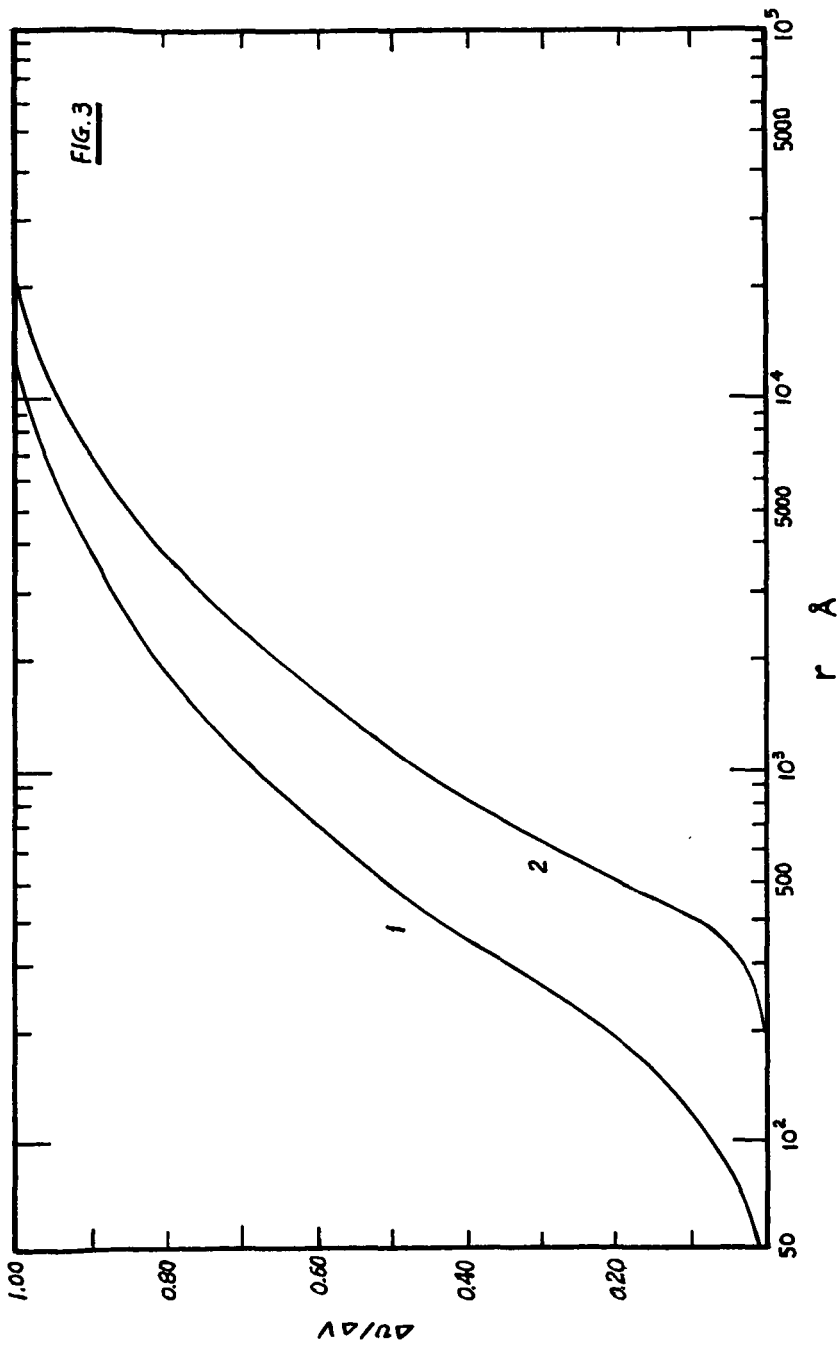


FIGURE 3 RELATION OF PORE RADIUS AND PORE VOLUME INCREMENT FRACTION

mentioned above, Maoming oil shale not only has a high porosity, but also has a very fine pore structure, so that the drying of the shale becomes a tedious process in practice.

Another example is the beneficiation of oil shale. Density of kerogen is nearly 1.0-1.1, density of minerals usually larger than 2.4. It seems to be a simple process to beneficiate the organic matter from shale by density difference, but practically, it is not the case. Many tests of this kind on Fushun and Maoming oil shale failed. It can be found from our present work that the organic matter is mingled so intimately with the minerals that, for Maoming oil shale, successful separation and beneficiation cannot be realized until it is powdered to the size smaller than $1\ \mu\text{m}$, and for Fushun shale, however, much more powdering is required to achieve the same result. It seems impractical for the conventional mechanical grinding and washing to meet such a requirement.

LITERATURE CITED

- (1) Robinson, W. E. and Cummins, J. J., *J. Chem. Eng. Data*, 5, 74 (1960).
- (2) Young, D. K. and Yen, T. F., *Geochim. et Cosmochim. Acta*, 41, 1411 (1977).
- (3) Wang, R. A., Jia, S. S. and Qin, K. Z., *J. East China Petro. Inst.* 6 (4), 87 (1982).
- (4) Tissot, B., Durand, B., Espitalie, J. and Combas, A., *Amer. Assoc. Petro. Geol. Bull.*, 58, 499 (1974).
- (5) Qin, K. Z., *J. East China Petro. Inst.*, 6 (2), 71 (1982).
- (6) Nutall, H. E., Private communication (1983).
- (7) Qin, K. Z., unpublished data.
- (8) Qin, K. Z., *Symp. of Oil Shale Research Works of East China Petro. Inst.*, in press (1983).
- (9) Yen, T. F., "Oil Shale", Chap. 7, 143, Elsevier, Amsterdam (1976).
- (10) Qin, K. Z., Wang, R. A. and Jia, S. S., *Energy Source* 7 (3), in press (1983).
- (11) Yang, R. T., Chen, D. R. and Qin, K. Z., *Symp. of Oil Shale Research Works of East China Petro. Inst.*, in press (1983).
- (12) Kombaz, A., *Kerogen*, Chap. 3, I. F. P. Paris (1980).
- (13) Tissot, P. R. and Murphy, W. I., *J. Chem. Eng. Data*, 5, 558 (1960).

SYMPOSIUM ON CHARACTERIZATION AND CHEMISTRY OF OIL SHALES
PRESENTED BEFORE THE DIVISIONS OF FUEL CHEMISTRY AND
PETROLEUM CHEMISTRY, INC.
AMERICAN CHEMICAL SOCIETY
ST. LOUIS MEETING, APRIL 8 - 13, 1984

CHARACTERIZATION AND GEOCHEMISTRY OF DEVONIAN OIL SHALE
NORTH ALABAMA - SOUTH CENTRAL TENNESSEE

By

K. F. Rheams and T. L. Neathery
Geological Survey of Alabama, P. O. Drawer O, University, Alabama 35486

INTRODUCTION

For the past three years, the Geological Survey of Alabama, in cooperation with the U. S. Department of Energy, has conducted a regional oil shale resource assessment of the Chattanooga Shale in north Alabama, northwest Georgia and south-central Tennessee (Figure 1). The work has involved an extensive outcrop sampling program, a limited drilling program in Alabama for subsurface data and a program to determine the physiochemical properties of the oil shale, and to analyze the shale for a series of trace metals of possible commercial value or environmental hazard.

Results from this study have delineated a four-county area in north Alabama and south-central Tennessee as having the best oil potential of the Devonian Chattanooga Shale in the southernmost part of the Highland Rim section. These four counties, Limestone and Madison Counties, Alabama, and Giles and Lincoln Counties, Tennessee, have an average oil yield of 13.9 gallons per ton (gal/t) with a maximum value of 23.9 gal/t. Within this area, more than 45 outcrops were sampled on 2 foot intervals upward from the lower contact of the shale. A limited drilling program of nine core holes provided 388 feet of shale, which were sampled at 2 foot increments or at distinct lithologic changes (1, 2).

GEOLOGIC SETTING

The Chattanooga Shale of Late Devonian age occurs on the surface and in the subsurface over almost all of the regional study area. The general outcrop line of the shale is shown in Figure 1.

In northern Tennessee, the Chattanooga Shale is subdivided into the upper Gassaway Member, the lower Dowlletown Member, with the Hardin Sandstone at the base. In Alabama, Georgia and south-central Tennessee, only the upper Gassaway Member appears to be present.

Stratigraphically, the Chattanooga Shale unconformably overlies Ordovician or Silurian age sandstone, shale and limestone and itself is overlain with local disconformity by the Maury Formation of Late Devonian to Early Mississippian age or by the Early Mississippian Fort Payne Chert.

Surface exposures of the Chattanooga Shale thicken away from the margin of the Highland Rim towards the fold belt provinces to the east and into the Warrior Basin on the south-southwest, with 82 feet of Chattanooga Shale recorded from a deep test well in northern Greene County, Alabama.

Depositional environment of the Chattanooga Shale was clearly marine, as indicated by the presence of marine fossils including brachiopods and conodonts and the local occurrence of phosphate. Generally high V:Ni ratios in the extracted oil also help substantiate a marine deposition for this shale. Deposition of the shale was apparently irregular, since it may vary greatly in thickness and lithologic composition between adjacent outcrops and is absent over pre-Chattanooga structural highs.

CHARACTERIZATION AND GEOCHEMISTRY

Mineralogy

In hand specimen, the Chattanooga Shale is typically a dark grey to black, organic, pyritiferous, marine shale with thin lenses and interbeds of sandstone, siltstone and silty shale. Phosphate nodules and cherty layers occur locally. Rock slabs cut from drill cores show the distinctive dark color of the shale, the thin discontinuous siltstone laminae, thin pyrite laminae and typical elongate pyrite blebs.

The characteristic black color is derived primarily from hydrogen-rich ($H/C = 1.42$) sapropelic matter apparently derived from algae and lesser amounts of spores and pollen. In outcrop,

the silt laminae appear to weather slightly faster than the clay laminae, imparting a finely fissile character to the shale. Freshly broken shale samples typically emit a strong, petroliferous odor. Locally samples from highly petroliferous zones will support combustion and have been used for heating fuel.

Mineralogically, the Chattanooga Shale is composed of 22% organic matter (kerogen), 31% clay minerals (illite and kaolinite), 22% quartz, 9% feldspars and 11% pyrite and marcasite. Accessory minerals such as calcite, apatite, tourmaline and zircon are also known to occur. In thin section, the kerogen occurs as coatings on the larger mineral grains as well as stringlike concentrations and globules along laminae.

X-Ray diffraction analyses show little mineralogical variation between shale samples. Detailed X-ray analysis of the shale interval from one of the core holes indicates the following mineralogy: chlorite, illite, feldspar, kaolinite, quartz, pyrite, calcite and dolomite. A series of X-ray diffractograms of 1-foot increments of shale from one of the cored intervals suggest that some minor vertical mineralogical changes occur within the interval (Figure 2). In general, there is an increase in calcite and dolomite and a decrease in the pyrite content from top to bottom.

Shale samples from the core hole were also analyzed for mineral composition using a scanning electron microscope (SEM). Uncoated square cut shale samples were mounted on aluminum stubs with silver paint and stored in a desiccator under vacuum until placed in the SEM. The SEM analyses were performed on an Etec-Auto Scan unit worked at 20 kilovolts. SEM mineral identifications are based on visual comparisons to standard reference images. Identifications have not been confirmed by microprobe analysis. Typical images observed are shown in Figure 3.

Figure 3A shows a dickite grain; a well-crystallized member of the kaolin group encased in a matrix of mixed-layered clays. Figure 3B shows pyrite occurring as closely packed clusters of pyritohedrons common to almost all of the scanned shale samples. Well structured sheets of kaolinite (Figure 3C) are also commonly observed associated with the undifferentiated mixed-layered clays. Amorphous appearing irregularly shaped zones of material (Figure 3D) are intimately associated with the mixed-layered clays and are interpreted to be organic matter. Other minerals identified using SEM include illite, halloysite, quartz and feldspar.

Fischer Assay

Shale samples collected from surface exposures and core samples from the drilling program were crushed and sized to produce representative 500 gram samples. All samples were submitted for analysis of shale oil content by modified Fischer Assay methods. Assays were performed at the Colorado School of Mines and the Alabama Mineral Research Institute. Average oil yields for samples in the four-county area range from 6.9 to 19.2 gal/t (Table I).

Whole Rock and Trace Metal Geochemistry

Chemical characterization of the Chattanooga Shale involved whole rock and trace metal analyses on shale samples having more than 7 gal/t oil yield from the four-county area. These analyses were done to ascertain the chemical character of the spent shale as it might affect the environment or add to the economic process.

Preliminary whole rock analyses of samples from 42 shale sections indicate an average shale composition of 43.33% SiO₂, 11.60% Al₂O₃ and 9.79% Fe₂O₃, with minor amounts of MgO, CaO, MnO, Na₂O, K₂O, TiO₂ and P₂O₅ (Table II). These analyses compare favorably to analyses of other Devonian organic shales, but the Chattanooga Shale samples of north Alabama and south-central Tennessee are anomalously lower in silica and higher in iron and titanium (Table III).

Ultimate and proximate analyses were also run on all shale samples having more than 7 gal/t oil. Average values are 1.12% moisture, 72.60% ash, 16.59% volatiles, 9.85% fixed carbon and 2,765 BTU's. Average elemental composition of the 42 sampled sections is 16.08% total carbon, 0.50% nitrogen, 6.57% sulfur, 1.85% hydrogen and 2.91% oxygen.

Trace metals examined during the characterization study include cobalt, chromium, molybdenum, nickel, vanadium and zinc. Uranium determinations were also made on each sample as part of evaluating the full energy resource potential of the shale (3). Average trace metal contents and value ranges for the 42 shale sections analyzed are given in Table III.

Organic Geochemistry

Rock eval pyrolysis analyses were made on nine samples of 13 gal/t plus rock from five locations within the study area (Table IV). Average total organic carbon content for the nine samples is 16.27 wt. % with an average hydrogen index of 323 mg hydrocarbon (HC)/g of organic carbon at an average pyrolysis temperature of 423°C. Free hydrocarbon averages 2.33 mg/g of rock for the nine samples, with an average residual hydrocarbon potential of 52.58 mg/g of rock. CO₂ produced from the kerogen pyrolysis is approximately 3.67 mg/g of rock for these samples.

The hydrocarbon fractions of five samples from three locations within the study area were also analyzed. Saturated hydrocarbon analyses average 5.2% paraffin, 0.80% isoprenoid and 94%

naphthene (Table V). Average composition of the extracted oil is 7.2% paraffins-naphthenes, 25.6% aromatics, 6.0% sulfur, 41.0% precipitated asphaltene, 16.8% eluted NSO's and 3.6% non-eluted NSO's (Table VI).

TABLE I

SAMPLE LOCATIONS AND AVERAGE OIL YIELD PER SAMPLE FOR CHATTANOOGA SHALE IN LIMESTONE AND MADISON COUNTIES, ALABAMA, AND GILES AND LINCOLN COUNTIES, TENNESSEE

<u>Sample Number</u>	<u>Oil Yield (g/t)</u>	<u>Sample Number</u>	<u>Oil Yield (g/t)</u>
LIM-1	11.1	GIL-10	19.2
LIM-2	9.8	GIL-11	15.7
LIM-3	15.5	GIL-12	15.7
LIM-4	13.1	GIL-13	14.7
LIM-5	11.5	GIL-14	14.8
MAD-1	10.4	GIL-15	15.5
MAD-2	11.9	LIN-1	19.2
MAD-3	8.7	LIN-2	14.2
MAD-5	14.3	LIN-3	12.0
MAD-6	11.6	LIN-4	9.7
MAD-7	12.0	LIN-5	6.9
MAD-8	11.9	LIN-6	16.5
GIL-1	15.5	LIN-7	16.7
GIL-2	18.2	LIN-8	16.9
GIL-3	19.2	LIN-9	11.3
GIL-4	14.3	LIN-10	11.5
GIL-5	15.6	LIN-11	14.7
GIL-6	15.2	LIN-12	11.0
GIL-7	16.6	LIN-13	14.5
GIL-8	14.8	LIN-14	13.6
GIL-9	11.5	LIN-15	12.1

TABLE II

WHOLE ROCK ANALYSES OF DEVONIAN SHALES (1, 6-9)

	<u>AL</u>	<u>WV</u>	<u>WV</u>	<u>TX</u>	<u>TN</u>	<u>OH</u>
	(percent)					
SiO ₂	43.33	56.92	58.39	50.3	49.30	60.65
Al ₂ O ₃	11.60	16.42	16.50	4.6	10.71	11.62
Fe ₂ O ₃	9.79	6.58	6.45	10.0	9.60	.36
MgO	1.61	1.54	1.70	2.6	1.22	1.90
CaO	.95	1.43	.82	7.4	.36	1.44
MnO	.02	.05	--	--	--	.04
Na ₂ O	.49	.68	.47	.29	.33	.60
K ₂ O	3.98	3.65	3.83	1.6	4.03	3.10
TiO ₂	1.26	.72	.70	--	.69	.62
P ₂ O ₅	.25	.01	.14	--	.12	.18
LOI	26.81	--	--	--	23.0	19.01

A gas chromatograph of the C₁₅₊ fraction of the saturated hydrocarbon component indicates that the major compound distribution, C₁₅ to C₂₀, makes up 68.9% of the total fraction

(Figure 4).

TABLE III
TRACE ELEMENTS IN DEVONIAN SHALE (1, 7, 10)

	Alabama		Texas	Tenn.
	Range (ppm)	Avg. (ppm)	Avg. (ppm)	Avg. (ppm)
Co	80-325	134	140	22
Cr	70-140	97	55	69
Mo	100-530	320	76	71
Ni	160-890	320	490	89
V	210-680	342	210	200
Ti	3000-10000	7341	1200	1900
Zn	50-1100	300	92	--
U	10-36	20	--	51

TABLE IV
ROCK EVAL PYROLYSIS RESULTS

Sample Number	Tmax (°C)	S ₁ (mg/g)	S ₂ (mg/g)	S ₃ (mg/g)	T. O. C. (wt %)	Hydrogen Index
MAD-8A	429	2.32	49.04	2.16	16.05	305
LIM-3A	422	1.78	47.73	2.82	15.40	311
LIM-3B	422	1.70	40.89	2.46	13.31	308
LIM-4B	421	2.11	50.08	4.83	17.12	296
GIL-10A	422	2.50	56.63	4.51	17.92	316
LIN-1-83-1	422	3.45	67.53	3.15	17.94	376
LIN-1-83-2	422	2.01	44.29	4.89	16.42	270
LIN-1-83-3	423	2.66	59.52	3.52	15.65	380
LIN-1-83-4	423	2.44	57.51	4.67	16.58	346

Tmax - Temperature index (degrees Celsius)
 S₁ - Free hydrocarbons (mg HC/g of rock)
 S₂ - Residual hydrocarbon potential (mg HC/g of rock)
 S₃ - CO₂ produced from kerogen pyrolysis (mg CO₂/g of rock)
 T. O. C. - Total organic carbon (wt %)
 Hydrogen Index - mg HC/g organic carbon

TABLE V
SATURATE HYDROCARBON ANALYSES: SUMMARY OF PARAFFIN-NAPHTHENE DISTRIBUTION

Sample Number	Paraffin (%)	Isoprenoid (%)	Naphthene (%)
MAD-8A	4.6	0.4	95.0
LIM-3A	6.2	1.0	92.8
LIM-3B	6.2	1.1	92.7
LIN-1-83-1	4.7	0.7	94.6
LIN-1-83-2	5.0	0.8	94.1
LIN-1-83-3	6.1	1.0	93.0
LIN-1-83-4	3.9	0.6	95.5

Whole oil characterization was performed using gas chromatographic/mass spectrometric (GC/MS) techniques. The whole oil analysis by GC/MS is presented in Figure 5. Major compounds and isomers identified in the whole oil samples are listed in Table VII. Compound identification is

based on the best fit of 31,331 spectra, available standards and evaluation by a mass spectral analyst. The concentration of each compound or isomer is calculated in ppm of the whole oil (weight/weight). Major components of the GC/MS scan are C₁₄ (974 ppm), C₁₅ (1,048 ppm), C₁₆ (1,069 ppm), C₁₇ (868 ppm), Dibenzothiophene (1,309 ppm) and Methylbenzothiophene isomer (836 ppm).

TABLE VI
COMPOSITION OF C₁₅₊ EXTRACTS

Sample Number	Paraffin-Naphthene (%)	Aromatic (%)	Sulfur (%)	Precipitated Asphaltene (%)	Eluted NSO's (%)	Non-eluted NSO's (%)
MAD-8A	11.0	45.7	4.2	11.7	25.9	1.5
LIM-3A	4.2	13.4	3.5	65.1	7.7	6.1
LIM-3B	3.9	13.3	6.3	65.8	6.9	4.0
LIN-1-83-1	9.1	30.6	2.6	36.6	18.9	2.6
LIN-1-83-2 ^a	3.4	10.2	10.9	57.8	13.2	4.8
LIN-1-83-3	10.1	35.4	3.6	26.8	23.2	0.9
LIN-1-83-4	8.4	30.8	10.9	23.2	21.5	5.3

a. Average of two separate sample fraction analyses.

TABLE VII
WHOLE OIL COMPOUND IDENTIFICATION

Scan Number	Compound Identification	(ppm)
832	Tetralin	54
927	n-C ₁₃	563
984	Dimethyltetralin isomer	25
1014	n-C ₁₄	974
1055	C ₂ -Alkyl-naphthalene isomer	462
1094	n-C ₁₅	1048
1170	n-C ₁₆	1069
1213	C ₂ -Alkylbiphenyl isomer	723
1242	n-C ₁₇	868
1309	n-C ₁₈	482
1314	Dibenzothiophene	1309
1373	n-C ₁₉	331
1381	Methylbenzothiophene isomer	836
1411	2-Methylphenanthrene	243
1458	C ₂ -Alkyldibenzothiophene isomer	296
1493	C ₂ -Alkylphenanthrene isomer	189
1611	C ₃ -Alkylphenanthrene isomer	69
1654	n-C ₂₄	67

Non-Destructive Analyses

Non-destructive analytical determinations during this phase of investigation of the Devonian Chattanooga Shale, have included energy dispersive X-ray analyses (EDS) and ¹³C neutron magnetic resonance analyses (NMR) (1, 3).

EDS analyses of five different depth intervals of Chattanooga Shale from core hole #8, Madison County, Alabama, were performed on a TN2000 energy dispersive X-ray analysis unit. Eight scans were run for 300 sec each at a tilt angle of 45° and a working distance of 18 mm to 20 mm. Magnification levels varied from 20X to 8,000X.

Major and minor elements indicated by the EDS analyses are Si, Al, K, Ca, Fe, S, Ti and Mg (Table VIII). The elemental identifications show good correlation to previously run X-ray analyses and SEM photomicrograph interpretations of the same shale samples.

TABLE VIII

QUALITATIVE ELEMENT IDENTIFICATION, CHATTANOOGA SHALE, CORE HOLE #8,
MADISON COUNTY, ALABAMA

Sample Depth (ft.)	Mineral Identification	Elemental Constituents	
		K α Line	K β Line
30.5	quartz	Fe, Si	
31.5	pyrite	Al, Fe, K, S, Si	Fe, K
31.5	clay mineral	Al, Fe, Si	
32.5	pyrite	Al, Fe, K, S, Si	Fe
34.8	clay mineral	Al, Fe, K, Mg, Si, Ti	Fe, K
34.8	clay mineral	Al, Fe, K, S, Si	Fe, K
34.8	clay matrix	Al, Fe, K, S, Si	Fe, K
36.7	clay matrix	Al, Ca, Fe, K, Si, Ti	Ca, Fe, Ti

¹³C NMR spectra of samples from core hole #9, Madison County, Alabama (Figures 6 and 7), compare favorably to other eastern oil shales in most aspects. However, carbon aromaticity values, *f_a*, are slightly higher (0.53 to 0.58) than most eastern shales (4). Alabama Devonian oil shale contains approximately 0.51 aliphatic carbon, of which 0.25 appears to be convertible to oil (1). This conversion to oil relative to organic carbon content of the shale appears to be in agreement with data given by Miknis and Smith (1982) (5).

SUMMARY

Based on the physical and chemical data obtained to date, the Devonian oil shale rock of north Alabama and south-central Tennessee appears to offer an attractive potential for future resource development. The shale rock appears to have formed in a restrictive marine environment which provided opportunity for the accumulation of marine organic matter to form sufficient kerogen. The shale contains approximately 18% to 22% organic matter which is primarily kerogen. The kerogen has a relatively high H:C ratio indicative of an alginite and/or exinite source (Type 1 and Type II kerogen) and a high proportion of alkane and saturated ring hydrocarbons. However, a few samples have low H:C ratio values and are interpreted to have been formed in a shallow water oxidizing environment. Also, there is a possibility that these low H:C values may represent mixtures of terrestrial and marine organic material suggesting lateral facies changes of the rock from marine to near shore depositional environments. Trace metal values for both the whole rock and the shale oil fraction indicate a generally high V:Ni ratio, also indicative of a marine environment. Other trace metal values are in good agreement with data from other Devonian shales. Throughout the north Alabama and south-central Tennessee study area, the average oil yield from the shale is 13.9 gallon per ton. The highest oil yield values were obtained from the middle and upper parts of the shale sequence. Based on the crude oil composition diagram (11), the Alabama-Tennessee shale oil is classified as a aromatic-intermediate oil. Estimated reserves of inplace shale oil resources in the principal study area, under less than 200 feet of overburden, exceeds 12.5 billion barrels.

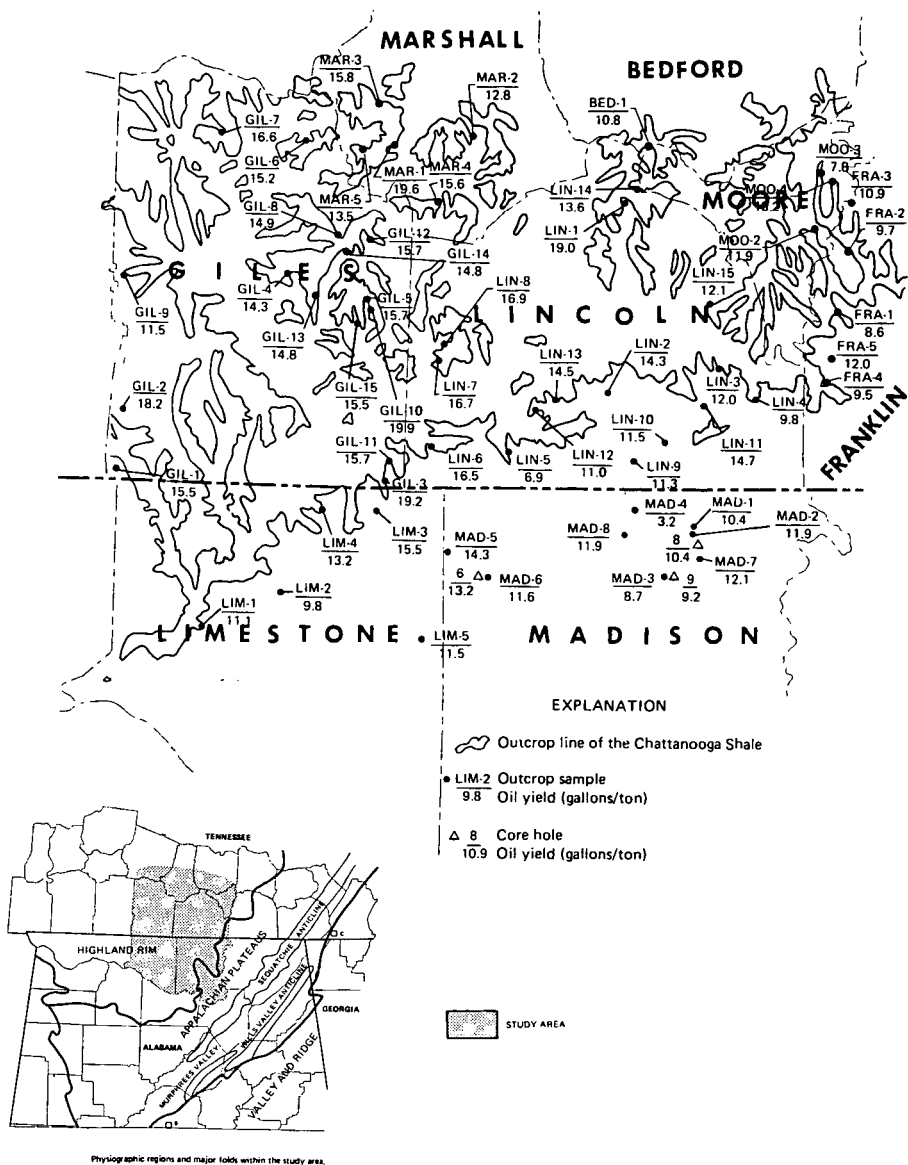


Figure 1.--Study area and general outcrop line of the Chattanooga Shale, north Alabama and south-central Tennessee.

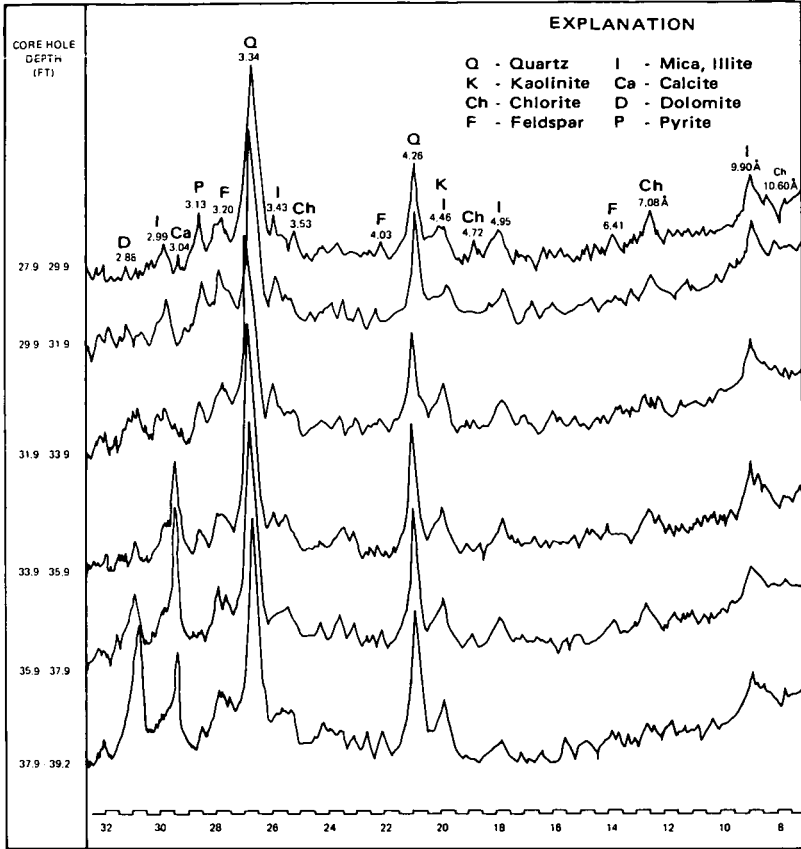


Figure 2.--X-ray diffractogram of Chattanooga Shale, core hole #8, Madison County, Alabama.

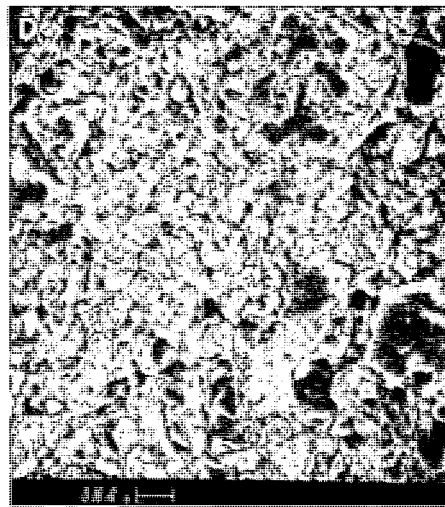


Figure 3.--Scanning electron photomicrographs of selected samples of Chattanooga Shale, core hole #8, Madison County, Alabama.

SATURATE HYDROCARBON ANALYSIS
NORMALIZED PARAFFIN DISTRIBUTION

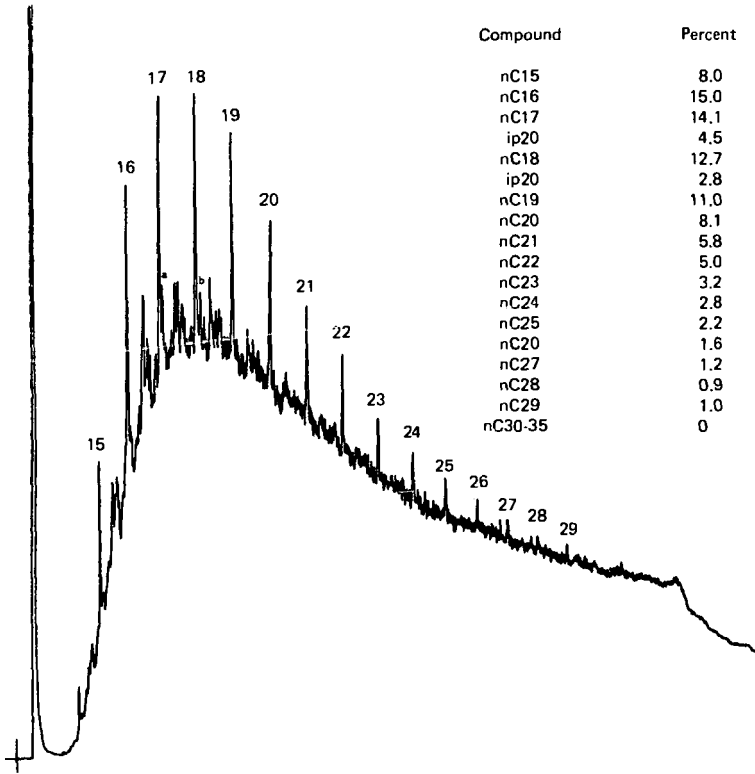


Figure 4.--Saturate hydrocarbon analysis-normalized paraffin distribution.

GC/MS WHOLE OIL ANALYSIS OF DEVONIAN SHALE, ALABAMA

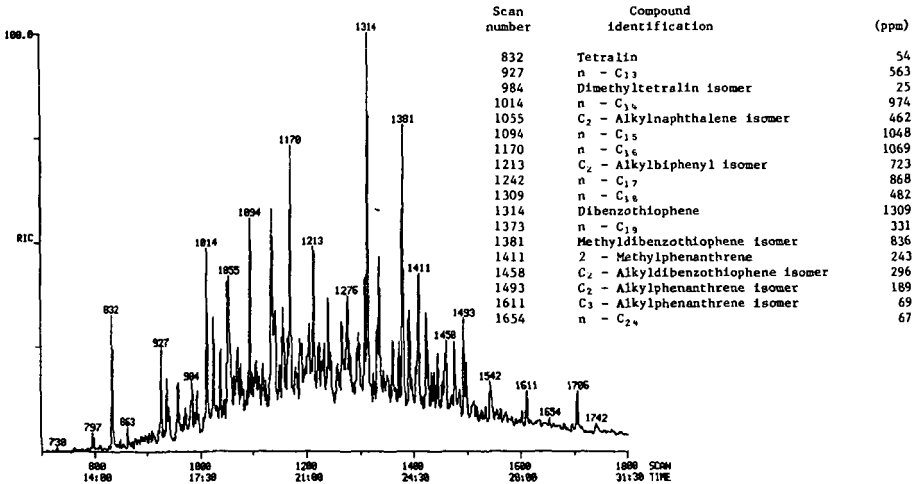


Figure 5.--GC/MS whole oil analysis of Devonian Shale, Alabama.

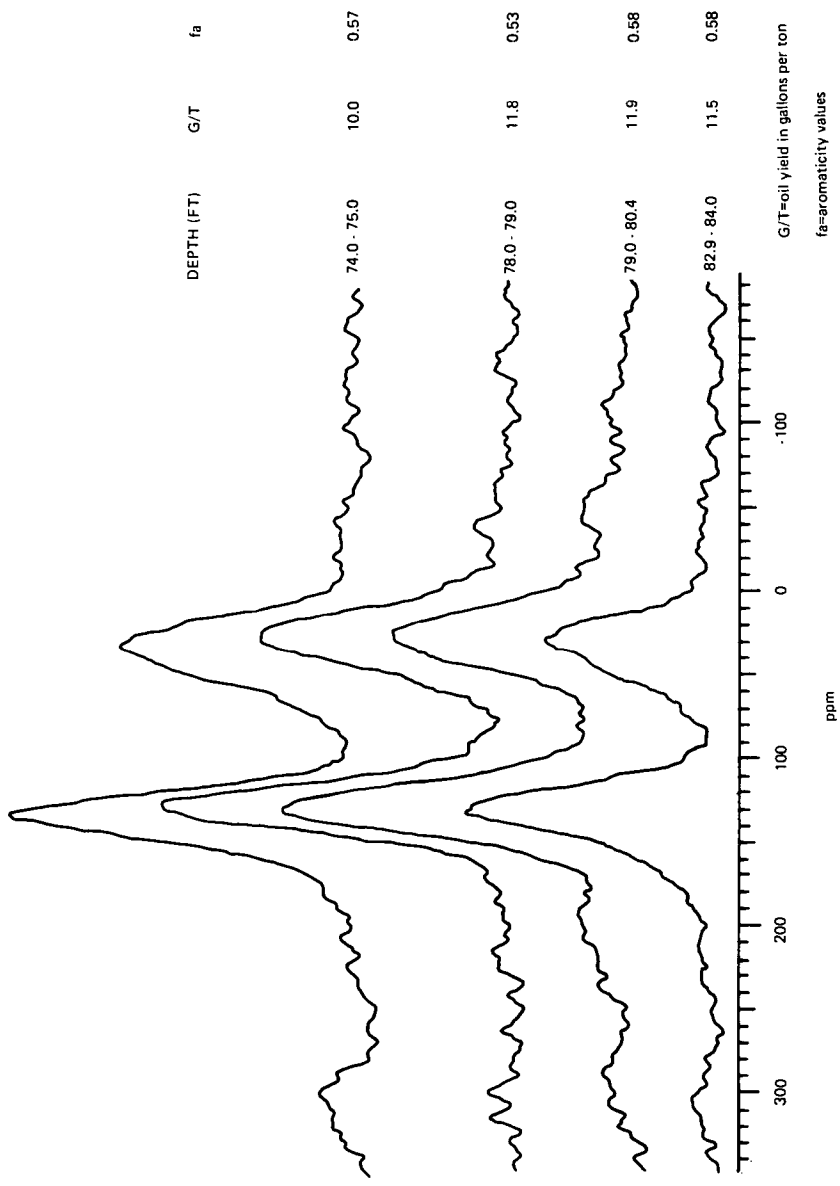


Figure 6. -- ^{13}C NMR spectra of Chattanooga Shale samples, core hole #9, Madison County, Alabama.

DEVONIAN OIL SHALES

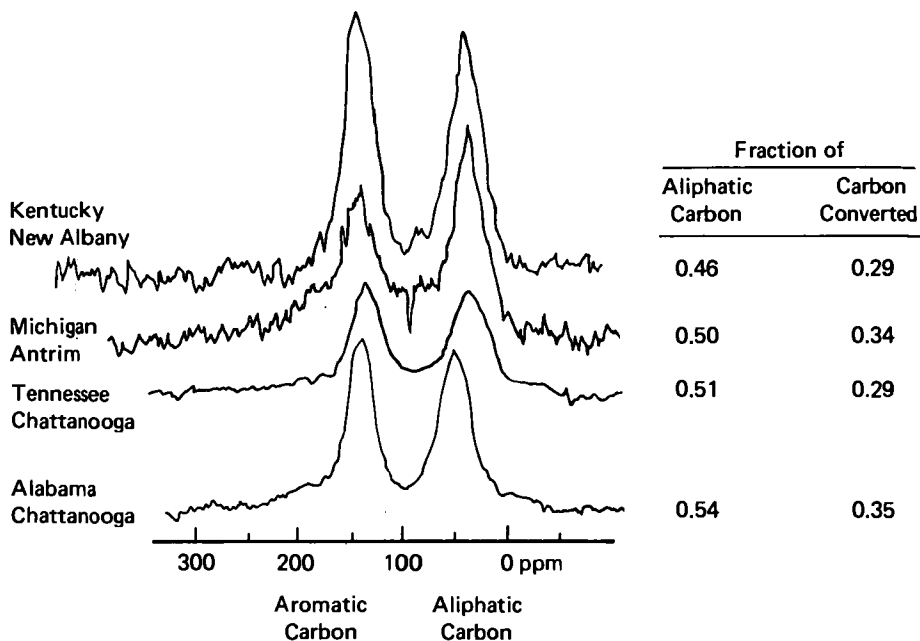


Figure 7.--Comparison of solid state ^{13}C NMR spectra for eastern Devonian Shales (1,5).

LITERATURE CITED

- (1) Rheams, K. F., Neathery, T. L., Rheams, L. J. and Copeland, C. W., Proc. 2nd Eastern Oil Shale Symp., in press.
- (2) Rheams, K. F., Neathery, T. L., Copeland, C. W. and Rheams, L. J., Geol. Soc. Am. Abs. with Programs, 15 (2), 68 (1983).
- (3) Rheams, K. F., Neathery, T. L., Copeland, C. W. and Rheams, L. J., AAPG Bull. 67 (3), 539 (1983).
- (4) Miknis, F. P., pers. comm. (1983).
- (5) Miknis, F. P. and Smith, J. W., Proc. 15th Ann. Oil Shale Symp. (1982).
- (6) Bialobok, S. J., Lamey, S. C. and Sumartojo, J., Proc. 1st Eastern Gas Shales Symp., 297 (1978).
- (7) Vine, J. D., Tourtelot, E. B. and Keith, J. F., USGS Bull. 1214-H, 38 (1969).
- (8) Conant, L. C. and Swanson, V. E., USGS Prof. Paper 357, 91 (1961).
- (9) Pettijohn, F. J., Sedimentary Rocks, 2nd ed., 718 (1957).
- (10) Vine, J. D., USGS Bull. 1214-G, 32 (1969).
- (11) Tissot, B. P. and Welte, D. H., Petroleum Formation and Occurrence, 538 (1978).

SYMPOSIUM ON CHARACTERIZATION AND CHEMISTRY OF OIL SHALES
PRESENTED BEFORE THE DIVISIONS OF FUEL CHEMISTRY AND
PETROLEUM CHEMISTRY, INC.
AMERICAN CHEMICAL SOCIETY
ST. LOUIS MEETING, APRIL 8 - 13, 1984

REACTION RATE KINETICS FOR IN SITU COMBUSTION RETORTING OF
MICHIGAN ANTRIM OIL SHALE

By

M. Rostam-Abadi
Illinois State Geological Survey, Champaign, Illinois 61820
and
R. W. Mickelson
Chemical Engineering Department
Wayne State University, Detroit, Michigan 48202

ABSTRACT

The intrinsic reaction rate kinetics for the pyrolysis of Michigan Antrim oil shale and the oxidation of the carbonaceous residue of this shale have been determined using a thermogravimetric analysis method. The kinetics of the pyrolysis reaction were evaluated from both isothermal and nonisothermal rate data. The reaction was found to be second-order with an activation energy of 252.2 kJ/mole, and with a frequency factor of $9.25 \times 10^{15} \text{ sec}^{-1}$. Pyrolysis kinetics were not affected by heating rates between 0.01 to 0.67°K/s.

No evidence of any reactions among the oil shale mineral constituents was observed at temperatures below 1173°K. However, it was found that the presence of pyrite in oil shale reduces the primary devolatilization rate of kerogen and increases the amount of residual char in the spent shale.

Carbonaceous residues which were prepared by heating the oil shale at a rate of 0.166°K/s to temperatures between 923°K and 1073°K, had the highest reactivities when oxidized at 0.166°K/s in a gas having 21 volume percent oxygen.

Oxygen chemisorption was found to be the initial precursor to the oxidation process. The kinetics governing oxygen chemisorption is

$$\frac{dX}{dt} = 176 e^{17.9X} e^{-(42+104X)/RT} (\text{sec}^{-1})$$

where X is the fractional coverage.

The oxidation of the carbonaceous residue was found also to be second-order. The activation energy and the frequency factor determined from isothermal experiments were 147 kJ/mole and $9.18 \times 10^7 \text{ sec}^{-1}$ respectively, while the values of these parameters obtained from a nonisothermal experiment were 212 kJ/mole and $1.5 \times 10^{13} \text{ sec}^{-1}$. The variation in the rate constants is attributed to the fact that isothermal and nonisothermal analyses represent two different aspects of the combustion process.

SYMPOSIUM ON CHARACTERIZATION AND CHEMISTRY OF OIL SHALES
PRESENTED BEFORE THE DIVISIONS OF FUEL CHEMISTRY AND
PETROLEUM CHEMISTRY, INC.
AMERICAN CHEMICAL SOCIETY
ST. LOUIS MEETING, APRIL 8 - 13, 1984

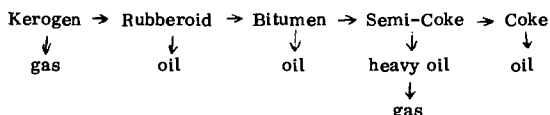
ANALYSIS OF PYROLYSIS KINETICS OF EASTERN OIL SHALES

By

M. S. Shen, L-S. Fan* and K. H. Casleton
Morgantown Energy Technology Center, P. O. Box 880, Morgantown, West Virginia 26505

INTRODUCTION

The kinetics of pyrolysis of Western oil shale has been studied by a number of investigators (1-6). Several reaction mechanisms have been proposed to account for the pyrolysis kinetics of Colorado shale. Hubbard and Robinson (4) postulated a two-step mechanism for the decomposition of kerogen to bitumen and subsequently bitumen to oil and gas. Johnson, et al. (5) concluded the following mechanism which was partially verified with experimental data:



Details of these mechanisms were documented in a review by Fisher (6). Relatively little is known regarding the pyrolysis kinetics of Eastern shale. The present work was undertaken to measure the rate of organic matter decomposition during pyrolysis of Kentucky Sunbury oil shale. Thermoanalytical methods are used to obtain the kinetics data. It should be noted, however, that the thermogravimetric analyzer (TGA) utilized in the present experiment is not equipped with G. C. or I. R. for gas composition measurement. Only the weight variation can be obtained from the TGA. Thus, the model developed here is only for the weight variation of solid reactants in the course of pyrolysis. Furthermore, the proposed model does not require consideration of the activation energy distribution function for the reactions. By heating the oil shale, gaseous and liquid products are formed which result from the many different reactions involving these components. The reported pyrolysis kinetics are, thus, an average for these many different reactions that take place. The representation of the decomposition rate would become very complex if all the mechanistic reactions were to be identified and accounted for. Thus, a global first order rate expression is assumed for simplicity's sake (2, 3, 7). For this reason, the activation energy and the frequency factor are the only "representative" kinetic values for a complicated reaction system. These values are, however, useful from the engineering standpoint of oil shale retorting and can be used in a mathematical model to represent the process.

EXPERIMENTAL

The oil shale used in the present study was Kentucky Sunbury shale. Ultimate analysis (wt %) of the oil shale: hydrogen - 1.55; nitrogen - 0.53; sulfur - 3.41; total carbon - 14.07; oxygen - 3.30; moisture - 2.18; ash - 74.96; with a Fischer Assay oil yield 9.3 gallons/ton. The samples were crushed and sieved to 16/20 U. S. mesh.

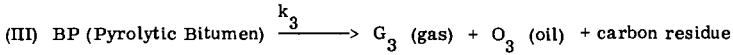
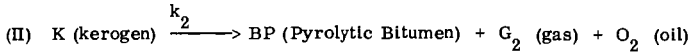
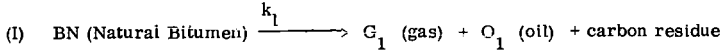
A Du Pont 951 thermogravimetric balance interfaced to a Du Pont 1090 thermal analyzer was used to obtain the weight-loss data as a function of time and temperature. The TGA experiments were carried out by heating the sample from ambient temperature to 600°C. The heating rates of 5°, 10°, 15° and 20°C/min were employed. Differential scanning calorimetric (DSC) data were obtained with a Du Pont cell base and the 1090 thermal analyzer. An aluminium pan containing the sample was placed on the raised platform in the DSC cell and an empty pan was placed on the reference platform. A known weight of sample was subjected to a linear heating rate in a flow of nitrogen or CO₂. DSC scans for the samples were obtained from 150° to 600°C at a linear heating rate of 10°C/min. A non-isothermal technique was utilized for determining the kinetics of oil shale pyrolysis.

* Permanent Address: Department of Chemical Engineering, Ohio State University, Columbus, Ohio 43210.

RESULTS AND ANALYSIS

Scrima, et al. (8) compared the bitumen removed thermally from oil shale (the shale sample was heated to 300°C at 28°C/min) with those removed by benzene extraction. Based on thermal chromatography of Green River oil shale, the two chromatograms appear identical, demonstrating that natural bitumen could be thermally removed at about 300°C.

Consider the following pyrolysis mechanism for oil shale which consists of two decomposable materials, i. e., bitumen (natural) and kerogen:



Reaction (I) takes place at a temperature from 100°C to 300°C and reactions (II) and (III) take place at temperatures beyond 300°C. Assuming first order kinetics for each step of reaction, we have

$$\frac{dW_{\text{BN}}}{dt} = -k_1 W_{\text{BN}} \quad 1)$$

$$\frac{dW_{\text{k}}}{dt} = -k_2 W_{\text{k}} \quad 2)$$

$$\frac{dW_{\text{BP}}}{dt} = k_2 f W_{\text{k}} - k_3 W_{\text{BP}} \quad 3)$$

where W_{BN} , W_{k} and W_{BP} are the weight of natural bitumen, kerogen and pyrolytic bitumen, respectively; f is the weight fraction of the decomposed kerogen which yields bitumen (2).

For a non-isothermal reaction condition in which the heating rate is linear, we have

$$\frac{dT}{dt} = \text{Hr} \quad 4)$$

where Hr is the heating rate. Equations 1 through 3 yield

$$\frac{dW_{\text{BN}}}{dt} = \frac{-k_1}{\text{Hr}} W_{\text{BN}} \quad 5)$$

$$\frac{dW_{\text{k}}}{dT} = \frac{-k_2}{\text{Hr}} = W_{\text{k}} \quad 6)$$

$$\frac{dW_{\text{BP}}}{dT} = \frac{1}{\text{Hr}} (k_2 f W_{\text{k}} - k_3 W_{\text{BP}}) \quad 7)$$

The Arrhenius forms for the variation of k_1 , k_2 , k_3 with temperature are

$$k_1 = k_{10} \exp\left(\frac{-E_1}{RT}\right) \quad 8)$$

$$k_2 = k_{20} \exp\left(\frac{-E_2}{RT}\right) \quad 9)$$

$$k_3 = k_{30} \exp\left(\frac{-E_3}{RT}\right) \quad 10)$$

Thus, Equations 5 through 7 can be rewritten as

$$\frac{dW_{BN}}{dT} = - \frac{k_{10}}{Hr} \exp \left(\frac{-E_1}{RT} \right) W_{BN} \quad (11)$$

$$\frac{dW_{BN}}{dT} = - \frac{k_{20}}{Hr} \exp \left(\frac{-E_2}{RT} \right) W_k \quad (12)$$

$$\frac{dW_{BP}}{dT} = \frac{1}{Hr} \left(k_{20} \exp \frac{-E_2}{RT} f W_k - k_{30} \exp \frac{-E_3}{RT} W_{BP} \right) \quad (13)$$

The boundary conditions for Equations 11 through 13 are, respectively,

$$T = 100^\circ\text{C}: W_{BN} = W_{BNO}; \quad T = 300^\circ\text{C}: W_k = W_{k0}, \quad W_{BP} = 0. \quad (14)$$

The total weight of the sample W is related to W_{BN} , W_k and W_{BP} by

$$W = W_i + W_{BN} + W_k + W_{BP} \quad (15)$$

Equations 11 through 13 subject to the boundary conditions of Equation 14 require a numerical scheme for solution.

Figure 1 shows an oil shale thermal histogram of weight loss and derivative weight loss versus temperature in a nitrogen flow at a heating rate of $5^\circ\text{C}/\text{min}$. There are two major peaks from the derivative weight loss - temperature curve. The first peak begins about 20°C and ends about 100°C while the second peak begins about 350°C and ends about 550°C . It is likely that the first peak represents the devolatilization of water, while the second peak represents the decomposition of pyrolytic bitumen. The differential weight variation between two peaks is considered to be the decomposition of natural bitumen and kerogen. The natural bitumen was extracted by benzene and the weight percent of natural bitumen in the oil shale was measured to be $\sim 2\%$. There is about 2% weight loss which occurred from 100°C to $\sim 300^\circ\text{C}$. This weight loss suggests that nearly all the natural bitumen decomposes in this low temperature range. Similarly, Figures 2, 3 and 4 show the histograms of weight loss and derivative weight loss versus temperature for the heating rate of $10^\circ\text{C}/\text{min}$, $15^\circ\text{C}/\text{min}$ and $20^\circ\text{C}/\text{min}$, respectively. The heating rate has moderate effects on the variation of weight loss. The results indicate the systematic shift in the rate maxima to lower temperatures with decreasing heating rate. Figures 5 and 6 summarize the experimental results on extent of conversion over the temperature range 165°C to 280°C and 365°C to 550°C , respectively.

The experimental results given in Figures 1 through 4 support the basic pyrolysis mechanism proposed in the present kinetics study. Figures 1 through 4 also show the comparison between the model prediction and the experimental data for the weight loss-versus-temperature relationship. The frequency factor and activation energy based on the best fit of the model to the experimental data are found to be

$$k_{10} = 1,040 \text{ 1/min}; \quad E_1 = 33.5 \text{ kJ/mole}$$

$$k_{20} = 900 \text{ 1/min}; \quad E_2 = 41.9 \text{ kJ/mole}$$

$$k_{30} = 1.2 \times 10^{12} \text{ 1/min}; \quad E_3 = 173.7 \text{ kJ/mole}$$

$$f = 0.9$$

Note that in the calculation based on the model, the weight loss due to water devolatilization is assumed to be known. As can be seen from these figures, the comparison is satisfactory. The closeness of the fit is a good indication of the adequacy of assuming a first order decomposition mechanism. It is noted that the values for frequency factor and activation energy obtained for kerogen decomposition are comparable to those reported for Colorado oil shale (2, 3, 5, 7).

Figure 7 shows DSC thermal histogram. The data were analyzed by Borchardt/Daniels DSC Kinetics (1957) Program. A reaction order of 0.88 with $E_3 = 151 \text{ kJ/mole}$ were obtained. E_3 would be 160 kJ/mole assuming a first order reaction. These results compare favorably with TGA

Sample: KENTUCKY SHALE
Size: 60.32 mg
Rate: 5 DEG/MIN 100CC N2/MIN

TGA

Date: 8-Oct-83 Time: 11:50:57
File: SUNBURY.01
Operator: M. SHEN

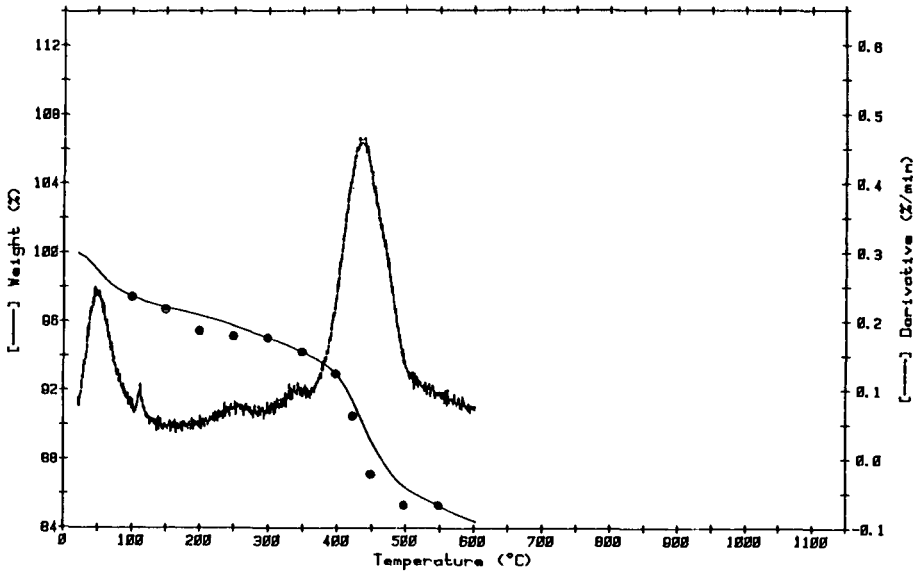


Figure 1. Non-isothermal histogram of weight loss versus temperature at 5°C/min.

Sample: KENTUCKY SHALE
Size: 59.96 mg
Rate: 10 DEG/MIN 100CC N2/MIN

TGA

Date: 8-Oct-83 Time: 22:45:45
File: SUNBURY.07
Operator: M. SHEN

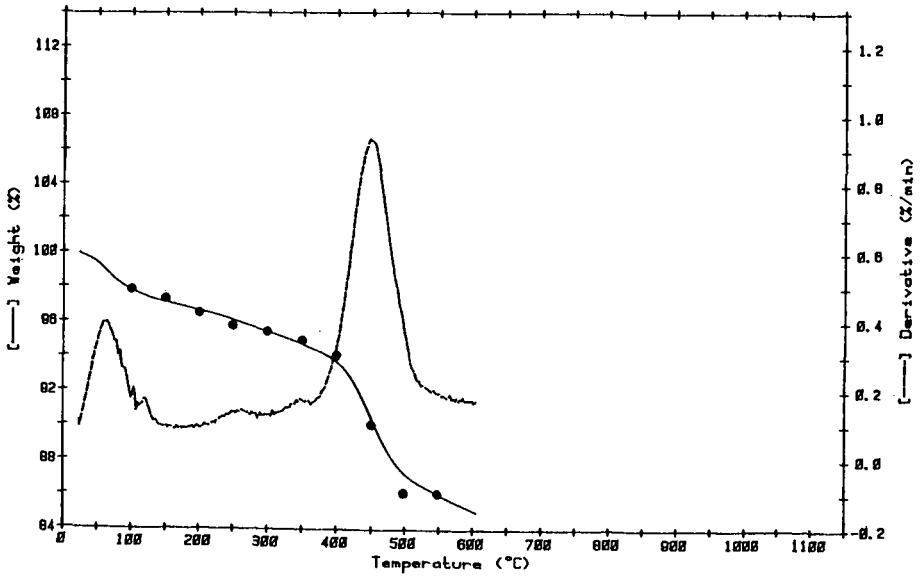


Figure 2 Non-isothermal histogram of weight loss versus temperature at 10°C/min

Sample: KENTUCKY SHALE
Size: 88.55 mg
Rate: 15 DEG/MIN 100CC N2/MIN

TGA

Date: 6-Oct-83 Time: 20:50:12
File: SUNBURY.08
Operator: M. SHEN

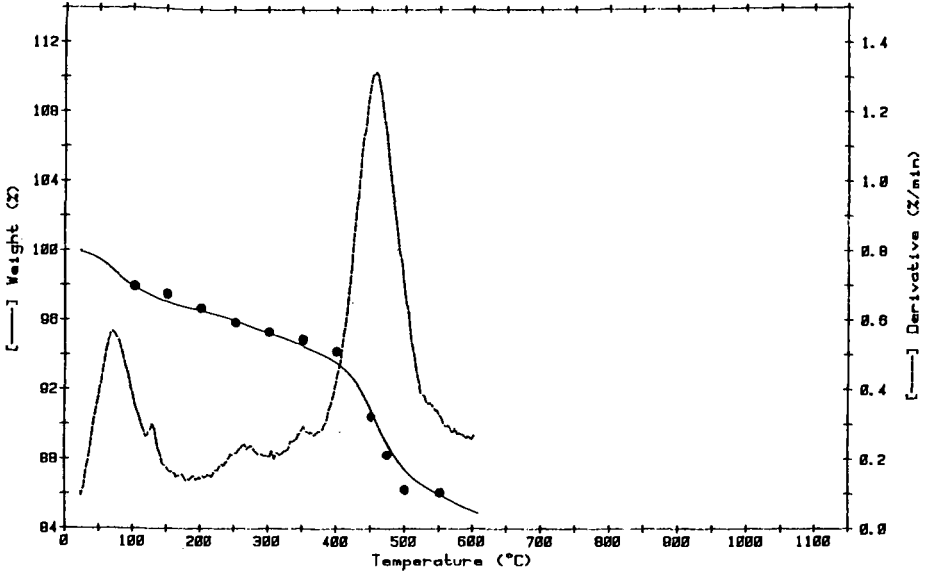


Figure 3 Non-isothermal histogram of weight loss versus temperature at 15°C/min

Sample: KENTUCKY SHALE
Size: 68.83 mg
Rate: 20 DEG/MIN 100CC N2/MIN

TGA

Date: 6-Oct-83 Time: 19:44:14
File: SUNBURY.05
Operator: M. SHEN

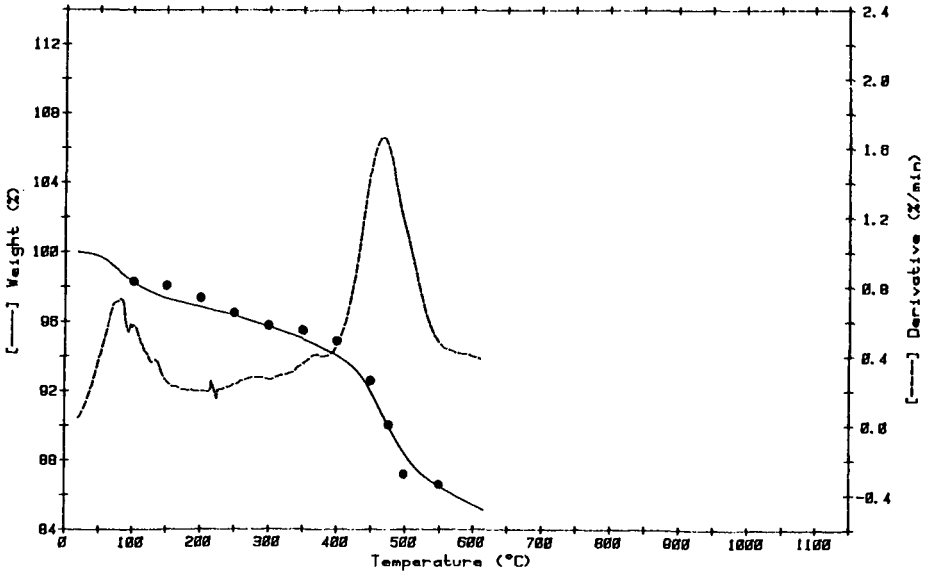


Figure 4 Non-isothermal histogram of weight loss versus temperature at 20°C/min

Sample: KENTUCKY SHALE

Date: 6-Oct-83 Time: 19:44:14

TGA

Program: TGA Kinetics V1.0

Operator: M. SHEN
Plotted: 7-Oct-83 10:12:10

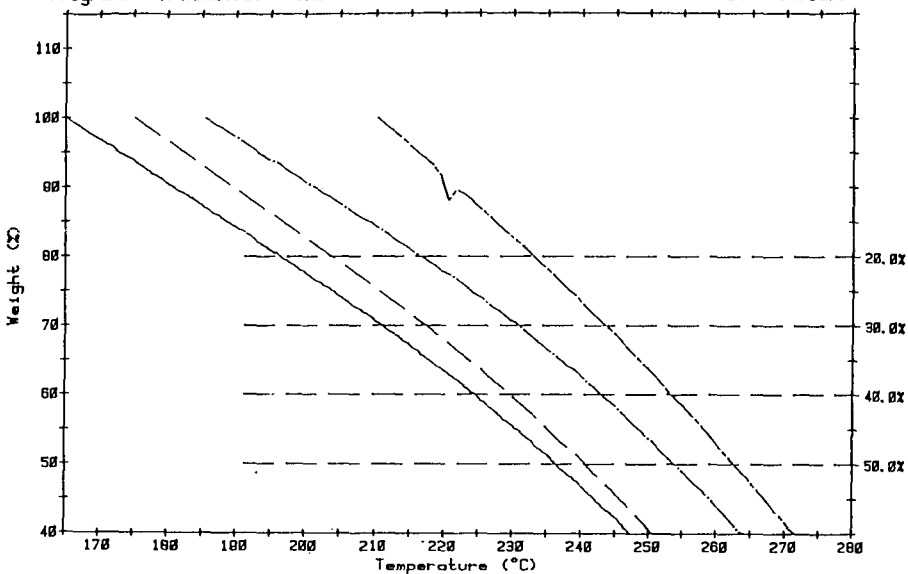


Figure 5 Extent of conversion versus temperature at various heating rates

Sample: KENTUCKY SHALE

Date: 6-Oct-83 Time: 19:44:14

TGA

Program: TGA Kinetics V1.0

Operator: M. SHEN
Plotted: 7-Oct-83 10:34:32

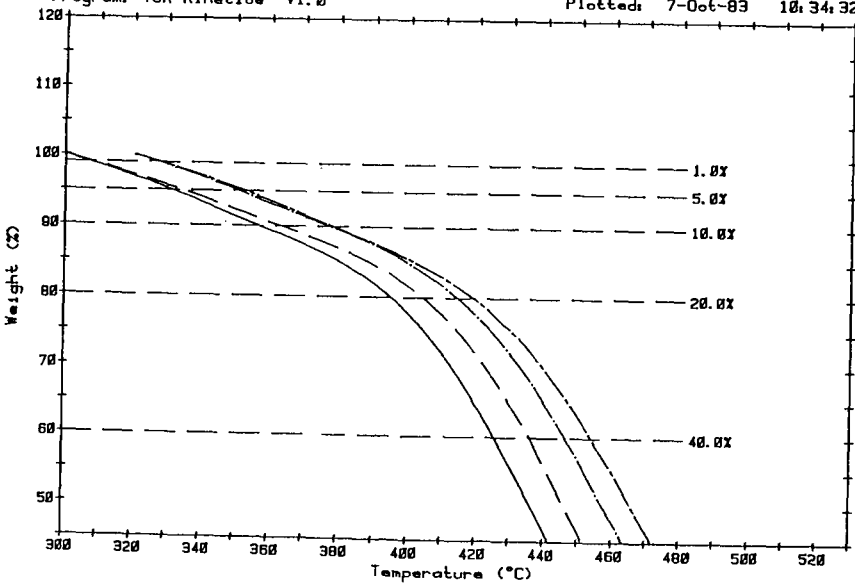


Figure 6 Extent of conversion versus temperature at various heating rates

Sample: SF-KENTUCKY SHALE
 Size: 26.94 MG
 Rate: 10 DEG/MIN 75CC C02/MIN
 Program: DSC Kinetics V1.0
 Date: 6-Oct-83 Time: 16:32:37
 File: INSUNBURY.04
 Operator: M. SIEN
 Plotted: 6-Oct-83 19:48:26

DSC

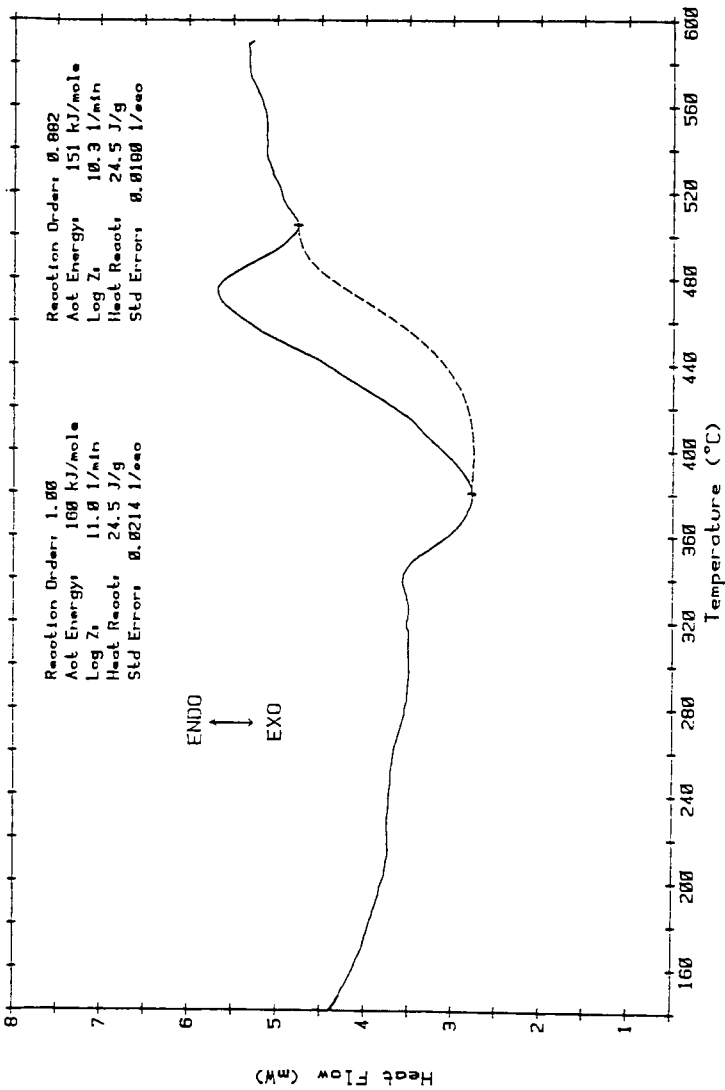


Figure 7 DSC curve for Kentucky Oil Shale at 10°C/min

data reported here.

NOMENCLATURE

A_1	frequency factor for bitumen decomposition
A_2	frequency factor for kerogen decomposition
E_1	activation energy for bitumen decomposition
E_2	activation energy for kerogen decomposition
f	fraction of mass of decomposed kerogen that yields bitumen
Hr	heating rate
k_1	kinetic constant for bitumen decomposition
k_2	kinetic constant for kerogen decomposition
R	gas constant
t	time
T	temperature
W_1	weight of bitumen
W_2	weight of kerogen
W_{10}	initial weight of bitumen
W_{20}	initial weight of kerogen
W_i	weight of inert material
W	total weight of oil shale

LITERATURE CITED

- (1) Allred, V. D. , Chem. Eng. Prog. , 62, 55-60 (1966).
- (2) Borchardt, H. L. and Daniels, F. , J. Am. Chem. Soc. , 79, 41 (1957).
- (3) Braun, R. L. and Rothman, A. J. , Fuel, 54, 129-131 (1975).
- (4) Campbell, J. H. , Koskinas, G. and Stout, N. , Fuel, 57, 372-376 (1978).
- (5) Fisher, E. R. , "A Review of Oil Shale Decomposition Kinetics", Wayne State University Report (1977).
- (6) Hubbard, A. B. and Robinson, W. E. , Rep. Invest. U. S. Bur. Mines, No. 4744 (1950).
- (7) Johnson, W. F. , Walton, D. K. , Keller, H. H. and Couch, E. J. , J. Colo. Sch. Mines Q. , 70, 237-272 (1975).
- (8) Scrima, D. A. , Yen, T. F. and Warren, P. L. , Energy Sources, Vol. 1, No. 3, 321-336 (1974).
- (9) Shih, S. M. and Sohn, H. Y. , Ind. Eng. Chem. Process Des. Dev. , 19, 420-426 (1980).

SYMPOSIUM ON CHARACTERIZATION AND CHEMISTRY OF OIL SHALES
PRESENTED BEFORE THE DIVISIONS OF FUEL CHEMISTRY AND
PETROLEUM CHEMISTRY, INC.
AMERICAN CHEMICAL SOCIETY
ST. LOUIS MEETING, APRIL 8 - 13, 1984

EPR AND FTIR STUDY OF METALS IN BITUMEN AND MINERAL COMPONENTS OF
CIRCLE CLIFFS, UTAH TAR SAND

By

R. A. Shepherd and W. R. M. Graham

Department of Physics, Texas Christian University, P. O. Box 32915, Fort Worth, Texas 76129

INTRODUCTION

The presence of certain metals in oil extracted from tar sands can have undesirable catalytic effects on refining and combustion. The cumulative effect of some of these metals on refining makes even trace amounts a serious problem. The technique of electron paramagnetic resonance (EPR) provides a sensitive means of detecting metal ions which exhibit the property of paramagnetism such as V^{4+} , Mn^{2+} and Fe^{3+} .

Numerous authors (1-4) have applied the technique to petroleum and observed an EPR spectrum which they attribute to the paramagnetic vanadium ion V^{4+} in the form of the vanadyl cation VO^{2+} bound in a porphyrin complex. Similar spectra have been observed for tar sand samples from the Athabasca deposit in Alberta, Canada (5, 6). Vanadium concentrations in various U. S. tar sands have been investigated by Branthaver and Dorrence (7) using optical colorimetry and UV spectroscopy. Using EPR on a tar sand sample from the P. R. Spring outcrop in Utah, Malhotra and Graham (8) have shown that no vanadium is present in the organic fraction in the V^{4+} state, but that there is inorganically bound vanadium in the clay fraction. This is consistent with the findings of Branthaver and Dorrence (7).

In the present study, the EPR technique has been applied to a tar sand sample originating from Circle Cliffs, Utah which, like P. R. Spring, is also one of the areas from which samples were taken for the Branthaver and Dorrence study (7). For Circle Cliffs, they reported the organic fraction to contain some vanadium but none that was porphyrin-bound.

PROCEDURE

The tar sand sample (USBM-3851) was separated into various fractions by Soxhlet extraction using the method described in (9). The whole tar sand was separated into an organic fraction (bitumen) and an inorganic fraction (mineral matter) using benzene. The bitumen was further separated using heptane into a heavy end fraction (asphaltene) and a light end fraction (petrolene).

EPR measurements were made by placing the various fractions into 3 mm O.D. quartz sample tubes in a rectangular TE_{102} mode cavity of a 9.1 GHz (Varian V-4500) spectrometer with 100 kHz magnetic field modulation.

The mineral matter was dried in an oven at 110°C for several hours. Fourier transform infrared (FTIR) spectra of this fraction were obtained by grinding a small sample of mineral with KBr in a 1:100 ratio (by weight) using a Wig-L-Bug, pressing the mixture into a pellet and scanning with a Nicolet 5-DXE FTIR spectrometer.

RESULTS AND DISCUSSION

The EPR spectrum of the asphaltene is shown in Figure 1. Aside from the strong free radical signal at $g=2.00$ common to all asphaltenes, the only other feature is a powder pattern spectrum characteristic of an ion with an electronic spin $S=1/2$ and a nuclear spin $I=7/2$, located at a site with axial symmetry. The spin Hamiltonian describing such a system is

$$H = g_{||} \beta S_Z H_Z + g_{\perp} \beta (S_X H_X + S_Y H_Y) + A_{||} S_Z I_Z + A_{\perp} (S_X I_X + S_Y I_Y) \quad 1)$$

$g_{||}$ and g_{\perp} are the components of the g -factor parallel and perpendicular to the symmetry axis Z and A and A are the corresponding components of the hyperfine splitting constant. The second order solution giving the line positions are

$$H_{||} (m) = H_{||} - \frac{A_{||}}{g_{||}\beta} m - \frac{A_{\perp}^2}{2H_{||} (g_{||}\beta)^2} [\Gamma (I+1) - m^2] \quad 2)$$

for

$$H_{\perp} (m) = H_{\perp} - \frac{A_{\perp}}{g_{\perp}\beta} m - \frac{A_{||}^2 + A_{\perp}^2}{4H_{\perp} (g_{\perp}\beta)^2} [\Gamma (I+1) - m^2] \quad 3)$$

The line positions measured from the spectrum in Figure 1 were fitted to Equations 2 and 3 and the values of the spin Hamiltonian determined. They are listed in Table I along with EPR data on several synthetic vanadyl porphyrins. A comparison indicates that the source of the EPR spectrum is vanadyl etioporphyrin. Etioporphyrin is one of the most common porphyrins found in tar sands, oil shale and petroleum (15).

TABLE I

EXPERIMENTAL EPR PARAMETERS FOR VARIOUS VANADYL PORPHYRINS

Complex	$g_{ }$	g_{\perp}	$A_{ }$ (mT)	A_{\perp} (mT)	Reference
Circle Cliffs asphaltene	1.962 (3)	1.986 (1)	17.20 (8)	6.08 (6)	Present work
VO Etioporphyrin	1.9629	1.9862	17.13	6.01	10
VO Porphin in triphenylene	1.964	1.985	17.4	5.9	11
VO Mesoporphyrin dimethyl ester	1.947	1.988	15.8	5.4	12
VO Octamethyltetrabenzoporphyrin	1.944	1.980	16.3	5.8	11
VO Tetrabenzoporphyrin	1.962	1.985	15.0	5.0	11
VO Tetrapyrindylporphyrin	1.961	1.984	15.7	5.4	11
VO Tetraphenylporphyrin	1.961	1.986	16.0	5.7	13
VO Phthalocyanine	1.966	1.989	15.8	5.6	11

There are at least two possible explanations for the detection by EPR of a vanadyl porphyrin in Circle Cliffs tar sand in the present study when it remained undetected in the earlier work (7). First, the porphyrin content may be quite variable in the Circle Cliffs deposit. Secondly, UV spectroscopy is not as intrinsically sensitive as the EPR technique. In a recent study, Shultz and Selucky (6) have applied both methods to samples of Athabasca tar sand and found that they could observe the 410 nm Soret band characteristic of vanadyl porphyrins, in fractions in which high concentrations of V^{4+} were detected by EPR; however, in fractions with low vanadyl porphyrin concentrations (as determined by the V^{4+} EPR signals), no optical absorption could be observed.

In order to obtain a powder pattern spectrum of the petrolene which is a viscous fluid, it was necessary to solidify the sample at $-20^{\circ}C$. The EPR spectrum of the fraction also indicates the presence of vanadyl etioporphyrin.

Figure 2 shows the EPR spectrum of the mineral matter at $g \approx 2.0$. Of interest are the 6 intense, broad lines (labelled I) and the 6 intense, sharp lines (labelled II). The average hyperfine splitting of the two series is ≈ 9.3 mT which is characteristic of Mn^{2+} ($S=5/2, I=5/2$) in the tetragonal symmetry of a carbonate lattice (16). The carbonates common to the minerals associated with tar sands are calcite, dolomite, magnesite, aragonite and rhodochrosite. The last two can be eliminated from the list of candidates since their spectra do not show any hyperfine splitting. Of the three remaining possibilities, an FTIR analysis of the mineral matter shows dolomite to be the most likely.

Figure 3 shows the FTIR spectrum of the mineral fraction and the spectrum of dolomite for comparison. As can be seen, the characteristic broad line at 1441 cm^{-1} and the two sharp lines at 880 and 729 cm^{-1} indicate that dolomite is one of the components of the mineral matter. Absent, however, are the characteristic lines of calcite at $1429, 876$ and 710 cm^{-1} and of magnesite at $1449, 885$ and 746 cm^{-1} (17).

The appropriate spin Hamiltonian for Mn^{2+} at a tetragonal site in carbonates is

$$H = g\beta H \cdot S + D[S_z - S(S+1)] + A S \cdot I \quad 4)$$

where D is the zero field splitting constant. Since there is significant disagreement in the literature between the values of g, A and D reported for single crystal dolomite (18, 19) and those

obtained for polycrystalline samples (20), we have derived a revised set of EPR parameters for a sample of dolomite for comparison with the tar sand mineral fraction spectrum.

The powder pattern spectrum of a polycrystalline dolomite sample from the Arbuckle Mountain Range in Oklahoma was recorded and is shown in Figure 4a. The observed spectrum is actually a superposition of two spectra due to Mn^{2+} occupying two inequivalent sites in the $MgCa(CO_3)_2$ crystal lattice. The six more intense lines labelled "Mg" in Figure 4a, are the allowed ($\Delta m=0$) transition lines for Mn^{2+} substituted at Mg sites and the six less intense lines labelled "Ca", are the allowed lines for Mn^{2+} at Ca sites (18-20).

The computer simulation shown in Figure 4b was calculated for the allowed transitions using a third order solution of the spin Hamiltonian derived by De Wijn and Van Balderen (21) for line positions and an equation derived by Allen (22) for the line intensities. As can be seen by comparison with Figure 4a, agreement with the observed spectrum is very good with line positions reproduced to within ± 0.07 mT. The values thus obtained for the EPR parameters are given in Table II.

TABLE II
EPR PARAMETERS FOR Mn^{2+} IN VARIOUS CARBONATES AND IN THE
MINERAL FRACTION OF CIRCLE CLIFFS TAR SAND

Sample	g	A (mT)	Δ (mT)	Reference
Mineral Matter I	2.003 \pm .001	-9.26 \pm .01	14.8 \pm .3	Present work
Mineral Matter II	2.003 \pm .001	-9.48 \pm .01	---	Present work
Dolomite Mg site	2.0028 \pm .0001	-9.27 \pm .01	14.60 \pm .05	Present work
Dolomite Ca site	2.0028 \pm .0001	-9.48 \pm .01	---	Present work
Calcite	2.002 \pm .001	-9.55 \pm .05	8.0 \pm .1	(24)
Magnesite	2.0018 \pm .0006	-9.22 \pm .01	9.0 \pm .1	(20)

The spectrum of the mineral matter fraction of the tar sand sample (Figure 2) is complicated by severe broadening and overlap; however, values of the magnetic parameters g, and A, have been obtained by fitting the peak line positions to the third order solution (21). D was obtained using the equation by Bleaney and Rubins (23)

$$\delta H = x \left[z + \frac{y^2}{4(y+z)} \right] \quad (5)$$

where

$$\begin{aligned} x &= 2D^2/g\beta H \\ y &= 8(1-9m/g\beta H) \end{aligned} \quad (6)$$

and

$$z = 1 + Am/g\beta H$$

which gives the splitting δH , between the main allowed transition lines and their corresponding "anomalous" lines in the powder pattern. The value of D for Mn^{2+} at an Mg-site is such that only two anomalous lines can be observed (labelled "A" in Figure 4a); in the case of the mineral matter, because of severe broadening and overlapping, only one line is resolved (labelled "A" in Figure 2).

The values of the EPR parameters derived from the mineral matter spectrum are given in Table II together with results for magnesite, calcite and dolomite for comparison. It is obvious from the data that the spectrum can only be that of Mn^{2+} in dolomite with the lines designated as I and II corresponding to substitutions at Mg and Ca sites, respectively.

Another feature in the mineral matter spectrum is a line at $g=4.2$, shown in Figure 5. This is characteristic of Fe^{3+} which in this case is probably located at a site in clay.

CONCLUSIONS

The results of this study suggest that EPR, supplemented by FTIR, is a particularly sensitive technique in the identification and characterization of paramagnetic metal ions in the complex mixture of organic and mineral matter comprising tar sands. As demonstrated in the present work, EPR has the additional advantage of permitting a determination of the site of metals, either

EPR SPECTRUM OF
CIRCLE CLIFFS ASPHALTENE

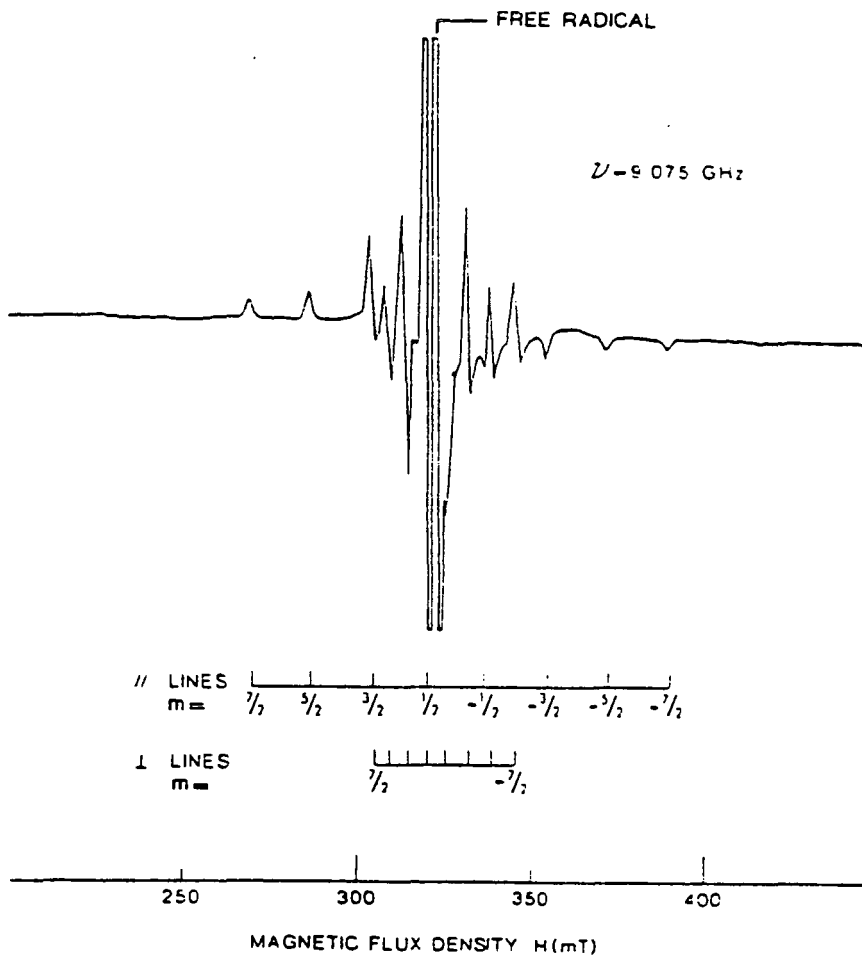


Figure 1. EPR spectrum of Circle Cliffs tar sand asphaltene.

CIRCLE CLIFFS MINERAL MATTER : HIGH FIELD

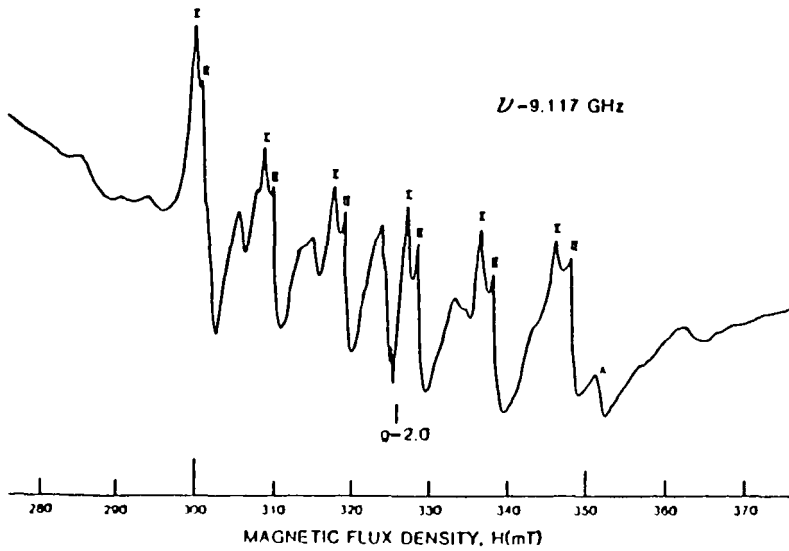


Figure 2. EPR spectrum of Circle Cliffs tar sand mineral matter at $g \approx 2$.

FTIR SPECTRUM OF (A) MINERAL MATTER (B) DOLOMITE.

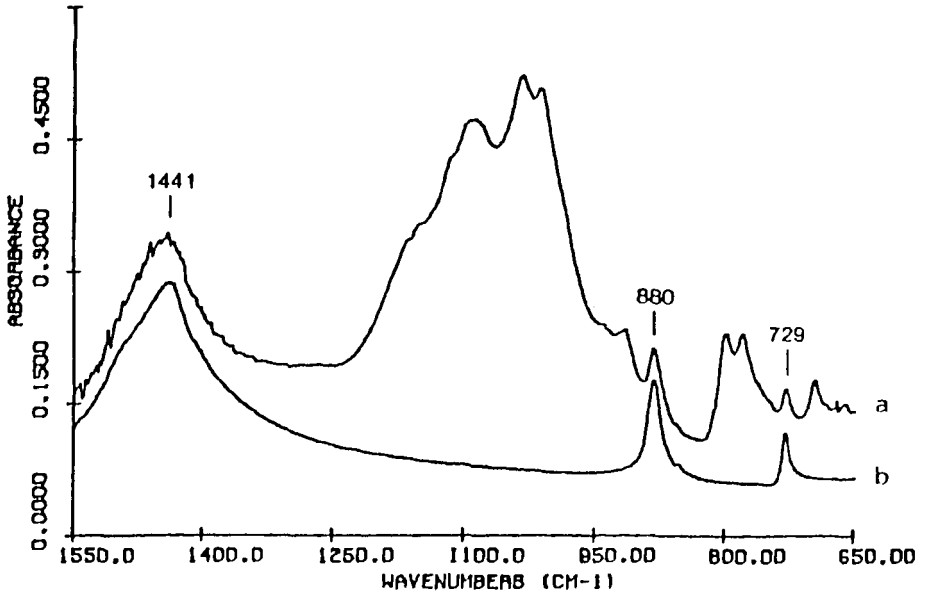


Figure 3. FTIR spectrum of (a) Circle Cliffs tar sand mineral matter (b) dolomite.

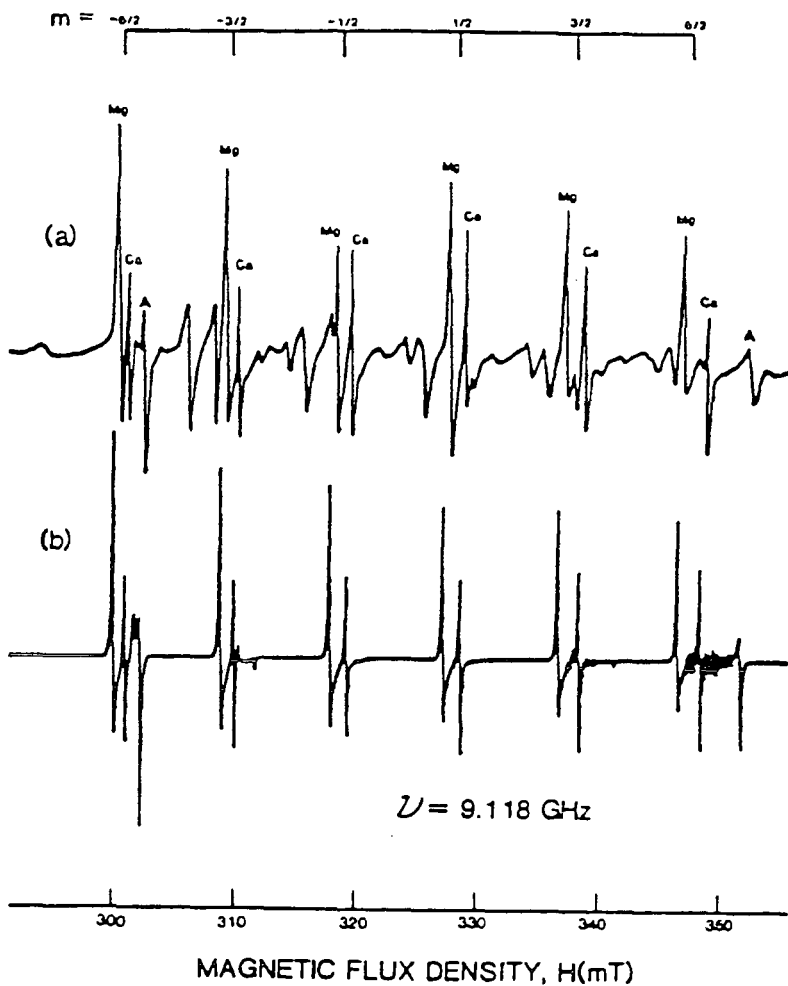


Figure 4. (a) EPR spectrum of polycrystalline dolomite. (b) simulation of (a).

CIRCLE CLIFFS
MINERAL MATTER : LOW FIELD

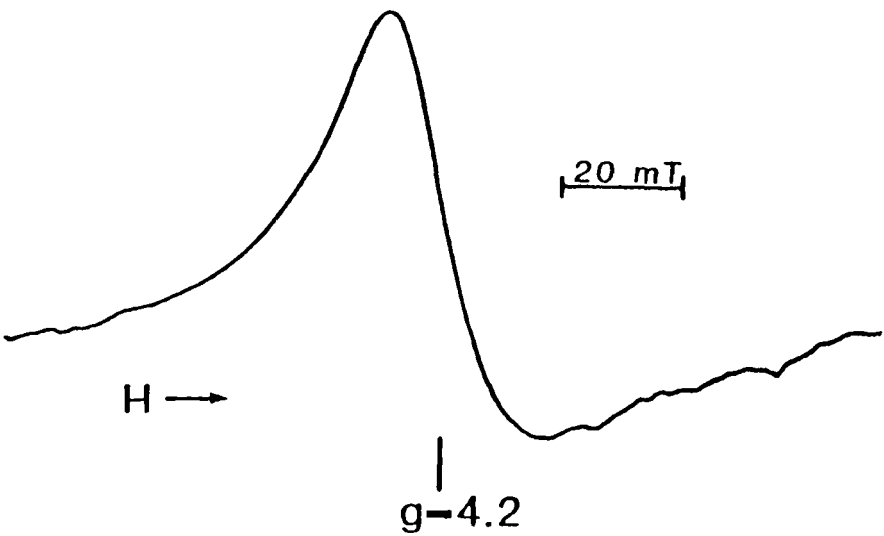


Figure 5. EPR spectrum of Circle Cliffs tar sand mineral matter at $g=4$.

occurring in minerals or bound in organic complexes. This may be particularly useful when the mineral phase and bitumen are not readily separable and their interactions have consequences for recovery processes (9).

ACKNOWLEDGMENTS

The authors express their thanks to Dr. J. F. Branthaver for providing the Circle Cliffs tar sand sample and to Dr. A. J. Ehlmann of the TCU Geology Department for the dolomite sample. This research was supported by the TCU Research Fund and in part by The Robert A. Welch Foundation.

LITERATURE CITED

- (1) Yen, T. F., Vaughan, G. B. and Boucher, L. J., "Spectroscopy of Fuels", Plenum, NY, pp. 187-201 (1970).
- (2) Dickson, F. E., Kunesh, C. J., McGinnis, E. L. and Petrakis, L., *Anal. Chem.*, 44, 978 (1972).
- (3) Saraceno, A. J., Fanale, D. T. and Coggeshall, N. D., *Anal. Chem.*, 33, 500 (1961).
- (4) Nasirov, R., Solodovnikov, S. P. and Urazgaliev, B. U., *Khim. Tekhnol. Topl. Masel*, No. 1, 56 (1978).
- (5) Niizuma, S., Steele, C. T., Gunning, H. E. and Strausz, O. P., *Fuel*, 56, 249 (1977).
- (6) Schultz, K. F. and Selucky, M. L., *Fuel*, 60, 951 (1981).
- (7) Branthaver, J. F. and Dorrence, S. M., "Analytical Chemistry of Liquid Fuel Sources - Tar Sands, Oil Shale and Petroleum", *Advances in Chem.*, No. 170, ACS, pp. 143-149 (1978).
- (8) Malhotra, V. M. and Graham, W. R. M., "Study of Mineral Fines in Tar Sand Bitumen and Their Acid Sensitivity Using EPR and FTIR Techniques", accompanying paper.
- (9) Malhotra, V. M. and Graham, W. R. M., "The Characterization of P. R. Spring (Utah) Tar Sand Bitumen by the EPR Technique: Free Radicals", *Fuel*, in press (1983).
- (10) Tynan, E. C. and Yen, T. F., *J. Mag. Res.*, 3, 327 (1970).
- (11) Lau, P. W. and Lin, W. C., *J. Inorg. Nucl. Chem.*, 37, 2389 (1975).
- (12) Roberts, E. M., Kosky, W. S. and Caughey, W. S., *J. Chem. Phys.*, 34, 591 (1961).
- (13) Sato, M. and Kwan, T., *Bull. Chem. Soc., Japan*, 47, 1353 (1974).
- (14) Assour, J. M., Goldmacher, J. and Harrison, S. E., *J. Chem. Phys.*, 43, 159 (1965).
- (15) Baker, E. W., Yen, T. F., Dickie, J. P., Rhodes, R. E. and Clark, L. F., *J. Amer. Chem. Soc.*, 89 (14), 3631 (1967).
- (16) Van Wieringen, J. S., *Disc. Faraday Soc.*, 19, 118 (1955).
- (17) Chester, R. and Elderfield, H., *Sedimentology*, 9, 5 (1967).
- (18) Schindler, P. and Ghose, S., *Trans. Am. Geophys. Union*, 50, 357 (1969).
- (19) Vinokurov, W. M., Zaripov, M. M. and Stepanov, V. G., *Soviet Phys. Cryst.*, 6, 83 (1961).
- (20) Wildeman, T. R., *Chem. Geol.*, 5, 167 (1969).
- (21) De Wijn, H. W. and Van Balderen, R. F., *J. Chem. Phys.*, 46, 1381 (1967).
- (22) Allen, B. T., *J. Chem. Phys.*, 43, 3820 (1963).
- (23) Belaney, B. and Rubins, R. S., *Proc. Phys. Soc.*, 77, 103 (1961).
- (24) Malhotra, V. M. and Graham, W. R. M., "The Origin of the Mn^{2+} EPR Spectrum in Pittsburgh No. 8 Bituminous Coal", submitted to *Fuel* (1983).

SYMPOSIUM ON CHARACTERIZATION AND CHEMISTRY OF OIL SHALES
PRESENTED BEFORE THE DIVISIONS OF FUEL CHEMISTRY AND
PETROLEUM CHEMISTRY, INC.
AMERICAN CHEMICAL SOCIETY
ST. LOUIS MEETING, APRIL 8 - 13, 1984

KINETIC STUDY ON HYDROCARBON FORMING PYROLYSIS OF
FUSHUN AND MAOMING OIL SHALES

By

J. Q. Wang and J. L. Qian
Beijing Graduate School of East China Petroleum Institute, P. O. Box 902, Beijing, China
and
L. Y. Wu
Research Institute of Petroleum Exploration and Development, Beijing, China

INTRODUCTION

There are many different experimental techniques for studying the pyrolysis kinetics of oil shale. The differential thermal analysis (DTA) method is based on the change in the quantity of heat absorbed and the thermogravimetric (TGA) method, on the loss of the sample weight accompanying the heating of oil shale sample (1, 2). However, by using these methods, when kerogen is pyrolyzed by heating, the mineral matter contained in oil shale will also be decomposed, with heat liberation and weight loss, which affects the kinetic parameter study. The main purpose of the oil shale retorting is to produce shale oil and hydrocarbon gases, so it is necessary to study the hydrocarbon forming pyrolysis of oil shale. Some researchers designed special apparatus for this purpose (3).

In this paper, "Rock Eval." pyrolysis apparatus is used for studying hydrocarbon forming pyrolysis kinetics. In general, this apparatus has been designed and used only for evaluation of source rocks, not for kinetic studies.

EXPERIMENTAL

The apparatus used is called "Rock-Eval", Type I, designed by I. F. P. and manufactured by Gridal Corp., in France. It is shown schematically in literature (4). A 100-mg sample with the size of less than 80 mesh is heated with constant rate to about 550°C. During heating, inert gas is passed through the sample layer in order to carry out the gaseous product evolved. The hydrocarbons already present in the sample in a free or adsorbed state are first volatilized at a moderate temperature. The amount of these hydrocarbons (S_1) is measured by a flame ionization detector (FID) which eliminates the interference of mineral matter decomposition. Then, pyrolysis of kerogen results in generating hydrocarbons and hydrocarbon-like compounds (S_2) and oxygen-containing volatiles, i. e., carbon dioxide (S_3) and water. The volatile compounds generated are split into two streams passing respectively through a FID (detector) measuring S_2 and a thermal conductivity detector measuring S_3 . An adequate temperature program allows a good separation of S_1 and S_2 peaks on the FID detector. In this paper, we are interested in the amount of the hydrocarbons (S_2) generated.

The experimental conditions used in this study are as follows: carrier gas is helium; constant heating rate is 5°C per minute.

Four Chinese oil shale samples are used: Fushun oil shale with rich kerogen content; Fushun oil shale with lean kerogen content; Maoming Jin Tang oil shale; and Maoming Yang Jiao oil shale.

RESULTS

Evaluation data of the samples are shown in Table I.

Kinetic data are shown in Tables II-V. In these tables, S_i means the sum of the integrated area indicating the sum of the amounts of pyrolysis hydrocarbon obtained from the beginning of the experiment to certain definite time, (or temperature); S_{oc} means the total amount of the integrated area, indicating the total amount of the hydrocarbon obtained in the whole run; and $x_i\%$ = S_i/S_{oc} indicates the percentage of the hydrocarbon obtained from the beginning to the time t_i sec. (or $T_i^\circ\text{C}$).

The data obtained are treated by using the kinetic equation of overall first order reaction,

$$\frac{dx}{dt} = A e^{-E/RT} (1-x) \quad (1)$$

TABLE I

EVALUATION DATA OF FUSHUN AND MAOMING OIL SHALE

Oil Shale	Organic Carbon	Adsorbed Hydrocarbon	Pyrolysis Hydrocarbon	CO ₂ Content
	COT Wt %	S ₁ mg/gm	S ₂ mg/gm	S ₃ mg/gm
Fushun (rich)	18.92	1.98	204.71	0.71
Fushun (lean)	9.28	0.82	87.67	0.39
Maoming Jin Tang	20.15	1.35	158.09	2.11
Maoming Yang Jiao	22.29	2.14	135.24	5.49

TABLE II

PYROLYSIS DATA OF FUSHUN RICH OIL SHALE

Time sec.	Temp. °C	S _i	x _i %
480	287	52	0.15
600	298	110	0.32
720	308	171	0.50
840	319	247	0.72
960	330	343	1.00
1080	340	506	1.47
1200	351	792	2.31
1320	361	1324	3.86
1440	372	2342	6.82
1560	383	4359	12.69
1680	393	8981	26.15
1800	404	16364	47.65
1920	414	25089	73.06
2040	425	31519	91.38
2160	436	33601	97.85
2280	446	33964	98.90
2400	457	34102	99.30
		S _α 34341	100.00

For constant heating rate, i. e., $dt=dT/C$, Equation 1 can be rewritten in logarithmic form:

$$\log \left[\frac{dx}{(1-x)dT} \right] = \log \frac{A}{C} - \frac{E}{2.303R} \cdot \frac{1}{T} \quad (2)$$

where C: heating rate, 0.0833°C/sec. in this work;

R: 1.987 cal/mol K;

E: apparent activation energy, cal/mol;

A: apparent frequency factor, 1/sec;

x: percentage of hydrocarbon formed from beginning to a certain temp.

T: pyrolysis temperature, K.

By assuming $\Delta x/\Delta T = dx/dT$, from the data given in Tables II-V, a series of different sets of $1/T_i$ and

$$\log \left[\frac{x_i}{(1-x_i)T_i} \right]$$

at different T_i is calculated. From these values, an interactive regression analysis allows the

calculation of the slope $-E/2.303R$ and intercept $\log A/C$ of Equation 2. Then E and A can be obtained, which are given in Table VI.

TABLE III
PYROLYSIS DATA OF FUSHUN LEAN OIL SHALE

Time sec.	Temp. °C	S_i	$\frac{x_i}{\%}$
540	300	66	0.29
660	310	135	0.59
780	320	214	0.94
900	330	341	1.34
1020	340	418	1.84
1140	350	582	2.56
1260	360	838	3.69
1380	370	1259	5.54
1500	380	2025	8.91
1620	390	3500	15.40
1740	400	5648	24.90
1860	410	9117	40.10
1980	420	14100	62.10
2100	430	18970	83.50
2220	440	20954	92.20
2340	450	22298	98.10
2460	460	22510	99.10
		S_∞ 22723	100.00

TABLE IV
PYROLYSIS DATA OF MAOMING JIN TANG OIL SHALE

Time sec.	Temp. °C	S_i	$\frac{x_i}{\%}$
420	282	588	1.07
540	292	677	1.23
660	302	790	1.43
780	312	952	1.73
900	322	1195	2.17
1020	332	1595	2.89
1140	342	2226	4.04
1260	352	3249	5.90
1380	362	5000	9.08
1500	372	8003	14.53
1620	382	12964	23.53
1740	392	20400	37.04
1860	402	30340	55.09
1980	412	40052	72.72
2100	422	48561	88.17
2220	432	52246	94.86
2340	442	53717	97.53
2460	452	54357	98.69
		S_∞ 55078	100.0

The reaction rate constant k at a definite temperature may be calculated by using Equation 3:

$$K = Ae^{-E/RT} \quad 3)$$

The time required for pyrolysis at constant pyrolysis temperature can be calculated by using Equation 4:

$$t = \frac{1}{k} \ln(1-x)$$

4)

Both results are shown in Table VII.

TABLE V
PYROLYSIS DATA OF MAOMING YANG JIAO OIL SHALE

Time sec.	Temp. °C	S ₁	x ₁ %
480		119	0.53
600		303	1.34
720		538	2.37
840		928	4.10
960		1388	6.10
1080		2201	9.72
1200		3186	14.06
1320		4761	21.02
1440		6678	29.45
1560		9178	40.52
1680		13125	57.94
1800		17031	75.18
1920		19757	87.22
2042		21275	93.92
2160		21840	96.41
2280		22136	97.18
2400		22310	98.48
		S _∞ 22653	100.0

TABLE VI

APPARENT ACTIVATION ENERGY AND APPARENT FREQUENCY FACTOR

Oil Shale	% of H. C. produced x %	Apparent Activation Energy E Kcal/mol	Apparent Frequency Factor A 1/sec	Correlation Factor r
Fushun (rich)	0.7-97.9	55.72	3.21x10 ¹⁵	0.989
Fushun (lean)	1.2-90.6	47.63	3.98x10 ¹²	0.988
Maoming Jin Tang	1-93	38.76	9.35x10 ⁹	0.990
Maoming Yang Jiao	0.5-94	31.20	4.67x10 ⁷	0.993

CONCLUSIONS

It is feasible to use the Rock Eval apparatus for studying hydrocarbon-forming kinetics of oil shales. Four Chinese oil shale samples are used. Under experimental conditions, the main stage of hydrocarbon formation during pyrolysis may be treated as an overall first order kinetic model. The experimental data are well fitted with the kinetic equations obtained with calculated apparent activation energy and frequency factor. The time required for pyrolysis under constant temperature are also calculated. These results may be used for the design of the pyrolysis retort, especially for fine particles of oil shales.

TABLE VII

REACTION CONSTANT AND PYROLYSIS TIME REQUIRED AT CONSTANT TEMPERATURE

Oil Shale	Pyrolysis Temp.	Reaction Rate Constant	Pyrolysis Time required for	Pyrolysis Time required for
	T °C	K 1/sec.	x=95% sec.	x=98% sec.
Fushun (rich)	400	0.00257	1165	1522
	425	0.0114	262	343
	450	0.0459	65	85
Fushun (lean)	400	0.00135	2218	2898
	425	0.00485	617	807
	450	0.0159	188	246
Maoming Jin Tang	400	0.0024	1247	1630
	425	0.0068	440	675
	450	0.0171	167	218
Maoming Yan Jiao	400	0.00344	870	1137
	425	0.00794	377	492
	450	0.017	176	230

LITERATURE CITED

- (1) Haddadin, R. A. and Tawarah, K. M., *Fuel* 59, 539 (1980).
- (2) Granoff, B. and Nuttal, H. E., *Fuel* 56, 234 (1977).
- (3) Shih, S. M. and Sohn, H. Y., *Ind. Eng. Chem. Proc. and Devel.* 19, 420 (1980).
- (4) Tissot, B. P. and Welte, D. H., *Petroleum Formation and Occurrence*, Springer-Verlag, Berlin, Heidelberg, New York, p. 443 (1978).

SYMPOSIUM ON CHARACTERIZATION AND CHEMISTRY OF OIL SHALES
PRESENTED BEFORE THE DIVISIONS OF FUEL CHEMISTRY AND
PETROLEUM CHEMISTRY, INC.
AMERICAN CHEMICAL SOCIETY
ST. LOUIS MEETING, APRIL 8 - 13, 1984

REACTIVITY OF OIL SHALE TOWARDS SOLVENT HYDROGENATION

By

R. M. Baldwin, D. P. Bennett and R. A. Briley
Chemical Engineering Department, Colorado School of Mines, Golden, Colorado 80401

INTRODUCTION

Oil may be extracted from oil shale by a number of different techniques. Of the several procedures available, only pyrolysis (retorting) has received the attention required to develop a commercial processing technology (1). Direct hydrogenation, or hydrogenation in slurry systems, is a well developed technology for conversion of coal to liquid fuels, but application of this technique to oil shale has only recently begun to receive attention. Kerogen in oil shale is known to be relatively insoluble in most organic solvents at their normal boiling points, but when oil shale is heated to temperatures above 600 K, the organic matter in shale may be solvent extracted in high yield (2, 3). Several early patents describe solvent processing of torbanite and other shale-like materials at elevated temperatures both with and without hydrogen gas atmospheres (4-7). In an extensive study, Jensen et al. (8) reported on hydroprocessing of a Green River oil shale in both batch and continuous reactors. Their results indicated that very high organic carbon conversions could be attained. Recently, patents on direct hydrogenation processes in vehicle oils have been granted to Gregoli (9), Patzer (10) and Greene (11). Results on hydroprocessing of an Australian oil shale have also been published by Baldwin et al. (12).

The objective of the work described in this paper was to compare the effect of direct hydrogenation operating conditions on the yield of oil and gas from a sapropelic oil shale (Australian Stuart A) and a humic oil shale (Montgomery County, Kentucky). These data were developed from batch autoclave experiments using both a pure hydrogen donor solvent (tetralin) and non-donor solvents (toluene and 1-methylnaphthalene).

EXPERIMENTAL APPARATUS AND METHODS

All experiments for this study were conducted in a 300 cc batch stirred autoclave reactor, manufactured by Autoclave Engineers, Inc. A schematic of the reactor and associated piping are shown in Figure 1. Shales from the upper part of the Kerosene Creek seam in the Stuart Deposit and from the Cleveland Member, Ohio Shale, Montgomery County, Kentucky were wet ground in a rod mill, sieved to 100% minus 74 micron (minus 200 mesh) and vacuum dried at 40°C prior to use. The Stuart shale was beneficiated by de-sliming prior to grinding, while the Kentucky shale was essentially run-of-mine. Fischer Assays of the feed shales used for this study are presented in Table I. Two different types of solvents were used for this study; 1,2,3,4-tetrahydronaphthalene (tetralin) was used as a hydrogen donor solvent and toluene and 1-methylnaphthalene were employed as non-donor solvents. Hydrogen used was 95% H₂ with a 5% argon tracer added to facilitate gas made calculations.

TABLE I
FISCHER ASSAY, PARENT SHALES

	% Spent Shale	Product Yield			Oil, gpt	OCC ^b
		% Oil	% Water	% Gas+Loss		
Kentucky ^a	91.6	4.6	1.5	2.3	11.6	
Stuart ^a	72.4	16.3	5.3	6.0	44.0	44.7

a. Analysis performed by Commercial Testing and Engineering, Golden, CO.

b. OCC = organic carbon conversion, %.

Reaction products were analyzed by several different techniques. Reaction product gases were determined on a Carle model 111-H gas chromatograph, with hydrogen, hydrocarbon gases

(through C₅) and carbon oxide gases quantified. Liquids were separated by acetone washing of the product slurry and soxhlet extraction of the residue with a solution of 50% benzene/50% methanol. The liquids were analyzed by chromatographic simulated distillation on an HP model 5840 gas chromatograph to determine the boiling range and by elemental analysis on a Carlo-Erba elemental analyzer. The spent shale was analyzed for total and inorganic carbon using a Coulometrics system and then ashed in a muffle furnace. Hydrocarbons were speciated with an Extranuclear model EL mass spectrometer, interfaced to a Carlo-Erba model 4100 capillary column gas chromatograph. The GC/MS system was operated in the electron impact mode, at 70 eV.

DISCUSSION OF RESULTS

Results of the experimental runs on the shales are presented in Tables II through V. In all cases, data on organic carbon conversion (OCC) and oil yield (OY) are shown at the applicable reaction conditions. The data given for oil selectivity represent carbon conversion to oil, determined by a quantitative gas analysis followed by a carbon balance on the reaction system. The selectivity reflects the carbon conversion to oil, relative to total carbon converted (expressed as a percentage of the total carbon conversion). Discussion of these data follows.

TABLE II
EFFECT OF TEMPERATURE AND SOLVENT TYPE, STUART SHALE

Temperature	Solvent	
	Tetralin	1-Methylnaphthalene
350°C	OCC: 32.3	OCC: 43.6
	OY: 91.8	OY: 95.9
425°C	OCC: 83.3	OCC: 81.6
	OY: 93.9	OY: 91.2

OCC = organic carbon conversion, %

OY = oil yield, % of total carbon converted

All runs at 800 psi H₂ initial pressure, 1 hour nominal residence time, 1:1 solvent-to-shale ratio.

TABLE III
EFFECT OF TEMPERATURE AND SOLVENT TYPE, KENTUCKY SHALE

Temperature	Solvent	
	Tetralin	Toluene
375	OCC: 38.0	OCC: 44.0
	OY: 96.2	OY: 98.5
425	OCC: 79.6	OCC: 80.9
	OY: 95.1	OY: 95.1
450	OCC: 85.6	NA
	OY: 97.2	

All runs at 800 psi initial H₂ pressure, 1 hour nominal residence time, 2:1 solvent-to-shale ratio.

Temperature

Temperature effects both organic carbon conversion and selectivity for oil formation. For both shales studied, increasing temperature raises organic carbon conversion. However, in the case of Kentucky shale, the reactivity towards conversion in both the donor and non-donor solvents is lower. This is reflected in the conversions found at the lower temperature levels. In tetralin, conversion of organic carbon is approximately 32% at 350°C for Stuart shale, while comparable conversions are achieved for Kentucky shale at 375°C (38%). In the non-donor solvents, the same temperature sensitivity is seen. This is undoubtedly due to the relative reaction rates of the two shales, with the more paraffinic Stuart shale reacting quicker and, thus, giving higher yields of oil at lower temperatures. It should be noted that since the reactor was operated in the true batch

mode, the actual reaction time was different for runs made at 350° and 375°C. Approximately 5 to 8 minutes was required to heat the reactor from 350° to 375°C and, thus, the comparisons of temperature sensitivity are even more pronounced than indicated by the data due to this confounding effect of heat-up time. At the higher temperature levels, reaction time is sufficiently long that the reaction has proceeded essentially to completion and the temperature sensitivity and reactivity differences noted between the two shales at the lower temperature levels are no longer apparent.

TABLE IV

EFFECT OF SOLVENT AND HYDROGEN PARTIAL PRESSURE, STUART SHALE

Solvent	Gas Atmosphere			
	Hydrogen		Nitrogen	
	800	300	800	300 ^a
Tetralin	OCC: 83.3	OCC: 83.7	OCC: 77.9	OCC: 83.3
	OY: 93.9	OY: 92.2	OY: 90.8	OY: 90.7
1-Methylnaphthalene	OCC: 81.6	OCC: 68.6	NA	NA
	OY: 91.2	OY: 88.0		

a. Initial total pressure at room temperature.

All runs at 425°C, 1 hour nominal residence time, 1:1 solvent-to-shale ratio.

TABLE V

EFFECT OF SOLVENT AND HYDROGEN PARTIAL PRESSURE, KENTUCKY SHALE

Solvent	Gas Atmosphere			
	Hydrogen		Helium	
	800	300	800	300 ^a
Tetralin	OCC: 79.6	NA	OCC: 76.57	NA
	OY: 95.1		OY: 97.35	
Toluene	OCC: 80.9	OCC: 72.6	OCC: 44.01	NA
	OY: 95.1	OY: 95.9	OY: 91.59	

a. Initial total pressure at room temperature.

All runs at 425°C, 1 hour nominal residence time, 1:1 solvent-to-shale ratio.

Somewhat surprisingly, for both shales temperature has little effect on selectivity for oil formation. This could be due to the relatively low temperatures employed in the study, although even at 450°C, selectivity for oil formation in tetralin was extremely high. It is also possible that reactions responsible for hydrocarbon gas formation in this reaction system have very high activation energies, requiring temperatures in excess of 450°C in order to proceed at an appreciable rate. The hydrogen activity of the system could also be a factor here, especially in inhibiting free-radical cracking reactions. Selectivities are somewhat lower in the non-donor systems, or where an inert gas rather than hydrogen is used for the reaction gas atmosphere, but overall oil yields are extraordinarily high for this reaction system.

Organic carbon conversions for these shales retorted under Fischer Assay conditions are as reported in Table I. Comparison of these conversions with those shown in Tables II through V points out the extreme differences in carbon utilization between these two reaction schemes. While retorting leaves behind in excess of 50% of the organic carbon on the spent shale, hydroprocessing successfully converts in excess of 80% of the carbon and at lower temperatures with a resulting higher selectivity for oil forming reactions.

Solvent and Hydrogen Partial Pressure

Solvent type (hydrogen donor or non-donor) has a marked effect on carbon conversion, but only in the absence of gas phase molecular hydrogen. When molecular hydrogen is present in the reactor, organic carbon conversion and the yield structure are nearly independent of the type of solvent used. In the absence of gaseous hydrogen, however, the nature of the solvent becomes very important, with high conversions only obtainable using the hydrogen donor solvent (tetralin). This

interdependency of solvent efficacy with hydrogen partial pressure is most clearly shown in Tables IV and V, where data on runs made with variable gas atmospheres is shown. As may be seen, hydrogen in some form is required to achieve the level of organic carbon conversions being obtained under these reaction conditions. With neither molecular hydrogen in the gas phase or donatable hydrogen in the solvent, low carbon conversions (typically on the order of the pyrolysis yields at these temperatures) are realized.

Product Oil Characterization

Sample total ion intensity (TII) chromatograms for a shale oil produced by hydrogenation of Stuart shale are shown in Figure 2. The chromatograms represent the whole oil and several fractions generated by open column elution chromatography. Although work is still in progress on identification of individual components in the two oils, several general features have been elucidated by GC/MS. In the case of Stuart shale oil, the spectrum is dominated by a homologous series of normal paraffins, commencing at approximately C₇ and continuing past C₃₀. Clustered around each normal paraffin peak are two smaller peaks, which represent mono-olefinic hydrocarbons with the same carbon number as the paraffin. Between the paraffin/olefin clusters, the peaks shown on the chromatogram for Stuart shale are largely comprised of iso-paraffins with a low degree of branching, alkyl-substituted aromatics and cycloparaffins and nitrogen moieties.

Further separation work on the Stuart shale is in progress, with attention being given to specification of the nitrogen compounds present. To date, a homologous series of nitriles from C₇ through C₃₀ and nitrogen-containing heterocycles have been speculated. The nitrogen heterocycles are predominately alkyl-substituted pyrrolidines, quinolines and isoquinolines. No evidence of amines or amides has been found, although under the conditions of reaction, amides are most probably converted to nitriles. This could explain the high concentration of nitriles found in the product oil, as these species are not normally present in shale oils. Regtop et al. (13) have reported the identification of a nitrile series in a Fischer Assay oil from Rundle shale.

Identification of chemical species in the Kentucky shale oil by GC/MS also indicates a homologous paraffin series starting at C₉ and terminating at C₃₀ or higher. In this case, however, the product distribution is much more complex and is not dominated by the paraffin series to the extent of the Stuart shale oil. The remaining compounds seem to consist predominately of alkyl-substituted benzenes and cycloparaffins and nitrogen moieties.

Simulated chromatographic distillation of the product oils is being used to determine the effect of operating variables on the boiling range distribution. At this time, data analysis is incomplete, preventing a comprehensive evaluation of the differences in distillation characteristics. Preliminary comparisons with Stuart Fischer Assay oil indicate that the shale oil produced by this process has approximately the same boiling range distribution, even though the highest temperature experienced in producing the oil was some 75°C lower than the final Fischer Assay temperature (500°C).

CONCLUSIONS

The results of this study indicate that sapropelic shales, such as the Australian Stuart A, are moderately more reactive towards oil extraction by direct hydrogenation than humic shales. This result is not surprising considering the aromaticity and hydrogen deficiency of humic shales relative to sapropelic shales. Both types of shale exhibit the same sensitivity to solvent type and hydrogen partial pressure, with the humic shale showing a lower temperature sensitivity (e.g., slower rate of reaction). Finally, the product spectra are substantially different, as would be expected due to the differing source materials for the organics in these shales.

ACKNOWLEDGMENT

The authors would like to express their gratitude to Southern Pacific Petroleum, N. L., Sydney, Australia for financial support of this work.

Figure 1
Reaction System Schematic

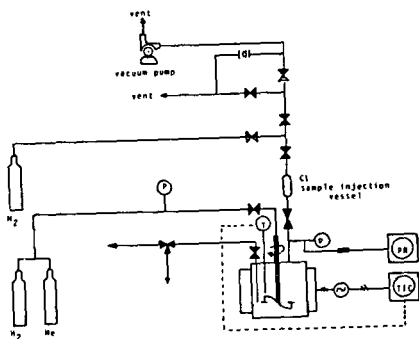
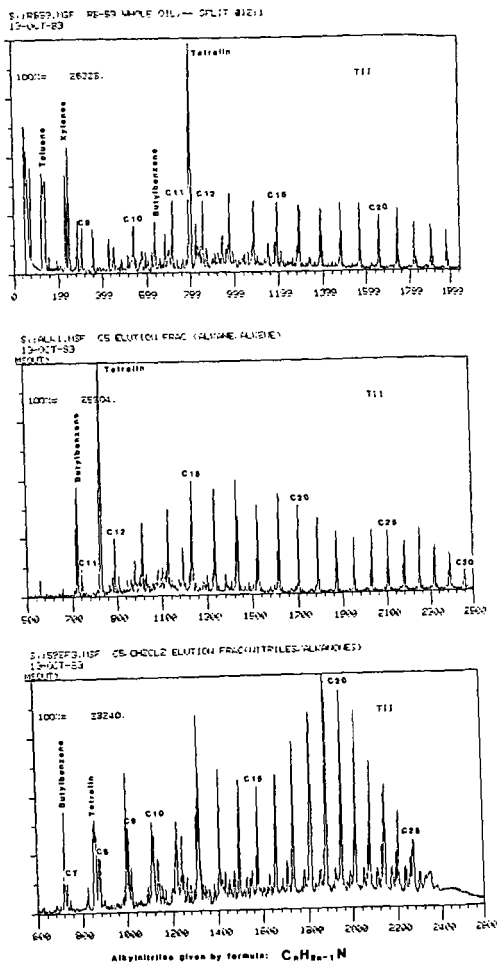


Figure 2
T11 Chromatograms of Whole Shale Oil and Elution Fractions



LITERATURE CITED

- (1) Baughman, G. L., Synthetic Fuels Data Handbook, second edition, Cameron Engineers, Inc. (1978).
- (2) Gavin, M. J. and Aydelotte, J. T., "Solubilities of Oil Shales in Solvents for Petroleum", U. S. B. M. Report of Investigation 2313 (1922).
- (3) Dulhunty, J. A., "Solvent Extraction of Torbanite", Proc. Linnean Soc., New South Wales, vol. 67 (1942).
- (4) Ryan, H. D., "Bituminous Material from Shale", U. S. Patent 1327572, January 6, 1920.
- (5) Hampton, H., "Hydrocarbons from Bituminous Shale-Like Material", U. S. Patent 1668898, May 8, 1928.
- (6) Fisher, A., "Pyrolytic Conversion and Coking of Finely Divided Bituminous Material and Hydrocarbon Oil", U. S. Patent 2073367, March 9, 1937.
- (7) Buchan, F. E., "Processing Oil Shale", U. S. Patent 2487788, November 15, 1949.
- (8) Jensen, H. B., Barnett, W. I. and Murphy, W. I. R., "Thermal Solution and Hydrogenation of Green River Oil Shale", U. S. B. M. Bulletin 533 (1953).
- (9) Gregoli, A. A., "Fluidized Bed Hydroretorting of Oil Shale", U. S. Patent 4075081, February 21, 1978.
- (10) Pätzer, J. F., "Recovery of Oil from Oil Shale", U. S. Patent 4238315, December 9, 1980.
- (11) Greene, M. I., "Process for Hydrogenation/Extraction of Organics Contained in Rock", U. S. Patent 4325803, April 20, 1982.
- (12) Baldwin, R. M., Frank, W. L., Baughman, G. L. and Minden, C. S., "Hydroprocessing of Australian (Stuart A) Oil Shale", Proc. 16th Oil Shale Symp., Golden, CO (1983).
- (13) Regtop, R. A., Crisp, P. T. and Ellis, J., "Chemical Characterization of Shale Oil from Rundle, Queensland", Fuel, Vol. 61, February, 1982.

SYMPOSIUM ON CHARACTERIZATION AND CHEMISTRY OF OIL SHALES
PRESENTED BEFORE THE DIVISIONS OF FUEL CHEMISTRY AND
PETROLEUM CHEMISTRY, INC.
AMERICAN CHEMICAL SOCIETY
ST. LOUIS MEETING, APRIL 8 - 13, 1984

PROCESSING OF OIL SHALE IN MOLTEN HYDROXIDES

By

A. D. Hues, C. K. Rofer-DePoorter and R. N. Rogers
Los Alamos National Laboratory, P. O. Box 1663, MS D462, Los Alamos, New Mexico 87545

INTRODUCTION

Current processes for the production of organics from oil shale are all variations of high-temperature pyrolysis. All such processes are subject to similar problems: handling solids is more difficult than handling liquids; much of the carbon is unrecoverable owing to the nature of organic pyrolysis; and the product is primarily a synthetic petroleum that must be further refined before it can be used as a fuel. The use of a molten-salt medium at lower temperatures may ameliorate these problem areas.

An earlier survey study to identify suitable salts for solvents gave no promising candidate systems (1). Processing in a tetrachloroaluminate melt at 320°C gave a variety of products soluble in organic solvents (2), but this temperature is still relatively high and carbon conversion was apparently limited by hydrogen disproportionation. Aqueous alkali has been shown to decompose coal to lower molecular weight products at somewhat lower temperatures (3).

The preliminary studies herein described have identified a candidate molten salt, a mixture of lithium, sodium and potassium hydroxides and some of its processing characteristics have been identified. Preliminary results on the effects of temperature, time and presence of oxygen show that processing at 200-225°C in the presence of oxygen and water gives an organic product consisting of a hydrocarbon fraction in the gasoline-diesel fuel range and an acid fraction that may be useful for plastics or resin manufacture. Very little further refining appears to be necessary for these products. A potential problem is the dissolution of silica and other mineral matter in the molten salt.

METHOD

A combustion furnace was set up to allow the shale to be heated in a controlled atmosphere (Figure 1). A glass liner for the furnace was fitted to a flowmeter and tanks of the gases to be used. A glass U-tube was used to collect the product fraction condensable in a dry-ice-methanol slush. Gases were not collected, but they appear to have been a minor product. Noncondensable gases would have been CO, CO₂, methane, ethylene and acetylene. Shale and hydroxide mix 1 NaOH: 1 KOH: 0.5 LiOH were measured into a nickel liner in a stainless steel boat and inserted into the furnace for various times, which were measured from the insertion of the boat to its removal. Duplicates were performed for most runs. The melting point of the hydroxide mix alone was 147-151°C.

All of the solids to be processed were ground into relatively small particles. In particular, the oil shale was ground in a ball mill and sieved to give fractions of less than 495 microns particle diameter. Grinding was necessary only for reproducibility, however. Chunks of shale up to a few centimeters diameter were easily dissolved in liquid hydroxide.

This apparatus has some heat and mass transfer limitations. Some dependence of apparent reaction rate on sample size was observed, with 200- and 500-mg samples of shale giving different results than 1-g samples when processed with hydroxide in a 1:5 shale:hydroxide ratio. A 2-g sample gave a similar result to the 1-g sample. This same effect was observed in pyrolysis of shale without hydroxide. In addition, condensate collected from the hydroxide mixture heated alone at 200°C for 30 min was independent of hydroxide mass, giving essentially the same amount of condensate for 1, 2.5, 5 and 10 g of hydroxide. The rate of absorbed water loss by the hydroxide mixture under these conditions is evidently more of a function of the surface area of the melt than of the quantity of hydroxide present.

A 1-g portion of shale was heated with 10 g of hydroxide for 30 min, to determine the effect of a change in the shale-to-hydroxide ratio. No change was observed from the results for the 1:5 ratio.

Products were contained both in the condensate and in the shale-hydroxide melt, which

upon cooling formed a brick. Separation of the solid products consisted of

1. dissolving the brick in distilled water,
2. filtration of solids,
3. extraction of the filtrate with diethyl ether,
4. acidification of the aqueous fraction with HCl,
5. removal of precipitates by filtration,
6. extraction of acidified filtrate with ether.

The filtrate was then evaporated, as were the ether extracts, and the residues retained.

The organic products were recovered mainly in the ether extracts, but the evaporated salt from the acidified filtrate also appeared to contain acids. This method must be considered semi-quantitative, as not all the variables are well known. For example, one of the precipitates that forms upon acidification is apparently a carbonate; at some low pH, it decomposes to CO₂ gas and soluble species. The decomposition point seems to vary from one set of processing conditions to another. Thus, comparable quantities and compositions of these precipitates could not be obtained.

Analysis of the separated organic components was by NMR and GC-MS. Spot tests (4) were attempted for sulfur and other inorganic components in the aqueous solution from the processed brick, but results were not interpretable, probably because of the presence of organic complexants.

RESULTS AND DISCUSSION

Effect of Process on Different Materials

Several types of oil shale and other materials were processed with the 1 NaOH: 1 KOH: 0.5 LiOH mix at 200°C. The oil shales were Green River, Cleveland (Kentucky), Gassaway, Huron and Dowelltown. Fruitland subbituminous coal, wood sawdust and Santa Rosa tar sand were also treated. Samples of each of these materials were also heated without hydroxide. Processing with hydroxide doubled the condensate yield from the coal and tripled the yield from the sawdust. In addition, the sawdust was converted almost completely to water-soluble products. The effect of the hydroxide on the tar sand appeared to be negligible; both in hydroxide yield and in organics contained in the melt.

The shales all gave markedly increased yields of condensate when processed with hydroxide at 200°C for 60 min. The amounts of condensate from shale only and the shale-hydroxide mix are given in Table I. Only qualitative observations have been made of the products contained in the melt. Filtrates from Green River and Cleveland shales are a light yellow. The filtrates from the other Eastern shales are much darker, suggesting increased amounts of aromatic acids, particularly phenols and possibly some complexing of metals liberated from the inorganic fraction. The filtrates from all of the shales but Dowelltown and Green River have strong, petroleum-like odors, while the shales before processing have little odor.

TABLE I

CONDENSIBLES FROM OIL SHALE PROCESSING (mg/g Shale)

<u>Shale Type</u>	<u>Shale Alone</u>	<u>Shale and Hydroxide</u>
Green River	22.0	94.2
Cleveland	18.7	101.3
	16.7	103.6
Gassaway	14.2	101.2
Huron	17.8	114.2
Dowelltown	15.7	103.0

Upon acidification, the filtrates give off a gas that has an H₂S odor and blackens lead acetate paper. This suggests that the sulfur in the shales is being retained in the melt in a water-soluble form. Standard spot tests (4) for sulfur in the filtrates were inconclusive, however.

GC-MS analysis of the condensate from Green River shale shows hydrocarbons with molecular weights up to about 200. These include relatively unbranched alkanes and alkenes, cycloalkanes and possibly aromatics. Proton and ¹³C NMR of the ether extract from the basic solution shows a similar group of compounds, presumably of higher molecular weight, since they were not distilled from the melt. The NMR spectrum is clean enough to suggest that the molecular weights are probably not extremely high, or that the molecular structure is relatively regular. NMR analysis of the ether extract from the acid solution shows acids, some of which may have complex structures involving bridged rings. No other heteroatom-containing functional groups were observed.

The coal filtrate precipitated a black organic solid upon acidification. This solid gave a proton NMR spectrum with a broad absorption in the aromatic region, suggesting that the compounds are highly aromatic and of high molecular weight, similar to humic acids.

Although both GC-MS and NMR are fairly reliable, stand-alone methods of analysis, these identifications must be regarded as preliminary until they are confirmed by at least one other method, such as IR spectroscopy.

Processing Conditions

To ascertain the ranges of atmospheric composition and processing temperature, Green River shale was used. Samples consisting of 1 g shale and 5 g hydroxide mix, shale only and hydroxide only were heated to temperatures of 200, 225 and 250°C in an atmosphere of 95% Ar and 5% O₂ at a flow of 500 cm³/min for times up to 2 h. The results plotted in Figure 2 represent the net amount of condensate obtained from the shale after correcting for the condensate from a hydroxide blank. An increase in temperature from 200 to 225°C resulted in an increase in the reaction products from the shale-hydroxide mixture, although the temperature effect is small after 2 hours. At 250°C, condensate weights from the shale-hydroxide mixture were erratic because of foaming and swelling of the samples during heating. The pyrolysis rate of the shale alone also increases with heating, but not as rapidly.

Because of the heat and mass transfer properties of the apparatus, these data must be taken as indicative of trends, rather than absolute. The error is not well known, but it seems likely to be +10%.

Yields of the hydrocarbons and acids extracted from the melt also increased with time. However, the yields of the acids appear to be higher for processing at 200°C than at 225°C. Dissolved mineral matter, in the form of the inorganic precipitates that form upon acidification, is much higher for processing at 225°C than at 200°C. These results are semi-quantitative only.

Heating of a 1:5 shale:hydroxide sample in Ar alone yielded only 63% of the amount of condensate obtained when the atmosphere contained 5% O₂. An unusually dry batch of hydroxide mix has much less effect on the reaction of the shale than a wetter batch. Portions of the dry hydroxide were exposed to the laboratory atmosphere for times of one and two hours to absorb moisture, after which they were used in processing Green River shale. Although the blank values varied with exposure time, the condensate yields from the shale processed with the wetter hydroxide agreed well with previous values. The reaction, therefore, appears to involve an oxidative attack on the kerogen structure, with water required for the reaction.

Yields of hydrocarbon in the condensate could not be directly measured. The condensate contains significant amounts of water, which cannot be estimated because of uncertainties in the amounts of water liberated from the oil shale minerals and from the hydroxide by additional bubbling caused by decomposition of the kerogen into gaseous products. However, a minimum value for the yield of organic products can be estimated from the amounts of organics extracted from the melt. A typical value for hydrocarbons extracted from the melt is 15 mg/g shale and for acids, 10 mg/g shale. The total converts to 8 gallons/ton shale, for an assumed density of the organics of 0.72. The shale used in these experiments has a Fischer Assay of 25 gallons/ton shale. The real yield, including the condensable hydrocarbons and the acids left in the filtrate, must be larger than 8 gallons/ton and is made up of compounds having a relatively high H:C ratio in the case of Green River shale.

CONCLUSIONS

Green River oil shale can be processed in a molten NaOH-KOH-LiOH mix in the presence of oxygen and water at temperatures near 200°C to give hydrocarbon and acid products. There appears to be no reason that the process should not work for Eastern oil shales, coal, wood waste and other materials, although it is ineffective for tar sands. A mechanism consistent with the observations would be oxidative attack on kerogen to form carboxylic acid salts, followed by decarboxylation of the salts to hydrocarbons. However, more work is necessary to prove this mechanism. Dissolution of mineral matter appears to be strongly temperature dependent. Nitrogen and sulfur appear to be absent from the products.

ACKNOWLEDGMENTS

We thank D. Ott for performing and interpreting the NMR analyses and R. E. Hermes for performing the GC-MS analyses.

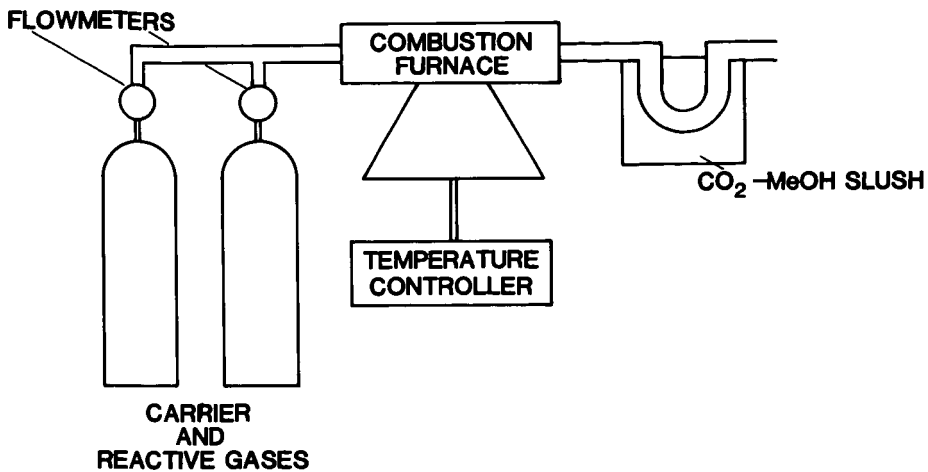


Figure 1. Experimental Apparatus

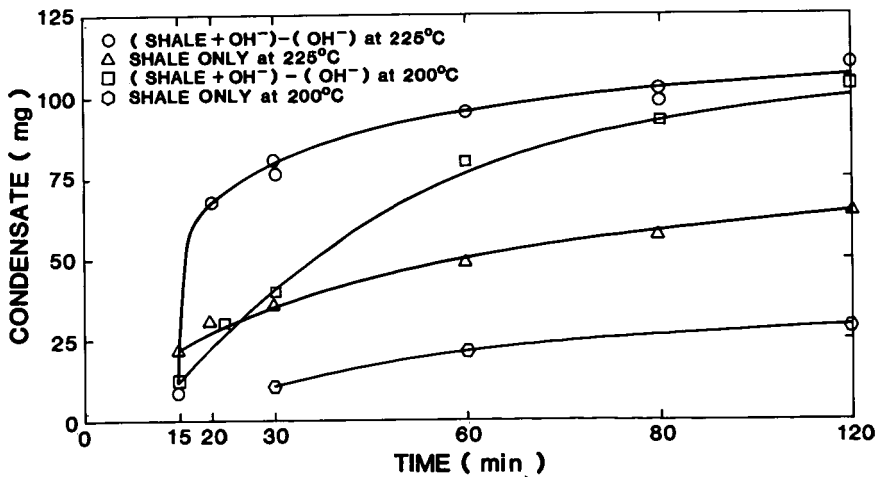


Figure 2. Dependence of condensate product on temperature and time.

LITERATURE CITED

- (1) Fritz, G. T. , "The Effects of Various Pyrolysis Conditions on the Release of Products from Green River Oil Shale", Los Alamos Natl. Lab. Report LA-7118-T (1978).
- (2) Bugle, R. C. , Wilson, K. , Olsen, F. , Wade, L. G. , Jr. and Osteryoung, R. A. , *Nature*, 274, 578 (1978).
- (3) Kasehagen, L. , *Ind. Eng. Chem.* , 29, 600 (1937).
- (4) Feigl, F. and Anger, V. , *Spot Tests in Inorganic Analysis*, Elsevier, Amsterdam (1972).

SYMPOSIUM ON CHARACTERIZATION AND CHEMISTRY OF OIL SHALES
PRESENTED BEFORE THE DIVISIONS OF FUEL CHEMISTRY AND
PETROLEUM CHEMISTRY, INC.
AMERICAN CHEMICAL SOCIETY
ST. LOUIS MEETING, APRIL 8 - 13, 1984

PHYSICOCHEMICAL PROPERTIES OF MAGNETICALLY SEPARATED SHALE OIL SOLIDS

By

K. M. Jeong and L. Petrakis
Gulf Research and Development Company, Pittsburgh, Pennsylvania 15230
and
M. Takayasu and F. J. Friedlaender
School of Electrical Engineering, Purdue University, West Lafayette, Indiana 47097

INTRODUCTION

The application of high gradient magnetic separation (HGMS) to shale oil has been shown by the authors (1) to be an effective method for the removal of solid particles from these hydrocarbon streams. Typical ash removal results indicated that the solids concentration was reduced by 90-100% in several different types of shale oils and that temperature effects can be significant. Similar studies (2-5) of coal and other synthetic fuels have demonstrated the usefulness of this technique in removing inorganic particulates, such as iron sulfides and pyrite, from liquid hydrocarbon streams. The application of magnetic separation methods to coal-derived liquids has been prompted by the large concentrations of iron-containing compounds present in coal ash. By comparison, the mineral matter composition of most oil shales is not as rich in iron. However, the iron composition appears to be fairly evenly distributed enabling even very small solid particles to be efficiently separated from shale oil streams.

The separation of solids from shale oil is believed to substantially simplify shale oil processing and upgrading technologies through the reduction of concomitant plugging, stability and pollution problems. An earlier paper by the authors (1) discussed the major features of the magnetic separation procedure and presented preliminary solids characterization data. The purpose of this study was to further define the nature of the separated solids and apply these results not only to the development of improved shale oil processing methods, but also to a better fundamental understanding of other organic/mineral matter systems.

In contrast to other magnetic separation techniques, HGMS is capable of separating weakly paramagnetic particles in addition to the ferromagnetic components from a bulk fluid, such as the hydrocarbon streams derived from oil shale. Magnetic separation is a physical separation process based on the interaction of four types of competing forces: tractive magnetic, gravitational, hydrodynamic and interparticle. Therefore, the quantity and quality of the separation depend both on the nature of the feed and the variable HGMS operating parameters, such as velocity, temperature, magnetic field strength, etc. Important properties of the feed to be considered include particle radius, kinematic viscosity, fluid density and the magnetic susceptibility of the particle and fluid. These latter parameters are particularly relevant to this solids characterization study. (The effects of HGMS process variables were discussed in (1)).

The typical HGMS apparatus consists of a canister filled with a ferromagnetic matrix and surrounded by a solenoid magnet. This type of separator is frequently referred to as an induced pole device, because the magnet acts upon the matrix to produce strong inhomogeneous magnetic fields which in turn generate high field gradients at the edges of the matrix filaments. These high field gradients then attract magnetic particles to the filaments, thereby trapping and separating them. Both the solids-free fluid and the trapped particles are recoverable.

The shale oil solids were characterized using several analytical techniques, including X-ray diffraction, X-ray fluorescence and thermomagnetic measurements. Similar studies of coal liquefaction mineral particulates (5) and coal filter cake solids (6) have been published. At the completion of this work, a brief report (7) describing the removal of mineral particles from shale oil by magnetic separation became available. Their proposed method (7) consists of heating the oil shale feed to at least the magnetic transformation temperature of the majority of the solids and then applying a magnetic field to the retorted shale oil in order to separate the solids from the hydrocarbon stream. Their magnetization measurements were of Green River oil shale (7), whereas this study is the first to report on the physicochemical properties of the magnetically separated shale oil solids. Certain fundamental characteristics of the separation of solids from shale oil have been obtained from single wire HGMS experiments investigating the buildup process itself (8).

Takayasu et al. (8) also presented preliminary magnetization data of the solids separated in those experiments.

EXPERIMENTAL

The HGMS apparatus and the shale oil feed samples have been described previously (1) and only a brief summary will be given here. Samples of shale oil effluent were treated using a pilot-scale commercial HGMS system. The canister volume was filled with a stainless steel wool matrix (Type 430) to which magnetic fields as large as 2T (20 kOe) were applied. The HGMS unit was equipped with various flow, temperature and pressure controllers such that fluctuations in the experimental conditions were small. Typical process variable conditions were as follows: flow rate, 10-700 ml/min; temperature, 50-250°C; pressure, 0.17 MPa. Trapped solid particles were removed from the matrix material at the completion of the separation cycle using a fixed toluene back-flush flow with the magnetic field turned off.

Three different types of shale oils were studied representing a range of mineral matter composition, organic carbon content and retorting conditions: Paraho, Addington and Moroccan. These oils were obtained from Western U. S., Eastern U. S. and Moroccan oil shales, respectively (1). The initial ash contents of these shale oils were found to vary from 130 to 9500 ppm. As mentioned earlier, the ash removal efficiencies were generally very good, as high as 100% for the Addington sample (see Table I, Reference 1).

TABLE I
BULK MINERALOGY OF SHALE OIL SOLIDS

Shale Oil	Clay	SiO ₂	FeO(OH) (wt %)	Feldspar	Amorphous ^a
Paraho	6	3	trace	trace	90
Moroccan	4	2	14	trace	80
Addington ^b	40	16	--	2	42

a. Mostly iron sulfide.

b. Pyrrhotite (Fe_{1-x}S) was identified in this sample.

The bulk mineralogy and elemental composition of the solids were determined using X-ray diffraction and X-ray fluorescence, respectively. Magnetic measurements were based on the Faraday technique using Sucksmith type pole pieces (9). Low temperature data were obtained using a 12-inch electromagnet from Pacific Electric Motor Company (type 12A-HI-A). The high temperature magnetic measurements involved a Varian Model V-400T electromagnet and a Cahn electrobalance.

CHARACTERIZATION OF SHALE OIL SOLIDS

X-Ray and Elemental Analysis

The Western (Green River Formation) oil shale, Paraho, contains relatively large concentrations of carbonate and silicate minerals in its natural state prior to retorting. The Moroccan oil shale has a similar bulk mineralogy, but in contrast to these oil shales, the Addington sample is predominantly composed of silicate minerals. These mineral compositions can be compared with the bulk mineralogy of the various separated solids summarized in Table I. The major minerals identified in the solids were clay, quartz, FeO(OH) and iron sulfide. Not surprisingly, the silicate-based Addington oil shale generated shale oil solids containing relatively large concentrations of clay and SiO₂. Since these minerals are not inherently magnetic, the data suggest a uniform distribution of iron sulfide and ferrimagnetic pyrrhotite (mass magnetic susceptibility ~0.125 emu/g) among the mineral solids and a close chemical/physical association between silicate minerals and iron-containing compounds, such as iron sulfide and pyrrhotite.

Relatively larger concentrations of amorphous material, mostly iron sulfides, were identified in the Paraho and Moroccan solids than the Addington solids. These results are consistent with the elemental composition data which indicate a substantially smaller Fe content for the Addington solids (see Table II). Although 100% ash removal was obtained from the Addington shale oil, the separated solids are relatively deficient in iron-containing compounds. Thus, factors in addition to magnetic susceptibility (e.g., average particle diameter) need to be considered in the separation of shale oil solids using HGMS (1). The major elemental constituent of the Addington solids was Si, further suggesting the possibility of an iron-silicon association. In addition, these

solids had a relatively larger concentration of elemental Al, K and Ti. The magnetic susceptibilities of such compounds are not insignificant, although substantially less than that of most Fe-containing compounds.

The organic C, H, O, N and S concentrations in the original shale oil feed compared to the separated solids were determined by conventional elemental analysis. These results (see Table III) indicate that the relative heteroatom concentration in the organic matter separated along with the solid particles is significantly enhanced. The reported increases in the O/C, N/C and S/C ratios are not due solely to a mechanical filtration procedure, but rather demonstrate the added usefulness of the HGMS method (Mechanical filtration involved passing a 1:200 shale oil : hexane mixture through a 0.125 micron filter). Thus, in addition to removing solid particles from shale oil streams, the overall quality of the resulting oil may also be improved.

TABLE II
ELEMENTAL COMPOSITION OF SHALE OIL SOLIDS

Element (Wt %)	Paraho	Moroccan	Addington
Ash	41.4	50.6	60.1
Al	0.7	0.6	1.3
Ca	4.6	0.6	0.6
Cr	<0.1	1.1	<0.1
Fe	11.4	22.2	4.5
K	1.5	0.6	3.3
Mn	0.2	0.2	0.1
P	0.8	0.6	0.4
S	10.2	7.8	3.1
Si	4.5	1.8	7.5
Ti	0.7	0.5	0.8
Others	As, Cu, μ g, Ni, Zn	As, Cu, μ g, Zn	As, Cu, μ g, Ni, Zn

TABLE III
ELEMENTAL ANALYSIS OF ORIGINAL SHALE OIL AND
MAGNETICALLY SEPARATED SHALE OIL SOLIDS

Element/ Atomic Ratio	Paraho		Moroccan		Addington	
	Original	Solids	Original	Solids	Original	Solids
Ash (wt %)	0.039	41.4 (----)	0.013	50.6	0.95	60.1
C (wt %)	83.4	29.4 (61.8)	79.5	25.7	-	30.1
H (wt %)	11.1	3.3 (6.6)	9.6	2.3	-	2.1
O (wt %)	2.2	17.4 (----)	2.2	12.3	-	5.0
N (wt %)	2.1	3.7 (3.6)	1.3	2.6	-	1.4
S (wt %)	0.88	5.7 (5.1)	7.7	6.6	-	2.3
H/C	1.59	1.33 (1.27)	1.44	1.07	-	0.83
O/C (x100)	2.0	4.4 (-----)	2.1	36	-	12
N/C (x100)	2.2	11 (5.0)	1.4	8.7	-	4.0
S/C (x100)	0.4	7.3 (3.1)	3.6	9.6	-	2.9

() Solids obtained using 0.125 micron filter.

Thermomagnetic Studies

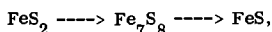
The thermomagnetic behavior of the shale oil solids was studied in the temperature range 4.2 to 1000K and in applied fields, H, up to 20 kOe. The accuracy of the experimental results are estimated to be approximately $\pm 6\%$. A typical experimental data plot of pulling force versus temperature is shown in Figure 1 for the Paraho solids at H=0 and 5 kOe. The pulling force at H=5 kOe was found to decrease with increasing temperature reflecting mainly thermal decomposition processes of organic matter and carbonate minerals which are essentially complete by about 900°C as is evidenced by the H=0 kOe data (i.e., standard thermogravimetric analysis (TGA)). Typical weight loss values due to thermal decomposition were about 40-60% (see Tables II and III).

The dependence of magnetization, σ (emu/g), on temperature and external magnetic field

are shown in Figures 2-4. The $\sigma(T)$ plots, Figures 2 and 3, were calculated based on the differences in pulling force with the magnetic field on and off (see Figure 1) at each temperature and the standard calibration between pulling force and magnetization. The magnetizations per gram at room temperature and 5 kOe for each sample were determined to be the following: Paraho - 0.85, Moroccan - 0.77 and Addington - 0.42.

The magnetizations of the Paraho and Moroccan solids, as a function of temperature over the range 25 to 900°C, were qualitatively similar (see Figure 2). Three distinct peaks were observed at an applied field of 5 kOe, although the magnetization was significantly larger for the Moroccan solids at temperatures above ~250°C, a magnetic transformation temperature (the Moroccan solids also contained the highest relative Fe concentration). This higher magnetization may be attributed to an intrinsically larger concentration of materials with higher magnetic susceptibilities at elevated temperatures. For example, it is believed that certain components, such as pyrites, interact with water present in other minerals at the magnetic transformation temperature or higher temperatures to form materials having a higher magnetization (7).

The data suggest that as the temperature is increased, the solids undergo various decomposition, chemically reactive and/or inductive processes resulting in the formation of magnetically active material. The highest temperature peak, 700-800°C, is attributed to the formation of Fe⁰ and the onset of the phase transition at the Curie point from paramagnetic to ferromagnetic character. The origin of the iron may involve the reduction of Fe⁺³ or Fe⁺² species by carbon-containing compounds present in the shale oil stream. The two peaks at lower temperatures, ~300 and 500°C, do not appear to be directly attributable to specific iron carbide or iron oxide compounds, although mineral matter effects or carbon-hydrogen bonding could possibly account for the shift of standard Curie points. The lower temperature peak may correspond to the reaction sequence



since pyrrhotite, Fe₇S₈, is strongly ferrimagnetic (Curie point ~300°C) and FeS₂ and FeS have zero and very low magnetizations, respectively (10). Pyrrhotite was identified in the Addington samples. The sharp increase in magnetization between ~400-500°C for the Paraho and Moroccan solids may be due to the transformation of iron sulfides, FeS or FeS₂, to Fe₃O₄ or gamma - Fe₂O₃ and the subsequent decline to the formation of alpha-Fe₂O₃ or FeO.

As Figure 2 indicates, the Addington thermomagnetograph differs distinctly from that of the Paraho and Moroccan solids. In general, the magnetization was observed to be essentially constant with temperature. The absence of pronounced maxima at ~500 and 750°C, as in the case of the Paraho and Moroccan samples, probably reflects the relatively low concentrations of iron sulfides and Fe-containing compounds in the Addington oil shale solids. However, the Addington solids did exhibit a Curie point for α -Fe upon cooling. The magnetization at room temperature for these solids was found to increase to 0.86 emu/g after the temperature treatment. If the magnetic pull is due entirely to Fe, then 7.0 x 10⁻⁶ g of ferromagnetic iron in 25.6 mg of sample, or 0.03 wt % Fe, was produced during the heating process assuming no weight loss.

Low temperature data, 4 to 273K, were obtained at two different field strengths, 4 and 20 kOe (see Figure 3). Analogous to the higher temperature results, the Paraho and Moroccan solids exhibit similar thermomagnetic behavior, however, the magnetization is significantly larger between 4 and 30K for the Paraho solids at both field strengths. The 4 and 20 kOe data for these two samples are distinctly displaced from one another, with larger magnetizations associated with the 20 kOe curves, but in contrast, essentially identical $\sigma(T)$ dependences were obtained for the Addington solids, with the exception of the small temperature range from 4 to 30K. In general, the Addington solids have a lower magnetization in the low temperature regime, although the magnetization increases and approaches that of the Moroccan solids with H=4 kOe between 4 and 60K. The upper temperature portion of the curves in Figure 3 confirm the earlier room temperature magnetization results reported above (see Figure 2) indicating the data to be self-consistent.

The similarity of the Addington and Moroccan magnetizations between 4 and 60K was observed to remain essentially unchanged as a function of external field. Plots of magnetization versus external field at 4.2K are shown in Figure 4. Whereas the Addington and Moroccan curves are almost superimposable, the Paraho solids exhibit much larger magnetizations over the entire range of external field studied. However, the relative increase in magnetization with temperature is comparable for all three samples.

On the basis of the magnetometric data, it appears that all the solid samples are a mixture of a weak ferromagnetic phase, indicated by the low field portion of the $\sigma(H)$ curves in Figure 4, and a paramagnetic phase. The paramagnetic phase seems to reflect the behavior characteristic of Curie-Weiss type materials and appears to be more pronounced than the ferromagnetic phase. The Paraho and Moroccan samples showed significantly larger magnetizations than the Addington solids. This weak magnetization was particularly evident by the almost flat dependence of the magnetization on temperature. In addition, the magnetization versus external field curve for the Addington solids

Figure 1

**THERMOMAGNETIC and THERMOGRAVIMETRIC BEHAVIOR of
PARAHO SHALE OIL SOLIDS from 25 °C to 920 °C (CYCLES in Ar)**

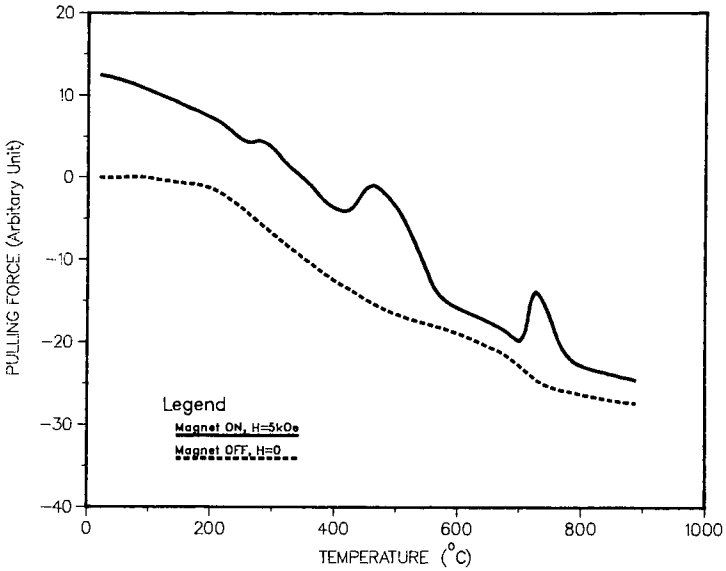


Figure 2

**PLOTS of MAGNETIZATION vs TEMPERATURE
for SHALE OIL SOLIDS**

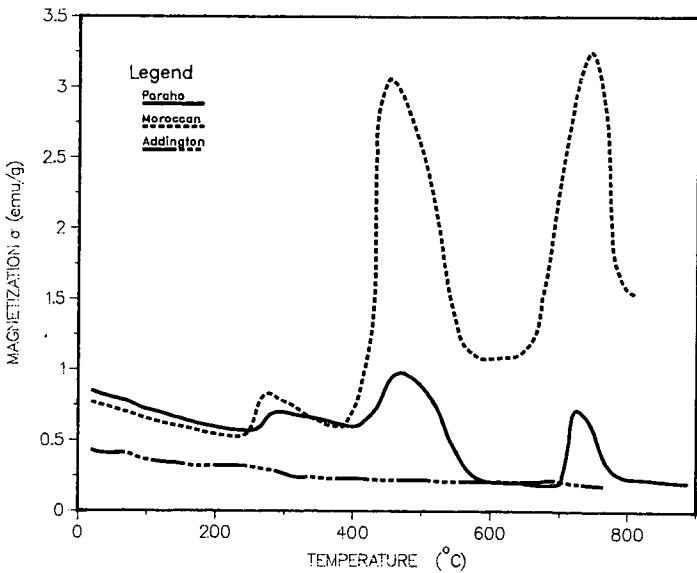


Figure 3

MAGNETIZATION - TEMPERATURE CURVES for SHALE OIL SOLIDS at LOW and HIGH EXTERNAL FIELDS (4 & 20 kOe)

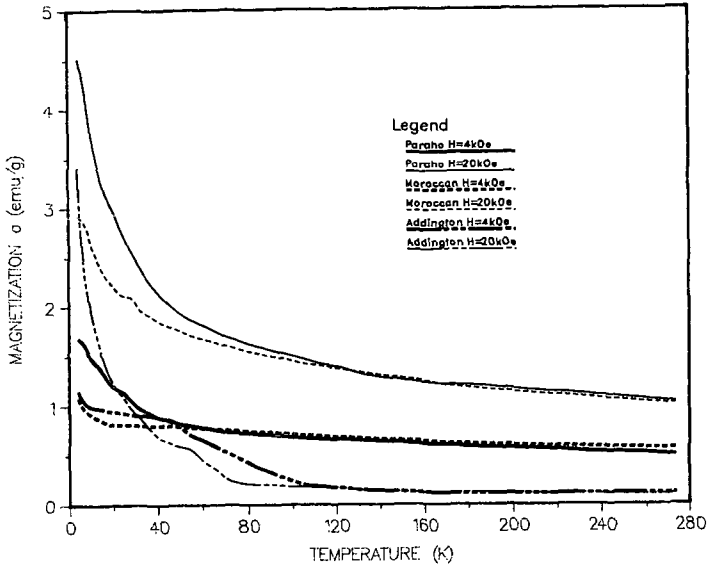
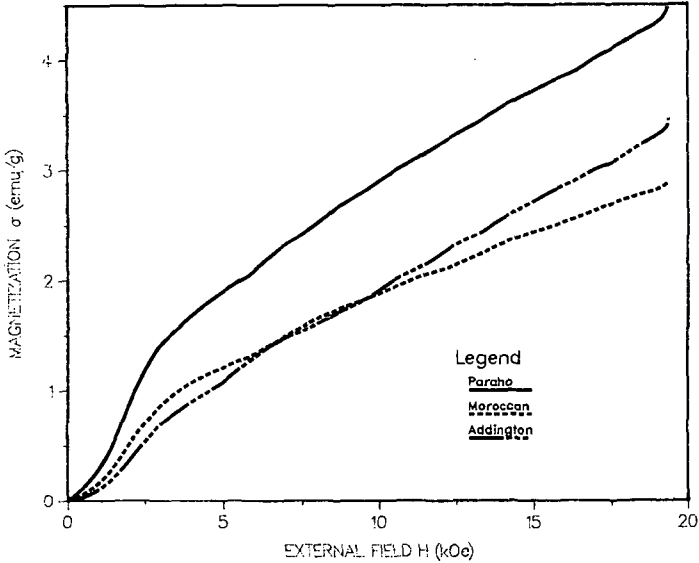


Figure 4

MAGNETIZATION - FIELD STRENGTH CURVES for SHALE OIL SOLIDS



was nearly linear, in contrast to some degree of curvature for the Paraho and Moroccan solids. This suggests that the Addington solids are mainly paramagnetic, consistent with the bulk mineralogy and elemental composition results discussed above. It should be noted that magnetometric measurements reflect the average bulk magnetic moment of the sample as a whole. Therefore, when considering mixtures of different magnetic phases, the results are representative of averaged quantities over all phases.

SUMMARY AND CONCLUSIONS

Thermomagnetic and X-ray studies have shown that the composition of shale oil solids magnetically separated from three different shale oil feeds are distinctly varied, but that high ash removal efficiencies are, nonetheless, obtainable under appropriate conditions for all three shale oils investigated. A clear example is the Addington sample which yielded 100% ash removal due to high average particle diameters, despite the lowest magnetization as a function of temperature among the three shale oil solids. On the basis of the magnetic behavior exhibited by the shale oil solids, a qualitative measure of the different phase transformations and the species present was obtained. These data reflected the general occurrence of a paramagnetic phase mixed with a trace amount of a ferromagnetic component. This conclusion is consistent with the bulk mineralogy and elemental composition results for the shale oil solids. These results may have potential application to the design of a larger scale magnetic separation system and the choice of operating parameters.

ACKNOWLEDGMENTS

This work was partially supported by the National Science Foundation. The authors appreciate the technical work done by Mr. D. L. Bash and the thermomagnetic measurements obtained by Dr. J. E. France at the University of Pittsburgh. We also acknowledge Dr. R. A. Martel of Laramie Energy Technology Center for obtaining the Moroccan shale oil sample used in this study.

LITERATURE CITED

- (1) Jeong, K. M., Petrakis, L., Takayasu, M. and Friedlaender, F. J., *IEEE Trans. Magn. Mag.*-18, 1692 (1982).
- (2) Maxwell, E. and Kelland, D. R., *IEEE Trans. Magn. Mag.*-14, 482 (1978).
- (3) Liu, Y. A. and Crow, G. E., *Fuel*, 58, 345 (1979).
- (4) Petrakis, L., Ahner, P. F. and Kiviat, F. F., *Sep. Science and Tech.*, 16, 745 (1981).
- (5) Maxwell, E., Kelland, D. R., Jacobs, I. S. and Levinson, L. M., *Fuel*, 61, 369 (1982).
- (6) Petrakis, L., Ahner, P. F. and Grandy, D. W., *Fuel*, 59, 587 (1980).
- (7) Lewis, R. T., U. S. Patent No. 4,388,179, issued June 14, 1983.
- (8) Takayasu, M., Friedlaender, F. J., Jeong, K. M. and Petrakis, L., *IEEE Trans. Magn. Mag.*-18, 1695 (1982).
- (9) Bechman, C. A., Narasimhan, K. S. V. L., Wallace, W. E., Craig, R. S. and Butera, R. A., *J. Phys. Chem. Solids*, 37, 245 (1976).
- (10) Richardson, J. T., *Fuel*, 51, 150 (1972).

SYMPOSIUM ON CHARACTERIZATION AND CHEMISTRY OF OIL SHALES
PRESENTED BEFORE THE DIVISIONS OF FUEL CHEMISTRY AND
PETROLEUM CHEMISTRY, INC.
AMERICAN CHEMICAL SOCIETY
ST. LOUIS MEETING, APRIL 8 - 13, 1984

COMPOUND-TYPE DISTRIBUTION IN SHALE OILS PRODUCED BY
FLASH HYDROPYROLYSIS OF EASTERN U. S. OIL SHALE

By

D. R. Kahn and V. H. Dayan
Energy Systems Group, Rockwell International, 8900 De Soto Avenue
Canoga Park, California 91304
and

S. A. Holmes and L. F. Thompson
Western Research Institute, P. O. Box 3395, Laramie, Wyoming 82071

INTRODUCTION

Rockwell International has been developing technology for the flash hydrolysis (FHP) of carbonaceous feedstocks under U. S. Department of Energy (DOE) sponsorship since 1975. FHP is based on the high-temperature (1100 to 1900°F) reaction of pulverized solid carbonaceous feedstocks with hydrogen in a single-stage, short-residence-time, entrained-flow reactor. Gases and liquids are produced in the reactor and unreacted material forms a dry, free-flowing char. Following product gas quench, liquid products are separated and gases are processed for recycle and product recovery. By varying the reactor operating conditions, the makeup of the product slate can be controlled over a broad range - from predominately a syncrude oil with SNG byproduct, to SNG with a relatively pure benzene byproduct, to SNG alone as the sole hydrocarbon product.

A key element of FHP is the injector/reactor technology pioneered and developed by Rockwell. This technology, first used in liquid-fueled rocket engines, has several distinctive features that make it superior to alternative means of achieving hydrolysis of carbonaceous feedstocks. These include extremely rapid mixing and heating of reactants (10 to 20 ms), precise and uniform control of temperature and reaction time, rapid startup and shutdown, unrestricted choice of feedstock and simple scaleup. In addition, because FHP operates in a short-residence-time (20 ms to 5 s), high-pressure (500 to 1500 psig), entrained-flow mode, the reactor is inherently compact.

The major oil shale development within the United States has focused on western oil shale and on recovery by pyrolytic methods. Eastern shales are hydrogen deficient compared with western shales and the corresponding oil yields produced by pyrolytic methods are much lower. The Rockwell FHP reactor seems particularly well suited for processing eastern shales, since oil yields are substantially increased by operating under a high hydrogen partial pressure.

In September, 1982, Rockwell International was awarded a DOE contract entitled "Investigation into the Application of Hydrolysis to the Hydroconversion of Eastern Oil Shale". The project had two major objectives: (a) testing, data reduction and chemical analysis to determine the performance of eastern oil shale in an FHP reactor and (b) selection of an operating point suited to high yields of shale oil and performance of a preliminary process analysis and economic assessment of the process.

A series of six tests was performed between January and March, 1983. Testing was conducted in Rockwell's existing 1-ton/h process development unit (PDU). A simplified schematic of this unit is shown in Figure 1. Three liquid products were obtained from each test: a heavy oil, a light oil and a BTX fraction.

The eastern oil shale used during the reactor testing was a blend of nine stockpiles taken from various depths in the Cleveland Member of the Ohio shale. The shale was obtained from the University of Kentucky's Institute for Mining and Minerals Research (IMMR) and pulverized to 70% through 200 mesh in an inert (nitrogen) atmosphere by Kennedy Van Saun Company, Danville, Pennsylvania. The tested shale had an average carbon content of 12.7 wt % and a Fischer Assay of ~13 gal/ton.

Key results and findings on the program were presented at the 1983 Eastern Oil Shale Symposium (1), while full details on the six tests are covered in the final report submitted to the Department of Energy, Laramie Project Office (2). Test results showed total carbon conversions as high as 70.0% and carbon conversions to liquid as high as 55.5%. Production of raw shale oil ranged from ~13.5 to 19.0 gal/ton of shale fed.

The composition of shale oil is dependent on the geographic origin of the oil shale and the pyrolysis method of extracting the liquid product (3, 4). This paper reports on the effect of process conditions in the Rockwell hydrolysis PDU on the composition of the resulting shale oil. Elemental carbon, hydrogen, nitrogen and sulfur values in each of the three liquid products were determined and H/C ratios were related to process conditions. Liquid products from three tests were further characterized by nuclear magnetic resonance (NMR) to report carbon and hydrogen aromaticities and the approximate level of aromatics, olefins and aliphatics. Nitrogen basicity was determined on the same liquid products. Finally, light-oil products from two tests representing moderate and severe process conditions were fractionated by chromatography to compare the effect of process conditions on the nitrogen compound distribution in the oil.

EXPERIMENTAL

Testing

To fulfill program objectives, two reactors were tested over a 1100 to 1400°F reactor temperature range. All tests were conducted at a nominal reactor pressure of 1000 psig and a nominal oil shale flow rate of 3/4 ton/h. The first reactor, used in tests 1 through 3, produced a nominal residence time of 200 ms; the second, used in tests 4 through 6, produced a nominal residence time of 75 ms. An average total of 1688 lb of oil shale (~212 lb of carbon) was fed per test for an average test duration of 68 min. Test conditions are summarized in Table I. At the conclusion of each test, the heavy oil product was removed from the flash drum while it was fluid and duplicate samples were taken for chemical analysis. The light-oil/water mixture was drained from the decanter after each test into 55-gal drums and duplicate representative samples were taken from each drum for analysis. The activated carbon-bed adsorber recovery system provided for recovery of vapor phase BTX and other light hydrocarbon oils in the product gas stream leaving the light-oil condenser. After each test, the bed was steamstripped to desorb the "BTX fraction". The BTX and condensed water were separated by decantation and duplicate samples were taken for chemical analysis. One set of samples was sent to the Rockwell Analytical Labs, the other to the Western Research Institute (WRI).

TABLE I
SUMMARY OF 1-TON/H PDU TEST CONDITIONS

Test	Pressure (psig)	Reactor Outlet Temp. (°F)	Residence Time (ms)	Test Duration (min)	Total Oil Shale Flowed (lbm)
OS-83-1	998	1198	198	75.1	1742
OS-83-2	1001	1329	185	68.4	1500
OS-83-3	999	1098	211	66.1	1753
OS-83-4	999	1203	74	70.2	1811
OS-83-5	1000	1422	67	60.3	1398
OS-83-6	998	1115	78	71.1	1925

Analytical Methods

The heavy-oil and BTX samples were analyzed as received, while the light-oil samples were centrifuged at 15,000 rpm at 12°C in a Sorvall Superspeed Centrifuge to separate the oil from the water. Heavy oils were analyzed for moisture content by the ASTM method for moisture in coal, while the light oils and BTX were analyzed by a Karl Fischer titration. The ash content was determined by evaporation in stages, followed by combustion at 750°C. The carbon, hydrogen and nitrogen contents of all three fractions were determined using a Perkin-Elmer 240B semimicrocombustion apparatus. Sulfur was determined by a Parr bomb combustion followed by gravimetric precipitation as barium sulfate.

The ¹H and ¹³C nuclear magnetic resonance (NMR) spectra were obtained on a JEOL FX-270 spectrometer under short-pulse delay times (2.5 s and 10 s, respectively). Shale oil samples were prepared in 5-mm tubes for the ¹H and ¹³C experiments. Deuteriochloroform (CDCl₃) was used as solvent for all samples and tetramethylsilane (TMS) was used as reference. 1% TMS in CDCl₃ provided the lock signal for ¹H and the solvent CDCl₃ provided the lock signal for ¹³C NMR spectra. Average molecular structure parameters for the shale oil samples were calculated from the normalized ¹H and ¹³C spectral areas according to equations used by Netzel and Miknis (3).

Solvent-compensated infrared spectra were recorded in the absorbance mode on a Perkin-Elmer Model 621 grating infrared spectrophotometer. High-resolution mass spectra were obtained

with a VG-ZAB mass spectrometer (accelerating voltage 8 kV, ionizing voltage 70 V and resolution at 20,000). A Finnigan-Incos data system was used to acquire and analyze the data. Samples were introduced under reduced pressure at 200°C via an oven.

At WRI, elemental nitrogen was determined by chemiluminescence using an Antek Model 771 pyroreactor with an Antek Model 720 digital nitrogen detector. A Mettler potentiometric titrator was used to titrate basic nitrogen. Titrations were done in acetic anhydride:toluene (2:1) and in acetonitrile:toluene (2:1) with perchloric acid in dioxane as titrant.

Fractionation by Adsorption Chromatography

Light-oil samples were fractionated into eight compound-type fractions using basic alumina and silica adsorption chromatography according to the procedures by Holmes (5). Linear solvent gradients of 0 to 100% methyl *tert*-butyl ether in cyclohexane and 0 to 100% methylene chloride in hexane were pumped via a Waters Model 600 solvent programmer onto basic alumina and silica gel, respectively. A variable wavelength UV/visible detector was used to indicate fraction collection end points. The chromatographic scheme is presented in Figure 2. The eight fractions were named for characteristic compound types identified by spectroscopic and titration analyses and corroborated by model compounds. Alkylpyridine-type compounds have a wide range of adsorptivity values on alumina and silica. Hindered alkylpyridine-type compounds elute early from alumina (pyridine I), whereas nonhindered alkylpyridine-type compounds elute late (pyridine III).

RESULTS AND DISCUSSION

Carbon Conversions

Experimental values of overall carbon conversion, carbon conversions to gases (total and methane only) and liquids and the distribution among the collected liquid products (heavy oil, light oil and stripped BTX oil) are summarized in Table II. Based on Rockwell's FHP experience in related fossil fuels programs, a convenient dependent variable that correlates much of the carbon conversion data is carbon conversion to methane. As temperature and residence time are increased in FHP reactors (i. e., higher reactor severity), more carbon in the feedstock is converted to methane. When the conversion and methane data in Table II are plotted in Figure 3, all data points fall along a single curve, providing an excellent correlation. Hereafter, all references to reactor severity are based on the relative conversion of carbon in shale to methane. Tests 3 and 6 had the lowest severity; tests 2 and 5 had the highest.

TABLE II
SUMMARY OF CARBON CONVERSION RESULTS

Test	Overall	To Char	To Gases		To Liquids By Difference	Liquids Distribution		
			Total	Methane Only		Stripped BTX Oil	Light Oil	Heavy Oil
OS-83-1	67.74	32.26	17.08	3.45	50.66	1.62	24.43	24.61
OS-83-2	69.99	30.01	26.11	7.39	43.88	2.43	26.61	14.84
OS-83-3	62.56	37.44	7.11	1.30	55.46	2.97	28.26	24.23
OS-83-4	67.27	32.73	14.35	2.72	52.92	4.93	24.76	23.23
OS-83-5	69.79	30.21	28.62	8.51	41.17	2.74	26.47	11.96
OS-83-6	61.43	38.57	7.15	1.19	54.28	1.02	24.52	28.74

Elemental Characterization of Oils

The chemical composition (carbon, hydrogen, nitrogen, sulfur and ash content) of the heavy oils, light oils and BTX oils are reported on a dry basis in Tables III, IV and V, respectively. A significant amount of spent shale (char) was carried into the heavy-oil collection system, as evidenced by the high ash contents (4.75 to 17.5 wt %) listed in Table III. The elemental composition of the heavy oils on a spent shale-free basis is, therefore, also presented in Table III. Nitrogen values increase from low-severity tests (tests 3 and 6) to high-severity tests (tests 2 and 5). The light oils (Table IV) show the same moderate effect of reactor severity on nitrogen content. The BTX oils (Table V) were all too low in nitrogen content to demonstrate an effect.

Compound-Type Distribution Produced Under Different Process Conditions

Liquid products produced by Rockwell oil shale FHP tests 3, 4 and 5 representing low, moderate and high processing severities (see Figure 3) were analyzed by ¹H and ¹³C NMR spectroscopy and potentiometric titration. Light oils from tests 4 and 5 were fractionated and compound types were determined by data from infrared spectroscopy, potentiometric titration and mass

spectrometry. The following discussion will focus on hydrocarbon and nitrogen compound-type distributions; ketones, ethers, sulfoxides and phenols were observed but are not reported here.

TABLE III
COMPOSITION OF HEAVY OILS

<u>Test</u>	<u>OS-83-1</u>	<u>OS-83-2</u>	<u>OS-83-3</u>	<u>OS-83-4</u>	<u>OS-83-5</u>	<u>OS-83-6</u>
<u>Wt % (dry)</u>						
Carbon	75.1	70.2	80.3	76.8	72.9	80.9
Hydrogen	5.76	4.76	6.89	6.53	5.02	7.56
Nitrogen	2.96	2.87	2.53	2.85	3.20	2.55
Sulfur	1.53	1.34	1.52	1.64	1.45	1.45
Ash	6.58	17.5	6.34	10.7	14.9	4.75
Atom H/C	0.91	0.81	1.02	1.01	0.82	1.11
Heavy Oils (Char-free)						
Carbon	80.5	85.4	85.8	86.2	85.7	85.0
Hydrogen	6.17	5.76	7.37	7.33	5.88	7.94
Nitrogen	3.17	3.48	2.70	3.19	3.75	2.67
Sulfur	1.56	1.35	1.54	1.70	1.50	1.46
Atom H/C	0.91	0.80	1.02	1.01	0.82	1.11

TABLE IV
COMPOSITION OF LIGHT OILS

<u>Test</u>	<u>OS-83-1</u>	<u>OS-83-2</u>	<u>OS-83-3</u>	<u>OS-83-4</u>	<u>OS-83-5</u>	<u>OS-83-6</u>
<u>Wt % (dry)</u>						
Carbon	85.2	86.1	85.2	85.3	86.4	85.3
Hydrogen	9.23	8.00	10.36	9.82	7.79	10.58
Nitrogen	1.61	2.16	1.43	1.43	2.14	1.06
Sulfur	1.82	2.11	1.73	1.72	2.42	1.92
Ash	0.05	0.07	0.08	0.04	0.27	0.13
Atom H/C	1.29	1.11	1.45	1.37	1.07	1.48

TABLE V
COMPOSITION OF BTX OILS

<u>Test</u>	<u>OS-83-1</u>	<u>OS-83-2</u>	<u>OS-83-3</u>	<u>OS-83-4</u>	<u>OS-83-5</u>	<u>OS-83-6</u>
<u>Wt % (dry)</u>						
Carbon	87.1	87.4	86.8	86.4	87.2	87.0
Hydrogen	11.83	10.35	11.89	12.54	10.81	10.84
Nitrogen	0.05	0.16	0.12	0.00	0.00	0.01
Sulfur	1.17	2.01	1.33	1.08	2.41	2.22
Ash	<0.01	<0.01	<0.01	<0.01	<0.01	<0.01
Atom H/C	1.62	1.41	1.63	1.73	1.48	1.48

^1H and ^{13}C NMR Spectrometric Analyses - Average molecular structure parameters calculated from the normalized proton and carbon-13 spectral areas are presented for the BTX and light oils in Table VI. As the severity of test conditions increased, hydrogen and carbon aromaticity values increased in the light oils produced from tests 3, 4 and 5. Amounts of aromatics were 54, 70 and 91 mol % in the oils from tests 3, 4 and 5, respectively. Significantly greater amounts of monoaromatics than diaromatics were present. The amount of olefins did not follow that pattern. Olefinic content was greater in the light oil produced under conditions of intermediate reactor temperature and short residence time (test 4). The aromaticities of the BTX products did not increase with reactor severity; the hydrogen and carbon aromaticities of test 4 BTX were lower than either test 3 or 5 products, while the corresponding olefinic and aliphatic contents of test 4 BTX were higher. Because of paramagnetic material resulting from the inclusion of spent shale in the heavy

oils, uncertainty in the calculations preclude determining average molecular structure parameters for the heavy-oil products. However, Table VII presents the ^1H and ^{13}C NMR data for these oils. Again, process conditions of increasing severity produced heavy oils with increased aromatic content and decreased olefinic content. To reduce the effect of the paramagnetic material, the heavy oils were benzene-extracted; NMR data on these oils are also presented in Table VII. The benzene-soluble fraction represents 87, 93 and 75%, respectively, of the char-free heavy oils for tests 3, 4 and 5.

TABLE VI
COMPOSITION OF BTX AND LIGHT OILS DETERMINED FROM NMR ANALYSIS

Test	BTX			Light Oil		
	3	4	5	3	4	5
Hydrogen aromaticity	0.22	0.13	0.29	0.16	0.18	0.43
Olefinic hydrogen	0.06	0.08	0.06	0.03	0.04	0.01
Carbon aromaticity ^a	0.48	0.38	0.56	0.34	0.45	0.73
Mol % aromatics	49	34	64	54	70	91
% mono-	48	33	63	40	62	69
% di-	1	1	1	14	8	22
Mol % olefins	11	15	10	6	10	2
Mol % alkanes	41	51	26	39	20	6
Total atomic H/C	1.63	1.73	1.48	1.45	1.37	1.07
Aromatic H/C	0.74	0.61	0.76	0.67	0.55	0.63
Aliphatic H/C	2.44	2.42	2.39	1.84	2.05	2.29

a. Uncertainty is ± 0.05 . Includes olefinic carbons.

TABLE VII
NMR ANALYSIS OF HEAVY OILS PRODUCED BY FHP

Test	Heavy Oil		
	3	4	5
Total Heavy Oil			
Hydrogen aromaticity	0.23	0.28	0.37
Olefinic hydrogen	0.03	0.01	0.00
Carbon aromaticity ^a	0.59	0.56	0.88
Benzene-Extracted Heavy Oil			
Hydrogen aromaticity	0.28	0.31	0.47
Olefinic hydrogen	0.04	trace	0.00
Carbon aromaticity ^a	0.53	0.56	0.76

a. Includes olefinic carbons.

Potentiometric Titration Analysis - Potentiometric titration measures basicities in oils. Different classes of nitrogen compounds often display different basicities, which then provide general information regarding the distribution of nitrogen compound types. An alkylamine is more basic than an arylamine, which is much more basic than alkylindole.

Measurements of wt % nitrogen were obtained by chemiluminescence detection for the BTX, light oil and heavy oils produced from tests 3, 4 and 5 and these values are presented in Table VIII. The heavy oil values are the nitrogen content of the benzene-soluble material. These results demonstrate that nitrogen is concentrated in the heavier oil fractions. In general, the amount of nitrogen increases in the corresponding oils from tests 3, 4 and 5 as reactor severity increases.

Results of the potentiometric titration analyses are also shown in Table VIII. Except for the BTX liquids, as the severity of processing conditions increased, the amount of basic nitrogen in corresponding oils also increased. The percent of total nitrogen which is weak base I (pKa of the conjugate acid 7 to 9), primarily pyridine-type compounds, generally increased from heavy oil to light oil to BTX. The percent of total nitrogen which is weak base II (pKa of the conjugate acid 2 to 7), primarily alkylarylamines, was very low. These compound types were probably reaction intermediates resulting from hydrogenation of reactive nitrogen-containing compounds during processing.

For heavy and light oils, the percent of total nitrogen that was nonbasic nitrogen was equal to or greater than the amounts of basic nitrogen and represents compound types such as alkylindoles and alkylamides.

TABLE VIII
POTENTIOMETRIC TITRATION RESULTS OF SHALE OILS
PRODUCED BY FLASH HYDROPYROLYSIS

Test	Wt % Nitrogen	% of Total Nitrogen			
		Basic			Nonbasic (pka >2)
		Weak Base I (pka 7 to 9)	Weak Base II (pka 2 to 7)		
BTX					
3	0.065	45	0	55	
4	0.018	87	0	13	
5	0.036	69	0	31	
Light Oil					
3	1.22	36	2	62	
4	1.36	40	<1	59	
5	1.87	48	4	48	
Heavy Oil					
3	2.42	26	2	72	
4	2.78	31	2	67	
5	3.04	49	3	48	

Compound-Type Fractionation Analysis - Chromatographic techniques were used to fractionate the complex matrix of two light oils into simpler compound-type fractions. Although overlap of similar compound types occurred in successive fractions, characterization of these fractions by spectroscopic and titration analyses helped to determine the compound-type distribution in each oil. In the following discussion, emphasis is on the nitrogen compound-type distributions determined in the light oils from tests 4 and 5.

As shown earlier in Figure 2, adsorption chromatography generated eight compound-type fractions displaying distinct infrared absorbances characteristic of major compound types: hydrocarbon, pyridine I, pyridine III/phenol, pyridine III/amide, pyrrole, ketone/pyrrole, diazaaromatic and pyridine II. Each light oil was comprised of significant amounts of neutral hydrocarbons with 46 and 54 wt % of the oil from tests 4 and 5, respectively, composed of nonhydrocarbon fractions (nitrogen-containing). The nonhydrocarbon fractions from test 5 oil were considerably more aromatic, as indicated from infrared and mass spectrometric analyses, than those from the test 4 oil. For example, quinolines and their homologs composed 17 wt % of the pyridine I fractions from the light oils of tests 5 and only 9 wt % in the same fraction from test 4. Quinolines were not found in the pyridine III/phenol fraction from the test 4 oil, but they amounted to 4 wt % in a similar fraction from the test 5 oil.

Each fraction was further characterized by methods previously reported by Holmes and Thompson (4) that allowed determining the nitrogen compound distribution in the light oils from tests 4 and 5. Table IX presents these results. About 94 and 92% of the nitrogen in oils from tests 4 and 5, respectively, was characterized; the remaining nitrogen was either lost by fraction drying or irreversible adsorption onto the chromatographic adsorbents. Strong bases such as alkylamines/piperidines were found only in the test 4 oil and in very small amounts. Lesser amounts of alkylpyridines/quinolines were found in the test 4 oil than in the test 5 oil. Significantly greater amounts of alkylhydroxypyridines and alkylazaindoles/diazaaromatics were found in the test 4 oil, but greater amounts of alkylpyrroles/indoles/carbazoles/nitriles and N-alkylcarbazoles were found in the test 5 oil.

The more severe processing conditions employed in test 5 produced a light oil containing a greater amount of total nitrogen, the most being in the form of weak base I nitrogen compounds (37%). Generally, greater amounts of the reaction intermediates weak base II such as N-alkarylamines and alkarylamines were present in the test 5 oil. The significantly greater amounts of N-alkylcarbazoles and alkylpyrroles/indoles/carbazoles/nitriles present in the test 5 oil may have resulted from more organic material having been converted from the kerogen under severe processing conditions. These latter compound types are relatively more stable, especially compared with amide-type compounds, as hydrogenation accompanies processing. The differences in the distribution of nitrogen compound types in these two light oils may affect hydrotreating conditions necessary to reduce nitrogen content to produce a viable transportation fuel or chemical feedstock.

TABLE IX

NITROGEN COMPOUND-TYPE DISTRIBUTION IN LIGHT OILS FROM TESTS 4 AND 5

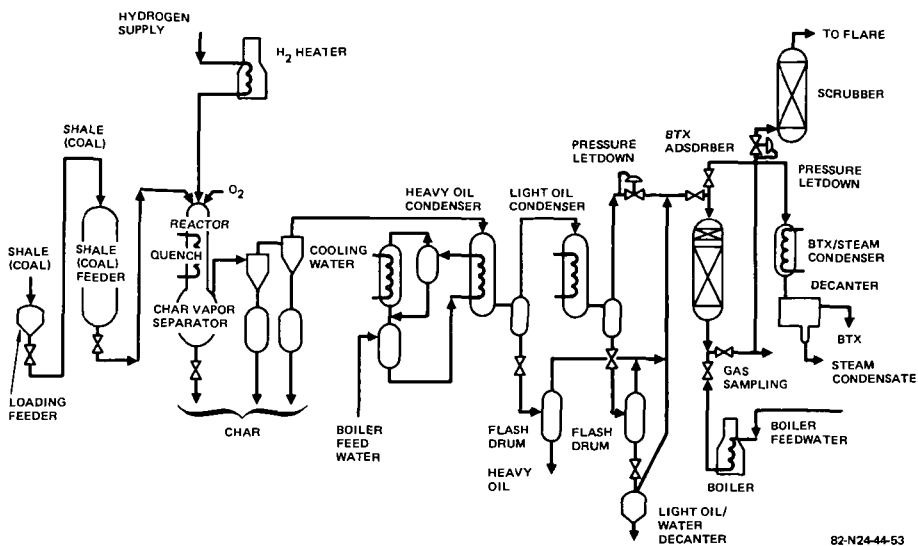
Compound Type	Wt % Nitrogen		% of Total Nitrogen	
	Test		Test	
	4	5	4	5
Strong Base				
Alkylamines/piperidines	0.005	-	0.4	-
Weak Base I				
Hindered alkylpyridines/quinolines	0.167	0.228	12.3	12.2
Less hindered alkylpyridines/quinolines	0.161	0.254	11.9	13.6
Nonhindered alkylpyridines/quinolines	0.134	0.214	9.9	11.4
Weak Base II				
Unknown	0.030	0.044	2.2	2.4
N-alkylarylamines	0.002	0.036	0.2	1.9
Alkylarylamines	0.046	0.056	3.4	3.0
Very Weak Base				
N-alkylindoles	0.032	0.027	2.4	1.4
Alkylpyrroles/indoles	0.178	0.283	13.2	15.1
Alkylloxazoles	0.008	0.007	0.6	0.4
Alkylhydroxypyridines	0.148	0.069	10.9	3.7
Alkylazaindoles/diazaaromatics	0.031	0.023	2.2	1.2
Nonbasic				
N-alkylcarbazoles	0.012	0.047	0.8	2.5
Alkylpyrroles/indoles/carbazoles/nitriles	0.171	0.312	12.6	16.7
Alkylanilides/N-acetylindoles	0.006	-	0.5	-
Alkylbenzamides	0.100	0.114	7.3	6.1
Alkylazaindoles/diazaaromatics	0.044	-	3.3	-
Total	1.28	1.71	94	92

Effect of Catalytic Hydrotreatment on Nitrogen Compound Types - In earlier work (3), different nitrogen compound types were shown to have different reactivities toward catalytic hydro-treatment. The ease of hydrogenation of nitrogen types from least to most difficult are: amides, pyridines, pyrroles and hindered alkylpyridines. Amounts of these compound types in the light oils from tests 4 and 5, respectively, are determined from Table IX: amides (19 and 10%), pyridines (22 and 25%), pyrroles (29 and 36%), hindered pyridines (12 and 12%). Earlier compositional studies (4) of crude and hydrotreated western (Green River) and eastern (Sunbury and New Albany) shale oils produced by IGT in the Hystort Process Development Unit were used to establish the amount of nitrogen removal by catalytic hydrotreatment as a function of the nitrogen compound-type distribution in the crude shale oil (HDN factor). The hydrotreating conditions used in establishing the relationship were: 2000 psia (13.8 MPa) hydrogen pressure, 800°F (428°C) catalyst temperature, LHSV of 0.4 and nickel/molybdenum catalyst. Details of deriving the relationship are summarized elsewhere (7). Allowing for differences in the total nitrogen content of the light oils, the HDN factors for these oils from tests 4 and 5 were calculated to be 1.02 and 0.69, respectively. Projections of the amount of nitrogen removal based on Figure 4 and the calculated HDN factors show that at the quoted hydrotreatment conditions about 95% of the nitrogen in the light oil from test 4 and 84% of the nitrogen in the light oil from test 5 may be removed. Presumably, the greater severity of processing conditions employed in test 5 produces a light oil containing more nitrogen in more nonreactive nitrogen compounds than that in the oil from test 4. This may result in decreased nitrogen removal during catalytic hydrotreatment of test 5 light oil.

SUMMARY AND CONCLUSIONS

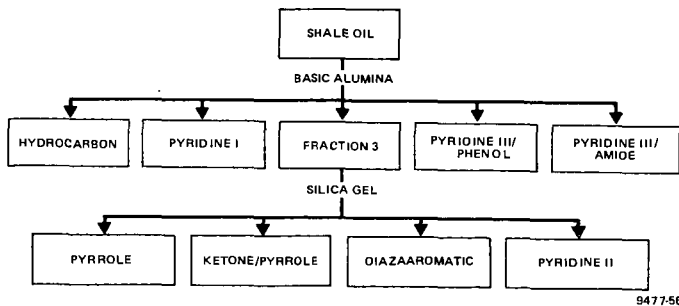
The chemical composition of shale oils produced by flash hydrolysis is dependent on process conditions. The atomic H/C ratios of light and heavy oils decrease with increasing process severity, while the nitrogen content increases. In contrast, process severity seems to have little effect on either H/C or nitrogen content with the BTX oils, which comprise less than 10% of the liquid products. For light, heavy and BTX oils, olefinic content decreases, aromatic content increases, aliphatic content decreases and basic nitrogen increases with increasing severity.

Increasing process severity converts more refractory compounds of the kerogen in shale to liquids and simultaneously converts labile liquids to gases by cleaving alkyl groups from aromatic



82-N24-44-53

Figure 1. Simplified schematic of Rockwell 1-ton/h liquefaction PDU



9477-56

Figure 2. Scheme for the fractionation of shale oils from Rockwell FHP Tests 4 and 5 into compound-type fractions.

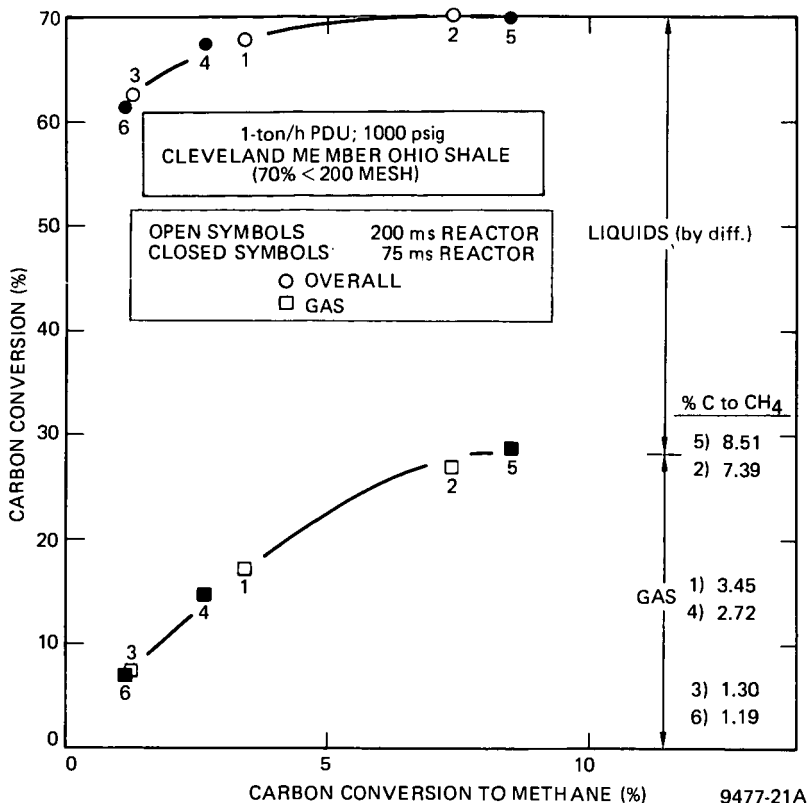


Figure 3. The effect of reactor severity on carbon conversion.

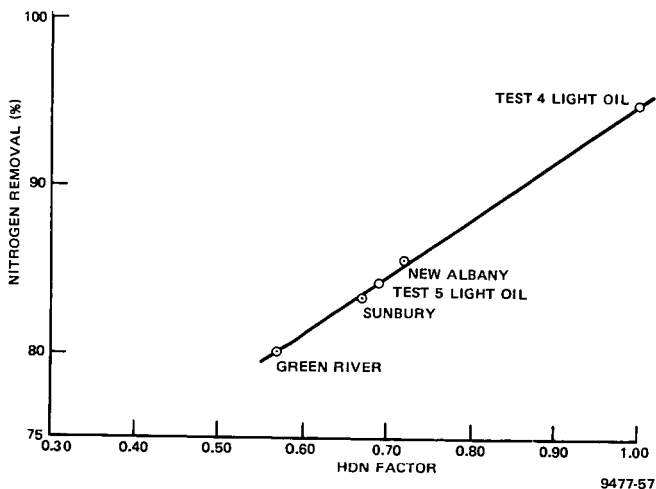


Figure 4. Relative ease of nitrogen removal from light oils from Tests 4 and 5 by catalytic hydrotreatment.

rings. This results in liquids of high-aromatic, low-olefinic and low-aliphatic content. In general, increasing process severity produces oils containing greater amounts of nitrogen in compounds less susceptible to hydrogenitrogenation. It suggests that increasing the severity of hydrotreating will be required to reduce their nitrogen content.

LITERATURE CITED

- (1) Kahn, D. R., Falk, A. Y. and Garey, M. P., "Flash Hydropyrolysis of Eastern Oil Shale", presented at the 1983 Eastern Oil Shale Symp., Lexington, Kentucky, November 13-16, 1983.
- (2) Falk, A. Y., Garey, M. P. and Rosemary, J. K., "Application of Hydropyrolysis to the Hydroconversion of Eastern Oil Shale", Final Report, ESG-DOE-13406, Rockwell International Corp., Environmental and Energy Systems Div., November, 1983.
- (3) Netzel, D. A. and Miknis, F. P., "NMR Study of U. S. Eastern and Western Shale Oils Produced by Pyrolysis and Hydropyrolysis", Fuel, 61, 1101-1110 (1982).
- (4) Holmes, S. A. and Thompson, L. F., "Nitrogen Compound Distribution in Eastern and Western U. S. Shale Oils Produced by Hydropyrolysis", 1982 Eastern Oil Shale Symp., Lexington, Kentucky, October, 1982.
- (5) Holmes, S. A., "Low Pressure Liquid Chromatography of Nitrogen Compounds in Shale Oil", 37th Ann. Northwest Regional Meeting of the ACS, p. 20, June, 1982.
- (6) Shale Oil Upgrading and Refining, S. A. Newman, Ed., Butterworth Publishers, Boston, pp. 159-181 (1983).
- (7) Holmes, S. A. and Thompson, L. F., "Shale Oil Upgrading: Effect of Nitrogen Compound Types on Catalytic Hydrotreatment", to be presented at the 188th Natl. ACS Meeting, St. Louis, Missouri, April 8-13, 1984.

SYMPOSIUM ON CHARACTERIZATION AND CHEMISTRY OF OIL SHALES
PRESENTED BEFORE THE DIVISIONS OF FUEL CHEMISTRY AND
PETROLEUM CHEMISTRY, INC.
AMERICAN CHEMICAL SOCIETY
ST. LOUIS MEETING, APRIL 8 - 13, 1984

INTERACTION OF TETRAHYDROFURAN WITH ATHABASCA BITUMEN

By

A. Majid and J. Woods

Division of Chemistry, National Research Council of Canada, Ottawa, Ontario, Canada K1A 0R9

INTRODUCTION

Athabasca bitumen has been the subject of numerous investigations with attention usually focussing on the structure and chemical composition. Important works related to this subject have been extensively reviewed by Bunger et al. (1).

Separation of bitumen into a number of fractions is always the first step in these studies. Subsequently, the fractions are characterized by chemical and spectroscopic techniques. In most published work, the separations are based on different solubilities of bitumen fractions in various solvents. Combinations of solubility effects and chromatographic fractionation of bitumen are also frequently used.

Recently, Furinsky et al. (2) have fractionated an athabasca bitumen in tetrahydrofuran by gel permeation chromatography (GPC), which separates molecules on the basis of their molecular size. Structural parameters were determined from proton nmr. Elemental, nickel and vanadium analyses of the fractions were also reported. All of these fractions had exceptionally high oxygen content compared with that of the feed. As THF is known to form hydrogen bonded complexes with a number of compounds (3), this anomalous oxygen content could be caused by the interaction of THF with some bitumen components. We, therefore, undertook to investigate the interaction of tetrahydrofuran with bitumen both as an eluent in the GPC fractionation and as a solvent. The fractions have been characterized using elemental analyses and infrared and ^{13}C nmr spectroscopy.

EXPERIMENTAL

The sample of Athabasca bitumen was obtained from the Alberta Research Council sample bank. This was a standard bitumen sample used recently in a round robin study (4).

Gel Permeation Chromatography

Equipment - The liquid chromatographic system consisted of a microprocessor controlled solvent delivery system (series 3B), an auto sampler (model ISS-100), a variable wavelength scanning uv detector (LC 75/AC) and a refractive index (RI) detector (LC-25), all from the Perkin-Elmer Corp.

Column - Fractionation of bitumen was performed using a μ -styragel column (30 cm x 7.8 mm I. D., Waters Associates) of pore size 500Å.

Solvents - All solvents used in this study were of analytical grade or HPLC grade and were used without further purification.

Procedure - Bitumen solutions in THF were filtered using micro pore filters (Millipore; pore size $\sim 0.45\ \mu\text{m}$) prior to transferring into the vials. Concentration of bitumen solution was $\sim 4\%$. $50\ \mu\text{l}$ of the sample was injected using a flow rate of $1\ \text{ml}^{\text{L}}$ per minute. The fractionation in THF was carried out with the uv detector set at 254 nm and in toluene, at 290 nm.

Solvent Evaporation

The greater part of the solvent was removed in a Brinkman rotary evaporator at 50°C for THF, or 80°C for toluene, under reduced pressure. The remaining solvent was removed on a Brinkman model SC/24R sample concentrator, under nitrogen.

In a separate experiment, 0.5 g of bitumen was dissolved in 1 litre of THF. Solvent was then removed from half of this solution at 50°C and the other half at room temperature using the procedure outlined above.

Elemental Analyses

C, H and N analyses were performed using a Perkin-Elmer model 240 CHN analyzer. Sulfur was analyzed as total sulfur X-ray fluorescence spectroscopy. Oxygen was determined by

difference.

Instrumental Analyses

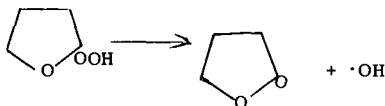
Infrared spectra were recorded using a Perkin-Elmer model 683 IR spectrometer. Samples were run as thin films on KBr plates.

^{13}C nmr spectra were obtained at 45.26 MHz on a Bruker CXPI80 nmr spectrometer under ^1H decoupling conditions and 5000-30,000 puses at intervals of 2 seconds.

RESULTS AND DISCUSSION

GPC elution curves of Athabasca bitumen in both tetrahydrofuran and toluene obtained using uv detector are shown in Figure 1. The sample was separated into two fractions as shown in the figure. Fraction 1 should contain the higher molecular weight material, which was confirmed by the molecular weights determinations on the two fractions. Polydispersity, the ratio of the weight average molecular weight to the number average molecular weight indicates a wider distribution of molecular sizes in fraction 1 compared with fraction 2.

Elemental composition of bitumen fractions, obtained from GPC and after treating with THF in both air and nitrogen, are given in Table I. Since oxygen content was determined by difference, all the errors in the determinations of carbon, hydrogen, nitrogen and sulfur will accumulate in the oxygen results. Elemental composition of GPC fractions in toluene indicates higher heteroatom (N, S, O) content of fraction 1 compared with fraction 2. This is again consistent with fraction 1 being a heavier fraction because heavier fractions of bitumen are known to contain higher heteroatom content (5). Elemental composition of the GPC fractions in THF cannot be rationalized simply on the basis of heavier and lighter fractions. Whereas there is no significant difference in the chemical compositions of fraction 2 in THF or toluene, the fractions 1 have very different chemical compositions. Most of the nitrogen is concentrated in fraction 1 for toluene solutions, whereas the corresponding fraction in THF has no detectable nitrogen. Also, the oxygen content of fraction 1 in THF is much higher than the corresponding fraction in toluene. THF is well known to form an unstable hydroperoxide which decomposes according to (6-8):



It has been previously reported that in the presence of free radical initiators THF and other ethers are not inert solvents and they act both as reactant and solvent (9). Incorporation of THF during the reductive alkylation of coal has also been noticed. The nature of the interaction between THF and the alkylated coal was said to be mysterious (10). Carson et al. (11) have reported the formation of trace quantities of an unidentified compound during the reaction of 1,2,3,4-tetrahydronaphthalene with THF. Cleavage of THF by benzene has long been observed (12). Therefore, in view of the reactivity of THF, particularly in the presence of free radical initiators, the interaction of THF or THF hydroperoxide decomposition products with bitumen components would not be surprising. Interaction of bitumen with THF was, therefore, investigated both in the presence of air and nitrogen. Elemental composition of bitumen treated with THF in the presence of air suggests the possibility of such an interaction. This bitumen has an unexpectedly high oxygen content that cannot be explained on the basis of experimental errors. The loss of nitrogen on heating bitumen with THF in air is consistent with the GPC results, where the absence of nitrogen was also found in the heavier fraction from THF solution.

HPLC grade THF used in this investigation contained no inhibitor. On treating with acidified KI, it liberated trace quantities of iodine indicating the presence of small quantities of hydroperoxide. Therefore, in a separate experiment, THF was freshly distilled from LiAlH_4 to remove hydroperoxide. This freshly distilled THF, when treated with bitumen under nitrogen, gave elemental analysis very similar to that of untreated bitumen. This demonstrates the significance of THF hydroperoxide during the interaction of bitumen with THF.

Infrared Spectra

Infrared spectra of Athabasca bitumen, its GPC fractions in THF and bitumen treated with THF in air, are shown in Figure 2. Infrared spectra of bitumen treated with freshly distilled THF in nitrogen and its GPC fractions in toluene were similar to that of the untreated bitumen. The infrared spectrum of GPC fraction 2 in THF is also similar to the infrared spectrum of untreated bitumen. However, the infrared spectra of GPC fraction 1 in THF and of bitumen treated with THF in

air contain characteristic absorption bands assignable to oxygen functions. Both exhibit a broad absorption band in the 3100-3500 cm^{-1} region due to the presence of hydrogen bonded -OH (13). Two sharp bands at 1725 and 1770 cm^{-1} present in the infrared spectra of GPC fraction 1 from THF and bitumen treated with THF in air have previously been assigned to six membered ring anhydrides (14, 15), acyl and aryl peroxides (16) and to α -hydroxytetrahydrofuran and butyrolactone (17), which are the decomposition products of tetrahydrofuran hydroperoxide (18). However, a definite assignment for the carbonyl absorption is difficult because a number of oxygen containing functions including aldehydes, ketones, acids and esters absorb in this region (19) and all of these species are said to be produced during the oxidation of bitumen and asphaltic materials (14, 15, 20-23).

TABLE I
CHEMICAL COMPOSITION OF BITUMEN FRACTIONS

Fraction	Elemental Analyses (Wt %)					Polydispersity ^e
	C	H	N	S	O ^d	
Athabasca bitumen (feed)	83.01	10.48	0.44	4.74	1.33	6.0
GPC-fraction 1 in toluene ^a	80.44	9.97	0.42	5.10	4.07	7.8
GPC-fraction 2 in toluene ^b	82.92	10.79	0.11	3.88	2.30	1.0
GPC-fraction 1 in THF ^a	76.08	9.80	-	4.58	9.54	4.3
GPC-fraction 2 in THF ^b	81.83	9.70	0.20	5.06	3.21	1.1
Bitumen treated with THF ^c						
at 30°C in air	70.88	8.83	0.32	3.48	16.49	N. D.
Bitumen treated with THF ^c						
at 50°C in air	65.21	8.60	-	4.5	21.69	N. D.
Bitumen treated with THF ^c						
at 50°C in N ₂	81.08	9.98	0.34	5.19	3.41	N. D.

a. Collected between 0 and 26 minutes.

b. Collected between 26 and 33.5 minutes.

c. 0.5 g of bitumen dissolved in 1L of HPLC grade THF and then solvent removed under reduced pressure at 30°C in one case and 50°C in the other two cases.

d. Determined by difference.

e. Ratio of wt average molecular wt to no. average molecular wt determined by GPC.

N. D.: Not determined.

¹³C NMR

¹³C nmr spectra of Athabasca bitumen, its GPC fractions in toluene and THF, and bitumen treated with THF in air are shown in Figure 3. The ¹³C nmr spectrum of bitumen treated with freshly distilled THF under nitrogen was similar to the nmr spectrum of the untreated bitumen. Also, it is obvious from the spectra in Figure 3 that GPC fractions in toluene have similar spectra to that of untreated bitumen. GPC fraction 2 in THF has a much simpler spectrum resembling the spectrum of untreated bitumen except that the long chain methylene peak at ca. 29.7 ppm is less intense and the low field broad absorption in the aromatic region has disappeared. This suggests that GPC fraction 2 has much simpler aromatic systems with none or very few branched substituents.

The ¹³C nmr spectra of GPC fraction 2 in THF and bitumen treated with THF in air at 30°C and 50°C contain a number of resonances characteristic of oxygen functions (24-28). All three fractions exhibit signals over the ranges 60-68 and 98-109 ppm that can be assigned to the α -alkyl carbon of alcohols, ethers and esters. The sets of signals at 161-163 ppm, 175-178 ppm and 201-202 ppm exhibited by GPC fraction 2 in THF and by bitumen treated with THF in air at 50°C, are due to anhydrides, esters, acids, aldehydes, ketones and quinones. The resonances of 130-136 and 143-146 ppm exhibited by the bitumen treated with THF in air at 50°C are most likely due to the presence of peri- and cata-condensed systems.

The presence of butyrolactone, a decomposition product of THF hydroperoxide (18), is indicated by the resonances of 178, 69, 28 and 22 ppm in the spectra of GPC fraction 2 in THF and of the bitumen treated with THF in air at 50°C.

Based on the results of the spectroscopic studies and elemental analyses of the GPC fractions of bitumen and bitumen treated with THF, the following conclusions can be drawn.

1. Bitumen reacts with THF in presence of air producing considerable quantities of oxygen containing functional groups. Oxidation of bitumen by THF results in the initial formation of THF hydroperoxide which decomposes giving

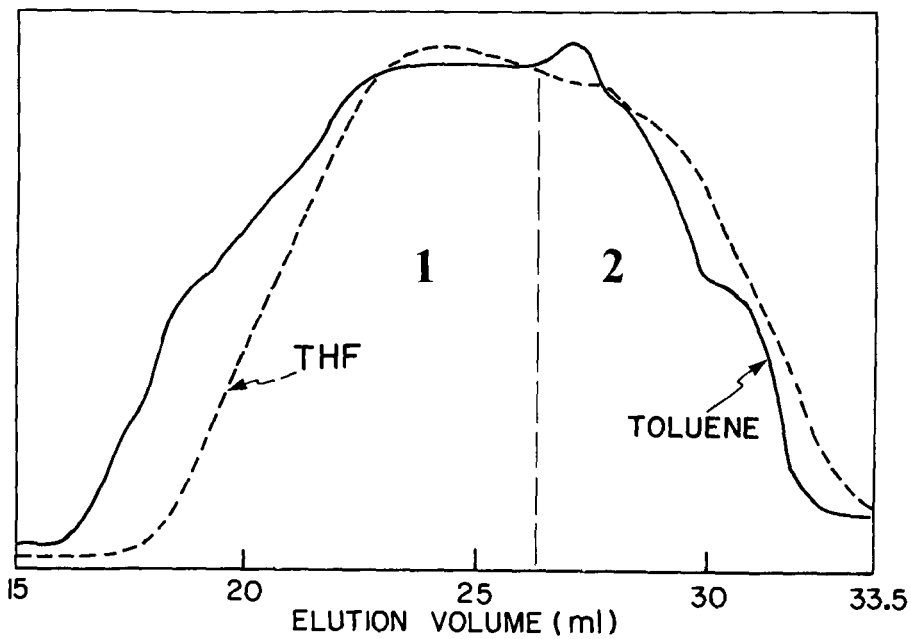


Figure 1. GPC chromatogram of Athabasca bitumen obtained using uv detector. — in toluene; - - - - in THF.

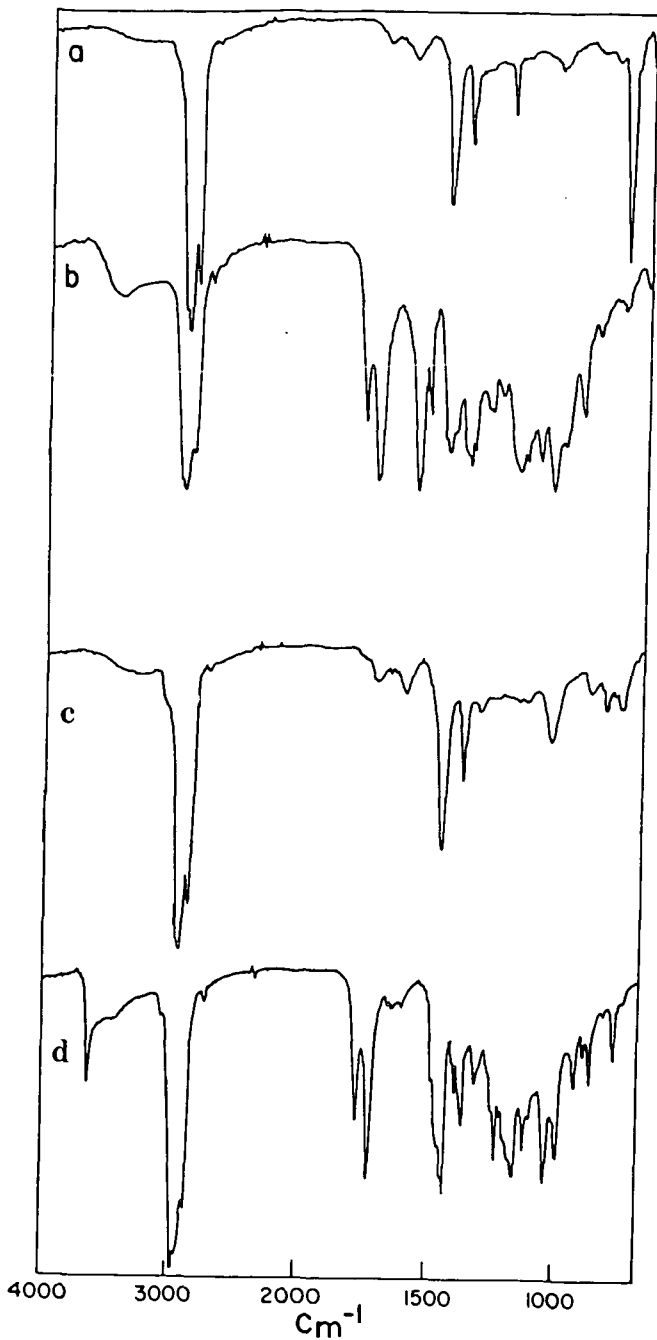


Figure 2. Infrared spectra of a) Athabasca bitumen; b) Bitumen dissolved in THF and solvent removed under reduced pressure; c) GPC fraction in THF collected between 26 and 33.5 minutes; d) GPC fraction in THF collected between 0 and 26 minutes.

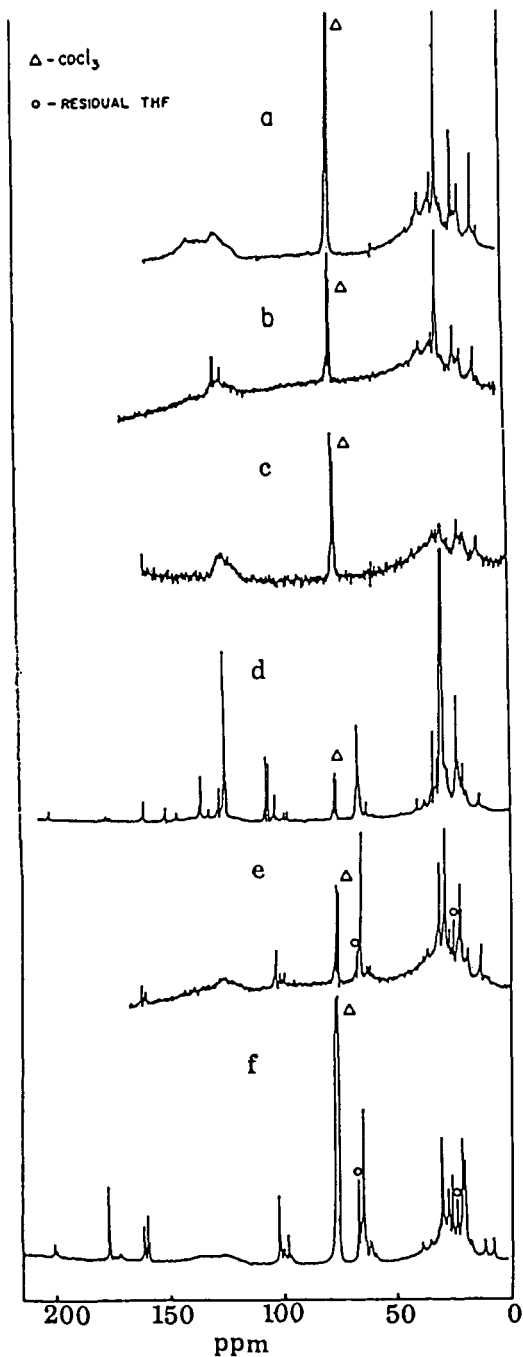


Figure 3. ^{13}C nmr spectra of a) Athabasca bitumen; b) a typical GPC fraction in toluene; c) GPC fraction in THF collected between 26 and 33.5 minutes; d) GPC fraction in THF treated with THF at 30°C in air and 26 minutes; e) Bitumen treated with THF at 30°C in air and f) Bitumen treated with THF at 50°C in air.



and $\cdot\text{OH}$ radicals that act as initiators.

2. Oxidation of bitumen by THF is faster at 50°C than at room temperature.
3. THF only oxidizes heavier fractions of bitumen which are rich in heteroatom content (N, O, S). This is consistent with the previous results for the oxidation of bitumen (29, 30).
4. Oxidation of bitumen by THF can be prevented by using freshly distilled THF containing no hydroperoxide.

ACKNOWLEDGMENTS

The authors are grateful to a number of colleagues for helpful discussions and experimental assistance. We are particularly indebted to Dr. D. W. Davidson for reading the manuscript and numerous useful comments, J. H. R. Seguin for elemental analysis, V. Clancy for infrared spectra, Dr. C. I. Ratcliffe for C-13 nmr spectra and Dr. Bryan D. Sparks and J. A. Ripmeester for many helpful discussions.

LITERATURE CITED

- (1) Bunger, J. W., Thomas, K. P. and Dorrence, S. M., *Fuel*, **58**, 183 (1979).
- (2) Furimsky, E. and Champagne, P. J., *Fuel Processing Technology*, **9**, 269 (1982).
- (3) Phillip, V. P. and Anthony, R. G., *Fuel*, **61**, 357 (1982).
- (4) Alberta Committee on Oil Sands Analysis, Bitumen Round Robin No. 2, Final Report.
- (5) Strausz, O. P., 1st Internatl. Conf. on the Future of Heavy Crude Oils and Tar Sands, June 4-12, 1979, p. 187.
- (6) Robertson, A., *Nature* **162**, 153 (1948).
- (7) Hawkins, E. G. E., "Organic Peroxides", E. and F. Spon Ltd., London (1961).
- (8) Ilin, Y. V., Plakhotnik, V. A., Glukhovtsev, V. G. and Nikishin, G. I., *Izv. Akad. Nauk. USSR, Ser. Khim* **2243** (1982), cf. *Chemical Abstracts* 98:71302j.
- (9) Grochowski, E., Boleslawska, T. and Jurczak, J., *Synthesis*, **718** (1977).
- (10) Larson, J. W. and Urban, L. O., *J. Org. Chem.*, **44**, 3219 (1979).
- (11) Carson, D. W. and Ignasiak, B. S., *Fuel*, **59**, 757 (1980).
- (12) Wolthuis, E., Bouma, M., Madderman, J. and Sysma, L., *Tetrahedron Letters*, p. 407 (1970).
- (13) Moschopedis, S. E. and Speight, J. G., *Fuel*, **55**, 187 (1976).
- (14) Peterson, J. C., Barbour, F. A. and Dorrence, S. M., *Anal. Chem.*, **47**, 107 (1975).
- (15) Moschopedis, S. E. and Speight, J. G., *Fuel*, **57**, 647 (1978).
- (16) "Spectroscopic Identification of Organic Compounds", R. M. Silverstein, G. C. Bassler and T. C. Morrill, eds., John Wiley and Sons, NY (1981).
- (17) Rabek, J. F., Skowronski, T. A. and Ranby, B., *Polymer*, **21**, 226 (1980).
- (18) Stenberg, V. J., Wang, C. T. and Kulevsky, N., *J. Org. Chem.*, **35**, 1774 (1970).
- (19) Bellamy, L. J., "The Infrared Spectra of Complex Organic Molecules", John Wiley and Sons, Inc., NY (1966).
- (20) Knotnerus, J., *J. Inst. Petrol.*, **52**, 355 (1956).
- (21) Campbell, P. G. and Wright, J. R., *J. Res. Nat. Bur. Stand.*, **680**, 115 (1964).
- (22) Moschopedis, S. E. and Speight, J. G., *Fuel*, **54**, 210 (1975).
- (23) Moschopedis, S. E. and Speight, J. G., *Proc. Asphalt Paving Technologists*, **45**, 78 (1976).
- (24) "Atlas of Carbon-13 NMR Data", E. Breitmaier, G. Haas and W. Voelter, eds., Heyden, London (1979).
- (25) "Carbon-13 NMR Spectroscopy", G. C. Levy, R. L. Lichter and G. L. Nelson, eds., John Wiley and Sons, NY (1972).
- (26) Barron, P. F. and Wilson, M. A., *Nature*, **289**, 275 (1981).
- (27) Pugnaire, J. R., Grant, D. M., Zilm, K. W., Anderson, L. L., Oblad, A. G. and Wood, R. E., *Fuel*, **56**, 295 (1977).
- (28) Snape, C. E. and Ladner, W. R., *Anal. Chem.*, **51**, 2189 (1979).
- (29) Speight, J. G. and Moschopedis, S. E., *Fuel*, **57**, 235 (1978).
- (30) Speight, J. G. and Moschopedis, J., *Can. Pet. Techn.*, **73** and references therein (1978).

SYMPOSIUM ON CHARACTERIZATION AND CHEMISTRY OF OIL SHALES
PRESENTED BEFORE THE DIVISIONS OF FUEL CHEMISTRY AND
PETROLEUM CHEMISTRY, INC.
AMERICAN CHEMICAL SOCIETY
ST. LOUIS MEETING, APRIL 8 - 13, 1984

FLUIDIZED-BED RETORTING OF OIL SHALE: EFFECT OF
AMBIENT GAS ATMOSPHERE ON OIL YIELD

By

J. Y. Shang and J. S. Mei
U. S. Department of Energy, Morgantown Energy Technology Center
Morgantown, West Virginia 26505
and
Y. S. Wang and G. Q. Zhang
Department of Mechanical Engineering, West Virginia University
Morgantown, West Virginia 26506

ABSTRACT

Fluidized-bed technology, due to its inherent advantages of good solid mixing and high solid heat transfer rate, has widely been used for the thermal processing of fossil fuels. Recently, the Morgantown Energy Technology Center (METC) has employed the fluidized-bed process to investigate the retorting characteristics of various oil shales. Design and operating parameters such as solid residence time, retorting temperature, particle size, fluidization velocity, and ambient gas atmosphere were investigated using the 2-inch diameter, laboratory-scale, electrically-heated, fluidized-bed retorting system to determine their effects on oil yield.

This paper presents the recent results of a series of experiments on the effect of ambient gas atmosphere on oil yield. Western oil shale from Colorado and eastern oil shale from Kentucky were studied at various ambient gas atmospheres. The characteristic feature of retorting for both oil shales in the presence of nitrogen, carbon dioxide, and nitrogen-steam, carbon-dioxide steam gas mixtures at various gas compositions was investigated in these experiments. Experimental results indicate significantly as 10 percent or more steam was present in the nitrogen-steam or carbon-dioxide steam gas mixtures. The amount of oil yield increased considerably for Colorado oil shale when it was retorted in a carbon dioxide gas atmosphere. The sensitivity of oil yields to carbon dioxide levels in the retorting gas, however, was much less for the Kentucky than the Colorado oil shale.

SYMPOSIUM ON CHARACTERIZATION AND CHEMISTRY OF OIL SHALES
PRESENTED BEFORE THE DIVISIONS OF FUEL CHEMISTRY AND
PETROLEUM CHEMISTRY, INC.
AMERICAN CHEMICAL SOCIETY
ST. LOUIS MEETING, APRIL 8 - 13, 1984

CONCEPTUAL VERIFICATION OF A TWIN FLUIDIZED-BED
REACTOR FOR OIL SHALE RETORT/COMBUSTION

By

J. Y. Shang and J. S. Mei

U. S. Department of Energy, Morgantown Energy Technology Center
Morgantown, West Virginia 26505
and

L. W. Zeng and R. Y. K. Yang

Department of Chemical Engineering, West Virginia University
Morgantown, West Virginia 26505
and

A. Lul

EG and G Washington Analytical Services Center, Inc.
Morgantown, West Virginia 26505

ABSTRACT

Fluidization technology, owing to its inherent ability of vigorous solid mixing has widely been applied in industry for various applications such as surface coating, blending, gasification and combustion of coals. During the past decades oil shale retorting employing fluidized-bed process has also been investigated; however, retorting processes using fluidization technology have not yet been demonstrated on a large scale of operation. Review of current literature on oil shale retorting using fluidized-bed technology revealed that directed-heated type processes result in the loss of residual carbon in spent shale. The indirected-heated type process, on the other hand, required separated reactors to isolate the retort and combustion process; as a consequence, higher capital investment and loss of thermal efficiency became inevitable.

A novel concept which combines both the retorting and combustion process in a single reactor is presented in this paper. In this new concept, the reactor is separated in two side-by-side twin compartments; one for fresh raw shale retorting and the other for spent shale combustion. In view of the close proximity of the two beds, thermal efficiency of the twin fluidized-bed is expected to be considerably higher than the conventional technology, and simple and compact facilities can be contemplated. A 9-inch diameter twin fluidized-bed oil shale retort/combustion reactor was designed, constructed, and operated based on the data generated from a 6-inch by 7-inch cold model. Experiments using low-grade Colorado oil shale were conducted in the twin-bed. Experimental data obtained from a series of tests at various operating conditions are presented. Preliminary results from these data demonstrate successfully the feasibility of the twin fluidized-bed concept.

SYMPOSIUM ON CHARACTERIZATION AND CHEMISTRY OF OIL SHALES
PRESENTED BEFORE THE DIVISIONS OF FUEL CHEMISTRY AND
PETROLEUM CHEMISTRY, INC.
AMERICAN CHEMICAL SOCIETY
ST. LOUIS MEETING, APRIL 8 - 13, 1984

AN ECONOMIC COMPARISON OF FIVE PROCESS CONCEPTS FOR USING EASTERN OIL SHALE

By

W. J. Parkinson, T. T. Phillips and J. W. Barnes
Los Alamos National Laboratory, Los Alamos, New Mexico 87545

INTRODUCTION

This study compared costs of retorting eastern oil shales using western shale retorting technologies that need no more development with the cost of processing the same shales using technologies designed specifically for eastern shales. The eastern shale technologies need more development. The study was designed to answer the question: Does process development work need to be done for eastern oil shale or will the existing western techniques suffice?

A calculation for a power plant that burned eastern oil shale to produce electricity was included in the study. We studied the following processes:

- the Institute of Gas Technology's (IGT) HYTORT (eastern shale process),
- the Paraho C-H (combination heated) (eastern shale process),
- the Paraho D-H (direct heated) (western shale process),
- the TOSCO II (western shale process), and
- power plant.

Our study achieves a different result than the report entitled "Synthetic Fuels from Eastern Oil Shale", (1) (also known as the Buffalo Trace Area Development District Study (BTADDS)). The BTADDS compared the HYTORT and the Paraho C-H processes using a shale with a higher Fischer Assay than the one used in this study.

BASIC OF CALCULATION

A Kentucky Sunbury shale, from IGT test Run 80BSU-11 (2) provided a material balance for the HYTORT process. This shale is similar in organic carbon content to the one used in the BTADDS. Table I gives the material balance data from Run 80BSU-11.

To make the comparisons as fair as possible, an effort was made to obtain a Fischer Assay from the shale used in Run 80BSU-11 (2). Unfortunately, shale from Run 80BSU-11 was not available, so the Fischer Assay was done on shale from Run 80BSU-10 (2). The shale from Run 80BSU-10 is a Kentucky Sunbury shale that has a higher organic carbon content than the shale from Run 80BSU-11. The Fischer Assay data were not received until the time-consuming HYTORT calculations with data from 80BSU-11 were nearly completed. Rather than change the calculations, we extrapolated the Fischer Assay data from Run 80BSU-10 to an 80BSU-11 basis predicted on shale carbon content. The extrapolated oil yield was 9.2 gallons per ton. Table II compares some of the most important material balance variables from Runs 80BSU-10 and 80BSU-11.

The material balance Fischer Assay yields for the shale from 80BSU-10 are given in Table III. These Fischer Assay data were obtained independently by Laramie Energy Technology Center. The Fischer Assay report indicates that the organic carbon content of this shale was 14.2 wt %. This value is slightly lower than the value of 15.04 wt % given in Table II.

Janka and Dennison (3) present a graphical correlation of Fischer Assay oil yield vs organic carbon content for eastern oil shales. Our value of 9.2 gallons per ton falls below this line, but it was well within the data scatter about the line.

For western shales, the product yields from the Paraho and TOSCO II retorts are comparable to the Fischer Assay product yields. We assumed that this would also be true for eastern shales. The Table I data were the basis for the HYTORT study and the extrapolated Fischer Assay data were used as the basis for the TOSCO II, the Paraho C-H and the Paraho D-H studies.

RESULTS

The product oil costs for each process in dollars per barrel are listed below.

- HYTORT \$48.0
- Paraho C-H \$70.0

- TSO CO II \$ 75.0
- Paraho D-H \$106.0
- Power plant \$107.0 (\$0.0607/kWh)

TABLE I

BASIC MATERIAL BALANCE DATA FROM IGT RUN 80BSU-11

Oil Shale			Gas		
Ultimate Analysis (Wt %)	Feed	Residue	Composition (Mole %)	Feed	Product
Organic carbon	13.40	4.52	H ₂ S		3.18
Mineral carbon	0.82	0.31	N ₂	0.7	1.26
Hydrogen	1.61	0.33	CO		2.02
Nitrogen	0.42	0.24	CO ₂		1.12
Oxygen	3.41	0.94	H ₂	99.3	76.81
Sulfur	4.02	3.10	CH ₄		9.34
Ash	<u>75.17</u>	<u>92.17</u>	C ₂ ⁺		4.67
Total	97.85	101.61	C ₂ ⁺		1.57
			C ₆ H ₆		0.03
			Total	<u>100.0</u>	<u>100.0</u>
			Shale Oil	Residue	Gas
C/H weight ratio			10.02		
Sulfur, wt %			1.89		
Nitrogen, wt %			2.18		
Specific gravity (60/60°F)			0.996		
Liquid hydrocarbon yield, lb/lb shale fed			0.0755		
Water yield, lb/lb shale fed			0.0518		
Residue shale yield, lb/lb shale fed					
By direct measurement				0.791	
By ash balance, scf/lb shale fed				0.811	
Product gas yield, scf/lb shale fed					3.83
Feed gas, scf/lb shale fed					4.77

TABLE II

COMPARISON OF MATERIAL BALANCE VARIABLES FROM RUNS 80BSU-10 AND 80BSU-11^a

Variable	IGT Run 80BSU-10	IGT Run 80BSU-11
Organic carbon content, wt % (dry)	15.04	13.4
Liquid hydrocarbon yield, lb/lb shale fed	0.0829	0.0755
Product gas yield, scf/lb shale fed	6.22	3.83

a. Numbers obtained from (2).

The Paraho C-H process combines, in one vessel, a retorting step and a combustion step. The combustion step uses the carbon on the spent shale to produce steam and electricity. The combustion section of the Paraho C-H retort was simulated using RETORT, a shale retort modeling program written by R. L. Braun (4). RETORT calculations show that when large amounts of carbon are left in the spent shale, as in this Fischer Assay, the large quantities of oxygen and diluent

gases required to burn all of the residual carbon from the shale actually quench the combustion.

TABLE III
MATERIAL BALANCE FISCHER ASSAY YIELD FOR 80BSU-10 SHALE

(Organic carbon content - 14.2 wt %)

<u>Fischer Assay</u>	<u>Original Run</u>	<u>Second Run</u>
Oil, wt %	3.07	3.79
Water, wt %	6.06	5.97
Gas plus loss, wt %	2.09	3.74
Retorted shale, wt %	88.18	86.5
Oil, C/H weight ratio	8.89	8.73
Oil, sulfur, wt %	2.41	2.40
Oil, nitrogen, wt %	1.06	1.14
Oil, sp gr 60/60°F	0.938	0.953
Oil, gal/ton	9.4	9.5
Gas Analysis		
cf/ton	516	516
Btu/cf	946	960
Vol % - H ₂	40.79	41.17
CO	4.32	3.23
CH ₄	13.45	13.89
CO ₂	10.46	9.80
C ₂ H ₄	1.21	1.24
C ₂ H ₆	6.19	6.38
C ₃ H ₆	2.05	2.10
C ₃ H ₈	3.10	3.21
C ₄ 's	3.66	4.19
C ₅ 's	2.16	2.51
C ₆ 's	0.94	1.00
C ₇ 's	1.59	0.86
H ₂ S	9.76	10.09
NH ₃	0.32	0.33

By introducing the combustion feed gas at several points within the combustion section, we achieved a design for which RETORT predicts stable combustion.

The TOSCO II retorting process design was based on Fischer Assay data from Table III. Because of the large amount of residual carbon that is discarded with the spent shale, the cost of oil from this process is very high.

The material balance for the Paraho D-H retorting process was computed using RETORT to extrapolate the Fischer Assay data from Table III to direct heating conditions. The costs are high for two reasons: first, because the residual carbon is discarded; second, because of the large quantities of dilute gases that must be processed, the acid gas cleanup is very costly.

A process for burning eastern shale to produce electric power was simulated with the ASPEN computer program. The capital costs for this process were estimated based on a similar Electric Power Research Institute (EPRI) study (5). The power costs were converted to dollars per barrel equivalent fuel oil.

The presentation of flow sheets and material balances for each of the processes is beyond the scope of this paper. This information with capital cost information and a discussion of each

process module is given in (6). Some of the more important factors that are required to compute product costs are given in Table IV.

TABLE IV
COSTS FACTORS

	Total Capital Cost (\$10 ⁶)	Oil Production (bbl/stream day)	Operating Costs (\$10 ⁶ /yr)	By-Product Income (\$10 ⁶ /yr)
HYTORT	2187.5	58,575	428.2	63.0
Paraho C-H	2220.2	34,740	390.8	159.8
TOSCO II	2240.0	36,620	389.8	69.0
Paraho D-H	3140.0	29,220	428.2	220.7
Power plant	577.0	7,277 ^a	49.9	-

a. Equivalent oil computed at 1758 Kwh/bbl.

PROCESS ECONOMICS

We made the following assumptions. The retorts in each case processed 145,764 tons of shale per stream day. This number was picked to produce oil at a rate of approximately 50,000 barrels per stream day for the better producing systems. The plants are located near a mine. The delivered shale is purchased at \$4.00/ton (7).

The capital costs are based on mid-1981 dollars. Our approach to capital cost calculation was to survey the literature and make up-to-date charts of plant capacity vs direct capital costs. We estimated maintenance and operating costs to be a percentage of the capital costs.

The following economic parameters were used to determine the product oil and power cost:

- 90% stream factor,
- 20-year plant life,
- debt-to-equity ratio of 75/25,
- 12% interest on debt, and
- 18% rate of return on equity.

(This rate of return is high, but it fits the mid-1981 time frame.)

Several areas that affect product price need more study. The five areas of greatest uncertainty are the following:

- retort capital costs,
- acid gas removal,
- product oil hydrotreating,
- sulfur remaining in the burned shale, and
- actual retort oil yield.

Retort Capital Costs

Large discrepancies in retort costs exist in the literature (1, 2). Because of this, we computed the effect of uncertainty in the retort module capital costs upon the selling price of the oil produced. The calculations were made for retort module capital costs of 50 and 200% of the best estimate. They were made for the HYTORT, Paraho C-H, TOSCO II and Paraho D-H cases. Figure 1 is a graphical representation of these calculations.

Figure 1 shows that the relative positions of the best and worst cases, HYTORT and Paraho D-H, are not changed.

The graphical method described above for computing capital costs does not work well with large field-fabricated items like retorts. Chicago Bridge and Iron (CBI) gave us some helpful suggestions for computing the capital cost for vessels like the retorts. The technique is based on dollars per pound of retort. We also obtained a written cost estimate from IGT that they had obtained from CBI. It included a sketch of the vessel. The CBI estimate was used as a basis for the HYTORT retort costs. Our HYTORT retort costs compare very well with those in (2), but are much lower than those in the BTADDS.

Staff members from the design engineering section of our Technical Engineering Support Group estimated the vessel weight for the Paraho retort based on the drawings in the BTADDS report. The Paraho C-H retort module costs on a dollar per pound basis were also less than those in the BTADDS. The Paraho D-H retort module cost was lower than we expected, but because of the uncertainty involved, this estimation method was assumed to be the best available and most consistent.

Not enough information was available to compute the retort costs for the TOSCO II retort

module by this method. These costs were computed by scaling cost information from (8). These costs seem high relative to our other costs.

Acid Gas Removal Systems

Acid gas removal for these processes is expensive. In all cases, capital costs are high. Acid gas removal also has high operating costs. Process optimization would require finding the best acid gas removal scheme for each retorting process; however, optimization was beyond the scope of this study. For the HYTORT process, we used amine absorption for acid gas removal and the U. S. Steel Corporation Phosam Process (1, 9) for ammonia removal. The Phosam process is good for high-pressure use (9). Hence, it was used for the HYTORT process as it was in the BTADDS.

The other low-pressure retorting schemes use the SULFAMMON process, which was used in the BTADDS for Paraho C-H acid gas and ammonia removal. The low ammonia and carbon dioxide contents of the BTADDS sour gas make the low capital cost SULFAMMON process look ideal. The sour gas compositions used in our study are derived from the Fischer Assay data in Table III. Ammonia-laden off-gas from the hydrotreater must also be cleaned in the acid gas plant in our study. This combination of sour gases presents a tougher acid gas removal problem for the SULFAMMON plant than occurred in the BTADDS. Some modifications had to be made to the BTADDS scheme for the SULFAMMON process to work on our gases.

Large quantities of low-Btu sour gas are produced in the Paraho D-H retort. Cleaning this gas so that it can be burned in an environmentally acceptable manner is expensive. The SULFAMMON process was used because of the low capital cost. In spite of this, the capital costs for cleaning large quantities of dilute gas are staggering.

Hydrotreating

Hydrotreating and the production of hydrogen for hydrotreating add significantly to the cost of the product shale oil (10). To prepare the shale oil for refinery use, the nitrogen content must be reduced by hydrotreating. A product oil containing 500 ppm nitrogen was assumed to be a suitable refinery feedstock.

In this study, an empirical technique based on very little data was used to estimate the hydrogen consumption and, therefore, the costs of this expensive process.

Raw eastern shale oil presents a different hydrotreating problem than does raw western shale oil produced by the same retorting method. One reason is the lower hydrogen-to-carbon ratio in the eastern shale oil. Furthermore, eastern shale oil produced by a Fischer Assay technique presents a different hydrotreating problem than eastern shale oil produced by the HYTORT method (11).

Hydrotreating data are available for oils produced from Colorado shale by the Paraho technique (10), but the data are not for eastern shale oil. Hydrotreating data are available for oils produced from eastern Sunbury shales, but they do not cover the oil nitrogen ranges used in this study (2, 12). These data were combined to estimate the hydrogen consumption required by the hydrotreaters in this study. Details of these calculations are given in (6).

Table V lists some assumptions and results of the hydrotreater calculations.

TABLE V

HYDROTREATER ASSUMPTIONS AND RESULTS

	<u>HYTORT OIL</u>	<u>Fischer Assay Oil (Paraho and TOSCO)</u>
Feed oil nitrogen	2.2 wt %	1.5 wt %
Feed oil gravity	10.5° API	19.3° API
Product oil nitrogen	500 ppm	500 ppm
Product gravity	36.2° API	47.0° API
Hydrogen consumption	2300 scf/bbl	1600 scf/bbl

Sulfur Retention in the Burned Spent Shale (Paraho C-H Case)

Sulfur retention in the burned spent shale in the Paraho C-H case is an important economic parameter. Disposing of the sulfur in the gaseous and liquid streams is expensive. In the Paraho C-H process, all sulfur that does not go into the gaseous and liquid streams is carried with the retorted shale to the combustion section. This sulfur must be removed as SO₂ or retained in the burned spent shale. Removing SO₂ from the flue gas stream is expensive. The more sulfur that is retained in the burned spent shale, the more economical the total process is. Again, the information that most strongly affects the cost of an expensive process (sulfur retention in the burned spent

shale) had to be estimated based on very little data. The only data found for sulfur retention in burned spent shale were in the BTADDS. The plant material balance in the BTADDS, however, did not reflect the actual data in the same report. The discrepancy was never resolved, so an independent source, an EPRI study of a lignite-fired fluidized bed power plant (13), was consulted. The EPRI report indicates that sulfur retention is a function of combustion temperature, CaO and possibly some of the other alkali oxides present. CaCO₃, often reported as a function of the mineral carbon (see Table I), will decompose to CaO and CO₂. This CaO and any other CaO in the shale can combine with the sulfur to form CaSO₄, which will remain in the burned spent shale.

Our estimate for the burned spent shale sulfur retention is based on the data in the EPRI report and the mineral carbon content in 80BSU-11 shale. The details of the calculation are presented in (6).

Retort Oil Yield

The amount of oil produced from each retort is a very important parameter for computing the cost of the product oil. With western shales, the Fischer Assay oil yield is predictable if the organic carbon content is known. This may not be true for eastern shales.

Janka and Dennison (3) give a plot of Fischer Assay oil yield vs organic carbon content for eastern oil shale, as does the BTADDS. There is a significant difference between the two plots (see Figure 2). Rather than choosing between these two correlations, we chose to have a Fischer Assay done independently on a sample of shale that had also been retorted by the IGT HYTORT process. The value obtained by the independent Fischer Assay is plotted in Figure 2. The value is within the data scatter about the lower line. Therefore, we assumed that this Fischer Assay was a fair basis for our study. We used 98% Fischer Assay oil yield for Paraho C-H and 100% for TOSCO II, based on 9.2 gallons per ton.

Shortly before this study ended, we obtained some data indicating that thermal retorting of eastern shales can produce higher oil yields than normal Fischer Assay (14, 15). Figure 3 is taken from (14). Some of the information on the original drawing was removed for clarity. Figure 3 indicates that heating rates above the Fischer Assay heat-up rate can increase the oil yield from eastern shales. These data suggest that eastern shales should not be treated as low-grade western shales. Yields greater than Fischer Assay can be obtained from eastern shales by thermal retorting methods. We do not know the economic benefits or penalties associated with these heating rates in full-scale equipment. Reference (15) states that proper thermal retorting may produce oil yields of up to 125% Fischer Assay from eastern shales.

It is only fair, however, to note the 80BSU-11 run (2) is not an optimum for the HYTORT case either. When compared on a normalized basis, Run 80BSU-10 produces a higher oil yield than Run 80BSU-11. Both runs are for Sunbury shale. Based on this observation, it is possible that the HYTORT process could produce 2 to 5% more oil than we estimated in our study.

The oil selling price was recalculated for the following processes using the increased oil yield percentages shown below:

- HYTORT (102% and 105%),
- Paraho C-H (110% and 125%),
- TOSCO II (110% and 125%), and
- Paraho D-H (110% and 125%).

The results of these calculations are given in Figure 4.

The 1.25 multiplying factor applied to the Paraho C-H case increases the oil production to nearly 11.3 gallons per ton. This value is close to the top Fischer Assay line in Figure 2. It is lower than the 12.5 gallons per ton used in the BTADDS calculations.

Increased oil production will bring down the selling price of the product oil significantly and will reduce the differences in the selling prices between the cases, but the relative ranking of the cases remains unchanged.

SUMMARY

We have tried to analyze each process impartially and believe that, based on our input data, the relative rankings shown earlier are correct. The oil yield data in (14) and (15) do, however, indicate that the differences between the HYTORT, Paraho and TOSCO II processes may not be as great as we have indicated.

Our oil costs are different from those of the BTADDS. There are several reasons for this.

1. Economy of Scale. The plants in this study are roughly five times the size of the plants in the BTADDS. Some economic benefit can be gained by going to plants larger than those in the BTADDS.

2. Capital Costs. Most of the capital costs from the BTADDS for individual process units are higher than those predicted by our correlations. On a cost vs capacity basis, our retort capital costs were significantly less than the BTADDS retorts. Overall, our capital costs are lower.

FIGURE 1

OIL SELLING PRICES FOR VARIOUS PROCESSES WITH DIFFERENT RETORT MODULE CAPITAL COSTS

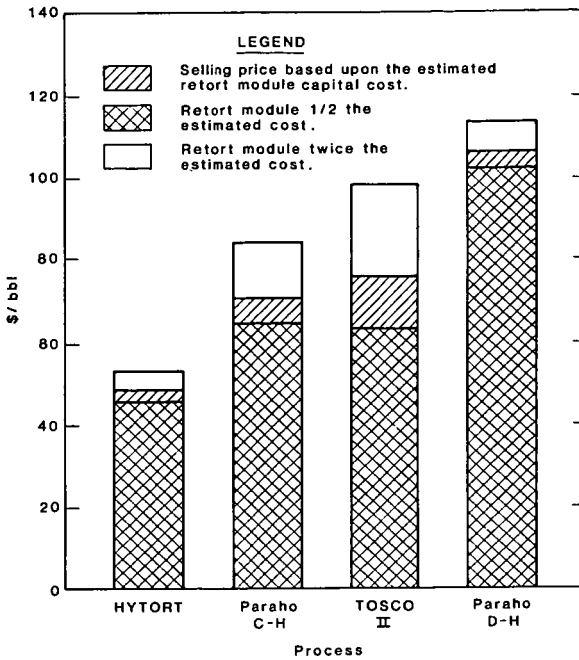


FIGURE 2

TWO DIFFERENT PLOTS OF FISCHER ASSAY OIL YIELD VS WT% ORGANIC CARBON FOR EASTERN OIL SHALE

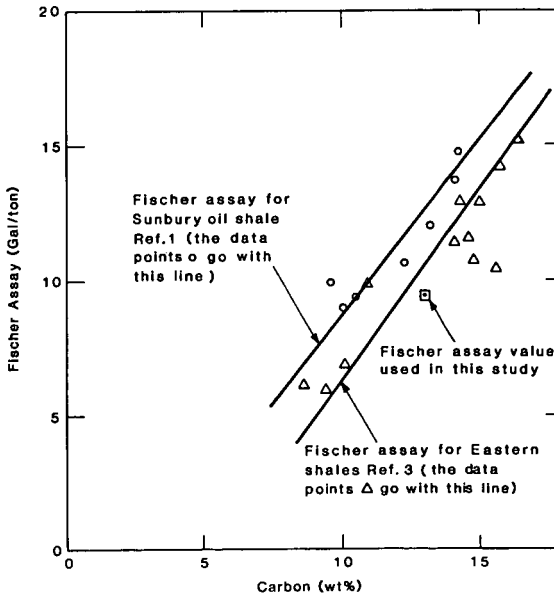


FIGURE 3

EFFECT OF HEATING RATE ON OIL YIELD FROM EASTERN AND WESTERN OIL SHALE (TAKEN FROM REF. 14).

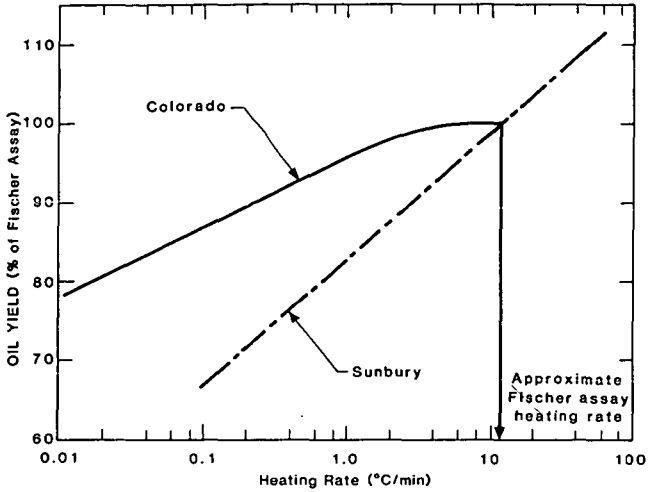
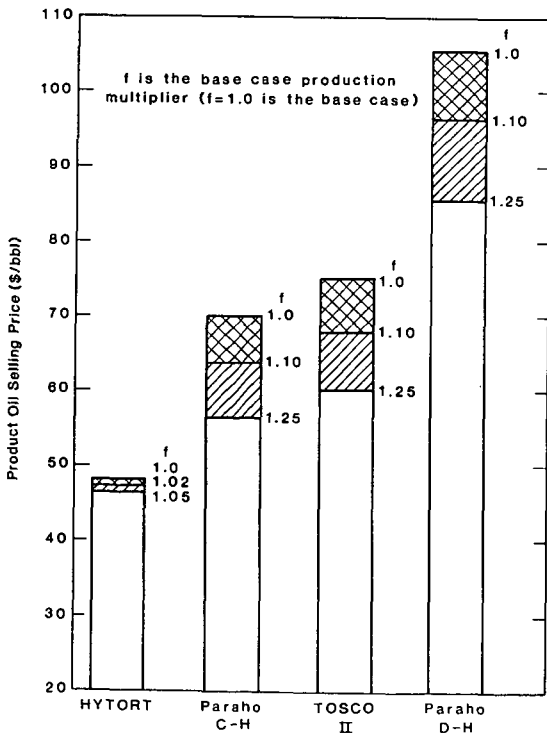


FIGURE 4

PRODUCT OIL SELLING PRICE FOR FOUR CASE STUDIES WITH INCREASED OIL PRODUCTION.



3. Mined vs Purchased Feed Shale. Our study uses shale purchased and delivered at \$4.00 per ton. The BTADDS included the mine as part of their plant.

4. Hydrotreated Oil. Our design included oil hydrotreaters. The major product from the BTADDS was raw shale oil.

5. Different Financial Factors. The capital cost basis for this study was mid-1981. The capital cost basis for the BTADDS was fourth quarter 1980. Our study used an 18% return on equity. The BTADDS used what appears to be a 12% return on equity.

6. Different Oil Yield Input. We used a higher HYTORT oil yield, based on Run 80BSU-11 (Table I), than was used in the BTADDS. We used a lower Paraho C-H oil yield, based on extrapolated Fischer Assay data (Table III). These two factors explain why our study predicted that HYTORT produced a lower cost oil than Paraho C-H and the BTADDS predicted the reverse.

CONCLUSIONS

Our study, based on the input data used, indicates the following.

- Without further development, western shale retorting processes are not adequate for use with eastern shales.
- As described here, the HYTORT process produces oil at a cost nearly competitive with oil produced from western shale using western retorting techniques.
- Increasing oil yield with thermal retorting techniques by increasing the heat-up rate looks promising for processes like the Paraho C-H and TOSCO II.

LITERATURE CITED

- (1) Vyas, K. C., Aho, G. D. and Robl, T. L., "Synthetic Fuels from Eastern Oil Shale", project NC-5477, Federal Grant No. DE-FG-4480R410185, Vol. 1 (1981).
- (2) "Synthetic Fuels from US Oil Shale - A Technical and Economic Verification of the HYTORT Process", Project 61040 Annual Report - US Dept. of Energy Contract Number DE-AC01-79ET14102 (1981).
- (3) Janka, J. C. and Dennison, J. M., "Devonian Oil Shale A Major American Energy Resource", paper presented at the Synthetic Fuels from Oil Shale Symp. I, Atlanta, GA (1979).
- (4) Braun, R. L., "Mathematical Modeling of Modified In Situ and Above-Ground Oil Shale Retorting", Lawrence Livermore Natl. Laboratory report UCRL-53119 (1981).
- (5) McGowin, C. R., Bardley, W. J., Panico, S., Ulerich, N. H., Newby, R.A. and Keairns, D. L., "Conceptual Design of a Gulf Coast Lignite-Fired Atmospheric Fluidized-Bed Power Plant", AICHE Annual Meeting, San Francisco, CA (1979).
- (6) Parkinson, W. J., Phillips, T. T. and Barnes, J. W., "An Economic Comparison of Five Process Concepts for Using Eastern Oil Shale", Los Alamos Natl. Laboratory report, publication in progress.
- (7) Feldkirchner, H. L. and Janka, J. C., "The HYTORT Process", paper presented at the Synthetic Fuels from Oil Shale Symp. I, Atlanta, GA (1979).
- (8) Allred, V. D., *Oil Shale Processing Technology*, Center for Professional Advancement, E. Brunswick, NJ (1982).
- (9) Kohl, A. L. and Riesenfeld, F. C., *Gas Purification*, 3rd ed., Gulf Publishing Company, Houston, TX (1979).
- (10) Sullivan, R. F., Strangeland, B. E., Rudy, C. E., Green, D. C. and Frumkin, H. A., "Refining and Upgrading of Synfuels from Coal and Oil Shales by Advanced Catalytic Processes", First interim report, processing of Paraho Shale Oil, DOE Report - Contract No. EF-76-C-01-2315 (1978).
- (11) Netzel, D. A. and Miknis, F. P., "Hydrocarbon Type Analysis of Eastern and Western Shale Oils Produced by the IGT HYTORT and Fischer Assay Processes", paper presented at the Synthetic Fuels from Oil Shale Symp. II, Nashville, TN (1981).
- (12) Feldkirchner, H. L. and Miller, R. L., "Upgrading Shale Oils Produced by the HYTORT Process", paper presented at the Synthetic Fuels from Oil Shale Symp. II, Nashville, TN (1981).
- (13) Burns and Roe, Inc., "Conceptual Design of a Gulf Coast Lignite-Fired Atmospheric Fluidized-Bed Power Plant", Final Report to the Electric Power Research Insti. on Projects 1180-1 and 1179-1, EPRIFP-1173 (1979).
- (14) Burnham, A. K., Huss, E. B. and Coburn, T. T., "Kinetics of Oil Shale Pyrolysis", paper presented at the Fourth Briefing on Oil Shale Research, conducted at Lawrence Livermore Natl. Laboratory, Livermore, CA (1982).
- (15) Rubel, A. M. and Coburn, T. T., "Influence of Retorting Parameters on Oil Yield from Sunbury and Ohio Oil Shales from Northeastern Kentucky", proceedings of the 1981 Eastern Oil Shale Symp.

SYMPOSIUM ON CHARACTERIZATION AND CHEMISTRY OF OIL SHALES
PRESENTED BEFORE THE DIVISIONS OF FUEL CHEMISTRY AND
PETROLEUM CHEMISTRY, INC.
AMERICAN CHEMICAL SOCIETY
ST. LOUIS MEETING, APRIL 8 - 13, 1984

EASTERN SHALE HYDRORETORTING

By

M. J. Roberts, H. L. Feldkirchner and D. V. Punwani
Institute of Gas Technology, 3424 South State Street, Chicago, Illinois 60616
and

R. C. Rex, Jr.
HYCRUDE Corporation, 10 West 35th Street, Chicago, Illinois 60616

INTRODUCTION

The Institute of Gas Technology (IGT), under a subcontract to HYCRUDE Corporation, participated in a feasibility study (Commercialization of the HYTORT Process), funded by Phillips Petroleum Company from December 1980 through May 1983. The overall objective of the Bench-Scale Unit (BSU) test program, which was one of the activities conducted, was to determine the effects of major process variables on conversion of organic carbon, yields and properties of oil and gas and consumption of hydrogen for hydroretorting of a specific Indiana New Albany shale. As part of the BSU program, an improved method was developed for measuring reactable organic oxygen in these shales, which resulted in greatly improved oxygen balances (1). The effects of particle size on product yields from hydroretorting a similar oil shale were measured in a high-pressure thermo-balance unit and a semi-batch unit; the results of this work have been presented in earlier publications (2, 3).

Before the BSU hydroretorting tests were begun, a preliminary error-propagation analysis was performed to identify possible improvements in BSU measurements that could lead to better overall material and elemental balances. A list of additional potential sources of uncertainty (primarily due to the operating procedures used) was compiled. Based on the identification of these possible sources of uncertainty, additional equipment was ordered and installed and existing operating procedures and calculation methods were modified. The result was excellent overall material balance closures ($100\% \pm 1\%$).

EQUIPMENT AND PROCEDURES

A flow diagram of the BSU after modification is shown in Figure 1. The BSU equipment consists primarily of a reactor with associated equipment for feeding and measuring the flow rates of feed shale and feed gas and for collecting and measuring the flow rates of residue shale, liquid product and product gas. Simple analog controllers are used to maintain reactor temperatures at the desired values, to maintain feed rates at constant values and to maintain the reactor pressure constant. Representative samples of the spent shale and feed and product gases are taken every 15 minutes during steady-state operation. The capacity of the unit is 250 lb/h of shale. Shale-gas contacting occurs in a truly continuous, countercurrent manner. Additional details of construction and operation of the BSU are available in earlier publications (4, 5).

The addition of mass flow meters (in series with orifice meters), a second product gas meter (in series with the first meter) and a helium tracer system contributed to improved gas flow measurements. The following equipment was added to improve product sampling and analyses:

- Sampling train for trace sulfur and nitrogen species
- "Cold Finger" for product gas freeze-out sample
- Steady-state product shale sampler
- On-line infrared gas analyzers
- On-line gas chromatograph
- Flash gas measurement system

Additional equipment installed to improve operation and data analysis included a closed-loop bed level control system, electronic feed and discharge screw RPM indicators, a multipoint digital pressure gauge (0.1% accuracy) and an electronic temperature profiler.

BSU TEST PROGRAM

Two "blank" or zeroing tests were conducted before the hydroretorting tests were begun. The first test was made with an "empty" reactor (at reaction temperature and pressurized with hydrogen) to determine the accuracy of the metered gas flows into and out of the reactor system. Gas flows were measured with an accuracy of $\pm 1\%$. The second test was similar to the first except that gravel was fed to the reactor to simulate shale movement without the complication of heat effects due to chemical reactions. Temperature controllers were also set to obtain a nearly linear temperature profile in the reactor. The results of this test indicated that solids flow rates could be measured with an accuracy of $\pm 0.25\%$.

Like oil hydrotreating and hydrocracking, oil shale hydroretorting requires that a large excess of hydrogen-rich gas be passed through the reactor. In commercial designs, this gas is recycled as a heat carrier. The quantity required for that purpose is such that only 8.5% of the hydrogen it contains actually reacts on one pass through the reactor. Therefore, determination of the level of chemical hydrogen consumption done in the obvious way (by subtracting the measured hydrogen gas flow rate leaving the reactor from that entering) can be subject to considerable uncertainty. This is because the resulting figure is a small difference between two large numbers. In order to provide measurements of chemical hydrogen consumption at an acceptable ($\pm 10\%$) level of confidence, it was necessary to obtain mutually-supporting measurements using several different and independent techniques as well as to improve the accuracy of the conventional methods.

Four methods were used to calculate H_2 consumption: the appearance of combined hydrogen in the product, forcing an oxygen balance, taking direct measurements (difference between H_2 fed and H_2 in the product) and using a helium tracer. The basis of each method is described below:

Appearance of Combined Hydrogen - The total chemically combined hydrogen in all reactants is subtracted from the total combined hydrogen in all products to obtain the chemical hydrogen consumption. This method depends on correct measurements of shale moisture contents and water production rates.

Forced Oxygen Balance - This calculational method assumes that oxygen analyses of feed and spent shale, oil and gas are correct. The hydrogen consumption is then calculated from the water yield which has been calculated by a forced oxygen balance.

Direct Measurement (by difference) - In this calculational procedure, the hydrogen (as H_2) flow rate in the product gas stream is subtracted from the hydrogen (as H_2) feed gas flow rate to determine hydrogen consumption. Improved accuracy is realized by duplication of gas flow metering equipment.

Helium Tracer - To utilize the helium tracer technique in the BSU test program, approximately 5 mole % of helium was dynamically blended with the BSU feed hydrogen. Ratios of He/H_2 in the feed and product streams were used to calculate hydrogen consumption.

The BSU hydroretorting test program was divided into three phases. Phase I was designed to investigate the effects of two independent variables, shale heat-up rate and maximum bed temperature, at two levels. In this phase, four replicate runs were also conducted. The replicate runs provided an indication of the experimental error and of the precision of the experiments. The implicit assumption here was that, by maintaining the same test procedures throughout the BSU program, the experimental error would remain constant. Phase II was designed to study the effects of lower maximum shale bed temperatures and shorter shale residence times. The experimental matrix was composed of two bed temperature levels at two shale residence times. Phase III was designed to investigate the combined effects of high shale mass flux, shale residence time at temperature, shale preheat and hydrogen partial pressure.

The properties of the Indiana New Albany shale employed in the study are shown in Table I.

TABLE I
CHARACTERISTICS OF FEASIBILITY STUDY SHALE

Shale source	Henryville, Indiana
Stratigraphic unit	Late Devonian (New Albany)
Pay thickness, ft	40
Organic carbon content, wt %	11.9 to 12.7
Fischer Assay oil yield, gal/ton	11 to 13

RESULTS AND CONCLUSIONS

Some standard deviations of selected resultant variables from the Phase I test results are shown in Table II. The reported standard deviations of the resultant variables incorporate both experimental uncertainty and the degree of precision in setting replicate run conditions. It is

important to note that the standard deviation of hydrogen consumption of ± 170 SCF/ton of dry shale is within the desired accuracy limits of $\pm 10\%$.

TABLE II
RESULTS OF STATISTICAL ANALYSIS OF PHASE I TEST DATA

Variable	Standard Deviation
Hydrogen consumption, SCF/ton ^b	170 ^a
Gross oil yield, gal/ton ^b	0.3
Adjusted oil yield, gal/ton ^b	0.2
Carbon conversion, %	1.3
Selectivity to oil, $(\frac{\text{Oil}}{\text{Oil} + \text{Gas}})$, %	0.9

- a. Calculated by the forced oxygen balance method.
b. On a dry shale basis.

The Phase I test results clearly indicate that lower maximum bed temperatures (1000°F versus 1250°F) —

- Decreased hydrogen consumption
- Increased oil production
- Improved oil quality

API gravity and sulfur content were used as an index of oil quality. Use of lower heat-up rates (15°F/min versus 100°F/min) also favors increased oil production and improved oil quality but does not appear to affect the hydrogen consumption within the temperature range employed in Phase I of the program.

Figure 2 indicates the range of hydrogen consumption values calculated by the various methods for some typical BSU runs. The direct method for measuring hydrogen consumption tended to give values with greater variability from the mean values. This is typical of methods that involve the calculation of a relatively small difference between two large numbers. There was generally good agreement between the hydrogen consumption figures calculated by the above methods. Use of four different methods provided an excellent cross-check of the hydrogen consumption values and increased our confidence in the experimental results. Additionally, sufficient experimental and analytical data were generated from each BSU run, to enable identification of plausible reasons for occasional differences in calculated hydrogen consumption values.

Analysis of the Phase II results indicates that the higher maximum bed temperature (1000°F versus 850°F) had the following statistically significant effects:

- Increased oil production
- Increased carbon conversion
- Increased hydrocarbon gas yield

The use of a longer shale residence time (60 minutes versus 30 minutes) results in an increase in carbon conversion, the major part of which goes into an increase in hydrocarbon gas yield.

The final phase of the test program showed that the yield of oil product increased continuously as the hydrogen partial pressure was increased. This effect is depicted graphically in Figure 3. The BSU tests indicated that oil yields of up to 230% of the Fischer Assay yield can be achieved. It should be pointed out that these higher oil yields were achieved without an appreciable reduction in oil quality. Choice of a design hydrogen partial pressure for commercial operation was based on a cost tradeoff study of yields against pressure.

Another aspect of commercial importance is the effect of hydroretorting time (shale residence time) on the oil product yield. The BSU program results indicate that there is essentially no change in volumetric oil yield when the shale residence time is reduced from 60 minutes to 15 minutes. The relatively short shale residence time requirement means that retorts smaller than originally estimated may be used commercially. This results in reduced capital expenditures and lower operating costs.

The Phase III study addressed the specific commercial plant design areas identified by the Bechtel Group, Inc., as having the greatest potential for reducing product oil costs. The variables studied were mass flux, purge gas preheat and shale residence time. Because more than one variable was changed at a time, it was not statistically possible to isolate the individual effects of high shale mass flux and purge gas preheat from the Phase III test results. However, judicious selection of operating conditions provided acceptable design points for the conceptual commercial plant design.

The stability of HYTORT product shale oil (Table III) was evaluated (in terms of API

gravity, kinematic viscosity at 100°F, pour point and amount of precipitated solids) over a period of 16 weeks. Storage stability was evaluated under four separate sets of storage conditions. One group of samples was refrigerated at 4°C, a second sample set was held at 50°C (to accelerate any potential changes) and two groups of samples were stored at ambient temperature (25°C). An anti-oxidant (DuPont Anti-Oxidant No. 22) was added to one subsample of the two ambient temperature groups. All samples were shielded from light during storage. The results of the oil stability tests, shown in Table IV, indicate no significant change in properties over a 16-week period. Thus, HYTORT oil can be stored prior to upgrading for several months without significant degradation.

TABLE III

ANALYSIS AND PROPERTIES OF RAW HYTORT SHALE OIL USED IN STABILITY TESTS

Ultimate Analysis, Wt %	
Carbon	86.38
Hydrogen	10.24
Sulfur	1.28
Nitrogen	2.13
Ash	0.0
Viscosity, cSt @ 100°F	16.0
Specific Gravity (60/60°F)	0.968
API Gravity, °API	14.7
Distillation, °F	
IBP	159
50%	653
EP	760
Heating value, Btu/lb	17,698
Pour point, °F	-25

TABLE IV

RESULTS OF HYTORT OIL STORAGE STABILITY TESTS

Storage Conditions	Analysis	Elapsed Time, Weeks		Analytical Method Accuracy
		0	16	
Refrigerated (4°C)	API gravity, °API	14.7	14.6	+0.1
	Viscosity, cSt @ 100°F	16.0	17.6	+0.1
	Pour point, °F	-25	-20	+2.5
	Precipitated solids, ppm	40	45	+2.5
Ambient (25°C)	API gravity, °API	14.7	14.1	+0.1
	Viscosity, cSt @ 100°F	16.0	18.1	+0.1
	Pour point, °F	-25	-20	+2.5
	Precipitated solids, ppm	40	40	+2.5
Heated (50°C)	API gravity, °API	14.7	14.3	+0.1
	Viscosity, cSt @ 100°F	16.0	18.8	+0.1
	Pour point, °F	-25	-20	+2.5
	Precipitated solids, ppm	40	35	+2.5
Ambient (Anti-oxidant added)(25°C)	API gravity, °API	14.7	14.5	+0.1
	Viscosity, cSt @ 100°F	16.0	19.7	+0.1
	Pour point, °F	-25	-15	+2.5
	Precipitated solids, ppm	40	40	+2.5

ACKNOWLEDGMENT

The authors gratefully acknowledge the support of Phillips Petroleum Company in conducting this work.

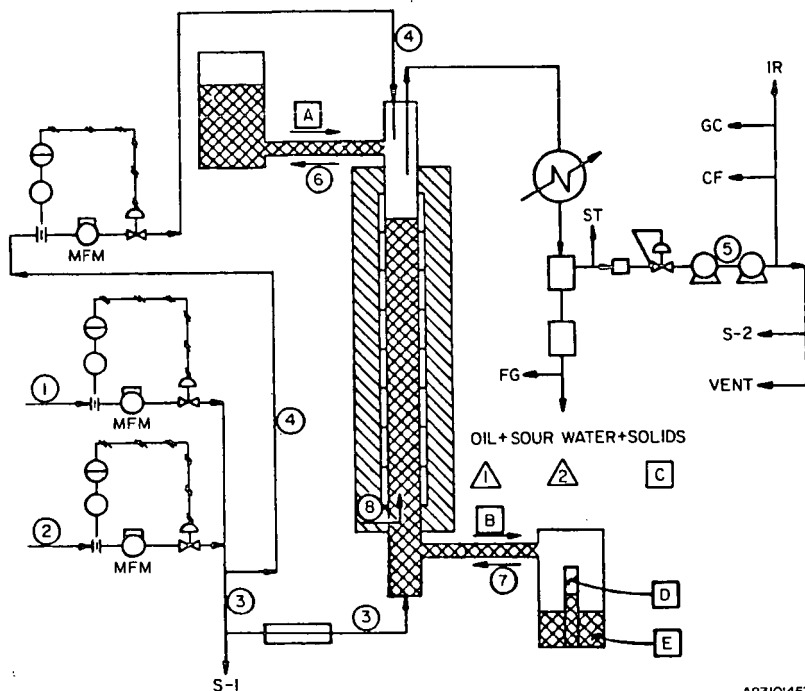


Figure 1. BENCH-SCALE UNIT (BSU)

LEGEND FOR FIGURE 1

- | | |
|--|--|
| ① main hydrogen supply to retort system | [E] Spent shale sample from residue receiver |
| ② Helium tracer supply to retort system | ▲ Product oil |
| ③ Pre-mixed hydrogen/helium flow to bottom of retort | ▲ Sour water |
| ④ Pre-mixed hydrogen/helium purge to top of retort | S-1 Feed gas sample point |
| ⑤ Product gas | S-2 Product gas sample point |
| ⑥ Purge gas mixture | ST Sampling train |
| ⑦ Pressurization gas mixture (H_2/He) | FG Flash gas system |
| ⑧ Purge nitrogen stream from shell to reactor | CF Cold finger for freeze-out sample |
| [A] Shale feed | GC Gas chromatograph |
| [B] Shale discharge | IR Infrared gas analyzers |
| [C] Solids in condensed liquids | Vent Product gas vent to atmosphere |
| [D] Spent shale sample from steady-state sampler | MFM Mass flow meter |

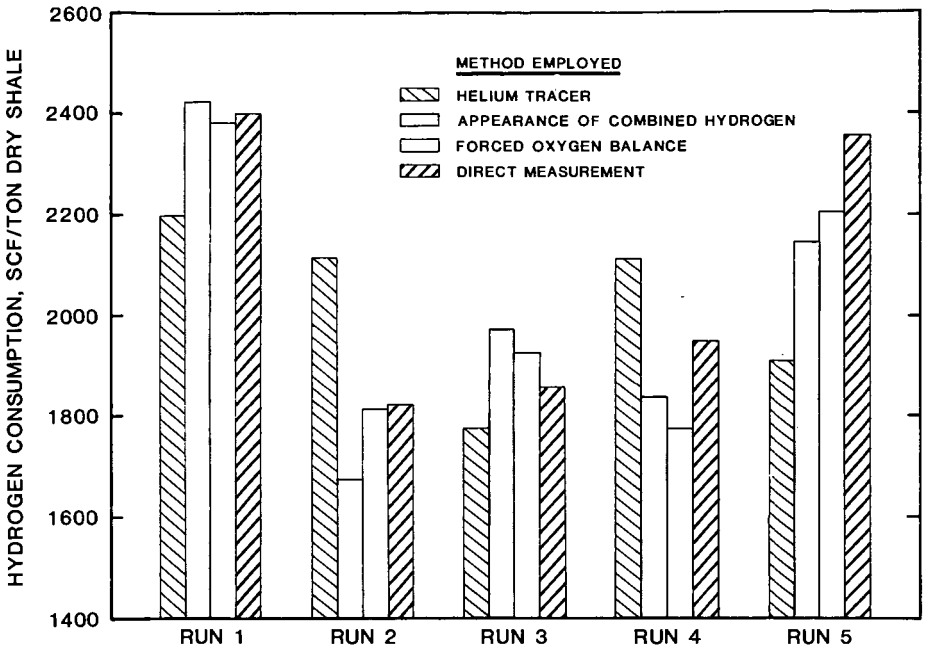


Figure 2. Comparison of hydrogen consumption calculated by various methods in selected BSU runs.

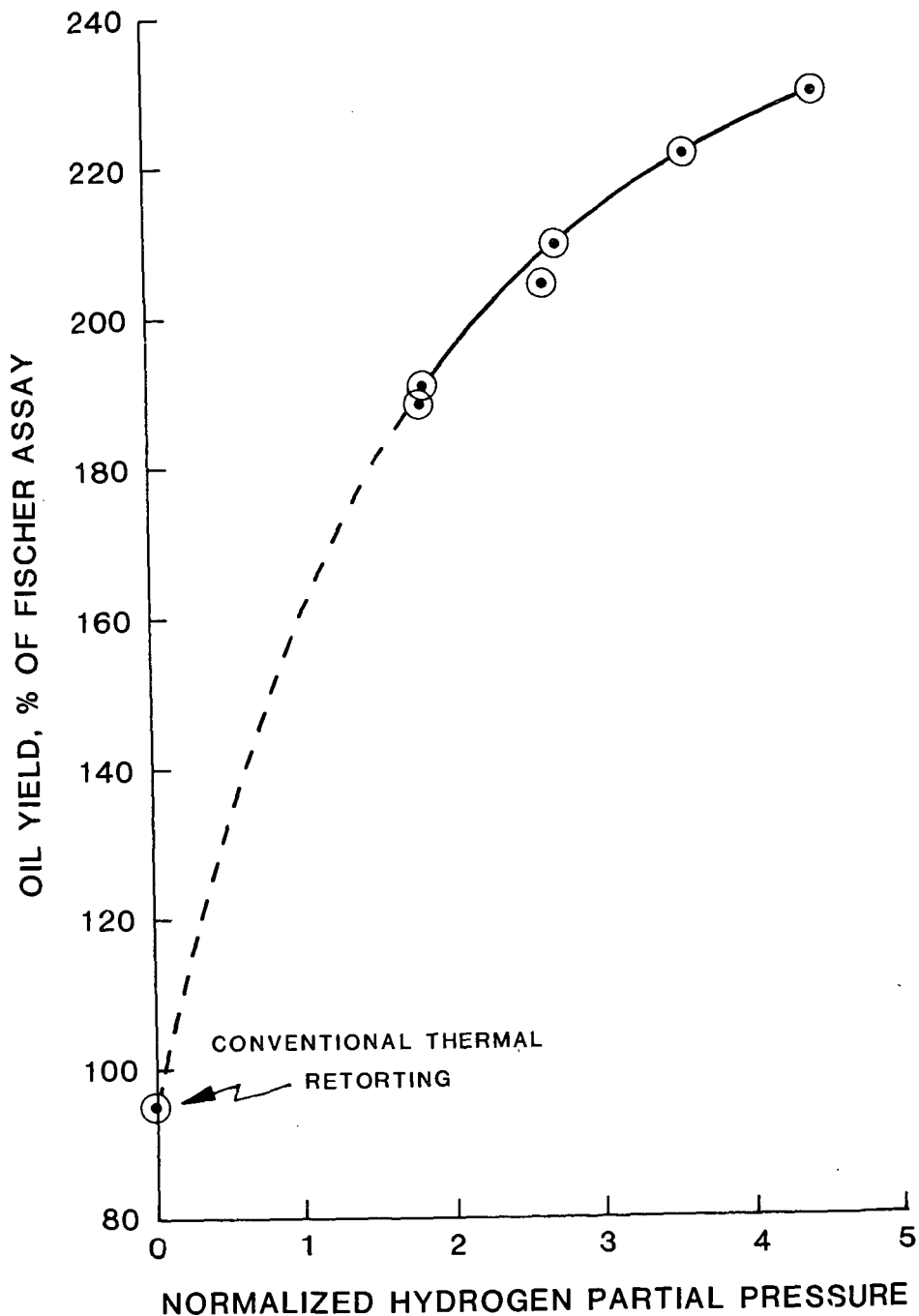


Figure 3. Oil yield (relative to Fischer Assay) as a function of hydrogen partial pressure.

LITERATURE CITED

- (1) Attari, et al. , "Determination of Organic Oxygen Content of Oil Shales", paper presented at the IM&R 1982 Eastern Oil Shale Symp. , Lexington, Kentucky (1982).
- (2) Weil, S. A. , et al. , "Oil Shale Hydroretorting Laboratory Studies at IGT", Paper No. 13 in Symp. Papers: Synthetic Fuels from Oil Shale, Chicago, Insti. of Gas Technology (1980).
- (3) Ewert, W. M. and Scinta, J. , "Hydrogen Retorting of Indiana Shale in a Loop Reactor System", Paper No. 19 in Symp. papers: Synthetic Fuels from Oil Shale and Tar Sands, Chicago, Insti. of Gas Technology (1983).
- (4) Roberts, M. J. , "Hydroretorting of Eastern Devonian and Western Eocene Shales", Paper No. 15 in Symp. papers: Synthetic Fuels from Oil Shale II, Chicago, Insti. of Gas Technology (1982).
- (5) Weil, S. A. , et al. , "Hydrogasification of Oil Shale", Paper presented at the ACS Fuel Chem. Div. Meeting in Los Angeles (1974).

SYMPOSIUM ON CHARACTERIZATION AND CHEMISTRY OF OIL SHALES
PRESENTED BEFORE THE DIVISIONS OF FUEL CHEMISTRY AND
PETROLEUM CHEMISTRY, INC.
AMERICAN CHEMICAL SOCIETY
ST. LOUIS MEETING, APRIL 8 - 13, 1984

BENCH SCALE RETORTING OF KENTUCKY OIL SHALE: COMPARISON OF
A FIXED BED TO 1 1/2 AND 3 INCH FLUID BED RETORTS

By

A. M. Rubel and S. D. Carter
Institute for Mining and Minerals Research, University of Kentucky, P. O. Box 13015
Lexington, Kentucky 40512

INTRODUCTION

Oil yields substantially in excess of Fischer Assay have been obtained for eastern U. S. oil shales by several different retorting technologies (1-5). The possibility of oil yield enhancement has now been confirmed by a number of researchers at different laboratories. However, the emphasis of most of the available information in the literature to date has been the determination of the maximum oil yield possible from eastern shales. The problem of how retorting under conditions such as fast heating, steam, sweep gases, or vacuum in a fixed bed retort and under fluid bed conditions, result in higher oil yield has not been addressed. Some of these retorting parameters might provide some kinetic advantages or they might enhance oil yield by the reduction of coking and cracking. Additionally, some combination of both of these explanations could be feasible as well as the possibility of the additional release of volatile matter from the shale by various retorting conditions. Comparison of information that has been obtained at the Institute for Mining and Minerals Research (IMMR) using a 1 1/2-inch diameter fixed bed retort and a 1 1/2-inch and 3-inch diameter fluid bed retort have provided insights to the mechanism of yield enhancement for eastern U. S. oil shales.

EXPERIMENTAL

Oil Shale

Several master batches of Kentucky oil shale were produced from bulk samples which were crushed, blended, sieved and riffled into representative aliquots for retorting. Samples were stored under argon in air-tight containers to retard aging prior to retorting. All samples used for this study were obtained from the Cleveland Member of the Ohio Shale and were mined in Fleming County, Kentucky. The master batch used for the 3-inch diameter fluid bed was 20-30 mesh particles and contained 12.2% carbon while the two samples of Ohio Shale used for the 1 1/2-inch fluid bed were 18-20 mesh particles and contained 11.6 and 11.0% carbon. These samples were also used in the fixed bed along with another sample containing 14.6% carbon.

Modified Fischer Assay and Fixed Bed Retorting Procedures

The bench scale fixed bed retort and the modified Fischer Assay procedures used at the IMMR have been described elsewhere (6, 7). Additional procedures used to operate the bench scale fixed bed retort under conditions of different heating rates, sweep gases, steam and vacuum are detailed in Rubel and Coburn (1).

Bench Scale Fluid Bed Retorts and Operating Procedures

A description of the 1 1/2-inch diameter fluid bed retort, the operating conditions and procedures and the product collection system used for this unit have been given in Rubel et al. (5). Similar information for the 3-inch diameter unit has been detailed in Carter et al. (4).

Retort Product Analysis

Gases from the fixed bed retort were analyzed on a Carle 311-H Gas Analyzer using Carle Application 357. Gases leaving the product collection apparatus from the fluid bed retorts were monitored on a Carle Gas Analyzer (Series SX-AGC) using Carle Application 397B. This enabled determination of off gas weight and carbon content. A Carlo-Erba 1106 Elemental Analyzer was used to determine C (total), H and N in the raw and spent shale and in the oil. Raw and spent shale and oil were also analyzed for moisture and ash (ASTM D3174). Raw and spent shale samples were subjected to thermogravimetric analysis on a Perkin Elmer TGS-2 for volatile matter and fixed

carbon determinations.

RESULTS AND DISCUSSION

Retort Products Distribution

Figure 1 compares the distribution of products for the fluid bed reactors versus the fixed bed retort operated under modified Fischer Assay conditions. Also given is the partitioning of carbon between spent shale, oil and gas. Material and carbon balances for both fluid bed retorts and the fixed bed retort were between 99 and 101%. The upper retorting temperature for all runs (both fixed and fluid bed) used for this comparison was between 533° and 550°C. Since gas yield has been shown to be dependent on upper retorting temperature (1, 5, 8) comparison of the distribution of products between spent shale, oil and gas can only be done between retorting runs with similar maximum temperatures. As can be seen from Figure 1, fluid bed retorting of Kentucky oil shale results in more oil and less gas yield in comparison to the same shale pyrolyzed in a fixed bed retort. In this case, oil yield weight was enhanced 36% and gas yield decreased 44%. These results are substantiated by the recovery of carbon in the products. Carbon recovered in the oil increased 33% while carbon in the gas decreased 17%. Also of significance is the fact that under fixed bed conditions 10% more carbon was recovered in the spent shale than under fluid bed conditions. As will be shown later, carbon recovered as coke is the likely source of this residual carbon.

Effect of Upper Retorting Temperature on Products

The most obvious effect of increasing the upper retorting temperature for both the fixed bed and fluid bed retorts is the substantial increase in gas make. Figure 2 is a plot of gas yield as percent of the raw shale versus maximum retorting temperature for the fluid bed units compared with fixed bed retorting at 12°C/min to different upper soak temperatures. Under both fixed bed and fluid bed retorting conditions there is a marked increase in the amount of off gas produced as the bed temperature is increased. However, the fluid beds produced considerably less gas than the fixed bed run at a similar retorting temperature. This is consistent with the fact that cracking of oil vapors in the fluid bed should be minimum due to their very rapid removal (0.6 sec) from the fluid bed retorts by the high sweep gas velocities required to maintain fluidization. Additionally, more cracking of oil vapor is expected as the bed temperature is increased under both retorting conditions which results in the observed increase in gases produced.

Evidence of oil cracking as the major source of the increased gas make is presented in Figure 3. In the 3-inch diameter fluid bed, a two fold increase in the amount of CH₄ (0.1 to 0.2 wt %) found in the off gas was noted as the bed temperature was increased from 470° to 530°C. This was accompanied by a shift in the composition of the gas as is shown in Figure 4. At a bed temperature of 478°C, the hydrocarbon off gas is 23 wt % CH₄ and 27 wt % C₄'s with intermediate amounts of C₂'s and C₃'s. At a bed temperature of 533°C, CH₄ composed 30 wt % of the gas and C₄'s 21 wt %. As the bed temperature increased, the hydrocarbon off gas composition shifted toward a higher concentration of the lower carbon number hydrocarbons. For comparison, the amount of CH₄ produced by a comparable sample of Ohio shale retorted in the fixed bed under modified Fischer Assay conditions was 0.3 wt % of the raw shale. This is greater than the amount produced (0.2 wt %) by the fluid bed at a comparable maximum temperature.

The information obtained from the off gas analysis implies that an optimum retorting temperature for maximum oil yield from Kentucky oil shales must be a balance between a temperature high enough to remove all volatile hydrocarbons from the shale but low enough to prevent excess cracking. This is verified by the oil yield results from the fluid bed retorts. Figure 5 indicates that there is a optimum bed temperature of 575°C for maximum oil recovery.

Effect of Bed Temperature on Volatile Matter Release

Figure 6 shows the effect of bed temperature on the release from the raw shale of volatile matter as determined by thermogravimetric analysis (TG). Included on this curve are points from both fixed and fluid beds. It is apparent that volatile matter release is dependent on the retorting temperature and not the method of retorting. Volatile matter by TG includes all volatile material (both organic and inorganic) in the shale. Also the amount of volatile matter removed from the raw shale includes the amount of organic carbon converted to fixed carbon. Therefore, the curve of bed temperature vs. volatile matter removed continues to increase beyond the point at which increased oil yield is no longer observed. However, the information of interest here is that both retorting technologies effect the same amount of volatile matter release, but the volatile matter goes to different products. This again implies that the reduction of cracking losses is the major factor in oil yield enhancement.

Oil Yield vs. Fixed Carbon Deposition

Further evidence for decreased cracking, as the major factor for increased oil yields

from Kentucky oil shales, is the relationship between oil yield and coking as monitored by the amount of fixed carbon in the shale determined by TG. Figure 7 gives the spent shale-to-raw shale fixed carbon ratio for several fluid bed runs at different bed temperatures compared to fixed-bed runs under modified Fischer Assay, inert sweep gas, steam and vacuum retorting conditions. In the fluid bed as bed temperature increases, CH_4 production increases, the percentage by weight of C4's in the hydrocarbon gas decreases, total gas make increases and fixed carbon (coke) deposition increases. All these factors point to increased oil vapor cracking with higher bed temperature. The difference in coke deposition between the fixed and fluid beds is dramatic; 30% more fixed carbon is deposited under Fischer Assay conditions. The relationship between fixed carbon deposition and oil yields from the fixed bed run under various conditions shows the dependence of oil yield enhancement on decreased coking. Inert sweep gas conditions produced an oil yield enhancement of 105% modified Fischer Assay with a 23% increase in fixed carbon whereas steam and vacuum runs produced between 115-120% Fischer Assay oil with only a 10% increase in the fixed carbon present in the spent shale over that found in the raw shale.

Comparison of volatile matter release (Figure 6), fixed carbon deposition (Figure 7) and oil yield provides an indication of the mechanism by which oil yield enhancement is obtained for eastern U. S. shale. For a fluid bed run at 475°C, less than maximum volatile matter is released but coke deposition is minimum with the resultant 120 wt % Fischer Assay oil yield produced. Fischer Assay conditions result in maximum organic volatile matter release and maximum fixed carbon deposition. Fixed-bed steam retorting again provides for maximum organic volatile matter release which, combined with moderate coking, produces an oil yield of approximately 120% of Fischer Assay. Fluidized bed retorting at 575°C was found to be optimum for maximum oil yields from the Ohio Oil Shale in this study. This allowed for maximum volatile release with minimum fixed carbon deposition and a resultant oil yield of 155-160 wt % Fischer Assay.

SUMMARY

Bench scale fluid bed and fixed bed retorting of Kentucky oil shale has provided evidence that for the small particle sizes used in this study increases in oil yield, which have been shown to be feasible for eastern U. S. shale, is primarily due to decreased cracking of oil vapors and that release of hydrocarbons from the shale depends on pyrolysis temperature and not the retorting technology used. The following information presented supports this statement: Under fluid bed conditions where oil vapors are rapidly removed from the retort more oil and less gas are produced than any fixed bed retorting conditions. Under fluid bed conditions, the proportion of CH_4 in the gas increases with increasing bed temperature at the expense of a lower proportion of C4's in the hydrocarbon gas. CH_4 produced under modified Fischer Assay conditions is greater than that obtained at a comparable bed temperature in the fluid bed. Oil yield from the fluid bed retorting of Ohio Oil Shale is maximized at a bed temperature of 575°C under retorting conditions used in this study. Removal of volatile matter as measured by TG from the shale depends on retorting temperature and not retorting method. Increases in the fixed carbon content of the spent shale relative to the raw shale are accompanied by decreased oil yields, increased gas make and increased CH_4 production in both fixed and fluid bed retorts. Under modified Fischer Assay conditions, 10% more carbon as determined by elemental analysis is left on the spent shale than a fluid bed run at the same maximum bed temperature; TG analysis of the spent shale indicates that this residual carbon is coke.

ACKNOWLEDGMENTS

The authors wish to acknowledge the support and technical assistance of many of their colleagues at IMMR and the assistance of the publication staff and Peggy Dundon for preparation of this manuscript. The work reported herein was supported by the Kentucky Energy Cabinet (KEC) through a grant from the University of Kentucky Institute for Mining and Minerals Research (IMMR).

FIGURE 1. MATERIAL AND CARBON BALANCES FOR THE FLUIDIZED BEDS COMPARED WITH MODIFIED FISCHER ASSAY

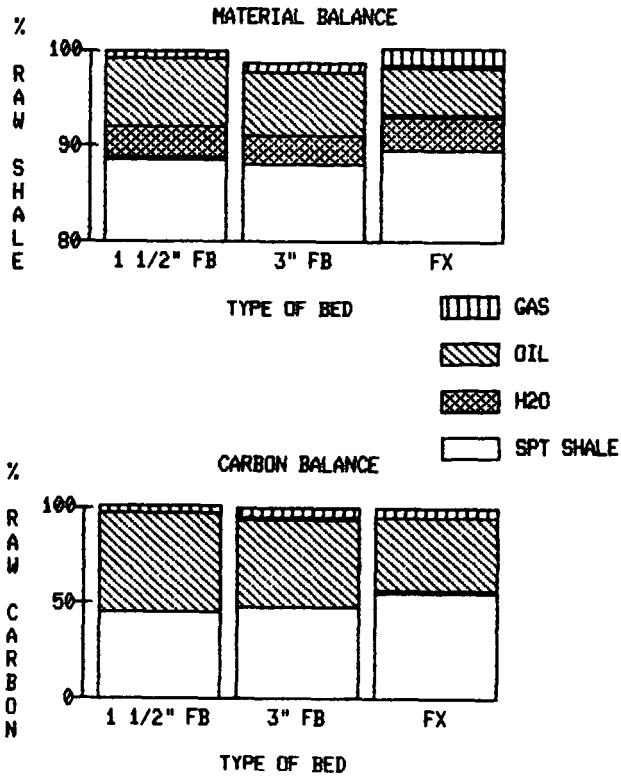


FIGURE 2. EFFECT OF TEMPERATURE ON GAS EVOLUTION

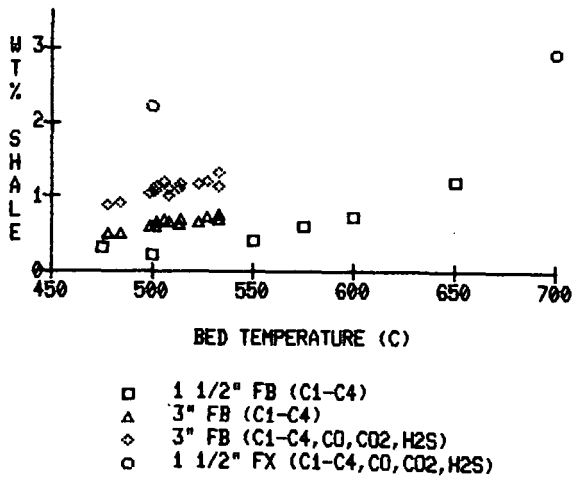


FIGURE 3. EFFECT OF BED TEMPERATURE ON METHANE EVOLUTION

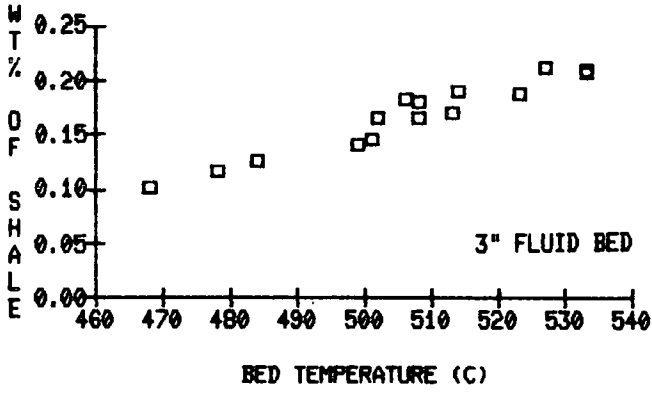


FIGURE 4. EFFECT OF TEMPERATURE ON HYDROCARBON GAS COMPOSITION

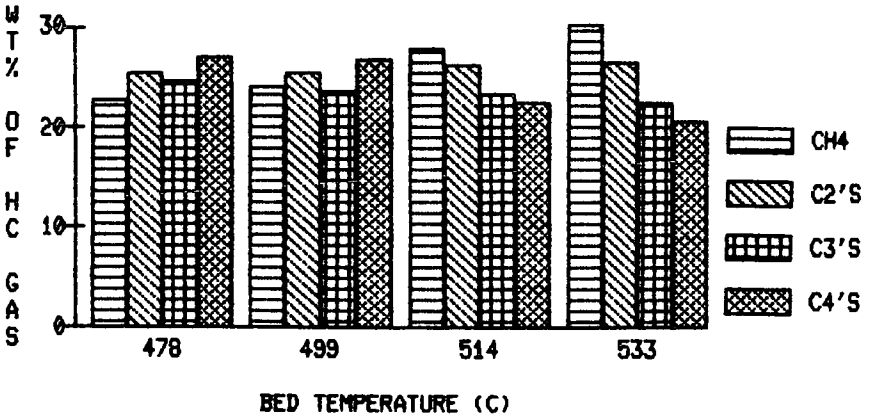


FIGURE 5. EFFECT OF BED TEMPERATURE ON OIL YIELD

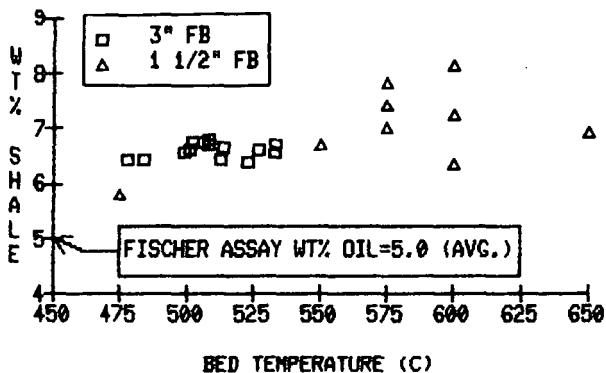


FIGURE 6. EFFECT OF BED TEMPERATURE ON VOLATILE MATTER BY TG REMOVAL IN THE FIXED AND FLUID BEDS

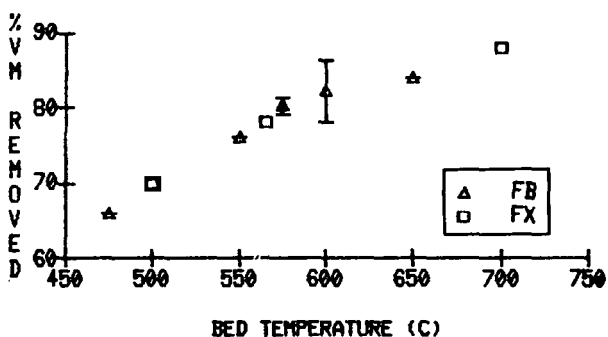
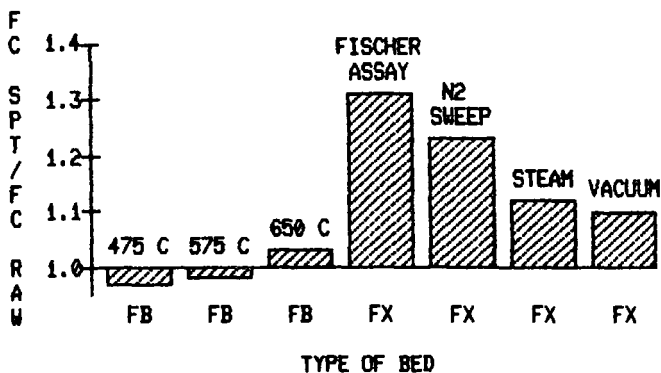


FIGURE 7. FIXED CARBON IN SPENT SHALE FROM DIFFERENT TYPES OF RETORTING CONDITIONS



LITERATURE CITED

- (1) Rubel, A. M. and Coburn, T. T., Proceedings of the 1981 Eastern Oil Shale Symp., University of Kentucky, Lexington, Kentucky, 21 (1981).
- (2) Richardson, J. H., Nuss, E. B., Ott, L. L., Clarkson, J. E., Bishop, M. O., Gregory, L. J. and Morris, C. J., UCID-19548, Lawrence Livermore Natl. Laboratory (1982).
- (3) Feldkirchner, H. L. and Janka, J. C., Symp. Papers: Synthetic Fuels from Oil Shale, Instl. of Gas Technology, Chapter 21, Atlant (1979).
- (4) Carter, S., Taulbee, D., Margolis, M., Saenz, A. and Cummins, W., Proceedings of the 1983 Eastern Oil Shale Symp., University of Kentucky, Lexington, Kentucky (1983).
- (5) Rubel, A. M., Margolis, M.J., Haley, J. K. and Davis, B. H., Proceedings of the 1983 Eastern Oil Shale Symp., Lexington, Kentucky (1983).
- (6) Coburn, T. T., Rubel, A. M. and Henson, T. S., IMMR Report No. IMMR 81/062, University of Kentucky, Lexington, Kentucky (1981).
- (7) Coburn, T. T. and Rubel, A. M., Fuel Processing Technology, 8 (1), 1 (1983).
- (8) Rubel, A., Taulbee, D., Coburn, T., Thomas, G. and Yates, L., Proceedings of the 1982 Eastern Oil Shale Symp., University of Kentucky, Lexington, Kentucky (1982).

SYMPOSIUM ON CHARACTERIZATION AND CHEMISTRY OF OIL SHALES
PRESENTED BEFORE THE DIVISIONS OF FUEL CHEMISTRY AND
PETROLEUM CHEMISTRY, INC.
AMERICAN CHEMICAL SOCIETY
ST. LOUIS MEETING, APRIL 8 - 13, 1984

INTERFACIAL CHEMISTRY OF THE HOT WATER PROCESS FOR RECOVERING BITUMEN
FROM THE ATHABASCA OIL SANDS

By

L. L. Schramm, R. G. Smith and J. A. Stone
Syncrude Canada Ltd., Research Department, P. O. Box 5790
Edmonton, Alberta, Canada, T6C 4G3

INTRODUCTION

In the Athabasca oil sands, bitumen is separated from the quartz sand grain matrix by (at least) a thin film of water. This separation distinguishes the oil sand from other oil sands such as those found in Utah, for example. This feature is also of crucial importance to the commercial success of the hot water extraction process as it is currently being practiced in the Fort McMurray region of Alberta.

In the hot water process, oil sand is slurried with water and sodium hydroxide at about 80°C. The slurry is then conditioned in a horizontal rotating drum into which steam is injected. After conditioning the slurry is screened, then diluted with additional water and transported to a flotation vessel. In this vessel, aerated bitumen droplets float to form a froth which is subsequently collected. The greater part of the recoverable bitumen is obtained in this primary process step although froth and other streams from this vessel are further treated. Additional details can be found elsewhere (1-3).

An understanding of the mechanisms involved in the hot water process is still evolving. In view of the wide array of interfaces present in the air, oil, water, sand and clay system it is not surprising to find that interfacial phenomena appear to play a major role in the process.

It was learned at an early stage, for example, that the process is adversely affected by clay minerals, that alkaline reagents are required to maintain near neutral solutions and that the presence of surface active agents is needed (4-6). Subsequent research has demonstrated that the alkaline reagents are required principally to generate naphthenic carboxylate surfactants from the bitumen and that these surfactants are in turn the active agents in the process (7-12). It further emerges that complex interactions take place. Thus, the dosage of alkaline reagents required depends upon the fine solids (clay) content in the oil sand (10, 12).

The surfactants generated by the alkaline reagent appear not only to promote bitumen separation and aeration but to promote solids flotation as well, having thus both positive and negative contributions to the process (7-9, 11). Unifying principles of process operation which hold for the complete range of Athabasca oil sands which vary in grade, age after mining and depositional environment have thus far been elusive; Sanford's correlation between oil sand fines content and process aid requirements (12) being the closest approach which is used in practice. In this paper, we discuss some results from investigations into the role of the natural surfactants in the hot water process.

EXPERIMENTAL

Oil Sands

We will focus mainly on three oil sand samples which were used in this work. All were obtained from the Syncrude Mildred Lake oil sands operation. The compositions of these oil sands are given in Table I. In this work, the oil sands are distinguished by their bitumen content. A rich ore would contain about 12-14% (w/w) bitumen, an average grade 10-11% and a lean grade 6-9%. As the grade improves the fraction of water decreases and the relative amount of fines (clays) also decreases (12).

Bench-Scale Processing

A laboratory-scale batch extraction unit and operating procedure developed by Sanford and Seyer (10) was used for studying the oil sands hot water process. The procedure involves slurrying 500g charges of oil sand and simulates the conditioning (tumbler) step and the primary and secondary recovery steps of the continuous commercial process. Samples collected from each extraction

were assayed for oil, water and solids content by standard methods (13). From the assays, primary and secondary recoveries as well as a mass balance were obtained for each extraction. Replicate extraction samples were isolated for surfactant and electrophoretic mobility determinations.

TABLE I
COMPOSITIONS OF OIL SANDS STUDIED

Oil Sand	Bitumen	Water	Solids	Fines ^a
		(% w/w)		
Rich	13	2	85	9
Average	11	3	86	19
Lean	6	11	83	21

- a. The fines level is defined as the weight fraction of solids smaller than 44 μm and is expressed as a percentage of total solids.

Primary oil recoveries obtained with this unit have been found to be good indicators of the primary oil recovery obtainable with a 2270kg/h continuous pilot unit, which is a scaled-down version of the Syncrude commercial plant.

Surfactant Determination

Secondary tailings is a process stream from the batch extractor (above) and contains the suspended clays and the bitumen not initially floated. Samples of this stream were centrifuged at 15,000 G to remove the bitumen and solids. The concentration of carboxylate-functional surfactant was then determined using a foam fractionation/acid titration technique described elsewhere (14).

The method is based on the tendency of surfactants to concentrate at interfaces. A sample is sparged with gas (such as a nitrogen/carbon dioxide mixture). The foam which is produced is then drawn off. When the process is complete all of the surfactants will have been carried over in the foam. Meanwhile, the non-surface active salts will remain present in both foam and residue. By potentiometrically titrating each phase with HCl, the total carboxylate salt content of each phase is obtained. The carboxylate surfactant concentration in the original sample can then be calculated.

Electrokinetic Determinations

Suspensions of fine solids were prepared for microelectrophoresis measurements by diluting a small portion of original secondary tailings with supernatant solution from a previously centrifuged aliquot. In some cases, a further filtration of the supernatant was required in order to remove all suspended material. In this manner, dispersions of about 0.1% or less solids were obtained in the original equilibrium solution (thus, preserving the original ionic strength and electrolyte composition).

Emulsions of bitumen in the same original equilibrium solution were prepared as follows. A sample of bitumen obtained from the Syncrude oil sands operation, having less than 1% combined solids and water, was stored at 4°C and used as a reference material. A small amount of bitumen was dispersed in the clarified secondary tailings solution with an ultrasound generator. In some cases, emulsions were prepared using instead primary froth from the corresponding batch extraction run to confirm the validity of employing emulsions prepared with the reference bitumen. The bitumen-in-water emulsions prepared had droplet radii of $4.9 \pm 2.4 \mu\text{m}$ as measured using a calibrated reference grid in the microelectrophoresis apparatus microscope (using dark-field illumination).

Microelectrophoresis Measurements

The apparatus used for these studies was a Rank Brothers' Microelectrophoresis Apparatus Mark II (Rank Brothers, Cambridge, England) fitted with a rotating prism and video-viewing system. In the present work, a rectangular cell was employed, fitted with hydrogen-charged palladium electrodes. The cell was used and stored in a constantly water wet condition. Detergent washing procedures proved to be satisfactory, except for the occasional need to rinse bitumen out with toluene and then re-wet the cell.

RESULTS AND DISCUSSION

Surfactants

Of the total amount of sodium hydroxide added during processing perhaps only 5% reacts to

produce the carboxylate surfactants (14). Figure 1 shows the relationship which is typically observed between the equilibrium concentration of carboxylate surfactants and the amount of sodium hydroxide used in the extraction. These surfactant correlations correspond to the supernatant equilibrium solution in secondary tailings slurry from the bench extractions. As indicated in the figure we commonly observe a linear relationship between the amount of sodium hydroxide added during processing and the amount of equilibrium surfactant appearing in solution. It is apparent that some oil sands yield a high concentration of surfactants in solution even when no sodium hydroxide is used while others yield low concentrations of surfactants even when fairly high levels of sodium hydroxide are employed.

Processibility curves for the oil sands investigated in the present work are given in Figure 2. They span the range of processibilities commonly observed from that for rich ore where addition of any base reduces recovery to that for lean ore where maximum oil recovery is achieved only at very high addition of base.

The relationship between the equilibrium concentration of carboxylate surfactant in solution and primary oil recovery from the bench extraction test is shown in Figure 3. In addition to the results from oil sands used in the present work, recoveries obtained in previous investigations of other grades and ages of oil sand are included for comparison. It can be seen that there exists a critical concentration of carboxylate surfactant at which maximum oil recovery is obtained from the hot water process. The value of this critical concentration is about 1.2×10^{-4} N (+15%). For further discussion see (14).

Interfacial Charges

In the present work, the dispersed particles and droplets can be considered to be large, with thin electrical double layers ($l \sim 1$ to 5×10^{-3} M). By isolating process samples and reducing the solution pH it was found that the fine solids (clays) exhibited negative electrophoretic mobilities at all pH conditions (down to pH 2). In the case of the dispersed bitumen droplets, the electrophoretic mobility decreased with decreasing solution pH to an apparent isoelectric point at a pH of about 3. Similar behavior has been observed by Takamura and Chow (15). It appears that the charge at the bitumen/solution interface is primarily determined by the presence of ionized carboxylic acid groups. This would be the logical result of the generation and/or adsorption of carboxylate surfactants at this interface.

The following discussion refers to process samples isolated and studied at the equilibrium pH levels which were reached during processing.

The electrophoretic mobilities of the solids and bitumen droplets are shown as functions of the process solution pH in Figure 4. It can be seen that in general the interfacial charges increase (negative) with solution pH.

The electrophoretic mobilities of the solids and bitumen droplets are shown as functions of the process equilibrium carboxylate surfactant concentration in Figure 5. As the carboxylate surfactants will be fully ionized about pH 7, the increases in interfacial charge depicted in Figures 4 and 5 appear to be due to surfactant adsorption at the interfaces.

It appears that the solid (clay) surfaces become saturated with respect to surfactant adsorption in the range of process conditions investigated. It further appears that, in the case of the bitumen droplets, a pronounced maximum in the interfacial charge occurs as a function of surfactant concentration in the process. The surfactant concentration at which this maximum is observed is very nearly the same as the critical surfactant concentration of Figure 3.

Comparison of Figures 3 and 5 reveals that the maximum in oil recoveries and the corresponding critical surfactant concentration all correlate with a maximum in the bitumen/solution interfacial charge. We now have two common threads which apparently link oil sands and their processing behavior. That is, maximum bitumen recovery obtained using the hot water process corresponds to a single critical surfactant concentration in solution which, in turn, corresponds to a maximum in the bitumen/solution interfacial charge.

DISCUSSION

The occurrence of a maximum in the electrophoretic mobility versus surfactant concentration curve (Figure 5) indicates a marked change in the manner in which the surfactants are adsorbing at the interface. The maximum in surface charge likely corresponds to completion of a conventional monolayer coverage. It is possible that, beyond this point, some form of hemimicelle formation takes place. For the present purpose, we will consider some implications of the experimental results.

That maximum bitumen recovery from the process is associated with a maximum in the charge at the bitumen/solution interface is a rather surprising discovery and in direct contradiction to previous theories of the mechanism of the hot water process advanced by Levine (11) and by Bowman and Leja (7, 9). It is of interest to discuss how this arises.

The earlier theories cited begin with the assumption that some charging of the bitumen and solids surfaces is necessary to prevent mutual agglomeration. Beyond this requirement, they go on to predict that a minimum in bitumen surface charge will be the optimum condition for air attachment and flotation. This will be the point at which the bitumen is most hydrophobic and it was thought that hydrophobic bitumen droplets and gas bubbles attached and rose to form a bituminous froth layer. The major weakness in these treatments is the description of the carboxylic surfactant deprotonation equilibria. Here significant dissociation effects are assumed to be prominent in the solution pH range 7-10, in which the process is operated. In fact, the surfactants will be nearly fully dissociated (>90%) by a pH of 6 (see also the discussion by Hall and Tollefson (16)). The carboxylate dissociation reaction aside, Levine's prediction that a minimum in bitumen surface charge should correspond to a maximum flotation efficiency is not unreasonable if the bitumen aeration process is indeed one in which hydrophobic bitumen and air bubbles contact and adhere to each other.

The present results indicate that another mechanism is operative. Maximizing the droplet charge will reduce the hydrophobicity of bitumen. If the bitumen surface is charged by the surfactants, it is reasonable to assume that any gas (air) bubbles in the process slurry will become charged as well. The studies of Sato et al. (17) support this hypothesis.

As recognized in virtually all process mechanism theories to date, the first step in the process must be to enhance the already present-but-small separation of bitumen from the solids. Charging the bitumen/solution and solid/solution interfaces can likely generate sufficient electrostatic potentials to accomplish this. Having done so, the interfacial tension will cause the bitumen to form droplets. Conceptually, the remaining step is to selectively float the bitumen, over the solids, to form a froth. It is possible that charged air (or gas) bubbles, with an associated aqueous film, become dispersed in the bitumen. The bitumen droplets would become, in effect, globules of bituminous foam which would have a sufficiently reduced density for them to rise in the flotation vessel. The process as just described would promote bitumen flotation over solids flotation by virtue of the fact that there will be a trade-off between the repulsive forces between the air, bitumen and solid moieties and the influence of the mechanical energy which is applied in the conditioning step. The importance of optimizing mechanical energy input to the system has been emphasized by Sanford (12).

The notion that bitumen aeration consists of producing a dispersion of air or gas bubbles in the bitumen droplets is also consistent with the studies of Miller and co-authors (18-21). In Miller's studies of Asphalt Ridge bitumen in hot water processing, a zero contact angle for air-bitumen attachment was observed in the alkaline solution pH range. Having found bitumen to have lost its hydrophobicity under efficient processing conditions, these authors concluded that polar fatty acid salts (surfactants) stabilize a dispersion of air bubbles in bitumen.

CONCLUSION

The natural carboxylate surfactants generated in the hot water extraction process appear to play a critical role in determining the ultimate bitumen recovery. There apparently exists a single equilibrium solution concentration of surfactant which corresponds to maximum oil recovery from the process. This relationship appears to hold irrespective of factors such as the oil sand's grade, age after mining or depositional environment.

It has also been shown that natural surfactants adsorb at the mineral and bitumen surfaces. The interfacial charges increase, in general, with increasing solution pH and surfactant concentration. The bitumen/solution interfacial charge, however, passes through a distinct maximum and is entirely determined by surfactant adsorption.

The maximum in bitumen droplet charge corresponds to the critical surfactant concentration for maximum bitumen recovery from the process. This means that maximum recovery in the process is not associated with minimum surface charges as had previously been supposed.

The present results support a theory of the hot water process in which electrostatic forces drive the separation of bitumen from the oil sand matrix and in which bitumen is aerated by a dispersive rather than an attachment mechanism.

ACKNOWLEDGMENTS

The authors wish to thank Dr. E. C. Sanford for his contribution to the design and interpretation of this research. The careful experimental work of A. Lemke, J. M. Severyn, J. B. Turnbull and M. Tyckowsky is also gratefully acknowledged. The authors are grateful to Syncrude Canada Ltd. for permission to publish this work.

Figure 2. Processibility curves for three oil sands as obtained from laboratory scale batch extractions.

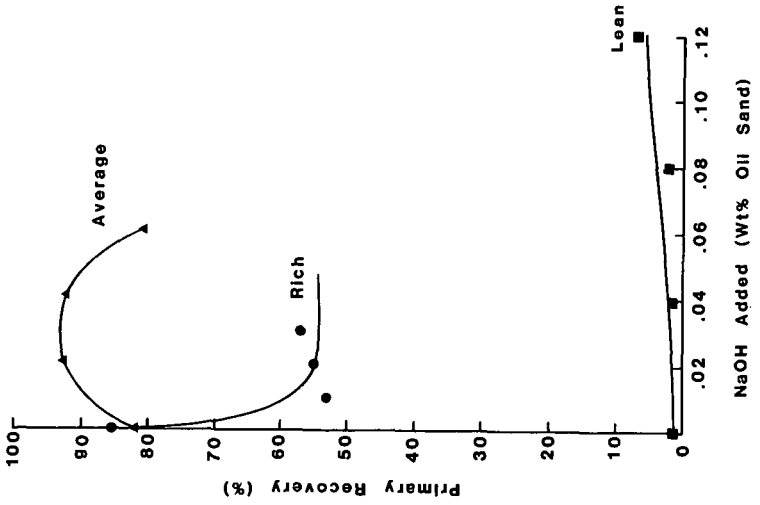


Figure 1. The equilibrium concentrations of carboxylate surfactant produced in processing oil sands by using various amounts of sodium hydroxide. The data refer to process stream extracts.

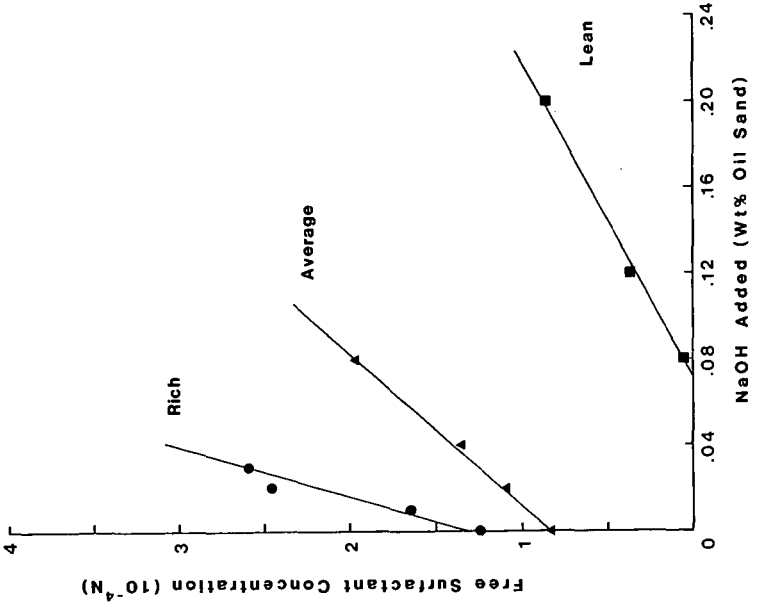


Figure 4. Electrophoretic mobilities observed for fine solids (filled symbols) and bitumen droplets (open symbols) as functions of process solution pH. The data are for average (●,○), lean (▲,△) and a mixture of the average and lean (■,□) ores extracted at various NaOH addition levels.

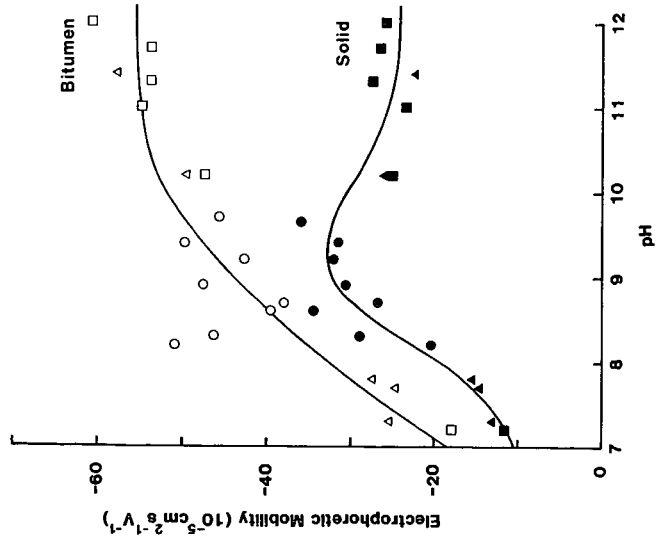


Figure 3. Primary oil recoveries obtained from processing various oil sands versus the equilibrium carboxylate surfactant concentrations observed in process stream extracts. The symbols indicate the rich (●), average (▲) and lean (■) ores of the present work.

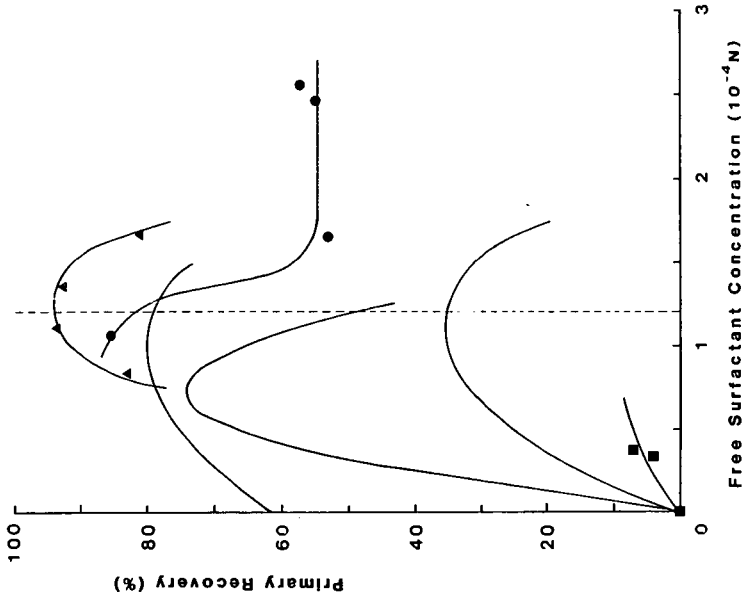
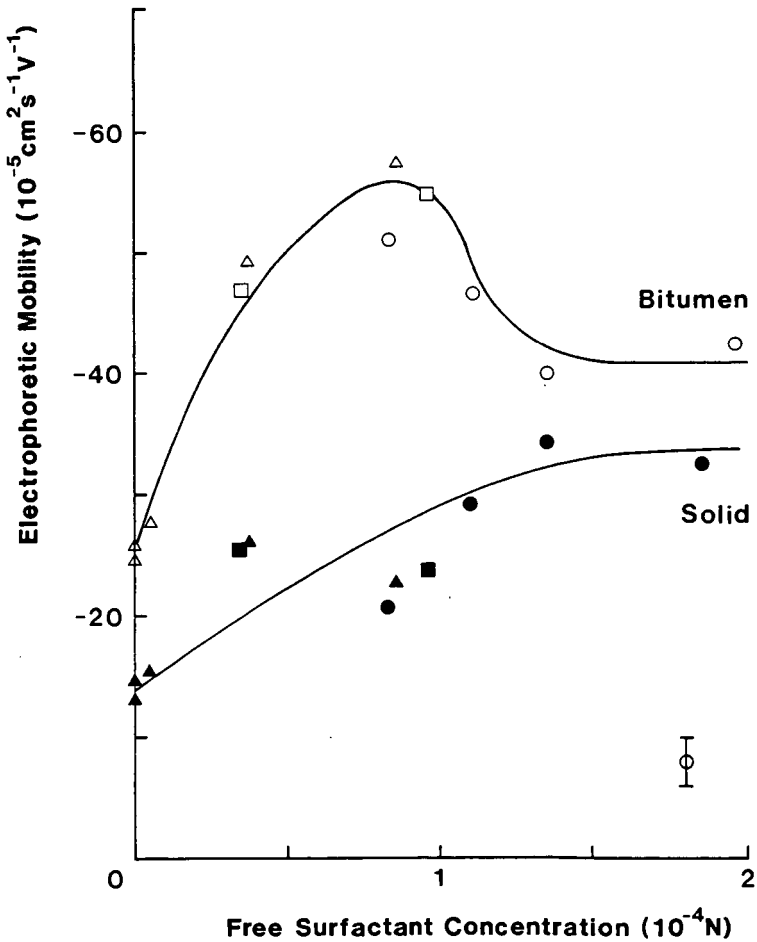


Figure 5. Electrophoretic mobilities of fine solids (filled symbols) and bitumen droplets (open symbols) as functions of the equilibrium carboxylate surfactant concentration in process stream extracts. The data are for average (●,○) lean (▲,△) and a mixture of the average and lean (■,□) ores extracted at various NaOH addition levels.



LITERATURE CITED

- (1) M. M. Schumacher, ed., "Heavy Oil and Tar Sands Recovery and Upgrading", Noyes Data Corp., Park Ridge (1982).
- (2) Schutte, R. and Ashworth, R. W., "Oil Sands", English Language translation of Olsande in Ullmanns Encyklopadie der technischen Chemie, Vol. 17, Verlag, Weinheim, pp. 423-436 (1979).
- (3) Ranney, M. W., "Oil Shale and Tar Sands Technology", Noyes Data Corp., Park Ridge (1979).
- (4) Clark, K. A. and Pasternack, D. S., Ind. and Eng. Chem., 24, 1410 (1932).
- (5) Pasternack, D. S. and Clark, K. A., Report No. 58, Research Council of Alberta, Edmonton, Alberta (1951).
- (6) Clark, K. A. and Pasternack, D. S., Report No. 53, Research Council of Alberta, Edmonton, Alberta (1949).
- (7) Bowman, C. W., Proc. 7th World Petrol. Congr., 3, 583 (1967).
- (8) Baptista, M. V. and Bowman, C. W., Preprint, 19th Can. Chem. Eng. Conf., Edmonton, Alberta (1969).
- (9) Leja, J. and Bowman, C. W., Can. J. Chem. Eng., 46, 479 (1968).
- (10) Sanford, E. C. and Seyer, F. A., CIM Bulletin, 72, 164 (1979).
- (11) Levine, S. and Sanford, E. C., Proc. 30th Can. Chem. Eng. Conf., 1112 (1980).
- (12) Sanford, E. C., Can. J. Chem. Eng., 61, 554 (1983).
- (13) Syncrude Canada Ltd., "Syncrude Analytical Methods for Oil Sand and Bitumen Processing", AO STRA, Edmonton, Alberta (1979).
- (14) Schramm, L. L., Smith, R. G. and Stone, J. A., AO STRA J. Research, in press (1984).
- (15) Takamura, K. and Chow, R. S., Preprint, 33rd Ann. Tech. Meeting Petrol. Soc. of CIM, Calgary, Alberta (1982).
- (16) Hall, E. S. and Tollefson, E. L., Can. J. Chem. Eng., 60, 812 (1982).
- (17) Sato, Y., Murakami, Y., Hirose, T., Yamamoto, H. and Uryu, Y., J. Chem. Eng. Japan, 12, 454 (1979).
- (18) Smith, R. J. and Miller, J. D., Mining Engineering, 33, 1719 (1981).
- (19) Miller, J. D. and Misra, M., Int. J. Mineral Processing, 9, 269 (1982).
- (20) Sepulveda, J. E., Miller, J. D. and Oblad, A. G., PREPRINTS, ACS, Div. Petrol. Chem., 21, 110 (1976).
- (21) Miller, J. D. and Misra, M., Fuel Process. Technol., 6, 27 (1982).

SYMPOSIUM ON CHARACTERIZATION AND CHEMISTRY OF OIL SHALES
PRESENTED BEFORE THE DIVISIONS OF FUEL CHEMISTRY AND
PETROLEUM CHEMISTRY, INC.
AMERICAN CHEMICAL SOCIETY
ST. LOUIS MEETING, APRIL 8 - 13, 1984

FLASH PYROLYSIS OF OIL SHALE WITH VARIOUS GASES

By

M. Steinberg and P. T. Fallon
Department of Applied Science, Brookhaven National Laboratory, Upton, New York 11973

INTRODUCTION

The rapid heat-up rate (10^3 - 10^5 °C/sec) and short residence time pyrolysis (<10 sec) of carbonaceous materials such as coal (1, 2) and wood (3) particulates with high temperature (700° to 1000°C) gases has been shown to produce significantly higher yields of gaseous and liquid hydrocarbon products than conventional slow heat-up rate (1-10°C/sec) and longer residence time (mins to hrs) pyrolysis. In the flash pyrolysis of coal, it has been found that the yield of gaseous and liquid hydrocarbons for certain coals can be increased by as much as 36% beyond the Fischer Assay value (4). The principles of flash pyrolysis follow the sequence: (a) rapid heat-up, depolymerize and bond break the structure of the large polycyclic coal and wood cellulose and lignin polymer molecules to form smaller free radical units; (b) allow the lighter fraction molecules to react in the gas or liquid phases with each other or with a reactive pyrolysis gas such as hydrogen and (c) limit the residence time at pyrolysis temperature by rapidly cooling the reaction system to stabilize the reaction products and prevent repolymerization and charring of the hydrocarbon gases and liquids. These flash pyrolysis principles have been applied in several exploratory experiments performed with western oil shales and are described in this paper.

It is known that there are differences in the yield and type of liquid and gaseous hydrocarbon products that can be obtained depending on the thermal treatment and the origin of oil shale. It is well known that eastern (Devonian) U. S. Shales yield a lower Fischer Assay of organic material (~10 gal/ton) than western (Eocene) U. S. Shales (~30 gal/ton). The H/C molar ratio of organic matter in western shale runs around 1.5 while in eastern shale it runs approximately 1.0 (5). There is also evidence that the manner and the rate at which shale is heated up, as well as the residence time at temperature, can affect the yield and distribution of products. This information has been mainly obtained from thermogravimetric analysis (TGA) and in static (retort) experiments. There is also information available on hydrogenation (6) and superheated steam hydrolysis of oil shale (7). The work presented in this paper deals with the results of the flash pyrolysis of oil shale by heating with both reactive and non-reactive gases in an entrained tubular reactor.

EXPERIMENTAL EQUIPMENT AND PROCEDURE

The flash pyrolysis of oil shale was conducted in a highly instrumented 1" I. D. by 8 ft long entrained downflow tubular reactor system. The equipment has been previously described in detail (8). A schematic flowsheet of the system is shown in Figure 1. Ground oil shale in the particle-size range of 150 to 500 microns is fed by gravity into the top of the reactor from a feeder enclosed by a high pressure vessel connected to the reactor. The pyrolyzing gas is supplied from high pressure storage cylinders and is preheated in an electrically-heated stainless steel resistance tube prior to entering at the top of the reactor where it meets the shale particles. Gas temperatures up to 1000°C can be obtained. The reactor is constructed of Inconel, a high alloy metal, having an 0.5" wall thickness, capable of withstanding pressures ranging up to 3000 psi. The gas mixes, transfers heat, pyrolyzes and reacts with the shale particles as they concurrently flow down the 8 ft length of the reactor. Reactor temperatures can be controlled by four 2 ft long clam shell electrical heaters along the outside lengths of the 2" I. D. reactor. Below the heated length of the reactor, there is a 4 ft forced air finned cooling section in which the reaction system is rapidly cooled to temperatures between 250° and 300°C. This temperature range is sufficient to terminate the pyrolysis reaction and to prevent the liquid products from condensing and separating at this point. The gases enter a trap where the char and unvented shale is first separated and the effluent gas is then sent first through a water-cooled condenser (15°C) and then to a freon-cooled condenser (-40°C) where the liquid products are separated. The remaining gases are then reduced to atmospheric pressure, measured in a positive displacement meter and vented to the atmosphere. Flow rates of oil shale are in the order of 1 lb/hr and gases in the order of 1 or 2 SCFM. Steady state operation

in this flow system can usually be obtained in 10 to 15 mins.

Product analysis is obtained with an on-line programmable gas chromatograph which determines CH_4 , C_2H_4 , C_2H_6 , BTX (benzene, toluene, xylene) CO and CO_2 concentrations at 8 minute intervals. Gas sampling taps are provided every 2 ft along the length of the reactor. Products heavier than BTX (>C₉) are collected in the condenser traps and measured at the end of each experiment. The heavier hydrocarbons (naphthalene, anthracene, etc.) are collected, measured and analyzed. An analysis of the char is also made. From these data a complete mass balance can be made over the entire experimental run.

The shale residence times are calculated by summing the shale particle free fall velocity and the gas flow velocity. Heat-up rates are also estimated by calculations from the heat transfer of the gas to the particles.

The yields are based on the percent of organic carbon in the feed oil shale which is converted to product. A Western (Colorado Green River Formation) oil shale obtained from the Laramie Energy Technology Center was used in these experiments. An analysis of the oil shale is shown in Table I.

TABLE I
ANALYSIS^a OF COLORADO SHALE GREEN RIVER FORMATION

	<u>Wt %</u>
C	- 17.0
H	- 2.2
N	- 0.8
O	- 17.5
S	- 0.8
Ash	- 61.9
CO_2^b	- 16.5

a. Analysis made with organic C analyzer and TGA.

b. CO_2 based on % of elemental plus ash analysis.

RESULTS AND DISCUSSION

A series of runs were performed with three types of pyrolysis gases, methane, helium and hydrogen at a pressure of 500 psi. The flash pyrolyses with CH_4 and He were conducted at a reactor temperature of 800°C and the flash hydrolyses with H_2 gas are conducted at temperatures from 800° to 950°C. The reactor conditions, flow rates and residence times together with product yields including HC (hydrocarbon) gases, HC liquids and C oxides are summarized in Table II.

The data indicate that the inert gas He gave the lowest total HC gas and liquid yield (42.7%) followed by H_2 (61.7%) followed by CH_4 gas and which resulted in the highest yield (80.5%). There was no formation of ethylene with He or with H_2 , however, with CH_4 there was a significantly large yield amounting to 32.4% of the organic C in the shale converted to ethylene. In the case of H_2 , for the series of runs ranging from 800° to 950°C, the methane yield at 800°C (29.5%) is higher than with He (24.1%) and increases markedly as the temperature rises to 950°C at which point most of the organic C is converted to CH_4 (88.5%). Due to the high partial pressure of CH_4 in the CH_4 pyrolysis experiments, a CH_4 balance is difficult to make. However, within experimental error of the flow rate in and out of the reactor there does not appear to be any net production or destruction of methane. Blank and control experiments with oil shale feed before and after the experiments indicated no formation of ethylene or other products due to possible cracking of the methane on the walls of the reactor.

The liquid BTX (benzene, toluene, xylene) yield is highest with the methane pyrolysis (21.1%) which is about 2.5 times higher than with He (8.6%) or H_2 (8.9%). The improved yield with methane pyrolysis compared to the yield with the inert helium may be due to a free radical reaction such as CH_2 formed from the pyrolysis of the kerogen reacting with the CH_4 giving rise to ethylene. Another possibility may be attributed to preventing secondary reactions of ethylene and benzene by maintaining a high partial pressure of methane during methane pyrolysis.

The HC gaseous and liquid yields for the flash hydrolysis of Colorado Shale is plotted in Figure 2 as a function of reactor temperature. The trends show the high rate of increase of CH_4 yield with reactor temperature. The ethane yield decreases rapidly from 800°C (23.3%) to 900°C at which temperature ethane is no longer formed. The BTX (mainly benzene) goes through a maximum of 12.1% at 850°C.

TABLE II

MAXIMUM YIELDS BY FLASH PYROLYSIS OF GREEN RIVER COLORADO OIL SHALE
WITH VARIOUS PYROLYSIS GASES

Constant Reactor Pressure of 500 psi
Shale Particle Size 150-300 Micron

Pyrolysis Gas	CH ₄	He	H ₂	H ₂	H ₂	H ₂
Reactor Conditions						
Reactor temp. - °C	800	800	800	850	900	950
Gas flow rate - SCFM	1.13	1.13	1.52	1.52	1.52	1.52
- lbs/hr	2.85	0.71	0.48	0.48	0.48	0.48
Shale flow rate - lbs/hr	0.55	0.84	0.64	0.64	0.64	0.64
Residence time - sec	1.7	1.7	3.2	3.2	3.1	3.1
Product Yields (% Organic C Conversion)						
HC Gas						
CH ₄ , methane	-	24.1	29.5	49.9	72.7	88.5
C ₂ H ₄ , ethylene	32.4	0.0	0.0	0.0	0.0	0.0
C ₂ H ₆ , ethane	22.1	10.0	23.3	12.8	0.0	0.0
C ₃ H ₈ , propane	4.9	-	-	-	-	-
Total HC Gas	59.4	34.1	52.8	62.7	72.7	88.5
HC Liquids						
BTX	21.1	8.6	8.9	12.1	10.1	8.5
Total HC, Liq. and Gas	80.5	42.7	61.7	74.8	82.8	97.0
C Oxides						
CO	8.5	6.1	14.7	19.6	22.7	29.5
CO ₂	7.7	7.4	0.0	0.0	0.0	0.0
Total CO _x	16.2	13.5	14.7	19.6	22.7	29.5
Total HC and C Oxides	96.7	56.2	76.4	94.4	105.5	126.5

It should be noted that the oxides of carbon (CO and CO₂) only indicate relative yields since CO₂ is evolved from the inorganic carbonates present in the shale. The increased yields of CO (14.7% to 29.5%) with no CO₂ formation obtained in the H₂ pyrolysis experiments at increasing temperatures are probably due to the shift reaction between H₂ with CO₂, forming CO and H₂O.

A second set of flash pyrolysis experiments was performed with mixtures of the Colorado oil shale and a New Mexico sub-bituminous coal. The elemental composition of the coal was C-60%, H-4.2%, O-16.8%, N-1.2%, S-0.8% and Ash-17.0%. The purpose of these experiments was to determine whether there is an interaction effect of the kerogen in the shale with the coal. The H/C molar ratio in kerogen is >1 equivalent to the stoichiometric formula, CH_{1.5}O_{0.7}. Coal has an H/C ratio of <1 equal to the formula, CH_{0.8}O_{0.2}. The thought was that the hydrogen deficiency in coal might be made up with the excess in kerogen for producing HC gases and liquids. The results with hydrogen as a pyrolysis gas at 1000 psi reactor pressure and with CH₄ as pyrolysis gas at a reactor pressure of 500 psi for an 80% coal-20% shale mixture are summarized in Table III. The yields given are based on the conversion to product from the sum total of carbon fed to the reactor contained both in the coal and the shale.

In the hydrogen experiment, the most prominent product yield is methane. As the temperature increases from 750° to 800°C, the methane increases rapidly from 45.4% to 76.8% while the ethane decreases from 14.6% to 1.8%. Comparing these results to those previously with shale alone at a hydrolysis pressure of 500 psi and 800°C, there appears to be a significant improvement in the conversion to methane. The CH₄ yield from shale alone is 29.5%. From coal, it is 15.8% (9). A calculation based on these yields by partial summing for the 80/20 shale/coal mixture would

indicate a methane yield of 23.1%, whereas 76.8% was actually obtained. For the benzene, a slightly higher yield is predicted (8.9%) than was obtained (7.1%). Thus, there appears to be an interaction effect of shale and coal under flash hydrolysis conditions.

In the series of experiments with methane pyrolysis at 500 psi, the ethane yield goes through a maximum of 14.1% at 900°C; the ethylene decreases rapidly from 12.8% at 850°C to 4.3% at 950°C, while the BTX increases significantly from 13.5% at 800°C to 24.6% at 950°C. The trends can be seen graphically in Figure 3. The total carbon conversion, which also includes the CO and CO₂ formation, appears to level off at about 60%, however, this would also include the CO₂ from mineral matter in the shale.

Based on the yields of ethylene and benzene for the methane pyrolysis of coal alone (10) and the yield from oil shale alone shown in Table II, it is predicted by fractional summing calculation that an 80/20 mixture of shale and coal would give a much higher yield for ethylene (19.2%) than was obtained (11.7%) but a slightly lower benzene yield (12.9%) than was actually obtained (13.5%). An interactive effect between the coal and the oil shale under methane pyrolysis conditions, thus, also appears to exist.

The combination of the conversion of the natural resources of coal, shale and natural gas to synthetic fuels and chemical feedstocks in one process step is an incentive for further exploration of flash pyrolysis reactions.

TABLE III

FLASH PYROLYSIS OF A MIXTURE OF 20% COLORADO SHALE (17% C) AND 80% NEW MEXICO SUB-BITUMINOUS COAL (60% C) WITH HYDROGEN AND METHANE AS PYROLYSIS GAS

Solids Particle Size 150-300 Microns

Pyrolysis Gas	H ₂	H ₂	CH ₄	CH ₄	CH ₄	CH ₄
Reactor Conditions						
Pressure, psig	1000	1000	500	500	500	500
Temperature, °C						
Gas flow rate - SCFM	1.71	1.71	1.53	1.53	1.53	1.53
- lbs/hr	0.54	0.54	3.86	3.86	3.86	3.86
Shale flow rate - lbs/hr	0.94	0.94	1.04	1.04	1.04	1.04
Residence time - sec	3.5	3.5	3.2	3.2	3.1	3.1
Product Yields (% Org. Carbon Conversion, Shale and Coal)						
HC Gas						
CH ₄ , methane	45.4	76.8	ND	ND	ND	ND
C ₂ H ₆ , ethane	14.6	1.8	8.6	11.5	14.1	10.8
C ₃ H ₈ , propane	0.0	0.0	0.0	0.0	0.0	0.0
C ₂ H ₄ , ethylene	<u>0.0</u>	<u>0.0</u>	<u>11.7</u>	<u>12.8</u>	<u>8.9</u>	<u>4.3</u>
Total HC Gas	60.0	78.6	20.3	24.3	23.0	15.1
HC Liquids						
BTX	<u>7.3</u>	<u>7.1</u>	<u>13.5</u>	<u>17.7</u>	<u>21.0</u>	<u>24.6</u>
Total HC, Liq. and Gas	67.3	85.7	33.8	42.0	44.0	39.7
C Oxides						
CO	3.4	5.7	4.3	5.0	10.4	11.9
CO ₂	<u>0.0</u>	<u>0.0</u>	<u>3.8</u>	<u>4.2</u>	<u>4.9</u>	<u>5.0</u>
Total CO _x	3.4	5.7	8.1	9.2	15.3	16.9
Total HC and C Oxides	<u>70.7</u>	<u>91.4</u>	<u>41.9</u>	<u>51.2</u>	<u>59.3</u>	<u>56.6</u>

ND - Not determined.

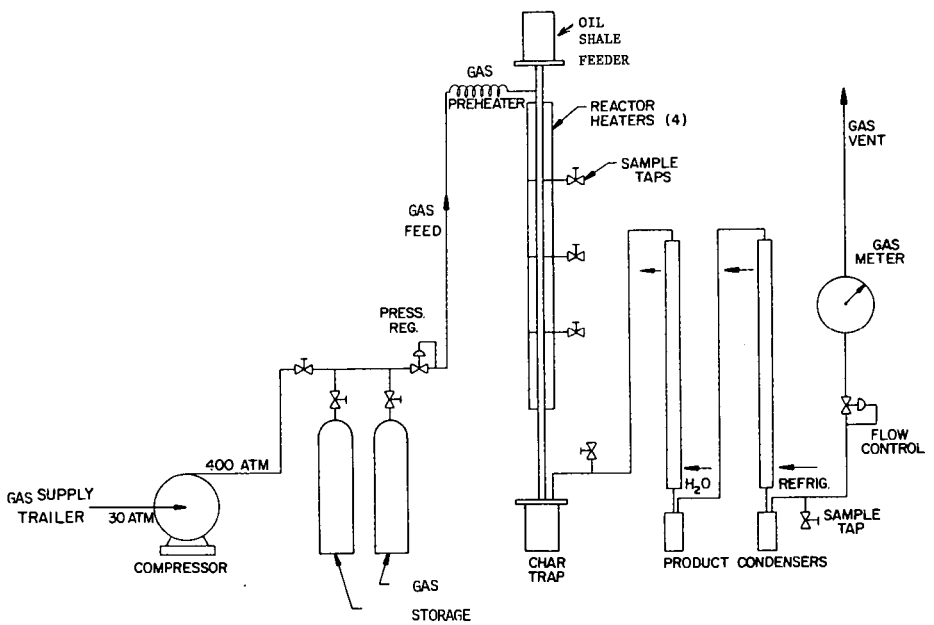


FIGURE 1. SCHEMATIC FLOWSHEET OF ENTRAINED TUBULAR REACTOR

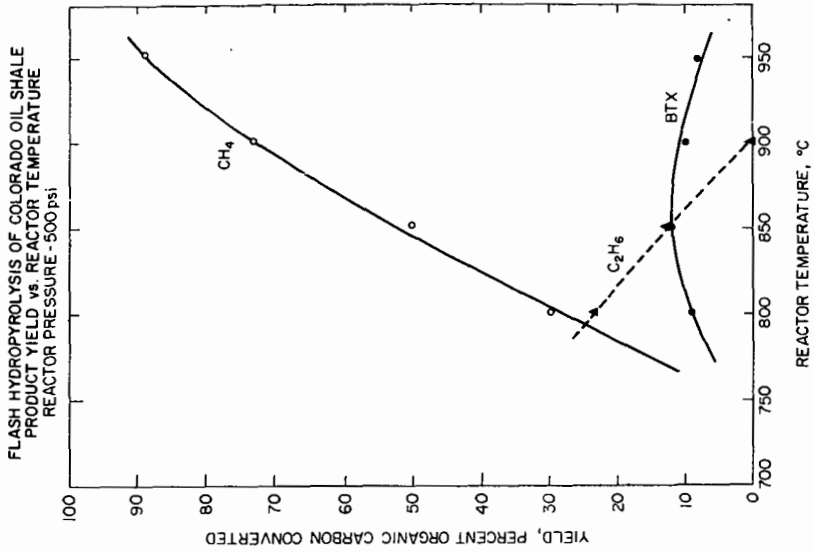


FIGURE 2

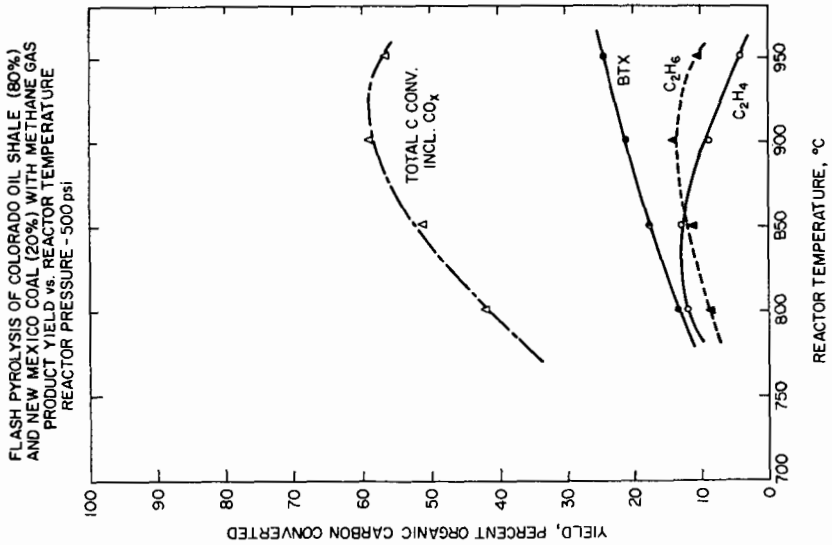


FIGURE 3

CONCLUSIONS

The flash pyrolysis of Colorado Oil Shale with methane at a temperature of 800°C and pressure of 500 psi appears to give the highest yield of hydrocarbon gas and liquid followed by yields with hydrogen and lowest with helium.

In the methane pyrolysis over 54.5% of the carbon in the kerogen is converted to ethylene and benzene. The flash pyrolysis with hydrogen (flash hydropyrolysis) of the oil shale at increasing temperatures showed a rapidly increasing amount of methane formed and a decrease in ethane formation, while the BTX (benzene mainly) yield remained at approximately 10%. At 950°C and 500 psi, almost all (97.0%) of the carbon in the kerogen is converted to liquid and gaseous hydrocarbons.

Experiments with a mixture of a New Mexico sub-bituminous coal and oil shale under flash hydropyrolysis and methane pyrolysis conditions indicated higher yields of methane and ethylene and slightly lower yields of benzene than predicted by partial additive calculations.

These exploratory experiments appear to be of sufficient interest to warrant a fuller investigation of the interaction of the natural resources, oil shale, coal and natural gas under flash pyrolysis conditions.

LITERATURE CITED

- (1) Steinberg, M. and Fallon, P. T., "Flash Pyrolysis of Coal", Chem. Eng. Progress, 75, No. 6, pp. 63-6 (1979) and BNL 25232, Brookhaven Natl. Laboratory, Upton, NY (1978).
- (2) Sundaram, M., Steinberg, M. and Fallon, P. T., "Flash Hydropyrolysis of Coal for Conversion to Liquid and Gaseous Fuel", Summary Report, DOE/METC/82-48, Morgantown Energy Technology Center, Morgantown, WV (1982).
- (3) Steinberg, M. and Fallon, P. T., "Flash Pyrolysis of Biomass with Reactive and Non-Reactive Gases", BNL 51560, Brookhaven Natl. Laboratory, Upton, NY (1982).
- (4) Belt, R. J. and Bissett, L. A., "Assessment of Flash Pyrolysis and Hydropyrolysis", METC/RI 79/2, Morgantown Energy Technology Center, WV (1978).
- (5) Smith, J. W. and Jensen, H. B., "Oil Shale", McGraw Hill Yearbook of Science and Technology, McGraw-Hill, NY (1977).
- (6) Will, S. A., Feldkirchner, H. L., Panwani, D. R. and Jenka, J. C., "The IGT Hybrid Process for Hydrogen Retorting of Devonian Oil Shales", presentation by Insti. of Gas Technol. at the Chattanooga Shale Conf., Oak Ridge Natl. Laboratory, Oak Ridge, TN (1978).
- (7) Allred, V. D., "Retorting Oil Shales with Superheated Water Vapor or Energy Process", presented by Marathon Oil Co. at Symp. on Synthetic Fuels from Oil Shales, Atlanta, GA (1979).
- (8) Fallon, P. T. and Steinberg, M., "Flash Hydropyrolysis of Coal: The Design, Construction, Operation and Initial Results of a Flash Hydropyrolysis Experimental Unit 4, BNL 50698, Brookhaven Natl. Laboratory, Upton, NY (1977).
- (9) Steinberg, M. and Fallon, P. T., "Flash Hydropyrolysis of Coal", Quarterly Report No. 9, BNL 51107, Brookhaven Natl. Laboratory, Upton, NY (1979).
- (10) Steinberg, M. and Fallon, P. T., "Flash Methanolysis of Coal for the Synthesis and Production of Ethylene, Benzene and Liquid Hydrocarbons", BNL 30624, Brookhaven Natl. Laboratory, Upton, NY (1981) and Hydrocarbon Processing 61, No. 11, 92-6 (1982).

SYMPOSIUM ON CHARACTERIZATION AND CHEMISTRY OF OIL SHALES
PRESENTED BEFORE THE DIVISIONS OF FUEL CHEMISTRY AND
PETROLEUM CHEMISTRY, INC.
AMERICAN CHEMICAL SOCIETY
ST. LOUIS MEETING, APRIL 8 - 13, 1984

SHALE OIL DELAYED COKING PRODUCTS UTILIZATION FOR MANUFACTURED GRAPHITES

By

M -A. Sadeghi, V. L. Weinberg and T. F. Yen
Civil and Environmental Engineering, School of Engineering, University of Southern California
Los Angeles, California 90089

INTRODUCTION

Carbon and graphite materials are required to withstand more and more severe conditions of thermal shock, stress and reactor irradiation in the steel making, aluminum, aerospace and nuclear industries. At the same time, the sources for the precursors of these manufactured carbons are being depleted, so that other sources are needed. The aim of this work is to demonstrate the applicability of new precursors from the delayed coking products of shale oil to graphite manufacture and to determine what chemical characteristics are required for those precursors.

It is known that the microstructure and properties of graphitic materials are determined by the characteristics of an ordered fluid, termed the "carbonaceous mesophase", which forms during pyrolysis, usually between the temperatures of 370°C and 500°C (1). It is the order developed in this mesophase below 500°C that determines the properties of the final product obtained after heating to graphitizing temperatures of 2800°C. The mesophase forms an optically anisotropic microstructure and the properties expected from the graphite can be related to the mesophase microstructure. An isotropic microstructure indicates a non-graphitizing carbon with poor graphite properties, whereas a flow type or fibrous structure indicates a needle coke morphology which tends to have good thermal and tensile properties (2). So the characteristics of the final product are controlled by the mesophase formed below 500°C and these characteristics can be measured in a qualitative way from the cross polarized micrographs of the pyrolysis product residues.

In this work, graphitizing and chemical properties of the delayed coking products from a Green River shale oil were examined. Samples were pyrolyzed, solvent fractionated and analyzed using elemental analysis, cross polarized microscopy, proton nuclear magnetic resonance, infrared spectroscopy, vapor pressure osmometry and gas chromatography.

EXPERIMENTAL

The crude shale oil was distilled at 0.05 mm Hg vacuum for 6 hours at a pot temperature of 190°C. The vacuum distillate bottoms were heat treated by refluxing under N₂ gas at a temperature of 285°C for 5 hrs, 25 hrs and 74 hrs. Then all the samples including the shale oil and vacuum bottoms were Soxhlet extracted using hexane followed by benzene. The purpose was to isolate and identify the fraction(s) that is responsible for the graphitizing properties of the sample(s). Each of the above prepared samples were pyrolyzed three times under nitrogen gas at atmospheric pressure. The samples (0.5g) were placed in pyrolysis cells made of aluminum tubes with 0.5 mm pin-hole openings for vapor escape. The tubes were placed in stainless steel cells, then put in a temperature-programmed furnace and purged with nitrogen gas controlled by flow meters at 15 L/hr. The temperature was programmed at 13°C/hr to 360°C and 5°C/hr to the desired final temperature of 465°C (3). It is in this region (465°C) where the principle features of graphitic and pregraphitic microstructures are established and can be detected by polarized light (2, 4).

The residues of the pyrolyzed samples were examined under polarized light using a Leitz SM-Lux-Pol Cross Polarizing Microscope. These residues were first cast in epoxy resin and polished until the surface were optically smooth, then micrographs were obtained.

In order to determine what changes were occurring with the processing, the samples (shale oil, vacuum distillate and heat treated vacuum bottoms) and hexane solubles along with benzene solubles were investigated using the following analytical methods:

1. Elemental Analysis: Elemental analysis was done by Huffman Laboratories (Wheat Ridge, Colorado) and some earlier samples were done by the California Institute of Technology (Pasadena, California).

2. Vapor Pressure Osmometry: Molecular weights of the precursor samples were obtained using a Mechrolab 301A Vapor Pressure Osmometer (VPO). Tetrahydrofuran was used as solvent.

3. **Infrared Spectroscopy:** A double-beamed infrared spectrophotometer (IR), Model Acculab 6-Beckman Instruments, was used with sets of potassium bromide matched liquid cells of 0.025 mm thicknesses at the concentration of 2.5 g/ml in carbon tetrachloride.

4. **Proton Nuclear Magnetic Resonance:** High resolution proton nuclear magnetic resonance of samples was done on a T-60 Varian spectrometer at a concentration 10 wt/vol % in deuterated chloroform. Due to overlapping of the resonance bands, the areas were separated using the method of Brown, et al. (5).

5. **Gas Chromatography:** Finally, the samples were further analyzed by gas chromatography using Hewlett-Packard Model 5880 on a 30 x 0.323 mm I. D. fused silica capillary column coated with SE-54. The oven temperature was programmed to an initial value set at 100°C (hold 2 min) and a linear heating rate of 5°C/min up to 270°C (hold 2 min). 1 Microliter of each sample was injected at a concentration of 2.5 wt/vol % in toluene. The peaks were assigned quantitatively by coinjecting standard n-alkanes.

RESULTS AND DISCUSSION

After vacuum distillation, up to 71% of heavy oil residua remained. Current operational and proposed refining practices of crude shale oil in recovery of high Btu volatile matter as useful fuels (aviation fuels) quantitatively produce similar heavy ends.

The shale oil and vacuum distillate pyrolyzed residues showed isotropic microstructures under light polarizers. Heat refluxing performed was to increase the aromaticity of materials. The aromaticity did not change much. However, optically active coarse mosaic textures were observed after 5 hrs of heat treating the vacuum bottoms. Also, the examined pyrolyzed results of hexane- and benzene-soluble fractions of the samples surprisingly showed that none of the benzene-soluble materials formed any optical activity. The hexane solubles, however, were optically active with all the heat-treated fractions forming coarse mosaic structures. The optical micrographs of polished surfaces of pyrolyzed prepared samples plus their solvent fractions are shown in Figure 1.

The normalized results of solvent-fractionated samples given in Table I, show that the 5 hrs heat treated vacuum bottoms has the highest cut of hexane solubles. With excess heat treatment of 74 hrs, it appears that cracking of resin to form asphaltene and preasphaltene takes effect.

TABLE I

PARAMETERS AND DATA OBTAINED BY SOLVENT FRACTIONATION, ELEMENTAL AND ANALYSIS (EA), ¹H NMR AND VPO OF PRECURSOR SAMPLES

Sample	Instrument and Parameter					
	Soxhlet Extraction (% wt)			EA	H NMR	VPO
	Hexane-Soluble	Benzene-Soluble	Benzene-Insoluble	H/C	Aromaticity fa	MW
Shale oil	96.7	1.4	1.9	1.81	0.15	270
Vacuum distilled bottoms	96.2	2.4	1.4	1.49	0.29	292
Heat treated						
5	96.7	2.6	1.4	1.54	0.27	295
vacuum bottoms	25	95.4	4.4	1.52	0.29	353
(hours)	74	85.7	10.0	1.50	0.29	315

The atomic H/C ratios of samples and their solvent fractions, calculated from elemental analysis results, showed a decrease after vacuum distillation but heat treatment caused slight changes. It is generally known that the lower the hydrogen-to-carbon ratio, the greater the degree of ring condensation regardless of whether the rings are aromatic or naphthenic in character.

From VPO studies, the average molecular weight of the samples increased with processing up to 25 hrs of heat treatment and decreased with 74 hrs of treatment.

Results from proton NMR and IR studies of all the samples revealed that percent naphthenicity is at minimum for shale oil and at maximum for 74 hrs heat treated vacuum bottoms. This explains that these cyclic compounds are the ones which form into mesophase as it was shown by the micrographs in Figure 1. The reason that the 25 hrs and 74 hrs treated samples did not form coarse mosaic microstructures is the increased presence of non-mesophase forming materials (hexane insolubles).

Some of the results obtained from elemental analysis, proton NMR and VPO are given in Table I. From these and other results obtained so far, a possible explanation of the changes with processing is that condensation or polymerization reactions followed by cracking of molecules and/or disproportionation reactions have occurred. Also, it was observed that, with proper control of processing conditions, the coarse mosaic microstructure can be obtained.

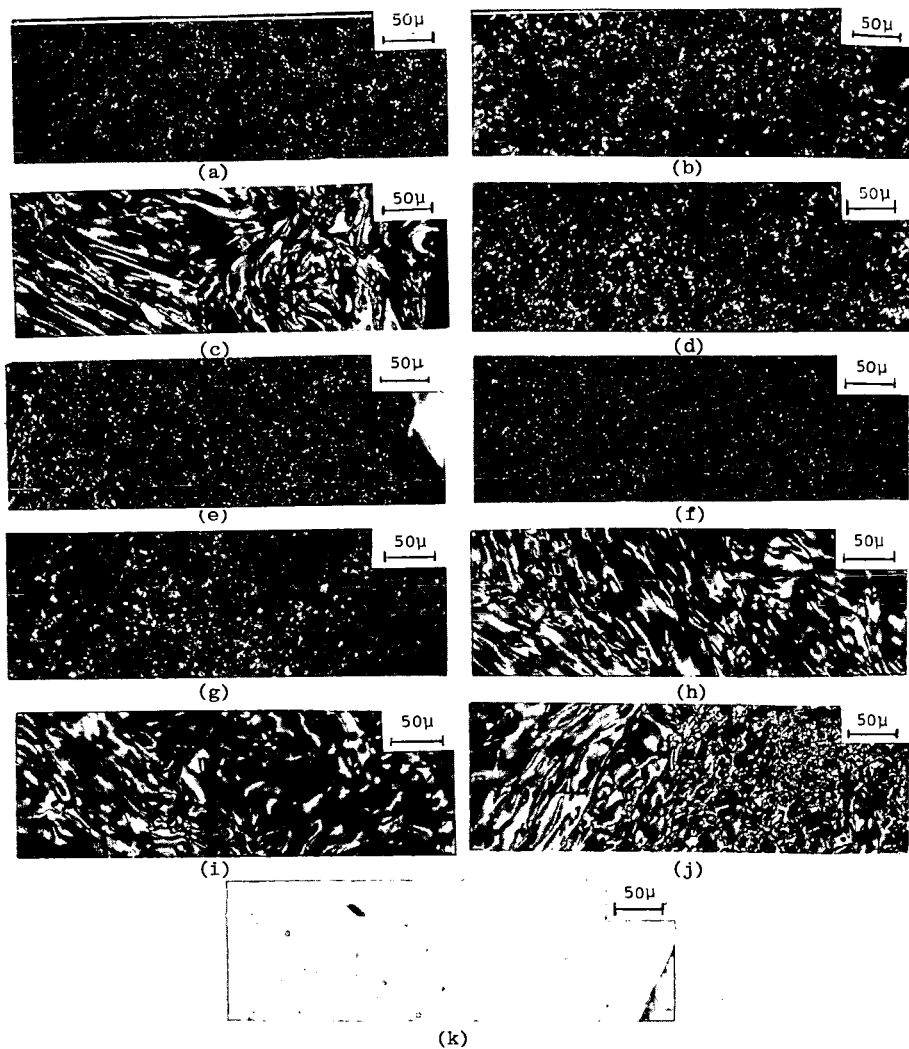
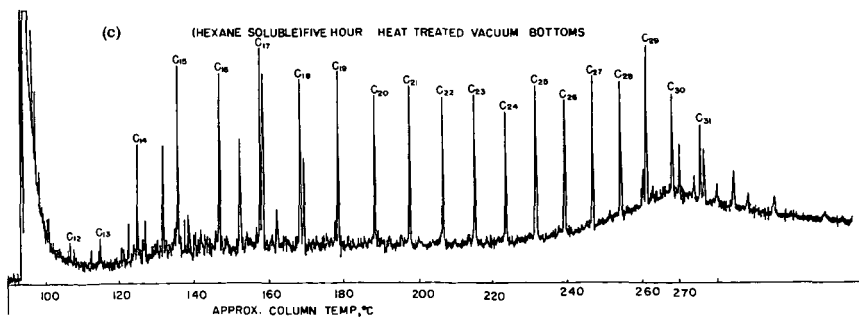
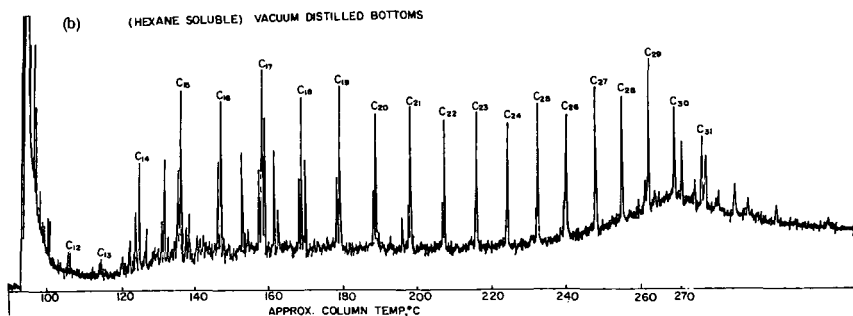
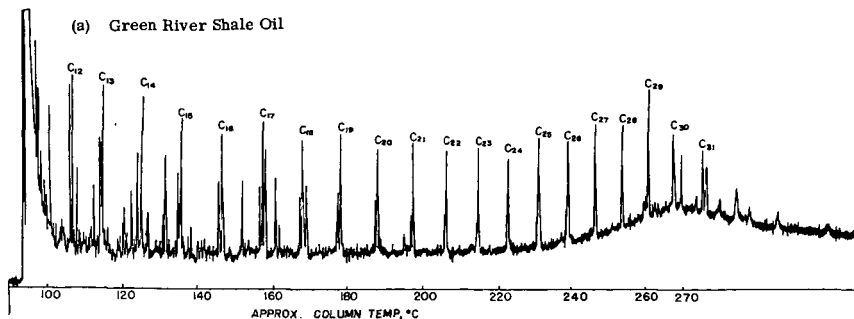


Figure 1. The Optical Micrographs of Polished Surfaces of Pyrolyzed Samples (a) Shale Oil, (b) Vacuum Distilled Bottoms and Heat Treated Vacuum Bottoms for (c) 5hrs., (d) 25 hrs. and (e) 74 hrs. Samples (f) to (j) are Hexane Solubles of Samples (a) to (e). And (k) Shale Oil Benzene Soluble Fraction. (Magnification is 200 Times).

Figure 2.
HEXANE SOLUBLE FRACTIONS OF SHALE OIL
ON 30Mx0.323 MM FUSED SILICA CAPILLARY COLUMN



Gas chromatograms of hexane-soluble matter of the shale oil, vacuum distillates and 5 hrs-heat-treated vacuum bottoms are shown in Figure 2. The chromatograms show the presence of certain branched aliphatic compounds attached to the left of most peaks in (a) shale oil and (b) vacuum distillates. These isocompounds disappeared with heat treatment as shown in (c) 5 hrs thermal treated sample. From the micrographs of Figure 1 (f-j), it can be concluded that the presence of such isocompounds act as suppressors to mesophase formation. This could be due to cracking of these highly unstable isocompounds at the branch level into smaller volatile molecules which, in turn, may interfere with the free radical aromatics that construct the matrix of the "Carbonaceous Mesophase".

CONCLUSIONS

The following conclusions may be drawn from the results of this preliminary research.

1. With 5 hrs of heat refluxing of shale oil vacuum distillate bottoms, coarse mosaic microstructures can be achieved. This shows that controlled processing will enhance the graphitizing properties of these organic products.

2. It is known that a good precursor for mesophase formation is a highly condensed organic compound with a large aromatic core and few and short aliphatic molecules. However, contrary to other precursors, proton NMR and IR studies revealed that the naphthenics are most likely responsible for mesophase formation. This phenomena was also shown by solvent fractionation of the samples. Only the hexane solubles which are of low aromaticity formed mesophase during the carbonization process.

3. Gas chromatography of the hexane-soluble fractions from shale oil and vacuum distillate bottoms indicates the existence of certain branched compounds. These isocompounds disappeared with heat treatments of 5 hrs, 25 hrs and 74 hrs. The micrographs of polished surfaces for these pyrolyzed hexane-soluble samples reveal that only the heat treated vacuum bottoms show anisotropic microstructures. Therefore, the presence of these branched compounds act as inhibitors to mesophase formation.

4. Shale oil delayed coking products utilization is indeed possible for manufactured graphites. However, scale-up procedures are required so that the cost of these carbon and graphite composites could be compared with those derived from petroleum and coal.

ACKNOWLEDGMENTS

Appreciation is made to National Science Foundation under grant No. DAR-8008755 and also for financial assistance from Bethlehem Steel Corporation.

LITERATURE CITED

- (1) White, J. L., "Mesophase Mechanisms in the Formation of the Microstructure of Petroleum Coke", ACS Symp. Series, 21, 282 (1975).
- (2) Mackowsky, M. Th., Fortschr. Mineral, 30, 10 (1951).
- (3) Weinberg, V. A., White, J. L. and Yen, T. F., "A Study of the Solvent Fractionation of Petroleum Pitch for Mesophase Formation", FUEL, accepted for publication (1983).
- (4) Weinberg, V. A., "Formation of the Carbonaceous Mesophase in Coal Liquid Fractions and Petroleum Pitch", Ph.D. Dissertation, University of Southern California (1981).
- (5) Schwager, I., Farmanian, P. A. and Yen, T. F., "Structural Characterization of Solvent Fractions from Five Major Coal Liquids by Proton Nuclear Magnetic Resonance", Advances in Chemistry Series, 170, 66 (1978).

SYMPOSIUM ON CHARACTERIZATION AND CHEMISTRY OF OIL SHALES
PRESENTED BEFORE THE DIVISIONS OF FUEL CHEMISTRY AND
PETROLEUM CHEMISTRY, INC.
AMERICAN CHEMICAL SOCIETY
ST. LOUIS MEETING, APRIL 8 - 13, 1984

NITROGEN-CONTAINING COMPONENTS FROM SHALE OIL AS MODIFIERS
IN PAVING APPLICATIONS

By

H. Plancher and J. C. Petersen
Western Research Institute, University of Wyoming Research Corporation, P. O. Box 3395
Laramie, Wyoming 82071

INTRODUCTION

One of the major causes of asphalt pavement failure is moisture-induced damage. The detrimental effects of moisture and/or repeated freeze-thaw cycles in asphalt concrete pavements have long been recognized by state and federal agencies and the motoring public. Moisture-induced damage has been studied in our laboratory from a chemical and mechanistic viewpoint related to the bonding and debonding of asphalt components from the aggregate surfaces (1-3). Results from these studies indicated that certain nitrogen-containing molecules naturally present in the asphalt might be involved in reducing the sensitivity of the asphalt-aggregate mixtures to moisture-induced damage. Infrared spectrometric (1, 3-6) and elemental nitrogen analyses (3) of asphalt components removed by hot pyridine extraction from previously benzene-extracted aggregates showed that nonpyrrolic nitrogen might, in part, be responsible for an increased resistance of the asphaltic pavements to moisture-induced damage.

During the development of a water susceptibility test (WST) to indicate the susceptibility of asphalt-aggregate mixtures to repeated freeze-thaw cycles, we found that WST briquets prepared from pyridine-pretreated aggregates were highly resistant to damage during the test (2). Evidence that pyridine-type compounds in shale oil retarded the detrimental effects of moisture resulted from the analysis of a 30-year-old pavement constructed from a shale oil residue (rich in pyridine-type compounds) and uncrushed river run gravel (7). Additional studies conducted at Texas A&M University (8) and in our laboratory (9-10) further indicated that pyridine-type nitrogen in asphalts reduced the effects of moisture damage in asphaltic pavements. Nitrogen of the pyridine type is naturally present in asphalts in varying small amounts; however, shale oil contains significant amounts (1.3 wt %) of pyridine-type homologs.

As part of our continuing research on moisture damage in asphaltic pavements, we began investigating the strength of nitrogen compound-aggregate interactions before and after subjecting the nitrogen compound-treated aggregates to a warm water-benzene soak. Temperature-programmed thermal desorption of the nitrogen compounds from the treated aggregate surfaces through three different temperature ranges was used to determine the relative strength or stability of the nitrogen-aggregate bond. Upon thermal desorption, nitrogen in the evolved gases was determined by a chemiluminescent detector (3, 9, 10).

Another area investigated was the ability of nitrogen-rich shale oil fractions to disperse asphaltenes in oxidatively-aged asphalts in anticipation of their use as potential recycle agents for aged petroleum asphalts. Pavement rehabilitation projects frequently add recycle or rejuvenating agents to aged asphaltic pavements to restore desired viscoelastic properties to the embrittled asphalt binder.

EXPERIMENTAL

Materials

Petroleum Asphalts - Four extensively studied (1, 6, 11-15) asphalts of widely varying composition and identified by code numbers B-2959, B-3036, B-3051 and B-3602 were supplied by the Federal Highway Administration (FHWA), Materials Division.

Aggregates - The aggregates, obtained from various asphalt paving projects, were crushed in a disk grinder equipped with ceramic plates, wet screened to 20 to 35 mesh size, rinsed with distilled water and dried at 150°C for 24 hours. Aggregates were heated again at 150°C prior to use. Identification of the aggregates appears in the text.

Solvents - Reagent-grade benzene and pyridine were dried by refluxing them for 8 hours over CaH_2 before final distillation through a Vigreux column.

Products Derived from Shale Oil and Petroleum Liquids - A shale oil basic nitrogen concentrate, a petroleum fraction from an AC-5 shale oil asphalt, a shale oil distillate fraction and several commercially available recycle agents (identified in the text) were used in the study. The shale oil basic nitrogen concentrate was obtained as a byproduct by Suntech, Inc., Marcus Hook, PA, during the experimental refining of shale oil produced by the Occidental vertical-modified in situ process. The oil sample was obtained from the U. S. Department of Energy's Anvil Points facility. The crude shale oil was first hydrotreated by Suntech (16) to reduce the nitrogen content from 1.5 to 0.5 wt % and then topped to 281°C by distillation. A portion of the distillation residue (4,826 L) was treated with 2.25 wt % anhydrous hydrochloric acid (HCl) in a glass-lined reactor at 43°C and 55.2 kPa to precipitate the hydrochloride salts of the nitrogen compounds. The salts were thermally decomposed at 300°C to liberate the HCl and yield the shale oil nitrogen concentrate. Total yield based on feed material was 13.3 wt %. The petroleum fraction (83.2 wt %) was prepared by digesting 100 g of an AC-5 shale oil asphalt (8) in 4 L n-pentane, removing the asphaltenes by filtration and evaporating the solvent. The shale oil distillate fraction produced from the Union gas combustion process had a corrected boiling range of 342-382°C at 1.013×10^5 Pa.

Solutions for Nitrogen Adsorption-Desorption Studies - 10% (weight/volume) Solutions of the various nitrogen-containing components used in the adsorption-desorption studies were prepared in benzene and used to treat the various aggregates.

Procedures

Nitrogen Compound-Treated Aggregates - One-gram lots of the 60-80 mesh sized aggregate particles were placed in vials containing 2 cc of the nitrogen compound-benzene solution. One hour later, the treated aggregates were recovered by vacuum filtration, washed with benzene and air dried for 48 hours prior to obtaining nitrogen analyses. One-half gram of the treated aggregate was further treated in a vial containing 25 cc of distilled water and 2 cc benzene for 6 hours at 60°C followed by vacuum filtration and water-benzene washings to remove water-displaced nitrogen compounds from the aggregate surfaces. The treated aggregates were air dried and analyzed for nitrogen, as described later.

Asphalt-Aggregate Briquets - Asphalt-coated aggregates used to prepare briquets for the water susceptibility test (WST) were prepared using previously reported procedures (2). Briefly, briquets mounted on a beveled stress pedestal and submerged in water were repeatedly subjected to freeze-thaw cycles until the briquet failed from crack propagation or fracture.

Nitrogen Analyses - Treated aggregates (0.2500 g) were placed in an Antek Model 772 microcomputer-controlled pyroreactor and the temperature was increased from 100 to 600°C at 50°C/minute with a 5-minute isothermal period at 100°C and 7-minute isothermal periods at 150, 300 and 600°C.

Asphaltene Settling Test - To conduct the test, 2 g of asphalt, or 2 g of aged asphalt plus 0.02 g of the recycle agent were digested in 50 cc n-hexane for 24 hours at 20°C. The resultant mixture was transferred into a 50-cc graduated cylinder and the rate at which the asphaltenes settled in the hexane solution was determined (2). The test result was reported as the time in minutes required for the asphaltene meniscus to reach the 25-cc mark on the graduated cylinder. Final volume of precipitated asphaltenes was recorded 24 hours later.

RESULTS AND DISCUSSION

As outlined in the Introduction, considerable evidence from previous studies indicated that pyridine-type compounds in bituminous mixtures reduce the sensitivity of the mixtures to moisture-induced damage. Because shale oil is rich in pyridine-type nitrogen compounds, the use of shale oil nitrogen components as modifiers in petroleum asphalt might be highly desirable. As part of a continuing study of the chemistry of asphalt-aggregate interactions, we examined the adsorption of a shale oil basic nitrogen concentrate on the surface of mineral aggregate and determined the relative sensitivity to displacement of the adsorbed compounds from the surface of the aggregate by water. Results were compared with the adsorption-desorption characteristics of the model nitrogen base, pyridine, on several aggregates of widely differing composition.

Adsorption-Desorption from Mineral Surfaces of Nitrogen Compounds in Shale Oil Basic Nitrogen Concentrate

Figure 1 illustrates the scheme used to evaluate the adsorption-desorption and water-displacement characteristics of the nitrogen compounds in the shale oil basic nitrogen concentrate that are strongly adsorbed on mineral aggregate surfaces. Briefly, nitrogen components adsorbed on mineral aggregate particles from a dilute benzene solution of the concentrate are thermally desorbed both before and after subjecting the treated aggregates to a warm water-benzene soak to displace water-sensitive components. Thermal desorption is accomplished in a temperature-programmed furnace and the displaced nitrogen is detected as a function of temperature by a nitrogen

detector.

A shale oil basic nitrogen concentrate produced as a byproduct during stream cleanup in the experimental refining of shale oil by Suntech, Inc. (16) was used to evaluate the interactions of shale oil nitrogen compounds with mineral aggregate surfaces. Properties of the concentrate are summarized in Table I. The material was a semiviscous liquid at ambient temperature. Infrared analysis of the byproduct in tetrahydrofuran showed strong doublet bands at about 1600 and 1560 cm^{-1} , which on treatment with HCl were replaced by a new band at about 1230 cm^{-1} . This behavior is typical of pyridines and indicates a high concentration of pyridine types in the concentrate. This, of course, is not surprising because its isolation from the experimental refining stream was by HCl extraction followed by springing of the HCl from the basic adduct by thermal treatment.

TABLE I

PROPERTIES OF SHALE OIL BASIC NITROGEN CONCENTRATE FROM STREAM CLEANUP DURING EXPERIMENTAL REFINING OF SHALE OIL

Gravity, °API	16.0
5% boiling point, °C	297
95% boiling point, °C	524
Carbon, wt %	84.03
Hydrogen, wt %	11.06
Nitrogen, wt %	3.97
Chlorine, wt %	0.045
Aromatics, ^{13}C NMR, %	27

Figure 2 shows the desorption thermograms of the nitrogen components from the shale oil basic nitrogen concentrate that had been adsorbed on two paving aggregates—one from Colorado and one from FHWA Region 10 (Oregon) (3, 17). Note that most of the nitrogen was desorbed in the 300 to 600°C range, indicating a strong bond with the aggregate surface. Subjecting the treated aggregates to a warm water soak in the presence of benzene to solubilize water-displaced components reduced the amount of strongly adsorbed nitrogen components on the aggregate surfaces; however, significant amounts were resistant to water displacement, as indicated by the thermograms. A considerable amount of the nitrogen desorbed from the FHWA Region 10 aggregate in the 300 to 600°C range was particularly resistant to displacement by water. Because pyridine-type compounds are suspect as the dominant type in the shale oil basic nitrogen concentrate contributing to the nitrogen thermogram, model compound studies using the parent compound pyridine were conducted to further elucidate the role of pyridine compounds in reducing moisture damage in asphalt pavements.

Adsorption-Desorption from Mineral Surfaces of Model Compound Pyridine

The Colorado and FHWA Region 10 aggregates were treated with a dilute solution of pyridine in benzene in a manner similar to their treatment with the shale oil basic nitrogen concentrate and thermograms of the nitrogen desorption obtained. Figure 3 shows the thermograms obtained both before and after subjecting the pyridine-treated aggregates to the warm water-benzene soak. Note the similarities between these thermograms for pyridine and those for the shale oil basic nitrogen concentrate shown in Figure 2. The Colorado aggregate had a greater affinity for nitrogen found to desorb in the 150 to 300°C range than did the FHWA Region 10 aggregate and the nitrogen in this desorption region was quite resistant to water displacement. The Colorado aggregate showed a reduced amount of adsorption in the 300 to 600°C range compared with the FHWA Region 10 aggregate.

Of potential significance to moisture-induced damage is the relative amounts of nitrogen desorbed within each temperature range and the resistance of that nitrogen to displacement to water. This can best be described by quantification of the data from Figure 3 as displayed in Table II. Even though the Colorado aggregate showed a higher total relative surface density (RSD) of adsorbed pyridine molecules than the FHWA aggregate before water displacement (40.6 vs 33.3, respectively), the adsorbed pyridine was more easily displaced from the Colorado aggregate surface by water as indicated by comparing the total RSD's of the same two aggregates after water treatment (7.4 vs 17.7, respectively). Also, the RSD of nitrogen in the 300 to 600°C range after water treatment was 13.6 for the FHWA Region 10 aggregate compared with 4.9 for the Colorado aggregate. Related studies using these aggregates in laboratory-prepared asphalt-aggregate mixtures have shown a relationship between the relative amount of nitrogen desorbed in the 300 to 600°C range and its resistance to water displacement to the resistance of the asphalt-aggregate mixtures to moisture damage. This is illustrated for the two aggregates in question by the data in Table III. Note the greatest tensile strength retention ratio of pavement mixtures and increased cycles to failure in the WST for the FHWA Region 10 asphalt-aggregate mixture when subjected to the

accelerated laboratory moisture damage conditioning. These data, together with data on additional asphalt-aggregate systems published elsewhere, support the proposition that adsorption of those pyridine-type nitrogen compounds in petroleum asphalts, although in much lower concentrations than in shale oil products, are important to the resistance of asphalt-aggregate mixtures to moisture damage. Thus, pyridine-type nitrogen components from shale oil should have potential value as asphalt modifiers in improving the moisture resistance of pavement mixtures.

TABLE II

THERMAL DESORPTION OF PYRIDINE FROM AGGREGATE SURFACES BEFORE AND AFTER WATER TREATMENT

Aggregate Source	Surface Area m ² /g	Water- Benzene Soak	Nitrogen Detector Readout	Relative Surface Densities ^a in Temperature Range, °C			
				<150	150-300	300-600	Total
FHWA							
Region 10	1.92	no	64,019	2.6	19.2	21.5	33.3
		yes	43,021	0	4.1	13.6	17.7
Colorado	1.95	no	79,340	9.6	19.5	11.5	40.6
		yes	14,463	0	2.5	4.9	7.4

a. Nitrogen detector readout counts divided by aggregate surface area.

TABLE III

RESISTANCE OF ASPHALT-AGGREGATE MIXTURES TO MOISTURE-INDUCED DAMAGE^a

Aggregate-Asphalt System	Tensile Strength Ratio from Accelerated Moisture Conditioning	Cycles-to-Failure in Water Susceptibility Test
FHWA Region 10	0.6	5
Colorado	0.2	3

a. Data from (3).

Laboratory Evaluation of Shale Oil Products in Asphalt Paving Applications

Three different shale oil-derived products were evaluated in our laboratory for their potential application in asphalt paving. These included a shale oil AC-5 asphalt prepared by a vacuum distillation of a gas combustion shale oil, the shale oil basic nitrogen concentrate discussed earlier and a 342 to 382°C distillate fraction from a partially hydrotreated shale oil. The nitrogen concentrate was evaluated both as an antistripping agent and for potential use as a recycle agent and the distillate fraction was analyzed only as a recycle agent. Pavement rehabilitation projects frequently add recycle agents to the aged asphaltic pavements being recycled to restore desired viscoelastic properties to the embrittled asphalt binder.

Evaluation of Petroleum- and Shale Oil-Derived Asphalts by WST Procedure - Data in

Table IV summarize the results obtained during the WST evaluation of several asphalt-aggregate mixtures prepared from petroleum and shale oil-derived asphalts using the same limestone aggregate. This particular aggregate was selected because previous studies showed that it produced moisture-sensitive mixtures (1). Comparisons between the number of freeze-thaw cycles in the WST required to induce failure in petroleum vs shale oil asphalt briquets using this aggregate clearly showed that the shale oil asphalt significantly improved the briquet water resistance compared to its petroleum counterparts. The shale oil asphalt briquet showed no signs of failure after 100-plus cycles, after which the test was finally terminated. The petroleum asphalt briquets failed in seven or fewer cycles. Related studies conducted at Texas A&M University using the same shale oil asphalt showed superior moisture-damage resistance for laboratory paving mixtures (8). These WST and Texas results lend support to the previous proposition that pyridine-type compounds in shale oil produce asphalt-aggregate bonds that resist the detrimental action of water.

Evaluation of Shale Oil Basic Nitrogen Concentrate as an Additive to Petroleum Asphalts to Improve Moisture Resistance of Asphalt-Aggregate Mixtures -

WST briquets were prepared using a Venezuelan asphalt and a quartzite aggregate that produced water-sensitive mixtures in a section of I-80 in eastern Wyoming. This section of interstate highway began to show signs of moisture-induced damage shortly after it was constructed. Addition of 5 wt % (based on asphalt content) of

the shale oil basic nitrogen concentrate to the asphalt-aggregate mixture in the laboratory resulted in an increase in briquet cycles-to-failure from less than one complete freeze-thaw cycle for the untreated briquet to five cycles before the shale oil-modified briquet developed cracks. This is a significant increase and demonstrated the value of using a shale oil basic nitrogen concentrate as an antistripping agent in petroleum asphalts.

TABLE IV
EVALUATION OF BRIQUETS PREPARED FROM PETROLEUM AND
SHALE OIL-DERIVED ASPHALTS

Petroleum Asphalts ^a	Briquet ^b Wt, g	Cycles-to-Failure,
		WST
B-2959	50	1
B-3036	50	2
B-3051	50	7
B-3602	50	2
Shale oil asphalt	50	>100

a. Asphalts obtained from FHWA.

b. All briquets prepared using 5% asphalt and 95% Hol limestone (7).

In another experiment, two different silicate aggregates from Texas that had produced moderate to severe stripping problems in pavements were evaluated using the nitrogen thermal desorption analysis technique previously described and the WST procedure. Although both aggregates showed relatively low interactions of the aggregate with model nitrogen compounds, the moderate stripping aggregate showed more interaction than the severely stripping aggregate. The shale oil basic nitrogen concentrate was compared with two commercial antistripping agents for its ability to reduce moisture damage using these two aggregates. Briquets containing 6 wt % AC-20 asphalt modified with 1 wt % (based on asphalt content) of the antistripping agents and 5 wt % shale oil basic nitrogen concentrate were prepared. The shale oil basic nitrogen concentrate was added at 5 wt % because its nitrogen content was correspondingly lower than that of the antistripping agents. Test results are shown in Table V. The commercial antistripping agents showed erratic response and sometimes increased rather than decreased the sensitivity of the briquet to moisture damage. The shale oil basic nitrogen concentrate was the only additive that was beneficial in the test on both aggregates when compared with the control.

TABLE V
EFFECT OF ADDITIVES ON SILICATE AGGREGATES

Additive	% Added	WST, Cycles to Failure	
		Severe Stripping Aggregate	Moderate Stripping Aggregate
-0-	-	5	17
Amidoamine	1	4	7
Imidazole	1	10	6
Shale oil basic nitrogen concentrate	5	23	25

Evaluation of Shale Oil Fractions as Potential Recycling Agents for Aged Asphalts

Important criteria for the recycling of asphaltic pavements are the restoration of pavement flexibility and durability. Restoration of these properties depends upon the ability of recycle agents to improve compatibility by softening the aged asphalts and dispersing the highly associated asphaltene-like components in the aged asphalt. The asphaltene settling test (AST) was developed as a potential indicator of asphalt compatibility (18). In the test, the asphalt is dispersed in hexane and the settling time of the resultant asphaltenes is measured. In theory, an observed increase in the asphaltene settling time from the addition of a recycle agent to an aged asphalt is indicative of the ability of the recycle agent to disperse polar components of the asphalt and improve its compatibility.

Data in Table VI show AST results using 6 different potential recycle agents on an 85- to 100- pen Midcontinent (Hawkins) asphalt that was previously laboratory-aged from a viscosity value

of 6.7×10^4 Pa. s (at 25°C) to 4.3×10^6 Pa. s to simulate pavement aging. Cyclopave and the shale oil distillate fraction caused about a 42 and a 25% decrease in asphaltene settling time, respectively. The three remaining commercial additives (Paxole, Dutrex and Ashland) showed similar settling times to the control, suggesting minimum interactions of those additives with the polar components of the asphalt. Only the shale oil basic nitrogen concentrate significantly increased the asphaltene settling time. Although asphaltene settling time reflected the dispersion characteristics of asphaltenes in a dilute hexane mixture, the solvent power of the additive on the neat mixture, although important to flow properties, may not be reflected in the settling time results.

TABLE VI

LIST OF PROPERTIES MEASURED FOR AGED ASPHALT TREATED WITH SIX RECYCLE AGENTS

<u>Recycle Agent^a</u>	<u>AST^b</u> <u>min.</u>	<u>Final</u> <u>vol, cc</u>
None (control)	76.1	10.0
Cyclopave	43.9	9.0
Shale oil distillate	56.8	9.3
Paxole 1009	72.6	10.1
Ashland 100	73.0	9.8
Dutrex 739	77.6	10.3
Shale oil basic nitrogen concentrate	93.5	11.0

a. 1 wt % additive, based on asphalt content.

b. Asphaltene settling time in minutes.

A correlation between the increase in asphaltene settling time and the final volume of precipitated asphaltenes was observed while conducting the AST. Data from Table VI are plotted in Figure 4. The increase in volume with increased settling time is attributed to a better dispersion of the asphaltenes, which become more flocculent in the hexane solution.

Based on measurements using asphalts from varying sources, mildly aged asphalts usually showed an increase in asphaltene settling time on addition of most commercial and shale oil-derived liquid additives. The shale oil distillate fraction usually produced longer settling times than the other additives. When the level of aging was increased, greater variations in the asphaltene settling times were obtained with the different recycle agents. On moderately or highly aged asphalts, the shale oil basic nitrogen concentrate and the shale oil petroleum fraction were more effective in dispersing asphaltenes than the commercial agents.

SUMMARY

Previous evidence that pyridine-type compounds may be responsible for increased resistance of asphalt-aggregate mixtures to moisture damage were reinforced by several recently completed studies. Experiments utilizing selected shale oil fractions known to contain pyridine compound types showed that these fractions were effective as petroleum-asphalt modifiers in reducing the sensitivity of the asphalt-aggregate mixtures to moisture damage and also showed potential as recycling agents for restoring desired viscoelastic properties to aged asphaltic pavements. The use of shale oil products in this vital application would likely be of economic importance in a synthetic fuels industry by utilizing these less fuel-desirable components in nonfuel uses and make available equivalent amounts of more energy-desirable petroleum counterparts for use as fuels.

ACKNOWLEDGMENTS

The authors gratefully acknowledge the financial support provided this project by the Department of Energy and the Federal Highway Administration in a cooperative program designed to make effective use of our natural resources and conserve the energy value of our fossil fuels. The authors are indebted to Dr. Abe Schneider, Suntech, Inc. and to Mr. Edgar B. Smith, Western Research Institute, who were instrumental in the procurement of the shale oil basic nitrogen concentrate sample.

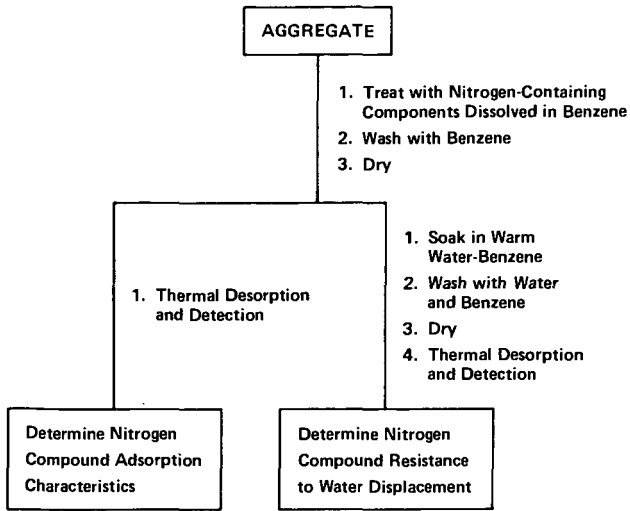


Figure 1. Scheme for studying adsorption-desorption and water displacement characteristics of nitrogen compounds on aggregate surfaces.

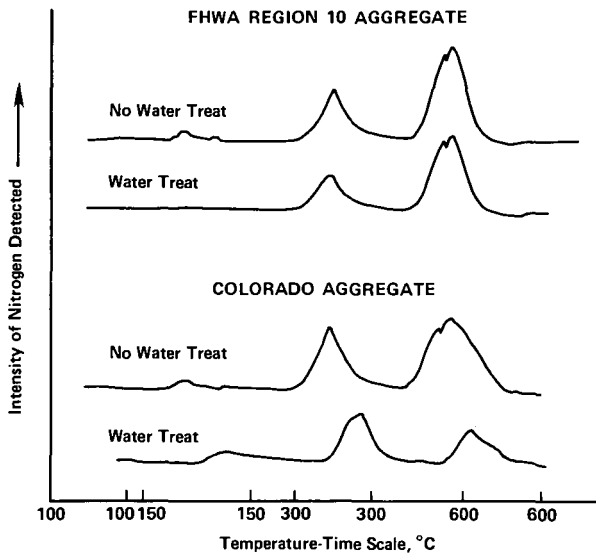


Figure 2. Adsorption-desorption of shale oil nitrogen compounds from FHWA Region 10 and Colorado aggregates.

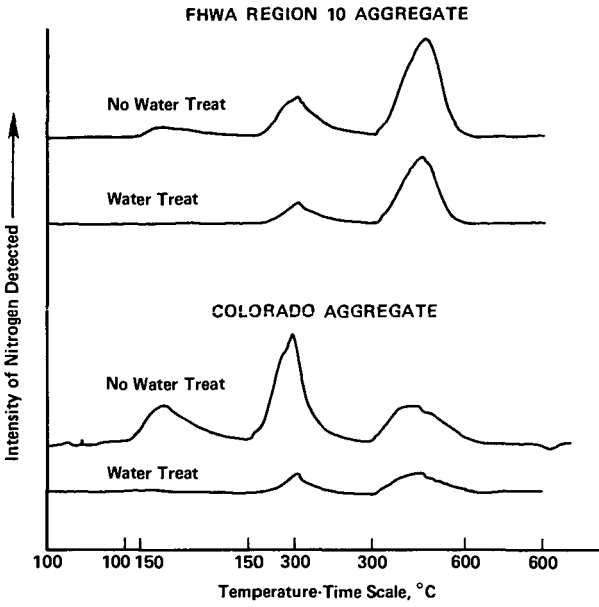


Figure 3. Nitrogen desorption thermograms of pyridine adsorbed on paving aggregates.

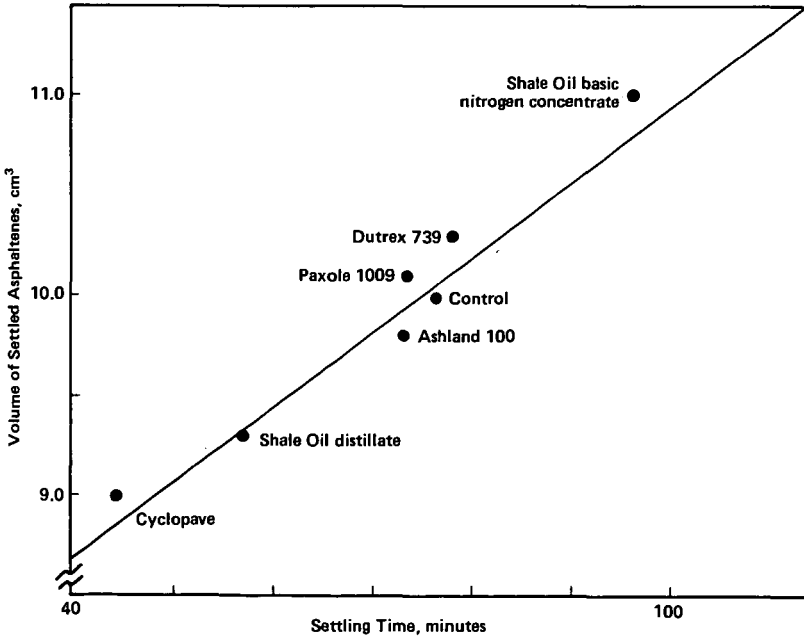


Figure 4. Relationship between asphaltene settling time and final asphaltene volume for aged Hawkins asphalt.

LITERATURE CITED

- (1) Plancher, H., Dorrence, S. M. and Petersen, J. C., Proc. Assoc. Asphalt Paving Technol., 46, 151-175 (1977).
- (2) Plancher, H., Miyake, G., Venable, R. L. and Petersen, J. C., Proc. Can. Tech. Asphalt Assoc., 25, 246-262 (1980).
- (3) Petersen, J. C., Plancher, H., Ensley, E. K., Venable, R. L. and Miyake, G., Trans. Res. Rec. No. 843, 95-104 (1982).
- (4) Petersen, J. C., Anal. Chem., 47, 112-117 (1975).
- (5) Petersen, J. C. and Plancher, H., Ibid., 53, 786-789 (1981).
- (6) Plancher, H. and Petersen, J. C., Proc. Assoc. Asphalt Paving Technol., 45, 1-24 (1976).
- (7) Plancher, H., Miyake, G. and Petersen, J. C., Proc. 13th Oil Shale Symp., Colorado School of Mines, 261-268 (1980).
- (8) Button, J. W., Epps, J. A. and Galloway, B. M., NTIS UC-92b, 121 pp. (1978).
- (9) Plancher, H., Chow, C., Holmes, S. A. and Petersen, J. C., Proc. Internl. Symp., Progressi Nella Technologie Dei Bitumi, Stazione Sperimentale per i Combustibili (Milano, Italy), 263-273 (1981).
- (10) Plancher, H., Smith, E. B., Petersen, J. C. and Anagnos, J. N., Proc. Pan-Pacific Synfuels Conf., Japan Petrol. Inst. (Tokyo, Japan), 2, 684-694 (1982).
- (11) Schmidt, R. J. and Scntucci, L. E., Proc. Assoc. Asphalt Paving Technol., 35, 61-90 (1966).
- (12) Welborn, J. Y., Oglio, E. R. and Zenewitz, J. A., Ibid., 19-60.
- (13) Halstead, W. J., Rostler, F. S. and White, R. M., Ibid., 91-138.
- (14) Petersen, J. C., Barbour, F. A. and Dorrence, S. M., Ibid., 43, 162-177 (1974).
- (15) Ensley, E. K., J. Inst. Petrol., 59, No. 570, 279-289 (1973).
- (16) Lander, H. R., Jr., Tech. Report AFWAL-TR 2135, Wright-Patterson AFB, Ohio (1981).
- (17) Lottman, R. P., NCHRP, Project 4-8(3)/1 Summary Interim Report (1979).
- (18) Plancher, H., Hoiberg, A. J., Subaka, S. C. and Petersen, J. C., Proc. Assoc. Asphalt Paving Technol., 48, 351-374 (1979).

SYMPOSIUM ON CHARACTERIZATION AND CHEMISTRY OF OIL SHALES
PRESENTED BEFORE THE DIVISIONS OF FUEL CHEMISTRY AND
PETROLEUM CHEMISTRY, INC.
AMERICAN CHEMICAL SOCIETY
ST. LOUIS MEETING, APRIL 8 - 13, 1984

OIL SHALE DEVELOPMENT IN MOROCCO

By

C. Y. Cha

Paraho Development Corporation, Englewood, Colorado 80112
and

A. Bekri

Office National de Recherche et, d'Exploitation de Hydrocarbures
Rabat, Kingdom of Morocco

ABSTRACT

The kingdom of Morocco has embarked on development of their extensive oil shale resources to decrease further dependence on foreign petroleum imports and to support internal industrial growth. The Office National de Recherche et d'Exploitation des Hydrocarbures (ONAREP) has elected to develop the T cube semi-continuous retorting process.

The presentation will review the retorting characteristics of Moroccan oil shale, the research and development program, and the current status of T cube process pilot plant construction. The presentation will also review the oil shale resources in Morocco, as well as some of the past ONAREP's oil shale activities.

SYMPOSIUM ON CHARACTERIZATION AND CHEMISTRY OF OIL SHALES
PRESENTED BEFORE THE DIVISIONS OF FUEL CHEMISTRY AND
PETROLEUM CHEMISTRY, INC.
AMERICAN CHEMICAL SOCIETY
ST. LOUIS MEETING, APRIL 8 - 13, 1984

DIFFERENTIAL THERMAL ANALYSIS OF THE REACTION PROPERTIES OF
RAW AND RETORTED OIL SHALE WITH AIR

By

T. F. Wang
Beijing Graduate School of East China Petroleum Institute, P. O. Box 902, Beijing, China

INTRODUCTION

Oil shale can burn directly in the furnace to produce steam and electricity. Recently, in U.S.S.R. probably 75% of their oil shale which was excavated was burned in the boiler (1). In our country, there is only one small power station in Huang county, Shandong, using oil shale as a boiler fuel to produce electricity. When oil shale is pyrolyzed in retort to produce shale oil, the retorted shale char may be treated to react with air in order to supply heat energy for retorting. It is necessary to know the combustion properties of oil shale and its char in order to get kinetic equations.

The kinetics of the oil shale char combustion have been determined in a number of investigations (2-7). Most of the previous work has dealt with the combustion of oil shale char at high temperatures and in large samples. H. Y. Sohn (8) reported the results of an investigation to determine the intrinsic kinetics of the reaction between oxygen and char by using the TG method. In their experiment, the mass transfer and diffusional effects were eliminated by using a sufficiently high flow rate of gas and a small amount of solid particles spread thinly on the sample pan.

There are two discrete peaks in the DTA curve of oil shale combustion. It is easy to determine two reaction steps in the oil shale combustion. In this paper, the results of study to determine the kinetics of combustion of oil shale and its char by using DTA are reported.

EXPERIMENTAL SECTION

In this work, we used the Japanese "Rigaku" type thermal analysis apparatus. It is a combined apparatus of TGA and DTA. A platinum/platinum-rhodium thermocouple was used to measure the sample temperature. Both the sample and reference holders are made of platinum and are 5 mm in diameter and 2 mm thick.

Oil shale samples used were Fushun oil shale, Maoming oil shale, Huang county oil shale and Colorado oil shale. The char is a residue of oil shale which is retorted for 10 minutes at 510°C as in a Fischer Assay. The analysis data of oil shales and their chars used in this work are shown in Table I and Table II.

TABLE I
ANALYSIS DATA OF OIL SHALE USED IN THIS WORK (WT %)

No.	Place	Fischer Analysis						CO ₂	Organic Carbon %
		Oil	Char	H ₂ O	Gas	V	A		
M812	Maoming (low grade)	4.5	85.2	8.0	2.3				13.52
M811 ^a	Maoming (high grade)	8.8	84.1	3.7	3.4	22.8	71.9	1.4	17.47
M821	Maoming Jin Tang	8.2	84.0	3.8	4.0				17.27
F812 ^a	Fushun	9.8	83.3	3.4	3.5	23.8	72.2	2.9	16.30
W821	Huang County	16.5	67.1	10.3	6.1	38.9	45	10.4	35.37
A811 ^a	Colorado	6.4	89.9	1.8	1.9			15.0	

a. Analytical data were taken from Ass. Prof. Qin's work and allowed to use through his kindness.

In order to remove water which was contained in the oil shale, sample particles (-200 mesh) were dried for 2 hrs under 60°C and vacuum (600 mm Hg) condition.

TABLE II

CARBON AMOUNT IN THE CHAR USED IN THIS WORK (WT %)

No.	Place	Carbon %
M811C	Maoming oil shale (high grade) char	8.51
M821C	Maoming Jin Tang oil shale char	8.86
W821C	Huang county oil shale char	31.38

In order to compare the experimental parallel results, all experiments have been done with the same operating conditions:

Working atmosphere	air
Reference substance	$\alpha\text{-Al}_2\text{O}_3$
Heating rate	10°C/min
DTA measuring range	+100 μv
Recording-paper speed	2.5 mm/min

THEORETICAL CONSIDERATION

The intrinsic kinetics for the reaction of a solid with a gas can be written as:

$$\frac{dx}{dt} = k \cdot f(P_A) (1-x)^n \quad 1)$$

Where

- t - time (min)
- x - the fractional conversion of the solid reactant (%)
- k - the reaction rate constant
- $f(P_A)$ - the dependence of rate on gaseous reactant concentration
- n - order of reaction.

In this work, temperature is raised linearly with time during the run. Thus, we have:

$$T = T_0 + a \cdot t, \quad dt = a \cdot dt \quad 2)$$

- T_0 - initial temperature
- a - heating rate

and k is no longer a constant in non-isothermal case:

$$k = A \cdot \exp(-E/RT) \quad 3)$$

Combining Equation 1, 2 and 3 and integrating, we obtain

$$\int_0^x \frac{dx}{(1-x)^n} = \frac{A \cdot f(P_A)}{a} \int_{T_0}^T \exp(-E/RT) dT \cong \frac{A \cdot f(P_A)}{a} \int_0^T \exp(-E/RT) dT \quad 4)$$

For greater values of E/RT , the integral on the right-hand side can be replaced by an approximate solution as follows:

$$\frac{A \cdot f(P_A)}{a} \int_0^T \exp(-E/RT) dT = \frac{A \cdot f(P_A)}{a} \cdot \frac{RT^2}{E} \left(1 - \frac{2RT}{E}\right) \exp(-E/RT) \quad 4a)$$

The left-hand side can be integrated and combined with 4a. So, when $n = 1$,

$$-\ln(1-x) = \frac{A \cdot f(P_A)}{a} \cdot \frac{RT^2}{E} \left(1 - \frac{2RT}{E}\right) \exp(-E/RT) \quad 5)$$

when $n \neq 1$

$$\frac{(1-x)^{1-n} - 1}{n-1} = \frac{A \cdot f(P_A)}{a} \cdot \frac{RT^2}{E} \left(1 - \frac{2RT}{E}\right) \exp(-E/RT) \quad (6)$$

H. Y. Sohn (1980) reported that the best value of A was obtained by using the value of T at $x = 0.5$ in the term

$$\left(1 - \frac{2RT}{E}\right),$$

and the first reaction order might be assumed so far the partial pressure of oxygen was concerned. Thus,

$$f(P_{O_2}) = P_{O_2} \quad (7)$$

A straight-line plot of

$$\ln\left(\frac{-\ln(1-x)}{T^2}\right) \text{ vs. } \frac{1}{T} \text{ (or } \ln\left[\frac{(1-x)^{1-n} - 1}{(n-1) T^2}\right] \text{ vs. } \frac{1}{T})$$

will give birth to the apparent activation energy E and the straight-line interception with the ordinate axis. Substituting Equation 7 into the intercept thus obtained, we can calculate the preexponential factor A value.

RESULTS AND DISCUSSION

The Reaction of Oil Shale with Air

The DTA curves of six oil shales' combustion are shown in Figure 1. When oil shale reacts with air, there are two large peaks on the above mentioned DTA curve. The temperature of the first peak is 316°-356°C, the temperature of the second peak is 382°-454°C.

According to the obtained DTA curve, one can get the X - T curve (9, 10) shown in Figure 2.

A straight-line plot of

$$\ln\left[\frac{-\ln(1-x)}{T^2}\right] \text{ vs. } \frac{1}{T}$$

(shown in Figure 3) yields the apparent activation energy E and preexponential factor A. The kinetic equations of oil shale combustion are shown in Table III.

TABLE III

THE KINETIC EQUATIONS OF OIL SHALE COMBUSTION

No	$k_1 \text{ (atm min)}^{-1}$	$k_2 \text{ (atm min)}^{-1}$
M812	$4.750 \cdot 10^6 \exp(-18390/RT)$	$1.495 \cdot 10^3 \exp(-9462/RT)$
M811	$5.134 \cdot 10^5 \exp(-16420/RT)$	$1.593 \cdot 10^3 \exp(-9833/RT)$
M821	$7.387 \cdot 10^4 \exp(-14720/RT)$	$2.866 \cdot 10^3 \exp(-10880/RT)$
F811	$3.765 \cdot 10^4 \exp(-14080/RT)$	$2.08 \cdot 10^2 \exp(-7887/RT)$
W821	$7.806 \cdot 10^3 \exp(-12320/RT)$	$9.933 \cdot 10^3 \exp(-12300/RT)$
A811	$k=3.786 \cdot 10^5 \exp(-15890/RT)$	

Table III shows that most of oil shales used in this work have two combustion kinetic Equations. It indicates that there are two reactions in the oil shale combustion process. But, for Colorado oil shale, the two peaks are too close. Only one combustion kinetic equation to express its combustion property can be formulated.

The Reaction of Char with Air

The DTA curves of char combustion are shown in Figure 4. It can be seen from Figure 4 that there is only one peak for each oil shale, the obtained DTA curve. The temperatures of the peaks lie in the range from 360°C to 410°C.

According to the obtained DTA curve, one can draw a plot of

$$\ln \left[\frac{-\ln(1-x)}{T^2} \right] \text{ vs. } \frac{1}{T}$$

and get their apparent activation energy E and preexponential factor A (the same method mentioned above).

Table IV displays these obtained kinetic parameters. It can be seen that the combustion rate of Colorado oil shale char is extraordinarily faster than that of other chars; the combustion rate of two Maoming oil shale chars is found to be the same and the combustion rate of Huang county oil shale char is faster than Maoming oil shale char.

TABLE IV

THE KINETIC PARAMETERS OF CHAR COMBUSTION

No.	Correlation Coefficient	n	k (atm min) ⁻¹
M811C-2	0.9950	1	1.267 · 10 ⁴ exp(-13360/RT)
M821C	0.9942	1	9.872 · 10 ³ exp(-13010/RT)
W821C	0.9944	1	6.380 · 10 ³ exp(-12180/RT)
A811C	0.9952	1	2.190 · 10 ⁶ exp(-18250/RT)

The Effect of the Sample Quantity on the Experiment

In order to inspect the effect of diffusion on the experiment, several sample quantities in milligrams of Maoming oil shale char were taken in this work. Results are in Table V.

TABLE V

THE RELATION BETWEEN SAMPLE QUANTITIES AND SAMPLE THICKNESS

No.	Sample Quantity (mg)	Sample Thickness in the Holder (mm)
M811C-1	6.3	0.38
M811C-2	9.1	0.54
M811C-3	18.1	1.08
M811C-4	27.0	1.62

Figure 5 shows the TG-DTA curve of four sample quantities of Maoming oil shale char. It can be seen from Figure 5 that the obtained peak temperatures are the same (about 438°C). It means that the peak temperature relates only to the sample property and bears no relationship to the sample quantity. According to Figure 5, one can get their kinetic parameters (same method as mentioned).

Table VI displays the obtained combustion kinetic parameters of four samples of Maoming oil shale char. It can be seen from Figure 5 and Table VI that, when the sample quantity is between 6.3 and 18 mg, the obtained kinetic parameters are nearly the same. But, when the sample quantity is 27 mg, its kinetic parameter differs greatly from the others. An effect of diffusion can be elicited only when the sample amount is more than 27 mg.

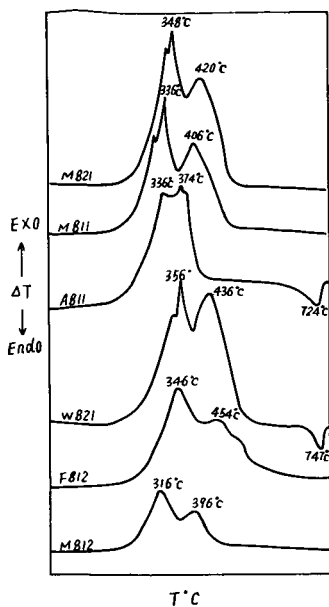


Figure 1. Six oil shale combustion DTA curves

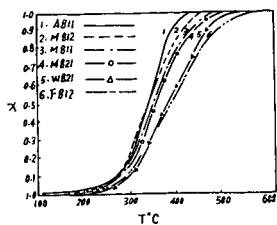


Figure 2. X-T curve of six samples of oil shale.

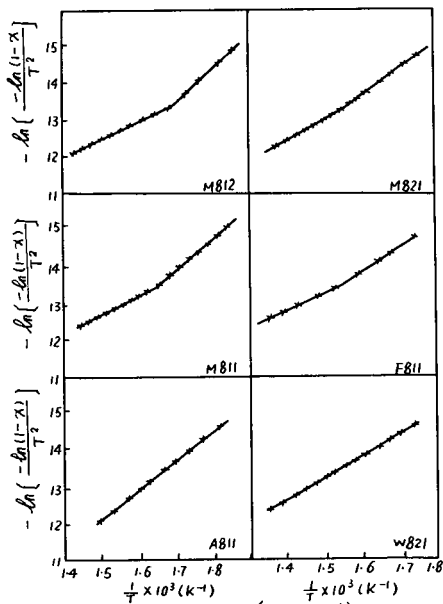


Figure 3. A plot of $\ln\left(\frac{-\ln(1-x)}{T^2}\right)$ vs. $\frac{1}{T}$

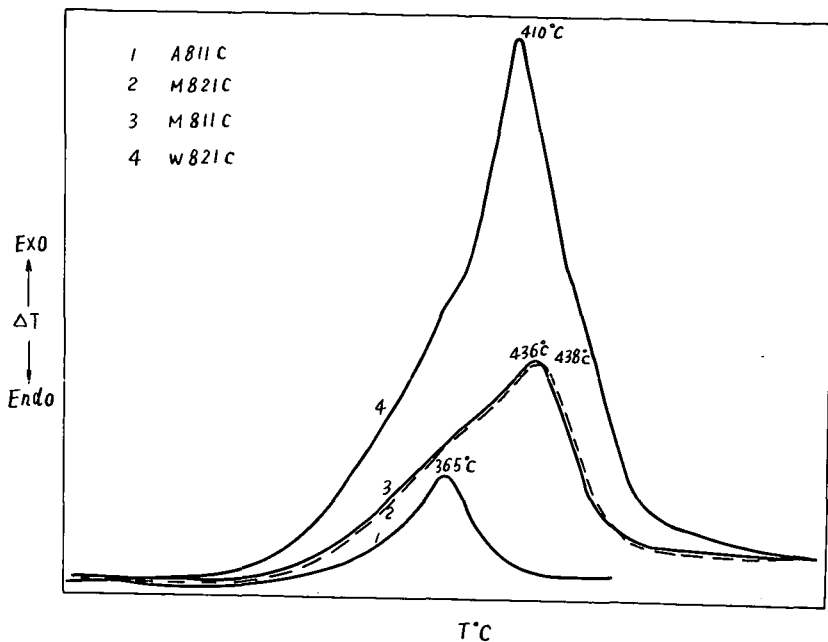


Figure 4. The combustion DTA curves of the chars used in this work

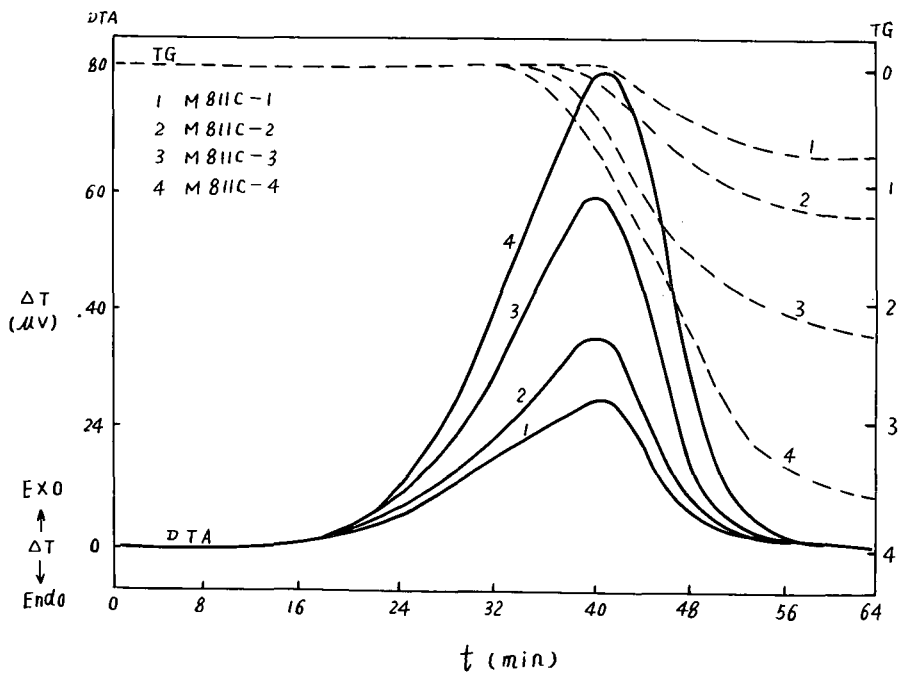


Figure 5. The TG-DTA curve of several sample amount of Maoming oil shale char

TABLE VI

THE COMBUSTION KINETICS OF SEVERAL SAMPLE AMOUNTS OF MAOMING OIL SHALE CHAR

No.	Correlation Coefficient	n	K
M811C-1	0.9979	1	$1.754 \cdot 10^4 \exp(-13770/RT)$
M811C-2	0.9950	1	$1.267 \cdot 10^4 \exp(-13360/RT)$
M811C-3	0.9960	1	$1.018 \cdot 10^4 \exp(-13090/RT)$
M811C-4	0.9954	1	$4.990 \cdot 10^3 \exp(-12210/RT)$

CONCLUDING REMARKS

There are two large peaks on the oil shale combustion DTA curve, but there is only one peak on its char combustion DTA curve.

Oil shale and its char combustion reaction is of the first order. The kinetic parameters of six oil shales and their char used in this work are shown in Tables III and IV. It indicates that Colorado oil shale and its char combustion rate is the fastest while Fushun oil shale and its char combustion rate is the slowest among the six oil shales used in this work.

Under experimental conditions as mentioned, when the sample quantity is less than 18 mg and the temperature is below 500°C, the sample quantity have no significant effect on the combustion rate.

ACKNOWLEDGMENT

Thanks are due Mr. B. X. Xiao, Y. Y. Zhang and A. M. Huang, who have participated in part of the present work.

LITERATURE CITED

- (1) Qian, J. L. and Wang, J. Q., Journal of East China Petroleum Insti., 3, 126 (1981).
- (2) Johnson, D. R., Young, N. B. and Smith, J. W., Energy Research and Development Administration Laramie Energy Research Center, Laramie, WYLER D/R 1-77/6.
- (3) Hguyen, K. and Branch, M. C., Journal of Energy Resource Technology, 133, 103 (1981).
- (4) Mallon, R. C. and Miller, W.C., Quarterly of the Colorado School of Mines, 222 (1975).
- (5) Tyler, A. L., Quarterly of the Colorado School of Mines, 207 (1976).
- (6) Smith, J. W. and Johnson, D. R., ACS, Preprints, Div. of Fuel Chem., 21, 25 (1976).
- (7) Dockter, L., AICHE Symp. Ser., 72, 155, 24 (1976).
- (8) Sohn, H. Y. and Kim, K. S., I. E. C. pro. Des. Dev., 19, 4, 550 (1980).
- (9) Haddadin, R. A. and Tawarak, K. M., Fuel, 59, 539 (1980).
- (10) Wang, T. F. and Lu, S. X., Journal of East China Petroleum Insti., 3, 118 (1981).

SYMPOSIUM ON CHARACTERIZATION AND CHEMISTRY OF OIL SHALES
PRESENTED BEFORE THE DIVISIONS OF FUEL CHEMISTRY AND
PETROLEUM CHEMISTRY, INC.
AMERICAN CHEMICAL SOCIETY
ST. LOUIS MEETING, APRIL 8 - 13, 1984

THE COMBUSTION OF OIL SHALES BY THE
CERCHAR FBC PROCESS

By

R. Puff, J-C. Kita and M. Bendif
Plate-Forme Nationale d'Essais des Carbons Mazingarbe
f 62160 Bully Les Mines, France

ABSTRACT

The CERCHAR experience is wide and relatively ancient in the area of coal refuses FBC combustion. Since 1976, CERCHAR has undertaken laboratory tests on different oil shales, more particularly Lorraine (North-east of France) and Brazilian oil shales.

These tests have been carried out in a 500 mm diameter fluidized-bed fitted with the "CERCHAR" pyramid distributor, principal component of the CERCHAR FBC Process. This paper presents the CERCHAR FBC Process, the test rig, the oil shales tested and the results obtained. The results show that these oil shales can be burned in a FBC boiler with a good combustion efficiency and allow a further development of the process, but for instance, the required economical conditions are not yet reached in France. However, a demonstration unit, able to burn oil shales, is now under construction in France. This unit will burn high ash (80%) coal shales in order to produce 15 t/h of 300°C/30 bar steam. Start-up is scheduled for October 1984.

SYMPOSIUM ON CHARACTERIZATION AND CHEMISTRY OF OIL SHALES
PRESENTED BEFORE THE DIVISIONS OF FUEL CHEMISTRY AND
PETROLEUM CHEMISTRY, INC.
AMERICAN CHEMICAL SOCIETY
ST. LOUIS MEETING, APRIL 8-13, 1984

EXAMINATION OF SHALE-DERIVED POLAR COMPOUNDS AND
THEIR EFFECTS ON DIESEL FUEL STABILITY

By

J. V. Cooney, E. J. Beal and R. N. Hazlett
Naval Research Laboratory, Code 6180, Washington, D. C. 20375

INTRODUCTION

Polar heterocyclic compounds present in middle distillate fuels have been implicated in the chemical processes involved in fuel instability. Nitrogen-containing aromatics (e.g., pyrroles, pyridines, quinolines, indoles) are often intimately involved in the reactions leading to deposition of insoluble sediments and gums in both petroleum and shale-derived fuels (1, 2). Although results of fuel dopant studies are useful in screening potentially active compounds, the results must be taken with caution (3, 4). For example, the particular accelerated (i.e., high temperature) stress regimen employed may have a variable effect upon the results obtained. Additionally, interactive effects between labile species need to be assessed in greater detail (2, 4).

One of the approaches we have used in the study of diesel fuel storage stability has been to examine the effects of adding shale-derived polar fractions to a stable shale base fuel. Thus, we have isolated polar compounds from two different shale sources by mild acid extraction followed by adsorption on silica gel. The identification of the extract components by combined gas chromatography - mass spectrometry, as well as the results of accelerated storage stability tests, are described in this paper.

EXPERIMENTAL

Storage Test Techniques

The accelerated storage stability test method used has been described in detail (3). In summary, 300 ml samples of filtered fuel were stressed in the dark in 500 ml screw-cap borosilicate Erlenmeyer flasks (Teflon-lined caps). All samples were run in duplicate and appropriate blank flask/filter holder corrections were applied. Both filterable sediment and adherent gum values were determined after stress.

Hydroperoxide levels were determined in samples of filtered, stressed fuel by iodometric titration (ASTM D1583-60).

Instrumental Methods

The nitrogen compound extracts were examined by combined GC/MS (EI mode). The GC/MS unit consisted of a Hewlett-Packard Model 5710 GC, a H-P Model 5982A mass spectrometer and a Ribermag SADR GC/MS data system. An all-glass GC inlet system was used in conjunction with a 0.31 mm x 50 m SP2100 (similar to OV-101) fused silica capillary column (5). Operational parameters included: sample size - 2 to 3 microliters split at 60:1, column flow - 1.1 to 1.2 ml/min at a head pressure of 10.5 PSI, detector gain - 9 X LOW, injection port - 250°C, temperature program - 70°C (2 min hold), 4°C/min programmed temperature rise, 220°C (16 min final hold).

Nitrogen concentration levels in fuel samples were determined with an Antek Model 720 nitrogen analyzer using a Dohrmann Model S-300 combustion furnace operating at 1000°C. Three-microliter samples were analyzed in quadruplicate (at the minimum) with the actual nitrogen concentration calculated by comparison with nitrogen calibration standards.

Base Fuel

The base fuel for the present study was diesel fuel marine (DFM) refined from Paraho crude shale oil by SOHIO. This fuel was produced in the U.S. Navy's Shale-II demonstration and is well-characterized (2). A quantity of this fuel was available which contained no additives (sample "D-1"). The D-1 fuel contained 15 ppm N (w./v.) and exhibited good storage stability (2).

Nitrogen Compound Source Fuels

Two high-nitrogen middle distillate fuels produced in U. S. Navy shale programs were selected for extraction studies. Sample "Shale-I DFM" was produced by a delayed coking process

followed by fractionation and was finished by extraction with high strength sulfuric acid (6-8). Sample "Shale-II DFM Composite" was produced by moderate hydrotreatment of the total crude followed by fractionation. This sample was a composite of several streams from the refining run prior to acid extraction. A final extraction with 92% sulfuric acid was used to produce the finished Shale-II DFM (which is the same as sample D-1, the base fuel in the present study) (9, 10).

Extraction Procedure

As shown in Figure 1, the Shale-I DFM and Shale-II DFM Composite fuels were initially subjected to extraction with a 25% molar excess of 0.20 N HCl. The quantity of acid used was calculated by assuming that all of the nitrogen present in the fuel was basic or extractable. The extraction process was conducted for both fuels on a 10 liter scale. The single acid extractions were accomplished with 2 liters of fuel in a 4 liter separatory funnel. A portion of the fuel to be extracted was placed in the funnel with the appropriate quantity of 0.20 N HCl. The contents were vigorously swirled for 5 min, allowed to stand 5 min, gently swirled for 5 min (to reduce the number of emulsion particles) and allowed to stand for 10 min. After careful separation of the layers, traces of acid were removed from the fuel sample by washing with water. The "basic" nitrogen compounds (BNC extracts) were isolated by neutralizing the combined aqueous acid extracts to pH 8-9 (NaHCO₃), extracting the mixture twice with methylene chloride, drying the combined organic layer (anh. MgSO₄) and removing the solvent gently by rotary evaporation (verified by GC).

The residual polar material (including non-basic nitrogen compounds, the "NBNC" extracts) was removed from both acid-extracted fuels by batch silica gel adsorption. Again, it was decided to employ a relatively mild separation technique to avoid extensive chemical alteration of the polar species present. Thus, 2 liters of fuel were treated once with 400 g of fully activated Grade 923 silica gel (100-200 mesh, W. R. Grace) with stirring for a 3h period. Gravity filtration afforded ca. 1550 ml of silica-extracted fuel (filtrate) and a quantity of moist silica. Excess fuel was desorbed from the moist silica by several washings with pentane (ca. 2.5 liters). The silica was next equilibrated several times with methylene chloride (8 x 500 ml). The methylene chloride NBNC extracts were combined and retained. Following this treatment, the silica gel was treated with methanol (1 x 1 liter), filtered and the methanol wash was retained (methanolic NBNC extract).

RESULTS AND DISCUSSION

Preliminary accelerated storage stability tests at 43°C and 80°C indicated that both Shale-I DFM and Shale-II DFM Composite were relatively unstable (i. e., much greater than 1.0 mg/100 ml of total insolubles at 14 days - 80°C) middle distillate fuels. Although both fuels were "unstable", the Shale-I DFM was by far the less stable. Both fuels were found to be relatively high in nitrogen content (Table I). Thus, it was considered that the differences in stability of the fuels might result from the presence of different nitrogen compound types and/or interactive effects. The high nitrogen contents of the fuels made them convenient sources of extractable material for the doping experiments which followed.

TABLE I
STORAGE STABILITY OF NITROGEN COMPOUND SOURCE FUELS

<u>Fuel</u>	<u>N Conc.</u> <u>(ppm-w/v)</u>	<u>Conditions</u>	<u>Total</u> <u>Insolubles</u> <u>(mg/100 ml)</u>	<u>Std. Dev.</u> ^a
Shale-I DFM	1955	43°C/49d	58.6	30.0 (4)
		43°C/92d	113.6	59.5 (4)
		80°C/4d	52.2	8.2 (4)
		80°C/7d	76.8	24.4 (4)
		80°C/14d	138.9	57.5 (8)
Shale-II DFM Composite	3505	80°C/14d	20.5	0.8 (2)

a. Number of trials indicated in parentheses.

Extraction of Nitrogen Compounds

The separation scheme which was employed for the removal of polar, nitrogen-rich extracts from both source fuels is summarized in Figure 1. A single, mild acid extraction was selected (0.20 N HCl) so that the opportunity for chemical changes in the fuel would be minimized (e. g., alky pyrroles are known to be acid-sensitive (11)). The BNC extracts from both fuels were

obtained in methylene chloride solution. Subsequent treatment of the acid-extracted fuels with silica gel afforded two NBNC extracts for each fuel (methylene chloride and methanol).

Samples of Shale-I DFM and Shale-II DFM Composite were analyzed for soluble nitrogen content following treatment with acid and silica gel. The nitrogen balance data, which appear in Table II, indicate that well over 90% of the nitrogen originally present in the fuels was accounted for. The final entries (line 8) in the table may be explained by nitrogen compounds still adsorbed to the silica and/or analytical imprecision. Although several trial extractions (on a 10 ml scale) were able to remove the bulk of the nitrogen present in Shale-I DFM, the actual batch extraction processes were seen to be far less efficient. Thus, although 55% of the nitrogen in the Shale-II DFM Composite was acid extractable, only about 10% of the nitrogen in the Shale-I DFM was acid extractable under these conditions. Line 3 in Table II refers to data obtained immediately prior to treatment of the fuels with silica gel. Since there had been approximately a four month interval between the acid and silica gel treatments, it was necessary to refilter the fuels and redetermine soluble nitrogen levels.

TABLE II

NITROGEN ANALYSES FOR EXTRACTED NITROGEN COMPOUND SOURCE FUELS

Sample	N Concentration (ppm-w/v)	
	Shale-I DFM	Shale-II DFM Composite
1. Original	1955	3505
2. After acid extraction	1757	1570
3. Before silica treatment	1720	1560
4. Isolated in CH ₂ Cl ₂ wash of silica	246	685
5. Isolated in CH ₃ OH wash of silica	139	380
6. After acid and silica treatment	1286	370
7. Sum of 4-6	1671	1435
8. Deficit in N balance ^a	(49)	(125)

a. The difference of lines 3 and 7.

The accelerated storage stabilities of the extracted source fuels were examined (Table III). The results of duplicate trials indicated that the fuels remained relatively unstable despite the treatment with acid and silica. It is noteworthy that the mild acid treatment may have actually deteriorated the stability of both fuels by a small degree. In addition, Shale-II DFM Composite remained a fairly unstable fuel despite the removal of 89% of its original nitrogen content by the extractions.

TABLE III

STORAGE STABILITY OF EXTRACTED NITROGEN COMPOUND SOURCE FUELS
(14 day/80°C Stress)

Fuel	Sample	N Conc. (ppm-w/v)	Total Insolubles (mg/100 ml)	Std. Dev.
Shale-I DFM	Original	1955	138.9	57.5
	Acid extracted	1757	152.6	9.8
	Acid and silica extracted	1286	179.4	103.2
Shale-II DFM Composite	Original	3505	20.5	0.8
	Acid extracted	1570	33.8	0.2
	Acid and silica extracted	370	16.4	1.0

Examination of Nitrogen Compound Extracts

Compounds present in the BNC, NBNC (CH₂Cl₂) and NBNC (CH₃OH) extracts from both source fuels were examined by GC/MS. The conditions used permitted excellent separation of the compounds present. Both total and selected ion-counting techniques were employed, with peaks being identified on the basis of fragmentation pattern and Z-series (5). Frequently, two or more compounds would be present in a peak, so that the relative amount of each was approximated by the magnitude of the total ion count for a given fragmentation pattern. Peak areas were determined by integration of the total ion count over the entire peak.

The results for the acid extract components (BNC) from Shale-I DFM are summarized in Table IV. Sixty-eight well-resolved major peaks were analyzed and over 180 distinct nitrogen compounds were identified by class and carbon number. Substituted pyridines represented by far the largest class of compounds present, comprising about 87% of the material identified. Also present were quinolines and tetrahydroquinolines. Other nitrogen compounds comprised the remainder of the materials examined. The peaks which were examined represent at least 75% of the total sample peak area and are, thus, representative of the total sample.

TABLE IV
EXAMINATION OF BNC EXTRACT FROM SHALE-I DFM

<u>Compound Class^a</u>	<u>No. Isomers</u>	<u>Area %</u>
A. Pyridines	<u>(81)</u>	<u>(87.1)</u>
C ₇	2	1.5
C ₈	10	9.6
C ₉	24	24.5
C ₁₀	22	22.2
C ₁₁	15	17.6
C ₁₂	8	11.8
B. Quinolines	<u>(53)</u>	<u>(7.0)</u>
C ₂	1	<0.1
C ₃	3	0.6
C ₄	10	1.2
C ₅	17	2.7
C ₆	18	2.1
C ₇	4	0.3
C. Tetrahydroquinolines	<u>(40)</u>	<u>(4.1)</u>
C ₁	1	<0.1
C ₂	1	0.1
C ₄	9	0.9
C ₅	7	0.6
C ₆	10	1.0
C ₇	8	0.7
C ₈	4	0.8
D. Indoles	<u>(5)</u>	<u>(0.4)</u>
E. Others ^b	<u>(4)</u>	<u>(1.4)</u>

a. C_x listing under each class denotes the number of carbon atoms in substituents on the heterocyclic ring.

b. Triazines, alkylamines.

Results for the BNC extract of Shale-II DFM Composite appear in Table V. Again, alkylpyridines were the principal components (ca. 77% of the identified material) with a good amount of

tetrahydroquinolines present as well (18.5%). The larger amount of tetrahydroquinolines in the Shale-II DFM Composite (relative to the Shale-I DFM) is a reflection of the hydrotreatment which this fuel was subjected to during its processing.

TABLE V
EXAMINATION OF BNC EXTRACT FROM SHALE-II DFM COMPOSITE

<u>Compound Class</u> ^a	<u>No. Isomers</u>	<u>Area %</u>
A. Pyridines	<u>(48)</u>	<u>(77.5)</u>
C ₃	2	2.0
C ₄	2	2.6
C ₅	3	2.8
C ₆	7	5.6
C ₇	7	9.6
C ₈	9	24.3
C ₉	12	20.7
C ₁₀	5	8.9
C ₁₁	1	1.1
B. Tetrahydroquinolines	<u>(40)</u>	<u>(18.5)</u>
C ₀	2	0.2
C ₁	2	0.5
C ₂	3	1.0
C ₃	9	5.6
C ₄	14	9.5
C ₅	9	1.8
C ₆	1	0.1
C. Quinolines	<u>(15)</u>	<u>(2.2)</u>
C ₁	1	<0.1
C ₂	1	0.2
C ₃	5	1.2
C ₄	7	0.7
C ₅	1	<0.1
D. Indoles	<u>(9)</u>	<u>(1.3)</u>
E. Indolines	<u>(2)</u>	<u>(0.5)</u>

a. C_x listing under each class denotes the number of carbon atoms in substituents on the heterocyclic ring.

Table VI indicates the identifications of the ten largest peaks present in the BNC extracts from both fuels. As can be seen, tri- and tetra-alkylpyridines were prevalent in both extracts.

Two components (denoted by asterisks) appeared to be common to both fuels. The ten largest peaks correspond to approximately 32% of the total identified area for the Shale-I DFM and 45% for the Shale-II DFM Composite.

TABLE VI

A. TEN LARGEST PEAKS - BNC EXTRACT FROM SHALE-I DFM

Rank	Rel. Area	Main Component	Retention Time (min.)
1	1000	Dimethylheptylpyridine	30:49*
2	754	Dimethylnonylpyridine	37:50
3	740	Dimethylheptylpyridine	36:59
4	663	Trimethylheptylpyridine	32:53*
5	659	Dimethyloctylpyridine	34:49
6	630	Dimethylheptylpyridine	31:40
7	607	Dimethyloctylpyridine	33:57
8	586	a C ₁₂ Pyridine	38:35
9	537	Trimethyloctylpyridine	35:57
10	513	Trimethylhexylpyridine	36:30

B. TEN LARGEST PEAKS - BNC EXTRACT FROM SHALE-II DFM COMPOSITE

Rank	Rel. Area	Main Component	Retention Time (min.)
1	1000	Dimethylheptylpyridine	30:47*
2	908	Dimethylhexylpyridine	27:32
3	682	Trimethylpentylpyridine	26:31
4	662	Dimethylhexylpyridine	28:25
5	639	Dimethylpentylpyridine	24:06
6	635	Methylpropyltetrahydroquinoline	26:42
7	508	Dimethylpentylpyridine	27:24
8	450	Trimethylpentylpyridine	30:19
9	432	Trimethylheptylpyridine	32:53*
10	427	Trimethylhexylpyridine	29:46

* These two components are common to both BNC extracts.

Both NBNC extracts (i. e., CH₂Cl₂ and CH₃OH solubles from silica gel treatment) for both source fuels were found to be exceedingly complex. The methylene chloride NBNC extract for Shale-I DFM consisted primarily of alkylbenzenes, indenenes, tetralins, naphthalenes and other hydrocarbons. A good variety of substituted indoles was present together with lesser amounts of pyridines, tetrahydroquinolines and quinolines. Trace quantities of alkylpyrroles were detected. The methanolic NBNC extract for this fuel was for the most part a mixture of straight-chain carboxylic acids and alkylpyridines. Small amounts of alcohols, indoles, amines, quinolines and pyrroles were detected.

The methylene chloride NBNC extract for Shale-II DFM Composite consisted largely of alkylbenzenes, indenenes, naphthalenes and hydrocarbons. A good variety of oxygen-containing species was found (esters and ketones). Most of the nitrogen in this extract appeared in the form of substituted indoles. Lesser amounts of carbazoles and pyridines were detected; no alkylpyrroles were found. The methanolic NBNC extract was found to be rich in alkylpyridines with trace levels of indoles detected. Once again, alkylpyrroles did not appear to be present. The presence of pyridines in the methanolic NBNC extracts from both source fuels is indicative of the inefficiency of the mild, batch acid extraction employed. Adsorption chromatography techniques have recently been applied to samples of Shale-I DFM (12) and Shale-II DFM Composite (13) in efforts to achieve analytical separations. Results obtained by these workers are consistent with the GC/MS and nitrogen concentration analyses reported in this paper.

Results of Doping Experiments

Nitrogen compound extracts (BNC, NBNC (CH₂Cl₂), NBNC (CH₃OH) from both source fuels were added as dopants to a stable shale DFM base, fuel D-1. The extracts which were added were solvent-free (verified by GC) and were immediately taken up in the appropriate quantity of D-1 following solvent-stripping. Nitrogen concentrations in the doped D-1 were then determined, with the amount of added nitrogen being calculated by subtracting the 15 ppm N (w/v) present in the

undoped base fuel. Stress conditions employed temperatures of 80°C and 43°C for periods of time ranging up to 14 and 96 days, respectively (3).

The results of doping experiments with the BNC extracts are shown in Table VII. The amount of total insoluble material reported is the mean of three experimental trials. On a ppm N basis, the BNC extract derived from Shale-I DFM was the more potent sediment promoter; however, relatively low levels of insoluble material were generally observed in all trials. Hydroperoxide levels were also determined in the filtrates of stressed samples. Samples of D-1 which had been doped with BNC from Shale-I DFM showed the highest peroxide numbers.

TABLE VII
STORAGE STABILITY OF D-1 WITH ADDED BNC EXTRACTS

BNC Source	Stress Conditions	N Added (ppm-w/v)	Total Insolubles (mg/100 ml)	Peroxide Number ^a (meq ROOH/kg fuel)
Shale-I DFM	43°C/49d	72	1.2	106.8 (2.2)
	43°C/92d	72	1.2	180.0 (8.1)
	80°C/7d	72	2.2	40.1 (8.1)
	80°C/14d	72	5.9	52.8 (52.5)
Shale-II DFM Composite	43°C/49d	545	3.4	15.5 (9.5)
	43°C/96d	545	4.8	25.1 (15.4)
	80°C/7d	545	2.5	22.0 (19.1)
	80°C/14d	545	4.2	13.1 (52.5)

a. Fuel blank values (i. e., undoped D-1) in parentheses.

In a similar manner, accelerated storage stability tests were conducted with the NBNC extracts from both sources in fuel D-1. The results, summarized in Table VIII, indicate that the methanolic NBNC extracts were active sediment promoters in D-1. On a ppm N (w/v) basis, the Shale-I DFM NBNC (CH₃OH) extract was 58% as effective as 2,5-dimethylpyrrole in promoting the formation of insoluble material (3). Since this extract was rich in alkylpyridines and carboxylic acids, it is possible that interactive effects between active species defined the efficacy of the dopant as an agent of fuel instability. All NBNC extract trials indicated that those extracts derived from Shale-I DFM were more active in promoting sediment.

TABLE VIII
STORAGE STABILITY OF D-1 WITH ADDED NBNC EXTRACTS

NBNC Source	Extraction Solvent	Stress Conditions	N Added (ppm-w/v)	Total Insolubles (mg/100 ml)
Shale-I DFM	CH ₂ Cl ₂	43°C/49d	120	6.2
		43°C/91d	120	6.7
		80°C/7d	120	8.7
		80°C/14d	120	12.2
	CH ₃ OH	80°C/14d	155	35.1
Shale-II DFM Composite	CH ₂ Cl ₂	43°C/49d	370	1.5
		43°C/91d	370	1.4
		80°C/7d	370	0.9
		80°C/14d	370	1.2
	CH ₃ OH	80°C/14d	398	16.9

CONCLUSIONS

Nitrogen-rich polar fractions have been isolated and characterized from two unstable shale diesel liquids. When these extracts were doped into a stable shale DFM and stressed at elevated temperatures, the formation of insoluble material was observed. The activity of a given polar extract in the promotion of instability behavior in a stable base fuel was a complex function of interactive effects between active species in the fuel.

NITROGEN COMPOUND EXTRACTION SCHEME

NITROGEN COMPOUND
SOURCE FUEL

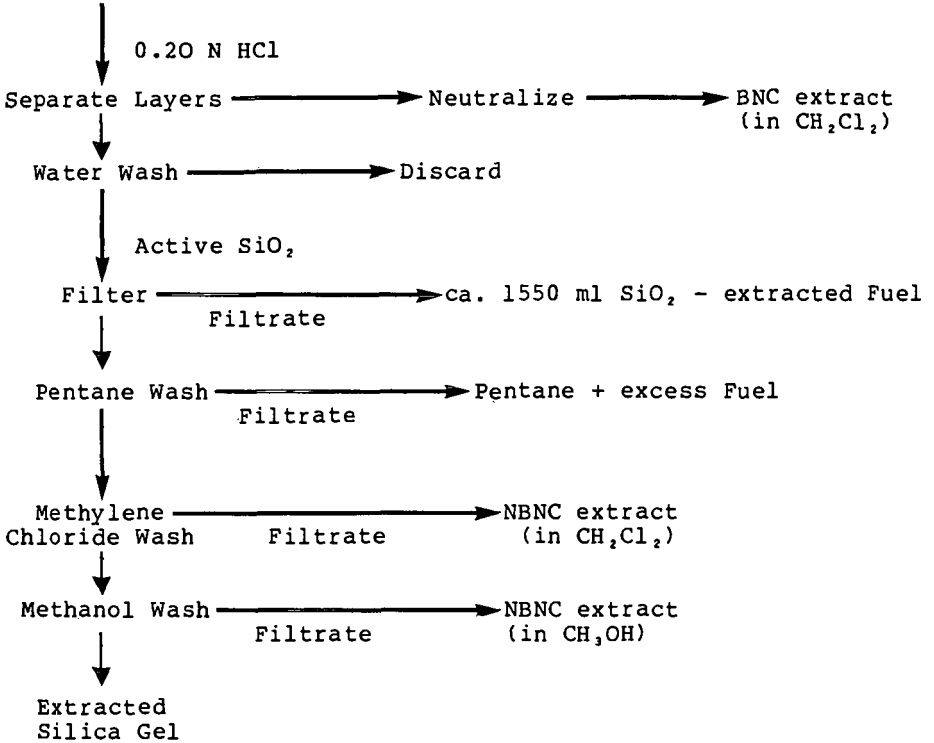


Figure 1

ACKNOWLEDGMENT

The authors thank Dr. Dennis W. Brinkman of the Bartlesville Energy Technology Center, Department of Energy (DOE), for sponsoring this work under DOE contract DE-AI19-81BC10525. References to brand names were made for identification only and do not imply endorsement by DOE or NRL.

LITERATURE CITED

- (1) Frankenfeld, J. W., Taylor, W. F. and Brinkman, D. W., Exxon R and E Co., U. S. Dept. of Energy Contract Report No. DOE/BC/10045-12 (1981).
- (2) Hazlett, R. N., Cooney, J. V. and Beal, E. J., Naval Research Laboratory, U. S. Dept. of Energy Contract Report No. DOE/BC/10525-4 (1983).
- (3) Cooney, J. V., Beal, E. J. and Hazlett, R. N., PREPRINTS, Div. of Petrol. Chem., ACS, 28 (5), 1139 (1983).
- (4) Frankenfeld, J. W., Taylor, W. F. and Brinkman, D. W., Exxon R and E Co., U. S. Dept. of Energy Contract Report No. DOE/BC/10045-23 (1982).
- (5) Hardy, D., Hazlett, R. N. and Solash, J., Preprints, Div. of Fuel Chem., ACS, 27 (2), 201 (1982).
- (6) Bartick, H., Kunchal, K., Switzer, D., Bowen, R. and Edwards, R., Allied Systems Corp., Office of Naval Research Contract Report No. N-00014-75-C-0055 (1975).
- (7) Solash, J., Hazlett, R. N., Hall, J. M. and Nowack, C. J., Fuel, 57, 521 (1978).
- (8) Nowack, C. J., Delfosse, R. J., Speck, G., Solash, J. and Hazlett, R. N., ACS Symp. Series, 163, 267 (1981).
- (9) Solash, J., Hazlett, R. N., Burnett, J. C., Beal, E. and Hall, J. M., ACS Symp. Series 163, 237 (1981).
- (10) Affens, W. A., Hall, J. M., Beal, E., Hazlett, R. N., Leonard, J. T., Nowack, C. J. and Speck, G., ACS Symp. Series, 163, 253 (1981).
- (11) Jones, R. A. and Bean, G. P., "The Chemistry of Pyrroles", Academic Press, NY, NY (1977).
- (12) Personal communication, D. W. Brinkman.
- (13) Holmes, S. A. and Thompson, L. F., Fuel, 62, 709 (1983).

SYMPOSIUM ON CHARACTERIZATION AND CHEMISTRY OF OIL SHALES
PRESENTED BEFORE THE DIVISIONS OF FUEL CHEMISTRY AND
PETROLEUM CHEMISTRY, INC.
AMERICAN CHEMICAL SOCIETY
ST. LOUIS MEETING, APRIL 8 - 13, 1984

HYDROTREATING OF OIL FROM EASTERN OIL SHALE

By

J. Scinta and J. W. Garner
Phillips Petroleum Company, Bartlesville, Oklahoma 74004

INTRODUCTION

Oil shale provides one of the major fossil energy reserves for the United States. The quantity of reserves in oil shale is less than the quantity in coal, but is much greater (by at least an order of magnitude) than the quantity of crude oil reserves. With so much oil potentially available from oil shale, efforts have been made to develop techniques for its utilization. In these efforts, hydrotreating has proved to be an acceptable technique for upgrading raw shale oil to make usable products (1). The present work demonstrated the use of the hydrotreating technique for upgrading an oil from Eastern oil shale.

DESCRIPTION OF TESTS

The pilot plant, which had a capacity of slightly over one gallon per day, approached isothermal operation using conventional fixed-bed, trickle-flow hydrotreating. Hydrogen was recycled and the pilot plant had necessary provisions to avoid plugging by ammonium sulfides.

Tests were made using a commercial catalyst at 2300 psig and 0.4 LHSV (i. e., volumes of hydrocarbon feed/volume of catalyst/hour) with a hydrogen flow rate of 6000 SCF/B. The temperature was varied between 720 and 800°F.

The feed for these tests was an oil recovered from Indiana New Albany shale using the Hytort Process. (Details of retorting are outside the scope of this paper.) Although this oil is probably different from that which would be obtained in an optimized process, its key properties are representative of those one would expect to obtain. These properties are given in Table I. In addition, properties of a Western shale oil, obtained by Phillips, are shown for comparison. Many of the properties of the Eastern oil are similar to the properties of the Western oil, but differences are present. The most significant differences are that the Eastern oil has lower viscosity, lower pour point, lower elemental hydrogen content, lower arsenic content, lower portion boiling above 1000°F and higher portion boiling below 400°F than does the Western oil.

DISCUSSION OF RESULTS

Excellent removal of nitrogen was obtained in single-stage hydrotreating without feed pre-processing. As shown by the data in Figure 1, the total nitrogen content of the product decreased from 800 to 70 wppm (96 to 99.6% removal) as the temperature was increased from 720 to 800°F. A temperature of 783°F was needed to reduce the nitrogen content of the shale oil from the 1.89 wt % in the feed to 0.01 wt % in the product. In other Phillips tests with oil from Western shale, the nitrogen content was reduced to 0.01 wt % at slightly milder operating conditions.

The basic nitrogen content of the product was approximately half the total nitrogen content. Since the basic nitrogen content of the feed was 47% of the total nitrogen content, reductions in basic and total nitrogen were comparable in these tests. Removals might not be comparable, however, at a significantly different operating pressure.

A correlation between temperature and hydrogen consumption is shown in Figure 2. As the temperature was increased from 720 to 800°F, chemical hydrogen consumption increased from 1950 to 2300 SCF/B. To produce product with a nitrogen content of 100 wppm, chemical hydrogen consumptions are lower than those obtained with the Eastern oil. However, the Eastern oil has a lower boiling range; thus, it may be a more valuable synthetic crude.

Data on yields are shown in Figure 2. On a weight basis, the yield of liquid product decreased as the temperature was increased (from 97 to 94 wt % of feed as temperature increased from 720 to 800°F). On a volume basis, the maximum yield of liquid product (almost 107 vol % of feed) was obtained at about 740°F, with only slightly lower yields at higher or lower temperatures. As temperature was increased (thereby giving more severe operating conditions), smaller

percentages of the liquid product were in the higher boiling ranges. The amount of material boiling above 650°F decreased by about 18 wt % of feed to the hydrotreater when operating at 720°F and by about 30 wt % of feed when operating at 800°F. The material cracked into all lower boiling ranges. At a temperature of 720°F, the amount boiling in the C₅-400°F boiling range increased by 12 wt % of the feed and at 800°F it increased by 19 wt % of the feed. At 720°F about 1.5 wt % of feed was cracked to C₁ through C₄ hydrocarbons. This amount increased to about 4.7 wt % when temperature increased to 800°F. The amount in the 400 through 650°F boiling range appeared to increase by 3 or 4 wt % of the feed. Data scatter obscured any possible correlation between variation in amount of increase in 400-650°F fraction and severity of hydrotreating.

TABLE I
PROPERTIES OF SHALE OILS

	From Eastern Oil Shale	From Western Oil Shale
API gravity at 60/60°F ^a	17.0	19.1
Ramsbottom carbon residue, wt %	1.45	2.77
Viscosity, cSt at 40°C	7.65	45.57
Bromine no.	68	56
Pour point, °F	-9	80
Total nitrogen content, wt %	1.89	2.12
Basic nitrogen, content, wt %	0.88	1.10
Sulfur content, wt %	0.99	0.85
Oxygen content, wt %	1.25	1.39
Water content, wt %	0.39	0.59
Elemental carbon content, wt %	85.08	83.83
Elemental hydrogen content, wt %	10.05	11.23
Nickel content, wppm	2.3	6.7
Vanadium content, wppm	0.3	1.4
Arsenic content, wppm	10.3	34.5
Portion boiling below 400°F, wt %	19.5	3.2
Portion boiling between 400 and 650°F, wt %	36.4	25.9
Portion boiling between 650 and 1000°F, wt %	41.6	48.4
Portion boiling above 1000°F, wt %	2.5	22.5

a. Corrected to 60/60°F from the measurement temperature of 33.5°C using API Measurement Tables for petroleum.

The data point at 800°F was largely ignored in drawing some of the curves (i. e. , yield of C₁ to C₄ hydrocarbons, yield of C₅ and heavier and increase in amount of C₅ to 400°F material) in Figure 2 because the data are believed to be incorrect. An operating problem caused the light hydrocarbon stream to be caught in a non-cooled container, from which some of the light hydrocarbons weathered and were lost.

The cracking and removal of heteroatoms caused a significant increase in the API Gravity. As shown in Figure 2, the API Gravity of the liquid product varied between 31.5 and 36.7 as the temperature varied between 720 and 800°F.

CONCLUSIONS

1. An excellent synthetic crude can be produced by single-stage hydrotreating of oil from Eastern shale.

2. Operation to produce a product containing 100 ppm nitrogen (a) requires a temperature of about 783°F with new catalyst at 2300 psig, 0.4 LHSV and 6000 SCF/B flow of hydrogen; (b) chemically consumes 2250 SCF/B of hydrogen; (c) cracks about 4 wt % of feed into C₁ through C₄ hydrocarbons; and (d) reduces amount boiling above 650°F by about 27 wt % of feed.

3. In comparison with other Phillips tests using Western shale oil, the Eastern shale oil requires more severe hydrotreating conditions to lower the nitrogen content to 0.01 wt % than does the Western oil and chemical hydrogen consumption is higher when hydrotreating the Eastern oil to an equivalent nitrogen content.

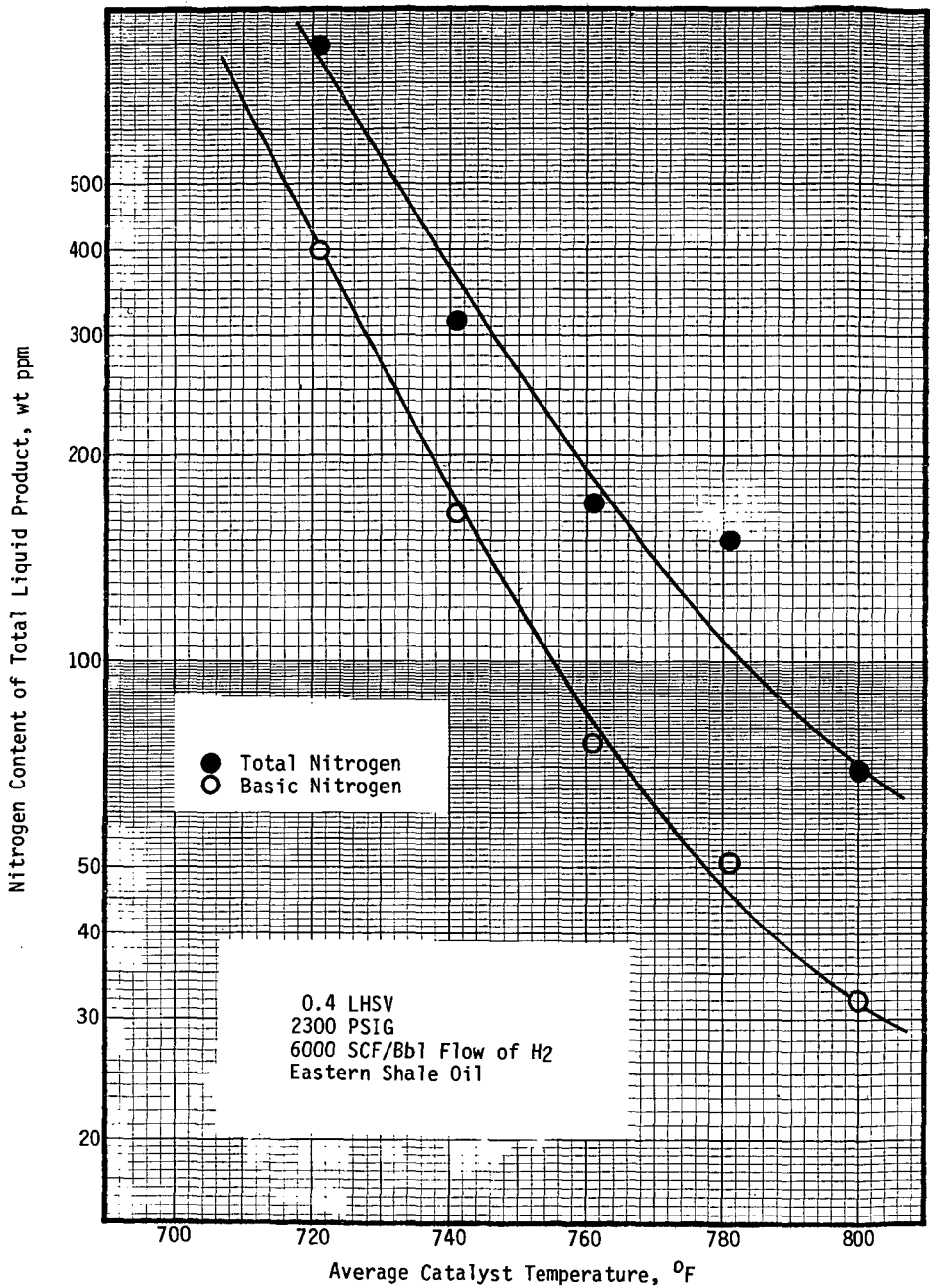


Figure 1

CORRELATION BETWEEN CATALYST TEMPERATURE AND NITROGEN CONTENT OF LIQUID PRODUCT

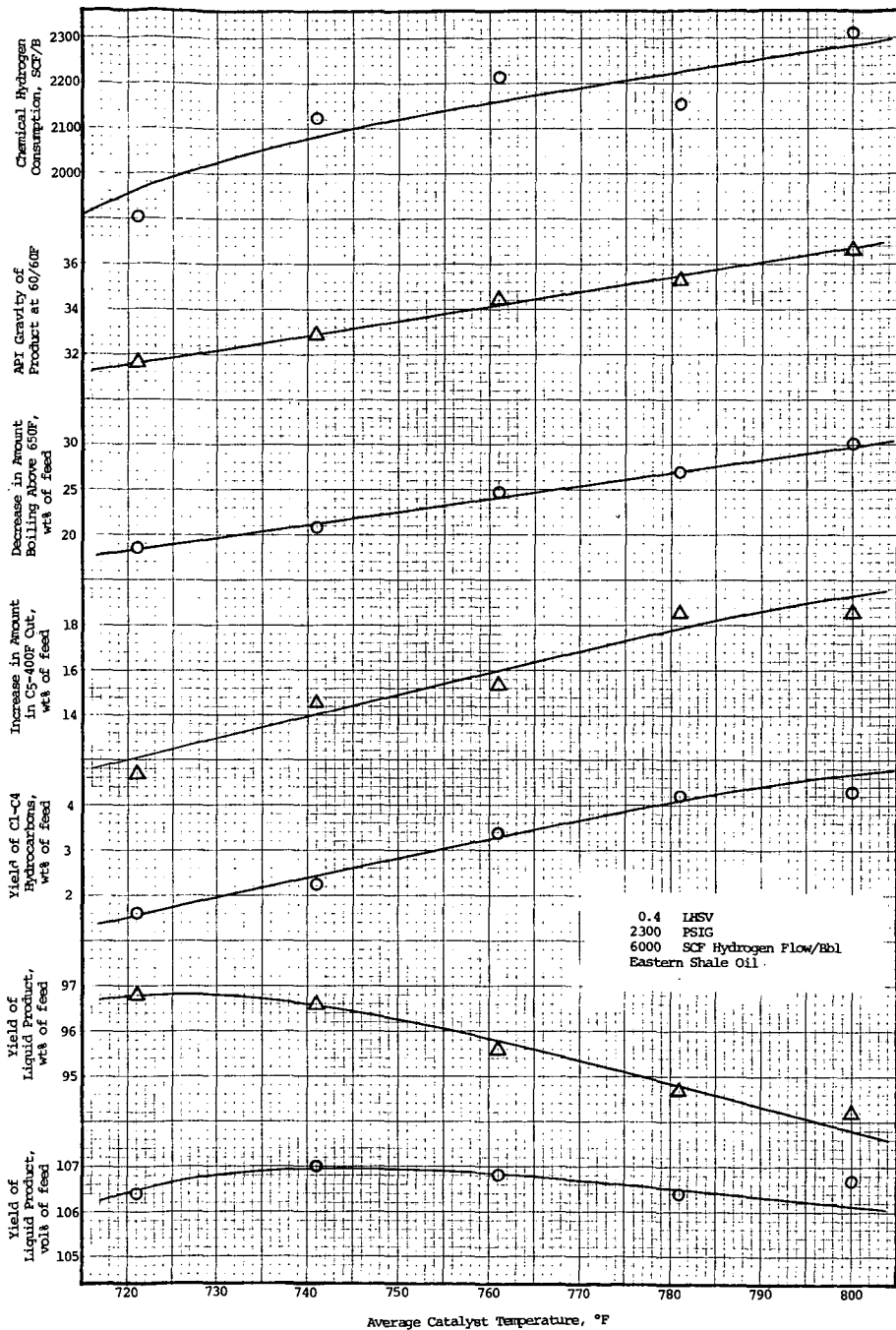


Figure 2

CORRELATION BETWEEN CATALYST TEMPERATURE AND SELECTED OTHER ITEMS

LITERATURE CITED

- (1) Sullivan, R. F. , Stangeland, B. E. , Rudy, C. E. , Green, D. C. and Frumkin, H. A. , "Refining and Upgrading of Synfuels From Coal and Oil Shales by Advanced Catalytic Process, DOE Contract EF-76-C-01-2315, Report FE-2315-25.

SYMPOSIUM ON CHARACTERIZATION AND CHEMISTRY OF OIL SHALES
PRESENTED BEFORE THE DIVISIONS OF FUEL CHEMISTRY AND
PETROLEUM CHEMISTRY, INC.
AMERICAN CHEMICAL SOCIETY
ST. LOUIS MEETING, APRIL 8 - 13, 1984

STUDY OF MINERAL FINES IN TAR SAND BITUMEN AND THEIR ACID SENSITIVITY
USING EPR AND FTIR TECHNIQUES

By

V. M. Malhotra* and W. R. M. Graham
Department of Physics, Texas Christian University, Fort Worth, Texas 76129

INTRODUCTION

The recovery of oil from tar sand deposits by conventional techniques is not possible because of the high viscosity of the bitumen. Processes which have been suggested for the *in situ* recovery of this heavy oil all require thermal and water injection treatment. Clementz (1) has found that asphaltenes are rapidly and irreversibly adsorbed on smectite, kaolinite and illite under near anhydrous laboratory conditions. Based on this observation, he has suggested that the adsorption of petroleum heavy ends on clay minerals would result in their stabilization against dispersion and subsequent migration. Since clay particles coated with heavy ends may be oil wettable, they may readily enter the oil phase, resulting in poor recoveries. The presence of minerals in conventional oil reservoir formations can reduce permeability and obstruct flow either by the expansion of smectite and illite clays to fill pore spaces or by the dispersion and lodging of very small amounts of clays in restrictions.

Recent results from studies on bitumen, extracted with benzene, from Utah (2) and Athabasca (3) tar sands have shown that it is impossible to remove coated clay particles from the bitumen, even when it is subjected to severe centrifuging conditions. Studies on tar sands which provide information on potential oil wettable minerals and the minimization of their negative effects on recovery are, therefore, of substantial importance.

EXPERIMENTAL PROCEDURES

The tar sand sample used in this study originated from the P. R. Spring Outcrop NE Sec. 32, T-Z5-1/2S, R23F, Uintah County, Utah, and was supplied by the Laramie Energy Technology Center through the courtesy of Dr. J. F. Branthaver. Free bitumen was separated from the heavy minerals in the raw tar sand by a Soxhlet extraction technique (4) using benzene as the solvent. Fine clay particles were observed to escape through the thimble during extraction; these could be removed only by further treatment. A 10% solution of bitumen redissolved in benzene was centrifuged at 8000 rev min⁻¹ for 35 min at 277 K, and then decanted. The fine clay particles remaining at the bottom of the tube were washed repeatedly with benzene until the solution was colorless in order to remove any remaining free bitumen. This centrifuged mineral residue (CMR) was the object of the present study.

Electron paramagnetic resonance (EPR) spectra were recorded with a Varian V4500 spectrometer operating at 9.2 GHz with 100 kHz magnetic field modulation. A Varian V-4557 variable temperature accessory was used in recording spectra at temperatures as low as 80 K. The sample temperature was continuously monitored by a chromel-constantan thermocouple attached to the sample tube.

Infrared spectra of samples prepared in KBr or CsI pellets and Nujol mulls were recorded in the range 4000-225 cm⁻¹ using a Nicolet 5DXE Fourier transform infrared (FTIR) spectrometer and a Beckman 4250 dispersive spectrometer.

RESULTS AND DISCUSSION

FTIR

The IR spectrum of the CMR shown in Figure 1 exhibits absorptions at 3000-2800, 1710, 1600 and 1500-1350 cm⁻¹, thereby providing evidence that bitumen remains after Soxhlet extraction, probably in the form of free bitumen which has not been adsorbed on mineral surfaces and also as

* Present address: Department of Physics, The University of Calgary, Calgary, Alberta
Canada T2N 1N4

bonded bitumen in mineral-organic complexes. The observation of a decrease in intensity of the 3000-2800 and 1500-1350 cm^{-1} bands on further treatment of the CMR with benzene indicates that additional free bitumen has been removed. A further reduction in the intensity of these bands when the stronger, chloroform-acetone (70:30) solvent is subsequently used, suggests that, in this step, adsorbed bitumen has been partially removed. In contrast to the aliphatic bands, the carbonyl and aromatic bands at 1710 and 1600 cm^{-1} are unaffected by the solvent treatment. This behavior indicates that stable complexes of these functional groups are formed with the mineral matter and are thus resistant to solvent extraction.

Utah tar sands consist of complex mixtures of organic matter and mineral material in which the sand grains are completely encompassed by bitumen. In contrast, the individual grains in the Athabasca deposits are surrounded by a thin water film. In the P. R. Spring deposit, which is of the consolidated type, bitumen is in direct contact with and bonded to the mineral particles.

Although a detailed study of the minerals present in P. R. Spring tar sands has apparently not been reported, quartz grains, mica flakes, calcite and clay particles were recognizable in the mineral fraction remaining after bitumen extraction and clays would be expected to be the major constituent of the CMR. IR and, more recently, FTIR spectroscopy have proved to be invaluable in the identification both of functional groups and of minerals in coals (5) and tar sands (2, 3). Figure 1 shows the spectrum of the CMR recorded in the ranges 4000-2000 and 1800-225 cm^{-1} . Typical, prominent carbonate features (6) include a broad band in the 1400-1500 cm^{-1} region and sharper bands at ~ 870 and 720 cm^{-1} . Treatment with dilute H_2SO_4 of a sample of the CMR fraction which had been cleaned with a chloroform-acetone solution resulted in the complete removal of the 1450 cm^{-1} band, in agreement with the assignment of this band to carbonates. Si-O vibrations are responsible for broad bands in the 900-1100 cm^{-1} region and sharper features in the 700-800 and 400-530 cm^{-1} regions. Characteristic quartz features are strong, broad bands at 1172 and 1082 cm^{-1} , originating from Si-O stretching modes, as well as bands in the vicinity of 460 cm^{-1} from Si-O bending vibrations.

The IR spectra show that the CMR, as expected, consists principally of a mixture of clays (7). The presence of kaolinite can be discounted, at least at concentrations $>1\%$, because of the absence of the higher-frequency member of the characteristic pair of O-H stretching bands at 3694 and 3620 cm^{-1} (8). The single band at 3620 cm^{-1} is characteristic, however, of smectite and illite clays. As shown in Figure 1, other typical bands of these clays are also observed. The very broad band at 3400 cm^{-1} and the sharper band at 1625 cm^{-1} , which are O-H stretching and bending vibrations, respectively, are attributable to the loosely bound, interlayer water contained in smectite or hydrous illite. The broad band at ~ 3200 cm^{-1} is characteristic of water molecules tightly bonded to particle surfaces in a monolayer. Weak bands appearing at 835 and 795 cm^{-1} are (Al, Mg)-O-H vibrations which can be assigned to smectite. Clays also absorb strongly at 900-1100 cm^{-1} , but overlapping bands in this region prevent analysis of these features in detail.

A further diagnostic test was made in order to verify the identification of smectite by forming a complex with 2,2'-dipyridyl, which is specific to smectite clay and results in a band at 1435 cm^{-1} (9). For this test, the CMR was treated with a chloroform-acetone mixture and then with dilute H_2SO_4 and HCl acid to remove carbonate minerals. After drying for 24 h at 383 K, the sample was ground for 15 min with 2,2'-dipyridyl and ethanol in a steel ball mill vibrator, washed with ethanol to remove any unreacted 2,2'-dipyridyl, and air dried. A KBr pellet was made and the FTIR spectrum shown in Figure 2 was recorded. The appearance of a band at 1435 cm^{-1} confirms the presence of smectite clay in the CMR fraction. The close similarity of the IR spectra of illite and smectite clays precludes further, detailed analysis; however, based on the preceding discussion it can be concluded that these clays along with carbonates are undoubtedly the principal constituents of the CMR.

EPR

The EPR spectrum of the CMR shown in Figure 3(a) exhibits four main features: (a) an intense broad signal at $g=2$ which is probably due to iron oxide and/or hydroxide, either in the form of discrete particles or on the surface of illite and smectite clay particles, (b) a partially resolved, six-peak signal typical of Mn^{2+} which is superimposed on the broad signal, (c) a sharp line at $g=2.003$ which can be assigned to organic free radicals, and (d) an absorption at $g=4.3$ characteristic of Fe^{3+} at sites of rhombic symmetry.

The intense, broad signal at $g=2$ is probably due to Fe_2O_3 . A similar spectrum has been observed by Griscom and Marquardt (10) for finely ground ferrites in lunar soil samples and attributed to the oxidation of Fe^{2+} to Fe^{3+} . EPR spectra of the CMR following treatment with either H_2SO_4 or HCl acid and of the acid extract (see Figure 3(b)) show that the broad signal has largely disappeared from the CMR spectrum, confirming that it originates with adsorbed or free iron oxide.

The six-peak spectrum superimposed on the Fe_2O_3 spectrum at $g=2.0$ is characteristic of Mn^{2+} ; here the site is expected to be in carbonates or clays. Since drying the CMR at temperatures

up to 573 K had no effect on the spectrum, the possibility that it originates with hydrated Mn^{2+} in smectite clays (11) can be ruled out. Malhotra and Graham (12) have reported a well resolved hyperfine spectrum of Mn^{2+} in coal-derived calcite. The partly resolved, smeared appearance of the spectrum may indicate that $MnCO_3$ is responsible, since, in that case, broadening of the hyperfine lines because of dipolar interaction is expected. Treatment with dilute HCl or H_2SO_4 acid resulted in the removal of the Mn^{2+} signal from the CMR spectrum and the appearance of a well resolved spectrum in the acid extract (Figure 3(c)). This behavior is consistent with the assignment to $MnCO_3$. Shepherd and Graham (13) have observed an EPR spectrum of Mn^{2+} at two sites in the mineral fraction of a sample of Circle Cliffs tar sand; however, detailed analysis of that spectrum shows that the Mn^{2+} occurs in dolomite.

When the CMR was treated with large quantities of a chloroform-acetone solution, the sharp, isotropic line at $g \approx 2.0028$ was reduced in intensity while the g -value and line-width were unaffected. This behavior is consistent with its assignment to organic free radicals and rules out the possibility of the cause being a defect in the smectite or illite clay structures. A detailed study of the application of the EPR technique to free radicals in P. R. Spring tar sand has been reported elsewhere by Malhotra and Graham (4). The downward shift in g -value from 2.0034 to 2.0028 and the increase in linewidth (see Table I) observed for the CMR in comparison to free bitumen reflects the selective removal of certain organic fractions during Soxhlet extraction. Treating the CMR with dilute H_2SO_4 reduces the linewidth and indicates further, selective removal of organic fractions. The g -values and linewidths for P. R. Spring organic fractions and for the CMR are summarized in Table I. Since g -values for aromatic hydrocarbons are typically 2.0026-2.0028, but higher for heteroatomic π -electron radicals, it is likely that the former contribute to the CMR free radical signal. As noted earlier, the persistence of the 1600 cm^{-1} aromatic band in the FTIR spectrum even after the CMR fraction was subjected to various treatments, suggests that the aromatic groups are strongly bound to the surfaces of the illite and smectite clays. These observations are, thus, consistent with the report by Clementz (1) that aromatic fractions are selectively adsorbed on clays. A bitumen covering on clay particles would render them hydrophobic and, hence, they may readily enter the bitumen phase during *in situ* recovery processes.

TABLE I

FREE RADICAL EPR PARAMETERS FOR P. R. SPRING TAR SAND FRACTIONS

Sample	g	ΔH (mT)	Reference
Bitumen	2.0034	0.53	4
Petrolene	2.0035	0.57	4
Asphaltene	2.0034	0.54	4
CMR ^a	2.0028	1.33	Present work
CMR treated with H_2SO_4	2.0027	0.63	Present work
CMR treated with acid and washed with chloroform-acetone	2.0031	0.69	Present work

a. Centrifuged mineral residue.

Many clay minerals and carbonates common to hydrocarbon fields contain iron which is released when the minerals are dissolved in the acids which are used to treat oil fields (14). Released iron forms a ferric gel which blocks pores and reduces permeability; consequently, it is important to know the amount of iron released. If, as suggested by Clementz, treatment with heavy ends of oil is used to stabilize formation, it is of interest to know the effect of acids on bitumen coated minerals during subsequent treatment.

The EPR spectra at 25-275 mT of the CMR residue following treatment with 1N H_2SO_4 and the acid extract appear in Figure 4. The signals at $g \approx 4.3$ and 9.5 originate with Fe^{3+} at octahedral sites of rhombic symmetry (15). Of the clays, kaolinite can be disallowed since EPR spectra of both natural and synthetic kaolinites exhibit 3 lines in the vicinity of $g \approx 4$ (16, 17). This finding differs from the results for the centrifuged residue from an Athabasca asphaltene in which kaolinite has been reported as the major clay constituent (3), but is consistent with the IR results which, as has been noted, indicate no evidence of kaolinite in the P. R. Spring sample. The observed powder pattern spectra were fitted to the spin-Hamiltonian

$$H = g\beta H \cdot S + D[S_z^2 - \frac{1}{3}S(S+1)] + E[S_x^2 - S_y^2] \quad 1)$$

where the first term is the Zeeman splitting, the second and third terms represent the axial and rhombic components of the zero field splitting and $S=5/2$ and $I=0$ for Fe^{3+} . The derived spin-Hamiltonian parameters shown in Table II for comparison with results for various clays indicate that the observed Fe^{3+} EPR spectrum arises from illite (16) and smectite (18) clays. The EPR spectrum of Fe^{3+} in the H_2SO_4 gives a measure of the iron released by the acid treatment and may be of potential use as a diagnostic tool in determining the amount of iron released when formations are treated, from the EPR spectrum of core samples.

TABLE II
EPR SPIN HAMILTONIAN PARAMETERS FOR Fe^{3+} IN P. R. SPRING CMR^a SAMPLES AND VARIOUS CLAYS

Sample	g	ΔH (mT)	$\lambda = E/D$	Reference
P. R. Spring CMR	~2 ~4.3	91		Present work
P. R. Spring CMR	4.18	21.7	~0.333	Present work
H_2SO_4 treated	9.65	16.3		
P. R. Spring CMR	4.32	14.3	~0.333	Present work
H_2SO_4 extract	9.65	8.2		
Kaolinite Clay				
Center I	4.2		0.333	16, 17
Iia	4.9			
Iib	{ 3.5 3.7		<0.333	
Mica				
	4.17		0.333	15
	4.29			
Smectite				
	4.33		0.333	18
	9.6			

a. Centrifuged mineral residue.

A complex spectrum, observed at $g \approx 1.99$ for a sample of CMR from which Fe_2O_3 and carbonates had been removed by acid treatment, exhibited eight peaks characteristic of a vanadyl complex and is similar to spectra observed for Athabasca and Boscan asphaltenes. The CMR and Boscan spectra are shown in Figure 5. Vanadyl is known to occur in a wide variety of carbonaceous deposits in both porphyrin and non-porphyrin complexes (19, 20). The spectrum was fitted to the axially symmetric spin Hamiltonian

$$H = \rho [g_{\parallel} H_z S_z + g_{\perp} (H_x S_x + H_y S_y)] + A_{\parallel} S_z I_z + A_{\perp} (S_x I_x + S_y I_y) \quad 2)$$

where A_{\parallel} and A_{\perp} are the parallel and perpendicular hyperfine constants. The derived EPR parameters are shown in Table III together with the spin-Hamiltonian parameters for various vanadyl porphyrins and VO^{2+} in Mg^{2+} -hectorite clay, SiO_2 and Al_2O_3 . Comparison indicates that the presence of VO^{2+} in porphyrins is unlikely and the observation that the vanadyl complex is not removed on treatment with H_2SO_4 implies an inorganic environment. The derived parameters are in better agreement with the data for inorganic complexes, particularly in the case where VO^{2+} is doped into Mg^{2+} -hectorite at the 5% level (22). The observation that the spectrum can be removed by bonding with HCl further supports the tentative suggestion that VO^{2+} is in clays. These results for P. R. Spring tar sand are in marked contrast to a study of a sample of Circle Cliffs tar sand in which vanadyl porphyrin has been identified, but no evidence has been found for VO^{2+} in inorganic fractions (13).

CONCLUSION

The results from this work suggest that the EPR and FTIR techniques are important tools in the study of fine clay particles in tar sand and petroleum deposits and have application in understanding the role of clays and their effect on recovery processes.

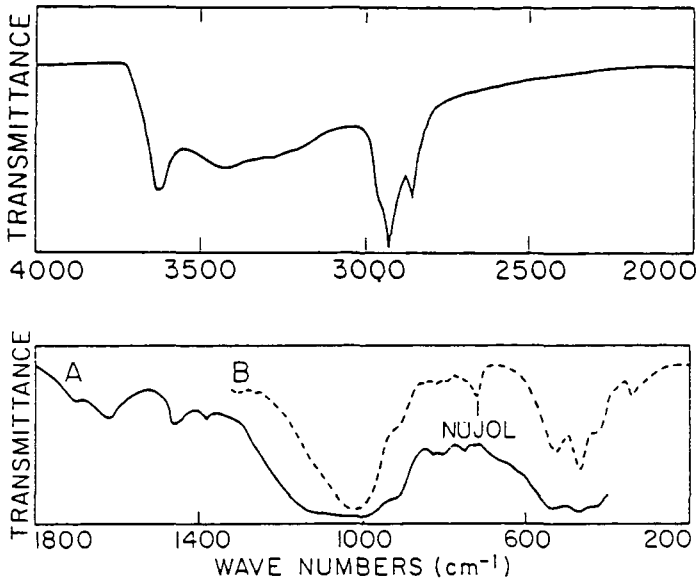


Figure 1. IR spectra of the centrifuged mineral residue in the 2000-4000 and 1800-200 cm^{-1} regions.

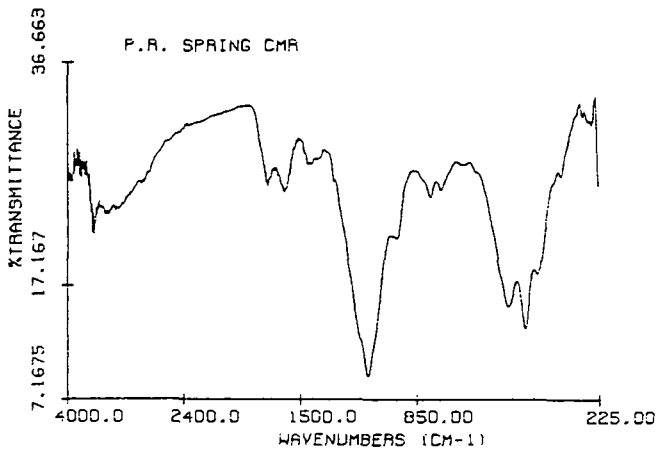


Figure 2. FTIR spectrum of centrifuged mineral residue which had been washed with acetone and chloroform-acetone, and then treated with 2,2'-dipyridyl showing the appearance of the 1435 cm^{-1} band which is specific to the formation of a complex between 2,2'-dipyridyl and smectite.

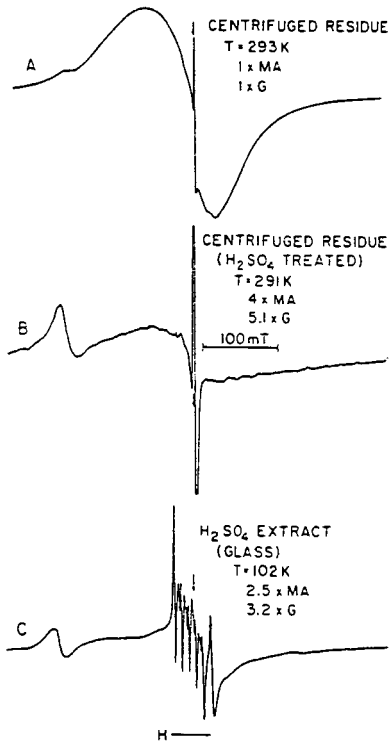


Figure 3. EPR spectrum of (a) the centrifuged mineral residue, (b) the CMR following treatment with dilute H_2SO_4 and (c) a glass of the acid extract. MA = modulation amplitude. G = gain.

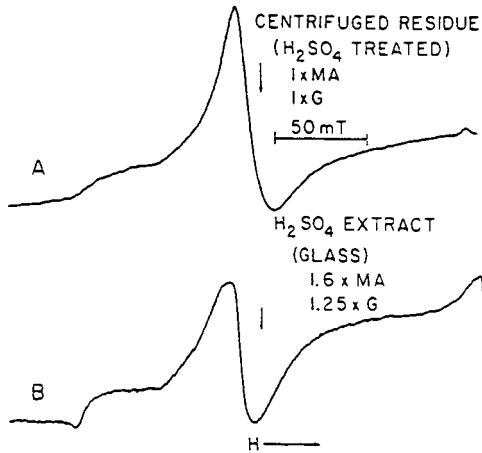


Figure 4. EPR spectra of (a) acid treated EMR and (b) its acid extract in the 25-275 mT region.

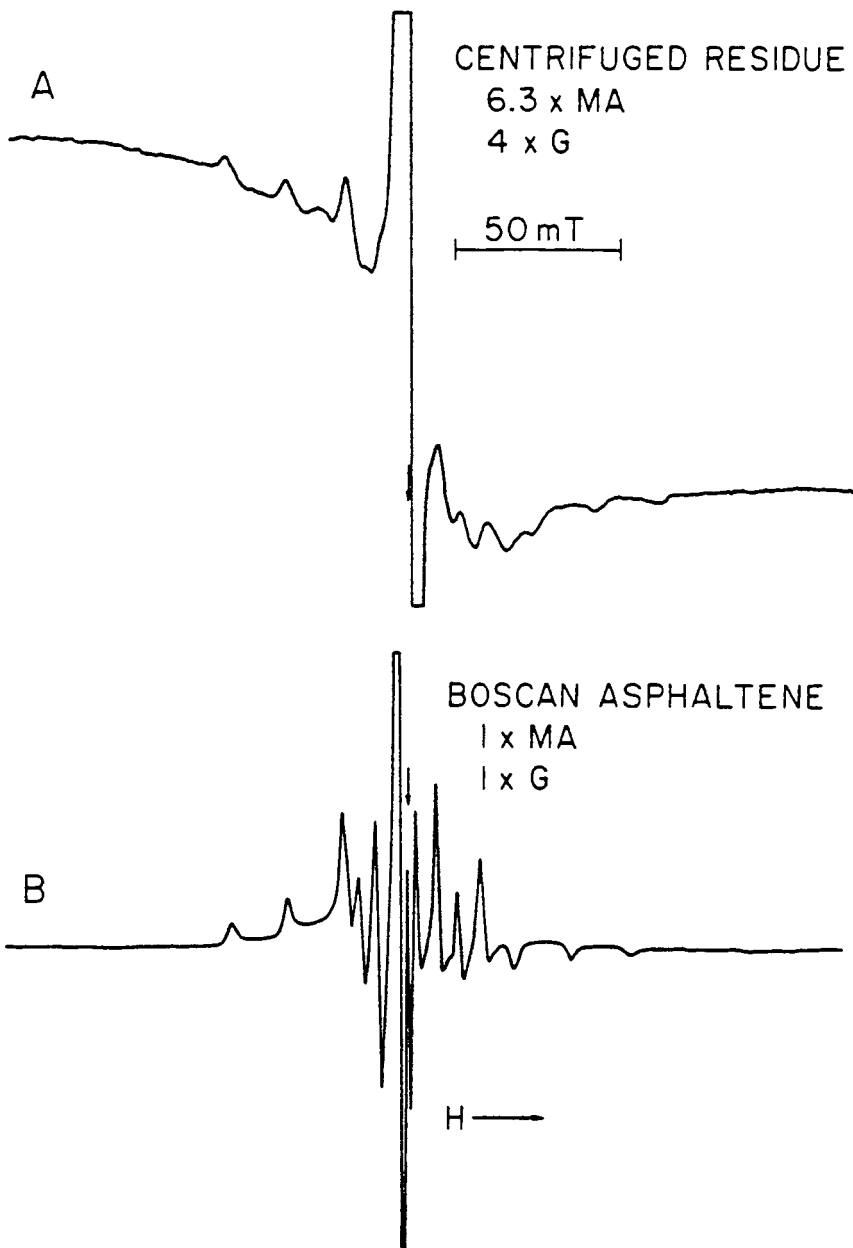


Figure 5. The EPR spectrum of (a) acid treated CMR and (b) Boscan asphaltene.

TABLE III

EPR PARAMETERS FOR VO^{2+} IN P. R. SPRING CMAR^a AND VARIOUS MINERALS

Sample	g_{\perp}	g_{\parallel}	A_{\perp} (mT)	A_{\parallel} (mT)	Reference
P. R. Spring C <small>MA</small> R	1.9928	1.9432	7.26	18.51	Present work
Boscan asphaltene	1.9861	1.9598	5.93	17.30	Present work
Etioporphyrin I	1.987	1.948	5.61	17.48	19
Etioporphyrin II	1.9823	1.9590	6.13	17.17	21
Mg^{2+} -hectorite (5% VO^{2+})			7.1	19.4	22
- Al_2O_3	1.989	1.916	7.08	18.12	23
SiO_2	1.982	1.922	7.72	19.51	23

a. Centrifuged mineral residue.

ACKNOWLEDGMENTS

The authors express their thanks to Dr. J. F. Branthaver for supplying tar sand samples and for useful discussions. The research has been supported by the TCU Research Fund and in part by The Robert A. Welch Foundation.

LITERATURE CITED

- (1) Clementz, D. M., *J. Petrol. Technol.*, **29**, 1061 (1977).
- (2) Malhotra, V. M. and Graham, W. R. M., *Bull. Amer. Phys. Soc.*, **28**, 202 (1983).
- (3) Ignasiak, T. M., Kotlyar, L., Longstaffe, F. J., Strausz, O. P. and Montgomery, D. A., *Fuel*, **62**, 353 (1983).
- (4) Malhotra, V. M. and Graham, W. R. M., "Characterization of P. R. Spring (Utah) Tar Sand Bitumen by the EPR Technique: Free Radicals", *Fuel*, in press (1983).
- (5) Painter, P. C., Coleman, M. M., Jenkins, R. G., Whang, P. W. and Walker, P. L., *Fuel*, **57**, 337 (1978).
- (6) Chester, R. and Elderfield, H., *Sedimentology*, **9**, 5 (1967).
- (7) Van der Marel, H. W. and Beutelspacher, H., "Atlas of Infrared Spectroscopy of Clay Minerals and Their Admixtures", Elsevier, NY (1976).
- (8) Olnuma, K., *Amer. Miner.*, **50**, 1213 (1965).
- (9) Chester, R. and Elderfield, H., *Chem. Geol.*, **7**, 97 (1971).
- (10) Griscon, D. L. and Marquardt, C. L., *Proc. Third Lunar Sci. Conf., Geochim. Cosmochim. Acta Suppl. Vol. 3*, pp. 2397-2415 (1972).
- (11) McBride, M., Pinnavata, T. J. and Kortland, M. M., *Amer. Mineral*, **60**, 66 (1975).
- (12) Malhotra, V. M. and Graham, W. R. M., "The Origin of Mn^{2+} Spectrum in Pittsburgh No. 8 Bituminous Coal", submitted to *Fuel* (1983).
- (13) Shepherd, R. A. and Graham, W. R. M., "EPR and FTIR Study of Metals in the Bitumen and Mineral Components of Circle Cliffs, Utah Tar Sand", accompanying paper.
- (14) Watkins, D. R. and Roberts, G. E., *J. Petrol. Technol.*, **35**, 865 (1983).
- (15) Olivier, D., Vedrinc, J. C. and Pegerat, H., *Bull. Grpe, Fr. Argiles*, **27**, 153.
- (16) Angell, B. R. and Hall, P. L., *Proc. Int. Clay Conf.*, Madrid, pp. 47-60 (1973).
- (17) Angell, B. R., Cutler, A. H., Richards, K. and Vincent, W. E. J., *Clays Clay Miner.*, **25**, 381 (1977).
- (18) Goodman, B. A., *Clay Minerals*, **13**, 351 (1978).
- (19) O'Reilly, D. E., *J. Chem. Phys.*, **29**, 1188 (1958).
- (20) Tynan, E. C. and Yen, T. F., *PREPRINTS, Div. of Petrol. Chem., ACS*, **12**, 1489 (1967).
- (21) Tynan, E. C. and Yen, T. F., *J. Mag. Res.*, **3**, 327 (1970).
- (22) McBride, M. B., *Clays Clay Miner.*, **27**, 91 (1979).
- (23) Van Reigen, L. L. and Cossee, P., *Disc. Faraday Soc.*, **41**, 277 (1966).

SYMPOSIUM ON CHARACTERIZATION AND CHEMISTRY OF OIL SHALES
PRESENTED BEFORE THE DIVISIONS OF FUEL CHEMISTRY AND
PETROLEUM CHEMISTRY, INC.
AMERICAN CHEMICAL SOCIETY
ST. LOUIS MEETING, APRIL 8 - 13, 1984

SHALE OIL UPGRADING: EFFECT OF CATALYTIC HYDROTREATMENT
ON NITROGEN COMPOUND TYPES

By

S. A. Holmes and L. F. Thompson

Western Research Institute, P. O. Box 3395, University Station, Laramie, Wyoming 82071

INTRODUCTION

Inspection of the chemical composition of different shale oil feedstocks has become of increasing importance to the refiner by providing an indication of the oil's utilization potential as a fuel and/or petrochemical feedstock. Different retort processes applied to oil shale from different sources produce feedstocks requiring different upgrading conditions. Knowledge of the chemical composition of the retorted shale oil provides insight for selecting upgrading conditions. A summary of work recently presented (1) emphasizes the importance of determining chemical composition:

- i) the method of retorting has a minor effect on the hydrocarbon composition of syncrude from the same shale source;
- ii) retorting has a marked effect on the shale oil boiling range and on elemental nitrogen distribution;
- iii) boiling range end-point is a key control to catalyst activity; and
- iv) hydrogen consumption and catalyst performance are predictable from feed inspections.

Because nitrogen content is high (1.5 to 2.2 wt %) in retorted shale oil, it must be significantly reduced (<50 ppm) for use as a transportation fuel to meet environmental standards and to minimize storage instability problems. Catalytic hydrotreatment may be better optimized for nitrogen removal if nitrogen-containing compounds are known. Hydroprocessing Australian and Colorado shale oil showed that the nitrogen compound types in material boiling greater than 496°C were more difficult to remove than those in material boiling below 496°C, although hydrogen consumption increased (1). The rate of removal of three-ring hetero compounds was less than that for two-ring hetero compounds. Highly alkyl-substituted nitrogen-containing species were more difficult to remove than less alkyl-substituted species (2).

Differences in severity of hydrotreating conditions have been found to affect relative hydrodenitrogenation reactivities of nitrogen-containing compounds. For example, hydrotreating Green River shale oil over a wide range of temperature and hydrogen pressure over a cobalt-molybdena catalyst, investigators (3) found that hydrodenitrogenation of pyridine types was faster than pyrrole types at lower temperature and pressure but that the converse occurred at more severe temperatures >440°C and pressures >13.8 MPa.

In the present studies, nitrogen compound-type distributions in shale oils produced by direct retorting (direct-heat mode) and hydrotreating of eastern and western U. S. oil shales were determined by characterization techniques. Differences in the distribution of nitrogen types in catalytic hydrotreated oils and in the retorted oils provided information as to relative hydrodenitrogenation reactivities of different nitrogen types under hydrotreating conditions. A method for predicting the extent of catalytic hydrotreatment as a function of the nitrogen-type composition in the retorted shale oil is presented.

SHALE OIL PROCESSING

The retorted shale oils studied in this work had been produced by direct retorting or hydrotreating. Shale oils from Green River Formation oil shale of western Tertiary (Eocene) age produced by direct retorting (4) using Paraho, Geokinetics, or Occidental technologies and by hydrotreating using the Institute of Gas Technology (IGT) Hytort technology (5) were studied. Shale oils from the Kentucky New Albany and Sunbury oil shale of eastern Devonian and Mississippian age produced by hydrotreating using IGT Hytort technology were also studied.

The upgraded shale oils studied had been processed from the retorted oils by catalytic hydrotreatment. The hydrotreating conditions employed in upgrading Occidental, Paraho, Geokinetics and the IGT Hytort oils are shown in Table I. Shale oils from direct retorting were hydrotreated

over nickel-molybdena catalysts at similar hydrogen pressures (10.4 MPa). Space velocities (LHSV) were about 1.0 except for Sohio hydrotreatment in which the LHSV < 0.6. In the hydrotreatment of Occidental oil, the catalyst temperature was increased resulting in greater hydrogen consumption and nitrogen reduction. The hydrotreating conditions used in the LETC-2 process removed 68% of the nitrogen content in the Occidental oil, but a relatively lower temperature in the LETC-3 process removed 80% of the nitrogen content in the Paraho oil. Because Sohio hydrotreatment recycled the residuum, unreactive nitrogen compound types in the higher-boiling residuum were concentrated in the hydrotreated oil (6). A higher temperature and lower space velocity than that employed in the LETC-3 process were necessary to achieve 80% nitrogen reduction in the Paraho oil.

TABLE I
HYDROTREATING CONDITIONS USED IN UPGRADING SHALE OILS
USING NICKEL-MOLYBDENA CATALYSTS

Source	Process		LHSV	Temperature, °C	H ₂ Pressure, MPa	H ₂ Con- sumption, kmole/m ³	Nitrogen Removal, %
	Retort	Hydro- treating					
Green River	Occidental	LETC-1 ^a	1.0	350	10.4	7.5	51.7
Green River	Occidental	LETC-2	1.0	399	10.4	9.0	67.5
Green River	Paraho	Sohio ^b	<0.6	406	10.4	12.0	79.7
Green River	Paraho	LETC-3	1.0	385	10.4	8.3	80.3
Green River	Occidental	LETC-4	1.0	413	10.4	9.4	83.4
Green River	Geokinetics	LETC-5	1.1	413	10.4	9.8	80.6
Green River	Hytort-1	HTC-6 ^c	0.4	428	13.8	36.2	80.1
Sunbury	Hytort-2	HTS-8	0.4	437	13.8	36.7	83.4
New Albany	Hytort-3	HTNA-3	0.6	426	13.9	25.0	85.6

a. LETC processing utilized bench-scale equipment without residuum recycle at the Laramie Energy Technology Center.

b. Standard Oil of Ohio commercially hydrotreated 11622 m³ of oil and recycled about 1:3 residuum to fresh feed.

c. IGT processed the Hytort oils using a bench-scale catalytic hydrotreating unit without residuum recycle.

Shale oils retorted by IGT Hytort were also hydrotreated over nickel-molybdena catalysts. Significantly higher catalyst temperatures and hydrogen pressures and lower space velocities were used to achieve 80 to 86% nitrogen reduction in these oils. As expected of retorted oils having high aromatic content, hydrogen consumption significantly increased during the production of the hydrotreated oil.

CHARACTERIZATION TECHNIQUES

The results of the nitrogen compound-type distributions presented were determined by the following characterization techniques and discussed in detail in earlier work (7-9). The determination of nitrogen compound types in retorted and hydrotreated shale oils involved chromatographic and spectrometric techniques. The chromatographic procedure resulted in little compound alteration with good material recovery. It was also flexible--having applicability to samples of different aliphatic and aromatic content. The chromatographic procedures incorporated basic alumina adsorption chromatography of the whole shale oil followed by silica gel chromatography of one or more complex fractions generated by the alumina chromatography. Different adsorbent activities, sample loadings and solvent gradients were employed depending upon aromatic content of the shale oil. Several fractions generated from an oil often contained similar compound types which were differentiated by using spectrometric techniques. Each fraction was analyzed by infrared spectroscopy and mass spectrometry. ¹H and ¹³C NMR spectrometry were also utilized in the later stages of the work. Total nitrogen was measured by chemiluminescence detection and basic nitrogen was determined by differential potentiometric titration analysis.

NITROGEN COMPOUND-TYPE DISTRIBUTIONS

Approximately 90% of the nitrogen content in retorted whole shale oil was classified as

one of four nitrogen types: amides, pyridines, pyrroles and hindered pyridines. Amides include compound types such as alkyl-substituted hydroxypyridines, benzamides, oxazoles, anilides and acetylpyrroles. Pyridines include alkyl-substituted pyridines, quinolines and acridines. Pyrroles include alkyl-substituted indoles, carbazoles, diazaromatics and benzocarbazoles. Hindered pyridines are represented by pyridine-type compounds that have alkyl substitution sterically hindering the nitrogen atom. The above nitrogen types also include the respective alicyclic analogs. The remaining 10% of the nitrogen content was distributed in arylamines, nitriles and piperidines and also included losses associated with irreversible adsorption and sample drying during chromatography. Because these latter compound types are also formed as reaction intermediates during hydrotreatment, they are not discussed.

The amounts of major nitrogen types in six retorted and five hydrotreated shale oils are listed in Table II. The distribution of types is somewhat different in oils produced from Green River shale by the first four listed retorting processes. Amide-type nitrogen ranges from 0.97 wt % in the Paraho oil to 0.31 wt % in the Hytort-1 oil. Pyridine-type nitrogen ranges from 0.85 wt % in the Geokinetics oil to 0.32 wt % in the Hytort-1 oil. However, considerably larger amounts of nitrogen in pyrroles and hindered pyridines are found in the Hytort-1 oil than in any of the oils produced by direct retorting. The oils produced from the Sunbury and New Albany shales by Hytort-2 and Hytort-3 contain greater amounts of pyrrolic nitrogen than do the oils from the Green River shale.

TABLE II
DISTRIBUTION OF NITROGEN COMPOUND TYPES IN RETORTED AND
HYDROTREATED SHALE OILS

Process	Total in Sample	Wt % Nitrogen Compound Types			
		Amides	Pyridines	Pyrroles	Hindered Pyridines
<u>Retorted Oils</u>					
Paraho	2.19	0.97	0.77	0.23	0.15
Geokinetics	1.70	0.32	0.85	0.24	0.15
Occidental	1.51	0.38	0.63	0.22	0.13
Hytort-1	2.20	0.31	0.32	0.69	0.66
Hytort-2	1.95	0.25	0.33	0.83	0.31
Hytort-3	1.93	0.33	0.28	0.83	0.24
<u>Hydrotreated Oils</u>					
LETC-1	0.73	0.082	0.245	0.089	0.175
LETC-2	0.49	0.026	0.172	0.086	0.132
Sohio	0.44	0.032	0.157	0.143	0.098
LETC-3	0.42	0.009	0.128	0.123	0.113
LETC-4	0.25	0.025	0.063	0.049	0.076

The nitrogen-type distributions among the hydrotreated shale oils presented in the lower portion of Table II are also significantly different. With the exception of the oil from the LETC-3 process, total nitrogen contents in the oils decrease with increasing severity of hydrotreating conditions (Table I), but the distribution of amides, pyridines, pyrroles and hindered pyridines do not proportionally decrease. For example, the pyrrolic nitrogen in the Sohio and LETC-3 oils range from 0.143 to 0.123 wt % compared with 0.086 and 0.089 wt % for the LETC-2 and LETC-1 oils, respectively. However, total nitrogen removal was 80% during Sohio and LETC-3 hydrotreating compared with 68 and 52% nitrogen removal during LETC-2 and LETC-1 hydrotreatment. The nitrogen-type composition in the LETC-5 hydrotreated oil was not determined.

HYDRODENITROGENATION REACTIVITIES OF NITROGEN COMPOUND TYPES

As previously stated, amounts of different nitrogen types are not removed proportionally to the total nitrogen removal. On the basis of nitrogen removal in percent, Figure 1 shows the amounts of nitrogen removal for different compound types. For example, Sohio hydrotreatment removed about 80% of the nitrogen from the Paraho retorted oil, but it removed 97% of the amide-type, 80% of the pyridine-type, 50% of the pyrrole-type and only 36% of hindered pyridine-type

nitrogen. The nitrogen-type distribution assumes negligible interconversion of nitrogen compound types. This may not have been the case with LETC-1 or LETC-2 hydrotreatment. Actual increased amounts of hindered pyridine-type nitrogen was found in the LETC-1 and LETC-2 oils relative to that in the feedstock (Occidental retorted oil), probably from the buildup of reaction intermediates formed from partial hydrogenation of acridine or quinoline ring systems under mild hydrotreating conditions.

Differences in the amount of nitrogen removal for different nitrogen compound types resulting from hydrotreatment suggest that different compound types have different hydrodenitrogenation reactivities. Relative reactivities of the different nitrogen types expressed as percent nitrogen removal divided by 100 were determined from data used in Figure 1. These results for compound types in the Sohio, LETC-3 and LETC-4 oils are listed in the top portion of Table III. Only the results for these oils are listed because of similar total nitrogen removal (80 to 83%). Because oils were retorted and hydrotreated by different processes, each nitrogen type displays a range of reactivities. For data comparison, the average reactivity value was determined for each nitrogen type and normalized to that of the amide-type nitrogen (a relative value of 1.00 meaning the easiest nitrogen type to remove). Normalized values of reactivity are presented in the bottom portion of Table III. Results suggest amide- and pyridine-type nitrogens are relatively easy to remove, 1.00 and 0.876, respectively. Pyrrole-type nitrogen (0.637) is relatively more difficult to remove and hindered pyridine-type nitrogen (0.352) is the most difficult to remove. However, in the calculation of reactivity, one must not overlook possible contributions from nitrogen-type interconversions caused by hydrogenation. The hydrotreating conditions necessary for 80% nitrogen removal are suggested to minimize the amount of buildup of reaction intermediates.

TABLE III

RELATIVE HYDRODENITROGENATION REACTIVITIES OF NITROGEN COMPOUND TYPES IN OILS UNDER HYDROTREATING CONDITIONS FOR 80% NITROGEN REMOVAL

Hydrotreating Process	Compound Types			
	Amides	Pyridines	Pyrroles	Hindered Pyridines
Sohio	0.967	0.797	0.493	0.355
LETC-3	0.991	0.834	0.564	0.257
LETC-4	0.934	0.899	0.778	0.402
Average	0.964	0.843	0.612	0.338
Normalized Values ^a				
Sohio	1.00	0.824	0.510	0.367
LETC-3	1.00	0.842	0.569	0.259
LETC-4	1.00	0.963	0.833	0.430
Average	1.00	0.876	0.637	0.352

a. Reactivities relative to amide nitrogen which is the easiest nitrogen compound type to hydrodenitrogenate.

HDN FACTOR CALCULATIONS

The amount of nitrogen removal by catalytic hydrotreatment may be estimated from the nitrogen-type composition of the shale oil feedstock and hydrodenitrogenation reactivities. A hydrodenitrogenation (HDN) factor is determined for each nitrogen compound type by multiplying the normalized reactivity by the percent of total nitrogen for each compound type (i) as shown below:

$$\text{HDN Factor}_{(i)} = \frac{\text{Normalized Reactivity}_{(i)} \times \text{Percent of Total Nitrogen}_{(i)}}{100}$$

The summed HDN factor, which is the sum of individual HDN factors for the four different nitrogen compound types, suggests the degree of difficulty of nitrogen removal from a given feedstock during catalytic hydrotreatment.

The nitrogen compound-type distributions in six retorted shale oils are presented on the basis of percent of total nitrogen in the top portion of Table IV. Calculations of the HDN factors are presented in the bottom portion of Table IV. Summed HDN factors range from 0.747 to 0.830 for oils produced from Green River shale by direct retorting. However, these values are significantly different from that for the Hytort-1 oil (0.574) produced from Green River shale. The oils

produced from the Sunbury and New Albany shales by the Hytort-2 and -3 process have similar values (0.602 and 0.632) compared with that for the Hytort-1 oil.

TABLE IV
HDN FACTOR CALCULATIONS

Retorted Oils	% of Total Nitrogen					Total
	Amides	Pyridines	Pyrroles	Hindered Pyridines		
Paraho	44.3	35.2	12.8	6.8		99
Geokinetics	18.8	50.0	14.1	8.8		92
Occidental	25.2	41.7	14.6	8.6		90
Hytort-1	14.1	14.5	31.4	30.0		90
Hytort-2	12.8	16.9	42.6	15.6		88
Hytort-3	17.1	14.5	45.6	12.4		90

Retorted Oils	HDN Factors					Normalized Nitrogen Content ^a
	Amides	Pyridines	Pyrroles	Hindered Pyridines	Summed	
Paraho ^b						
Sohio	0.443	0.290	0.065	0.025	0.823	1.00
LETC-3	0.443	0.296	0.073	0.018	0.830	1.00
Geokinetics	0.188	0.438	0.090	0.031	0.747	1.29
Occidental	0.252	0.402	0.122	0.037	0.813	1.45
Hytort-1	0.141	0.127	0.200	0.106	0.574	1.00
Hytort-2	0.128	0.148	0.271	0.055	0.602	1.12
Hytort-3	0.171	0.127	0.290	0.044	0.632	1.14

- Nitrogen content for each retorted oil is normalized to the nitrogen content in the Paraho oil (2.19 wt % nitrogen).
- Normalized reactivity values from Table III used in the HDN factor calculations for the Paraho oil.

HDN FACTOR ANALYSIS

Relationships of the HDN factors generated from the nitrogen-type composition in a feedstock and the percent nitrogen removal under hydrotreating conditions were established. Because total nitrogen content affects percent nitrogen removal, the nitrogen contents in the retorted oils were normalized to that in the Paraho-retorted shale oil. These values are also presented in the bottom portion of Table IV. Summed HDN factors are adjusted for nitrogen content by multiplying by the normalized nitrogen content. The adjusted HDN factor for each oil feedstock is determined using the equation below.

$$\text{Adjusted HDN Factor} = \text{Summed HDN Factor} \times \text{Normalized Nitrogen Content}$$

Adjusted HDN factors for the oils were plotted versus nitrogen removal for different hydrotreating conditions. The resulting relationships are shown in Figure 2. Oils produced from Green River shale by direct retorting gave a nearly linear relationship ($r^2 = 0.934$) under moderate hydrotreating conditions. Oils produced by hydroretorting from either Green River or Sunbury and New Albany shales establish a different linear relationship ($r^2 = 0.988$) under severe hydrotreating conditions. In each case, about 80 to 86% nitrogen was removed.

Larger values of adjusted HDN factors indicate nitrogen compound-type compositions relatively more susceptible to hydrodenitrogenation. Smaller adjusted HDN factors for the hydroretorted oils suggest a nitrogen-type composition of more unreactive compound types compared with that in the oils produced by direct retorting. Greater amounts of more aromatic and sterically-hindered alkyl-substituted nitrogen compounds are present in oils produced by the Hytort process, particularly, greater amounts of pyrrole- and hindered pyridine-type nitrogen. During hydroretorting, a hydrogen atmosphere allows partial hydrogenation of unsaturated hetero compounds resulting in greater percentages of nitrogen in unreactive nitrogen compounds.

Using severe conditions, hydrotreatment of a Paraho oil removes an amount of nitrogen not defined by either relationship previously discussed. These data are shown in Figure 2.

Hydrotreatment of Paraho oil by LETC-3 or Sohio processes removes 80% of the nitrogen content under moderate conditions, but hydrotreatment under severe conditions, such as those used on the Hytort oils, removes 99% of Paraho oil's nitrogen content. The extent of nitrogen removal is very much dependent upon the conditions of catalytic hydrotreatment. Theoretically, a set of curves similar to those in Figure 2 could be generated for differently retorted oils subjected to different hydrotreating severity.

The relationships in Figure 2 may be used to estimate relative amounts of nitrogen removal from an oil feedstock under moderate or severe hydrotreating conditions. For example, Rockwell International recently produced six light oils from Ohio oil shale using different conditions of flash hydroprolysis temperatures and shale residence times (10). These hydroretorted oils differed in their nitrogen-type compositions. Adjusted HDN factors were calculated: 1.022 for an oil produced at a lower temperature (650°C) and 0.694 for an oil produced at a higher temperature (772°C). From the relationship generated by the Hytort data in Figure 2, the amounts of nitrogen removal estimated under severe hydrotreating conditions for upgrading the low and high temperature produced oils are 95 and 84%, respectively. ¹H and ¹³C NMR data indicated that the higher-temperature-produced oil contained about three times the amount of di- and polyaromatic compounds (22 mol %). A relatively greater aromaticity was also found in the nitrogen-containing compounds; the amount of quinolines was significantly greater than that of pyridines. It is expected that the more aromatic nitrogen compounds would be more difficult to hydrodenitrogenate.

SUMMARY

The ease of removing nitrogen from shale oil by catalytic hydrotreatment is dependent upon feedstock characteristics. Several characteristics related to nitrogen distribution which affect hydrodenitrogenation include the amount of nitrogen, nitrogen compound-type composition and distribution of nitrogen according to boiling point. Nitrogen compound-type distributions were significantly different in oils from eastern and western U. S. oil shales produced by direct retorting or hydroretorting.

This work has shown that the types of nitrogen compounds (functional group basis) display different hydrodenitrogenation reactivities. Upgraded oils studied had been hydrotreated over nickel-molybdena catalysts at moderate to severe temperatures <440°C and pressure <13.8 MPa. Reactivities of nitrogen compound types calculated at these conditions indicated that least to most difficult compound types to remove are, respectively: amides, pyridines, pyrroles and hindered pyridines.

The development of HDN factor analysis may allow estimation of the relative amount of nitrogen removal by catalytic hydrotreatment. HDN factors are calculated from nitrogen-type compositions of oil feedstocks and hydrodenitrogenation reactivity values. Adjusted HDN factors are dependent upon the source of the oil shale, retorting method of the oil shale and hydrotreating conditions. Nearly linear relationships result by plotting adjusted HDN factors versus nitrogen removal. Feedstocks hydrotreated by different conditions than described in this work may show different hydrodenitrogenation reactivities and the relationships of HDN factors and nitrogen removal may be different from those presented. Refinement of characterization techniques will better define nitrogen compound types resulting in improved HDN factor calculations. Compositional analyses of differently retorted and hydrotreated shale oils will provide additional data useful in the development of HDN factor analysis.

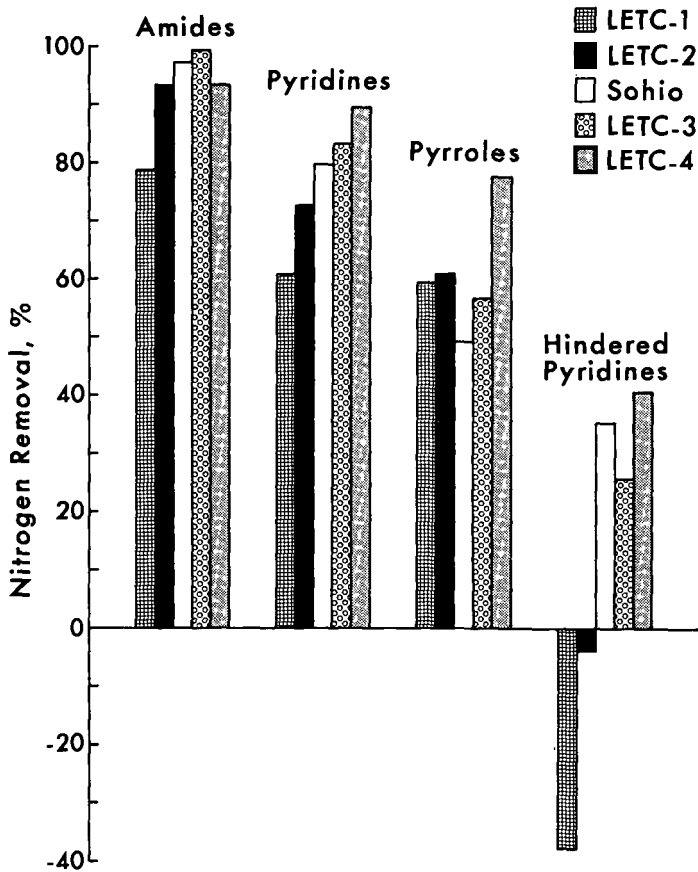


Figure 1. Nitrogen compound type removal by different hydrotreating processes.

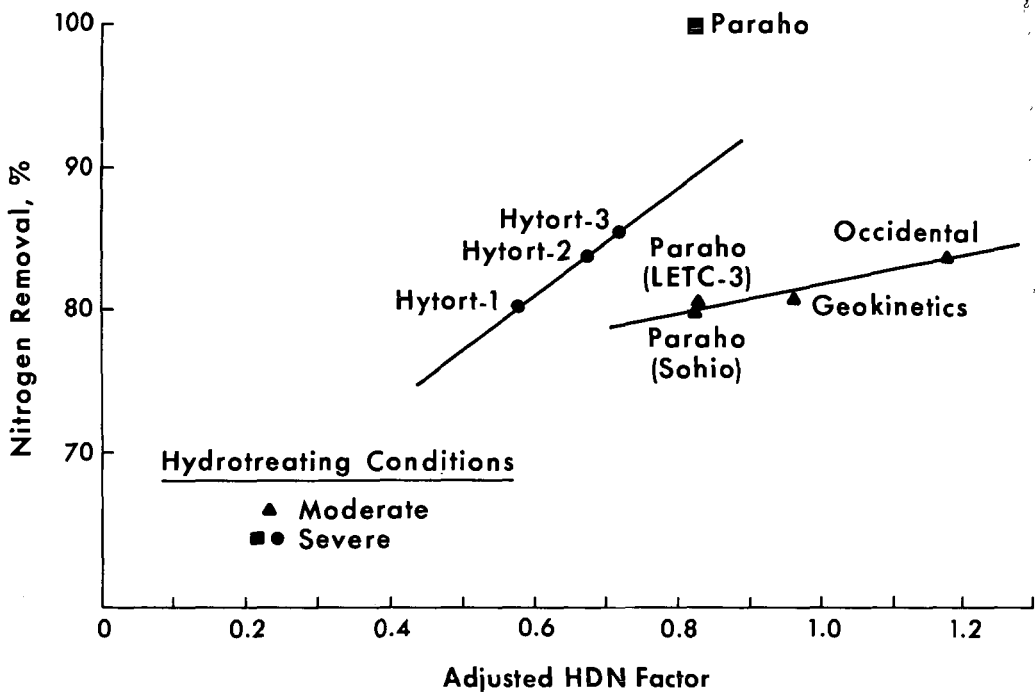


Figure 2. Relative ease of nitrogen removal from shale oils by catalytic hydrotreatment.

LITERATURE CITED

- (1) Hamner, G., Exxon Research, Baton Rouge, LA, private communication.
- (2) Drushel, H. V., Preprints, Div. of Analytical Chem., ACS, Anaheim, CA (1978).
- (3) Frost, C. M. and Jensen, H. B., PREPRINTS, Div. of Petrol. Chem., ACS, 18 (1), 119 (1973).
- (4) Smith, E. B., Laramie Energy Technology Center, private communication.
- (5) Weil, S. A., Proceedings of IGT Synthetic Fuels from Oil Shale Symp., 353, Atlanta, GA (1980).
- (6) Holmes, S. A. and Thompson, L. F., Fuel, 62 (6), 709 (1983).
- (7) Holmes, S. A. and Thompson, L. F., Proceedings, 1982 Eastern Oil Shale Symp., Lexington, KY (1983).
- (8) Holmes, S. A. and Thompson, L. F., Proceedings 14th Oil Shale Symp., Golden, CO, 235 (1981).
- (9) Holmes, S. A., Thompson, L. F. and Heppner, R. A., Proceedings 15th Oil Shale Symp., 424, Golden, CO (1982).
- (10) Falk, A. Y., Garey, M. P. and Rosemary, J. K., Report ESG-DOE-13406, Rockwell Internatl. Corp. (1983).

SYMPOSIUM ON CHARACTERIZATION AND CHEMISTRY OF OIL SHALES
PRESENTED BEFORE THE DIVISIONS OF FUEL CHEMISTRY AND
PETROLEUM CHEMISTRY, INC.
AMERICAN CHEMICAL SOCIETY
ST. LOUIS MEETING, APRIL 8 - 13, 1984

NITRIC OXIDE (NO) REDUCTION BY RETORTED OIL SHALE

By

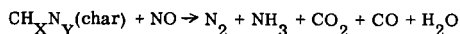
R. W. Taylor and C. J. Morris
Lawrence Livermore National Laboratory, Livermore, California 94550

INTRODUCTION

Oil shale, shale oil and retorted (spent) oil shale are rich in nitrogen. They contain 2 to 3 times as much nitrogen as found in coal, coal tar or coal char. Retorted oil shale contains char which can be burned. Some processes for recovering shale oil utilize the retorted shale as a fuel. The NO emission from the combustion of retorted shale has been measured by Lyon and Hardy (1) and by Taylor et al. (2). Lyon and Hardy's result suggests emissions of NO will probably exceed present standards for coal combustions (140 mg NO/MJ)*, but we found emissions of NO less than this value.

The concentration of NO and CO₂ in the exhaust gas as a function of time during the combustion of retorted shale in a fluidized bed has been reported (2). Only when the concentration of CO₂ decreased to 1/5 of its maximum value, signaling the end of char combustion, did the concentration of NO in the exhaust gas reach its maximum, as shown in Figure 1. The present work was initiated to explain this delay in NO emissions.

One explanation for the low NO emissions during most of the char combustion is that NO is reduced by the char. There are at least 5 possible products of this reduction as indicated by the following reaction:



Furusawa et al. (3) have found that coal char and activated petroleum coke reduce NO at elevated temperatures and they have measured the rates for the reduction reaction. They made the surprising discovery that char continues to reduce NO in the presence of oxygen even as the char is being consumed by oxidation. The principal products of the reaction at temperatures between 500 and 600°C were found to be N₂ and CO₂; above 775°C the concentration of CO exceeds CO₂ (4).

The object of the present work is to measure the rate of reduction of NO by retorted shale as a contribution to a general model of retorted shale combustion, leading to strategies for the control of NO emissions from retorted-shale combustors.

EXPERIMENTAL PROCEDURE AND RESULTS

Two kinds of experiments were performed to determine the rate of reduction of NO by retorted oil shale. In both kinds of experiments, NO, diluted in N₂, was passed through a shale bed and the decrease in NO concentration was measured. The rate was calculated from the transit (contact) time of NO through the bed. In one kind of experiment, the gas flow rate was held constant and the temperature was increased at a fixed rate. In the other experiments, the temperature was fixed and the gas flow rate was changed.

A fluidized bed was used both for the preparation of retorted shale and for reaction-rate measurements. It consisted of a silica-glass tube 4.2 cm inside diameter and 0.8 m long. The tube was mounted vertically inside an electric furnace. Preheated gas was passed upward through the tube. A perforated glass plate near the center of the tube retained the sample of crushed shale and distributed the gas flow. The sample of 104 L/Mg (24.8 gallons of oil per metric ton) shale came from Colorado tract C-a and had been crushed and sieved to a size distribution between 0.21 and 0.43 mm. A gas flow of approximately 3.5 L/min (STP) of nitrogen was sufficient to set the

* In the U. S. emission standards are written in units familiar to industry. For coal combustion, the NO_x standards are written in terms of pounds of NO₂ per 10⁶ Btu of fuel value in the coal, i. e., 0.5 lb NO₂/10⁶ Btu for new utility boilers. In metric units, this is equal to 140 mg NO/MJ. The standards are written in terms of NO₂ because NO is oxidized to NO₂ in the atmosphere.

100-g shale bed into a fluid like motion at a temperature of 500°C. Details of the bed are given in Table I.

TABLE I

Mass of raw shale bed	100.0 g
Mass of retorted shale bed	87 g
Organic carbon concentration (retorted)	2.9 wt %
Length of static bed	6.5 cm
Diameter of bed	4.2 cm
Volume of static bed (raw and retorted ^a)	90.0 cm ³
Shale density (raw)	2.22 g/cm ³
Shale density (retorted, calculated)	1.9
Bed void fraction (static, calculated)	0.50
Particle size range (diam.)	0.21 to 0.43 mm
Inlet concentration of NO	249 ppm

a. Particle size did not decrease with retorting; only the particle density decreased.

A 100-g sample of raw oil shale was retorted by heating it in flowing nitrogen to a temperature of 550°C at a rate of 25°C/min. The sample was kept at 550°C for 3 min and then cooled rapidly to room temperature in flowing nitrogen by opening the electric furnace. The retorted shale contained approximately 2.9 wt % organic carbon. The weight loss of the raw shale during retorting was 13%.

In all experiments, N₂ containing 249 ppm of NO was passed upward through the bed of retorted oil shale. The large amount of carbon (~3 g) and the low concentration of NO was planned to assure a nearly constant carbon concentration during each experiment. At the end of all the experiments, approximately 10% of the char could have been consumed.

The concentrations of NO and CO₂ in the gas stream from the reactor were measured by means of a mass spectrometer. The mass spectrometer was calibrated using purchased gas standards. Two standards for NO were purchased. When the mass spectrometer was calibrated by means of one standard, the concentration of NO in the other standard could be measured to within a few ppm.

In the first experiments, the temperature of the retorted shale was increased at the rate of 14.5 C/min in the NO-N₂ mixture flowing at 7.8 L/min (measured at 25° and 1 atm). At temperatures below approximately 175°C, the shale sample removed some of the NO from the gas stream by adsorption. As the temperature was increased above 175°C, the concentration of NO in the exit gas exceeded the inlet concentration of NO. At 200°C, the inlet and exit concentration were nearly equal and as the temperature was increased above 200°C, the concentration of NO decreased by reaction with the retorted shale as shown in Figure 2. The sample was again cooled to room temperature under pure N₂ and then reheated to 500°C at the same rate of heating and in the same gas mixture but at a flow rate of 4.9 L/min. A larger fraction of the NO was removed from the gas stream at the slower flow because of the 1.6 times longer period of contact between the solid sample and the gas.

In subsequent isothermal experiments using the same bed of retorted shale in the same apparatus, the temperature was held constant at various temperatures between 280°C and 400°C. The rate of flow of NO bearing N₂ gas through the bed was also kept constant. After measuring the exit gas concentration of NO at several flow rates, the temperature was changed and the process was repeated. In the course of these experiments, the bed was operated at a range of flow rates both below and above those required for fluidization. Whether or not the bed was fluidized made no discontinuity in the measured rate of reaction.

The effective rate constant (*k*) was evaluated at selected temperatures by the expression

$$k_{\text{eff}} (\text{s}^{-1}) = \frac{\ln \left[\frac{(\text{NO})_i}{(\text{NO})_o} \right]}{t}$$

where (NO)_i/(NO)_o is the ratio of the NO concentration into and out of the reactor and *t* is the actual transit time of the gas through the bed at temperature. The transit time was calculated from the bed volume, bed height and bed void volume (in a static, non fluidized condition, Table I), using the measured inlet gas flow rate and the bed temperature. The results of the nonisothermal experiments are given in Figure 3. Because the temperature of the reacting bed changes only about 5°C during the gas transit time, the nonisothermal experiments can be analyzed as a series of

isothermal experiments (Table II). The results of the isothermal experiments are given in Figure 4. The reaction rate from both the isothermal and nonisothermal experiments is plotted as a function of temperature on Figure 5. An average value of the rate as a function of temperature, the line in Figure 5, can be expressed as

$$k_{\text{eff}} (\text{s}^{-1}) = 4.0 \times 10^5 e^{-E/RT}$$

where E is 59.7 kJ/mole.

TABLE II

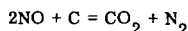
	Temperature of Fluidized Bed, °C								
	275	300	325	350	375	400	425	450	475
Flow = 7.8 L/min									
NO ^{out} , ppm	189	163	140	116	91	68	44	25	12
t, s	0.188	0.180	0.172	0.165	0.159	0.153	0.148	0.142	0.138
k, s ⁻¹	1.5	2.4	3.3	4.6	6.3	8.5	12	16	22
Flow = 4.9 L/min									
NO ^{out} , ppm	185	152	117	87	60	38	21	9	3
t, s	0.299	0.286	0.274	0.263	0.253	0.244	0.235	0.227	0.219
k, s ⁻¹	0.99	1.7	2.8	4.0	5.6	7.7	10	15	20

DISCUSSION

The results have been presented in terms of an effective rate constant for 87 g of a particular retorted oil shale. In order to make these results more general and to make comparisons to other measurements of NO reduction rates with other carbonaceous materials, it is necessary to take into account the amount and form of the agent effective in the NO reduction.

The principal reaction products of nitric oxide reduction by coal char are N₂ and CO₂ at temperatures from 502°C to 680°C. At 680°C, CO is also found and it becomes abundant at 775°C and the principal reaction product at 910°C, the maximum temperature investigated by Furusawa et al. (4).

We measured the concentration of CO₂ in the exit gas expecting to verify the principal NO reduction reaction as



However, the exit gas concentration of CO₂ was at most 45 ppm. This maximum concentration was found at the maximum temperature investigated (475°C), when all the NO flowing into the bed was reacted.

It appears possible that the principal agent for NO reduction by retorted oil shale at temperatures below 500°C is the hydrogen in the char. Oil shale retorted at 500°C contains a char of the approximate composition CH_{0.4}N_{0.07}. The coal char used by Furusawa et al. (4) had the composition CH_{0.17}N_{0.007}. The oil shale char used in this investigation has approximately twice the hydrogen concentration and ten times the nitrogen concentration of this coal char.

Furusawa et al. (4) measured the rate of reduction of NO by coal char in a packed bed reactor where the transit time was calculated from the "effective" length of the bed and the superficial gas velocity. The bed used was a mixture of inert aluminosilicate particles and char particles both approximately 0.6 mm in diameter. The "effective" length is the length of bed due to the char particles alone. The coal char contained 26% ash and it is not clear how this was taken into account. Retorted oil shale is also a mixture of "inert" silicate and carbonate minerals with char. The mixture is on a scale much smaller than the particle size; each particle contains many mineral particles and many zones or particles of char.

To calculate the effective residence time, Kunii, Wu and Furusawa (5) used the equation

$$Z = \frac{M_c}{\rho_b F}$$

where M_c is the mass of char, ρ_b is the bulk density of a pure char bed and F is the flow rate.

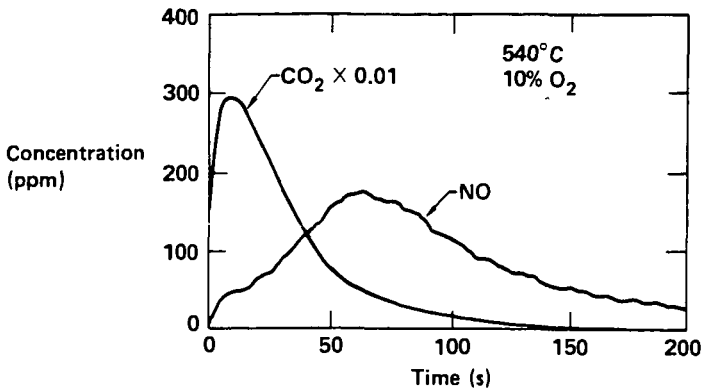


Fig. 1: Concentrations of CO₂ and NO as a function of time during the batch combustion of retorted Tract C-a oil shale in a fluidized bed.

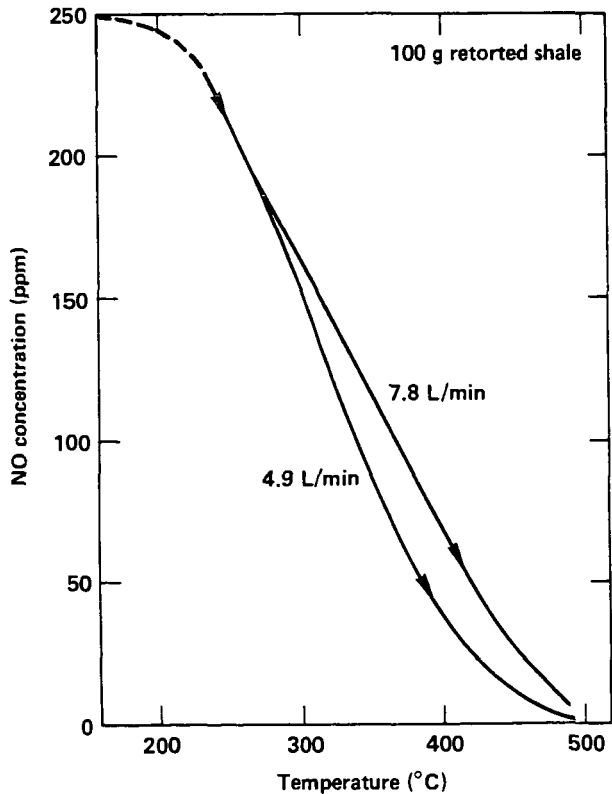


Fig. 2: Concentration of NO in the exit of a fluidized bed of retorted oil shale showing the removal of NO as the bed is heated (heating rate 14.5°C/minute). Inlet NO concentration, 249 ppm.

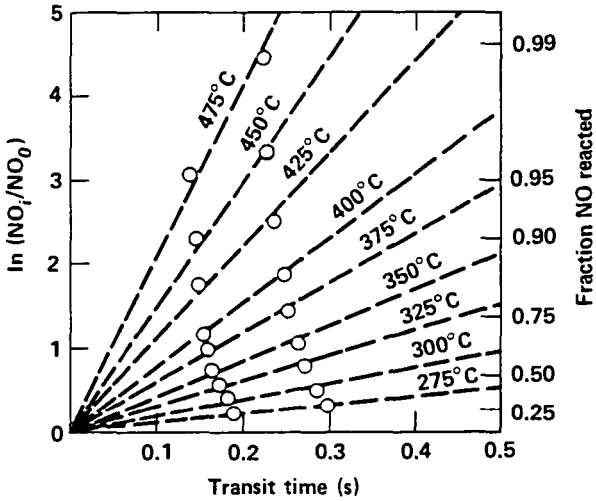


Fig. 3: Reduction of NO concentration as a function of transit time and temperature. The slope of these lines is equal to the reaction rate constant for the case of a constant rate of heating.

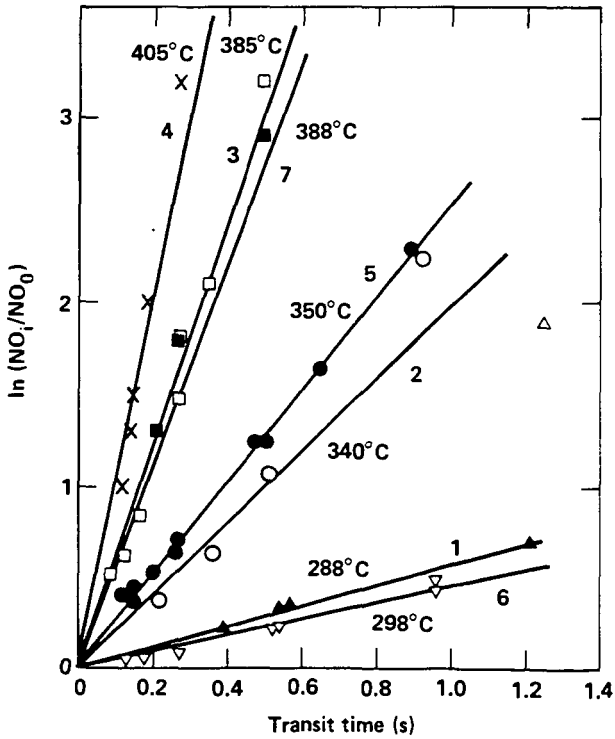


Fig. 4: Transit time (t) vs. $\ln(NO_0/NO_i)$ for isothermal experiments. The number on each line is the sequence in which the experiments were conducted.

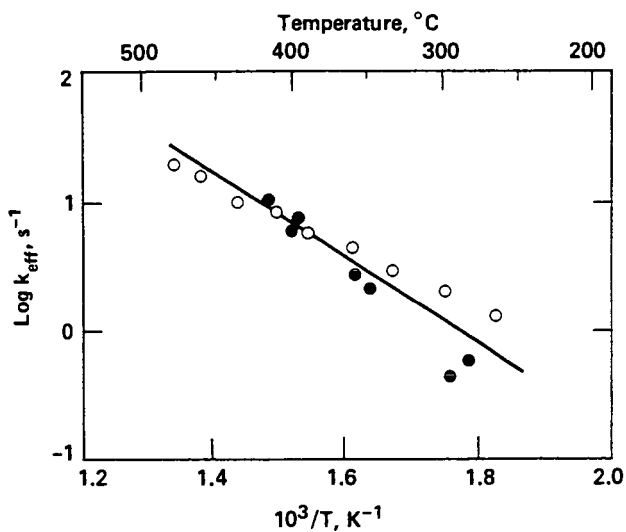


Fig. 5: Arrhenius Plot of effective rate constant for reduction of NO by retorted oil shale. The solid circles represent the results from heating the retorted shale bed at a constant rate; the open circles show the results when the bed was kept at the same temperature until a constant NO concentration was observed in the exit gas.

Using the same definition to calculate an effective residence time in our experiments results in residence times only 1/25 as long as those we used above, hence, a rate constant 25 x larger. Using this larger rate constant for comparison, we find that oil shale char is 10^3 times more reactive for NO reduction than is coal char.

An alternate approach for comparison is to convert the rate to units used by Chan, Sarofim and Beer (6) who show an Arrhenius plot indicating agreement of their results with those of Furusawa et al. We have not been able to make this comparison with certainty because of a confusing difference in units, but our preliminary comparison indicates oil shale char is $> 10^3$ times more reactive than the Montana Lignite Char used by Chan et al. While previous work (7, 8) has demonstrated that oil shale char is more reactive also towards oxidation and gasification than is coal char, the greater reactivity of oil shale char towards reduction of NO is more dramatic.

The reason for the greater activity is unknown. It may be due in part to the higher hydrogen content of oil shale char. The char in retorted oil shale (7) has a specific surface area of $\sim 360 \text{ M}^2/\text{g}$ which is similar to that of the coal char used by Chan et al. (6). However, the oil shale char may also be more accessible. Retorted oil shale is 97 wt % ash and contains 20 volume % interconnected porosity. The char in retorted oil shale is probably distributed primarily along these pores because they were created when the shale was retorted by the loss of volatile carbonaceous material. Thus, the char in retorted oil shale may be more available for NO reduction than char particles prepared by coal pyrolysis. Also, the great excess of ash in retorted oil shale may provide catalytic sites. Finally, we must not overlook the possibility that the NO is not reduced by char alone, but by some other reducing agent in the retorted shale, for example, iron-bearing minerals.

LITERATURE CITED

- (1) Lyon, R. K. and Hardy, J. E., "Combustion of Spent Shale and Other Nitrogenous Chars", *Combustion and Flame*, 51, 105 (1983).
- (2) Taylor, R. W., Morris, C. J. and Burnham, A. K., "Nitric Oxide Emissions from the Combustion of Retorted Shale", Lawrence Livermore Natl. Lab., Report under preparation (1983).
- (3) Furusawa, T., Kunii, D., Tsujimura, M. and Tsunoda, M., "Calcined Lignite and In Situ Formed Char as Catalysts for "NO" Reduction by Reducing Gases", *Proc. Int. Conf. Fluid. Bed Combustion*, 7 (1), 525 (1983).
- (4) Furusawa, T., Kunii, D., Oguma, A. and Yamada, N., "Rate of Reduction of Nitric Oxide by Char", *Internatl. Chem. Engineering*, 20 (2), 239 (1980).
- (5) Kunii, D., Wu, K. T. and Furusawa, T., "NO_x Emission Control From a Fluidized Bed Combustor of Coal. Effects of In Situ Formed Char on "NO" Reduction", *Chem. Eng. Sci.*, 35, 170 (1980).
- (6) Chan, L. A., Sarofim, A. F. and Beer, J. M., "Kinetics of the NO-Carbon Reaction at Fluidized Bed Combustor Conditions", *Combustion and Flame*, 52, 37 (1983).
- (7) Burnham, A. K., "Reaction Kinetics Between CO₂ and Oil Shale Residual Carbon". 1. Effect of Heating Rate on Reactivity, *Fuel*, 58, 285 (1979).
- (8) Sohn, H. Y. and Kim, S. K., "Intrinsic Kinetics of the Reaction Between Oxygen and Carbonaceous Residue in Retorted Oil Shale", *Ind. Eng. Chem. Process, Des. Dev.*, 10, 550 (1980).

SYMPOSIUM ON CHARACTERIZATION AND CHEMISTRY OF OIL SHALES
PRESENTED BEFORE THE DIVISIONS OF FUEL CHEMISTRY AND
PETROLEUM CHEMISTRY, INC.
AMERICAN CHEMICAL SOCIETY
ST. LOUIS MEETING, APRIL 8 - 13, 1984

SELECTED ASPECTS OF CATALYTIC REFINING OF MIDDLE DISTILLATES
FROM ATHABASCA SYNCRUDES

By

M. F. Wilson and J. F. Kriz

CANMET, Energy Research Laboratories, Department of Energy, Mines and Resources
555 Booth Street, Ottawa, Ontario K1A 0G1, Canada
and

I. P. Fisher

Gulf Canada Ltd., 2489 North Sheridan Way, Sheridan Park, Ontario L5K 1A8, Canada

INTRODUCTION

The two existing commercial processes for upgrading Athabasca bitumen use delayed coking and fluid coking, and produce synthetic crudes which are low in paraffins and relatively high in aromatics and naphthenes. The problems of producing specification transportation fuels from these feedstocks have been discussed in earlier reports (1, 2). In previous work, middle distillates from delayed coking of bitumen were catalytically refined by severe hydroprocessing using conventional hydrotreating catalysts. The aromatics conversion to naphthenes was monitored using C^{13} NMR analysis and the kinetics of hydrogenation was elucidated together with the effects of thermodynamic equilibria (2).

The present work deals with hydroprocessing of middle distillates from fluid coked bitumen and uses low resolution mass spectrometry to provide compositional analyses of the fuel products generated. The mass spectrometric method determines differences in reactivity of aromatic and saturated compound types including the effects of thermodynamic equilibria and cracking. Cetane numbers of fuel products were determined by engine tests and the relationships obtained between aromatic content and cetane rating are compared with previous results obtained for refined distillates from a delayed coking process.

EXPERIMENTAL

The feedstock used in this study was a middle distillate fraction from a synthetic crude produced by fluid coking of Athabasca bitumen. Table I presents properties of the feedstock. A commercial $NiO-WO_3/\gamma-Al_2O_3$ catalyst (Katalco Sphericat NI-550), tested in a previous study, was used for hydroprocessing the feed (2, 3).

A detailed description of the semi-pilot plant hydrotreating system is given in an earlier report (2). The experimental runs were carried out using 70 grams of catalyst in 100 cc of reactor volume. The catalyst was sulfided at 380°C and atmospheric pressure by passing a mixture of 10% H_2S in hydrogen over the bed for 2 hours. The volume of H_2S passed was equivalent to eight times the amount of sulfur required for the formation of sulfides. The continuous flow reactor was operated in the up-flow mode, the liquid feed and hydrogen were mixed, passed through a pre-heater and then over the fixed bed of catalyst. The unit was run for 8 hours on oil before the first steady-state sample was taken. Experimental runs were performed at temperatures of 340-440°C, liquid space velocities of 0.75 to 2.00 hr^{-1} and a hydrogen flow rate at STP of 530 L hydrogen per L of feedstock (3000 scf/bbl). All runs were at a pressure of 17.3 MPa (2500 psig). The reactor system was maintained at steady-state conditions for 1 hr prior to and 2 hrs during the period in which product was collected.

Compositional analysis of the feedstock and hydrotreated products was performed by low resolution mass spectrometry using a modification of the method of Robinson (4). The samples were run on a CEC 103 mass spectrometer. The aromatic carbon content was determined by C^{13} NMR analysis using a Varian SL-200 spectrometer. Sulfur content was analyzed by the Wickbold technique and carbon, hydrogen and nitrogen analysis was carried out using a Perkin Elmer 240B analyzer.

Cetane numbers were determined on a standard Cooperative Fuels Research (CFR) test engine using a constant compression ratio method.

TABLE I

PROPERTIES OF MIDDLE-DISTILLATE FEEDSTOCK FROM SYNTHETIC CRUDE A
(FLUID COKED BITUMEN)

Relative density, 15/15°C	0.862
Carbon	87.2 wt %
Hydrogen	11.7 wt %
Sulfur	97 ppm
Nitrogen	37 ppm
Average molecular weight	200
% Aromatic carbon by C ¹³ NMR	16.9
Cetane number (CCR method)	31
Distillation (D86)	
IBP°C	163
5%	183
10%	192
20%	210
50%	251
90%	296
FBP	318

RESULTS AND DISCUSSION

Hydrocarbon Compositions and Effects of Processing

The chemical characteristics of middle distillates from the Athabasca syncrudes are significantly different from those of conventional crudes. This is a consequence of the unique oil sands compositions and the upgrading processes employed. The mass spectrometric method used in this work allows the identification of a number of distinct hydrocarbon group types and the amount of each group type found in a particular fuel is a function of the feedstock source and processing conditions.

Table II shows compositional analyses of middle distillates from two Athabasca syncrudes produced by fluid and delayed coking of bitumen and designated A and B, respectively. Also included are compositions of products from secondary hydrotreating of the above distillates from this and previous work. The distillates are from approximately the same boiling range (2, 3).

TABLE II

COMPOSITIONAL ANALYSES (MASS %) OF MIDDLE DISTILLATES FROM
ATHABASCA SYNCRUDES BEFORE AND AFTER SECONDARY HYDROTREATING
(Experimental Conditions: 380°C, 17.3 MPa, LHSV 0.75)

	<u>Synthetic Crude A</u>	<u>Product from A</u>	<u>Synthetic Crude B</u>	<u>Product from B</u>
	Fluid Coked Bitumen with Primary Hydrotreating	Secondary Hydrotreating of Distillate from A (this work)	Delayed Coked Bitumen with Primary Hydrotreating	Secondary Hydrotreating of Distillate from B (2,3)
Paraffins	15.8	19.5	26.4	27.2
Total Cyclo paraffins	42.4	79.3	48.9	69.6
Non-condensed				
monocycloparaffins	20.5	39.2	24.5	32.2
Condensed				
dicycloparaffins	14.4	28.3	16.8	26.3
polycycloparaffins	7.5	11.8	7.6	11.1
Total Aromatics	41.9	1.3	24.8	3.1
Alkylbenzenes	17.3	-	11.3	0.9
Benzocycloparaffins	12.9	0.5	8.7	1.3
Benzodicycloparaffins	5.2	0.6	2.6	0.6
Naphthalenes	3.5	0.2	1.6	0.3
Naphocycloparaffins	1.6	-	0.1	-
Fluorenes	1.0	-	0.5	-
Triaromatics	0.4	-	-	-
Cetane Number	31	42.5	36	45

A comparison of distillates from syncrudes A and B shows some important differences in their chemical compositions. Syncrude A (from fluid coking) yields distillate which is significantly lower in paraffins (15.8%) than that from B (26.4%). (Distillate from A is also marginally lower in total cycloparaffins.) The aromatic contents of the two distillates are also significantly different with distillate from A having an amount which is approximately 17% higher. To some extent, this may be attributed to differences in severity of primary hydrotreating. These major differences in chemical composition are reflected in the cetane numbers 31 and 36 for A and B, respectively.

A comparison in Table II of products from the syncrudes after secondary hydrotreating (this work together with earlier results) shows almost complete elimination of aromatics under the given processing conditions and these results confirm previous analysis by C^{13} NMR. Both products show a marginal increase in paraffins which indicates some cracking, possibly ring scission of cycloparaffins.

An examination of the aromatic hydrocarbon group types in Table II shows major contributions from 4 predominant species in syncrude distillates (alkylbenzenes, benzocycloparaffins, benzodicycloparaffins and naphthalenes). The saturation of these species is, therefore, the major contributing factor in cetane improvement. Figure 1 shows summarized chemical changes for conversion of some of the aromatic group types to their corresponding naphthenes. This work also demonstrates that such reactions are controlled by thermodynamic equilibria.

In previous work, where C^{13} NMR was used to monitor the effects of changing experimental conditions on aromatics conversion, plots of aromatic carbon content vs. reaction temperature were made, the processing effects were "mapped out" with changing LHSV and optimum operating conditions were established (2, 3). In the present work, some of the implicit relationships between the kinetic and thermodynamic equilibrium effects (including cracking) are resolved by separately mapping out the individual hydrocarbon group types.

Figure 2 shows the effect of change of LHSV on the mass % of alkylbenzenes in product from secondary hydrotreating of syncrude A distillate over the complete temperature range. A series of smooth, round, almost symmetrical curves is obtained showing a minimum at 380-400°C. Above this temperature, the effect of thermodynamic equilibrium is observed as the concentration of alkylbenzenes increases again. It is assumed that cracking occurring under these processing conditions for this equilibrium reaction is not significant.

On the other hand, Figure 3, which is a similar plot for saturation of benzocycloparaffins, produces a series of v-shaped curves which show a marked loss of roundness above 380°C. Figure 3 may be linked with Figure 4 which shows corresponding plots for conversion of benzodicycloparaffins (see Figure 1). In this case, it is clear that extensive cracking during this particular equilibrium reaction occurs above 400°C and the curves pass through a maximum at 420°C. It is assumed that, in this high temperature range, ring scission in a 3-ring structure occurs with the generation of a corresponding 2-ring species.

Mass spectrometric analysis also suggests that some cleavage of two-ring structures occurs under extreme processing conditions. Figure 5 shows plots of condensed dicycloparaffin mass % vs LHSV over the complete temperature range. As expected, the curves produced are more or less the mirror image of Figure 3 (the corresponding plots for benzocycloparaffins) and pass through a maximum at 370-380°C as a result of the equilibrium shift. The curves indicate that, although the dicycloparaffins seem reasonably stable for most of the observed conditions, some cracking is likely at low space velocities (0.75 and 1.00) and at higher temperatures (crossing of curves in Figure 5). Figure 6 is a similar plot for the condensed polycycloparaffins in which case extensive cracking is observed at temperatures as low as 360-380°C. These reactions may be important for fuel quality improvement by ring opening of naphthenes.

Effect of Aromatic Content on Fuel Ignition Quality

Figure 7 shows a plot of % aromatic carbon content (determined by C^{13} NMR) versus cetane number for fuel products produced by secondary hydrotreating of distillates from syncrudes A and B under different conditions of temperature and LHSV. These plots reveal the processing severities required to produce fuels which meet the current Canadian diesel ignition specification (cetane number 40).

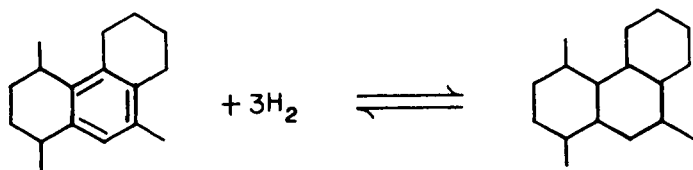
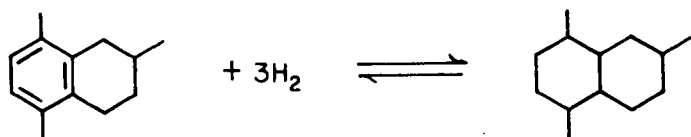
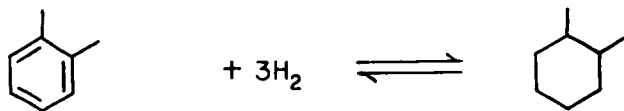
The curvature of these graphs has been attributed to the presence of very stable aromatic species which would appear to have a markedly adverse effect on diesel ignition quality (3).

The plots indicate qualitative differences between syncrudes A and B. For any level of aromatic content, the syncrude produced by delayed coking shows better cetane rating. Most likely, it is a consequence of the higher paraffin content in this feedstock.

SUMMARY

Secondary hydrotreating was performed on a middle distillate from a syncrude produced by fluid coking of Athabasca bitumen and products were analyzed by low resolution mass spectrometry.

1. MONOAROMATIC REDUCTION TO SATURATES



2. DIAROMATIC REDUCTION

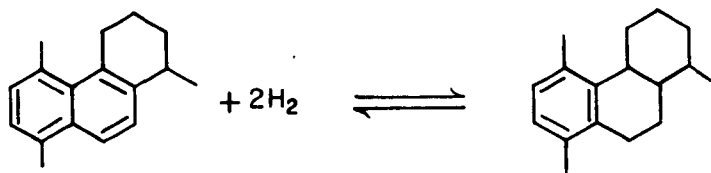
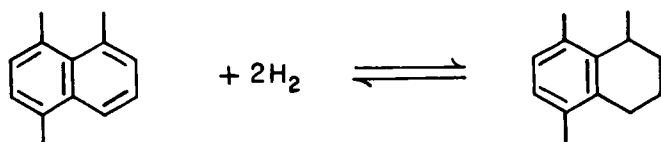


FIGURE 1. SUMMARIZED CHEMICAL CHANGES DURING HYDROTREATING OF MIDDLE DISTILLATES FROM SYNTHETIC CRUDE.

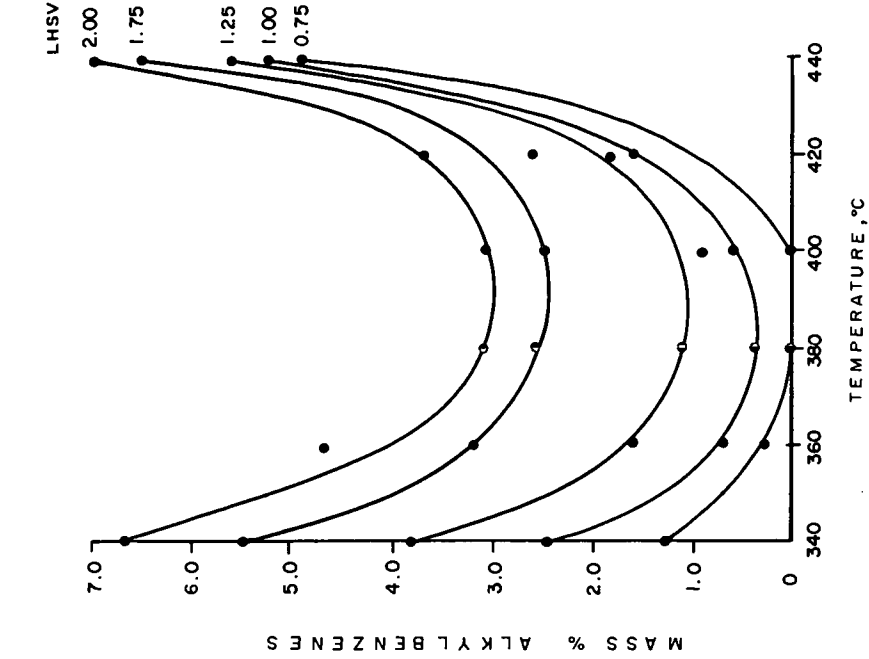


FIGURE 2. EFFECT OF LHSV ON SATURATION OF ALKYL BENZENES IN DISTILLATE FROM SYNCRUDE A (17.3 MPa).

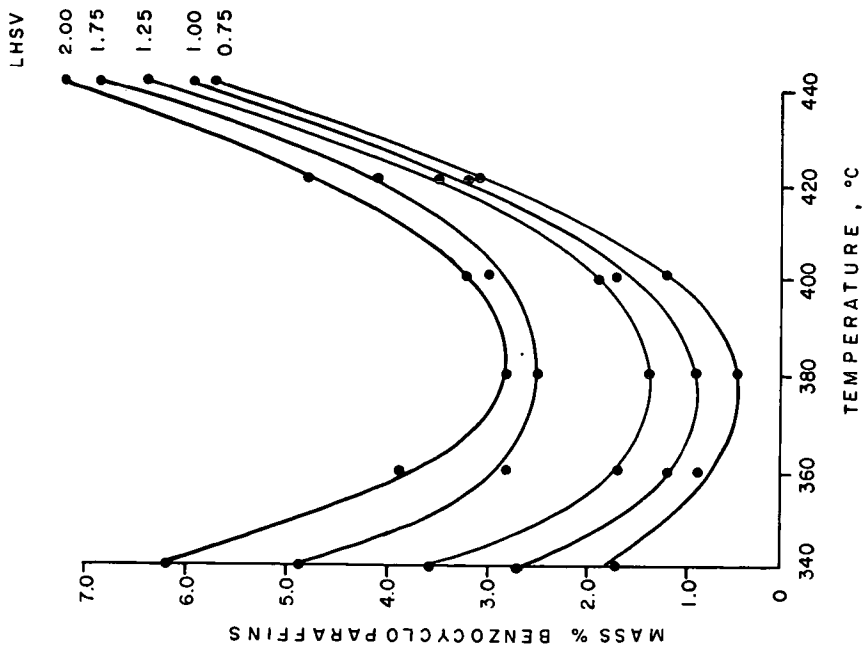


FIGURE 3. EFFECT OF LHSV ON SATURATION OF BENZOCYCLOPARAFFINS IN DISTILLATE FROM SYNCRUDE A (17.3 MPa).

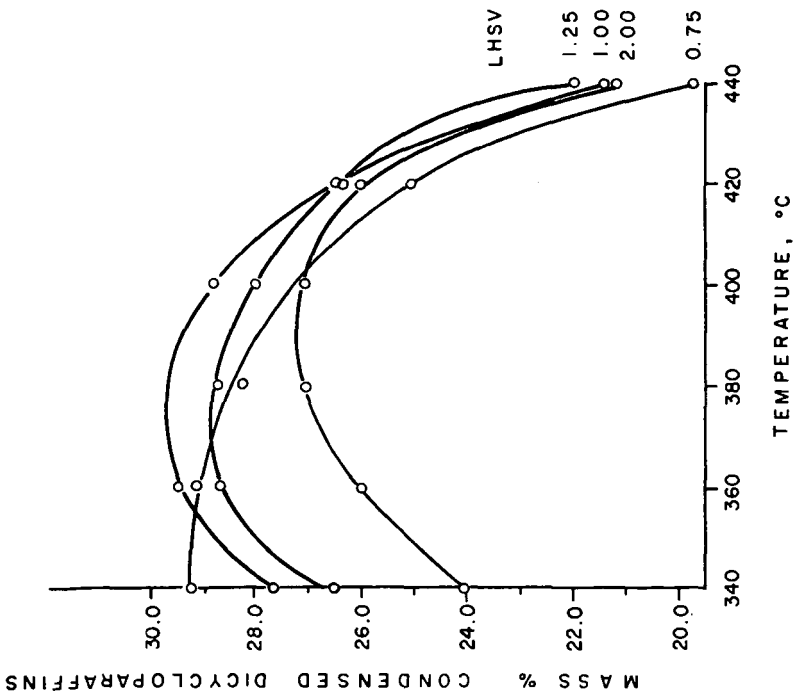


FIGURE 5. FORMATION AND DEHYDROGENATION OF CONDENSED DICYCLOPARAFFINS. EFFECT OF LHSV. (SYNCRUDE A DISTILLATE).

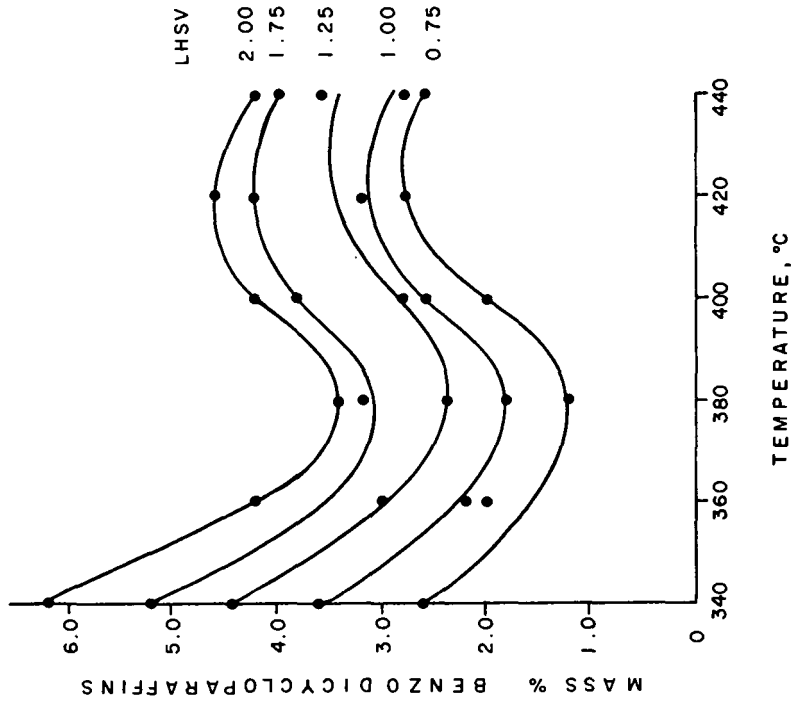


FIGURE 4. EFFECT OF LHSV ON SATURATION OF BENZODICYCLOPARAFF. IN DISTILLATE FROM SYNCRUDE A (17.3 MPa).

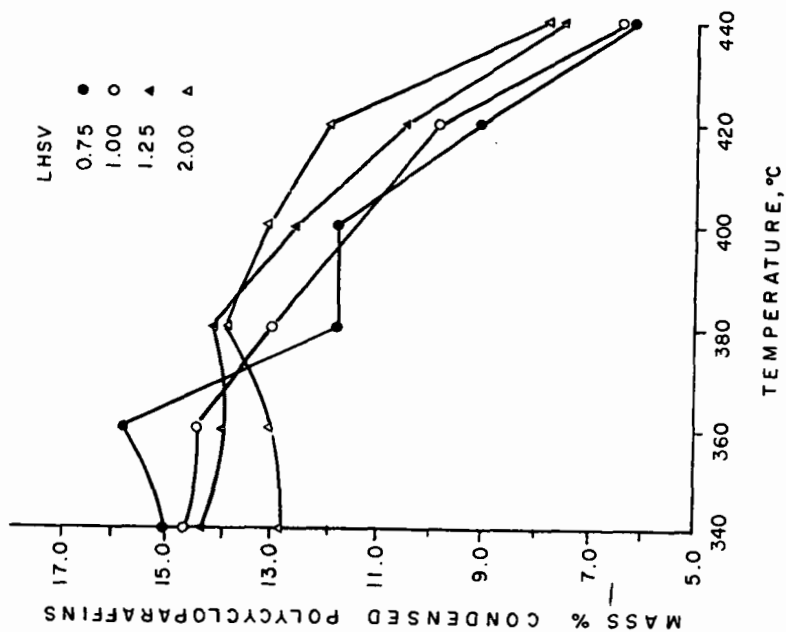


FIGURE 6. DEHYDROGENATION AND CRACKING OF CONDENSED POLYCYCLOPARAFFINS. EFFECT OF LHSV. (SYNCRUDE A DISTILLATE).

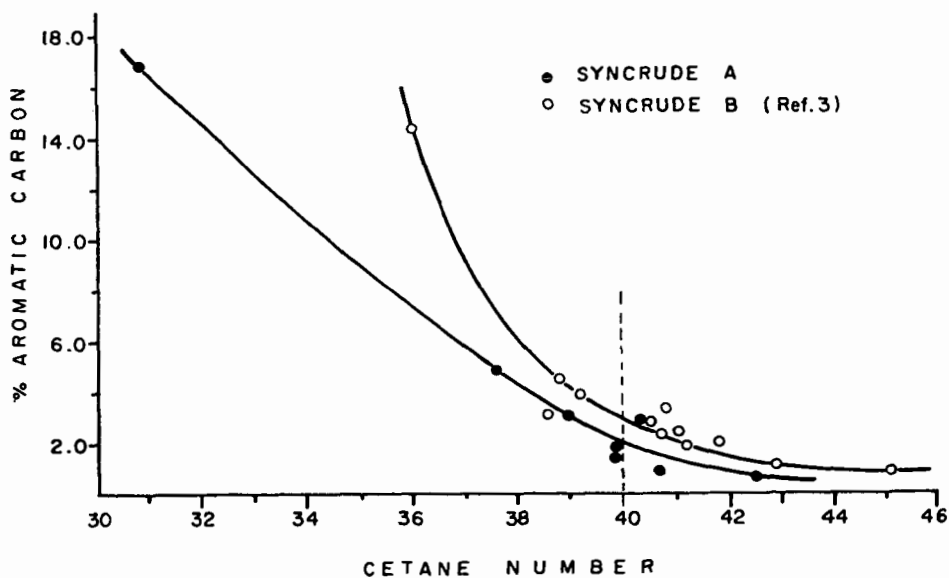


FIGURE 7. PERCENT AROMATIC CARBON (C^{13} NMR) VS. CETANE NUMBER FOR HYDROTREATED DISTILLATES FROM SYNCRUDES A AND B.

The processing effects on several hydrocarbon group types were "mapped out" in terms of temperature and LHSV. It was concluded that alkylbenzene and benzocycloparaffin saturation is accompanied by a minimum of cracking but for the equilibrium reaction involving saturation of benzodicycloparaffins, cracking was observed above 400°C at all space velocities. The cracking of polycycloparaffins was also found to be extensive by examining the corresponding plots for these hydrocarbon group types.

The effects of aromatic content on fuel ignition quality of the two syncrudes were compared. Although the trends were remarkably similar, consistent differences in quality were observed throughout the range.

ACKNOWLEDGMENTS

The authors wish to thank M. Stolovitsky for performing hydrotreating experiments, G. de Boer for mass spectrometric analyses and Professor G. W. Buchanan, Carleton University, Ottawa for C^{13} NMR determinations. We also thank N. Kallio of the National Research Council for cetane engine tests and the Alberta Research Council, Syncrude Canada Ltd. and Suncor Inc. for samples of synthetic crude oil.

LITERATURE CITED

- (1) Wilson, M. F., CANMET Report 82-2E, "Impact of Excessive Aromatics in Oil Sand Syncrudes on Production and Quality of Middle Distillate Fuels", (1981).
- (2) Wilson, M. F. and Kriz, J. F., "Upgrading of Middle Distillate Fractions of Syncrudes From Athabasca Oil Sands", PREPRINTS, Div. Petrol. Chem., ACS, 28, 640 (1983).
- (3) Wilson, M. F. and Kriz, J. F., Fuel, accepted.
- (4) Robinson, C. J., Anal. Chem., 43, 1425 (1971).

SYMPOSIUM ON CHARACTERIZATION AND CHEMISTRY OF OIL SHALES
PRESENTED BEFORE THE DIVISIONS OF FUEL CHEMISTRY AND
PETROLEUM CHEMISTRY, INC.
AMERICAN CHEMICAL SOCIETY
ST. LOUIS MEETING, APRIL 8 - 13, 1984

MORTALITY, MORBIDITY AND OTHER NIOSH HEALTH RELATED STUDIES OF
OIL SHALE WORKERS

By

J. Costello

Division of Respiratory Disease Studies, National Institute for Occupational Safety and Health
Morgantown, West Virginia 26505

INTRODUCTION

At the time of the conception of the NIOSH shale oil studies, oil prices were going up and there was renewed interest in synfuels, especially shale oil. Originally, most of oil shale extraction work was done on a demonstration project basis with a small work force (1). Then Union Oil Company of California and the COLONY project (2) of TOSCO and Exxon began commercial scale projects in shale oil production on the Colorado plateau. With an unfavorable change in the business climate, the Colony project was dropped and the Union Oil Company project was delayed. Union is now expected to go into production shortly. Thus, health considerations of exposure to kerogen become important. Three completed NIOSH studies involving this synfuel will be discussed. These include a mortality study, a case-control study and a morbidity study. In addition, two new studies involving shale oil will be presented.

METHODS

The first study to be done was the mortality study (3). The universe from which the sample was drawn was estimated to be about 800 people. The basis for this list was three employee groups: a) 294 employees of the U. S. Bureau of Mines who worked at the Anvil Points Oil Shale Facility near Rifle, Colorado from 1948 to 1956; b) 135 employees who worked at the Anvil Points facility from 1966 to 1969 for the joint venture of the Colorado School of Mines Research Institute and Colony; and c) 15 men who worked from 1956 to 1959 at the Union Oil Retort Facility at Grand Valley, Colorado. Leads to additional workers in these groups resulted in a master list of 1215. From this master group, a non-random sample consisting of 713 white males who worked in mining, retorting, maintenance or supervisory jobs involving actual production of shale oil was chosen for mortality follow-up. Clerical workers, short-term (less than one month) personnel and employees for whom we had only names and no other data were excluded from the final cohort. Of the 485 living subjects of this cohort, 321 men and 4 women were examined in the morbidity study. Table I gives the breakdown of the 713 subjects by vital status.

TABLE I

FINAL COHORT

	<u>In Morbidity Study</u>	<u>In Mortality Study</u>
Known living	325	485
Known deceased		205
(a) Death certificates		(181)
(b) No death certificates		(24)
Vital status unknown		23
 Grand Totals	 325	 713

Mortality

Standard populations for determining expected deaths were: (a) all white males in the states of Colorado and Utah, and (b) all white males in the United States. Mortality statistics were averaged for the years 1968, 1969 and 1970 to calculate expected death rates. The U.S. population was used only for all causes to check for the "healthy worker effect". Standardized Mortality

Ratios (SMR) were calculated using a modified life table procedure. Death certificates were coded by a nosologist utilizing the Elghth Revision International Classification of Diseases Adopted for Use in the United States (4).

Case-Control

During the course of the mortality study, it was determined that 16 men died of cancer of the trachea, bronchus and lungs, and 15 men died of cancer of the digestive organs and peritoneum. In an attempt to clarify the effects of certain risk factors, namely smoking, radioactive exposure and metal mining exposure, a case-control study of 12 oil shale workers dying from respiratory cancer and 15 workers dying from digestive cancer was done. Two separate control groups were used: the first was composed of 27 oil shale workers who had died from diseases of the circulatory system and the second was composed of 27 living oil shale workers. Workers were matched as closely as possible on the basis of age, job classification and length of service in that job. Odds ratios were calculated by the method of Guy (5).

Morbidity

The third study, the morbidity study, was related to the mortality study in that the 485 known living survivors from the mortality study formed the basis for the morbidity study. 321 men and 4 women agreed to participate, for a participation rate of 67%. The balance of 160 workers were untraceable, had moved to distant points that were too costly to visit, or declined to participate. Coal miners at 3 Utah mines were used for comparison because they worked on the Colorado plateau, did not work with oil shale materials, were readily available and could be matched by age. However, they were exposed to coal mine dust, a well documented cause of respiratory symptoms. We considered other sources of controls in the region such as uranium miners, smelter workers, metal miners, etc., but rejected them because of confounding cancer risks which was our primary objective to evaluate among the oil shale workers. Thus, it was felt that coal miners were the best of a poor choice for the control population. Each worker was questioned about his work history, smoking history and information on medical problems and respiratory symptoms, the respiratory symptoms are to be reported in a separate paper later. A complete dermatological examination was given by certified dermatologists and sputum and urine cytologies were done. Only results of skin examination, sputum and urine cytologies will be reported here.

RESULTS

Mortality Study

Table II presents a listing of the SMR's for all causes and several specific causes of death utilizing Colorado-Utah white males as controls. We also show an SMR for all causes using all U. S. males as a control. Statistically significant increases in SMR's are seen for all malignant neoplasms and cancer of the colon. Nonstatistically significant increases are seen for cancer of digestive organs and peritoneum, cancer of respiratory organs and cancer of the trachea, bronchus and lungs. Statistically significant decreases are seen for all causes (U.S. control), diseases of the circulatory system and ischemic heart disease. The significant decrease in all causes may be a consequence of the "healthy worker effect" and is a common characteristic of working populations (6).

Smoking is always an item of interest when increased SMR's for respiratory and lung cancer are seen. Table III presents a summary of the smoking history data that was available for this cohort. Unfortunately, these data were only available for 325 living workers and 53 deceased workers. Smokers and ex-smokers account for 307 of the 378 men or 81.2% of this group. However, the value of 37.8% for smokers is a low prevalence for smokers in an industrial population (7).

Employment in the oil shale industry has been erratic and lengths of employment have varied from weeks to months. Length of employment is skewed towards short-term employment with a median of 9 months and an arithmetic average of approximately 30 months. Over 50% of the workers have 2 years or less employment in oil shale work. This limits the implications of oil shale exposure as a causative agent in the development of chronic disease.

Case-Control Study

Table IV is a breakdown of the various categories of smoking by disease. It is quite apparent that smoking is an important factor in lung cancer. Smokers account for all but one case of lung cancer in both the case group and the deceased control group. In digestive cancer, smokers account for the majority in both the case group and the deceased control group.

The results of the case control study are numerically illustrated in Table V. Looking at the results for lung cancer, we see elevated odds ratios for radioactive exposure in the study group versus both control groups. The values are 7.9 using the living control. We also see an elevated odds ratio for smoking using the living control. Unsurprisingly, the odds ratio is 1.1 for

smoking using the deceased control group. As smoking is suspected as being associated with various diseases of the circulatory system (8), there would be competition by both lung cancer and circulatory system disease with the end result being a depressed odds ratio for smoking. Metal mining exposure was not related to lung cancer in this case control study.

TABLE II
STANDARDIZED MORTALITY RATIOS

<u>Cause of Death</u>	<u>Observed</u>	<u>Expected</u>	<u>SMR</u>
All causes (U.S. control)	205	246	83 ^b
All causes (CO and UT control)	205	221	93
All malignant neoplasms	49	36	136 ^a
Digestive Organs and Peritoneum	15	10	150
Colon	7	3.1	226 ^a
Respiratory Organs	16	11	145
Trachea, bronchus and lung	16	10	160
Diseases of circulatory system	76	102	75 ^b
Ischemic heart diseases	55	72	76 ^a
Diseases of respiratory system	18	18	100
Accidents	18	15	120

a. Statistically significant, $p .05$

b. Statistically significant, $p .01$

TABLE III
SMOKING DATA

MORBIDITY COHORT + CASE CONTROL COHORT

<u>Smoking Status</u>	<u>Number</u>	<u>Percent</u>
Ex-smokers	164	43.4
Smokers	143	37.8
Nonsmokers	71	18.8
Total	378	100.0

Smokers + Ex-Smokers = 307 or 81.2%

TABLE IV
SMOKING
CASE CONTROL STUDY

<u>Disease</u>	<u>Category</u>	<u>Case</u>	<u>Living Control</u>	<u>Deceased Control</u>
Lung cancer	Smokers	11	6	10
	Ex- and nonsmokers	1	6	1
Digestive cancer	Smokers	9	2	11
	Ex- and nonsmokers	6	13	3

A similar situation exists for digestive cancer. Again, we see elevated odds ratios due to radioactive exposure except that while both ratios are elevated, the ratio using the deceased control group is much higher, 7.2 versus 2.2. As we are concerned with relatively small numbers, an increase of two people makes a large change in the results. Smoking shows an elevated odds ratio for digestive cancer in the living control group of 9.8 and a depressed odds ratio of 0.4 in the deceased control group. As smoking is known to be associated with circulatory disease deaths (see above reference) and since the cause of death for the deceased population was circulatory system problems, the low odds ratio in this control group is expected. Metal mining exposure seems to

have little influence as far as digestive cancer is concerned.

TABLE V
ODDS RATIO
CASE CONTROL STUDY

<u>Cause of Death</u>	<u>Exposure</u>	<u>Odds Ratio</u>	
		<u>Living Controls</u>	<u>Deceased Controls</u>
Lung cancer	Smoking	11.0	1.1
	Radioactivity	7.9	7.1
	Metal Mining	1.3	0.3
Digestive cancer	Smoking	9.8	0.4
	Radioactivity	2.2	7.2
	Metal Mining	-	1.1

In summary, the case-control study suggests that smoking and radioactive exposure have stronger association with lung and digestive cancers than does oil shale exposure in this population.

Morbidity Study

Table VI presents a brief summary of important presumed risk factors in the morbidity study. Although the study group and the control group are well matched for age, the oil shale workers had worked more time in other oil work, uranium mining and farming. In addition, the oil shale workers had spent more of their working time outdoors than the controls. Fewer of the oil shale workers were current smokers but despite this, their pack years were considerably greater. These imbalances of risk factors, coupled with the short duration of exposure to oil shale, make interpretation difficult.

TABLE VI
AGE, SMOKING, OCCUPATION AND OTHER VARIABLES FOR
THE OIL SHALE AND CONTROL GROUPS

	<u>Oil Shale</u>	<u>Control</u>
Number	325	323
Mean age (years)	56	56
% current smokers	28	37
Mean pack years	35	27
Mean years in oil shale work	6.0	0
Mean years in oil shale production work	2.9	0
Mean years in other oil work	1.3	0.1
Mean years in uranium mining	1.9	0.2
Mean years in other mining	2.0	29.8
Mean years in farming	3.4	2.5
Mean percentage of time spent at work out of doors over last 20 years	47	23
Mean percentage of time spent off duty out of doors over last 20 years	58	51

The mean of 6 years conceals a rather skewed distribution of work in oil shale; 50% of the oil shale group had worked less than 4 years. For work in oil shale production, the figures were 2.9 years for the mean and 1.3 for the median, with 90% having worked less than 8.4 years.

Sixteen men in each of the study group and control group were suspected as having one or more tumors. Most of the suspected tumors were biopsied; eight basal cell and two squamous cell carcinomas were found in the oil shale group. The latter four tumors were on the nose, face, neck and finger, respectively. The corresponding exposures for these four men were: two years as office manager in oil shale for the first; two years in oil shale as miner and foreman, but 19 years in uranium mining for the second; three years in oil shale as powderman and carpenter, but nine years processing uranium and vanadium plus 38 years in ranching for the third; and four years in oil shale

in mechanical design for the latter.

The results of the dermatological examinations are shown in Table VII. Oil shale workers have a higher mean number per person of pigment changes and keratoses and a higher percentage of persons having nevi and keratoses. The control population has a higher mean per person of nevi, telangiectasiae and papillomata and a higher percentage of persons having pigment changes, telangiectasiae and papillomata.

TABLE VII
SUMMARY STATISTICS OF DERMATOLOGICAL EXAMINATION FINDINGS

Entity	Mean Number Per Person		Percentage with Entity	
	Oil Shale	Control	Oil Shale	Control
Nevi	4.3	5.4	77	64
Pigment change	0.8	0.7	31	34
Telangiectasiae	18.5	22.0	80	83
Keratoses	3.0	1.9	43	37
Papillomata	1.7	1.9	45	47

A logistic regression model showed a significantly increased prevalence of actinic keratoses associated with oil shale exposure ($p < 0.01$). However, hyperpigmentation did not show a significant trend with oil shale exposure. As one would expect, both age and sun exposure were also significantly correlated with the presence of actinic keratoses; papillomata were correlated with age and both pigment changes and telangiectasiae were correlated with sun exposure. Leukoplakia was noted on the lips and oral mucous membranes of 10 oil shale workers and 14 controls. Table VIII presents the cytology findings for controls and oil shale workers by smoking group. Among smokers, the oil shale group had a higher proportion with metaplasia than the controls. This did not constitute a statistically significant difference, however, ($\chi^2 = 2.48$). Correction for age and pack years did not reduce the observed disproportion to any great extent. The ex-smokers showed a similar tendency to have a higher rate of metaplasia while the nonsmokers revealed the opposite effect, though again nonsignificantly ($\chi^2 = 0.58$). For dysplasia, both smokers and ex-smokers showed slight excesses among the oil shale workers but nonsmoking controls had about twice the prevalence as the oil shale group. Statistical significance was not achieved, however, ($\chi^2 = 1.98$).

TABLE VIII
PULMONARY CYTOLOGY BY SMOKING HABITS AND STUDY GROUP

	Normal Cytology		Metaplasia		Dysplasia		n		
	Oil Shale	Control	No Dysplasia		Oil Shale	Control	Oil Shale	Control	
			Oil Shale	Control					
Smokers	40	51	34	24	26	25	88	105	
Ex-smokers	45	51	31	26	24	23	143	117	
Nonsmokers	68	53	22	28	10	19	58	67	
	TOTALS						289 ^a	289 ^b	

a. Fewer than overall totals because of missing and unsatisfactory samples.

b. One additional control had an invasive malignancy.

A logistic model relating years of work in oil shale production to presence or absence of signs of metaplasia and dysplasia was fitted to the oil shale group, divided into current smokers and non-smokers. For metaplasia there was a positive relation with production work in both smoking groups ($p < 0.05$ for both) and the two coefficients were similar in magnitude. For dysplasia, both smoking groups showed a negative trend with years of exposure although these were both statistically significant. One rather strange result of these analyses is that age did not appear to be related to either metaplasia or dysplasia. In addition, pack years was not significantly associated with these two factors among the smokers.

In summary, actinic keratoses showed a significant and positive association with oil shale exposure after allowing for age, sunlight and other exposures. In addition, the prevalence of metaplasia was positively associated with years of oil shale production work.

NEW PROJECTS

NIOSH is currently involved in two new oil shale projects, a feasibility study of community-based occupational health registry of oil shale workers and an extension of a DOE mortality contract with the Institute of Occupational Medicine in Edinburgh, Scotland to identify survivors of Scottish Oils Ltd. for the determination of the prevalences of shale workers pneumoconiosis and skin tumors. This second project will also look at mineralogical characterizations and documentation of the mining and retorting processes utilized in the Scottish shale industry.

The feasibility study of a community-based registry has been awarded to the National Jewish Hospital and Research Center in Denver. With this contract, we hope to accomplish the following work:

1. Abstract medical records of cases of cancer diagnosed in the period 1979 through 1981 in the counties in planning region XI -- Garfield, Rio Blanco, Mesa and Moffat Counties. This information will be offered to the Colorado State Tumor Registry.
2. Design and initiate a protocol for pulmonary function studies and questionnaire data from oil shale workers and appropriate controls, which can be used as base line data toward a future registry. The design will address the need for longitudinal study of workers and controls, especially with regard to quality assurance and research needs for early detection of respiratory hazards in the industry. Stability of personnel dictates the involvement of local medical facilities with collaboration of the Preventive Medicine Department of the University of Colorado Health Sciences Center. The outcome of this objective will depend, in part, on whether company cooperation is obtained, since the design of the study changes substantially if access to the workforce at the work site is not possible.
3. Assess the feasibility of a worker registry in the oil shale industry, in cooperation with currently active Western Slope oil shale companies or, independent of them, in a community-based effort. If coordination with industry-based efforts proves possible, means for such coordination will be developed. Data collection in the respiratory evaluation in item 2 will be evaluated for use in a community-based registry. Success and obstacles encountered in conducting pulmonary evaluation will be assessed for their implications for a long term registry of oil shale workers. A system of record keeping will be developed in an appropriate institution in Garfield County.

To date, item 1, the cancer case abstractions, have been completed and the data have been turned over to the Colorado State Cancer Registry. The Garfield County Health Officer, Dr. Mary Jo Jacobs, has been working on local funding to continue this work. Item 2, the design and initiation of a protocol for pulmonary function studies, is progressing well. Procedures and questionnaires have been developed and tried out on a group of molybdenum workers at Leadville, Colorado. Final revisions are in progress. Item 3, an industry-supported registry has suffered a setback because of the business recession and abandoning or backing off of companies interested in the developing of shale oil. The loss of the combined Exxon-TOSCO project was a big blow to shale oil development in general.

The Scottish project involves workers who formerly worked for Scottish Oils Ltd., a commercial producer of shale oil, until it shut down in the middle 1950's. The Institute of Occupational Medicine is currently involved in a mortality study of these workers for DOE. NIOSH recommended that a morbidity study of shale workers' pneumoconiosis and skin lesions be done on the survivor group of this cohort.

As of the writing of this report, 1605 men have agreed to participate in the dermatology portion of the study and 1324 of these men have agreed to have chest X-rays taken. Presently, 978 men have completed dermatology questionnaires and the first part of the chest X-ray survey involving 585 men has been completed. The study is to be completed by October 1, 1984.

CONCLUSIONS

Standardized Mortality Ratios were calculated for a cohort of 713 oil shale workers who were employed primarily at the U. S. Bureau of Mines Anvil Points Oil Shale Facility at Rifle, Colorado, from 1947 through 1969. In addition, 325 living oil shale workers from the above cohort were examined in a morbidity study primarily aimed at dermatological changes. The following conclusions were generated from the data collected:

1. Oil shale workers appear to exhibit the "healthy worker effect". With one major exception, noted below, the SMR's for major disease classification have either been normal or less than normal.
2. Oil shale workers show decreased deaths for all causes and for diseases of the circulatory system including ischemic heart disease. They show no difference in SMR for diseases of the respiratory system and a slight, but not significant, increase for accidents.
3. Oil shale workers show a significant increase of malignant neoplasms particularly for the colon and less so for cancer of the trachea, bronchus and lung. In light of the several other

carcinogenic risk factors previously mentioned and investigated in the case-control study, it is difficult to implicate oil shale exposure, per se, as responsible for the increase in SMR for respiratory cancer and digestive cancer. The case-control study indicates a stronger association between these cancers and exposure to radioactivity and smoking than with exposure to oil shale.

4. The prevalence of actinic keratoses was associated significantly and positively with oil shale work exposure after allowing for age, sunlight exposure and other exposures.

5. The prevalence of metaplasia was positively associated with years of production work in oil shale.

ACKNOWLEDGMENTS

The author gratefully acknowledges the following persons who assisted in the morbidity study: Dr. John Burkart and Mr. Eugene Turner of UBTL for the collection of data; Drs. G. Kruger, J. Zone and W. Rom of the University of Utah for dermatologic services and medical expertise, and Mr. Michael Attfield of NIOSH for statistical analysis.

LITERATURE CITED

- (1) Costello, J. , Morbidity and Mortality Study of Shale Oil Workers in the United States, *Environ. Health Perspect* 30, 205-208 (1979).
- (2) Anonymous, Firms Begin Major Synfuels Studies, *The Oil and Gas Journal*, 41-42 (1981).
- (3) Costello, J. , Retrospective Mortality Study of Oil Shale Workers, 1948-1977, 13th Oil Shale Symp. Proceedings, CSM, Golden, Colorado, pp. 369-375 (1980).
- (4) U. S. Dept. of Health, Education and Welfare, 8th Revision Internl. Classification of Diseases, adopted for use in the U. S. , Washington, D. C. , Natl. Center for Health Statistics, Public Health Service Publication No. 1693 (1967).
- (5) Guy, W. A. , Contributions to a Knowledge of the Influence of Employments on Health, *J. Roy Stat. Soc.* 6, 197-211, 1843.
- (6) McMichael, A. J. , Standardized Mortality Ratios and the "Healthy Worker Effect", *Scratching the Surface*, *JOM* 18, 3, 165-168.
- (7) Ortmeier, C. E. , Costello, J. , Morgan, W. K. C. , Swecker, S. and Petersen, M. , The Mortality of Appalachian Coal Miners, 1963-1971, *Arch Environ. Health* 29, 67-72 (1974).
- (8) U. S. Dept. of Health, Education and Welfare, Smoking and Health, a Report of the Surgeon General, Washington, D. C. , U. S. Public Health Services, DHEW Publication No. (PHS)79-50066, pp. 4-1 through 4-76 (1979).

SYMPOSIUM ON CHARACTERIZATION AND CHEMISTRY OF OIL SHALES
PRESENTED BEFORE THE DIVISIONS OF FUEL CHEMISTRY AND
PETROLEUM CHEMISTRY, INC.
AMERICAN CHEMICAL SOCIETY
ST. LOUIS MEETING, APRIL 8 - 10, 1984

CHARACTERIZATION OF TRACE ELEMENTS IN AUSTRALIAN OIL SHALES

By

L. S. Dale, J. J. Fardy and G. E. Batley
CSIRO, Division of Energy Chemistry, Lucas Heights Research Laboratories
Lucas Heights. NSW. 2232. Australia

INTRODUCTION

Australia's most extensive oil shale deposits are located in the state of Queensland (Figure 1), where oil reserves exceed 2000 billion barrels (1). Much of this is of low oil yield and located at considerable depths. A number of deposits are, however, being studied for commercial development, including one at Julia Creek in the north-west part of the large Toolebuc formation containing a Cretaceous oil shale. On the eastern coast, the Condor, Rundle and Nagoorin deposits of Tertiary oil shales have estimated recoverable reserves of 8500, 2000 and 3000 million barrels, respectively (2-4).

The depositional environments of these oil shales are very different. The three eastern deposits appear to be dominated by Pediastrum and other planktonic algae inhabiting what was a shallow lacustrine environment (5), together with high concentrations (up to 50%) of humic material. Julia Creek oil shale was deposited in a marine environment and contains cyanobacteria and other marine algal species, with humic acid comprising only a very small percentage of the organic matter (6). Evidence for these differing origins may be reflected in the trace element contents of the kerogens where elements, such as arsenic which preferentially accumulates in marine algae (7), should be more abundant in the marine deposit.

The trace element content of an oil shale is, however, likely to be dominated more by the mineral matrix binding the kerogen, rather than kerogen-associated elements. These minerals also differ significantly between deposits; in Julia Creek shale, calcite and quartz predominate, whereas the Tertiary shales contain primarily claystone, limestone and sandstone. Comprehensive elemental analyses were, therefore, carried out on the raw shales, to characterize them and to indicate differences in the environmental impact that might be posed by the products of oil shale retorting.

The latter have been more fully investigated in measurements of the partitioning of trace elements between retort waters, shale oils, gases and spent shale. Products for these studies were generated using the Fischer Assay procedure which yields products similar to those of some commercial retorting processes and, thus, provides a comparative product assessment.

While atmospheric emissions of volatile elements, or the accumulation of others in shale oil or retort water, may be undesirable from environmental or processing viewpoints, a further problem is created by those elements remaining in the retorted shale. The retorting process will concentrate non-volatile elements in this residue, while transforming others into soluble species on pyrolysis of the associated organics. Leaching of trace elements from both spent and raw shale storage heaps may pose a further environmental problem, with leaching conditions in the sub-tropical climate of north Queensland quite different to those encountered in the U. S. Column leaching studies on raw and spent shales have been carried out to define the extent of the problem.

Multi-element techniques were applied to the analysis of raw shales, retorted shales, oil, retort waters and leachates. Spark-source mass spectrometry (SSMS) and instrumental neutron activation analysis (INAA) together provided data for 65 elements. More precise data for specific elements were obtained using inductively-coupled plasma emission spectrometry (ICP) and atomic absorption spectrometry (AAS).

EXPERIMENTAL

Bulk samples (1-2 kg) of raw shale, for use in Fischer retorting and leaching studies, were ground to -2 mm particle size and dried at 110°C for 17 h. For chemical analyses, samples were further ground, using a tungsten carbide mill, to -74 µm.

For INAA, 100-200 mg shale samples were irradiated for two days in a thermal neutron flux of $5 \times 10^{12} \text{ n cm}^{-2} \text{ s}^{-1}$ in the Australian Atomic Energy Commission HIFAR reactor. Retort

waters were analyzed after freeze drying, while oils were analyzed directly. High resolution gamma spectrometric measurements were made after cooling periods of 5-7 days and 28-40 days.

Spark-source mass spectrometric analysis of the oil shales was carried out using photo-plate detection for maximum element coverage. Lutetium was added as an internal standard to provide quantitative data. Retort waters were analyzed via this procedure after evaporation onto a graphite substrate.

For partitioning studies, shales were retorted under standard Fischer Assay conditions (8) and the product oil, water and spent shales analyzed for trace element content. Off-gas samples were collected, but not analyzed. Oils for analysis by ICP and AAS were first digested with sulfuric acid-hydrogen peroxide to decompose the organic matter.

Analytical methods were checked for accuracy using the USGS Green River Shale SGR-1 and Coady Shale SC0-1 samples.

Leaching of raw and spent shales (150 g) was carried out in 50 cm x 2.5 cm diameter glass columns under saturated conditions, using distilled water drawn through the bed at 0.5 mL min⁻¹ by a peristaltic pump. Leachates were analyzed by INAA and SSMS using the procedures followed for retort waters. Specific elements were analyzed by ICP and AAS. Dissolved organic carbon was measured on a Beckman Carbon Analyzer, while selected anions were determined using standard wet chemical procedures (9).

RESULTS AND DISCUSSION

Elemental Composition of Raw Shales

Analytical data for raw shales from the four Australian deposits are shown in Table I. For comparison, data for Green River shale (10) and a Devonian eastern U. S. shale (11) are also included. Although it was possible to quantify 65 elements, the tabulated data contain only those elements which most reflected the differences between deposits.

TABLE I
ELEMENTAL COMPOSITION OF RAW SHALES

	(Dry Basis: $\mu\text{g g}^{-1}$ except as shown)					
	Julia Creek	Condor	Rundle	Nagoorin	Green River (10)	Antrim (11)
C(Org)	15.0 \pm 0.1 (%)	10.3 \pm 0.1 (%)	15.4 \pm 0.1 (%)	30.4 \pm 0.1 (%)	26.2 \pm 2.6 (%)	10.0 (%)
C(Inorg)	7.2 \pm 0.1 (%)	0.7 \pm 0.1 (%)	0.8 \pm 0.1 (%)	0.5 \pm 0.1 (%)	3.05 \pm 0.31 (%)	-
Na	0.19 \pm 0.01 (%)	0.47 \pm 0.03 (%)	0.83 \pm 0.05 (%)	0.39 \pm 0.02 (%)	2.36 \pm 0.06 (%)	0.39 (%)
Mg	0.18 \pm 0.01 (%)	0.76 \pm 0.18 (%)	1.86 \pm 0.54 (%)	0.51 \pm 0.03 (%)	2.87 \pm 0.06 (%)	1.14 (%)
Al	0.61 \pm 0.07 (%)	6.79 \pm 0.35 (%)	5.73 \pm 0.32 (%)	3.86 \pm 0.22 (%)	3.41 \pm 0.06 (%)	7.35 (%)
S	1.8 \pm 0.1 (%)	0.6 \pm 0.1 (%)	1.0 \pm 0.1 (%)	1.0 \pm 0.1 (%)	2.54 \pm 0.25 (%)	3.2 (%)
Cl	950 \pm 60	0.57 \pm 0.01 (%)	0.26 \pm 0.01 (%)	0.29 \pm 0.01 (%)	--	-
K	0.16 \pm 0.02 (%)	0.57 \pm 0.06 (%)	0.93 \pm 0.09 (%)	0.21 \pm 0.02 (%)	1.01 \pm 0.2 (%)	3.12 (%)
Ca	23.7 \pm 3.4 (%)	0.24 \pm 0.01 (%)	2.58 \pm 0.45 (%)	1.04 \pm 0.22 (%)	5.72 \pm 0.03 (%)	0.51 (%)
Ti	340 \pm 17	0.39 \pm 0.06 (%)	0.40 \pm 0.08 (%)	0.17 \pm 0.05 (%)	0.11 \pm 0.05 (%)	0.42 (%)
V	0.21 \pm 0.01 (%)	104 \pm 11	79 \pm 10	83 \pm 10	166 \pm 18	156
Cr	97 \pm 5	48 \pm 2	42 \pm 2	25 \pm 2	33.3 \pm 0.7	83
Mn	125 \pm 4	390 \pm 11	650 \pm 20	232 \pm 7	242 \pm 5	195
Fe	0.84 \pm 0.02 (%)	4.97 \pm 0.13 (%)	3.26 \pm 0.09 (%)	2.1 \pm 0.06 (%)	1.94 \pm 0.16 (%)	4.66 (%)
Co	10.8 \pm 0.3	38 \pm 1	17.5 \pm 0.4	12.1 \pm 0.3	13.3 \pm 0.3	24.4
Ni	237 \pm 12	108 \pm 5	53 \pm 10	37 \pm 2	24.2 \pm 3.2	81
Cu	65 \pm 3	32 \pm 2	43 \pm 2	41 \pm 2	51.2 \pm 2.4	79
Zn	1220 \pm 60	100 \pm 5	70 \pm 5	60 \pm 3	69.3 \pm 2.8	39
As	66 \pm 6	9.7 \pm 1.3	7.7 \pm 1.1	14 \pm 1	42.3 \pm 1.7	28
Se	26.7 \pm 0.5	4.2 \pm 0.4	<1	12 \pm 1	2.4 \pm 0.6	2.7
Br	8.2 \pm 2.7	32 \pm 9	10 \pm 3	19 \pm 5	--	-
Mo	295 \pm 30	1.3 \pm 0.4	1.6 \pm 0.4	4.3 \pm 1	31.8 \pm 2.5	114
Cd	28 \pm 3	0.6 \pm 0.2	1.8 \pm 0.4	2.2 \pm 0.5	1.20 \pm 0.06	0.67
Sb	29 \pm 3	0.2 \pm 0.1	0.2 \pm 0.1	0.7 \pm 0.2	2.50 \pm 0.19	4.00
U	38 \pm 3	1.8 \pm 0.9	0.9 \pm 0.4	4.3 \pm 0.9	4.79 \pm 0.05	28
Tl	6.4 \pm 1.5	1.1 \pm 0.2	0.4 \pm 0.2	0.4 \pm 0.2	--	-

The Julia Creek sample is distinctly different from the others. Calcium, inorganic carbon, zinc, vanadium, arsenic, selenium, thallium, molybdenum, cadmium, antimony and uranium

are all 1-2 orders of magnitude higher in concentration, while aluminium, titanium and iron are by comparison lower. The high calcite and quartz and relatively low clay mineral content explain many of these differences. Results for Sunbury and other U. S. marine-derived shales show similar elevated levels of uranium, molybdenum, zinc and arsenic (12). Vanadium concentrations are also high in these U. S. samples, but not to the extent of the Julia Creek sample.

There is considerable evidence for the uptake of arsenic by marine algae. In low phosphate seawater, arsenate is co-adsorbed by the algae and converted to a range of organoarsenic compounds (7). It has also been suggested that arsenic and selenium may replace sulfur in organo-sulfur compounds (13) and this may also be true for antimony. Antimony is also concentrated by some bacteria.

Uranium in Julia Creek shale is associated mainly with phosphatic fish skeletal remains and high concentrations have been identified in strata rich in fish debris (14). Arrhenius et al. (15) found that concentration of uranium occurs through complexation with phosphate ion after the death of the organism. Phosphate is present as apatite in the skeletal debris. In Chattanooga shales, uranium concentrations as high as 100 mg g⁻¹ have been found, present mainly as the oxide minerals, although some organic association was detected (16).

To examine trace element associations, concentration-depth profiles were studied for two Julia Creek drill core samples. In agreement with the findings of Ramsden (14), cadmium, zinc and thallium were found to be associated with pyritic sulfur, whereas uranium correlated well with organic carbon (17). Vanadium exhibits an association with both the clay and organic fractions. In the shallow core, arsenic, selenium, antimony and molybdenum showed a strong association with both organic sulfur and organic carbon (Figure 2). Data from the deeper core suggest that arsenic and selenium are predominantly associated with pyritic sulfur in the oil shale, but still associated with organic species in the coquinite.

Molybdenum is associated with pyritic sulfur in the coquinite but appears to be associated with organic species in the shale. It is needed by cyanobacteria as a catalyst for nitrogen fixation (18).

Vanadium, while also present as oxides, vanadates and silicates, is present in high concentrations as vanadyl porphyrins (19, 20). A range of both vanadium and nickel porphyrins have been isolated by Ekstrom et al. (21) and evidence has been found indicating a mild thermal history, but possibly a biological transformation from chlorophyll. Both vanadium and nickel form strong complexes with porphyrin-type molecules; however, a high V/Ni complex ratio is favored by oxidizing rather than anoxic conditions. Although the methanogenic bacteria would have created anoxic conditions in the sediments, overlying waters were most likely oxygenated and it is here that complexation would have occurred. Potter et al. (22) explained high V/Ni ratios in Kentucky shales on the basis of low sedimentation rates permitting high vanadium uptake from seawater by organic matter. The ratio of dissolved vanadium to nickel is at least 30 times greater in seawater than in river or lake waters (23). In addition, there are species of tunicates which are efficient concentrators of vanadium and these may have been present amongst the precursor organisms (18).

Trace element abundances in the three Australian Tertiary shales are very similar and approximate the values for average sedimentary shales as reported by Turekian and Wedepohl (24). Differences in minor element content of the shales are associated with slightly differing lithologies. Rundle shale, for example, is higher in calcium and magnesium than either Condor or Nagoorin shales, due to the presence of both calcite and dolomite. Green River shale contains even more carbonate, calcium and magnesium than Rundle shale, with measurably higher concentrations of arsenic, antimony, molybdenum and cadmium.

Trace Element Partitioning

Details of oil and water yields and total weight losses in Fischer Assays are shown in Table II and data for the concentrations of 19 trace elements found in oils and retort waters are given in Table III.

TABLE II
FISCHER ASSAY PRODUCT DETAILS OF OIL SHALES

Sample	Oil Yield (g/100 g Dried Raw Shale)	Water (mL/100 g Dried Raw Shale)	Weight Loss (g/100 g Dried Raw Shale)
Julia Creek	7.62	1.60	12.0
Condor	5.38	9.73	18.7
Rundle	10.64	2.68	21.7
Nagoorin	4.95	7.98	25.7

TABLE III

PARTITIONING OF TRACE ELEMENTS IN SHALE OIL AND RETORT WATERS

Element	Julia Creek			Condor			Rundle		
	Oil $\mu\text{g g}^{-1}$	Water $\mu\text{g L}^{-1}$	Mobility %	Oil $\mu\text{g g}^{-1}$	Water $\mu\text{g L}^{-1}$	Mobility %	Oil $\mu\text{g g}^{-1}$	Water $\mu\text{g L}^{-1}$	Mobility %
Al	37	<1	0.046	153	<1	0.012	25	<1	0.005
As	42	19	5.3	1.3	0.24	0.85	5.7	3.8	9.2
Br	0.3	1.1	0.49	0.12	2.4	0.72	0.18	0.95	0.5
Ca	60	50	0.002	22	19	0.088	35	18	0.016
Cl	66	370	1.15	49	2110	3.7	29	600	0.74
Co	0.16	1.6	0.37	0.42	4.8	1.3	0.26	2.7	0.57
Cr	1.2	0.29	0.093	6.7	1.0	0.96	3.5	0.08	0.88
Cu	0.49	0.08	0.063	0.41	0.27	0.16	0.32	0.57	0.12
Fe	17	0.22	0.015	6.9	5.4	0.002	16	0.7	0.005
K	33	15	0.17	20	10	0.016	26	8.8	0.032
Mg	9	3.2	0.041	14.4	10.7	0.023	22	8.7	0.0001
Mn	0.4	0.07	0.025	0.14	0.52	0.015	0.28	0.12	0.005
Na	3.6	11	0.024	3.9	11	0.028	6.1	6.5	0.01
Ni	1.9	4.2	0.089	3.5	8.4	0.93	1.4	5.2	0.55
Sb	1.8	0.04	0.48	<0.03	<0.03	0	<0.03	<0.03	0
Se	10	12	3.6	0.25	0.05	11.0	0.11	0.2	0.15
Ti	13	0.016	0.29	0.91	0.13	0.002	13.4	0.023	0.035
V	10.2	<0.1	0.037	<0.1	<0.1	<0.01	<0.1	<0.1	<0.01
Zn	5	<0.07	0.031	1.2	0.17	0.09	1.5	0.31	0.24

Element	Nagoorin			Green River (10)		
	Oil $\mu\text{g g}^{-1}$	Water $\mu\text{g L}^{-1}$	Mobility %	Oil $\mu\text{g g}^{-1}$	Water $\mu\text{g L}^{-1}$	Mobility %
Al	24	<1	0.003	9.7	<1	0.0062
As	9	1.5	4.1	4.1	3.4	3.8
Br	0.67	1.32	0.74	-	-	-
Ca	32	180	0.15	<1	6	0.003
Cl	240	1050	3.3	-	-	-
Co	0.78	4.9	3.6	2.0	0.21	3.8
Cr	1.2	0.36	0.36	0.22	0.01	0.38
Cu	0.46	0.12	0.073	<0.7	<0.1	0.27
Fe	23	18	0.012	60	1.2	0.084
K	8	83	0.34	5	5	0.023
Mg	7.1	95	0.16	8.2	<17	0.021
Mn	0.26	0.32	0.017	0.16	<0.10	0.056
Na	26	18	0.07	51.5	1360	0.19
Ni	1.3	11.4	2.6	4.1	1.3	4.7
Sb	0.4	<0.03	2.9	0.005	0.15	0.28
Se	0.58	0.37	0.5	0.81	1.25	5.1
Ti	2.4	0.43	0.009	<0.5	<0.6	0.009
V	<0.1	<0.1	<0.02	0.60	<0.07	0.11
Zn	1.6	0.80	0.23	0.69	0.09	0.27

On the basis of these data, mobilities of elements into the oil and water phases were calculated as the percentage by weight of the element transferred to these phases from the raw shale (Table III). Data for Green River shale are included for comparison (11).

During retorting, aluminium, arsenic, chromium, iron, titanium and zinc partitioned predominantly into the oil fraction. Vanadium was found in Julia Creek oil and antimony in both Julia Creek and Nagoorin oil. Cobalt, nickel and chlorine partitioned mainly in the retort waters in each case. Arsenic and selenium are the most mobile elements in all shales. Cobalt and nickel (except in Julia Creek shale) were also mobilized to greater than 1%, into the retort water. Apparent anomalies, such as the low mobilities of zinc, nickel and chromium in Julia Creek shale and the high mobilities of antimony in Nagoorin and titanium in Julia Creek shales, are the result of higher or

lower concentrations, respectively, of the element in the raw shale, when compared with the value for an average sedimentary shale (24).

Preferential mobility in the oil phase must be interpreted as arising from organic association of the element; this has already been demonstrated for vanadium, uranium, molybdenum, arsenic, selenium and antimony in Julia Creek Shale. The possibility that a small fraction of elements in either phase may result from the carryover of shale fines cannot be discarded.

Elements soluble in retort waters may be volatile organic complexes or inorganic species, including fines, which preferentially dissolve on contact with the weakly basic retort water. Typical analyses of these waters (Table IV) showed them to be primarily dilute solutions of ammonium carbonate, with high concentrations of chloride and thiosulfate ion. Dissolved organic carbon concentrations are also high, especially in the Nagoorin sample and are due to the presence of a plethora of metal-binding organic species, principally carboxylic acids, but also phenols, aromatic amines and heterocyclic bases.

In assessing the potential environmental impact posed by trace elements in retort waters and oils, it is their ultimate concentration rather than their mobility which is important. On the basis of recommended "safe" environmental concentration limits for waters (25) considerable treatment would be required to remove elements such as arsenic, selenium, cobalt, nickel and other heavy metals, in addition to toxic organic species, before discharge to a waterway would be permissible.

The chemical form and concentration of elements remaining in the spent shale will also be of concern, especially if the retorting process has rendered them readily leachable from the spent shale storage heaps. Concentrations of all but the mobile elements are altered little from those in the raw shale, but depending on retorting temperatures and conditions, non-volatile organic complexes may well be decomposed, while carbonates and other non-refractory minerals are transformed to oxides.

TABLE IV
CHEMICAL ANALYSIS OF RETORT WATERS

	<u>Julia Creek</u>	<u>Condor</u>	<u>Rundle</u>	<u>Nagoorin</u>
pH	8.4	9.5	8.6	8.8
Organic C, g L ⁻¹	2.3	4.1	2.2	7.4
Ammonia, g L ⁻¹	1.3	5.0	29	8.6
Alkalinity, g L ⁻¹ (CaCO ₃)	1.6	11.5	2.6	17.1
S ₂ O ₃ ⁼ , g L ⁻¹	1.1	0.01	0.3	0.05
SO ₄ ⁼ , mg L ⁻¹	72	100	26	212
SCN ⁻ , mg L ⁻¹	97	22	29	50
CN ⁻ , mg L ⁻¹	24	10	4	7
Phenolics, mg L ⁻¹	58	29	41	37

Leaching Studies

There have been many differing approaches to the study of leaching characteristics (26, 27) and standard batch leach tests have now been devised and accepted by the U. S. Environmental Protection Agency as a basis for the comparison of samples (28). Batch tests are, however, sensitive to the solution-to-solids ratio, give only a total leachable quantity and fail to reflect adequately the compositional changes that may occur in the leachate with time. More realistic data can be obtained by column testing, ideally conducted under non-saturated flow for extended periods of up to six months or more; however, data obtained from saturated flow experiments over a few days of continuous flow provide a useful estimate of potential pollutant release. In the present studies, the latter approach was adopted to enable a comparison of raw and spent shales from the four Australian deposits, since stockpiles of either will be potentially leachable.

The distribution of major ions in leachates from the raw and spent shales was similar to that reported previously for some U. S. shales (29) and for Rundle shale (30). The salt release was disturbingly high; the first pore volumes released from the Condor sample contained approximately 0.3 M sodium and chloride, accompanied by a high sulfate concentration (0.01 M). The

concentrations of these ions were lower in the other deposits, although they exhibited higher calcium concentrations consistent with its elevated levels in the shales.

The rate of trace element release was initially rapid except for calcium and sulfate whose solubility was a limiting factor in some shales. In most instances, the concentrations of trace elements in the leachates reduced to acceptable levels after the passage of 4-5 pore volumes. The pH values, however, diminished little. Values for raw shale leachates were near 7 (Table V); however, the Rundle and Julia Creek spent-shale leachates were more basic as a consequence of oxides, formed during retorting, which undergo partial hydrolysis during leaching.

TABLE V
COMPOSITION OF THE FIRST PORE VOLUME OF COLUMN LEACHATES

	Julia Creek		Condor		Rundle		Nagoorin	
	Raw	Retorted	Raw	Retorted	Raw	Retorted	Raw	Retorted
pH	7.7	10.7	6.5	6.1	7.5	9.7	5.2	7.5
Na, g L ⁻¹	1.4	1.3	6.7	5.0	3.7	2.3	1.2	3.6
Ca, g L ⁻¹	1.0	0.9	0.6	0.4	1.0	0.8	0.8	0.7
Cl ⁻ , g L ⁻¹	1.8	0.9	12.0	14.2	3.6	3.5	1.9	5.8
SO ₄ ⁼ , g L ⁻¹	5.5	2.3	7.4	2.5	7.1	2.9	5.4	2.2
Organic C, mg L ⁻¹	252	36	12	2	680	36	168	10
Mn, mg L ⁻¹	0.1	0.1	1.0	0.4	2.6	2.5	1.8	0.9
Ni, mg L ⁻¹	1.2	0.1	0.7	0.6	0.2	0.2	0.1	0.1
Cu, mg L ⁻¹	0.4	0.2	2.6	1.4	1.7	0.1	0.3	0.1
Zn, mg L ⁻¹	2.3	0.3	2.6	1.2	1.5	1.0	4.0	0.2
Cd, mg L ⁻¹	0.5	0.4	0.2	0.1	0.6	0.1	0.7	0.5
As, mg L ⁻¹	0.8	0.4	1.4	0.5	0.6	0.1	4.0	0.2
CN ⁻ , mg L ⁻¹	1.0	1.0	0.1	0.1	0.1	0.1	0.1	0.5
S ₂ O ₃ ⁼ , mg L ⁻¹	5.5	56	15.4	96	7.3	47	0.8	11.4

Leachates from Green River retorted shale are also basic (pH 8.2-9.5 (27)); however, those from Kentucky shales, both raw and retorted, are acidic (31). This acidity results from high pyrite yet low carbonate concentrations, unlike that of Julia Creek shale. Mobilization of trace elements during leaching will be pH dependent. Most heavy metals will be more readily leached under acidic conditions, while molybdenum, arsenic and selenium are more soluble in basic conditions. Low concentrations of these latter elements were found in leachates of Kentucky shales (31), but cadmium, zinc, copper and manganese concentrations were environmentally significant. Arsenic and molybdenum levels were higher in leachates of Green River shale (27, 32).

For the Australian shales, arsenic, cadmium, copper, nickel, zinc and manganese were found to exceed the recommended environmental limits (25) in the first pore volumes of leachates. Changes in the distributions of these species in the leachates depend not only on pH, but also on ionic strength and chemical form. Phenols and carboxylic acids, which are more soluble in basic solutions, are likely metal-binding agents. Preliminary results indicate that up to 60% of nickel and copper are in bound forms.

It was noticeable that cyanide and thiosulfate levels were also high for leachates from some of the retorted shales. The retorting process causes high concentrations of thiosulfate and ammonia to be driven off in the retort waters, together with cyanide, sulfide and thiocyanate (Table IV). Residues of these species may be released from the spent shale by aqueous leaching.

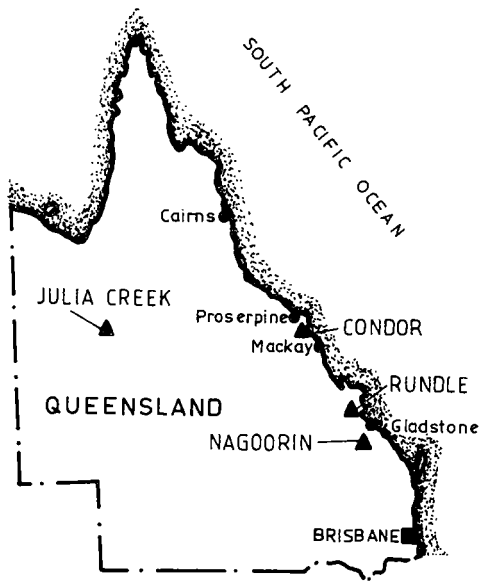


Figure 1. Major oil shale deposits in Queensland, Australia.

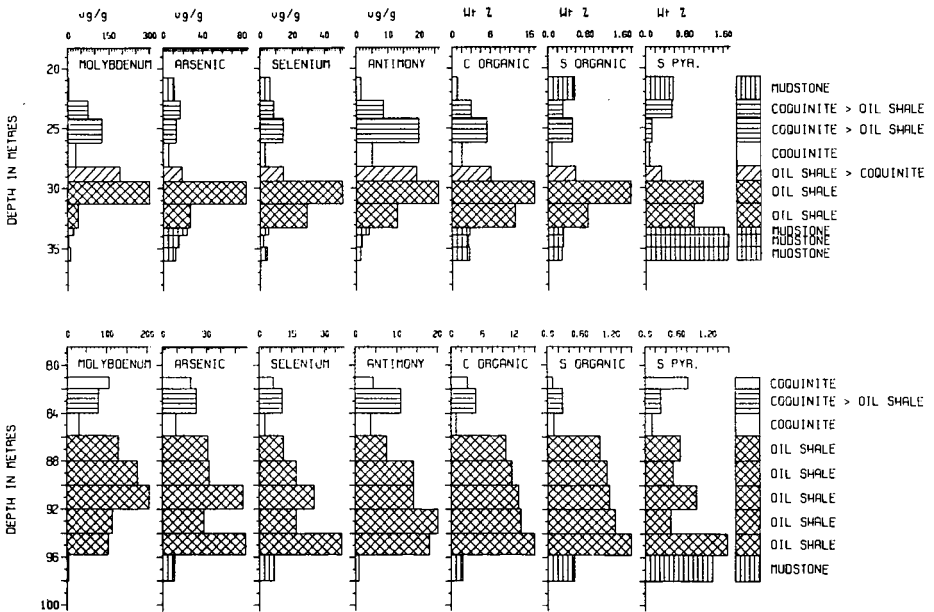


Figure 2. Concentration-depth profiles in Julia Creek drill core samples.

ACKNOWLEDGMENTS

The authors gratefully acknowledge the following staff of Analytical Chemistry Section for their contribution to this work: Y. Farrar, D. Alewood, K. Prescott, I. Warner, J. Buchanan, G. McOrist and J. Chapman. Fischer Assays were provided by G. C. Wall and R. Pearse. Southern Pacific Petroleum NL, CSR Ltd and Esso Australia Limited are thanked for providing raw shale samples.

LITERATURE CITED

- (1) Cane, R. F., 12th Oil Shale Symp. Proceedings, Colorado School of Mines, 17 (1979).
- (2) Jones, C. H., Thompson, D. J. and Moore, A. J., Proceedings 1st Australian Workshop on Oil Shale, Lucas Heights, N.S.W., 3 (1983).
- (3) Poole, D. R., *ibid.* 9 (1983).
- (4) Ivanac, J. F., *ibid.* 12 (1983).
- (5) Hutton, A. C., *ibid.* 31 (1983).
- (6) Glikson, M., *ibid.* 39 (1983).
- (7) Benson, A. A., Cooney, R. V. and Herrera-Lasso, J. M., *J. Plant Nutr.*, 3, 285 (1981).
- (8) ASTM Standard - D3907, Amer. Soc. for Testing and Materials, Philadelphia (1982).
- (9) Wallace, J. R., U. S. Environmental Protection Agency Report, EPA 600/7-81-084 (1981).
- (10) Fox, J. P., Mason, K. K. and Duvall, J. J., 12th Oil Shale Symp. Proceedings, Colorado School of Mines, 58 (1979).
- (11) Fox, J. P., "Partitioning of Major, Minor and Trace Elements During Simulated In-Situ Oil Shale Retorting", Thesis, University of California, LBL-9062 (1980).
- (12) Bland, A. E., Robl, T. L. and Koppenaal, D. W., 1981 Eastern Oil Shale Symp. Proceedings, Lexington, KY, 183 (1981).
- (13) Wilkerson, C. L., *Fuel*, 61, 63 (1982).
- (14) Ramsden, A. R., Personal communication.
- (15) Arrhenius, G., Bramlette, M. N. and Picciotto, E., *Nature*, 180, 85 (1957).
- (16) Judzis, A. and Williams, B., 12th Oil Shale Symp. Proceedings, Colorado School of Mines, 390 (1979).
- (17) Dale, L. S. and Fardy, J. J., Proceedings 1st Australian Workshop on Oil Shale, Lucas Heights, N.S.W., 57 (1983).
- (18) Glikson, M., Personal communication.
- (19) Riley, K. W. and Saxby, J. D., *Chem. Geol.*, 2, 187 (1982).
- (20) Ekstrom, A. J., Loeh, H. J. and Dale, L. S., *Proc. 187th ACS Symp. Series*, Seattle, in press (1983).
- (21) Ekstrom, A. J., Fookes, C. J. R., Hambly, T., Miller, S. A. and Taylor, J. C., *Nature*, in press (1983).
- (22) Potter, P. E., Magnard, J. B. and Pryor, W. A., U. S. Dept. of Energy EGSP Contract DE-AC21-76, Report MC05201.
- (23) Forstner, U., in "Metal Pollution in the Aquatic Environment", U. Forstner and G. T. W. Wittman, eds., Springer-Verlag, Berlin, 71 (1979).
- (24) Turekian, K. K. and Wedepohl, K. H., *Geol. Soc. Amer. Bull.*, 72, 175 (1961).
- (25) Cleland, J. G. and Kingsbury, G. L., U. S. Environmental Protection Agency Report EPA-600/7-77-136 (1977).
- (26) Amy, G. L., Hines, A. L., Thomas, J. F. and Selleck, R. E., *Environ. Sci. Technol.*, 14, 831 (1980).
- (27) Stollenwerk, K. G. and Runnells, D. D., *Environ. Sci. Technol.*, 15, 1370 (1981).
- (28) ASTM Standard D3987, Amer. Soc. for Testing and Materials, Philadelphia (1981).
- (29) Fransway, D. F. and Wagenet, R. J., *J. Environ. Qual.*, 10, 107 (1981).
- (30) Bell, P. R. F., Greenfield, P. F. and Nicklin, D. J., 16th Oil Shale Symp. Proceedings, Colorado School of Mines, 477 (1983).
- (31) Koppenaal, D. W., Cisler, K. and Thomas, G., 1981 Eastern Oil Shale Symp. Proceedings, Lexington, KY, 369 (1981).
- (32) Jackson, K. and Jackson, L., 13th Oil Shale Symp. Proceedings, Colorado School of Mines, 351 (1980).

SYMPOSIUM ON CHARACTERIZATION AND CHEMISTRY OF OIL SHALES
PRESENTED BEFORE THE DIVISIONS OF FUEL CHEMISTRY AND
PETROLEUM CHEMISTRY, INC.
AMERICAN CHEMICAL SOCIETY
ST. LOUIS MEETING, APRIL 8 - 13, 1984

THE PARTITIONING OF ARSENIC IN INDIGENOUS AND RETORTED OIL SHALE

By

K. M. Jeong and J. C. Montagna
Gulf Research and Development Company, Pittsburgh, Pennsylvania 15230

INTRODUCTION

The distribution of organometallic compounds in shale oils is somewhat variable, but typical analyses indicate the presence of elemental Cd, V, Hg, Sn, Se and As. Of these, the relatively high concentrations of arsenic have, in particular, presented problems for the processing and refining of oil shale into final oil products. Typically, approximately 30 ppm of arsenic compounds are present in Paraho-retorted (indirect mode) shale oils, with similar arsenic concentration ranges being found in shale oils obtained via other above-ground or *in situ* processing methods.

These arsenic concentration levels reduce the efficiency of current processing systems due to the rapid deactivation and/or poisoning of hydrogenation catalysts. The hydrogenitrogenation activity of a commercial nickel-molybdenum hydrotreating catalyst was found by Curtin, et al. (1), to decrease at a substantially slower rate when charging dearsenated shale oil. Thus, one factor in the development of an oil shale conversion/oil upgrading technology program is a detailed understanding of the arsenic chemistry.

The majority of the studies dealing with arsenic have been prompted by oil-upgrading considerations and have examined potential dearsenation methods which would be applicable prior to hydrotreating, e. g., reactive heat transfer solids, hydrovisbreaking, guard beds and caustic washing. From a processing standpoint, these methods have been moderately successful but various disadvantages remain. These efforts have been supplemented to a certain extent by studies directed at more fundamental questions of the arsenic chemistry in oil shale and shale oil. In this context, a topic of significant current interest is the identification and partitioning of these trace arsenic compounds.

The origin and identification of the arsenic components in shale oil have not been studied in detail; one exception is the recently reported work of Fish and Brinckman (2). Although various geochemical schemes have been advanced in the literature, certain analytical results (3) have suggested that arsenic exists in the indigenous oil shale primarily in inorganic forms. There have been numerous studies on the biogeochemical creation of kerogen and the role of ancient algae in this process. The uptake and metabolism of inorganic arsenic and other inorganic forms of elements by algae (5, 6) and other microflora (7) is well documented. It has been shown by Andrae and Klumpp (6) that the biomethylation of inorganic arsenic in the +5 oxidation state by marine algae produces both dimethylarsine and methylarsonate species. Concerning the origin of the arsenic compounds in shale oil, it has been suggested that (I) the arsenic is originally concentrated in the organic matter in the oil shale and is released with little decomposition during the pyrolysis process and (II) the inorganic arsenic compounds present as a fraction of the mineral matrix react with various hydrocarbons upon pyrolysis to form organoarsenic compounds.

The principal objective of this study was to characterize the arsenic distribution in both oil shale and shale oil. These obtained results can be used to develop a more complete description of the total As balance among products of a conversion process: shale oil, spent shale, gas and water products. For example, it has recently been shown by Fish, et al. (8) and Fox, et al. (9) that both inorganic and organic arsenic species are present in oil shale retort process waters. Results obtained by this study of the identification of specific arsenic compounds in Paraho shale oil are compared with the recent "fingerprinting" study of Fish and Brinckman (2). The details of the processes whereby arsenic compounds are formed in indigenous oil shale and retorted shale oil are beyond the scope of this study, but these data may provide added insight.

ARSENIC DISTRIBUTION IN OIL SHALE

Experimental

The oil shale samples used in this study were obtained from the Green River formation, C-a tract, Mahogany zone. Standard pulverizing and sieving procedures reduced these samples to

the -50 +325 mesh size range.

Two separation methods were investigated in an attempt to preferentially isolate and concentrate the arsenic constituents in these samples: heavy media liquids gravitational separation and isodynamic magnetic separation (Frantz, Model L-1). In the first method, heavy media separations at densities of ρ : >2.25, <2.25 and >1.65, <1.65 g cm⁻³ were utilized and oil shale fractions of the following three grades, as determined by Fischer Assay, 25, 31 and 44 GPT, were obtained.

Arsenic concentrations were determined by neutron activation analysis. Arsenic concentration measurements were performed for the original oil shale, bitumen-free oil shale and the bitumen fraction. The latter two fractions were obtained using the Soxhlet extraction method based on a 3:7 mixture of methanol:benzene. The mineral composition of the various samples was determined from X-ray diffraction data (Phillips, APD-3500).

Results and Discussion

Analysis of the three grades of oil shale indicated that the arsenic concentration is a function of oil shale richness and increases with increasing organic content. An increase of 102% in the arsenic content was determined between the 25 and 44 GPT samples, i. e., the arsenic concentration increased from 42 to 85 ppm. The major mineral constituents were identified to be ankerite, dolomite, aragonite, calcite, quartz, albite, analcime and illite. The mineral composition was essentially uniform among the three different shale grades and, therefore, no preferential of arsenic is expected on this basis.

The measurement of arsenic concentration as a function of the organic carbon content is not an absolute determination of the partitioning of arsenic between the organic and inorganic matter in oil shale. These results indicate an association between arsenic and the organic matter phase in Green River oil shale, but do not differentiate between indigenous organoarsenate compounds and inorganic As compounds which are intimately associated with the organic matter. Results are later presented which support the latter alternative.

The results of the Soxhlet extraction indicated that the bitumen accounted for a fairly constant fraction, approximately 20 wt %, of the total organic matter in these samples (see Table I). The arsenic concentration in the bitumen fractions was reasonably constant among the three different grades, although small, approximately 2 ppm. Thus, it appears that the arsenic fraction which may be organic in nature is intrinsically associated with the kerogen matrix and inseparable by simple, organic solvent extraction methods.

TABLE I

ARSENIC CONCENTRATION IN ORIGINAL AND TREATED OIL SHALE

Grade (GPT)	Fraction	Yield (Wt %)	[As] + δ^a (ppm)
25	Original	100	41.7 + 2.3
	Bitumen	3.2	1.7
	Bitumen free	96.8	39.3 + 5.3
	Low temp. ash	90.0	46.5 + 0.7
	Total organics	13.5	----
31	Original	100	49.7 + 0.9
	Bitumen	3.5	1.7
	Bitumen free	96.5	49.3 + 2.5
	Low temp. ash	86.8	55.0 + 4.2
	Total organics	16.2	----
44	Original	100	84.5 + 0.6
	Bitumen	3.9	2.3
	Bitumen free	96.1	84.6 + 5.0
	Low temp. ash	81.2	108.0 + 2.8
	Total organics	22.9	----

a. δ represents single standard deviation for several measurements.

The solid oil shale fractions insoluble in benzene (i. e., bitumen-free oil shale) were analyzed for both organic carbon and arsenic content and both sets of data increased with increasing oil richness (see Table I). For example, the organic carbon concentration increased by

approximately 20% between the 25 and 31 GPT oil shale samples and by about 41% from the 31 GPT to the 44 GPT sample. The corresponding values for the percent arsenic increase were 19% and 70%, respectively. Although the arsenic concentration is somewhat dependent on the organic carbon content of bitumen-free oil shale, it was determined that greater than 95% of the As is associated with either the kerogen or mineral matrix. This is based on the arsenic concentrations in the bitumen fractions and the original oil shale.

Since the arsenic distribution is largely concentrated in the naturally occurring mineral matrix which is closely associated with organic matter, the isodynamic magnetic separation procedure was applied to concentrate arsenic according to the magnetic properties of the oil shale for further characterization. The arsenic concentration was determined as a function of the transverse angle at which the fractions were collected, i. e., <10, 10, 15, 20 and >25 degrees, at a fixed longitudinal slope of 15° and a current of 1.2 A. The data obtained using this experimental configuration were directly related to the magnetic susceptibilities of each fraction. These results are summarized in Table II. The arsenic content was preferentially separated with respect to magnetic susceptibility and concentrated by about a factor of 2.5 relative to the original sample.

TABLE II

ISODYNAMIC MAGNETIC SEPARATION YIELDS AND [As], [C_{org}], [Fe] AND [S] DISTRIBUTIONS FOR GREEN RIVER OIL SHALE^a

Trans-verse Angle (degree)	25 GPT Oil Shale					44 GPT Oil Shale				
	Yield (Wt %)	[As] (ppm)	[C _{org}]	[Fe] (Wt %)	[S]	Yield (Wt %)	[As] (ppm)	[C _{org}]	[Fe] (Wt %)	[S]
Original	100	42	11.5	1.1	0.7 ^b	100	85	19.5	2.4	1.3 ^c
>25 (6.0)	1.4	144	11.4	2.4	0.9	19.3	136	18.6	3.5	1.4
25 to 20 (4.8)	19.2	47	10.5	1.7	0.8	14.4	100	20.5	2.6	1.3
20 to 15 (3.6)	27.4	37	11.1	1.2	0.6	20.8	84	21.2	2.2	1.2
15 to 10 (2.4)	38.2	37	11.0	0.8	0.6	22.0	78	20.9	2.1	1.2
<10 (1.2)	13.8	35	10.8	0.6	0.5	23.6	62	21.0	1.6	1.3

a. Mahogany zone, C-a tract, particle size: 100 x 200 mesh.

b. Pyritic sulfur, 0.40; organic sulfur, 0.12; sulfate sulfur, 0.14 wt %.

c. Pyritic sulfur, 0.97; organic sulfur, 0.31; sulfate sulfur, 0.02 wt %.

[As] determined by Instrumental Neutron Activation Analysis (INAA).

[Fe] and [S] measured by X-ray Fluorescence.

() estimated mass susceptibility, x 10⁻⁶ cgs.

The isodynamic magnetic separation results suggest an association between the arsenic content and iron containing sulfide minerals, e. g., Fe_{1-x}S, Fe(AsS)₂, etc., the principal magnetic materials in oil shale. This is consistent with the presence of a large arsenic fraction in the mineral matrix and the determination by derivative thermogravimetric analysis of a pyritic sulfur decomposition (10) temperature of about 510°C (see Figure 1). X-Ray diffraction results indicated that the more magnetic fractions contained relatively larger concentrations of ankerite, albite and analcime, whereas the predominantly nonmagnetic fractions contained more aragonite and calcite. The correlation of the arsenic concentration with constituents having a high magnetic susceptibility is probably the result of complex chemical interactions involving As, Fe and S containing species. This is indicated in Table II by the similar trends of the arsenic and iron concentrations as a function of the transverse angle. The sulfur concentration dependence is not as strong since the sulfur composition includes pyritic, organic and sulfate sulfur at various wt % in the 25 and 44 GPT samples. A previous study (11) has also suggested that the arsenic in oil shale is bound up with pyrite.

In addition to the herein reported results, scanning electron microscopy (SEM) data indicate that arsenic is mainly present in the form of inorganic compounds in indigenous oil shale. These data exhibited the same correlations with transverse angle as summarized in Table II. In view of the above suggested inorganic nature of the arsenic constituents and the strong correlation with organic carbon content, the arsenic distribution processes need to be examined in relation to the organic decomposition occurring during the pyrolysis of the oil shale and in the resulting products.

ARSENIC DISTRIBUTION IN SHALE OIL

The primary objective of these studies was to determine the arsenic distribution in shale oil distillates and residue according to boiling point ranges, molecular weight (size) ranges,

specific compounds and concentration ranges.

Experimental

A sample of Paraho shale oil was fractionally distilled into the following four cuts: (a) naphtha (B. P. IBP-191°C, 1.8 wt %), (b) furnace oil (B. P. 191-360°C, 35.7 wt %), (c) gas oil (B. P. 360-516°C, 46.6 wt %) and (d) residuum (B. P. >516°C, 15.9 wt %). These fractions, except for the naphtha cut and the original sample were passed through a GPC (Gel Permeation Chromatography) column with THF eluent to obtain molecular weight distributions. The residuum fraction was further separated using prep GPC into sixteen equal-volume oil-plus-eluent (CH₂Cl₂) fractions, since this fraction contained the highest arsenic concentration among the four separated samples.

High performance liquid chromatography (HPLC) was used to separate a sample of Paraho shale oil into five different classes of compounds: saturate, aromatic, polar, hexane insoluble and volatiles. In addition to the hexane-insoluble fraction, a hexane- and toluene-insoluble fraction was prepared. (See Table IV)

Semiquantitative product identification was obtained from X-ray photoelectron spectroscopy (XPS) data. XPS was employed to characterize the shale oil-insoluble fractions after extraction with hexane and hexane and toluene in order to identify the surface constituents in the hydrocarbon solvent-insoluble fractions. Spectra were obtained using a Perkin-Elmer PHI Model 550 ESCA/SAM/SIMS which operated at a base pressure of about 1×10^{-8} torr. The samples were irradiated with MgK α radiation at a power of 400 watts. All spectra were calibrated relative to the C(1s) line at 285.0 eV binding energy. The analysis method to determine relative concentrations in units of atomic percent is accurate to $\pm 20\%$ and precise to about one-tenth of the concentration.

Results and Discussion

Analysis of the four cuts obtained by fractional distillation indicated no significant correlation between the arsenic concentration and the boiling point range (see Table III). The arsenic levels in all the fractions were essentially constant, 25-33 ppm, except for the naphtha fraction which contained an arsenic concentration of ~ 2.7 ppm. Such a distribution suggests a fairly uniform mixture of organoarsenic compounds of varying structural complexity. The results in other studies (1, 12, 13) of shale oils indicate that the arsenic concentration profile may be dependent on the process used in recovering the oil. Paraho shale oil is obtained by an above-ground retorting technique, compared to other shale oils processed by *in situ* and other heat transfer methods.

TABLE III

ARSENIC DISTRIBUTION IN PARAHO SHALE OIL ACCORDING TO BOILING POINT RANGES

Fraction	Yield (Wt %)	[As] (ppm)
Whole shale oil	100	28
IBP - 191°C (naphtha)	1.8	2.7
191 - 360°C (furnace oil)	36	25
360 - 516°C (gas oil)	46	28
>516°C (residuum)	16	33

The GPC plots of wt % oil versus retention time of the furnace oil, gas oil and residuum fractions were displaced from one another according to the relationship retention time \propto (effective molecular size)⁻¹. Figure 2 shows the GPC curves of the three distillation fractions which are strongly overlapped and parallel the boiling point range results. The relative arsenic concentration was fairly constant among the three separated fractions, 25-33 ppm (see Table III). Therefore, no direct dependence was found between arsenic concentration and effective molecular size for the tested Paraho shale oil samples.

Due to the small displacement of the GPC curves in Figure 2, further separation of the residuum fraction using preparative GPC was done in order to obtain a more detailed characterization of the heavier molecular weight composition. The results of this separation were analogous to the previous data in that there was no direct dependence of relative arsenic concentration on molecular size with the exception of the first fraction (i.e., largest molecular size) which contained an unusually high concentration of arsenic, approximately 97 ppm. The remaining fractions centered around a mean of about 30 ppm. Thus, no direct correlation between the arsenic concentration and effective molecular size ranges was found, with the possible exception of very large molecular sizes which, in any case, amount to a small percentage of the total oil.

The HPLC physicochemical separation techniques were employed to obtain the following classes of compounds: saturate, aromatic, polar, hexane insoluble and volatiles. The hexane-insoluble fraction overwhelmingly contained the highest arsenic concentration, approximately 85

times more than the original sample. This fraction, however, accounted for only 0.7 wt % of the original sample. Based on these results, a hexane- and toluene-insoluble fraction was also obtained for comparison purposes.

The shale oil insolubles obtained by treatment with hexane, and hexane and toluene were analyzed using X-ray photoelectron spectroscopy to identify trace arsenic constituents. Spectra were scanned from 0 to 1000 eV binding energy and arsenic, magnesium, carbon, nitrogen, oxygen and sulfur were detected. Figure 3 shows the As(3d) and Mg(2p) spectra measured for the hexane- and toluene-insoluble oil shale fraction. An identical spectrum was obtained for the hexane-insoluble fraction. Arsenic was determined to be present on the surface at low concentrations of approximately 0.5% atomic. However, considering the toxicity of this element, these concentration levels are not insignificant.

Binding energies of reference arsenic compounds are available in the literature (14). Due to the low arsenic concentrations in the complex matrix structure on the surface of the shale oil insolubles, a definitive identification of specific arsenic compounds is difficult, but the data strongly suggest the presence of As_2O_5 and organic arsenic compounds, such as phenylarsonic acid. Fish and Brinckman (2) have recently identified methyl- and phenylarsonic acids and arsenate in methanol extracts of Green River oil shale using the HPLC-GFAA and GC-MS techniques. Since these authors used a much more rigorous experimental procedure, their results are considered to be more definitive than the XPS data of this study. Both sets of data, however, are consistent with each other and indicate organic as well as inorganic arsenic compounds in shale oil.

In order to further identify the major arsenic constituents in shale oil, a sample of the hexane and toluene extracted material was demineralized using an HCl/HF mixture. The XPS spectra detected aluminum, carbon, chlorine, magnesium, nitrogen, oxygen, sulfur and silicon. Arsenic was not detected after the HCl-HF treatment. Figure 3 shows the Mg(2p)-As(3d) region of the electron spectrum for the hydrocarbon insoluble fraction both before and after acid extraction and the absence of the arsenic peak is clearly evident in the demineralized sample. It is known that arsenic pentoxide is soluble in alcohol and both alkaline and acidic solutions, but it is not clear to what extent phenylarsonic acid is soluble or reactive in acidic solution.

CONCLUDING REMARKS

The trace metal composition of oil shale and its retort products is increasingly the subject of experimental investigation for reasons of: fundamental chemistry, processing and potential environmental effects. The relatively large concentration of arsenic in indigenous oil shale was found to be in the form of inorganic compounds, particularly in combination with other heteroatoms, such as O, Fe and S. In addition, its concentration in the oil shale was found to increase with organic carbon and higher magnetic susceptibility species, such as iron-containing compounds. The arsenic distribution in shale oil appears to be characterized by both organic and inorganic species, including arsenic pentoxide and phenylarsonic acid. The origin of the organoarsenic compounds is attributed to both organometallic addition and substitution reactions during the pyrolysis process.

In terms of arsenic removal, the results of this study indicate little possibility of significant arsenic reductions in the naturally occurring fossil fuel before the oil extraction (conversion step). The apparent intimate association of arsenic with the organic matter phase suggests that dissolution of arsenic by conventional chemical and/or physical separation methods is not feasible. The distribution of arsenic in the product oil is essentially uniform with respect to boiling point range and effective molecular size range. Conventional removal of arsenic compounds from the shale oil either before or during retorting/conversion remains the more promising approach.

TABLE IV
ARSENIC CONTENT OF PARAHO SHALE OIL HPLC FRACTIONS

	Yield (Wt %)	[As] (ppm)
Whole shale oil	100	33
Volatiles	18	---
Aromatics	34	5
Saturates	19	8
Polars	29	34
Hexane Insolubles	0.71	2800
Hexane/Toluene involubles	0.23	4600

[As] determined by INAA.

Figure 1
TG/DTG CURVES OF ISODYNAMIC MAGNETICALLY SEPARATED
GREEN RIVER OIL SHALE: a) > 25° TRANSVERSE ANGLE, b) 25-20°, c) < 10°

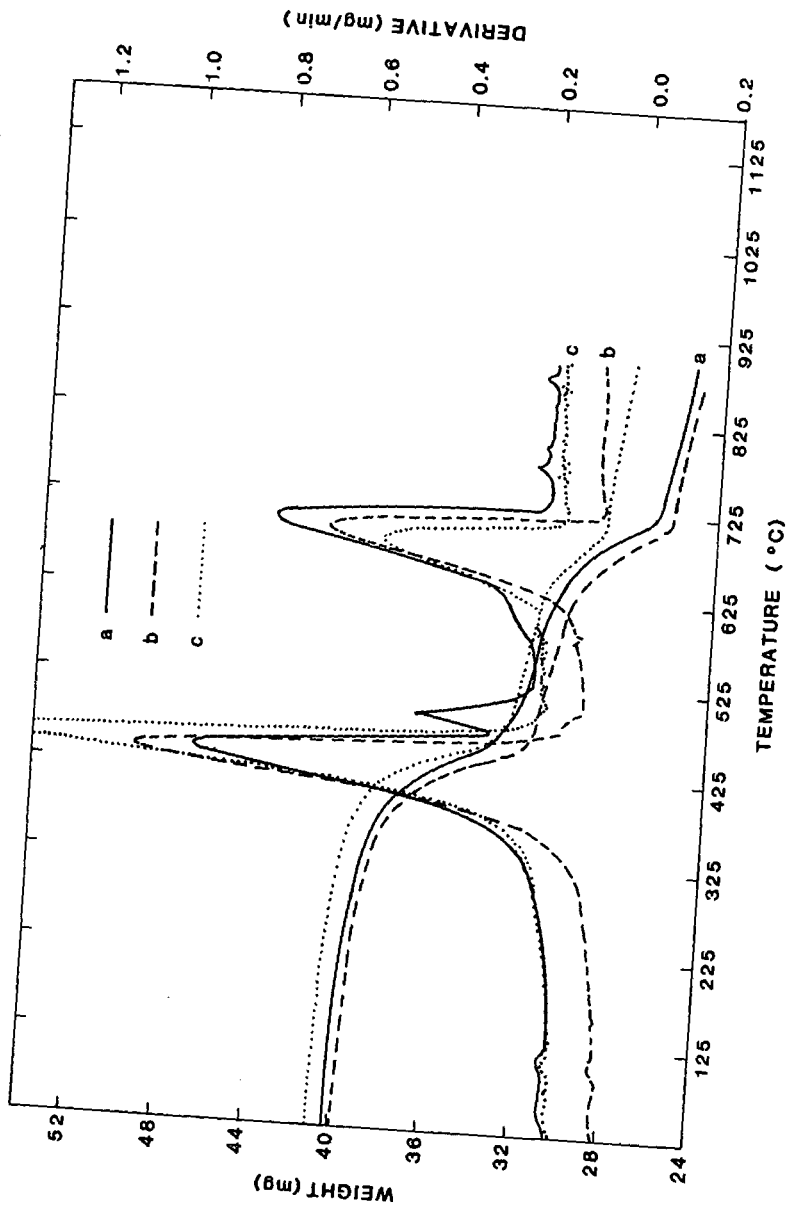


Figure 2

GPC PLOTS OF CONCENTRATION VS. RETENTION TIME
FOR PARAHO SHALE OIL AND DISTILLED FRACTIONS

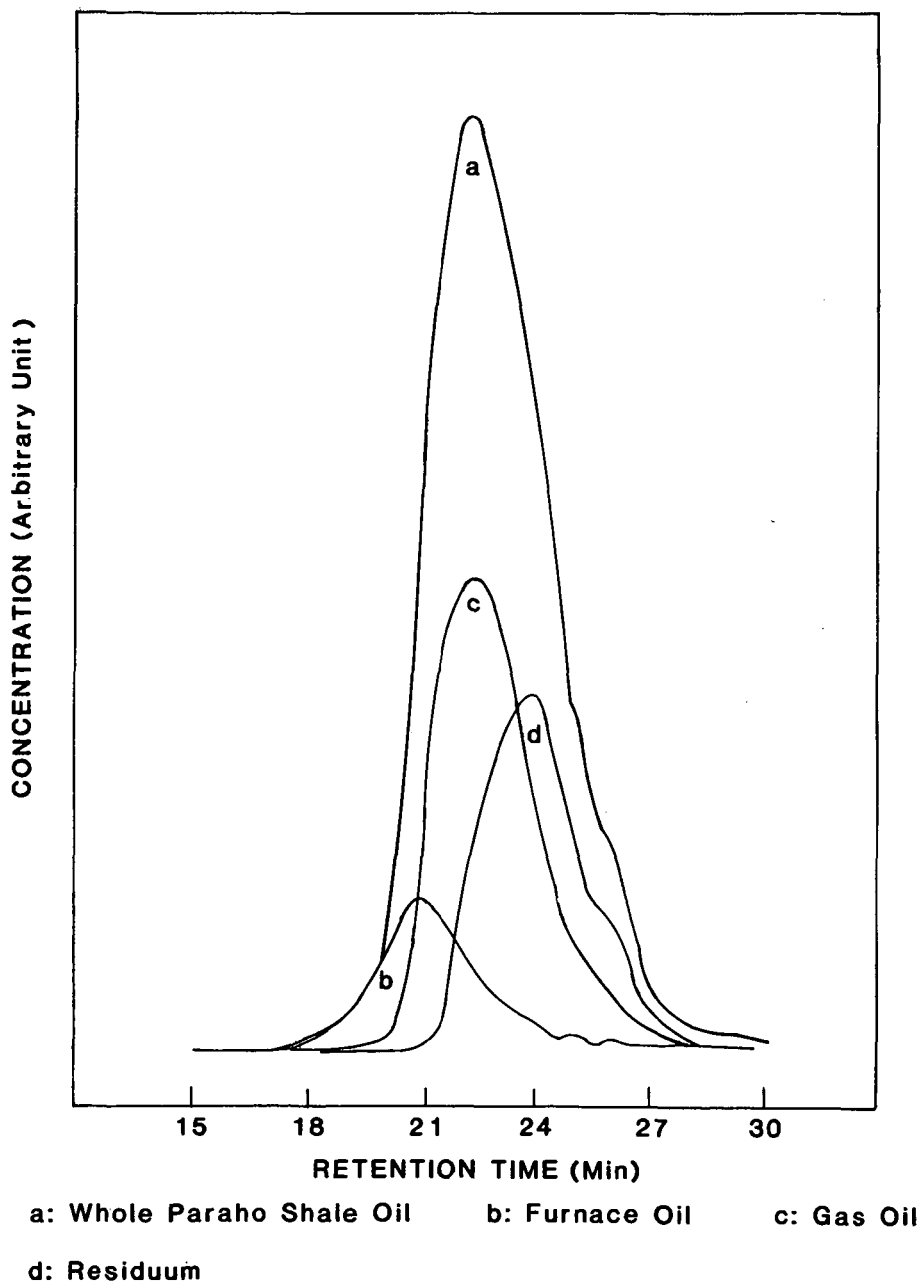
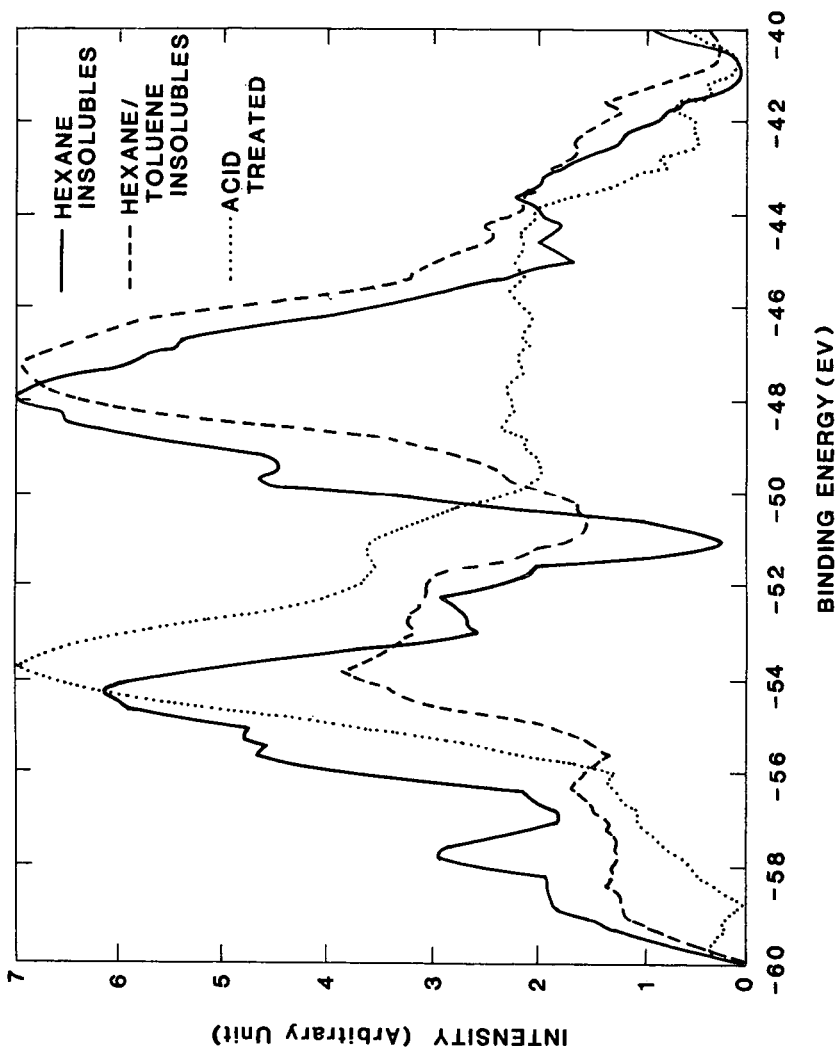


Figure 3

XPS SPECTRA OF HEXANE INSOLUBLES, HEXANE AND TOLUENE INSOLUBLES,
AND DEMINERALIZED FRACTIONS OF PARAHO SHALE OIL



ACKNOWLEDGMENTS

The authors gratefully acknowledge the technical assistance of Mr. D. L. Bash. We also appreciate the technical advice of Dr. T. P. Debies for the XPS Analysts and Mr. E. G. Miller for the INAA measurements.

LITERATURE CITED

- (1) Curtin, D. J., Dearth, J. D., Everett, G. L., Grosboll, M. P. and Myers, G. A., "Arsenic and Nitrogen Removal During Shale Oil Upgrading", ACS, Div. of Fuel Chem., Preprints, 23 (4), 18 (1978).
- (2) Fish, R. H. and Brinckman, F. E., "Organometallic Geochemistry. Isolation and Identification of Organoarsenic and Inorganic Arsenic Compounds from Green River Formation Oil Shale", ACS, Div. of Fuel Chem., Preprints, 28 (3), 177 (1983).
- (3) Wildeman, T. R. and Heistand, R. N., "Trace Element Variation in An Oil Shale Retorting Operation", ACS, Div. of Fuel Chem., Preprints, 24, 271 (1979).
- (4) Cane, R. F., in "Oil Shale", T. F. Yen, ed., Elsevier, Amsterdam, pp. 27-60 (1976).
- (5) Bottino, N. R., Cos, E. R., Irgolic, K. J., Maeda, S., McShane, W. J., Stockton, R. A. and Zingaro, R. A., "Organometals and Organometaloids Occurrence and Fate in the Environment", F. E. Brinckman and J. M. Bellama, eds., ACS, Symp. Ser. 82, Washington, D. C., pp. 116-129 (1978).
- (6) Andrae, M. O. and Klumpp, D., Environ. Sci. Technol. 13, 738 (1979).
- (7) a. Cheng, C. N. and Focht, D. D., Appl. Environ. Microbiol. 38, 494 (1979); b. Cullen, W. R., McBride, B. C. and Pickett, A. N., Can. J. Microbiol. 25, 1201 (1979).
- (8) Fish, R. H., Brinckman, F. E. and Jewett, K. L., Environ. Sci. Technol. 16, 174 (1982).
- (9) Fox, J. P., McLaughlin, R. D., Thomas, J. F. and Poulson, R. E., "The Partitioning of As, Cd, Cu, Hg, Pb and Zn During Simulated In-Situ Oil Shale Retorting", 10th Oil Shale Symp. Proceedings, Colorado School of Mines, pp. 223-237 (1977).
- (10) Jeong, K. M. and Patzer, J. F., II, "Indigenous Mineral Matter Effects in Pyrolysis of Green River Oil Shale", ACS Symp. Ser., 230, Seattle, Washington (1983).
- (11) Desborough, G. A., Pitman, J. K. and Huffman, C., Jr., Chem. Geol. 17, 13 (1973).
- (12) Lyzinski, D. and Vainieri, H., Gulf Rand D Co., private communication.
- (13) COT No. 5A, 23.1 API Occidental Shale Oil, July 16, 1979.
- (14) Handbook of X-Ray Photoelectron Spectroscopy, Perkin-Elmer Corp., Physical Electronics Div., Eden Prairie, MN (1979).

SYMPOSIUM ON CHARACTERIZATION AND CHEMISTRY OF OIL SHALES
PRESENTED BEFORE THE DIVISIONS OF FUEL CHEMISTRY AND
PETROLEUM CHEMISTRY, INC.
AMERICAN CHEMICAL SOCIETY
ST. LOUIS MEETING, APRIL 8 - 13, 1984

THE DETERMINATION OF SULFUR SPECIES IN
OIL SHALE RETORT GAS

By

J. R. Wallace
Denver Research Institute, University of Denver
Denver, Colorado
and
E. Sexton
Chemistry Department, Pennsylvania State University
University Park, Pennsylvania

ABSTRACT

Gas chromatography with flame photometric detection was developed as a means of measuring sulfur species in retort gas. Two potential problems were considered in detail: 1) quenching of the fluorescent signal by coeluting hydrocarbons, and 2) adequate separation of the large number of sulfur species which could potentially occur in retort gas. Fluorescent quenching effects were measured on two types of commercially available FPD's, a single-flame detector and a dual-flame detector. The latter exhibited no significant quenching effects over the concentration ranges of interest in retort gas. However, for the single-flame detector quenching effects cannot be ruled out entirely. Although hydrogen sulfide in retort gas is usually abundant enough to minimize quenching effect, the minor species (COS, CH₃SH, CS₂, and CH₃CH₂SH) could be subject to quenching effects unless precautions are taken. These precautions include operating the detector with the air and hydrogen flows reversed and measuring peak height rather than peak area. The single-flame detector exhibited both suppression and enhancement of the fluorescent signal. Columns were evaluated with respect to their ability to separate the sulfur species of primary interest--H₂S, COS, CH₃SH, SO₂, CS₂, and CH₃CH₂SH--from each other as well as from the later eluting sulfur compounds and the potentially interfering hydrocarbons. Columns were also tested with respect to their ability to tolerate water vapor and for their stability during tests with actual retort gas. A method is described for the primary sulfur species in the range 5-50,000 ppmv using a Carbopack B HT 100 column arranged in a backflush-to-detector configuration.